

***Geothermometry Mapping of Deep
Hydrothermal Reservoirs in Southeastern
Idaho: Final Report***

Earl D. Mattson¹, Mark E. Conrad²,
Ghanashayam Neupane¹, Travis L.
McLing¹, Thomas R. Wood³, Cody J.
Cannon³

August 2016



¹ Idaho National Laboratory

² Lawrence Berkeley National Laboratory

³ University of Idaho

The INL is a U.S. Department of Energy National Laboratory
operated by Battelle Energy Alliance

DISCLAIMER

This information was prepared as an account of work sponsored by an agency of the U.S. Government. Neither the U.S. Government nor any agency thereof, nor any of their employees, makes any warranty, expressed or implied, or assumes any legal liability or responsibility for the accuracy, completeness, or usefulness, of any information, apparatus, product, or process disclosed, or represents that its use would not infringe privately owned rights. References herein to any specific commercial product, process, or service by trade name, trade mark, manufacturer, or otherwise, does not necessarily constitute or imply its endorsement, recommendation, or favoring by the U.S. Government or any agency thereof. The views and opinions of authors expressed herein do not necessarily state or reflect those of the U.S. Government or any agency thereof.

***Geothermometry Mapping of Deep Hydrothermal Reservoirs
in Southeastern Idaho: Final Report***

**Idaho National Laboratory
Idaho Falls, Idaho 83415**

<http://www.inl.gov>

**Prepared for the
Battelle Memorial Institute, Inc.
Under DOE Idaho Operations Office
Contract DE-AC07-05ID14517**

EXECUTIVE SUMMARY

The Eastern Snake River Plain (ESRP) in southern Idaho is a region of high heat flow. Sustained volcanic activity in the wake of the passage of the Yellowstone Hotspot through the area created a region with great potential for geothermal resources. Numerous hot springs with temperatures up to 75 °C are scattered along the margins of the plain. Similarly, several hot water producing wells and a few hot springs are also present within the ESRP. The geothermal reservoirs in the area are likely to be hosted at depth in felsic volcanic rocks and/or Paleozoic rocks underneath the thick sequences of basalts within the ESRP. The heat source for these geothermal resources is thought to be a mid-crustal sill complex that sustains high heat flow in the ESRP. Several anomalous thermal areas are believed to be associated with local thermal perturbations caused by favorable structural settings. However, it is hypothesized that the thermal signatures of these deep-seated geothermal resources are masked by highly productive, cold-water aquifers in the basalts. The dilution of deeper thermal water and re-equilibration at lower temperatures represent significant challenges for the evaluation of potential resource areas in the ESRP.

To address this issue, this project used advanced geothermometry tools including temperature-dependent mineral and isotopic equilibria with mixing models that account for processes such as boiling and dilution with shallow groundwater that could affect calculated temperatures of underlying deep thermal waters. Over the past two years, we collected samples from approximately 100 springs/wells in and around the ESRP for chemical analysis. Similarly, the water chemistry data of several thermal features in the area that were not accessible for sampling during the current sampling campaign were assembled from previously published sources. To all thermal water compositions, we applied several geothermometric and geochemical modeling tools to estimate reservoir temperatures of the several geothermal prospects in the ESRP. Geothermometric calculations based on the principle of multicomponent equilibrium geothermometry with inverse geochemical modeling capability (e.g., Reservoir Temperature Estimator, RTest) have been useful for evaluation of reservoir temperatures. Similarly, sulfate-water oxygen isotope geothermometry was also applied to several samples in tandem with RTest. In addition, applications of other isotopic signatures of high-temperature water-rock interaction (e.g., shifts in $\delta^{18}\text{O}$ of water, isotopic signatures of magmatic CH_4) are also presented.

In summary, geothermometric calculations of ESRP thermal water samples indicated numerous potential geothermal areas with elevated reservoir temperatures. These areas are could be considered to be potentially economic geothermal resources. Specifically, areas around the southern and southwestern sides of the Mount Bennet Hills and within the Camas Prairie in the southwestern portion of the ESRP indicate reservoir temperatures of 140-190 °C. In the northern portion of the ESRP, Lidy Hot Springs, Ashton, Newdale, and areas east of Idaho Falls have expected reservoir temperature ≥ 140 °C. In the southern ESRP, areas near Buhl and Twin Falls with calculated reservoir temperatures as high as 160 °C. In most cases, the isotopic determined reservoir temperature generally agreed with the multicomponent equilibrium geothermometry derived temperatures giving greater confidence in the estimated reservoir temperatures. In a few cases, the sulfate-water isotope temperatures are significantly higher than the RTest temperatures. Although RTest and isotopic analyses suggest that many areas of the ESRP that have high reservoir temperatures, further detailed study at each site is necessary to evaluate their suitability for economic use

CONTENTS

EXECUTIVE SUMMARY	2
1. Introduction	5
2. Project objectives.....	5
3. Geologic and geothermal setting of eastern Snake River Plain.....	7
4. Geothermometry.....	8
5. Water samples	9
5.1 New data	9
5.2 Historical data	10
5.3 Hot springs and nearby hot wells	10
5.4 Geothermal prospects.....	10
6. Results	11
6.1 Water chemistry	11
6.2 Isotope data	12
6.3 Geothermometric assessments	13
6.3.1 Giggenbach diagram	13
6.3.2 Temperature estimates with traditional geothermometers	13
6.3.3 Temperature estimates with RTEst	15
6.3.4 Temperature estimates from sulfate-water oxygen isotope geothermometry	16
6.4 Some geothermal prospects and their reservoir temperatures.....	17
6.4.1 Lidy Hot Springs.....	18
6.4.2 Ashton Hot Spring	18
6.4.3 Newdale area.....	18
6.4.4 East Idaho Falls area	19
6.4.5 Magic Hot Spring.....	19
6.4.6 Camas Prairie area	20
6.4.7 South Mount Bennett Hills	21
6.4.8 Banbury Hot Springs-Twin Falls area.....	22
7. Summary	22
Acknowledgments.....	23
Appendices.....	23
References.....	24

FIGURES

- Figure 1. Map of potential geothermal prospects (stars and polygons) in the southern Idaho. The map was prepared by draping a heat flow map (Williams and DeAngelo, 2011) over digital elevation model (DEM) of the area. The thick red line demarcates the margins of the ESRP from the surrounding Basin and Range province. The codenames of the geothermal prospects are given in Table 1. The numeric value(s) numbers associated with each geothermal prospect is the RTest estimated reservoir temperature (°C)..... 6
- Figure 2. Schematic cross-section across the ESRP (modified from Hughes et al., 1999; Neupane et al., 2014) showing underlying rhyolitic ash-flow tuffs and overlying basalt flows with few sedimentary layers. The underlying rhyolite ash-flow tuffs are assumed to host the ESRP geothermal resources. 7
- Figure 3. Chemistry of the ESRP thermal water samples shown on a Piper diagram 11
- Figure 4. Hydrogen and oxygen isotopic compositions from ESRP water samples with the global meteoric water line for comparison. Most waters fall very close to the meteoric water line, but there are several samples that are significantly shifted to the right of the meteoric water line, which is an indication of oxygen isotope exchange during high-temperature water-rock interaction in hydrothermal systems. Abbreviations are- BW: Barron Well, CHS: Condie Hot Spring, ELHS2: Elk Creek Hot Spring 2, MRLW: Magic Reservoir Landing Well, and MRLWR: Magic Reservoir Landing Well runoff..... 12
- Figure 5. Giggenbach ternary diagram for the ESRP thermal water samples..... 13
- Figure 6. Graphical representation of RTest analysis of Miracle Hot Spring well located in the Banbury Hot Springs prospect (see Figure 1). a) $\log Q/K_T$ plot for assemblage minerals using observed fluid composition, b) $\log Q/K_T$ plot for assemblage minerals using RTest optimized fluid composition. Mineral assemblage includes: bei: beidellite-Mg, cal: calcite, cha: chalcedony, mor: mordenite-Na, and par: paragonite..... 15
- Figure 7. RTest temperature estimates versus sulfate-water oxygen isotope temperature estimates for the ESRP thermal water samples. The solid line represents a 1:1 comparison and the dashed lines indicate the range of temperatures within ± 30 °C of each other. The abbreviations in the figure are- HHS: Heise Hot Spring, GCHS: Green Canyon Hot Spring, MRLWR: Magic Reservoir Landing well runoff, MRLW: Magic Reservoir Landing well. The Barron well is not shown in this figure because of the sulfate-water oxygen temperature estimate is far above (419 °C) the maximum axis temperature..... 17

TABLES

- Table 1. Estimated temperatures (°C) for potential geothermal prospects in the ESRP 14

Geothermometry Mapping of Deep Hydrothermal Reservoirs in Southeastern Idaho: Final Report

Earl D. Mattson, Mark E. Conrad, Ghanashyam Neupane, Travis L. McLing, Thomas R. Wood, and Cody J. Cannon

1. Introduction

The eastern Snake River Plain (ESRP) in southeastern Idaho is a region of high heat flow with great potential for significant geothermal resources (Figure 1). A limited number of deep wells (such as INEL-1) and several hot springs and wells along the margin of ESRP also provide direct evidence of a high-temperature regime at depth in the area. However, most of the shallow wells within the ESRP generally exhibit low field-measured temperatures, likely due to the Eastern Snake River Plain Aquifer (ESRPA) obscuring the deep geothermal signature. The ESRPA is a prolific aquifer hosted in a thick sequence of thin-layered, highly transmissive basalt flows. The aquifer rapidly transports cold recharge from the Yellowstone Plateau and surrounding mountain basins to springs along the Snake River Canyon west of Twin Falls, Idaho. The flush of cold water through the overlying ESRPA masks the geothermal signature of the heat existing at depth (e.g., Smith, 2004). Importantly, the geothermal gradient below the ESRP aquifer system increases rapidly (Blackwell, 1989; McLing et al., 2002; Nielson et al., 2012) providing additional evidence of the presence of deep geothermal resources in the area.

2. Project objectives

This project uses advanced geochemical simulation tools that couple temperature-dependent mineral and isotopic equilibria with mixing models to estimate reservoir temperatures of potential geothermal resources in the ESRP. These tools help account for processes such as boiling and dilution with shallow groundwater that could affect calculated temperatures of deep geothermal reservoirs. Traditional as well as multicomponent geothermometry tools were applied to both existing data (e.g., Idaho Department of Water Resources, literature searches from the Web of Science, dissertations at the University of Idaho, and data located at the Idaho Geologic Survey) and new data collected as part of this study.

Specific objectives of this project were to obtain samples from thermal expressions (Appendix A), analyze samples for chemical and isotope compositions (Appendices B and C), use INL's geothermometry tool (RTEst), traditional geothermometers, and dissolved sulfate ($\delta^{34}\text{S}$ and $\delta^{18}\text{O}$) calculations (Appendix D), and identify potential geothermal areas (prospects) in the ESRP (Appendix E). Initially, we conducted a geothermometric assessment of the ESRP using previously published data from the region (Neupane et al., 2014; Cannon et al., 2014). That was followed by a series of field campaigns where an extensive set of new water samples from geothermal features in the ESRP and surrounding areas were collected and analyzed for chemical and isotopic compositions. These new data were used to expand our geothermometric assessment of the ESRP and have led to identification of several areas with promising potential for geothermal development. Specifically, we present calculated temperatures for geothermal areas distributed around southern/southwestern sides of the Mount Bennett Hills, Camas Prairie area, Lidy Hot Springs, Ashton area, Newdale area, and areas east of Idaho Falls. Similarly, we also present geothermometric results of geothermal areas around Buhl and Twin Falls area in the southern ESRP. The reservoir temperatures of these geothermal sites were estimated with traditional (e.g., Fournier et al., 1977) as well as multicomponent geothermometry tool [e.g., Reservoir Temperature Estimator (RTEst) (Palmer et al., 2014; Mattson et al., 2015)] based on the chemical composition of thermal water samples.

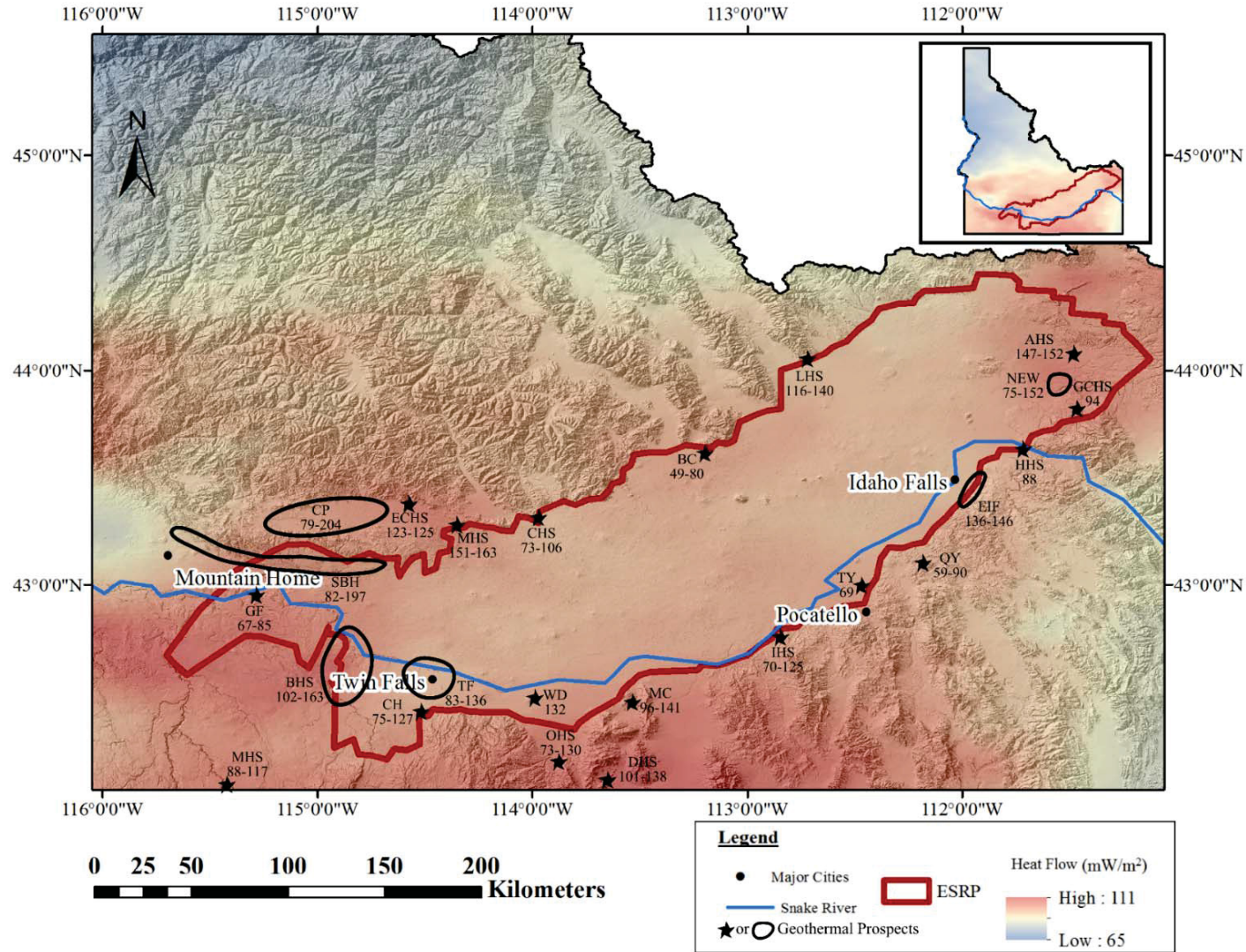


Figure 1. Map of potential geothermal prospects (stars and polygons) in the southern Idaho. The map was prepared by draping a heat flow map (Williams and DeAngelo, 2011) over digital elevation model (DEM) of the area. The thick red line demarcates the margins of the ESRP from the surrounding Basin and Range province. The codenames of the geothermal prospects are given in Table 1. The numeric value(s) numbers associated with each geothermal prospect is the RTEst estimated reservoir temperature (°C).

Isotopic compositions for a subset of the water samples collected were also measured. Specifically, the δD and $\delta^{18}O$ were measured. In addition, where concentrations were above the analytical requirements for isotopic analyses of dissolved sulfate ($\delta^{34}S$ and $\delta^{18}O$), total dissolved inorganic carbon ($\delta^{13}C$), and methane (δD and $\delta^{13}C$) analyses were done. Reservoir temperatures were calculated from the offset of the $\delta^{18}O$ values of the water and sulfate using the relationship published by Fowler et al. (2013) and compared with the results from the MEG values determined in this study.

3. Geologic and geothermal setting of eastern Snake River Plain

The Snake River Plain (SRP) is a topographic depression along the Snake River (Figure 1) in southern Idaho. The SRP is divided into two parts, the western Snake River Plain (WSRP) and the ESRP. The WSRP is a basalt- and sediment-filled tectonic feature defined by a normal fault-bounded graben whereas the ESRP is formed by crustal down-warping, faulting, and successive caldera formation that is linked to the middle Miocene to ongoing volcanic activities associated with the relative movement of the Yellowstone Hot Spot (Pierce and Morgan, 1992; Hughes et al., 1999; Rodgers et al., 2002). The 100 km wide ESRP extends over 600 km (Hughes et al., 1999). Four events in the late Tertiary are important for creating and shaping the ESRP (Hughes et al., 1999): (1) successive Miocene-Pliocene rhyolitic volcanic eruptive centers from the southwest near the common border of Idaho, Oregon, and Nevada trending northeast to Yellowstone National Park in northwest Wyoming, (2) Miocene to Holocene crustal extension which produced the Basin and Range province, (3) Quaternary basaltic flows, and (4) Quaternary glaciation and associated aeolian, fluvial, and lacustrine sedimentation and catastrophic flooding.

The ESRP consists of thick rhyolitic ash-flow tuffs, which are overlain by >1 km of Quaternary basaltic flows (Figure 2). The felsic volcanic rocks at depth are the product of super volcanic eruptions associated with the Yellowstone Hotspot. These rocks progressively become younger to the northeast towards the Yellowstone Plateau (Pierce and Morgan, 1992; Hughes et al., 1999). The younger basalt layers are the result of several low-volume, monogenetic shield-forming eruptions of short-duration that emanated from northwest trending volcanic rifts in the wake of the Yellowstone Hot Spot (Hughes et al., 1999). The thick sequences of coalescing basalt flows with interlayered fluvial and aeolian sediments in the ESRP constitute a very productive cold water aquifer system above the volcanic ash-flow tuffs (Whitehead, 1992).

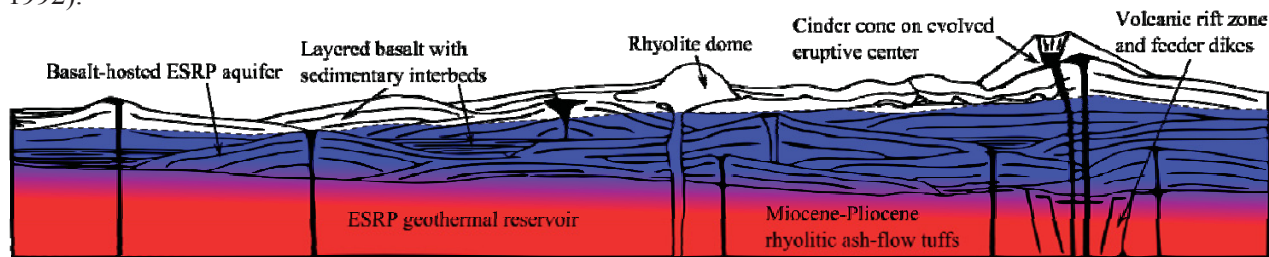


Figure 2. Schematic cross-section across the ESRP (modified from Hughes et al., 1999; Neupane et al., 2014) showing underlying rhyolitic ash-flow tuffs and overlying basalt flows with few sedimentary layers. The underlying rhyolite ash-flow tuffs are assumed to host the ESRP geothermal resources.

Recent volcanic activity, a high heat flux [$\sim 110 \text{ mW/m}^2$ (Blackwell, 1989; Smith, 2004)], and the occurrence of numerous peripheral hot springs suggest the presence of potential geothermal resources in the ESRP. In particular, we consider the lower welded rhyolite ash-flow tuff zone (Figure 2) to have exploitable heat sources that can be tapped by conventional or engineered geothermal development.

The ESRP system as a whole (including the deep geothermal reservoir and the overlying cold-water aquifer system) is an open and dynamic hydrogeologic system. Most water from shallow wells and

springs that exhibit a thermal expression in the ESRP are mixed waters of multiple sources, dominated by meteoric water with some deep-sourced thermal water (McLing et al., 2002; Smith, 2004; Welhan, 2015). The upwelling thermal waters interact with the basalt at the base of the regionally extensive cold water aquifer (Morse and McCurry, 2002), with the altered basalt forming a permeability barrier: this helps mask the expression of the deep thermal resource (Figure 2).

4. Geothermometry

One tool used to prospect for a geothermal resource is geothermometry, in which the chemical composition of water from springs and wells is used to estimate reservoir temperature. As an exploration tool, geothermometry offers a cost effective method to decrease exploration risk by evaluating a potential geothermal reservoir's temperature. To conduct geothermometry, the measured chemical compositions of water from wells and springs that exhibit some level of elevated temperatures are needed. The application of geothermometry requires several assumptions. The most important assumptions are that the reservoir minerals and fluid attain chemical equilibrium at reservoir temperatures and that as the water moves from the reservoir to the sample location, it retains its chemical composition (Fournier et al., 1974). The first assumption is generally valid for long residence times, but the second assumption is more likely to be violated because of composition altering processes, such as, re-equilibration at lower temperature, dilution (mixing), and loss of fluids (boiling) and gas degassing (e.g., CO₂) with the decrease in pressure.

Traditional geothermometers are mostly empirical (semi-empirical) relationships between temperatures and concentrations (or concentration ratios) of one or more components (e.g., such as the Na-K-Ca geothermometer) or based on temperature-dependent solubility of single-phase mineral (e.g., silica geothermometers). To apply a traditional geothermometer, a user needs to collect thermal water sample, conduct a chemical analysis to obtain the concentration of the desired component(s), and enter the measured concentration of certain component(s) into the geothermometer equation to estimate a reservoir temperature. The reliability, sensitivity, and responsiveness of traditional geothermometers to processes that effect the fluid compositions vary. For example, geothermometers based on cation concentration ratios (e.g., Na/K geothermometer) are minimally sensitive to boiling or mixing with dilute water, whereas geothermometers based on the concentration of a component(s) (e.g., quartz geothermometer) are highly sensitive to these processes (D'Amore and Arnórsson, 2000)). A drawback of many existing geothermometry approaches is that they do not adequately account for physical processes (e.g., mixing, boiling) and geochemical processes (e.g., mineral dissolution, precipitation, degassing, differences in actual mineral assemblages in the reservoir) that may alter the composition of specific chemical components. If these changes are not taken into account, predictions of *in-situ* reservoir conditions (e.g., temperature, fCO₂) based on the chemical composition of water samples taken from shallower depths or at the surface may be erroneous or too imprecise to be useful.

In addition, it is difficult to quantify uncertainties associated with temperatures estimated with these geothermometers. As a result, it is not uncommon to find diverse temperature estimates for the same water using multiple traditional geothermometers. Nevertheless, because these geothermometers are easy to use and sometimes provide good results, they are considered to be an essential part of the geothermal exploration toolkit (D'Amore and Arnórsson, 2000).

A more advanced geothermometric approach is multicomponent equilibrium geothermometry (MEG). The MEG approach of geothermometry utilizes multiple chemical constituents measured in water samples for inverse geochemical modeling considering a suite of selected minerals (selected based on some knowledge of the system) so as to provide more robust temperature estimates with quantifiable uncertainties. Geothermal temperature predictions using MEG provide apparent improvement in reliability and predictability of temperature over traditional geothermometers. The basic concept of this method was developed in 1980s (e.g., Michard and Roekens, 1983; Reed and Spycher, 1984). Some previous investigators (e.g., D'Amore et al., 1987; Hull et al., 1987; Tole et al., 1993) have used this

technique for predicting reservoir temperatures in various geothermal sites. Other researchers have used the basic principles of this method for reconstructing the composition of geothermal fluids and formation brines (Pang and Reed, 1998; Palandri and Reed, 2001). More recent efforts by some researchers (e.g., Bethke, 2008; Spycher et al., 2011; Smith et al., 2012; Cooper et al., 2013; Neupane et al., 2013, 2014; Cannon et al., 2014; Spycher et al., 2014; Peiffer et al., 2014; Palmer et al., 2014; Neupane et al., 2015a,b,c; Mattson et al., 2015; Neupane et al., 2016a,b) have been focused on improving temperature predictability of the MEG.

For this study, both traditional [e.g., quartz (no steam loss) (Fournier, 1977), chalcedony (Fournier, 1977), and Na-K-Ca (Truesdell and Fournier, 1973; Fournier and Potter, 1979)] and RTest (Palmer et al., 2014; Mattson et al., 2015) geothermometric approaches were applied to estimate reservoir temperatures. For the silica geothermometers, a pH correction on silica concentrations was not applied. While applying RTest to each water sample, a mineral assemblage consisting of 5-7 representative minerals (Mg bearing minerals – clinocllore, illite, saponite, beidellite, talc; Na bearing minerals – paragonite, saponite; K-bearing minerals – K-feldspar, clinoptilolite-K, illite; Ca bearing minerals – calcite; fluorite, and chalcedony) was used for the development of the reservoir temperature estimate for each sample. For each site, the same mineral assemblage was used for all samples using the same thermodynamic database (e.g., LNNL database based thermo.dat database of Geochemist's Workbench). In general, the mineral assemblage is selected based on available information such as water chemistry (e.g., pH), likely reservoir rock types and temperature range, etc. For more detailed information on selection of the mineral assemblage, see Palmer et al. (2014).

Another independent geothermometric approach is comparing the isotopic compositions of different components of the fluids to calculate the temperature at which the two components would have been in isotopic equilibrium (e.g., the oxygen isotopic composition of dissolved sulfate and the water or the carbon isotopic composition of dissolved inorganic carbon and methane). This approach can be very precise, but can also be affected by other processes including mixing with non-reservoir fluids or microbial metabolic processes that shift the isotopic compositions of the components of interest. Additionally, in some cases, the isotopic signatures of some fluid phases can also be used to identify interaction of fluids with rocks in high-temperature systems. For instance, the hydrogen and oxygen isotopic compositions of meteoric water are generally related to each other in a systematic way (Craig, 1961), but interaction with rocks at high temperatures will shift the oxygen isotopic composition of the water towards equilibrium with the rocks with little effect on the hydrogen isotopic composition of the water (Taylor, 1974) creating a distinctive water isotopic composition that can be used to infer high temperature interaction between the water and rocks. Similarly, the carbon and hydrogen isotopic compositions of dissolved methane can be used to distinguish formation in high temperature water-rock systems from methane formed from microbial processes (Welhan, 1988). The temperature estimates with isotope data were compared with temperature estimates with chemical data.

5. Water samples

5.1 New data

As a major part of this work, we initiated sampling campaigns during the spring and summer of 2014 and 2015 (Cannon et al., 2014; Dobson et al., 2015; Neupane et al., 2015c). The sampling campaigns were aimed at collecting samples from thermal features that have either incomplete available data or were not previously sampled/analyzed. Our goal was to develop an extensive thermal expression chemistry data set to be used for geothermometry calculations using RTest as well as for analyzing for other trace elements, isotopes and noble gases (working with Pat Dobson of LBNL, Appendix K). Over the course of the project period, we collected and analyzed about 100 samples from thermal features in the ESRP and surrounding area (Appendix A). With the exceptions of some samples from the Preston, Malad, and Sun Valley, Idaho area, new water samples are used for geothermometry reported here. The general chemical

compositions of water samples are given in Appendix B. The water chemistry data are also uploaded to the Geothermal Data Repository (GDR) web portal. Similarly, isotopic compositions of ESRP water samples are given in Appendix C.

5.2 Historical data

Existing southeast Idaho water composition data have been obtained from the Idaho Department of Water Resources, literature searches from the Web of Science, and dissertations the University of Idaho. Existing water composition data were evaluated for their quality (e.g., charge balance, etc.) and completeness (except Al) for MEG. Almost all of the historical data lacked measured concentrations of Al. For these samples, Al concentrations determined by assuming equilibrium with K-feldspar (Pang and Reed, 1998) was used in the geochemical modeling. In some instances, the Al values measured in new samples collected from nearby hot springs or hot wells were used. New and existing chemical data (Appendices B and C) were used for the estimation of reservoir temperatures with traditional geothermometers as well as with RTest (Appendix D). In the past, historical data were used for preliminary evaluation of geothermal resources along the margins of the ESRP (e.g., Neupane et al., 2014). Some of the geothermal features with available good quality and complete geochemical data were also sampled as a part of this project. For most of these features, the existing data were found to be similar to the new chemical data. However, despite having good quality and complete existing data, Appendix B only contains data for features sampled for this project.

5.3 Hot springs and nearby hot wells

Compositions of water samples collected from hot springs and shallow wells exhibiting a thermal expression were used for the temperature estimation of several geothermal prospects in the ESRP (Appendix E). It is generally assumed that geothermal systems manifest some kind of surface signals such as hot springs or fumaroles, however, there have been some hidden or blind geothermal systems. For example, the Raft River geothermal system was identified when shallow (120-150 m deep) wells that were drilled for domestic and stock use encountered boiling water (Williams et al., 1976). Similarly, in the ESRP, the Newdale prospect (NEW in Figure 1) was first identified by the presence of numerous hot shallow wells in the area. However, how useful hot shallow waters can be for geothermometric calculations in the southern Idaho was an issue for us when we started this work.

To address the viability of using hot shallow wells as sampling locations to collect water samples for MEG analysis, we compared the MEG temperature estimates from hot springs and nearby wells in southern Idaho (Neupane et al., 2015c, see Appendix F). This study indicated that the reservoir temperatures estimated using water compositions measured from surface thermal features and wells produce similar results. However, there are a few systems where the estimated reservoir temperatures based on water compositions measured from hot springs and hot wells are different. Neupane et al. (2015c) emphasized that when such differences exist, it is imperative to consider the consistency of the water types and distance between the sources when estimating reservoir temperatures. With the exception of the Durfee Hot Spring prospect [the same system was also noted by Neupane et al. (2015c) as one of two systems examined in southern Idaho that have divergent temperature estimates with hot spring and hot well compositions] (DHS in Figure 1), all other prospects with measured compositions from samples collected from hot springs and hot wells in the ESRP yielded similar results (see section 6).

5.4 Geothermal prospects

Based on the distribution of sampling features (Appendix A) and range of temperature estimates, 24 geothermal prospects with moderate to high reservoir temperatures have been identified (Figure 1 and Table 1). The number of samples from each prospect (Table 1) varies such that some prospects have multiple samples (e.g., Banbury Hot Springs prospect has 37 samples) from different sources whereas some prospects are based on the results for only a few samples (e.g., Wybenga Dairy prospect has only

one sample). Neupane et al. (2016a) (Appendix G) and Section 6.4 describes these geothermal prospects in the ESRP. More detailed descriptions of these prospects are provided in Appendix E.

6. Results

6.1 Water chemistry

The concentrations of major anions and cations in the water samples from hot/warm springs and wells in southeastern Idaho (Appendix B) are presented in Figure 3. All springs/wells (with a few exceptions such as the Spackman well in the Newdale prospect) that we sampled represent the expression of geothermal activities (field T > 20 °C) in the ESRP. The highest field temperature within and along the margins of ESRP was recorded at the Magic Hot Spring Landing well (75 °C) in the Magic Hot Spring prospect (MHS in Figure 1). The pH of ESRP thermal waters ranges from 6.3 to 9.6. These thermal waters show a large range in total dissolved solids (TDS) from about 106 mg/L (Sturm well in Ashton prospect, AHS in Figure 1) to more than 7,000 mg/L (Heise Hot Spring, HHS in Figure 1).

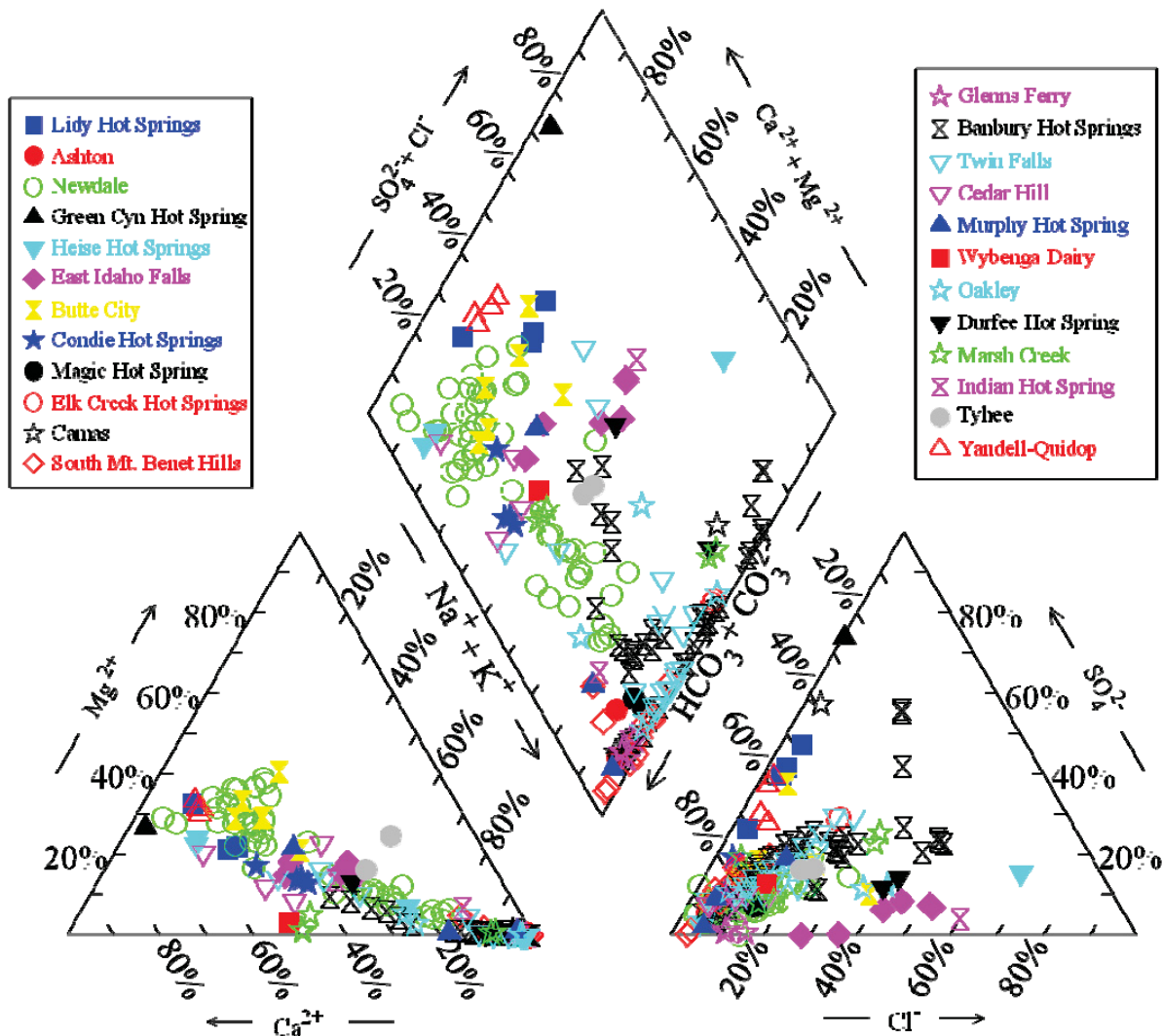


Figure 3. Chemistry of the ESRP thermal water samples shown on a Piper diagram

Based on the dominant ions (Figure 3) in water, ESRP waters can be grouped into 10 water types. These are Ca-HCO₃, Mg-HCO₃, Ca-Mg-HCO₃, Na-HCO₃, Ca-SO₄, Na-SO₄, Na-Cl, Na-K-HCO₃, Na-K-Cl-SO₄,

and Ca-Na-HCO₃ type waters. In general, ESRP waters have either Ca-Mg or Na as the dominant cations and HCO₃ as the dominant anion. The ESRP waters with dominant HCO₃ may have been the product of carbonated water-rock interaction at low to high temperatures. Specifically, Na-HCO₃ waters are considered deeper ESRP water whereas Ca-Mg-HCO₃ waters are shallower ESRPA water. The few water samples (e.g., Heise Hot Spring, Green Canyon Hot Spring, etc.) with Cl and/or SO₄ as dominant anions may have originated with water-rock interaction involving Paleozoic evaporite beds.

6.2 Isotope data

The isotopic compositions of samples collected for isotope analyses are included in Appendix C. Analyses were done of the δD and $\delta^{18}O$ of all samples and plotted in Figure 4. Most of the samples plot close to the meteoric water line (precipitation in this region tends to be slightly offset to the right of the global meteoric water line), but there are several samples that have oxygen isotope composition shifted 1-3‰ to the right of the meteoric water line (e.g., Barron Well, Condie Hot Spring, Elk Creek Hot Spring 2, Magic Reservoir Landing Well). In addition, where concentrations were above the analytical requirements for isotopic analyses of dissolved sulfate ($\delta^{34}S$ and $\delta^{18}O$), total dissolved inorganic carbon ($\delta^{13}C$), and methane (δD and $\delta^{13}C$) analyses were done. Reservoir temperatures were calculated from the offset of the $\delta^{18}O$ values of the water and sulfate using the relationship published by Fowler et al. (2013) and compared with the results from the other chemical geothermometers used for this study. Calculated temperatures for other isotopic geothermometers (e.g., carbon isotopes of dissolved inorganic carbon and methane and the hydrogen isotope compositions of water and methane) did not yield consistent results likely due to mixing with other sources of those compounds and are not presented here. The results of some of these data can be, however, useful indicators of potential deep, high-temperature systems.

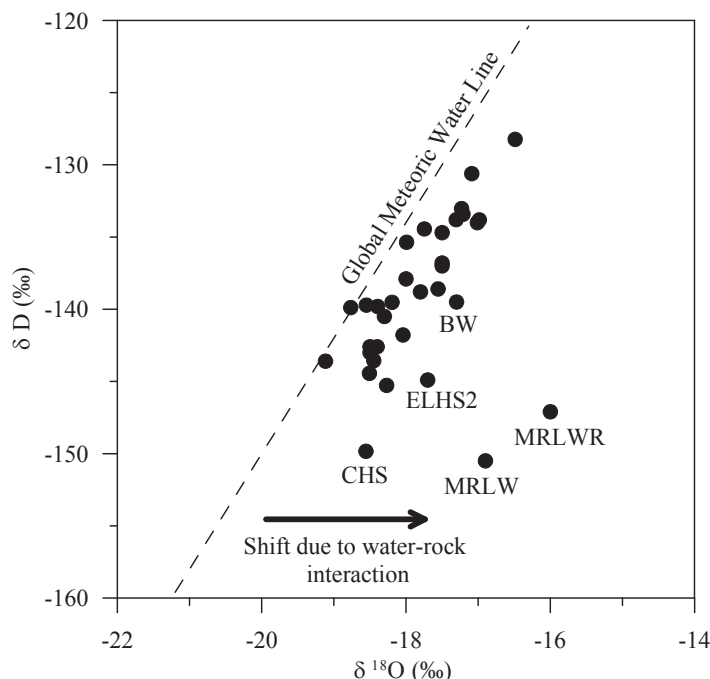


Figure 4. Hydrogen and oxygen isotopic compositions from ESRP water samples with the global meteoric water line for comparison. Most waters fall very close to the meteoric water line, but there are several samples that are significantly shifted to the right of the meteoric water line, which is an indication of oxygen isotope exchange during high-temperature water-rock interaction in hydrothermal systems. Abbreviations are- BW: Barron Well, CHS: Condie Hot Spring, ELHS2: Elk Creek Hot Spring 2, MRLW: Magic Reservoir Landing Well, and MRLWR: Magic Reservoir Landing Well runoff.

6.3 Geothermometric assessments

6.3.1 Giggenbach diagram

The sample compositions are plotted on a Giggenbach ternary diagram (Giggenbach, 1988) to determine evidence of equilibration and/or mixing (Figure 5) as well as to illustrate the likely water-rock interaction temperatures in the reservoirs. This plot is useful classifying waters as either fully equilibrated waters, partially equilibrated, or immature waters. The diagram uses the full range of equilibrium relationships between Na, K, and Mg to determine the degree of equilibration between the water and the rock at depth. The plot suggests that the waters from several ESRP wells and springs are partially equilibrated that may have interacted with the reservoir rocks at temperatures ranging from 100 °C to 180 °C. However, majority of the ESRP waters are immature waters, as indicated by elevated Mg contents (Appendix B, Figure 3). The immature waters may indicate significant mixing with cool meteoric waters, and traditional geothermometers may not be suitable tools for temperature estimation for these waters.

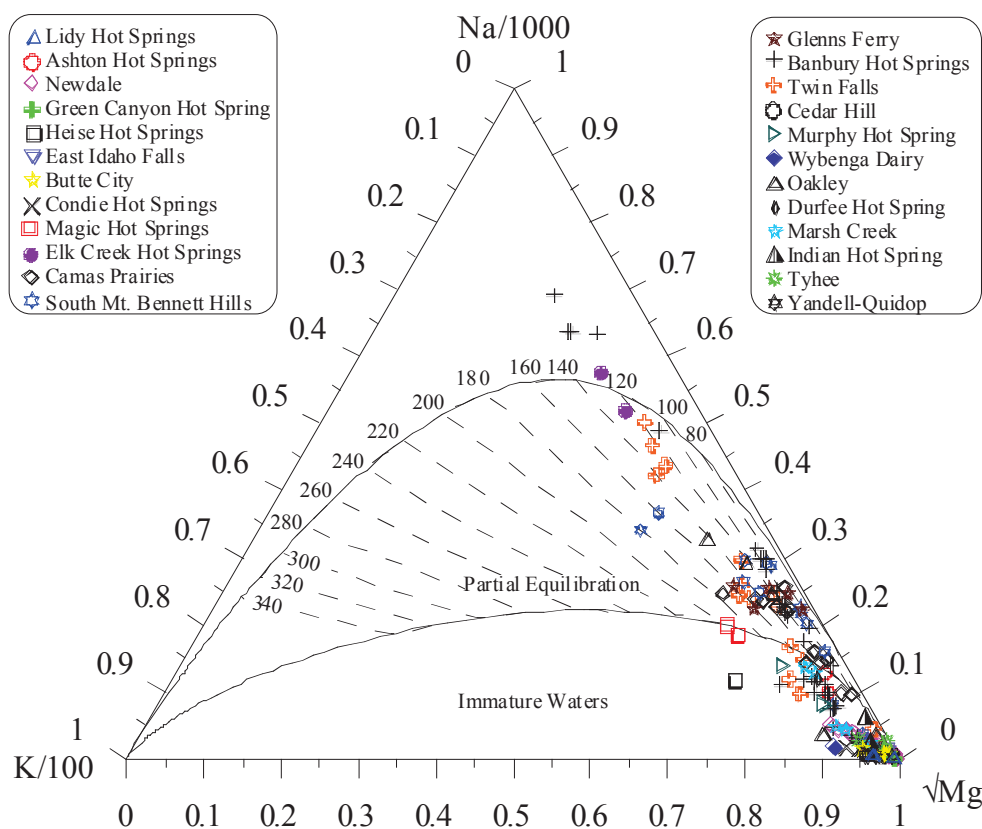


Figure 5. Giggenbach ternary diagram for the ESRP thermal water samples

6.3.2 Temperature estimates with traditional geothermometers

Traditional geothermometers were applied to measured water compositions for general assessment of the geothermal temperature at each sampling site. For the ESRP, the traditional geothermometer-based temperatures (Appendix D) can be difficult to use to assess the geothermal potential of prospects. For example, estimated temperature values for the Heise Hot Spring, range from 53 °C using chalcedony to 243 °C using Na/K ratios. Nevertheless, for some samples from other prospects, such as a well at the College of Southern Idaho (CSI Well2) representing the Twin Falls geothermal prospect, the estimated

Table 1. Estimated temperatures (°C) for potential geothermal prospects in the ESRP

Prospects	Map Code ^a	Measured ^b	RTEst ^c	SO ₄ -H ₂ O $\delta^{18}\text{O}^{\text{d}}$	Quartz (nsI) ^e	Chalcedony ^f	Na-K-Ca ^g	Silica-enthalpy ^h
Lidy Hot Springs	LHS	56	116-140	127	57-89	25-58	44-65	60 (130)
Ashton Hot Spring	AHS	66	147-152		113-143	84-116	109-117	
Newdale	NEW	87	75-152	87	66-134	26-112	29-111	174 (224)
Green Cyn Hot Spring	GCHS	44	94	29	75	44	65	
Heise Hot Spring	HHS	48	88	65	84	53	89	
East Idaho Falls	EIF	28	136-146		115-143	86-117	45-74	
Butte City	BC	41	49-80	92-95	70-106	38-77	37-43	75 (124)
Condie Hot Spring	CHS	51	73-106	102-105	71-82	40-51	71-83	52 (100)
Magic Hot Spring	MHS	75	151-163	233-237	139-142	113-116	143-149	
Elk Creek Hot Springs	ECHS	56	123-125	136	114-115	86	107-110	
Camas Prairie	CP	73	79-204	133- >300	103-128	74-100	70-124	133 (173)
South Mt. Bennett Hills	SBH	68	82-197	154	110-143	80-117	72-160	150 (182)
Glenn's Ferry	GF	39	67-85		80-109	48-79	74-138	108 (150)
Banbury Hot Springs	BHS	72	102-163	99-159	98-139	67-127	69-165	135 (171)
Twin Falls	TF	43	83-136	133	77-119	45-91	70-132	121 (157)
Cedar Hill	CH	38	75-127		62-116	29-87	50-129	
Murphy Hot Spring	MHS	55	88-117		119-148	90-122	57-144	
Oakley Hot Spring	OHS	47	73-130	92-157	77-125	45-97	45-155	
Durfee Hot Spring	DHS	45	101-138	104	96-117	66-88	46-131	
Marsh Creek	MC	60	96-141	142	96-113	66-83	48-89	
Wybenga Dairy	WD	34	132		118	89	189	
Indian Hot Spring	IHS	39	70	174	64	32	75	
Tyhee	TY	41	69		63-93	31-62	52	
Quidop-Yandell	QY	38	59-90		55-63	23-31	43-63	

^aThese map codes are used to represent geothermal prospects in Figure 1;

^bmaximum measured temperature for the prospects;

^cRTEst estimated temperature range;

^dsulfate-water ¹⁸O isotope geothermometer (Fowler et al., 2013);

^equartz (no steam loss) geothermometer temperature (Fournier, 1977);

^fchalcedony geothermometer temperature (Fournier, 1977);

^gMg-corrected (where applicable) Na-K-Ca geothermometer temperature (Fournier and Truesdell, 1973; Fournier and Potter II, 1979);

^htemperature with silica-enthalpy mixing model (where applicable) using chalcedony solubility (temperature with quartz solubility given in parenthesis) (Fournier, 1977).

temperatures range from 85 °C to 140 °C suggesting relatively good agreement between the traditional geothermometry temperature estimates. In general, we have found that in the ESRP, the estimated reservoir temperatures using the Na/K ratios are higher than estimated temperatures obtained [Na/K temperatures are not included (except Giggenbach diagram) in this report] with other geothermometers. However, for some systems (e.g., Driscoll Spring and Well, Banbury Hot Spring, etc.), Na/K estimated temperatures are cooler than temperatures with other geothermometers.

6.3.3 Temperature estimates with RTest

All water samples collected during the sampling campaigns of 2014 and 2015 as well as useful water compositions assembled from the literature for this study (Appendix B) were individually used for the temperature estimation with RTest (Table 1, Appendix D). For each sample, 5-7 minerals (consisting mainly of silica-polymorphs, clays, zeolites, carbonates, sulfates, feldspars, etc.) were selected as a mineral assemblage.

An example of the RTest results for a water sample collected from Miracle Hot Spring well located in Banbury Hot Springs prospect (BHS in Figure 1) is shown in Figure 6. Figure 6a shows $\log(Q/K_T)$ curves of the reservoir mineral assemblage RMA (calcite, chalcedony, beidellite, mordenite, and paragonite) used for the Miracle Hot Spring water composition. The $\log(Q/K_T)$ curves of these minerals intersect the $\log(Q/K_T) = 0$ at a wide range of temperatures, making the $\log(Q/K_T)$ curves derived from the reported water chemistry minimally useful for estimating temperature. The range of equilibration temperature for the assemblage minerals is a reflection of physical and chemical processes that may have modified the Miracle Hot Spring water composition during its ascent to the sampling point.

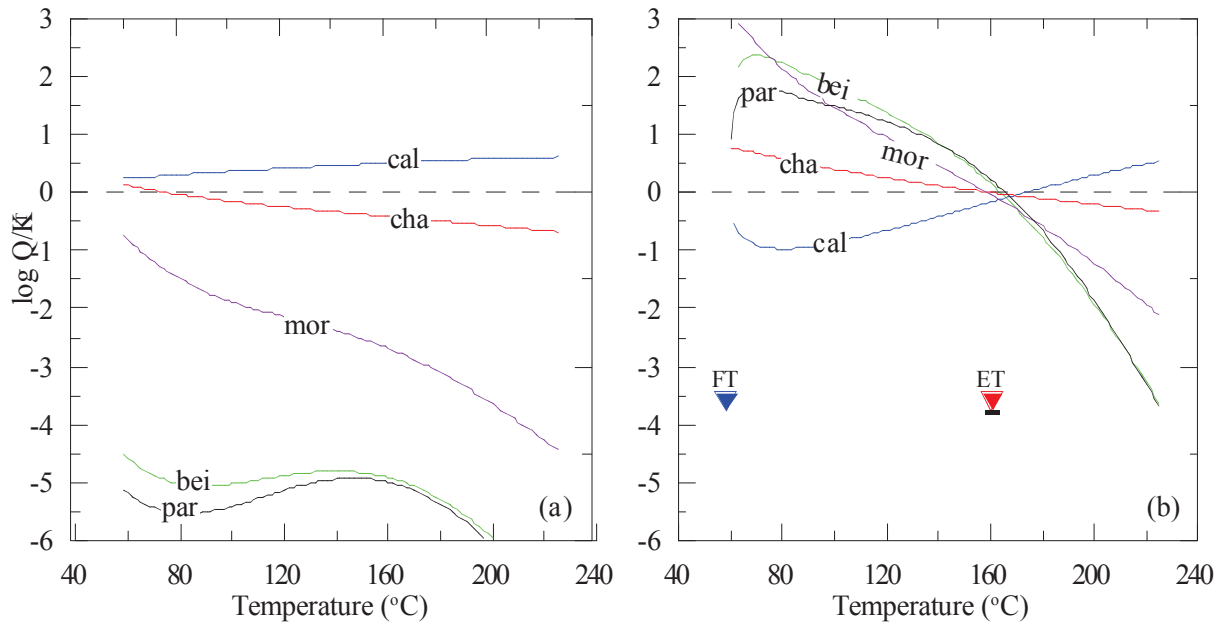


Figure 6. Graphical representation of RTest analysis of Miracle Hot Spring well located in the Banbury Hot Springs prospect (see Figure 1). a) $\log Q/K_T$ plot for assemblage minerals using observed fluid composition, b) $\log Q/K_T$ plot for assemblage minerals using RTest optimized fluid composition. Mineral assemblage includes: bei: beidellite-Mg, cal: calcite, cha: chalcedony, mor: mordenite-Na, and par: paragonite.

To account for possible composition altering processes, RTest was used to simultaneously estimate a reservoir temperature and optimize the amount of dilute near-surface H_2O mixed with the thermal water (a physical process) and the fugacity of CO_2 change (a chemical process) that may have occurred during

its ascent to the surface. Using these two additional optimization parameters, the results for the corrected fluid composition of Miracle Hot Spring are shown in Figure 6b. Compared to the $\log(Q/K_T)$ curves calculated using the reported water compositions (Figure 6a), the optimized curves (Figure 6b) converge to $\log(Q/K_T) = 0$ within a narrow temperature range (i.e., 161 ± 3 °C).

The optimized temperatures and composition parameters for the other ESRP waters were estimated using RTest in the same manner. The RTest estimated temperatures for the ESRP geothermal samples range from about 60 °C to 204 °C (Table 1). The hottest reservoir temperature estimate is obtained for Wardrop Hot Spring located in north-central part of Camas Prairie (CP in Figure 1). Similarly, hot springs located on the southern side of the Mount Bennett Hills (e.g., Prince Albert Hot Spring, Latty Hot Spring) (SBH in Figure 1) also have reservoir temperature estimates as high as 200 °C.

6.3.4 Temperature estimates from sulfate-water oxygen isotope geothermometry

Also included in Table 1 (and Appendix C) are estimated reservoir temperatures calculated from the relationship between the $\delta^{18}\text{O}$ values of dissolved sulfate and water in samples containing sufficient sulfate for these analyses. In general, the calculated RTest temperatures and sulfate-water oxygen isotope temperatures are similar (Figure 7). In some cases, most notably for some samples where there are thought to be other sources of subsurface sulfate present (e.g., Heise and Green Canyon samples where evaporite beds are believed to be present in the subsurface), the results are not consistent. In a few other instances, the sulfate-water isotope temperatures are significantly higher than the RTest temperatures [e.g., the Magic Reservoir Hot Springs well and the Barron's Well]. The isotope temperature could be closer to actual temperatures due to significant dilution with shallow groundwater that may have altered the water chemistry without adding sulfate to the water. Conversely, the oxygen isotope composition of the water may have been shifted due to boiling of the fluids in the subsurface leading to erroneously high temperature estimates. It is notable, however, that the samples in question also have other indicators of high temperature fluids in the form of magmatic methane and shifted water isotope compositions. In addition, many of these samples also contained high $^3\text{He}/^4\text{He}$ values for dissolved helium, another indicator of deep, magmatic systems (Dobson et al., 2015).

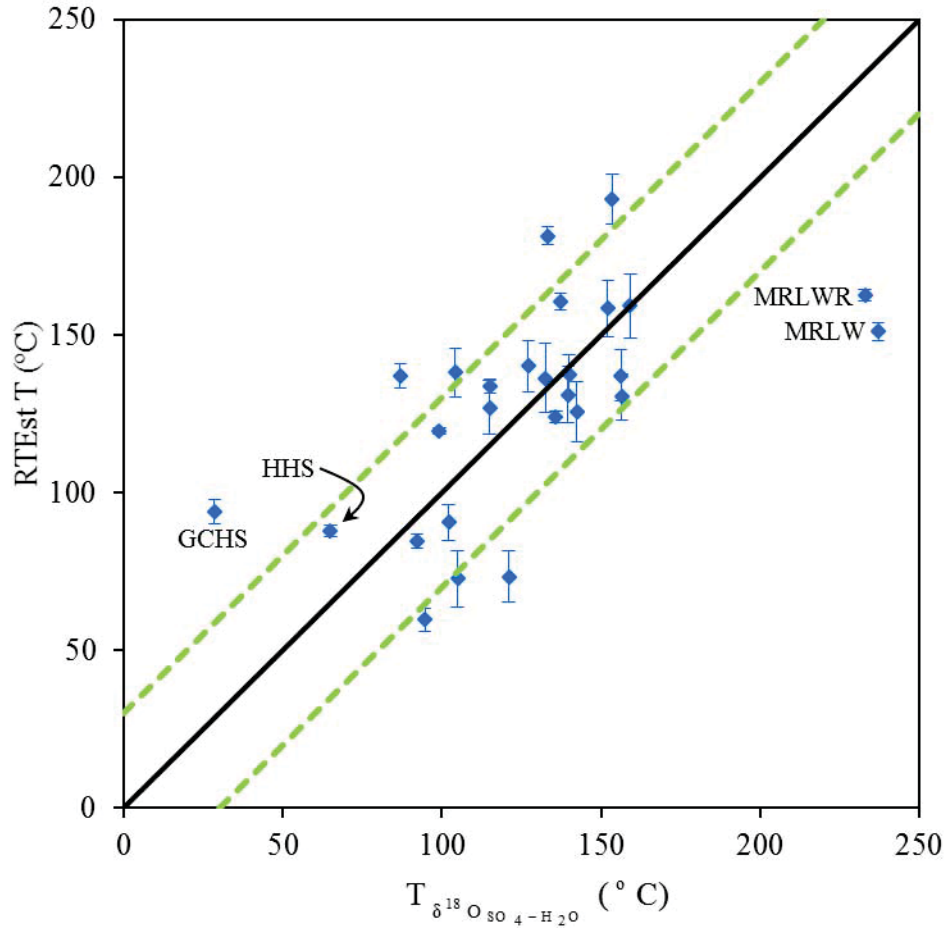


Figure 7. RTest temperature estimates versus sulfate-water oxygen isotope temperature estimates for the ESRP thermal water samples. The solid line represents a 1:1 comparison and the dashed lines indicate the range of temperatures within ± 30 °C of each other. The abbreviations in the figure are- HHS: Heise Hot Spring, GCHS: Green Canyon Hot Spring, MRLWR: Magic Reservoir Landing well runoff, MRLW: Magic Reservoir Landing well. The Barron well is not shown in this figure because of the sulfate-water oxygen temperature estimate is far above (419 °C) the maximum axis temperature.

6.4 Some geothermal prospects and their reservoir temperatures

Table 1 summarizes likely reservoir temperature range for all geothermal prospects within and along the margins of the ESRP identified in this study. The RTest estimated temperature range for each prospect is also given in Figure 1. Some of the highest temperature prospects in the ESRP region are Lidy Hot Springs (LHS), Magic Hot Spring (MHS), Camas Prairie (CP), south of Mount Bennett Hills (SBH), Banbury Hot Springs (BHS), east Idaho Falls (EIF), Newdale (NEW), and Ashton Hot Spring (AHS) (Figure 1). The geothermal potential of some of these prospects are also identified by the first phase of the SRP Play Fairway analysis (Shervais et al., 2015). Below we provide brief summaries for some of the promising geothermal prospects in the ESRP region. Detailed geologic and geothermal settings along with water chemistry and geothermometric results for all geothermal prospects are given in Appendix E.

6.4.1 Lidy Hot Springs

The Lidy Hot Springs prospect (LHS in Figure 1) is located at the southeastern end of the Beaverhead Mountains in Clark County in Idaho. Beginning in the early 20th century, the area was developed into a commercial recreation site that provided activities such as swimming, soaking, dancing, dining, and lodging to the public. However, with the transfer of ownership in the early 1960s, the site ceased to offer those services and started a travertine mining activity. Two hot springs in the area are still issuing thermal water (52-56 °C). In the vicinity of the Lidy Hot Springs, there are other springs (e.g., Warm Spring 29 °C) issuing warm to cooler waters.

Rocks underlying the Lidy Hot Springs area consist of young volcanics and older meta-sedimentary rocks (Link, 2002). The younger rocks (Upper Miocene and Pliocene) consist of fluvial and lacustrine deposits, felsic volcanic rocks, rhyolite flows, tuffs, and ignimbrites. Thick sequences of Paleozoic sedimentary rocks (Pz) underlie the Tertiary rock types, and likely constitute the geothermal reservoir in the area (see Appendix E for detailed information).

The RTEst estimated reservoir temperature for the Lidy Hot Springs prospect is about 140 °C (Table 1). RTEst modeling results show that the Lidy Hot Springs water may contain up to 60% cooler water and 40% deeper thermal water. Similarly, no-steam loss silica-enthalpy mixing model with the quartz solubility curve (Fournier, 1977; Fournier and Porter, 1982) yields a reservoir temperature of about 130°C. The sulfate-water $\delta^{18}\text{O}$ temperature calculated for this sample was in the same range as these temperatures at 127°C. However, silica-enthalpy mixing model with the chalcedony solubility curve (modified from Fournier, 1977; Fournier and Porter, 1982) yields a cooler temperature (about 60 °C).

6.4.2 Ashton Hot Spring

The Ashton Hot Spring and associated geothermal area (AHS in Figure 1) is located on the northern side of Ashton in Fremont County in Idaho. The existence of Ashton Hot Spring with a surface water temperature of 41 °C was previously reported by Mitchell et al. (1980). A 1220 m deep geothermal exploratory well (Sturm Well-1) was drilled about 2 km NE from the Ashton Hot Spring in 1979 (Occidental Geothermal Inc., 1979). Driller's records indicate a bottom-hole temperature of about 63 °C.

Geologic mapping of the area shows thin layers of Quaternary sediments covering underlying volcanic rocks (Link, 2002). Borehole records from the area reveal the presence of thick sequences of flood basalts and felsic volcanics. Specifically, along the Sturm Well-1, the Quaternary sediments near the surface are underlain by layers of flood basalts (up to a depth of 82 m), felsic volcanics (82-808 m), and again flood basalts (808 -1220+ m) with depth (Occidental Geothermal Inc., 1979) (see Appendix E for detailed information).

Quartz and chalcedony geothermometers yielded reservoir temperatures of 143 °C and 116 °C for Ashton Hot Spring and 113 °C and 84 °C for the Sturm Well, respectively. For these two sampled features, Na-K-Ca geothermometer resulted in 117 °C and 109 °C, respectively. Similarly, the RTEst produced reservoir temperatures for the Sturm Well and Ashton Hot Spring are 152±14 °C and 147±5°C, with nearly 70% and 35% admixing of cooler water, respectively. All of these temperatures are significantly higher than the bottom hole temperature measured for the Sturm Well (63 °C). Given the measured temperature gradient (48 °C/km, Blackwell, 1989), such temperature conditions might be found at depths of about 3 km. Samples for isotopic analyses were collected from both locations, but the sulfate concentrations were too low for analysis.

6.4.3 Newdale area

The Newdale geothermal prospect (NEW in Figure 1) in Madison and Fremont Counties in Idaho represents a blind geothermal system, as it has no hot springs. The geothermal potential of the Newdale area was identified in late 1970s by several researchers (e.g., Brott et al., 1976), based on the discovery of relatively high heat flow (167 mW/m²). The area between Newdale town to the NE across the Teton River

has been considered as a potential area for geothermal energy (Brott et al., 1976, GeothermEx, 2010; Neupane et al., 2016b)). During 1979-1981, Union Oil of California (Unocal) drilled several geothermal test wells in the area ranging in depth from 183 m (Newdale No. 79-3) to 1204 m (Madison Geothermal No.1 near Rexburg, ID). The highest recorded temperature in the Unocal wells was 87.2 °C (Well # State 2591-07-79-1).

A surficial geologic map of this area shows the presence of Quaternary sediments, Quaternary flood basalts, and Quaternary felsic volcanic rocks (Bond, 1978; Link, 2002; Embree et al., 2011). Early Pleistocene flood basalts are mapped around the town of Newdale whereas felsic volcanic rocks of similar ages (Huckleberry Ridge Tuff) are mapped NE from Newdale. In geologic cross-section, Embree et al. (2011) show Huckleberry Ridge Tuff lying underneath the Early Pleistocene basalt at Newdale. Below the Huckleberry Ridge Tuff lie the Tertiary sediments intercalated with Tertiary basalt. Subsurface lithologic records of numerous wells in the area as compiled by Idaho Geological Survey indicate the presence of thick sequences of rhyolites and tuff at greater depths (see Appendices E and H for detailed information).

Quartz, chalcedony, and Na-K-Ca (Mg corrected) geothermometers resulted reservoir temperatures in the range of 66-134 °C, 28-112 °C, 29-111 °C, respectively. A silica (chalcedony)-enthalpy mixing model using all Newdale area samples results in reservoir temperature of about 174 °C. Similar mixing models using quartz solubility results in even higher temperature estimates (224 °C). The RTest temperature estimates for the Newdale area samples range 75-152 °C (Table 1) and a sulfate-water oxygen isotope temperature obtained for a sample from the area was 87 °C. The lower end RTest temperature estimates and the isotope temperature for this area are similar to the bottom hole temperatures (83-87 °C) measured in two relatively deep (~1000 m) Unocal wells. Moreover, it is likely that the area hosts even higher temperatures at greater depths that would correspond to a hotter zone at depth reaching to the higher end RTest temperatures. Assuming an 80 °C/km thermal gradient (as indicated by two Unocal wells), the higher end RTest temperatures would be present at about 2 km below ground surface.

6.4.4 East Idaho Falls area

The foothills (1480-1580 m above sea level) along the margins of the ESRP east of Idaho Falls (EIF in Figure 1) in Bonneville County have been known to have some wells producing warm water. Ralston et al. (1981) initially reported the geothermal potential of the area. Specifically, they noted the existence of two wells in Rim Rock Estate that produce ≥ 20 °C water. Recently drilled shallow wells (depth up to 244 m) in the Comore Loma and Blackhawk communities few kilometers south from Rim Rock Estate also produce warm (21-28 °C) water.

The area lies on the edge of the SRP where pronounced volcanism has taken place throughout the past 6.5 Ma. The foothills to the east of Idaho Falls consist predominantly of tuffs, ignimbrites, and ash flows related to the Miocene-Pliocene Heise volcanic field (Morgan and McIntosh, 2005). Although all shallow wells in the area bottomed out within the volcanic rocks, the volcanic rocks in the area are thought to be about 300 m in thickness. Mesozoic sedimentary rocks that include the limestones, sandstones, siltstones, conglomerates, and evaporite beds underneath the young volcanic rocks are assumed to be the geothermal reservoir in this area (see Appendix E for detailed information).

Quartz, chalcedony, and Na-K-Ca temperature estimates for east Idaho Falls area range from 115-143 °C, 86-117 °C, and 45-74 °C, respectively. The Mg-corrected Na-K-Ca temperature estimates for these samples are lower because of the presence of high concentrations of Mg. The RTest temperature estimates of east Idaho Falls water samples are very similar with a range from 136-143 °C (Table 1). No isotope samples were collected from this area.

6.4.5 Magic Hot Spring

The Magic Hot Spring prospect (MHS in Figure 1) is located on the northern margin of the ESRP in Camas and Blaine Counties in Idaho. Until a 79 m deep well (Magic Reservoir landing well) was drilled

for direct use purposes in 1965, the hot spring issued 36°C water (Ross, 1970). However, with the operation of the well, the hot spring dried out (Mitchell, 1976). At the beginning, the well was producing water at 66°C, however, the water temperature subsequently increased to 74 °C by 1975 (Mitchell, 1976; Mitchell et al., 1980). The most recent (2014) temperature record for the surface discharge of the well (our data) is 75 °C.

The Magic Hot Spring area consists predominantly of Miocene-Quaternary silicic volcanic rocks and basalt flows (Struhsacker et al., 1982). The Pliocene-Miocene Poison Creek Tuff is the uppermost unit in the immediate vicinity of Magic Reservoir and is underlain by the Miocene Tuff of the Idavada Group. Other rhyolites and basalt flows are abundant in the surrounding areas but not shown in cross-section. The Cretaceous Idaho Batholith granitic rocks form the basement throughout the region (see Appendix D for detailed information).

Quartz (no steam loss), chalcedony, and Mg-corrected Na-K-Ca geothermometers resulted in 139 and 142 °C, and 113 and 116 °C, and 153 and 152 °C with compositions measured in water samples from the well leak and leak runoff channel, respectively. The chalcedony-enthalpy mixing model resulted in an estimated 145 °C reservoir temperature with about 50% dilution. Similarly, the quartz-enthalpy mixing model resulted in 181 °C reservoir temperature with about 60% dilution. The RTest results indicate that the Magic Hot Spring geothermal area has a reservoir temperature about 163 °C (Table 1).

The sulfate-water $\delta^{18}\text{O}$ temperature for this well is 237 °C, which is higher than the values calculated using the chemical geothermometers. However, the $\delta^{18}\text{O}$ of the waters were highly shifted from meteoric values (Figure 4), indicating extensive high temperature interaction with the reservoir rocks. In addition, the isotopic composition of dissolved CH_4 in the sample was typical of CH_4 produced in high-temperature magmatic systems (Appendix I). Taken together, these isotopic signals are all indicate a high-temperature system at depth (Conrad et al., 2016).

6.4.6 Camas Prairie area

Camas Prairie (CP in Figure 1) is an east-west elongated (about 50 km by 15 km) inter-montane valley in Camas and Elmore Counties in Idaho. The area has several hot springs [besides the Elk Creek Hot Springs (ECHS in Figure 1) in the northeastern part of the prairie]. The Sheep and Wolf Hot Springs are located in the western part of Camas Prairie, about 4 km north of Hill City in Idaho. These two hot springs, separated approximately 100 m from each other, issue hot water at about 50 °C. Two additional hot springs in the area are Wardrop Hot Springs (60°C), located on the northern side of prairie near the base of the Soldier Mountains, and Barron Hot Spring (73 °C), located on the southern side of the prairie near the base of the Mount Bennett Hills. The area also has several hot shallow wells, scattered mostly in the Wardrop Hot Springs and the Barron Hot Spring areas.

Camas Prairie is bounded by the Mount Bennett Hills to the south and the Soldier Mountains to the north (see Appendix D for detailed information). The Mount Bennett Hills are composed predominantly of Miocene rhyolitic ash flows and lava flows of the Idavada Volcanic Group that overlies granodiorite of the Idaho Batholith. Local basalt flows and fluvial/lacustrine sediments are also present. The Soldier Mountains are composed mostly of granodiorite of the Idaho Batholith with minor amounts of younger intrusive rocks. Camas Prairie is host to an unknown thickness of Quaternary alluvial, fluvial, and lacustrine sediments with local lenses of basalt encountered in the shallow subsurface (Cluer and Cluer, 1986). However, the preliminary results of the ongoing Snake River Plain Play Fairway phase II project data indicate that the valley-fill sediments may be in the range of few hundreds of meters at the deepest parts.

All Camas Prairie thermal water samples provide similar reservoir temperatures with the same traditional geothermometer. The quartz, chalcedony, and Na-K-Ca geothermometers result in temperature estimates

in the range of 103-128, 74-99, and 70-124 °C, respectively. The silica-enthalpy model with chalcedony solubility and quartz solubility curves resulted in temperature estimates of about 133 °C and 173 °C, respectively.

Unlike the traditional geothermometers, RTest temperature estimates for the Camas Prairie features have a bimodal distribution of higher temperatures for the samples from northern parts and lower temperatures for the samples from southern parts. Specifically, the hot springs from the areas along the northern part of Camas Prairie that abuts the prairie with the foothills of the Soldier Mountains (e.g., Wardrop Hot Spring, Wolf/Sheep Hot Spring) results in higher (181-204 °C) RTest reservoir temperatures. On the other hand, RTest reservoir temperature estimates for hot springs and wells (e.g., Barron Hot Spring) in the southern part of Camas Prairie are 79-108 °C.

Sulfate-water $\delta^{18}\text{O}$ temperatures calculated for the samples from the Camas Prairie range from 133°C to >300°C. The higher temperature is for the sample collected from the Barron Well which had a relatively low field temperature (37 °C), but used to have a very high temperature (approaching boiling) when it was initially drilled, suggesting that it has been significantly diluted by incursion of cool groundwater after years of production. Similar to the Magic Reservoir sample, all of these samples have $\delta^{18}\text{O}$ values shifted off the meteoric water line (Figure 4) and dissolved methane with isotopic signatures indicating a magmatic origin (Appendix I). This suggests that these samples may be indicating a significant geothermal resource related to a magmatic system at depth (Conrad et al., 2016).

6.4.7 South Mount Bennett Hills

Several hot springs located along the southern side of the Mount Bennett Hills in Elmore, Gooding, and Lincoln Counties in Idaho extending over 70 km represent this prospect (SBH in Figure 1). Some of the known hot springs in the area include the Prince Albert (Coyote) (58 °C), Latty (65 °C), and White Arrow (65 °C). The Bostic 1-A well (2950 m) drilled to the south from this area indicated the presence of hot (ca. 200 °C) rock at depths of about 3 km (Arney, 1982; Arney and Goff, 1982; Arney et al., 1984). The presence of several hot springs and hot rock at depth suggests that this part the SRP has great potential for geothermal resources.

Rocks in the area consist mainly of mafic and felsic volcanic rocks with thick sequences of sediments and gravels. The Mount Bennett Hills to the north consist of predominantly of Miocene rhyolitic ash flows and lava flows of the Idavada Volcanic Group that overlies Idaho Batholith granodiorite (see Appendix E for detailed information). At the base of the Mount Bennett Hills, the basalt flows are intercalated with quaternary lacustrine sediments deposited in the Pleistocene-Pliocene Lake Idaho and the sandstones and shales of the Tertiary Glenn's Ferry Formation. At depth, an older basalt unit (Banbury basalt) and Idavada volcanics are encountered at Bostic 1-A well (Arney et al., 1984). The basement rock in the area is considered to be the Idaho Batholith granodiorite.

Reservoir temperature estimates for this area calculated from the chemical compositions of several water samples are given in Table 1. Quartz (no steam loss), chalcedony, and Na-K-Ca geothermometers resulted in 110-143, and 80-117, and 72-160 °C, respectively. The Prince Albert and Latty Hot Springs resulted in highest temperatures for the area with these traditional geothermometers. Silica-enthalpy mixing models with chalcedony and quartz solubility curves resulted in 150 and 182 °C temperature estimates for the area. As with the traditional geothermometers, the RTest modeling of waters from hot springs yielded higher temperature. The three hot springs in the area, Prince Albert, Latty, and White Arrow Hot Springs resulted in reservoir temperatures at 193 ± 8 , 197 ± 5 , and 177 ± 6 °C, respectively. A sulfate-water oxygen isotope temperature for a sample from the Prince Albert Hot Spring yielded a high temperature of 154 °C. Similarly, RTest temperature estimate for a well (Shannon well) in the area is 137 ± 10 °C. All other wells resulted in lower reservoir temperature estimates (82-122 °C). The reservoir temperature estimates using

the hot spring waters are similar to the bottom hole temperature (~200 °C, Arney et al., 1984) measured in the Bostic 1-A well. It is likely that deep thermal waters that ascend along the range-forming faults are the source these hot springs.

6.4.8 Banbury Hot Springs-Twin Falls area

The southwestern periphery of the ESRP near Twin Falls and Buhl is one of the Known Geothermal Resource Areas in southern Idaho (see Appendix J for detailed information). The area is comprised of two dense clusters of geothermal surface manifestations, Banbury Hot Springs (BHS in Figure 1) and Twin Falls (TF in Figure 1). Discharging thermal waters range in temperature from 25 °C to 70 °C. At this time thermal waters are being used for space heating, agriculture, and recreation.

The Twin Falls and Banbury hydrothermal areas show characteristics of both the ESRP and Basin and Range regional extension. Tertiary rhyolitic volcanic rocks underlie younger Quaternary and Tertiary basaltic units throughout the study area. Paleozoic meta-sedimentary rocks are thought to underlie the entire area (Lewis and Young, 1989). The thermal aquifer system in the area is located beneath basalt units within the Idavada volcanics and is under artesian conditions with temperatures of the waters increasing to the northwest. Thermal waters are thought to originate from deep circulation paths from the Cassia Mountain recharge zone to the south and through fractures in the overlying basalts of the thermal area. The high regional thermal gradient coupled with the young volcanic sill complexes associated with the ESRP volcanism in the area then heat these waters resulting in the thermal features (McLing et al., 2014, Dobson et al., 2015).

Reservoir temperature estimate ranges obtained with traditional geothermometers and RTest are given in Table 1 for both the Banbury Hot Springs and Twin Falls prospects. The highest reservoir temperatures (ca. 160 °C) for the Banbury Hot Springs prospect are obtained for Banbury Hot Spring, Miracle Hot Spring well, and Salmon Falls Hot Spring with RTest as well as other geothermometers. Similarly, for the Twin Falls prospect, the highest reservoir temperatures (ca. 135 °C) are obtained for samples from two hot shallow wells (used for direct heating – Neely, 1996) within the premises of the College of Southern Idaho. Nearly identical temperatures were obtained using the sulfate-water oxygen isotope geothermometer. Two samples taken from the Banbury hot springs yielded temperatures of 159 and 152 °C and a sample from one of the College of Southern Idaho wells was 133 °C. Samples from 7 additional thermal features in the region ranged from 99 to 156 °C.

7. Summary

The specific objectives of this project were to obtain samples from thermal expressions (Appendix A), analyze samples for chemical and isotopic concentrations (Appendix B & C), use INL's geothermometry tool (RTest), traditional geothermometers, and dissolved sulfate ($\delta^{34}\text{S}$ and $\delta^{18}\text{O}$) calculations (Appendix D), and identify potential geothermal areas (prospects) in the ESRP (Appendix E). All objects for this project were accomplished and a map of the ESRP (Figure 1) was produced describing the locations and calculated reservoir temperatures of potential geothermal resource areas.

Geothermometric calculations of ESRP thermal water samples indicate numerous potential geothermal areas with elevated reservoir temperatures. Specifically, RTest results of thermal water samples from areas around the southern/southwestern side of the Mount Bennett Hills and within the Camas Prairie in the southwestern portion of the ESRP suggest temperatures of 140-200°C. In the northern portion of the ESRP, Lidy Hot Springs, Ashton, Newdale, and areas east of Idaho Falls have expected reservoir temperatures ≥ 140 °C. Resource temperatures in the southwestern ESRP, specifically, areas near Buhl and Twin Falls are estimated to as high as 160 °C. These areas are likely to host potentially economic geothermal resources; however, further detailed study is warranted for each site to evaluate their suitability for economic use.

Acknowledgments

This work was supported by funding by the Assistant Secretary for Energy Efficiency and Renewable Energy, Geothermal Technologies Office of the U.S. Department of Energy under the U.S. Department of Energy Contract Numbers DE-AC07-05ID14517 for Idaho National Laboratory and DE-AC02-05CH11231 for Lawrence Berkeley National Laboratory. We thank landowners who provided access to sampling locations. We also thank Dr. Ross Spackman (Brigham Young University-Idaho) for his assistance in coordinating with landowners and field work during summer 2014 sampling campaign. Ms. Debbie Lacroix (University of Idaho) at Center for Advanced Energy Studies (CAES) conducted chemical analyses of the samples. Dr. Pat Dobson (LBNL) and Wade Worthing (University of Idaho) helped during collection of thermal water samples. We appreciate the discussion with Drs. Bill Phillips (Idaho Geological Survey), Glenn Embree (BYU-Idaho), and Dan Moore (BYU-Idaho). Mr. Trevor Atkinson (Utah State University) helped construct geologic cross-sections of several prospects.

Appendices

- Appendix A. Map showing distribution of thermal features in and around the ESRP.
- Appendix B. Water chemistry data for thermal features in and around the ESRP.
- Appendix C. Water isotope data for thermal features in and around the ESRP.
- Appendix D. Geothermometric temperature estimates for thermal features in and around the ESRP.
- Appendix E. Descriptions of geothermal prospects in and around the ESRP.
- Appendix F. Neupane, G., Mattson, E.D., Mines, G.L., McLing, T.L., Dobson, P.F., Conrad, M.E., Wood, T.R., Cannon, C., Worthing, W., 2015c. Geothermometric temperature comparison of hot springs and wells in southern Idaho. GRC Transactions, 39, 495-502.
- Appendix G. Neupane, G., Mattson, E.D., Cannon, J.C., Atkinson, T.A., McLing, T.L., Wood, T.R., Worthing, W.C., Dobson, P.F., and Conrad, M.E., 2016b. Potential hydrothermal resource areas and their reservoir temperatures in the Eastern Snake River Plain, Idaho. Proceedings, 41st Workshop on Geothermal Reservoir Engineering, Stanford University, Stanford, CA.
- Appendix H. Neupane, G., Mattson, E.D., Cannon, J.C., Atkinson, T.A., McLing, T.L., Wood, T.R., Worthing, W.C., and Conrad, M.E., 2016b. Mixing effects on geothermometric calculations of the Newdale Geothermal area in the Eastern Snake River Plain, Idaho. Proceedings, 41st Workshop on Geothermal Reservoir Engineering, Stanford University, Stanford, CA.
- Appendix I. Conrad, M.E., Dobson, P.F., Sonnenthal, E.L., Kennedy, B.M., Cannon, C., Worthing, W., Wood, T., Neupane, G., Mattson E., and McLing, T., 2016. Application of isotopic approaches for identifying hidden geothermal systems in southern Idaho. Proceedings, 41st Workshop on Geothermal Reservoir Engineering, Stanford University, Stanford, CA.
- Appendix J. Cannon, C.J., 2015. Evidence for mixing and re-equilibration in the Twin Falls – Banbury hydrothermal system and its effects on reservoir temperature estimation. MS Thesis, University of Idaho, 184 p.
- Appendix K. Dobson, P.F., Kennedy, B.M., Conrad, M.E., McLing, T., Mattson, E., Wood, T., Cannon, C., Spackman, R., van Soest, M., and Robertson, M., 2015. The isotopic evidence for undiscovered geothermal systems in the Snake River Plain. Proceedings, 40th Workshop on Geothermal Reservoir Engineering, Stanford University, Stanford, CA.

References

- Arney, B., 1982. Evidence of former higher temperatures from alteration minerals, Bostic 1-A well, Mountain Home, Idaho. *GRC Transactions*, 6, 3-6.
- Arney, B.H., Gardner, J.N., and Belluomini, S.G., 1984. Petrographic analysis and correlation of volcanic rocks in Bostic 1-A well near Mountain Home, Idaho. LA-9966-HDR, Los Alamos National Laboratory.
- Arney, B.H. and Goff, F., 1982. Evaluation of the hot-dry-rock geothermal potential of an area near Mountain Home, Idaho. LA-9365-HDR, Los Alamos National Laboratory.
- Bethke, C.M., 2008. *Geochemical and Biogeochemical Reaction Modeling*. Cambridge University Press, 547 p.
- Blackwell, D.D., 1989. Regional implications of heat flow of the Snake River Plain, northwestern United States. *Tectonophysics*, 164, 323-343.
- Bond, J. G., Kauffman, J. D., Miller, D.A., and Venkatakrishnan, R., 1978. Geologic Map of Idaho: Moscow. Idaho, Idaho Bureau of Mines and Geology Map GM-1.
- Brott, C.A., Blackwell, D.D., and Mitchell J.C., 1976. Geothermal investigations in Idaho, Part 8: Heat flow study of the Snake River Plain, Idaho, Idaho Department of Water Resources. *Water Information Bulletin*, 30, 195 p.
- Cannon, C., Wood, T., Neupane, G., McLing, T., Mattson, E., Dobson, P., and Conrad, M., 2014. Geochemistry sampling for traditional and multicomponent equilibrium geothermometry in southeast Idaho. *GRC Transactions*, 38, 524-431.
- Cluer, J.K., Cluer, B.L., 1986. The late Cenozoic Camas Prairie Rift south-central Idaho, Contributions to Geology, University of Wyoming, 24(1), 91-101.
- Cooper, D.C., Palmer, C.D., Smith, R.W., and McLing, T.L., 2013. Multicomponent equilibrium models for testing geothermometry approaches. *Proceedings*, 38th Workshop on Geothermal Reservoir Engineering Stanford University, Stanford, CA.
- Conrad, M.E., Dobson, P.F., Sonnenthal, E.L., Kennedy, B.M., Cannon, C., Worthing, W., Wood, T., Neupane, G., Mattson E., and McLing, T., 2016. Application of isotopic approaches for identifying hidden geothermal systems in southern Idaho. *Proceedings*, 41st Workshop on Geothermal Reservoir Engineering, Stanford University, Stanford, CA.
- Craig, H., 1961. Isotopic variations in meteoric waters. *Science*, 133(3465), 1702-1703.
- D'Amore, F. and Arnórsson, S., 2000. Geothermometry, in *Isotopic and Chemical Techniques in Geothermal Exploration, Development and Use* (S. Arnórsson, ed.): IAEA (Editorial), Vienna, 152-199.
- D'Amore, F., Fancelli, R., and Caboi, R., 1987. Observations on the application of chemical geothermometers to some hydrothermal systems in Sardinia. *Geothermics*, 16, 271-282.
- Dobson, P.F., Kennedy, B.M., Conrad, M.E., McLing, T., Mattson, E., Wood, T., Cannon, C., Spackman, R., van Soest, M., and Robertson, M., 2015. The isotopic evidence for undiscovered geothermal systems in the Snake River Plain. *Proceedings*, 40th Workshop on Geothermal Reservoir Engineering, Stanford University, Stanford, CA.
- Embree, G.F., Phillips, W.M., and Welhan, J.A., 2011. Geologic map of the Newdale quadrangle, Fremont and Madison Counties, Idaho. Idaho Geological Survey, University of Idaho, Moscow, Idaho 83844-3014.

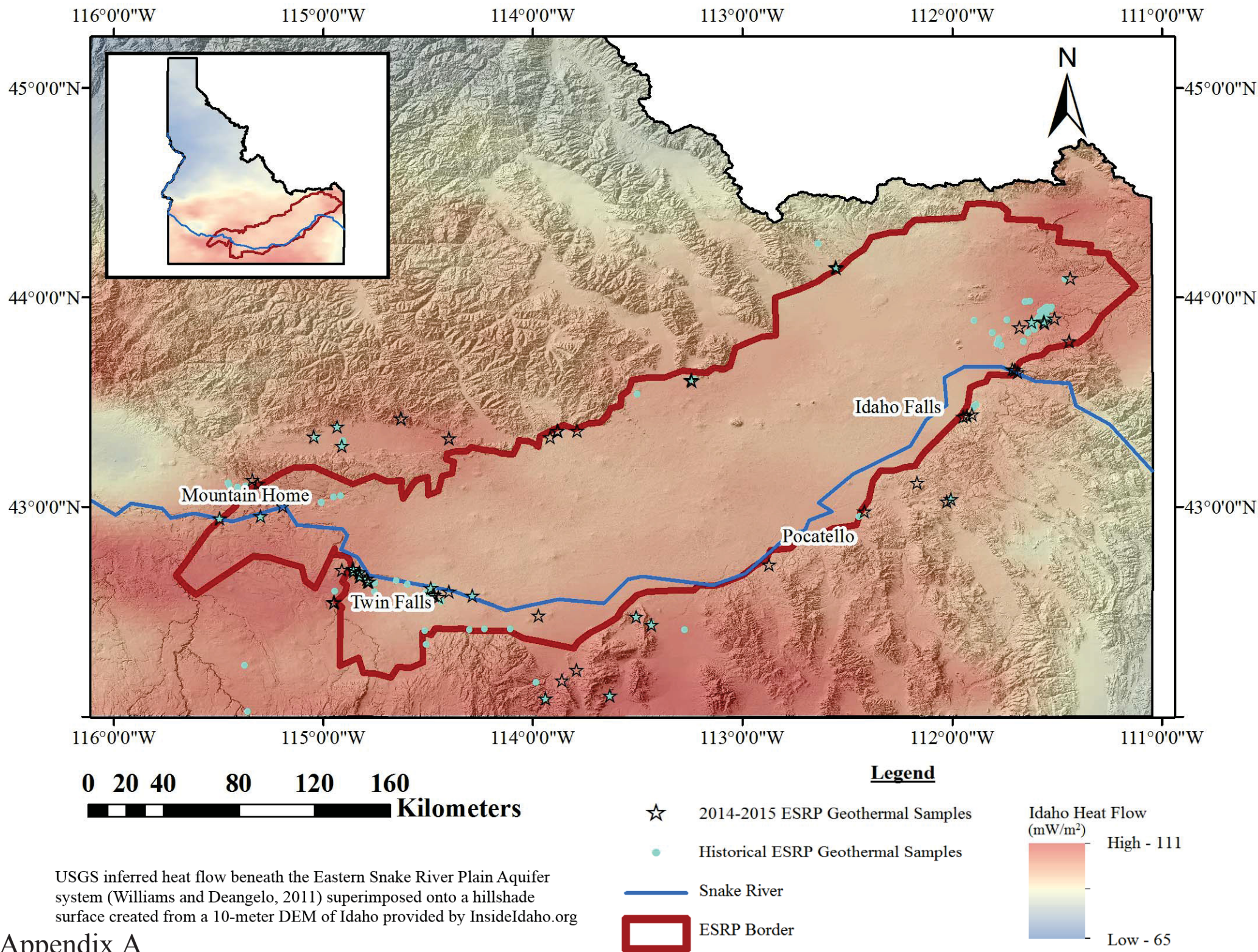
- Fournier, R.O. and Truesdell, A.H., 1973. An empirical Na-K-Ca geothermometer for natural waters. *Geochim. Cosmochim. Acta*, 37, 1255-1275.
- Fournier, R.O., 1977. Chemical geothermometers and mixing models for geothermal systems. *Geothermics*, 5, 41-50.
- Fournier, R.O., 1979. A revised equation for the Na/K geothermometer. *GRC Transactions*, 3, 221-224.
- Fournier, R.O. and Potter II, R.W., 1979. Magnesium correction to the Na-K-Ca chemical geothermometer. *Geochim. Cosmochim. Acta*, 43, 1543-1550.
- Fowler, A.P.G., Hackett, L.B., and Klein, C.W., 2013. Reformulation and Performance Evaluation of the Sulfate-Water Oxygen Isotope Geothermometer. *GRC Transactions* 9, p. 31.
- GeothermEx, Inc., 2010. Independent technical report: Resource evaluation of the Newdale geothermal prospect, Madison and Fremont Counties, Idaho, USA. Geothermix, Inc., Richmond, California, USA, 101 p.
- Giggenbach, W.F., 1988. Geothermal solute equilibria. Derivation of Na-K-Mg-Ca geoindicators. *Geochim. Cosmochim. Acta*, 52, 2749-2765.
- Hughes, S.S., Smith, R.P., Hackett, W.R., and Anderson, S. R., 1999. Mafic volcanism and environmental geology of the eastern Snake River Plain. *Idaho Guidebook to the Geology of Eastern Idaho*. Idaho Museum of Natural History, 143-168.
- Hull, C.D., Reed, M.H., and Fisher, K., 1987. Chemical geothermometry and numerical unmixing of the diluted geothermal waters of the San Bernardino Valley Region of Southern California. *GRC Transactions*, 11, 165-184.
- Lewis, R.E. and Young, H.W., 1989. The hydrothermal system in central Twin Falls County, Idaho: U.S. Geological Survey Water Resources Investigations Report 88-4152, 44 p.
- Link, P.K., 2002. Clark County, Idaho. Digital Atlas of Idaho, Idaho State University, Geosciences Department, p. 3.
- Mattson, E.D., Smith, R.W., Neupane, G., Palmer, C.D., Fujita, Y., McLing, T.L., Reed, D.W., Cooper, D.C., and Thompson, V.S., 2015. Improved geothermometry through multivariate reaction-path modeling and evaluation of geomicrobiological influences on geochemical temperature indicators: Final Report No. INL/EXT-14-33959, Idaho National Laboratory (INL), Idaho Falls, Idaho.
- McLing, T.L., Smith, R.W., and Johnson, T.M., 2002. Chemical characteristics of thermal water beneath the eastern Snake River Plain. In: *Geology, Hydrogeology, and Environmental Remediation: Idaho National Engineering and Environmental Laboratory, Eastern Snake River Plain, Idaho*, P.K. Link and L.L. Mink, eds. *GSA Special Paper*, **353**, 205-211.
- McLing, T., McCurry, M., Cannon, C., Neupane, G., Wood, T., Podgorney, R., Welhan, J., Mines, G., Mattson, E., Wood, R., Palmer, C. and Smith, R., 2014. David Blackwell's Forty Years in the Idaho Desert, The Foundation for 21st Century Geothermal Research. *GRC Transactions*, 38, 143-153.
- Michard, G. and Roekens, E., 1983. Modelling of the chemical components of alkaline hot waters. *Geothermics*, 12, 161-169.
- Mitchell, J.C., 1976. Geothermal Investigations in Idaho – Part 7: Geochemistry and geologic setting of the thermal waters of the Camas Prairie Area, Blaine and Camas Counties, Idaho. Idaho Department of Water Resources, *Water Information Bulletin* 30.
- Mitchell, J.C., Johnson, L.L., and Anderson, J.E., 1980. Geothermal Investigations in Idaho – Part 9: Potential for direct heat applications of geothermal resources. Idaho Department of Water Resources, *Water Information Bulletin* 30.

- Morgan, L.A., and McIntosh, W.C., 2005. Timing and development of the Heise volcanic field, Snake River Plain, Idaho, western USA. *GSA Bulletin*, 117, 288-306.
- Morse, L.H. and McCurry, M., 2002. Genesis of alteration of Quaternary basalts within a portion of the eastern Snake River Plain aquifer. *Special Papers Geological Society of America*, 213-224.
- Neely, K.W., 1996. Geothermal heat keeps students warm at the College of Southern Idaho. *GRC Transactions*, 20, 129-136.
- Neupane, G., Smith, R. W., Palmer, C. D., and McLing, T. L., 2013. Multicomponent equilibrium geothermometry applied to the Raft River geothermal area, Idaho: preliminary results. In *GSA Abstracts with Programs*, 45 (7).
- Neupane, G., Mattson, E.D., McLing, T.L., Palmer, C.D., Smith, R.W., and Wood, T.R., 2014. Deep geothermal reservoir temperatures in the Eastern Snake River Plain, Idaho using multicomponent geothermometry. *Proceedings, Thirty-Ninth Workshop on Geothermal Reservoir Engineering*, Stanford University, Stanford, CA.
- Neupane, G., Mattson, E.D., McLing, T.L., Palmer, C.D., Smith, R.W., Wood, T.R., and Podgorney, R.K., 2015a. Geothermal reservoir temperatures in southeastern Idaho using multicomponent geothermometry. *Proceedings, World Geothermal Congress 2015*, Melbourne, Australia, 19-25 April 2015.
- Neupane, G., Baum, J.S., Mattson, E.D., Mines, G.L., Palmer, C.D., and Smith, R.W., 2015b. Validation of multicomponent equilibrium geothermometry at four geothermal power plants. *Proceedings, Fortieth Workshop on Geothermal Reservoir Engineering* Stanford University, Stanford, CA.
- Neupane, G., Mattson, E.D., Mines, G.L., McLing, T.L., Dobson, P.F., Conrad, M.E., Wood, T.R., Cannon, C., Worthing, W., 2015c. Geothermometric temperature comparison of hot springs and wells in southern Idaho. *GRC Transactions*, 39, 495-502.
- Neupane, G., Mattson, E.D., McLing, T.L., Palmer, C.D., Smith, R.W., Wood, T.R., and Podgorney, R.K., 2016a. Geothermometric evaluation of geothermal resources in southeastern Idaho. *Geoth. Energ. Sci*, 4(1), 11-22.
- Neupane, G., Mattson, E.D., Cannon, J.C., Atkinson, T.A., McLing, T.L., Wood, T.R., Worthing, W.C., and Conrad, M.E., 2016b. Mixing effects on geothermometric calculations of the Newdale Geothermal area in the Eastern Snake River Plain, Idaho. *Proceedings, 41st Workshop on Geothermal Reservoir Engineering*, Stanford University, Stanford, CA.
- Nielson, D.L., Delahunty, C., and Shervais, J.W., 2012. Geothermal systems in the Snake River Plain, Idaho, characterized by the Hotspot project. *GRC Transactions*, 36, 727-730.
- Occidental Geothermal, Inc., 1979. Sturm 1, Computer Processed Log. Department of Water Resources, Idaho, 18 p.
- Palandri, J.L. and Reed, M.H., 2001. Reconstruction of in situ composition of sedimentary formation waters. *Geochim. Cosmochim. Acta*, 65, 1741-1767.
- Palmer, C.D., Ohly, S.R., Smith, R.W., Neupane, G., McLing, T., Mattson, E.: Mineral selection for multicomponent equilibrium geothermometry. *GRC Transactions*, 38, (2014), 453-459.
- Pang, Z.H. and Reed, M., 1998. Theoretical chemical thermometry on geothermal waters: Problems and methods. *Geochim. Cosmochim. Acta*, 62, 1083-1091.
- Peiffer, L., Wanner, C., Spycher, N., Sonnenthal, E., Kennedy, B.M., Iovenitti, J., 2014. Optimized multicomponent vs. classical geothermometry: insights from modeling studies at the Dixie Valley geothermal area. *Geothermics*, 51, 154-169.

- Pierce, K. L., and Morgan, L. A., 1992. The track of the Yellowstone hot spot: Volcanism, faulting, and uplift. *GSA Memoirs*, 179, 1-54.
- Ralston, D.R., Arrigo, J.L., Baglio, J.V. Jr., Coleman, L.M., Souder, K., and Mayo, A.L., 1981. Geothermal evaluation of the thrust area zone in southeastern Idaho, Idaho Water and Energy Research Institute, University of Idaho.
- Reed, M. and Spycher, N., 1984. Calculation of pH and mineral equilibria in hydrothermal waters with application to geothermometry and studies of boiling and dilution. *Geochim. Cosmochim. Acta*, 48, 1479-1492.
- Rodgers, D.W., Ore, H.T., Bobo, R.T., McQuarrie, N., and Zentner, N., 2002. Extension and subsidence of the eastern Snake River Plain, Idaho. Tectonic and Magmatic Evolution of the Snake River Plain Volcanic Province. *Idaho Geological Survey Bulletin*, 30, 121-155.
- Ross, S.H., 1970. Geothermal potential of Idaho. *Geothermics*, 2, 975-1008.
- Shervais, J.W., Glen, J.M., Liberty, L.M., Dobson, P., Gasperikova, E., Sonnenthal, E., Visser, C., Garg, S., Evans, J.P., Siler, D., DeAngelo, J., Athens, N., and Burns, E., 2015. Snake River Plain play fairway analysis – Phase 1 Report. *GRC Transactions*, 39, 761-769.
- Smith, R.P., 2004. Geologic setting of the Snake River Plain aquifer and vadose zone. *Vadose Zone Journal*, 3, 47-58.
- Smith, R.W., Palmer, C.D., and Cooper, D., 2012. Approaches for multicomponent equilibrium geothermometry as a tool for geothermal resource exploration. *Abstracts*, AGU Fall Meeting, San Francisco, CA.
- Spycher, N.F., Sonnenthal, E., and Kennedy, B.M., 2011. Integrating multicomponent chemical geothermometry with parameter estimation computations for geothermal exploration. *GRC Transactions*, 35, 663-666.
- Spycher, N., Peiffer, L., Sonnenthal, E. L., Saldi, G., Reed, M. H., and Kennedy, B. M., 2014. Integrated multicomponent solute geothermometry. *Geothermics*, 51, 113-123.
- Struhsacker, D.W., Jewell, P.W., Ziesloft, J., and Evans, S.H. Jr., 1982. The geology and geothermal setting of the Magic reservoir area, Blaine and Camas Counties, Idaho. In: *Cenozoic geology of Idaho*, B. Bonnicksen and R.M. Breckenridge, eds., Idaho Bureau of Mines and Geology Bulletin 26, 377-393.
- Taylor, H.P., 1974. Application of oxygen and hydrogen isotope studies to problems of hydrothermal alteration and ore deposition. *Econ. Geol.*, 69, 843-883.
- Tole, M.P., Ármannsson, H., Pang, Z.H., & Arnórsson, S., 1993. Fluid/mineral equilibrium calculations for geothermal fluids and chemical geothermometry. *Geothermics*, 22, 17-37.
- Welhan, J.A., 2015. Thermal and Trace-Element Anomalies in the Eastern Snake River Plain aquifer: toward a conceptual model of the EGS resource. *GRC Transactions*, 39, 363-375.
- Whitehead, R.L., 1992. Geohydrologic framework of the Snake River Plain regional aquifer system, Idaho and eastern Oregon. Regional aquifer system analysis-Snake River Plain, Idaho. *US Geological Survey Professional Paper 1408-B*.
- Williams, C.F., and DeAngelo, J., 2011. Evaluation of approaches and associated uncertainties in the estimation of temperatures in the upper crust of the western United States, *GRC Transactions*, 35, 1599-1605.
- Williams, P.L., Mabey, D.R., Zohdy, A.A.R., Ackermann, H., Hoover, D.B., Pierce, K.L., and Oriel, S.S., 1976. Geology and geophysics of the southern Raft River Valley geothermal area, Idaho, USA.

Proceedings, Second UN Symposium on the Development and Use of Geothermal Resources, San Francisco, Lawrence Berkeley National Laboratory, 1273

Appendix A. Map showing distribution of thermal features in and around the
Eastern Snake River Plain (ESRP)



Appendix B. Water chemistry data for thermal features in and around the Eastern
Snake River Plain (ESRP)

Appendix B. Water chemistry data for thermal features in and around the Eastern Snake River Plain (ESRP).

Sampling Features	Latitude	Longitude	T (°C)	pH	Ca	Mg	Na	K	HCO ₃	SO ₄	Cl	F	SiO ₂ (aq)	Al	Sr	Li	B	TDS (g/L)	Ref.
Lidy HS1	44.14558	-112.55494	56.1	7.17	66	16	25	13	132	102	7.3	4.6	38	0.001	0.60	0.05	0.09	0.36	TS
Lidy HS2	44.14166	-112.55240	52.3	7.21	64	16	28	14	163	98	6.9	4.7	34	0.001	0.61	0.05	0.09	0.38	TS
Lidy HS W	44.140500	-112.550167	59.0	7.60	55	14	24	12	180	100	7.1	4.4	37			0.04	0.09	0.34	M-80
Warm Spring WS	44.256500	-112.639167	29.0	7.00	54	19	10	2.9	209	62	5.3	1	17					0.27	YM-73
Sturm W	44.09325	-111.43534	31.4	8.73	3	0.0	33	0.9	66	5.8	3.3	2.1	63	0.005	0.005	0.05	0.04	0.11	TS
Ashton WS	44.091333	-111.4595	41.0	7.60	1	0.1	36	1.6	92	4.7	2.9	2.2	110	0.010	0.002	0.05	0.03	0.21	M-80
Warm River S1	44.098133	-111.368144	27.1	6.84	10.5	1.3	21.8	0.724	184.2	8.11	6.53	2.58	37.7	0.010	0.02	0.07	0.03	0.21	TS
Warm River S2	44.099381	-111.382628	21	6.73	27.5	2.5	36.3	1.56	82.4	7.62	5.87	2.05	51.7	0.010	0.04	0.1	0.04	0.21	TS
Newdale City W	43.88308	-111.6186	30.0	7.34	28	4.7	71	8.1	251	29.7	24.9	5.0	70	0.002	0.09	0.12	0.22	0.30	TS
Wanda Woods W2	43.861167	-111.608333	27.0	7.60	31	7.6	70	8.5	217	26	25	4.5	80					0.36	M-80
Walz Enterprises W	43.862167	-111.606833	26.0	7.70	31	6.9	65	9.0	232	26	27	3.7	65					0.35	M-80
Wanda Woods W1	43.868167	-111.617167	24.0	8.00	33	7.2	64	8.6	240		24	3.5	66					0.32	M-80
Wallace Little W	43.88308	-111.6186	36.0	7.90	28	6.3	78	8.6	240	33	24	5.4	75					0.38	M-80
Henry Harris W	43.890667	-111.598	33.0	7.60	25	5.9	69	6.9	204	26	22	5.7	64					0.33	M-80
Donald Trupp W	43.901333	-111.5735	32.0	7.80	23	3.3	88	12.0	181	26	25	6.2	76					0.35	M-80
Wayne Larson W	43.905667	-111.586667	22.0	8.10	19	2.7	93	12.0	243	23	28	7.1	94					0.40	M-80
Schwendiman W	43.87717	-111.55890	28.0	7.57	27	6.9	39	5.5	165	25.2	13.7	2.6	62	0.002	0.08	0.05	0.09	0.30	TS
Clyde W	43.88566	-111.55949	32.7	7.5	25	7.3	46	5.3	183	23.0	15.4	3.2	65	0.002	0.08	0.06	0.12	0.30	TS
Cinder Block W	43.90127	-111.50967	26.3	7.35	18	3.5	52	5.0	182	17.2	12.2	4.2	70	0.002	0.05	0.07	0.15	0.30	TS
G23	43.90150044	-111.53902	43	8.22	37	6.3	56	4.5	166	35.4	54.5		44					0.40	G-10
G25	43.92297413	-111.55408	51	8.03	16	4.2	92	9.1	241	22.3	25.1		102					0.51	G-10
G41	43.89159947	-111.55900	25	7.44	17	3.6	75	9.2	180	27.4	38.6		89					0.44	G-10
G43	43.88352634	-111.60607	32	6.60	34	6.9	76	8.5	230	31.0	27.0	5.3	71					0.47	G-10
G44	43.88983677	-111.57849	32	8.20	22	7.5	69	9.1	211	30.6	33.0		52					0.43	G-10
G50	43.89855088	-111.57878	39	7.80	22	3.1	95	12.2	243	22.5	28.3		91					0.52	G-10
G54	43.90885357	-111.57828	41	7.84	18	3.8	93	10.3	251	19.6	25.0		87					0.51	G-10

G80	43.85004832	-111.60480	22	7.90	32	8.6	58	7.9	217	22.2	24.0	3.5	66					0.44	G-10
Remington Produce W	43.914333	-111.554	26.0	7.90	35	17.0	15	2.2	144	22.0	24	2.2	65					0.22	M-80
Dean Swindelman W	43.948167	-111.529167	32.0	7.60	38	14.0	22	4.8	205	8.8	14.0	2.0	65					0.27	M-80
Pauline SW W	43.771833	-111.763333	21.0	8.00	37	15.0	14	2.7	189	11.0	16.0	0.6	40					0.23	M-80
Mark Ricks W	43.780000	-111.7835	26.0	7.60	33	11.0	20	3.9	170	12.0	12.0	1.7	50					0.23	M-80
Lavere Ricks W	43.790000	-111.658333	21.0	7.90	34	12.0	18	3.1	174	11.0	20.0	1.3	42					0.23	M-80
G21 W	43.89116621	-111.538604	35.56	8.47	21	4.7	50	5.2	189	11.6	12.1		69					0.36	G-10
G22 W	43.89412153	-111.543860	32.78	7.91	44	17.4	32	1.9	196	31.9	40.5		44					0.40	G-10
G24 W	43.90556757	-111.558298	26.67	7.89	41	8.0	25	6.4	182	15.5	13.4		74					0.36	G-10
G26 W	43.91244701	-111.558163	27.22	8.06	46	15.4	20	4.6	204	23.3	26.8		37					0.37	G-10
G28 W	43.91939558	-111.549334	21.11	8.03	34	18.7	19	4.0	194	16.4	23.9		30					0.33	G-10
G30 W	43.93306682	-111.548551	27.78	8.05	37	20.3	27	3.2	217	17.5	26.1		19					0.36	G-10
G31 W	43.94458406	-111.531049	25	7.76	46	22.1	18	2.2	244	11.4	13.1		34					0.38	G-10
G36 W	43.944632	-111.547598	27.22	7.78	34	21.1	22	2.4	213	12.2	16.6		40					0.36	G-10
G37 W	43.95167768	-111.554056	34.44	7.81	42	15.7	20	6.8	212	18.4	16.2		64					0.39	G-10
G38 W	43.95521336	-111.547147	26.11	7.65	46	18.9	22	2.5	198	22.5	24.8		34					0.36	G-10
G39 W	43.95584748	-111.525217	25	7.66	46	17.4	20	4.3	220	13.2	24.1		37					0.38	G-10
G56 W	43.92241041	-111.564397	28.89	7.90	42	15.0	26	1.8	180	20.0		2.3	37					0.32	G-10
G64 W	43.93370158	-111.578670	20	7.43	37	11.0	27	3.4	190	16.8	26.9		35					0.34	G-10
G65 W	43.92670316	-111.559305	28.33	7.83	52	22.1	20	2.6	224	19.9	33.5		36					0.40	G-10
G66 W	43.92669653	-111.567951	29.44	7.86	46	18.6	32	2.2	196	28.0	40.7		37					0.40	G-10
G67 W	43.93348517	-111.567965	30	7.88	51	30.2	34	2.7	228	59.1	45.8		39					0.48	G-10
G78 W	43.87852691	-111.55884	27.78	7.80	32	12.1	37	4.5	180	24.7	10.0	2.4	57					0.35	G-10
G83 W	43.8649129	-111.608294	26.5	7.70	47	19.0	13	2.6	207	13.0	21.0	0.4	33					0.35	G-10
Spackman W	43.85840	-111.67870	14.1	7.19	37	13.7	12	3.0	190	12.9	5.8	0.5	30	0.001	0.108	0.000	0.065	0.29	TS
GW1	43.80194444	-111.776667	17.5	8.00	36	13.0	20	3.2	180	14.0	13.0	1.1	45					0.32	WL-88
GW2	43.83333333	-111.806111	10	7.80	51	14.0	5	1.6	210	10.0	3.9	0.2	20					0.31	WL-88
GW3	43.83388889	-111.635556	8.5	7.70	29	8.4	17	3.1	150	13.0	10.0	1.5	46					0.27	WL-88
GW4	43.89083333	-111.892222	9	7.30	19	6.5	12	3.6	110	10.0	4.4	1.4	37					0.20	WL-88
GW5	43.89472222	-111.736389	11.5	8.00	41	11.0	6	1.6	190	8.3	3.1	0.8	19					0.27	WL-88
G6 W	43.9843592	-111.627456	12.39	7.60	22	6.6	14	2.9	140	3.6	5.4	1.4	43					0.23	G-10
G14 W	43.98185851	-111.648016	10.61	6.40	52	16.5	19	1.9	185	14.5	24.7	1.1	39					0.32	G-10

G16 W	43.98158212	-111.649123	13.22	7.40	26	6.6	12	3.3	116	4.5	4.7	1.3	43					0.21	G-10
Green Canyon HS	43.79211	-111.44009	44	7.2	144	33.8	5	4.5	137	314	0.9	1.5	27	0.0005	1.17	0.02	0.02	0.59	TS
Heise HS	43.64283	-111.68768	48.2	6.32	488	94	1540	206.2	986	712.3	2267.5	4.0	34	0.131	5.47	2.48	4.55	7.00	TS
Hawley WS	43.657882	-111.712868	16.4	6.93	39	9.7	10	3.2	214	6.0	6.2	0.7	56	0.010	0.11	0.02	0.01	0.22	TS
Elkhorn WS	43.654338	-111.701418	20.2	7.11	40	9.1	11	3.3	134	7.6	5.1	0.8	57	0.010	0.12	0.02	0.01	0.22	TS
Comore Loma W6	43.44244	-111.90484	20.9	6.7	51	15.2	97	16.0	222	32.2	126	0.4	65	0.002	0.31	0.12	0.22	0.59	TS
Comore Loma W5	43.43774	-111.93018	27.7	6.94	52	18.5	90	15.8	251	25.6	120	0.3	85	0.002	0.23	0.09	0.22	0.59	TS
Blackhawk W2	43.43142	-111.94501	26.8	6.64	77	22.1	124	17.3	271	37.0	205	0.2	84	0.002	0.41	0.13	0.34	0.84	TS
Blackhawk W1	43.43121	-11.94469	25.1	6.77	75	21.0	122	16.7	268	39.1	197	0.3	82	0.002	0.43	0.13	0.34	0.76	TS
Dyer W	43.4900	-111.8833	21	7.7	50	13	50	3	188	1	61	0.29	68					0.43	R-81
Anderson W	43.4790	-111.8970	20	7.7	50	10	45	7	199	0.0	45.0	0.44	111					0.47	R-81
Butte City W	43.60827	-113.24432	32.5	7.4	52	20.9	32	7.5	386	49.4	19.8	0.6	33	0.002	0.56	0.03	0.16	0.43	TS
Greenhouse W	43.60234	-113.24214	36.3	7.09	78	27.7	34	9.4	285	57.5	22.2	0.7	32	0.000	0.72	0.04	0.15	0.48	TS
E Butte City W	43.60911	-113.23064	22.8	7.4	65	28.7	31	5.8	228	35.3	95.2	0.4	24						NWIS
W Butte City W	43.60861	-113.24417	27	7.4	52	21.2	33	7.2	273	42.5	18.2	0.5	30						NWIS
Birch and 7th St W	43.60917	-113.24611	28	8.1	32	23.3	23	6.7	174	39.4	37.4	0.4	38						NWIS
Lewis Rothwell W	43.540500	-113.502	41	6.3	74	24.0	72	21.0	322	170.0	21.0	3.2	55						NWIS
Condie HS	43.33278	-113.91790	50.5	7.03	61	11.5	62	22.5	315	33.5	14.0	1.6	30	0.003	0.93	0.09	0.26	0.48	TS
Milford Sweat HS	43.36414	-113.78943	38.1	7.25	66	13.7	43	8.5	251	49.9	6.6	1.9	25	0.003	0.45	0.05	0.17	0.42	TS
Rush WS1	43.364911	-113.882168	29.5	6.65	48	9.8	47	14.5	278	27.4	13.4	1.5	30	0.010	0.84	0.05	0.16	0.40	TS
Rush WS2	43.36479	-113.882468	23.2	7.08	45	8.7	43	13.0	281	24.8	13.4	1.3	32	0.010	0.75	0.05	0.15	0.36	TS
Magic HS Landing W Runoff	43.32777	-114.39941	39.1	8.61	13	1.3	333	20.9	710	52.9	79.1	10.6	109	0.007	0.65	1.17	1.24	1.14	TS
Magic HS Landing W	43.32777	-114.39941	75.0	6.79	22	1.4	311	19.8	703	50.3	74.1	9.9	104	0.009	0.93	1.18	1.20	1.18	TS
Elk Creek HS1	43.42341	-114.62857	50.0	9.12	2	0.004	90	1.7	93	42.6	23.2	15.1	65	0.022	0.11	0.21	0.25	0.34	TS

Elk Creek HS2	43.42322	-114.62865	55.5	9.05	2	0.003	91	1.6	90	42.6	23.1	15.2	65	0.026	0.11	0.21	0.25	0.34	TS
Wardrop HS	43.38290	-114.93224	67.5	9	1.2	0.27	56	0.9	193	11.5	5.1	3.4	77	0.09	0.05	0.05	0.05	0.21	TS
Hot Spring Rnach HS1	43.382791	-114.932445	60	9.2	1	0.1	56	0.8	82	11	5.7	3.7	81						M-76
Hot Spring Rnach HS2	43.382791	-114.932445	67	9.2	1	0.1	56	2.0	89	12	5.7	3.3	78						M-76
Hot Spring Rnach HS3	43.382791	-114.932445	64	9.2	1.2	0.1	55	1.2	87	11	5.7	3.2	78						M-76
Sheep HS	43.333898	-115.033219	45	9.9	0.8		49	0.4	57	8.2	3.2	1.9	68						M-76
Wolf HS.	43.33723	-115.0443	50	9.48	1.4	0.019	52	2.3	71	6.5	3	1.9	64	0.08	0.02	0.02	0.02	0.19	TS
Barrons HS1	43.29365	-114.910036	49	8.3	3.4	0.1	106	2.7	211	12	14	13	84				0.11		M-76
Barrons HS2	43.29383333	-114.908667	73	8.2	3.6	0.1	108	3.1	227	13	13	13	84				0.11		M-76
Barron W1	43.29241	-114.91002	38	8.03	17	0.62	156	3.0	183	211	9.5	7.1	52	0.01	0.36	0.36	0.17	0.62	TS
Lee Barron W2	43.30166667	-114.909167	35	8	3	0.1	94	1.6	210	5.8	11	11	83				0.11		M-76
Lee Barron W3	43.30116667	-114.908333	45	8.5	2.2	0.1	99	2.0	215	9.1	12	10	64						M-76
Punkin Corner Area W	43.30216667	-114.906667	35	7.4	3.2	0.1	96	1.3	216	6.4	12	11	78						YM-73
Sun Valley Ranch W	43.317763	-114.90548	26	7.8	3	0.6	86	2.4	193	5.3	10	9.8	78						M-76
Prince Albert HS	43.12966	-115.33841	57.7	9.08	0.3	0.006	55	2.7	105	8.4	2.6	7	110	0.02	0.001	0.01	0.04	0.20	TS
Latty HS	43.11025	-115.31258	65.0	9.25	0.2	0.005	54	1.9	107	11.5	2.7	6.8	103	0.02	0.001	0.02	0.04	0.17	TS
White Arrow HS	43.04867	-114.95150	65	7.5	1.2	0.04	91	1.6	141	15.0	6.6	12	99					0.37	TS
Janns Farm W1	43.02467	-115.00917	38	7.8	3.2	0.2	160	3.7	447	5.4	10	3	86					0.72	YM-73
Dave Archer W	43.02444	-115.00944	43	8.6	1.6	0.1	90	0.8	83	19.0	8.4	19	62					0.28	YM-73
Shannon W	43.05333	-114.91600	47	7	9.8	1.2	100	5.9	278	19.0	8.2	12	92					0.53	YM-73
Leslie Beam W	43.114631	-115.452562	68	8.5	1.5	0.04	87	0.8	125	14.0	4.5	17	86					0.34	YM-73
Bill Davis W	43.09583	-115.40833	62	9.2	0.9	0.1	82	0.8	81	14.0	3.2	16	85					0.28	YM-73
Diamond Laundry W	42.95543	-115.29997	35.0	8.89	1.7	0.18	142	1.3	315	4.3	23.3	13.1	30	0.01	0.007	0.02	0.89	0.44	TS
Johnston Well W	43.00294	-115.19222	39.0	9.26	2.4	0.05	77	1.3	117	10.3	5.9	17	41	0.01	0.002	0.02	0.33	0.26	TS
Laib W	42.94632	-115.49423	32.5	7.64	9.4	0.6	292	9.8	886	10.4	66	1.7	58	0.18	0.09	0.34	2.17	0.92	TS
Charles Boyd W	42.946500	-115.493333	34.0	7.7	9.1	1	320	11	797	6.5	59	2.2	58					0.86	YM-73
Magic West CO W	42.947833	-115.295833	37.5	7.9	2.5	0.2	130	0.9	270	2.5	29	13	46					0.37	YM-73

Eckart Office W	42.69940	-114.91040	24.7	9.47	5.7	0.74	113	4.2	81	90.9	46.5	12.2	52	0.007	0.02	0.01	0.19	0.40	TS
Campbell W1	42.64497	-114.78706	34.5	7.98	23	3.0	58	7.7	144	40.5	23.1	2.2	72		0.16	0.06	0.11	0.25	TS
Campbell W2	42.64432	-114.78294	34.4	7.96	27	3.5	56	8.0	127	31.8	20.0	2.5	69		0.18	0.06	0.11	0.29	TS
Miracle HS W	42.69457	-114.85592	58.4	9.53	0.8	0.001	128	1.9	93	33.7	31.7	22.4	100	0.022	0.001	0.05	0.33	0.42	TS
Driscoll W	42.54479	-114.94855	37.5	8.59	11	0.36	149	1.4	95	188.0	53.3	2.4	46	0.005	0.06	0.19	0.12	0.56	TS
Driscoll S	42.54348	-114.94897	36.2	8.65	11	0.79	147	1.9	98	186.6	53.6	2.4	48	0.016	0.07	0.19	0.11	0.57	TS
Sligers W	42.70399	-114.85699	72.0	9.5	0.9	0.004	136	1.6	212	30.1	50.4	24.2	94	0.074	0.001	0.05	0.50	0.49	TS
Banbury HS W	42.68841	-114.82680	58.8	9	0.9	0.001	97	1.6	249	23.5	16.9	11.4	103	0.014	0.001	0.035	0.22	0.33	TS
Banbury HS	42.68841	-114.82680	58.5	9	1	0.001	95	1.6	168	23.5	16.8	11.4	103	0.015	0.001	0.034	0.22	0.33	TS
Leo Ray Hill W	42.66778	-114.82673	35.0	8.69	5.9	0.19	62	3.4	140	31.3	14.0	3.4	54	0.002	0.010	0.060	0.13	0.23	TS
Leo Ray Road W	42.66851	-114.82436	35.5	8.41	7.6	0.45	56	4.1	139	24.8	11.7	3.4	54	0.011	0.018	0.060	0.13	0.22	TS
Kanaka Rapids W	42.65772	-114.79054	30.1	7.98	18	1.86	50	6.7	120	29.4	16.2	2.7	68	0.020	0.118	0.057	0.14	0.25	TS
Hensley W	42.70501	-114.85701	31.8	9.55	1.9	0.01	122	1.6	232	33.1	51.9	24.1	83	0.011	0.007	0.043	0.58	0.43	TS
Unnamed W near Buhl	42.596667	-114.755833	29	7.9	36	5.4	61	10.0	170	61	31	1.9	66			0.070	0.12	0.36	LY-82
Unnamed W N of Balanced Rock	42.598667	-114.945	30	8	26	3.9	35	7.9	120	35	16	1.8	86			0.050	0.06	0.28	LY-82
Unnamed W Melon Valley	42.634333	-114.7775	25	8.1	17	1.1	53	7.5	160	22	14	2.4	87			0.050	0.12	0.29	LY-82
Unnamed W Buhl Wendell	42.637667	-114.753	26	8.3	7.4	0.2	62	5.6	140	21	9.9	4.8	82			0.080	0.14	0.26	LY-82
Kanaka Rapids W4	42.658667	-114.81	32	8.3	10	0.5	62	3.5	150	25	11	2.9	51			0.050	0.11	0.24	LY-82
Kanaka Rapids W 3	42.660500	-114.815	31.5	8.6	7.5	0.3	63	2.8	120	26	11	3.2	51			0.050	0.12	0.23	LY-82
Kanaka Rapids W1	42.661833	-114.811333	33	8.4	11	0.5	61	3.9	150	24	11	3.1	53			0.060	0.11	0.25	LY-82
Kanaka Rapids W2	42.661833	-114.8145	32	8.4	8	0.2	62	2.8	140	26	11	3.1	53			0.050	0.11	0.24	LY-82
Unnamed W3 Briggs Creek	42.667167	-114.816667	35	8.3	7.8	0.3	63	4.0	140	22	13	3.6	54			0.060	0.10	0.24	LY-82
Unnamed W2 Briggs Creek	42.670000	-114.825	34	8.7	5.4	0.2	66	2.9	110	30	13	3.7	56			0.050	0.12	0.24	LY-82
Unnamed W1 Briggs Creek	42.675167	-114.825	42.5	9.2	1.3	0.1	93	1.7	89	27	24	12	76			0.030	0.21	0.30	LY-82
Near Banbury Natatorium W5	42.682667	-114.8285	30	9.3	0.9	0.1	97	1.6	85	28	20	13	64			0.030	0.21	0.29	LY-82
Near Banbury Natatorium W2	42.683667	-114.833833	42.5	9.3	1.3	0.1	90	1.7	85	28	14	9.4	67			0.040	0.17	0.27	LY-82
Near Banbury Natatorium W4	42.686000	-114.826333	44.5	9.4	3.3	0.1	100	1.8	83	27	22	12	88			0.04	0.23	0.32	LY-82
Near Banbury Natatorium W3	42.686333	-114.825333	42	9.2	3.7	0.2	100	2.1	88	27	23	13	94			0.03	0.23	0.33	LY-82
Near Banbury Natatorium W1	42.688000	-114.831167	45.5	9.1	0.9	0.1	100	1.8	100	29	30	26	86			0.04	0.23	0.34	LY-82

Banbury Natatorium W	42.688500	-114.825833	59	9.3	1.1	0.1	110	1.6	78	30	23	15	88			0.04	0.26	0.34	LY-82
Harry Huttanus W2	42.688500	-114.825833	59	9	1.1	0.1	100	1.5	90	27	25	14	100			0.04	0.23	0.34	LY-82
Hot Sulphur Miracle HS	42.692000	-114.859333	57	9.4	0.9	0.1	130	1.5	59	34	34	21	86			0.04	0.34	0.38	LY-82
Unnamed W3 near Salmon Falls Creek HS	42.700667	-114.850333	62	9.4	0.7	0.1	150	1.4	56	35	48	15	84			0.05	0.49	0.40	LY-82
Unnamed W2 near Salmon Falls Creek HS	42.702500	-114.856667	71.5	9.5	1.5	0.1	140	1.5	56	33	51	27	82			0.06	0.51	0.40	LY-82
Unnamed W1 near Salmon Falls Creek HS	42.703667	-114.8555	72	9.3	0.9	0.1	140	1.2	59	35	51	27	86			0.06	0.47	0.41	LY-82
Salmon Falls Creek HS	42.703667	-114.8555	70.5	9.1	1.2	0.1	140	1.1	70	32	50	27	89			0.06	0.44	0.40	LY-82
CSI W2	42.58318	-114.47496	38.1	8.79	4.5	0.19	95	3.3	127	46.8	26.4	9.6	64	0.001	0.02	0.01	0.15	0.33	TS
CSI W1	42.58050	-114.47089	37.7	8.81	4.0	0.22	86	3.0	154	45.4	25.8	8.6	61	0.003	0.02	0.02	0.19	0.31	TS
Larry Anderson W1	42.59755	-114.40018	43.0	9.16	1.2	0.013	118	2.2	188	36.3	21.1	15.8	69	0.005	0.002	0.03	0.29	0.40	TS
Pristine S	42.61390	-114.48799	43.0	9.18	1.3	0.014	109	2.1	154	30.8	26.7	16.5	72	0.004	0.004	0.01	0.32	0.38	TS
Twin Falls High School W	42.57256	-114.45175	31.0	7.77	40	9	55	4.9	161	76	37.5	2.4	59	0.002	0.19	0.03	0.11	0.39	TS
Anderson Campground W	42.57750	-114.28870	37.0	9.05	1.5	0.02	126	3.1	246	37.4	34.4	23.4	66	0.024	0.004	0.07	0.50	0.42	TS
Unnamed W	42.410000	-114.513333	37.0	7.30	37	9.9	46	11	250	20	5.8	2.2	28			0.07	0.14	0.28	M-80
Cedar Hill W	42.415333	-114.3015	38.0	7.6	18	2.0	16	6.0	95	9.3	8	0.6	67					0.18	YM-73
Theodore Sturgill W	42.417500	-114.106	32.0	7.5	43	8.9	11	7.4	186	13	5	0.7	28					0.21	R-70
Sam High & Sons W	42.417667	-114.228833	33.0	6.6	27	3.9	17	8.6	118	12	15	0.3	63					0.21	M-1980
Nat-Soo-Pah HS	42.345833	-114.508	36.0	7.6	34	14.0	43	11.0	266	18	8	1.9	19					0.28	YM-73
Murphy HS	42.025333	-115.361667	54.5	8.5	6	0.1	30	2.1	56	4.7	2	3.6	120			0.03	0.03	0.20	YL-82
Unnamed W NE of Mosquito Lake Butte	42.245000	-115.375	26.5	7.9	31	10.0	30	5.4	140	32	19	1.0	71			0.02	0.07	0.28	YL-82
Wybenga Dairy	42.48216	-113.97341	33.9	7.45	25	1.1	21	8.7	115	16	13.1	0.7	69	0.002	0.21	0.01	0.05	0.18	TS
Unnamed W west of Lower Goose River	42.164833	-113.983833	43.0	8.00	14	1.1	44	9.6	144	15	7.0	1.3	47					0.21	TS
Basin Cemetery W	42.22333	-113.79167	30.7	7.85	18	2.4	58	2.0	122	21	47.4	3.6	40	0.001	0.17	0.008	0.06	0.28	TS
Oakley HS	42.17334	-113.86163	46.9	9.32	2.2	0.02	86	2.2	107	21	52.6	7.6	79	0.02	0.05	0.04	0.05	0.32	TS

References

- GeothermEx, Inc.: Independent technical report: Resource evaluation of the Newdale geothermal prospect, Madison and Fremont Counties, Idaho, USA. Geothermix, Inc., Richmond, California, USA, February 10, 2010, p. 101, (2010).
- Lewis, R.E. and Young, H.W. (1982) Geothermal resources in the Banbury Hot Springs Area, Twin Falls County, Idaho. USGS Water-Supply Paper 2186, p. 31.
- Mitchell, J.C., Johnson, L.L, and Anderson, J.E. (1980) Geothermal Investigations in Idaho – Part 9: Potential for direct heat applications of geothermal resources. Idaho Department of Water Resources, *Water Information Bulletin* **30**.
- NWIS (2016). USGS National Water Information System, <http://waterdata.usgs.gov/nwis>.
- Ralston, D.R., Arrigo, J.L., Baglio, J.V. Jr., Coleman, L.M., Souder, K., Mayo, A.L. (1981) Geothermal evaluation of the thrust area zone in southeastern Idaho, Idaho Water and Energy Research Institute, University of Idaho.
- Ross, S.H.: Geothermal potential of Idaho. *Geothermics Special Issue* **2**, (1970), 975-1008.
- Wood, W.W. and Low, W.H. (1988) Solute geochemistry of the Snake River Plain aquifer, Idaho and eastern Oregon. USGS Professional Paper 1408-D, p. 91.
- Young, H.W. and Lewis, R.E. (1982) Hydrology and geochemistry of thermal groundwater in southwestern Idaho and north-central Nevada. Geological Survey Professional Paper 1044-J, USGS, p. 26.
- Young, H. W., & Mitchell, J. C. (1973). Geothermal investigations in Idaho. Part 1. Geochemistry and geologic setting of selected thermal waters. *Idaho Dept. of Water Admin., Water Inj Bul*, 30, 24.

Appendix C. Water isotope data for thermal features in and around the Eastern
Snake River Plain (ESRP)

Appendix C. Water isotope data for thermal features in and around the Eastern Snake River Plain (ESRP)

Sampling Features	$\delta^{18}\text{O}$ H ₂ O	δD H ₂ O	d-excess (‰)	$\text{d}^{34}\text{S}_{\text{SO}_4}$ (‰)	$\delta^{18}\text{O}$ SO ₄	T $\delta^{18}\text{O}_{\text{SO}_4\text{-H}_2\text{O}}$ (°C)	DIC (mM)	$\delta^{13}\text{C}_{\text{DIC}}$ (‰)	Dissolved CH ₄ (uM)	Gas CH ₄ (ppm)	$\delta^{13}\text{C}_{\text{CH}_4}$ (‰)	$\delta\text{D}_{\text{CH}_4}$ (‰)
Lidy HS1	-18.2	-140	6.0	3.8	-3.4	127	5.4	-1.5	2.6		-19.7	-29
Sturm W	-18.6	-140	8.7				1.6	-11.6				
Schwendiman W	-19.1	-144	9.3		0.5	87	2.2	-6.5	BD			
Green Canyon HS	-18.8	-140	10.2	22.6	11.6	29	4.2	-2.8	0.4		-16.1	
Heise HS	-17.6	-139	1.9	20.3	5.4	65	21.4	3.7				
Greenhouse W	-18.4	-144	4.0	14.4	0.1	95	9.4	-3.5	BD			
Condie HS	-18.6	-150	-1.4	18.2	-0.9	102	9.9	-2.1	1.4		3.6	-9
Condie HS ^{GD}										1282	3.7	27
Milford Sweat HS	-18.3	-141	5.9	15.8	-1.0	105	3.2	-1.6	1.6		-55.5	
Magic HS Landing W Runoff	-16.0	-147	-19.1	21.6	-8.7	233						
Magic HS Landing W	-16.9	-151	-15.3	21.9	-9.8	237	13.1	-0.9				
Magic HS Landing W ^{GD}										3160	-22.0	-203
Elk Creek HS2	-17.7	-145	-3.3	13.1	-3.7	136	1.4	-4.2	6.8		-13.8	-189
Wardrop HS	-18.4	-143	4.6	7.0	-4.2	133	1.0	-7.0	2.8		-12.8	
Wardrop HS ^{GD}										2016	-15.8	-173
Barron W	-17.3	-140	-1.1	-8.3	-15.9	419	2.1	-6.9	2.6		-48.9	
Wolf HS	-18.4	-140	7.3		-		0.6	-9.1				
Wolf HS ^{GD}										491	-51.0	
Prince Albert HS	-18.5	-143	5.0	8.3	-6.1	154	0.9	-8.6	0.5		-23.7	
Diamond Laundry W	-18.5	-144	3.6								-54.9	-186
Laib W	-16.5	-128	3.7								-53.1	-168
Eckart Office W	-18.3	-145	0.9	5.5	-2.2	115	1.9	-3.1	BD			
Campbell W1	-17.0	-134	2.1	6.2	-3.4	140	3.7	-7.5	BD			
Campbell W2	-17.2	-133	4.3	6.3	-3.6	140	3.7	-7.2	BD			
Miracle HS W	-18.0	-142	2.6	6.6	-4.2	137	1.5	-4.6	2.2		-44.0	-195
Driscoll S	-17.0	-134	2.1	5.7	-4.8	156	2.9	-11.2	BD			

Banbury HS W	-17.5	-137	3.2	6.0	-5.6	159	1.9	-5.9	1.7		-51.3	
Banbury HS	-17.5	-137	3.0	4.7	-5.0	152				2140	-50.5	-242
Sligers W	-17.8	-139	3.6	11.6	-1.7	115	1.2	-4.2	2.2		-47.6	
Leo Ray Road W	-17.2	-133	4.8		0.8	99			BD			
CSI W2	-17.3	-134	4.6	6.6	-3.0	133	2.6	-7.2	BD			
Wybenga Dairy W	-18.0	-135	8.6				1.5	-2.5	BD			
Oakley WS	-18.0	-138	6.1	13.4	-5.9	157			BD			
Richard Austin W1	-18.5	-143	5.4	14.8	0.4	92	1.5	-2.7	12.9		-29.8	-186
Basin Cemetery W	-17.1	-131	6.1		-1.6	121	1.5	-6.2	BD			
Durfee HS	-17.7	-134	7.5	10.9	-0.4	104	1.2	-7.7	BD			
Marsh Creek W	-17.5	-135	5.3	10.2	-4.1	142	1.7	-4.4	2.4		-31.5	
Grush Dairy W							1.6	-2.2	BD			

BD: Below detection

GD: gas duplicate sample

HS: Hot spring

S: Spring

WS: Warm Spring

W: Well

Appendix D. Geothermometric temperature estimates for thermal features in and around the Eastern Snake River Plain (ESRP).

Appendix D. Geothermometric temperature estimates for thermal features in and around the Eastern Snake River Plain (ESRP).

Sampling Features	Field T (C)	RTes ¹	Sulfate -water ¹⁸ O ²	Temperature (°C)									
				Quartz (no steam loss) ³	Chalcedony ²	Quartz ⁴	Silica ⁵	Quartz ⁶	Na-K ⁷	Na-K ⁸	Na-K ⁹	Na-K ⁵	Na-K-Ca-(Mg) ¹⁰
Lidy HS1	56.1	140±8	127	89	58	90	60	75	477	416	410	457	67
Lidy HS2	52.3	138±6		85	54	85	56	71	459	405	401	442	69
Lidy HS W	59.0	140±5		88	57	89	60	74	466	409	405	448	67
Warm Spring WS	29.0	116±7		57	25	57	29	42	343	330	336	338	22
Sturm W	31.4	152±14		113	84	113	84	100	79	125	145	91	50
Ashton WS	41.0	147±5		143	116	143	114	131	114	156	175	125	130
Warm River S1	27.1	104±7		89	58	90	60	75	93	138	157	104	21
Warm River S2	21	111±5		103	74	104	75	90	112	154	173	122	28
Newdale City W	30.0	96±4		118	90	119	90	105	203	229	243	209	81
Wanda Woods W2	27.0	141±7		125	97	125	97	112	210	234	248	216	76
Walz Enterprises W	26.0	131±8		114	86	115	86	101	226	247	260	231	80
Wanda Woods W1	24.0	110±7		115	86	115	87	102	222	244	257	227	78
Wallace Little W	36.0	106±4		122	93	122	93	109	199	225	240	205	79
Henry Harris W	33.0	133±5		114	85	114	85	100	188	217	232	195	77
Donald Trupp W	32.0	115±3		122	94	123	94	109	224	245	258	229	98
Wayne Larson W	22.0	122±3		134	107	134	105	122	217	240	254	223	111
Schwendiman W	28.0	137±4	87	112	83	112	83	98	227	247	261	232	63
Clyde W	32.7	139±5		114	86	115	86	101	205	230	245	211	65
Cinder Block W	26.3	119±3		119	90	119	90	105	184	214	229	191	71
G23	43	75±6		96	65	96	67	82	164	198	215	173	54
G25	51	135±3		138	112	138	110	126	187	216	232	194	73
G41	25	138±3		131	103	131	102	118	212	236	250	218	83
G43	32	136±5		119	90	119	90	106	200	227	241	207	79
G44	32	102±4		104	74	104	75	90	220	242	256	226	60

G50	39	113±3		132	105	132	104	119	217	240	253	222	110
G54	41	118±2		130	102	130	101	117	199	226	241	206	83
G80	22	103±2		115	86	115	86	102	224	245	258	229	74
Remington Produce W	26.0	134±7		114	86	115	86	101	233	252	265	238	26
Dean Swindelman W	32.0	129±12		114	86	115	86	101	291	294	303	291	47
Pauline SW W	21.0	85±5		92	61	92	63	78	271	281	291	273	29
Mark Ricks W	26.0	125±4		102	72	102	73	88	273	282	292	275	43
Lavere Ricks W	21.0	116±8		94	63	94	65	80	255	268	280	258	36
G21	35.56	138±3		118	89	118	89	104	193	221	236	200	69
G22	32.78	104±10		96	66	97	68	82	138	176	194	147	24
G24	26.67	117±6		121	93	121	93	108	317	313	320	315	55
G26	27.22	118±13		88	57	89	60	74	298	300	308	298	42
G28	21.11	122±2		79	48	80	50	65	288	292	302	288	43
G30	27.78	101±10		61	28	61	32	46	205	231	245	211	38
G31	25	92±7		85	54	86	56	71	206	232	246	212	23
G36	27.22	110±8		92	61	92	63	78	198	225	240	205	31
G37	34.44	138±3		114	85	114	85	100	369	348	352	362	55
G38	26.11	98±3		85	54	86	56	71	205	230	245	211	28
G39	25	121±1		89	58	89	60	75	288	293	302	289	40
G56	28.89	102±8		88	57	89	60	74	151	187	205	160	22
G64	20	96±4		85	54	86	57	71	213	237	251	219	40
G65	28.33	89±7		87	56	88	58	73	219	241	255	224	26
G66	29.44	102±7		88	58	89	60	74	151	187	204	160	28
G67	30	134±12		90	59	91	61	76	163	197	214	171	31
G78	27.78	152±5		108	78	108	79	94	209	233	247	215	53
Green Canyon HS	44	94±4	29	75	44	76	47	61	671	521	499	622	12
Heise HS	48.2	88±2	65	84	53	85	56	70	222	243	257	227	86
Hawley WS	16.4	109±11		107	78	108	79	94	367	347	350	360	29
Elkhorn WS	20.2	117±6		108	79	108	79	94	353	337	342	347	30

Comore Loma W6	20.9	136±9		115	86	115	86	101	249	264	276	252	63
Comore Loma W5	27.7	138±11		128	101	129	100	116	258	271	282	261	56
Blackhawk W2	26.8	140±10		127	100	128	99	115	226	247	260	231	65
Blackhawk W1	25.1	140±10		126	99	127	98	114	224	246	259	229	66
Dyer W	21	146±7		117	88	117	88	104	139	177	195	148	37
Anderson W	20	143±7		143	117	143	115	132	241	258	270	245	59
Butte City W	32.5	61±4		84	52	84	55	69	301	302	310	300	58
Greenhouse W	36.3	60±4	95	82	50	82	53	67	332	323	329	328	56
E Butte City W	22.80	49±4		70	38	71	42	56	267	277	288	269	45
W Butte City W	27.00	57±4		80	49	80	51	66	288	293	302	289	57
Birch and 7th St W	28.00	66±8		90	59	90	61	76	339	328	333	335	
Lewis Rothwell W	41.00	80±3		106	77	107	78	93	342	330	335	337	60
Condie HS	50.5	91±6	102	79	47	79	50	64	385	359	361	376	85
Milford Sweat HS	38.1	73±9	105	71	40	72	43	57	275	283	293	276	59
Rush WS1	29.5	103±6		79	48	80	50	65	351	336	341	345	83
Rush WS2	23.2	97±2		83	51	83	54	68	351	336	341	346	80
Magic HS Landing W Runoff	39.1	163±2	233	142	116	142	114	131	143	180	198	152	143
Magic HS Landing W	75.0	151±3	237	139	113	139	111	127	144	181	199	153	149
Elk Creek HS1	50.0	126±2		114	86	115	86	101	57	105	126	69	86
Elk Creek HS2	55.5	124±2	136	115	86	115	86	101	53	102	122	65	85
Wardrop HS	67.5	181±3	133	123	95	123	95	110	48	97	118	60	74
Hot Spring Rnach HS1	60	188±3		126	98	126	97	113	44	93	113	56	75
Hot Spring Rnach HS2	67	194±2		124	96	124	95	111	98	142	162	109	130
Hot Spring Rnach HS3	64	188±1		124	96	124	95	111	67	114	134	78	114

Sheep HS	45	198±11		117	88	117	88	104	17	68	89	30	57
Wolf HS.	50	204±2		114	85	114	85	100	112	154	173	123	141
Barrons HS1	49	103±2		128	100	128	99	115	76	122	143	88	122
Barrons HS2	73	104±6		128	100	128	99	115	84	129	149	95	127
Barron W1	38	79±0	419	103	74	104	75	90	59	107	127	71	68
Lee Barron W2	35	104±4		127	99	127	99	114	53	101	122	65	79
Lee Barron W3	45	103±5		114	85	114	85	100	62	110	130	74	115
Punkin Corner Area W	35	105±6		122	94	123	94	109	43	92	113	55	71
Sun Valley Ranch W	26	108±4		124	96	124	95	111	82	128	148	93	90
Prince Albert HS	57.7	193±8	154	143	117	143	115	131	121	162	180	131	161
Latty HS	65.0	197±5		139	112	139	111	127	97	141	161	108	147
White Arrow HS	65	177±6		136	110	137	108	124	55	103	123	66	112
Janns Farm W1	38	88±5		129	101	129	101	116	70	117	137	82	124
Dave Archer W	43	101±2		112	83	112	84	99	21	71	93	33	70
Shannon W	47	137±10		133	105	133	104	120	137	176	193	147	110
Leslie Beam W	68	102±3		129	101	129	101	116	23	73	94	35	71
Bill Davis W	62	122±1		128	101	128	100	116	25	75	96	37	81
Diamond Laundry W	35.0	70±2		80	48	80	51	65	22	72	93	34	90
Johnston Well W	39.0	67±4		93	62	93	64	79	51	99	120	63	74
Laib W	32.5	83±1		109	79	109	80	95	94	139	158	105	138
Charles Boyd W	34.0	85±1		109	79	109	80	95	96	140	159	107	123
Magic West CO W	37.5	74±3		98	68	98	69	84	11	61	82	23	68
Eckart Office W	24.7	127±9	115	104	74	104	75	90	101	144	163	111	107
Campbell W1	34.5	137±6	140	120	91	120	91	106	221	243	257	227	80
Campbell W2	34.4	131±9	140	118	89	118	89	105	231	250	263	235	79
Miracle HS W	58.4	161±3	137	137	110	137	109	125	45	93	114	57	112
Driscoll W	37.5	134±8		98	67	98	69	84	23	73	94	35	53
Driscoll S	36.2	137±8	156	100	70	101	72	86	39	88	110	51	62

Sligers W	72.0	134±2	115	133	106	134	105	121	34	83	104	46	103
Banbury HS W	58.8	159±10	159	139	113	139	111	127	53	101	122	65	114
Banbury HS	58.5	159±9	152	139	112	139	111	127	52	101	121	64	112
Leo Ray Hill W	35.0	121±6		105	76	106	77	92	132	171	189	141	144
Leo Ray Road W	35.5	120±1	99	106	76	106	77	92	156	191	208	164	140
Kanaka Rapids W	30.1	112±7		117	88	117	89	104	222	244	257	227	121
Hensley W	31.8	138±17		127	100	127	99	115	40	89	110	52	102
Unnamed W near Buhl	29.0	130±11		115	86	115	87	102	248	263	275	251	80
Unnamed W N of Balanced Rock	30.0	163±6		129	101	129	101	116	296	298	307	296	102
Unnamed W Melon Valley	25.0	129±9		130	102	130	101	117	229	249	262	233	148
Unnamed W Buhl Wendell	26.0	127±3		126	99	127	98	114	177	208	224	185	165
Kanaka Rapids W4	32.5	102±2		103	73	103	74	89	133	172	190	143	136
Kanaka Rapids W 3	31.5	106±1		103	73	103	74	89	114	156	175	125	133
Kanaka Rapids W1	33.0	103±3		105	75	105	76	91	144	181	199	153	140
Kanaka Rapids W2	32.0	107±5		105	75	105	76	91	116	157	176	126	133
Unnamed W3 Briggs Creek	35.0	109±3		105	76	106	77	92	144	181	198	153	146
Unnamed W2 Briggs Creek	34.0	116±4		107	78	108	79	94	113	155	174	124	136
Unnamed W1 Briggs Creek	42.5	121±2		122	94	123	94	109	57	105	125	68	114
Near Banbury Natatorium W5	30.0	145±6		114	85	114	85	100	51	100	120	63	113
Near Banbury Natatorium W2	42.5	139±7		116	87	116	87	103	59	106	127	70	114
Near Banbury Natatorium W4	44.5	139±7		130	103	130	102	118	56	104	125	68	108
Near Banbury Natatorium W3	42.0	142±8		134	107	134	105	122	65	112	132	76	113
Near Banbury Natatorium W1	45.5	157±6		129	101	129	101	116	56	104	125	68	116
Banbury Natatorium W	59.0	148±6		130	103	130	102	118	45	93	114	57	108
Harry Huttanus W2	59.0	155±8		137	110	137	109	125	46	95	116	58	108
Hot Sulphur Miracle HS	57.0	150±4		129	101	129	101	116	33	83	104	45	103

Unnamed W3 near Salmon Falls Creek HS	62.0	152±2		128	100	128	99	115	23	73	95	35	98
Unnamed W2 near Salmon Falls Creek HS	71.5	135±5		126	99	127	98	114	30	79	101	42	98
Unnamed W1 near Salmon Falls Creek HS	72.0	150±3		129	101	129	101	116	20	70	91	32	93
Salmon Falls Creek HS	70.5	148±5		131	103	131	102	118	16	66	87	28	92
CSI W2	38.1	136±11	133	114	85	114	85	101	96	140	160	107	132
CSI W1	37.7	134±12		111	82	112	83	98	96	140	160	107	131
Larry Anderson W1	43.0	108±3		118	89	118	89	104	58	105	126	69	118
Pristine S	43.0	130±11		119	91	120	91	106	60	108	128	72	118
Twin Falls High School W	31.0	115±4		110	80	110	81	96	175	207	223	183	56
Anderson Campground W	37.0	123±3		115	86	116	87	102	74	120	141	85	129
Unnamed W	37.0	98±1		77	45	77	48	62	306	305	313	305	73
Cedar Hill W	38.0	122±5		116	87	116	87	103	394	364	366	384	65
Theodore Sturgill W	32.0	90±4		77	45	77	48	62	559	462	450	528	50
Sam High & Sons W	33.0	127±5		113	84	113	84	100	469	411	406	451	68
Nat-Soo-Pah HS	36.0	75±5		62	29	62	33	47	318	313	320	315	54
Murphy HS	54.5	117±4		148	122	148	120	136	152	188	205	161	62
Unnamed W NE of Mosquito Lake Butte	26.5	88±3		119	90	119	90	106	261	273	284	264	57
Wybenga Dairy W	33.9	132±3		118	89	118	89	105	419	380	379	406	72
Unnamed W west of Lower Goose River	43.0	84±5		99	69	99	70	85	291	294	303	291	155
Basin Cemetery W	30.7	73±8	121	92	61	92	63	78	95	140	159	106	45
Oakley HS	46.9	130±7	157	125	97	125	96	112	76	122	143	88	122
Richard Austin Well 1	45.7	85±2	92	79	48	80	50	65	55	103	124	67	111
Morris Mitchell W1	46.0	82±2		77	45	77	48	62	51	99	120	63	109

Harold Ward W	38.0	101±6		96	66	96	67	82	114	156	175	124	46
Durfee HS	44.9	138±8	104	117	88	117	88	103	105	148	167	116	80
Marsh Creek W	59.6	125±10	142	113	83	113	84	99	106	149	168	116	89
SKAGGS Ranch W1	60.0	141±11		111	81	111	82	97	98	142	161	109	88
Skaggs Ranch W	33.3	96±11		96	66	96	67	82	207	232	246	213	51
Critchfield Land & Cattle W	35.0			99	69	99	70	85	209	234	248	215	51
SKAGGS Ranch W2	32.0			98	68	98	69	84	200	227	241	207	48
Ruby Farms W	39.0	125±12		110	80	110	81	96	66	114	134	78	60
Indian HS	32.7	70±11		64	32	64	36	49	178	209	225	186	75
Robert Brown W2	25	69±2		93	62	93	64	79	52	101	121	64	
Robert Brown W1	41			63	31	64	35	49	227	248	261	232	52
Fort Hall Thermal W	21.1			102	72	102	73	88	309	308	315	308	54
Yandell WS	22.2	59±9		57	24	56	28	41	342	330	335	337	27
Alkali Flats WS	34.0	90±4		62	29	62	33	47	770	568	538	703	62
Quidop S1	21.0	75±7		55	23	55	27	40	629	499	481	586	65
Quidop S2	38.1	81±5		63	31	63	34	48	730	550	523	670	60
Sampling Features													
HS: Hot spring S: Spring WS: Warm Spring W: Well				1: Palmer et al. (2014); Mattson et al. (2015). 2: Fowler et al. (2013). 3: Fournier (1977). 4: Fournier and Potter II (1982). 5: Arnorsson et al. (1983) .				6: Arnorsson (2000). 7: Truesdell (1976). 8: Fournier (1979). 9: Giggenbach (1988). 10: Fournier and Truesdell (1973); Fournier and Potter II (1979).					

References

- Arnorsson, S., Gunnlaugsson, E., & Svavarsson, H. (1983). The chemistry of geothermal waters in Iceland. III. Chemical geothermometry in geothermal investigations. *Geochim. Cosmochim. Acta*, 47(3), 567-577.
- Arnorsson, S. (2000). The quartz-and Na/K geothermometers. I. New thermodynamic calibration. In *Proceedings of the World Geothermal Congress* (pp. 929-934).
- Fournier, R.O. and Truesdell, A.H. (1973) An empirical Na-K-Ca geothermometer for natural waters. *Geochim. Cosmochim. Acta*, **37**, 1255-1275.
- Fournier, R.O. (1977) Chemical geothermometers and mixing models for geothermal systems. *Geothermics*, **5**, 41-50.
- Fournier, R.O. (1979) A revised equation for the Na/K geothermometer. *GRC Transactions*, **3**, , 221-224.
- Fournier, R.O. and Potter II, R.W. (1979). Magnesium correction to the Na-K-Ca chemical geothermometer. *Geochim. Cosmochim. Acta*, **43**, 1543-1550.
- Fournier, R. O., & Potter II, R. W. (1982). Revised and expanded silica (quartz) geothermometer. *GRC Bulletin* 11(10), 3-12.
- Fowler, A. P. G., Hackett, L. B., & Klein, C. W. (2013). Reformulation and Performance Evaluation of the Sulfate-Water Oxygen Isotope Geothermometer. In *In: GRC Transactions. GRC Annual Meeting (Vol. 9, p. 31)*.
- Giggenbach, W.F.: Geothermal solute equilibria. Derivation of Na-K-Mg-Ca geoindicators. *Geochim. Cosmochim. Acta*, **52**, (1988), 2749-2765.
- Mattson, E.D., Smith, R.W., Neupane, G., Palmer, C.D., Fujita, Y., McLing, T.L., Reed, D.W., Cooper, D.C., and Thompson, V.S.: Improved geothermometry through multivariate reaction-path modeling and evaluation of geomicrobiological influences on geochemical temperature indicators: Final Report No. INL/EXT-14-33959, Idaho National Laboratory (INL), Idaho Falls, Idaho, (2015).
- Palmer, C.D., Ohly, S.R., Smith, R.W., Neupane, G., McLing, T., Mattson, E.: Mineral selection for multicomponent equilibrium geothermometry. *GRC Transactions*, **38**, (2014), 453-459.
- Truesdell, A. H., 1976, Summary of Section III Geochemical Techniques in Exploration, *Proceedings of the Second United Nations Symposium on the Development and Use of Geothermal Resources, San Francisco 1975*, v. 1, p. liii - lxxix .

Appendix E. Descriptions of geothermal prospects in and around the Eastern Snake
River Plain (ESRP)

Prospects

1.	Lidy Hot Springs	4
1.1	General	4
1.2	Geologic setting	4
1.3	Water chemistry	5
1.4	Geothermometric results	5
2.	Ashton Hot Spring	6
2.1	General	6
2.2	Geologic setting	6
2.3	Water chemistry	7
2.4	Geothermometric results	7
3.	Newdale area	8
3.1	General	8
3.2	Geologic setting	8
3.2.1	Water chemistry	10
3.2.2	Geothermometric results	14
4.	Green Canyon Hot Spring	16
4.1	General	16
4.2	Geologic setting	16
4.3	Water chemistry	17
4.4	Geothermometric results	17
5.	Heise Hot Spring	18
5.1	General	18
5.2	Geologic setting	18
5.3	Water chemistry	19
5.4	Geothermometric results	19
6.	East Idaho Falls area	20
6.1	General	20
6.2	Geologic setting	20
6.3	Water chemistry	21
6.4	Geothermometric results	21
7.	Butte City area	22
7.1	General	22
7.2	Geologic setting	23
7.3	Water chemistry	23
7.4	Geothermometric results	23

8.	Condie Hot Spring	25
8.1	General	25
8.2	Geologic setting	25
8.3	Water chemistry	26
8.4	Geothermometric results	26
9.	Magic Hot Spring	27
9.1	General	27
9.2	Geologic setting	27
9.3	Water chemistry	28
9.4	Geothermometric results	28
10.	Elk Creek Hot Springs	29
10.1	General	29
10.2	Geologic setting	29
10.3	Water chemistry	30
10.4	Geothermometric results	30
11.	Camas Prairie area	30
11.1	General	30
11.2	Geologic setting	31
11.3	Water chemistry	32
11.4	Geothermometric results	32
12.	South Mount Bennett Hills	33
12.1	General	33
12.2	Geologic setting	33
12.3	Water chemistry	34
12.4	Geothermometric results	35
13.	Glenns Ferry area	36
14.	Banbury Hot Springs-Twin Falls area	36
15.	Cedar Hill area	37
16.	Murphy Hot Spring	37
17.	Oakley Hot Spring	37
18.	Durfee Hot Spring	38
19.	Marsh Creek area	38
20.	Wybenga Dairy area	39
21.	Indian Hot Spring	39

22.	Tyhee area	40
23.	Quidop-Yandell Warm Springs	40
	References.....	41

1. Lidy Hot Springs

1.1 General

The Lidy Hot Springs (LHS) area (Figure 1) is located at the southeastern end of the Beaverhead Mountains on the northwestern margins of the ESRP in Clark County in Idaho. The area is about 27 km west from Dubois, Idaho along route 22. From the early 20th century, the area was gradually developed into a commercial recreation site that provided services such as swimming, soaking, dancing, dining, and lodging to public. However, with the transfer of ownership in the early 1960s, the site ceased to offer those recreational services, and started a travertine mining activity.

Two hot springs in the area are issuing thermal water (52-56 °C). Similarly, in the vicinity of the LHS, there are other springs [e.g., Warm Spring (29 °C)] issuing warmer to cooler waters.

1.2 Geologic setting

Rocks underlying the LHS area consist of young volcanics and older meta-sedimentary rocks (Bond et al., 1978; Link, 2002a). The younger rocks (Upper Miocene and Pliocene) consist of fluvial and lacustrine deposits, felsic volcanic rocks, rhyolite flows, tuffs, ignimbrites. Although massive ongoing travertine deposition is lacking, the area may have had greater hydrothermal activities in the past when the travertine currently being mined was deposited. Thick sequences of Paleozoic sedimentary rocks (Pz) underlie the Tertiary rock types, and likely constitute the geothermal reservoir in the area (Figure E1).

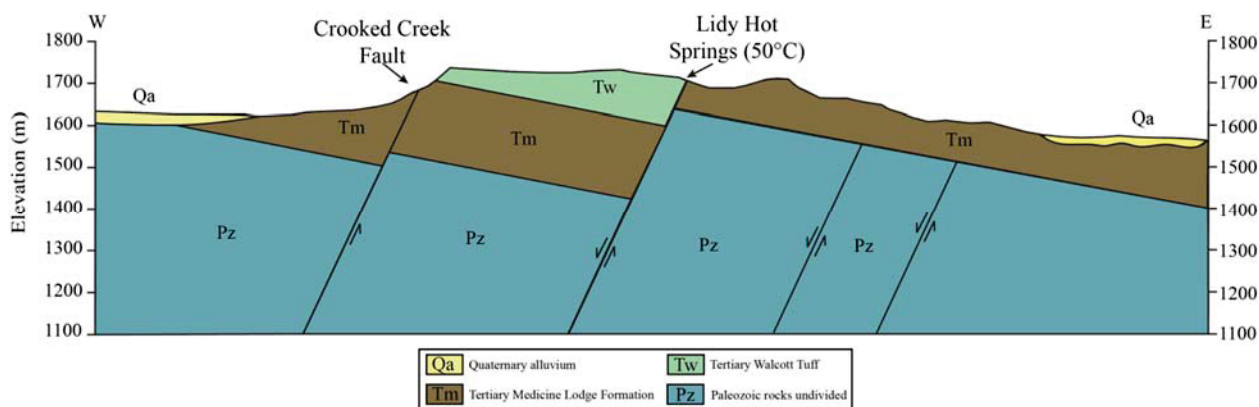


Figure E1. Geologic cross-section through Lidy Hot Springs area.

Regionally, the area represents the northwestward continuation of the Idaho-Wyoming thrust belt associated with Sevier orogeny. However, the physical continuation of this region to the Idaho-Wyoming thrust belt located southeast of the ESRP has been obscured by the middle Miocene to Recent volcanic activities associated with Yellowstone hot spot. Nevertheless, several extensional Tertiary-Quaternary normal faults truncate thrusts and folds of the Sevier orogeny (similar to that traced in Idaho-Wyoming thrust belts in southeastern Idaho and west-central Wyoming) have been mapped in the Beaverhead Mountains and other mountain ranges in the surrounding areas (Skipp, 1985).

Locally, the area has been intersected by numerous westward dipping imbricate faults that are believed to plunge into the Tertiary-Quaternary volcanic rocks of the ESRP to the southeast (Ross, 1970). Overlapping faults are reported to be one of the major geothermal settings in the Basin and Range Province (Faulds et al., 2011). As with the numerous geothermal sites of the Basin and Range Province, the hydrothermal activity in the area is also controlled by the fault-bound circulation of deep water.

1.3 Water chemistry

The two hot springs in the LHS area that were sampled are near-neutral (pH) water containing Ca, bicarbonate, and sulfate as the dominant ions (Appendix B). Water samples from these two features in the LHS area have been sampled multiple times since early 1970s for chemical analysis. The available data indicate that the composition of springs' water have remained constant over the last several decades. The higher content of Ca in water may have been related to carbonate-rich Paleozoic reservoir rocks in the area. The chemical analyses of water samples also show a significant amount of Mg. The total dissolved solid (TDS) level in these waters range from 360 to 400 mg/L.

A water sample from another spring (Warm Spring) in the area has lower TDS values. Specifically, the concentrations of $\text{SiO}_2(\text{aq})$, K, Na, in Warm Spring water are less than the concentrations in the samples from LHS. However, the Mg content is higher in Warm Spring water. When plotted on a Giggenbach plot (Giggenbach, 1988), water samples from LHS area plot in the immature zone (Figure E2). The immaturity of thermal water emerging from LHS area is likely to be related with higher concentration of Mg. The higher Mg content is believed to be the result of either mixing of cooler water groundwater or re-equilibration of the water at low temperature (or, that the reservoir temperature is low).

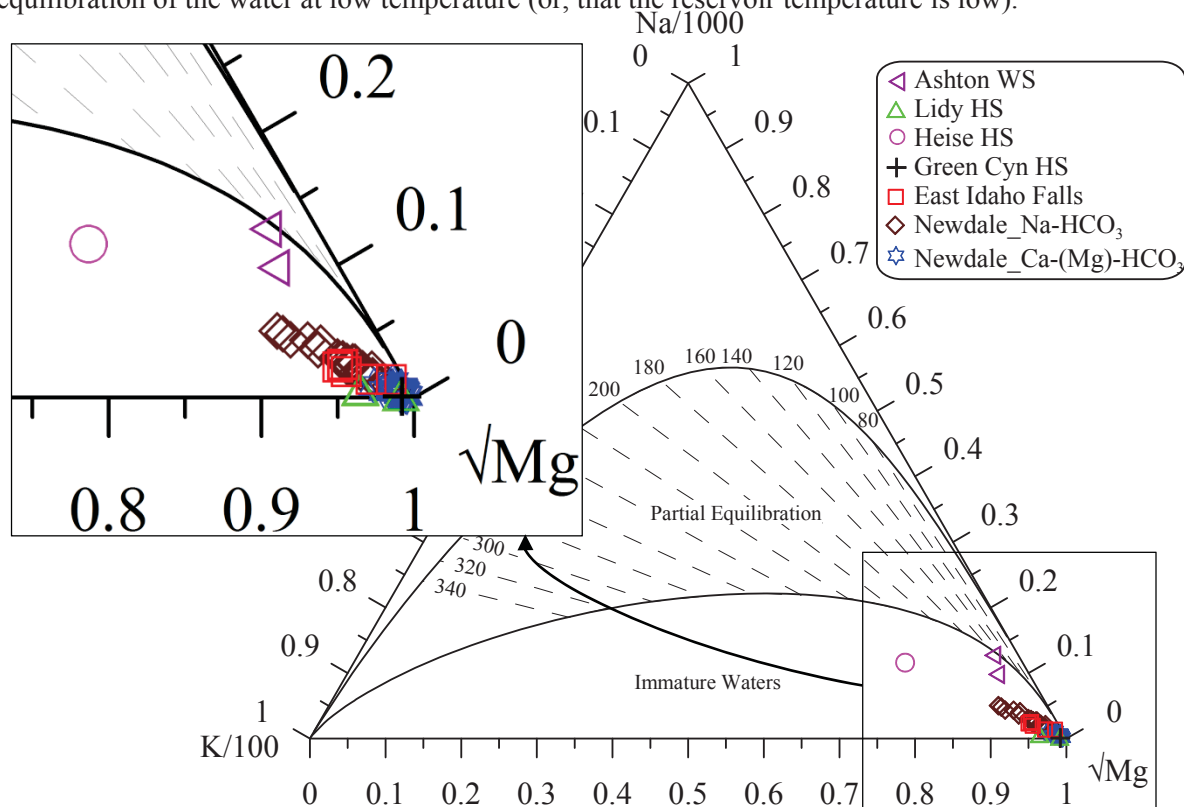


Figure E2. Northeastern ESRP water samples plotted on Giggenbach diagram.

1.4 Geothermometric results

Reservoir temperatures calculated for the LHS samples are given in Appendix D. Quartz (no steam loss) and chalcedony (Fournier, 1977) geothermometers resulted in 85-89 °C and 54-58 °C, respectively. Similarly, Mg-corrected Na-K-Ca reservoir temperatures for the area range from 60 to 67 °C. The reservoir temperature estimated for the Warm Spring sample is cooler than the temperatures calculated for the LHS samples.

The RTest (Palmer et al., 2014; Mattson et al., 2015) estimated reservoir temperatures for the LHS reservoir is about 140 °C (Appendix D). RTest modeling result shows that the LHS water may contain up to 60% cooler water and 40% deeper thermal water. Similarly, no-steam loss silica-enthalpy mixing model with quartz solubility curve yields a reservoir temperature of about 130°C. However, silica-enthalpy mixing model with chalcedony solubility curve yields a rather cooler temperature (about 60 °C). A sulfate-water oxygen isotope temperature of 127 °C calculated for one of the samples from the LHS are (Appendix D) is also in the same range as the RTest temperatures.

2. Ashton Hot Spring

2.1 General

The Ashton Hot Spring (AHS) and associated geothermal area (Figure 1) is located on the northern side of Ashton in Fremont County in Idaho. The existence of AHS with a water temperature 41 °C was previously reported by Mitchell et al. (1980). A 1220 m deep geothermal exploratory well (Sturm Well-1) was drilled about 2 km NE from the AHS in 1979 (Occidental Geothermal Inc., 1979). Driller's records indicate a bottom-hole temperature of about 63 °C. In March 2014, however, we recorded a water temperature of 31 °C. The lower temperature of the produced water may indicate that the well is currently tapping water from the upper section of the well. The Sturm well water is now used for space heating.

2.2 Geologic setting

The AHS is the one of the few hot spring that is located within the ESRP proper. A geologic map of the area shows thin layers of Quaternary sediments overlying volcanic rocks (Link, 2002b). Borehole records from the area reveal the presence of thick sequences of flood basalts and felsic volcanics. Specifically, for Sturm Well-1, the Quaternary sediments near the surface are underlain by layers of flood basalts (up to a depth of 82 m), felsic volcanics (82-808 m), and again flood basalts (808 -1220+ m) with depth (Occidental Geothermal Inc., 1979) (Figure E3).

It is not clear whether the AHS area is located in the inter-caldera zone or along the caldera ring fracture (Pierce and Morgan, 1992; Anders et al., 2014). This area is located outside, about 9 km south, of the overlapping Island Park area calderas [2.1 Ma Big Bend caldera and 1.3 Ma Henry's Fork Caldera (Christiansen, 2001)]. The gravimetrically and geologically inferred Rexburg caldera complex (RCC) zone (Heise volcanic field of Anders et al., 2014) has been mapped to the south of Ashton (Prostka and Embree, 1978; Mabey, 1978). However, some researchers (e.g., Malde, 1991; Blackwell et al., 1992; Anders et al., 2014) have mapped the rim of Kilgore caldera (4.61 Ma) passing through Ashton. Collectively, RCC represents the pre-2.1 Ma multiple nested and overlapping calderas to the south and southwest of the Island Park area (Prostka and Embree, 1978; Malde, 1991; Morgan and McIntosh, 2005). If these suggestions are valid, the AHS area may be a surface expression of the highly fractured zone at depth. However, the deeper zone with multiple fractures may have been buried underneath the 1220+ m thick layers of sediments and volcanics (both rhyolitic and basaltic rocks) in the Ashton area. Bond (1978) shows a left-lateral fault that extends from southern side of the Island Park/Henry's Fork caldera rim and ends near the AHS area. Either this fault or some other local fractures in rocks beneath the Quaternary sediments may act as a path for the hot water that emerges as the AHS (Figure E3).

Finally, we could also speculate that the pre-caldera Basin and Range type faults that would have been continued from the eastern side of Big Hole Mountain (or the western side of the Teton Range) to Centennial or Beaverhead range through Ashton and Spencer-High Point [this later segment represents an active rift zone in the ESRP, and Kuntz et al. (1992) suggest that the active rifting zone in the SRP may have been controlled by pre-caldera fault systems], and these fault systems may still provide pathways for deep circulation. Bond et al. (1978) shows a series of discontinuous faults striking NW-SE to the SE and NW of Ashton. However, the lack of seismicity in the area (Christiansen, 2001) makes it unlikely that the continuation (if any) of the pre-caldera fault through Ashton could be contributing to the hydrothermal activities in the area at present.

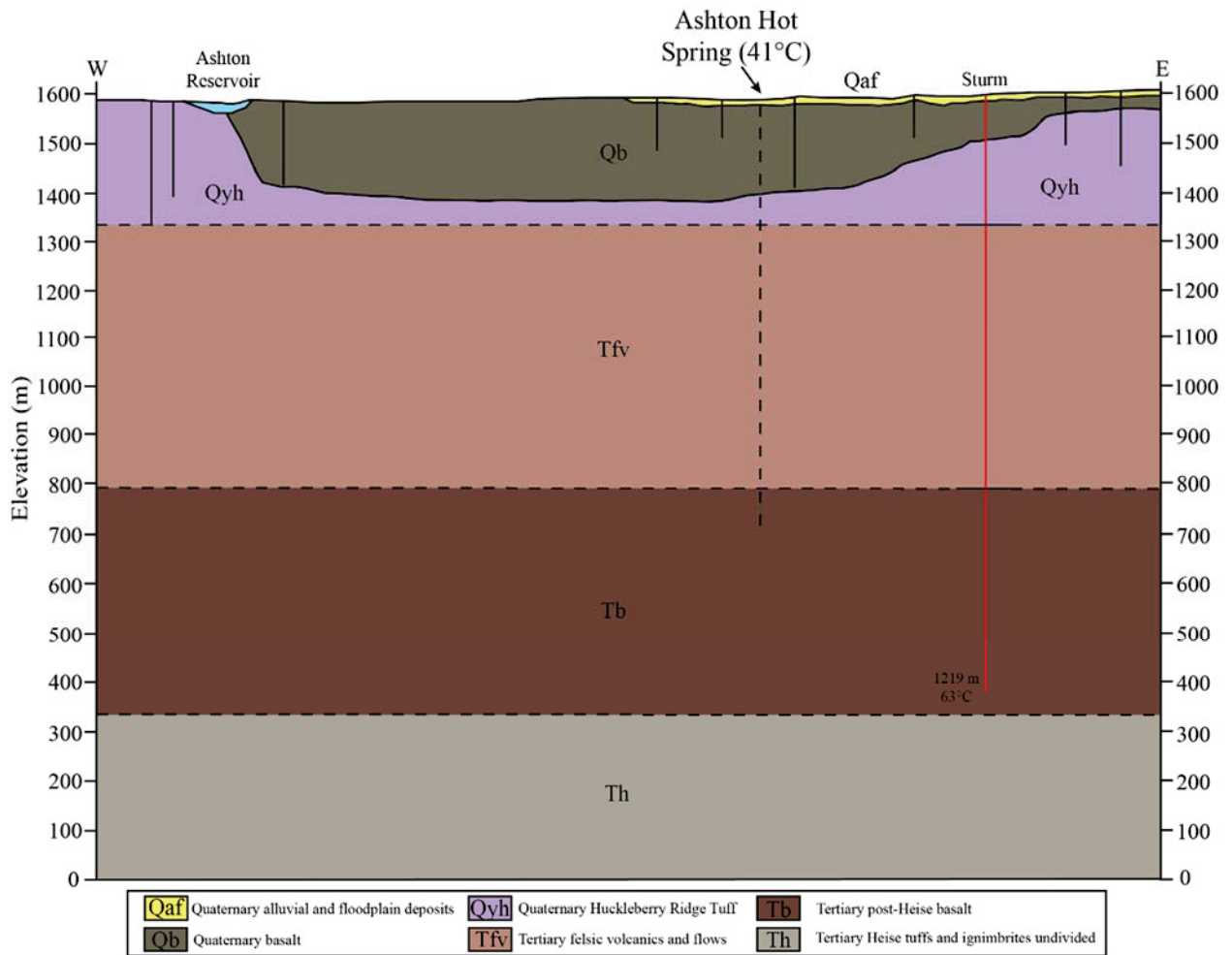


Figure E3. Geologic cross-section through Ashton Hot Spring and Sturm Well near Ashton, Idaho.

2.3 Water chemistry

Both AHS and Sturm Well produce slightly alkaline low TDS water. Relatively, the pH of water from Sturm Well is more alkaline (>1 unit of pH) than water from the neighboring Ashton Warm Spring (Appendix B). The AHS water contains higher concentrations of $\text{SiO}_2(\text{aq})$ and HCO_3^- . The higher concentration of $\text{SiO}_2(\text{aq})$ in hot spring water may indicate an elevated temperature at depth (Mitchell et al., 1980). On the other hand, waters from these two expressions have similar concentrations of Na, SO_4 , Cl, and F. On Giggenbach diagram (Figure E2), both the AHS and SW water samples plot in immature water field.

2.4 Geothermometric results

Quartz and chalcedony geothermometers gave reservoir temperatures of 143 °C and 116 °C for AHS and 113 °C and 84 °C for Sturm Well, respectively (Appendix D). For these two features, Na-K-Ca geothermometer resulted in temperatures of 117 °C and 109 °C, respectively. With the un-optimized (un-reconstructed) AHS composition, all these three traditional geothermometers resulted in slightly higher reservoir temperature than with the un-optimized Sturm Well composition. We applied RTest to both water compositions with the same modeling constraints such as the same mineral assemblage (beidellite, calcite, chalcedony, clinoptilolite, K-feldspar, and paragonite) and optimization parameters. For both water samples, pure water was used during RTest modeling to optimize mass of thermal water. Unlike

the traditional geothermometers, RTest provided similar reservoir temperatures based on the optimized (reconstructed) compositions of water from these two sources. The RTest produced reservoir temperatures for the Sturm well and AHS are 152 ± 14 °C and 147 ± 5 °C, with nearly 70% and 35% of cooler water, respectively. Although the Sturm well was drilled to over 1200 m depth, it may be tapping water from the upper cooler section. According to the owner, the well was originally cased only in the upper sections, and the lower portion of the well might have plugged because of caving. The temperature record (bottom hole temperature and temperature of produced water) over time for the Sturm well also indicates that the lower portion of the well might have caved in long ago. The initial recorded bottom-hole temperature of the well is 63 °C (Occidental Geothermal Inc., 1979). Blackwell et al. (1992) provide a temperature measured during early 1990s for the produced water at 38 °C. During our sampling campaign in 2014, the water was measured at 31 °C. Therefore, it is likely that the Sturm well is currently producing water from a shallower depth that may have higher fraction of cooler water. The sulfate concentrations of samples collected from both of these thermal features were too low for isotope geothermometry.

3. Newdale area

3.1 General

The Newdale geothermal area (Figure E4 and Figure 1) in Madison and Fremont Counties in Idaho represents a blind geothermal system. The geothermal potential of the Newdale area was identified in the late 1970s by several researchers, specifically, with the discovery of relatively higher heat flow (167 mW/m^2) (Brott et al. 1976). Subsequent studies of the area identified a zone called the Newdale thermal anomaly zone (Mabey, 1978; Prostka and Embree, 1978; Mitchel et al., 1980).

Specifically, the area from Newdale town to the NE across the Teton River has been considered as potential area for geothermal energy (Brott et al., 1976, GeothermEx, 2010). During 1979-1981, Union Oil of California (Unocal) drilled several geothermal test wells in the area ranging in depth from 183 m (Newdale No. 79-3) to 1204 m (Madison Geothermal No.1 near Rexburg, ID). The highest recorded temperature in Unocal wells was 87.2 °C (Well # State 2591-07-79-1). Currently, Standard Steam Trust LLC (SST) holds a set of leases for further exploration and development in an area of about 53.4 km^2 around Newdale and defines this area as 'Newdale geothermal energy prospect' (GeothermEx, 2010).

3.2 Geologic setting

A surficial geologic map of this area shows the presence of Quaternary sediments, flood basalts, and felsic volcanic rocks (Bond et al., 1978; Embree et al., 2011). Early Pleistocene flood basalts are mapped around the town of Newdale whereas felsic volcanic rocks of similar ages (Huckleberry Ridge Tuff) are mapped NE from Newdale. In a geologic cross-section, Embree et al. (2011) show the Huckleberry Ridge Tuff lying beneath the Early Pleistocene basalt in Newdale town. Below the Huckleberry Ridge Tuff are the Tertiary sediments intercalated with Tertiary basalt flows (Figure E5). Subsurface lithologic records of numerous wells in the area compiled by Idaho Geological Survey indicate the presence of thick sequences of rhyolites and tuff at greater depths.

Based on geologic, geomorphologic (Prostka and Embree, 1978) and gravity anomaly features (Mabey, 1978), a series of overlapping and intersecting calderas that developed 4.45-6.62 Ma (Morgan and McIntosh, 2005) have been inferred as the RCC around Rexburg, Teton, Sugar City, and Newdale areas that possibly extend further north to Ashton (Malde, 1991; Blackwell et al., 1992; Anders et al., 2014). Specifically, the Newdale geothermal area lies along the three inferred caldera margins (Prostka and Embree, 1978). Recently, Anders et al. (2014) mapped the Blacktail Creek Tuff caldera (a caldera unit of RCC) rim that passes through the Newdale geothermal area along the Teton River.

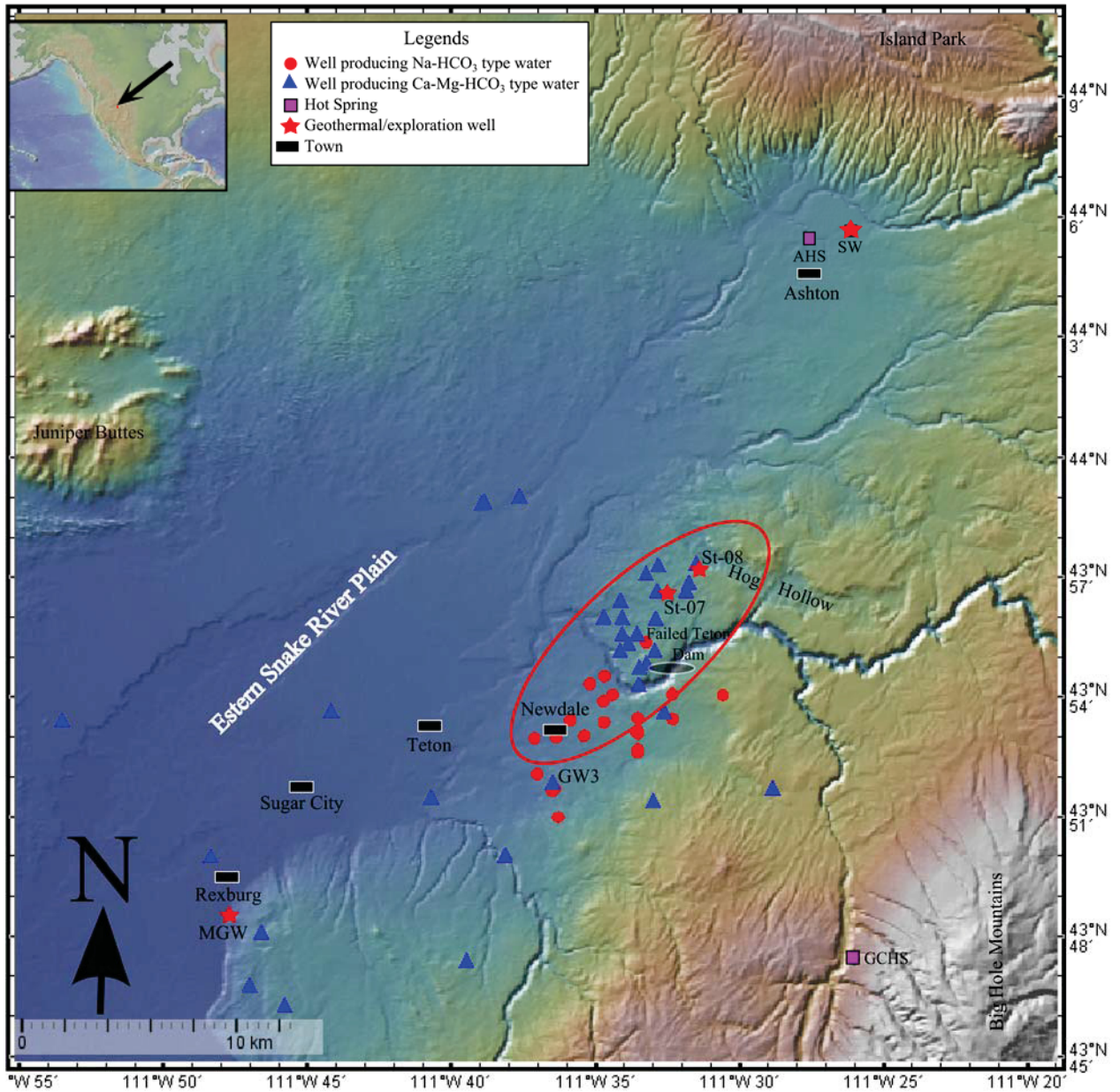


Figure E4. Location of sampling features around Newdale geothermal prospect. Red circles and blue triangles are two groups water with distinct chemistry and mixing trends. Ashton hot spring (AHS), Sturm well (SW), and Green Canyon Hot Spring (GCHS) are not included in the Newdale area samples. Wells St-08 and St-07 are two Unocal thermal wells in the prospect.

It is likely that this area has a highly fractured zone at depth that is buried beneath thick sequences of post-RCC volcanic and sedimentary rocks. Two NE trending parallel faults are also mapped in the area (Embree et al., 2011). Specifically, the Teton Dam Fault has been traced along a stretch of the Teton River near the failed Teton dam, and extended further to the NE and SW (Prostka and Embree, 1978; Embree et al., 2011). The other fault is located NW of the Teton Dam Fault. Both of these faults dip to the SE. Prostka and Embree (1978) also show a NW striking and SW dipping fault (Warm Creek Fault) that extends from the Big Hole Mountains to the SE and intersects the NE terminus of the Teton Dam Fault. However, this fault is not shown on the new geologic map (e.g., Embree et al., 2011). Moreover, Embree and Hoggan (1999) show a series of shallow and short faults that transect the Hog Hollow area located a

little further NE from the Newdale area. The significance of the Teton Dam Fault and other associated faults for the development of Newdale geothermal area is yet to be fully evaluated. In general, these faults may act structural control for the geothermal setting in the area by providing upward pathways for migration of hotter fluid from depth. However, the Teton Dam fault and the other fault in the area may have a limited role in circulating hotter fluids from depth to the surface such that these faults may be limited by the post-RCC zone and may lack to provide a continuous flow path from ring fracture zones to the surface. Moreover, the lack of surface expressions (e.g., hot springs) in the area may be related to lack of sufficient hydraulic/convective head such that the water table in the area is located several tens of meters below ground surface.

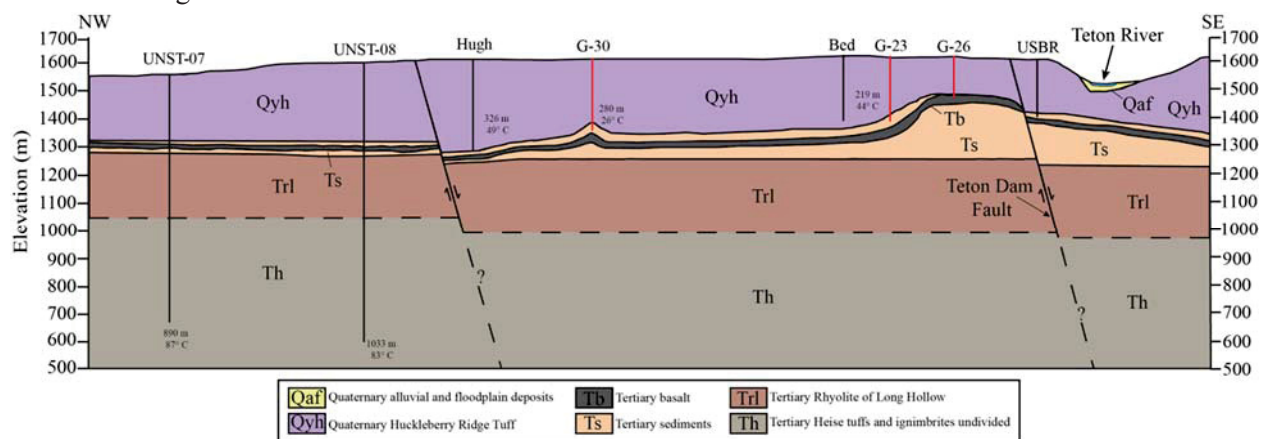


Figure E5. Geologic cross-section through Newdale geothermal area.

3.2.1 Water chemistry

The locations of Newdale water samples are shown in Figure E4. The compiled water composition dataset (Appendix B) includes wells producing waters at both elevated temperatures and cooler temperatures. The warmer wells have temperatures ranging from 21 to 51.1 °C whereas the temperatures of the cooler wells range from 8.5-17.5 °C. All Newdale area wells produce dilute (TDS ranging from 200 to 520 mg/kg with an average value 375 ± 80 mg/kg), immature (Figure E2), and near-neutral (pH 6.4 - 8.5) water. The major cations in water samples are Na, Ca, and Mg whereas major anions are HCO_3 , Cl, F, and SO_4 .

Water samples are either Na-HCO_3 or Ca-(Mg)-HCO_3 types (Figure E6). In the ESRP, the Na-HCO_3 and Ca-(Mg)-HCO_3 type waters are often related to deeper water that have interacted with rhyolite and shallower groundwater that have interacted with basalt, respectively (McLing et al., 2002). The Na-HCO_3 waters have slightly higher TDS (ranging from 340 to 520 mg/kg with average value 440 ± 60 mg/kg) than the Ca-(Mg)-HCO_3 waters (ranging from 200 to 480 mg/kg with average value 330 ± 60 mg/kg).

The cations ternary and the diamond plots in Figure E6 show that these two groups of water aligned along a trend from Na+K vertex to Ca-Mg baseline; however, such trend is missing in the anions ternary plot. Nevertheless, the anions ternary diagram shows a type-water independent trend from the HCO_3 vertex towards middle of the Cl- SO_4 base line. Similar type-water independent trend can be found on a bivariate plot constructed for HCO_3 and Cl (Figure E7a). The type-water independent trend depicted in Figure E7a is likely to reflect the intensity of water-rock interaction (regardless of the rock type) that a water might have interacted. In general, higher the degrees of water-rock interaction, higher the concentrations of HCO_3 and Cl in water are. Other bivariate plots (Figure E7b-f), however, show linear alignment of Na-HCO_3 and Ca-(Mg)-HCO_3 type water samples. Traditionally, such linear alignment of water samples on bivariate plots is considered to be the result of mixing of two end member water compositions in different proportions. Figure E7f also indicates that the original source water for both Na-HCO_3 and Ca-(Mg)-HCO_3 type waters is meteoric water.

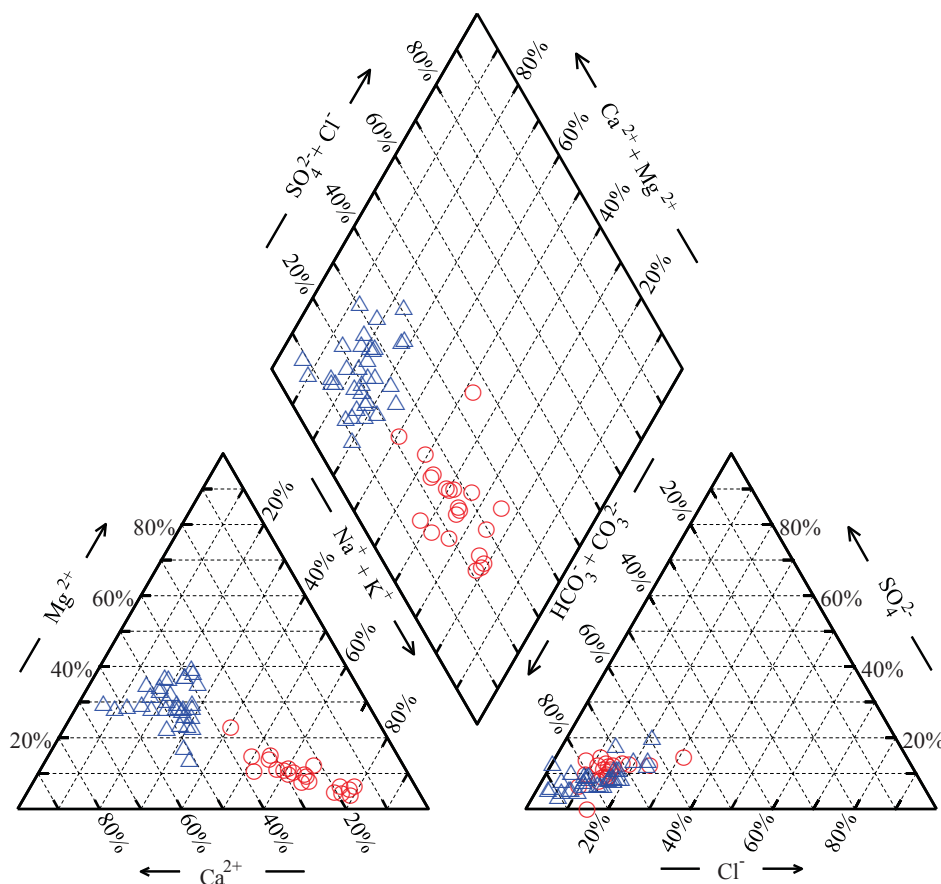


Figure E6. Piper diagram representing chemistry of water samples from Newdale geothermal prospect and surrounding areas

Although the bivariate plots shown in Figure E7b-f depict the apparent linear alignment of Na-HCO₃ and Ca-(Mg)-HCO₃ type waters, some additional bivariate plots with other components and ratios (Figure E8a-f) show two distinct mixing (and/or degree of water rock interaction) trends, one for Na-HCO₃ and the other for Ca-(Mg)-HCO₃ type waters. These diagrams indicate that for Ca-(Mg)-HCO₃ type waters, the dilute end-member can be represented by a pristine water (rain/snow melt). The composition of the higher TDS end member has not been directly measured, but this composition was inferred with RTest modeling for each sample. Intermediate waters are likely to be formed either by mixing of two end-member waters at various proportions, or by water-rock interactions of various intensities.

Some bivariate plots (e.g., Figure E8b, d, and f) that include Cl (concentration or as part of ratio) indicate (the low TDS trends of Na-HCO₃ type waters in these plots point towards origin) that the cooler end member water that mixed with the Na-HCO₃ type waters is a very dilute Ca-(Mg)-HCO₃ type water or even a pristine water. However, the other plots that do not include Cl (e.g., Figure E8a, c, and e) indicate (the low TDS trends of Na-HCO₃ type waters in these plots do not point towards origin) that the dilute end member water that might have mixed with Na-HCO₃ type waters may have a composition similar to some intermediate Ca-(Mg)-HCO₃ type water or such non-linear (trends not pointing towards origin) behavior is noticed because of non-conservative nature of non-Cl components. Since RTest does not handle precipitation, cation exchange, and so on, we assume that some variant of intermediate Ca-(Mg)-HCO₃ type water is the end member water that might have mixed with Na-HCO₃ type waters. As with the cases of Ca-(Mg)-HCO₃ type waters, the higher TDS end member compositions of Na-HCO₃ type waters are also not known, and for each sample, the original thermal water is reconstructed with RTest modeling.

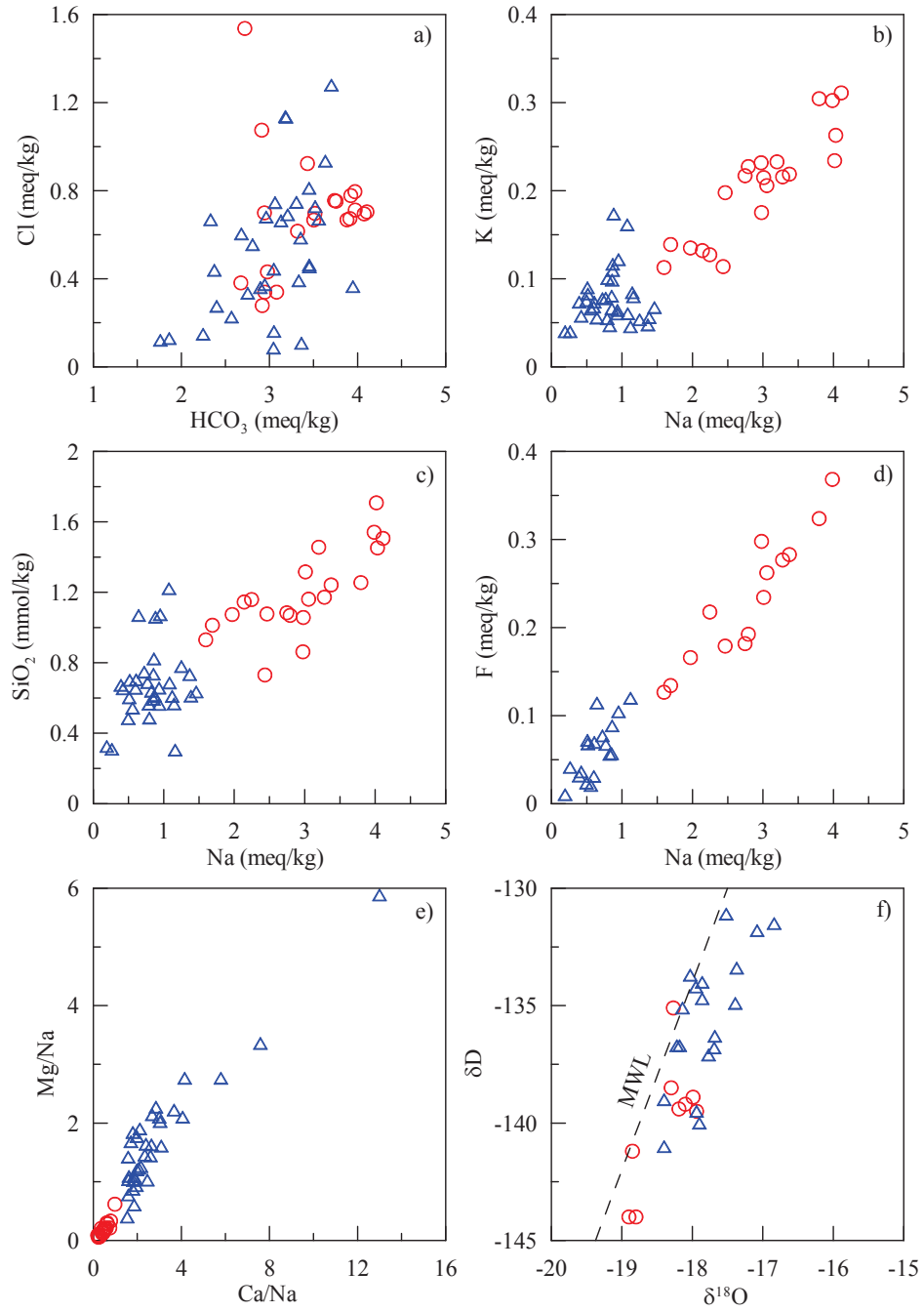


Figure E7. Bivariate diagrams constructed for some components, isotopes, and ratios for Newdale and surrounding area water samples.

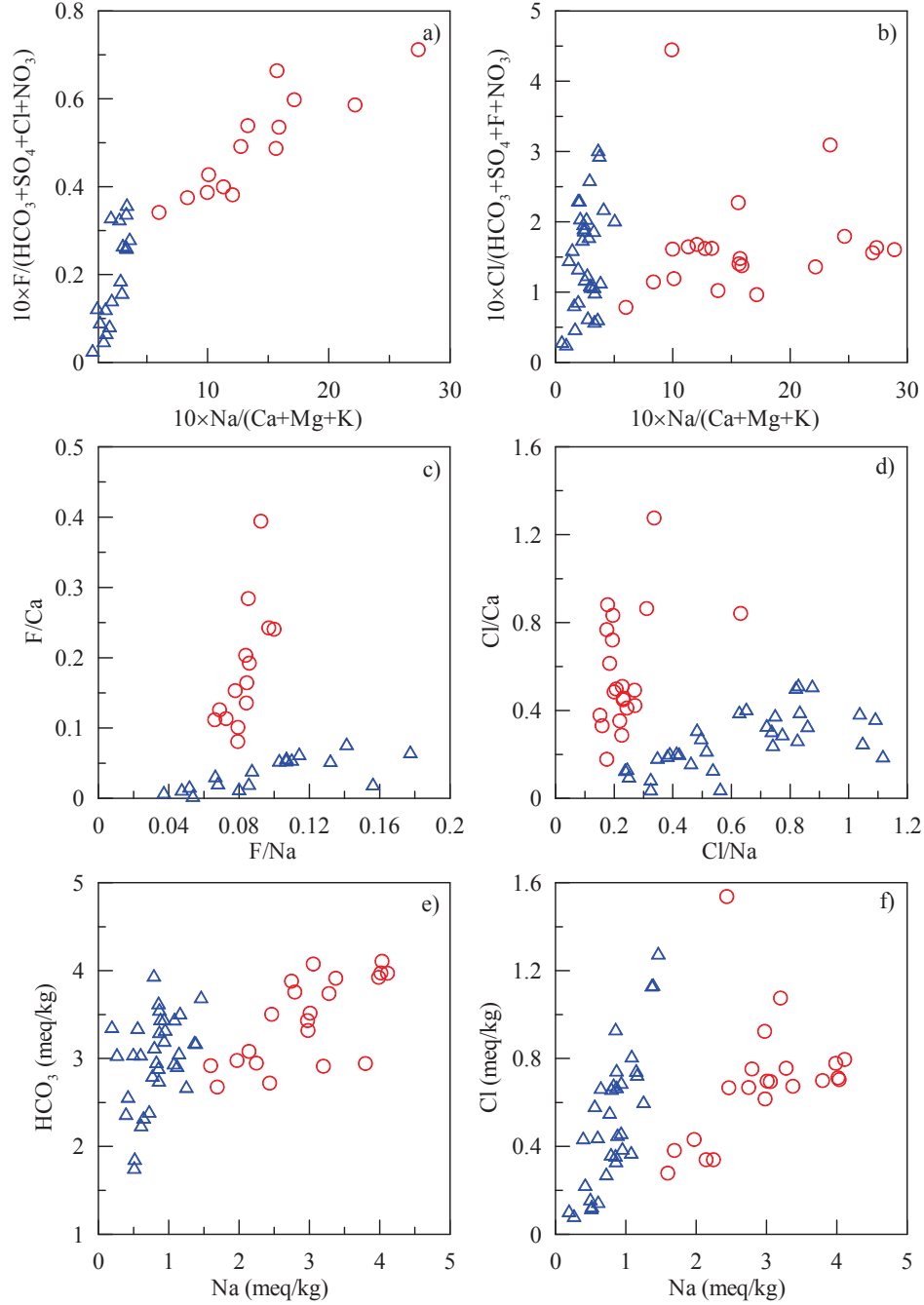


Figure E8. Bivariate diagrams constructed for some components and ratios for Newdale and surrounding area water samples.

The bivariate plots shown on Figure E9 also support the assumption that some intermediate Ca-(Mg)- HCO_3 type water is likely to be the dilute end-member water that might have mixed with Na- HCO_3 type waters at different proportions. Figure E9a also indicates that the Na- HCO_3 type water may be divided into two groups resulting in slightly different mixing trends. Figure E9b indicates that the Ca-(Mg)- HCO_3 waters may have two sub-groups with two mixing/water rock interaction trends- one group may have only interacted with basaltic rocks and may have not received any fraction Na- HCO_3 water whereas the other

group may have either weakly interacted with felsic volcanic rocks or received some fraction of Na-HCO₃ waters. The first group of Ca-(Mg)-HCO₃ type water samples has low F, and these water samples do not show further enrichment in F with progression of water-rock interaction. On the other hand, the second group of water samples show a tendency of slightly increasing F with increasing concentration of Ca (and TDS as well, figure not shown); however, it is may be difficult to discern whether the increasing F concentration merely reflects the fact that these waters may have limited water-rhyolite interaction or they receive increasing amount of Na-HCO₃ type water as they persistently interact with basalt.

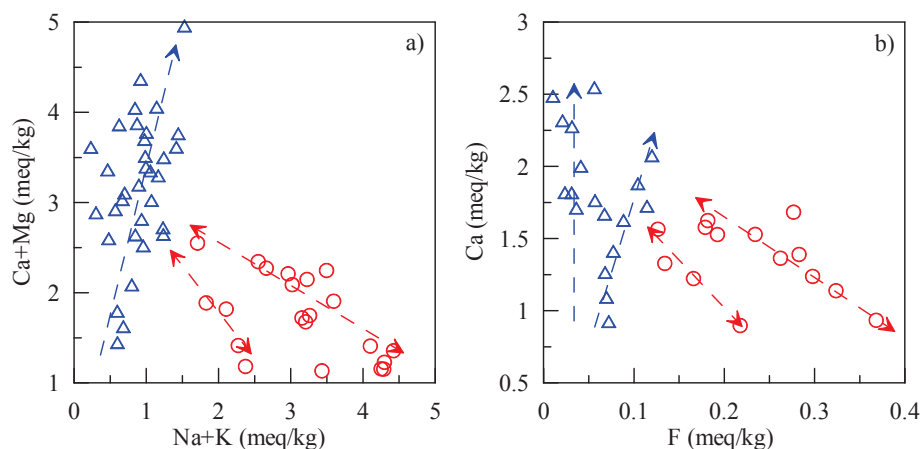


Figure E9. Bivariate diagrams constructed for some components for Newdale and surrounding area water samples.

The concentration of F in water samples is highly influenced by the degree of past interaction with felsic volcanic rocks. However, the majority of low F water samples are from the area north of the Teton River where the subsurface lithology is dominated with felsic rocks. At first, it appears odd with the near surface rock types, however, the wells located north of Teton River tap water from a sediment-basalt aquifer sandwiched between pre-Huckleberry Ridge and Huckleberry Ridge felsic volcanic rocks (Figure E5). Similarly, wells distributed on the southern side of the Teton River where near surface rocks are basalts mostly tap Na-HCO₃ type water from felsic volcanic rock units underneath the basalts.

3.2.2 Geothermometric results

Temperature estimates for the Newdale area samples are included in Appendix D. Quartz, chalcedony, and Na-K-Ca (Mg corrected) geothermometers resulted in lower reservoir temperatures for Ca-(Mg)-HCO₃ type waters compared to the temperatures for the Na-HCO₃ type waters. The range of temperatures with quartz, chalcedony, and Na-K-Ca (Mg corrected) geothermometers for Ca-(Mg)-HCO₃ type waters are 66-119 °C, 28-93 °C, 29-81 °C, respectively. Similarly, the range of estimated temperatures calculated with these geothermometers for Na-HCO₃ type waters are 97-134 °C, 65-112 °C, and 50-111 °C, respectively. A silica (chalcedony)-enthalpy mixing model using all Newdale area samples results in reservoir temperatures of around 174 °C (Figure E10). A similar model using quartz solubility results in even higher temperatures (224 °C).

Since Na-HCO₃ type waters show mixing trends (Figure E9) with a variant of Ca-(Mg)-HCO₃ type water; RTest modeling of the Newdale samples were performed using option that reconstructs thermal fluid using mixing, fugacity of CO₂, and T as optimization parameters. The GW3 water composition was selected to define the end member cooler water composition for RTest modeling of Na-HCO₃ type waters because of its close geographical location to the Newdale geothermal anomaly area. The GW3 is a Ca-

(Mg)-HCO₃ type water that approximately falls along the mixing trends for both types of water on some bivariate plots (Figure E7, Figure E8a,b,e,f). During RTest modeling, some variant of this water composition is found applicable to all Na-HCO₃ type waters as well as to the majority of Ca-(Mg)-HCO₃ type waters. Specifically, the SiO₂(aq) concentration of GW3, which has an unusually high concentration of 46 mg/L at 8.5 °C, was not included in the end member cooler water for RTest modeling. The same approach was used for most of the Ca-(Mg)-HCO₃ type waters, however, for some Ca-(Mg)-HCO₃ type waters (Remington Produce, Dean Swindelman, Pauline, Mark Rick, and Laverie Rick wells), RTest modeling was performed using pure water to account for the mixing. For these samples, use of the GW3 based end member water resulted in a similar estimated temperatures (similar temperature estimates obtained with the pure end member) but poor convergence (large standard error). As noted in the previous section, the assumption of some pristine water as end member cooler water for Ca-(Mg)-HCO₃ type waters is geochemically satisfactory to all bivariate plots (Figure E7, Figure E8, and Figure E9).

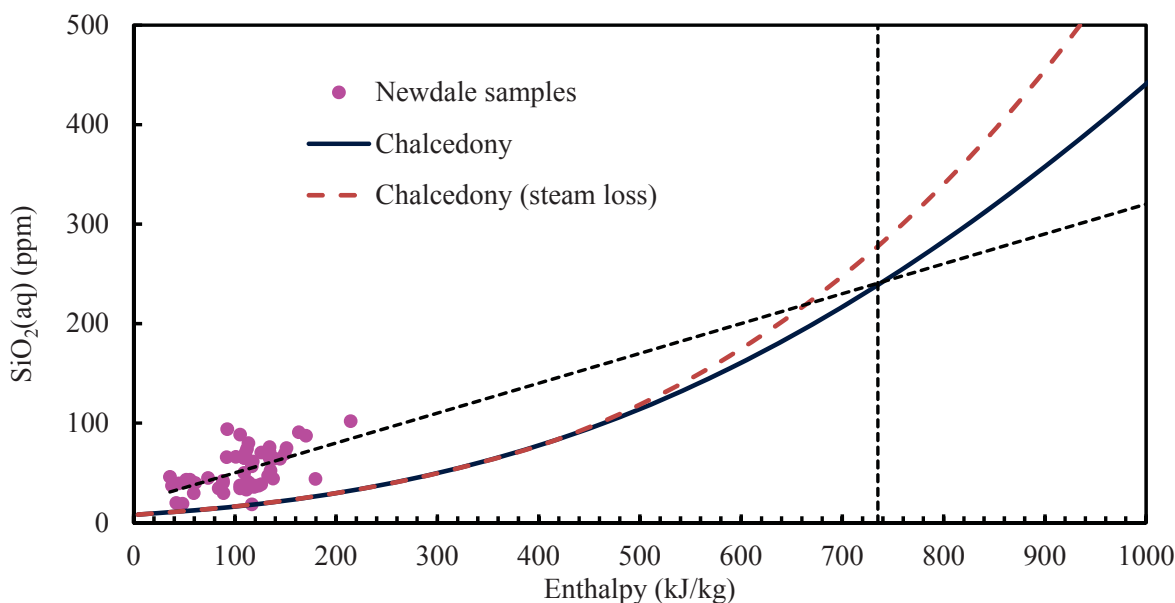


Figure E10. Silica (chalcedony)-enthalpy mixing model applied to all Newdale area samples.

The ranges of RTest temperature estimates for Na-HCO₃ and Ca-(Mg)-HCO₃ type waters are 85-152 °C and 75-141 °C, respectively. RTest results indicate that Newdale area samples contained 10 to 75% of cooler water fractions. Relatively, Ca-(Mg)-HCO₃ type waters have greater fractions (30-75%) of cooler water than Na-HCO₃ type waters (10-50%). The relatively cooler temperatures obtained with the traditional geothermometers for the Ca-(Mg)-HCO₃ type waters may have been resulted because of the fact that they are more diluted with cooler waters than the Na-HCO₃ type waters.

The lower end RTest temperature estimates of this area are similar to the bottom hole temperatures (83-87 °C) measured at two relatively deeper (~1000 m) Unocal wells. Moreover, it is likely that the area hosts hotter zone at depth reaching to the higher end RTest temperatures. Assuming an 80 °C thermal gradient (as indicated by two Unocal wells), the higher end RTest temperatures could occur at about a 2 km depth. A sulfate-water oxygen isotope temperature was calculated for a sample from the Schwendiman well in this area gave a relatively low temperature of 87 °C. The water isotope composition of this sample ($\delta^{18}\text{O} = -19.1\text{‰}$, $\delta\text{D} = -144\text{‰}$) indicates that the sample is dominated by relatively unaltered meteoric water and may not have circulated deeply through the system.

4. Green Canyon Hot Spring

4.1 General

The Green Canyon Hot Springs (GCHS) (Figure E4 and Figure 1) is located along the margin of the ESRP on the northwestern edge of Big Hole Mountains in Madison County, Idaho. It sits at approximately 1558 m above sea level and is approximately 28 km east of Rexburg and 20 km southeast from Newdale, Idaho. This area was originally developed as a local limestone mining location because of the large tufa/travertine deposits nearby. However, with the discovery of the hot spring, the area was later developed into a soaking facility in 1910. An upgraded commercial recreational facility is still in operation in the area. The GCHS issues water at 46°C from a vent located about 300 m to the east from the facility.

4.2 Geologic setting

The GCHS is located on the eastern margin of the inferred Heise caldera complex that produced many of the silicic eruptions from 6.5-4.4 Ma (Prostka and Embree, 1978; Christiansen, 2001; Morgan and McIntosh, 2005). These eruptions produced voluminous tuffs, ash flows, lava flows, and ignimbrites and are labeled as undivided Tertiary Heise (Th) volcanic rocks in Figure E11. A post-caldera rhyolite lava flow, Rhyolite of Long Hollow (Trl), is documented to only occur west of the GCHS area (Morgan and McIntosh, 2005). Quaternary basalt (Qb) is abundant to the north and documented in well logs in the shallow subsurface around GCHS. The Quaternary Huckleberry Ridge Tuff (Qyh) caps most of the hillsides throughout the area. A 50 m thick deposit of travertine is reported near the hot spring (Prostka and Embree, 1978).

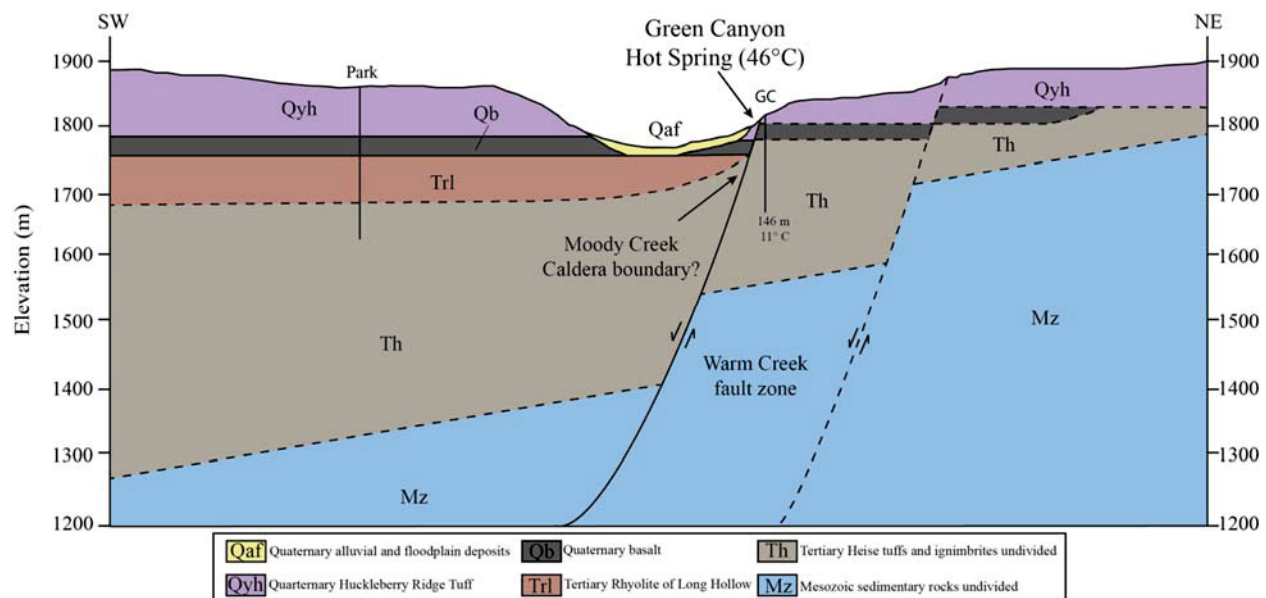


Figure E11. Geologic cross-section of the Green Canyon Hot Springs area; Wells used to constrain lithology are in black.

Mesozoic sedimentary rocks (Mz) are inferred from adjacent maps to extend into this area and form the basal units of the area. These include various limestones, sandstones, siltstones, conglomerates, and evaporite beds which are reported to have undergone extensive folding and faulting associated with the Sevier-Laramide orogeny (Prostka and Embree, 1978; Oriel and Platt, 1980). The northwest trending Warm Creek Fault Zone is the dominant structure controlling geothermal fluids in this area. This normal fault zone extends from the southeastern corner of the area and continues up Warm Creek where it intersects with a north trending normal fault that extends up Green Canyon. These faults have a down to

the west/southwest sense of displacement with unknown amount of slip. Anders et al. (2014) have recently modified the boundaries of the Blacktail Creek Tuff and Kilgore Tuff calderas which both intersect in the GCHS valley. The combination of intersecting faults with caldera ring fractures suggests that the increased fracture permeability gives rise to higher fluid flux from depth.

4.3 Water chemistry

GCHS issues near neutral water containing Ca, Mg, SO_4 , and HCO_3 as major ions. The measured TDS in water is 585 mg/L. On a Giggenbach diagram (Figure E2), the GCHS water plots in immature water field. The reported hydrogen ($\delta\text{-D}$: -136.2‰) and oxygen ($\delta\text{-}^{18}\text{O}$: -18.08‰) (GeothermEx, 2010) isotope values indicate that the GCHS issues heated meteoric water. The GCHS issues waters with low concentrations of Cl and Na with high concentrations of Ca and SO_4 . Similarly, the GCHS water has a lower F concentration than water that equilibrated with felsic volcanic rocks in the ESRP but higher than typical basalt-hosted ESRP water. Although high Ca and Mg waters in the ESRP are regarded as the product of water-basalt interaction, the presence of higher concentration of SO_4 in GCHS water indicate that it must have interacted with rocks other than basaltic rocks. The geologic cross-section (Figure E11) through GCHS shows a rather thin ca. 20 m thick basalt layer (Qb) sandwiched between Tertiary (Th, Trl) and Quaternary (Qyh) felsic volcanic rocks. Underneath the Tertiary felsic rocks are the Mz units comprising passive-margin sedimentary rocks (Mansfield, 1927; Oriol and Platt, 1980). It is apparent that the GCHS water has limited interaction with basaltic rocks, and its composition is largely shaped by the water-rock interaction in the Mz units, which may have been slightly changed by limited interaction with felsic volcanic rocks and mixing with shallow groundwater. Thick deposits of travertine in the area (Prostka and Embree, 1978) also support that the GCHS issues water that interacted with carbonates of the Mz units. The low concentration of Cl in GCHS water, however, precludes its interaction with Preuss Sandstone of the Jurassic Period that contains both halite and gypsum rich evaporite beds. It is, therefore, likely that the hot water from the reservoir migrates upward along the Warm River Fault zone interacting with felsic volcanic rocks before emanating as hot spring at the surface. However, the deeper water also mixes with dilute cooler shallow subsurface water.

The GCHS water appears to be similar to LHS water such that both features produce waters with low concentrations of Cl and Na along with higher concentrations of Ca and SO_4 . Similarly, there have been some other hot/warm springs [e.g., the Bear Lake Hot Springs (BLHS) near Idaho-Utah boarder and the Warm Spring near Big Elk Mountain] in the Idaho-Wyoming fold-thrust belt that produce Ca- SO_4 type water (Ralston et al., 1981; Neupane et al., 2015a). Geologically, the GCHS, BLHS, and Warm Spring (near Big Elk Mountain) areas share the same Mz stratigraphic units at depth. However, the Heise Hot Spring (HHS) which issues chemically distinct (high Na, Cl, and SO_4) water that is also interacted with Mz rocks in its reservoir at depth. It is likely that a fraction of the GCHS water (and similar other waters) may have interacted with Mz units containing SO_4 rich (and Cl poor) beds.

4.4 Geothermometric results

Quartz, chalcedony, and Na-K-Ca temperature estimates for GCHS are 75, 44, and 65 °C, respectively (Appendix D). However, these traditional geothermometer temperatures are obtained using un-optimized (un-reconstructed) composition of the GCHS. The fluid composition of this water was reconstructed with RTest using a mineral assemblage of chalcedony, clinoptilolite, fluorite, anhydrite, and calcite. As alluded in the water chemistry section, the intermediate concentration of F indicate that the GCHS water is likely to have mixed with dilute cooler water. Geochemical speciation calculations indicate that both anhydrite and fluorite are undersaturated at field temperature and composition. RTest modeling was performed to reconstruct GCHS thermal water composition using pure water as a substitute for dilute cooler water that may have mixed with along the flow path to the surface. RTest modeling results indicate that the GCHS water may contain up to 60% of cooler water and 40% thermal water with reservoir temperature at 94 ± 4 °C. Both fluorite and anhydrite are found to be at equilibrium in

reconstructed reservoir water. A sulfate-water oxygen isotope temperature of 29°C (Appendix D) was calculated for a sample from GCHS. This is likely indicating that the source of sulfate in the sample is coming from interaction of the fluids with anhydrite and/or gypsum in the subsurface and does not represent formation of the sulfate in a high temperature system. In addition, the $\delta^{34}\text{S}$ of the sulfate is high at 22.6‰, supporting a sedimentary sulfate origin.

5. Heise Hot Spring

5.1 General

The Heise Hot Springs (HHS) area (Figure 1) lies at the base of a cliff (Heise cliff) along the flanks of the Snake River at 1530 m above sea level in Jefferson County, Idaho. It is approximately 33 km northeast of Idaho Falls, along highway 26. Since the early 20th century, the area has been used for camping, swimming, and soaking. The facilities include a large swimming pool, a warm pool, and a hot pool for soaking. The spring that supplies the water to these facilities is issuing thermal waters at 48°C. Approximately 1.7 km and 3 km northwest of HHS, there are two additional warm springs [Hawley Spring (16 °C) and Elkhorn Spring (20°C)] issuing waters from higher elevations.

5.2 Geologic setting

Between 10 and 2 Ma, the area was blanketed by thick sequences of silicic volcanic rocks, including tuffs, rhyolite flows, and ignimbrites. These units include the Tertiary Arbon Valley Tuff (Tav) originating from the Picabo Caldera (Kellogg et al., 1994), and the Tertiary Heise volcanic field (Th) consisting of the Blacktail Tuff, Rhyolite of Kelly Canyon, Wolverine Creek Tuff, Tuff of Elkhorn Spring, Tuff of Hawley Gulch, and Kilgore Tuff (Morgan and McIntosh, 2005). Other minor units in the area include the Rhyolite of Long Hollow and various Tertiary and Quaternary basalt flows. The Quaternary Huckleberry Ridge Tuff (Qyh), associated with Yellowstone caldera volcanism (Christiansen, 2001), is the uppermost unit located throughout the area. A minor travertine deposit (ca. 10 m thick) is located near the HHS.

Underlying the volcanic rocks are Mesozoic sedimentary rocks (Mz) including the Jurassic Nuggett Sandstone, Twin Creek Limestone, Stump Formation, and Preuss Sandstone, and the Cretaceous Gannett Group (for simplicity, these units are lumped together in the cross-section shown in Figure E12). These units were extensively folded and faulted during the Sevier-Laramide orogeny.

This region represents the termination of the Idaho-Wyoming thrust belt as is evidenced by truncation of folded and thrust faulted Mesozoic sedimentary rocks as they enter the Snake River Plain volcanic province. The Jurassic units exposed in the area have been documented to have various dip angles and an overturned nature as part of a thrust package (Phillips et al., 2016a,b). The more recent Heise and Snake River faults, NW trending splays of the Grand Valley Fault Zone (Piety et al., 1992), have dropped the SW edge of the Big Hole Mountains down and raised the Rexburg Bench exposing the Heise volcanics and underlying Mesozoic rocks. There is an estimated 350 m of displacement along this fault system (Piety et al., 1992).

The springs in the area are located at the intersections of the NW trending Heise Fault and unnamed NE trending faults. Along with the faulted nature of the area, the tuffs and rhyolites associated with the Heise volcanic field are highly fractured and hydrothermally altered suggesting possible increased fracture permeability to allow for hydrothermal fluids to travel to the surface. Furthermore, the Kelly Mountain Caldera (Prostka and Embree, 1978) rim fractures may lie underneath the HHS. Similarly, the existence of a dense intrusive body [likely to be the lateral end of the mid-crustal sill complex (Sparlin et al., 1982; Peng and Humphreys 1998; Shervais et al., 2006)] is suggested by Mabey (1978) based on regional Bouguer gravity anomaly.

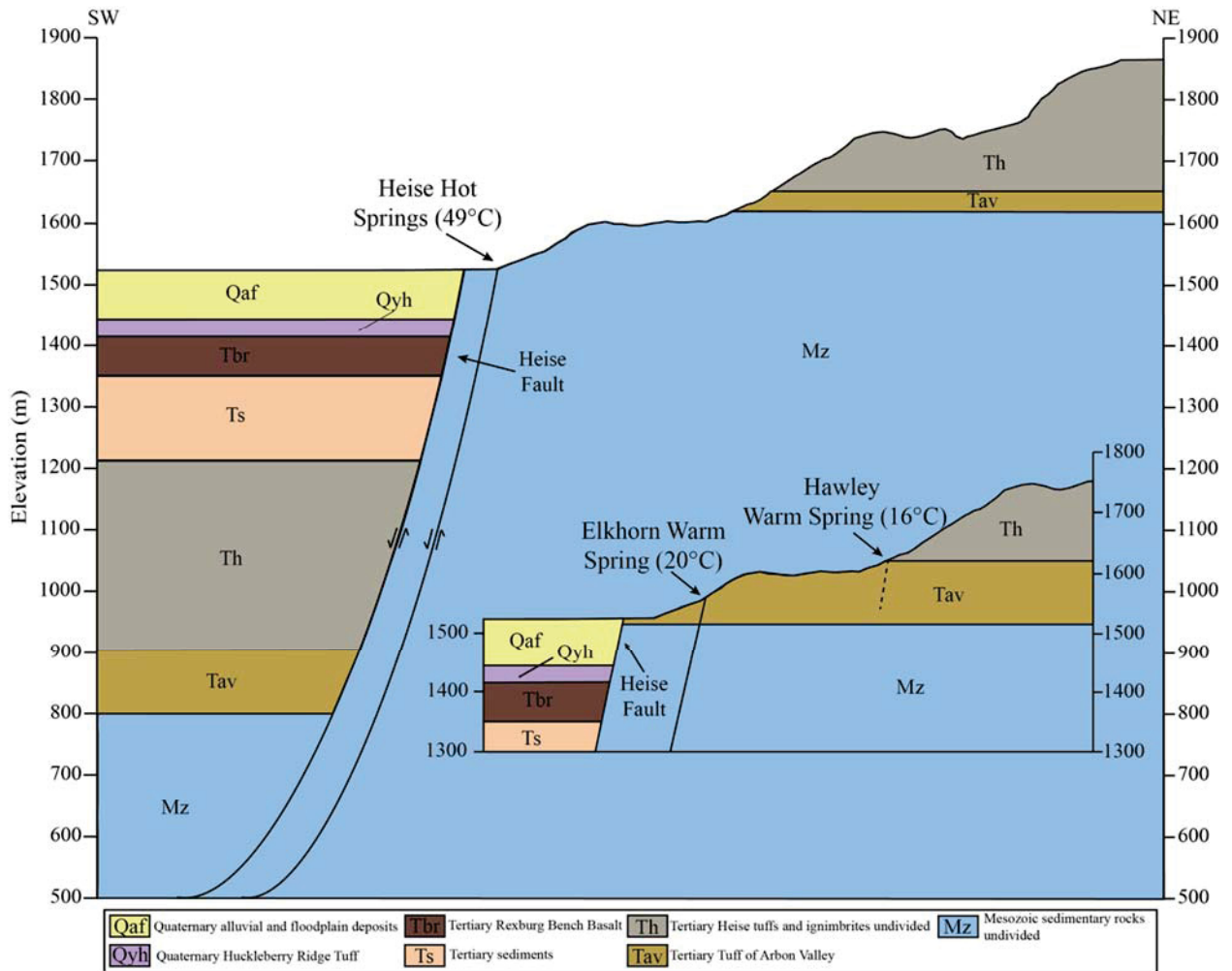


Figure E12. Geologic cross section of the Heise Hot Springs area; In-set cross section is representing the area NE of Heise showing Elkhorn and Hawley warm springs.

5.3 Water chemistry

The chemical property of HHS water makes it unique among the water samples from ESRP/ESRP margins hot springs and wells (Appendix B). This spring produces near neutral (pH 6.32) water with very high TDS (>7000 mg/L) and a strong hydrogen sulfide smell. Specifically, the HHS water is enriched in Cl, Na, HCO₃, and SO₄. It also contains significant amounts of K, Ca, and Mg. On Giggenbach diagram (Figure E2), the HHS water plots in immature water field. The evaporite beds in the Preuss Sandstone of the Mz units (Figure E12; Phillips et al., 2016a,b) are the likely source of elevated Cl and SO₄ in HHS water.

The two nearby springs (Hawley and Elk Horn Springs) produce chemically different water than the HHS. These two springs issue neutral water containing lower TDS content (~335 mg/L). The water of these two springs also have very low Cl and SO₄ concentrations, indicating that they do not interact with evaporite beds of the Mz units at depth.

5.4 Geothermometric results

Quartz, chalcedony, and Na-K-Ca temperature estimates for HHS field water composition are 84, 53, and 89 °C, respectively (Appendix D). The reservoir fluid composition for HHS was reconstructed with

RTest using a mineral assemblage of anhydrite, beidellite, chalcedony, clinoptilolite, illite, and K-feldspar. The reconstructed fluid resulted in a reservoir temperature of 88 ± 2 °C. RTest results also indicate that the HHS water is diluted by a factor of almost 2. As with GCHS, the calculated sulfate-water oxygen isotope temperature for this site was relatively low at 65° (Appendix D) compared to the RTest temperatures. This is probably also an artifact of interaction with anhydrite beds in the subsurface. In addition, as with the GCHS sulfate, the $\delta^{34}\text{S}$ of the sulfate is high at 20.3‰ supporting a sedimentary sulfate origin. However, unlike the GCHS sample, the concentration of dissolved inorganic carbon compounds (DIC) in the HHS sample was very high and had a high $\delta^{13}\text{C}$ suggesting a marine carbonate source.

The other two nearby warm springs provide 64-108 °C as reservoir temperatures based on field water composition applied to traditional geothermometers. Specifically, for field water compositions, quartz, chalcedony, and Na-K-Ca geothermometers resulted in very similar temperatures for both of these springs about 108 °C and 79 °C, and 64-68 °C, respectively. Because of the differences in the water compositions of these two springs relative to the HHS water, a slightly different minerals assemblage was used for the RTest modeling. Specifically, anhydrite that was used in the RTest modeling of HHS water was not included in the mineral assemblage for the RTest modeling of waters from these two springs. Specifically, a mineral assemblage consisting of calcite, chalcedony, clinoptilolite, saponite, paragonite, and disordered dolomite was used for these springs. For Hawley and Elkhorn springs, the RTest reservoir temperature estimates are 109 and 117 °C, respectively.

6. East Idaho Falls area

6.1 General

The foothills (1480-1580 m above sea level) along the margins of the ESRP east of Idaho Falls in Bonneville County have some wells that have been producing warm water since the early 1980s (Ralston et al. (1981). The geothermally anomalous area (Figure 1) along the foothills covers an area 10×3 km². Ralston et al. (1981) reported the existence of two wells in Rim Rock Estate that were producing water at ≥ 20 °C. Recently drilled shallow wells (depth up to 244 m) in the Comore Loma and Blackhawk communities a few kilometers south from Rim Rock Estate also produce warm water (21-28 °C). As a part of this study, we collected and analyzed several water samples from wells in the area.

6.2 Geologic setting

The area lies on the edge of the SRP where pronounced volcanism has taken place throughout the past 6.5 Ma. The foothills to the east of Idaho Falls consist predominantly of tuffs, ignimbrites, and ash flows related to the Miocene-Pliocene Heise volcanic field (Th; Morgan and McIntosh, 2005). To the west of the foothills, the SRP Quaternary basalts (Qb) become the dominant rock type with a thin layer of Quaternary sediments (Qs).

Beneath the Heise volcanic rocks and quaternary basalts are inferred Mesozoic sedimentary rocks (Mz) including limestones, sandstones, siltstones, conglomerates, and evaporite beds. For simplicity, these units are lumped together in the cross-section (Figure E13).

Although, there are no mapped faults in the area, reverse faults associated with the Idaho-Wyoming thrust belt have been mapped in the Mesozoic units to the south. Allmendinger (1982) has mapped multiple late Cenozoic normal faults in the northern Blackfoot Mountains, including the Gateway Fault. These north-northwest trending faults are associated with the oldest regional range front faults in the area and have been mapped both to the north and south with throws ranging from 775-1000 m. They faults have been projected into the study area showing offset within the Mesozoic units without continuing into the overlying Heise units. There is evidence, however, of late normal faulting having occurred in recent time within the Heise units to the east in the Ririe Reservoir area (Phillips et al., 2016b). These faults, as well as other north-northeast trending normal faults mapped by Allmendinger (1982), could represent the late

Cenozoic adjustments that occurred as the SRP downwarp developed. The faults along with the highly permeable nature of the Heise volcanics could be facilitating fluid flow for several wells in the area.

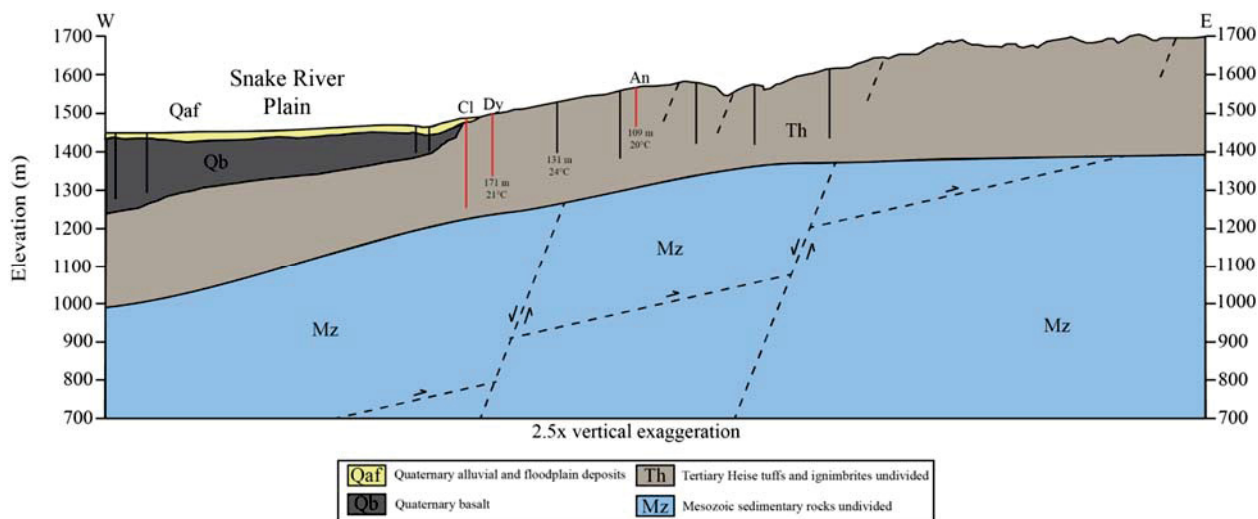


Figure E13. Geologic cross-section of an area east of Idaho Falls, ID; Black vertical lines indicate well logs used to constrain lithology and red lines indicate wells that were used for both lithology and geochemistry. (Cl: Comore Loma, Dy: Dyer, An: Anderson wells).

6.3 Water chemistry

All wells in the east Idaho Falls foothills produce neutral (pH from 6.7-7.7) water with TDS levels in the range of 430 to 835 mg/L (Appendix B). Chemically, water from these wells is Na-HCO₃ type (Figure E14), and contain relatively higher (compared to other ESRP waters except HHS water) concentration of Cl. Similarly, these water samples contain significant amount of Ca (50-77 mg/L). Wells in the northern part of the area (Rim Rock Estate) produce water containing very low concentration of SO₄ whereas wells in the southern part of the area (Comore Loma and Blackhawk communities) produce water containing >25 mg/L SO₄. Similarly, water from the southern part has relatively higher concentrations of Na and K. However, when plotted on a Giggenbach plot (Giggenbach, 1988), all water samples from this area plot in the immature zone (Figure E2) because of higher (10-22 mg/L) concentration of Mg. Despite all wells being drilled within the felsic volcanic rocks, they produce water having low (<0.5 mg/L) concentration of F. Low concentration of F in these water samples may indicate that the wells in the east Idaho Falls foothills are mostly getting water chemically influenced by the underlying Mz units containing carbonates. It is likely that the higher Cl and SO₄ concentrations in the waters from these wells are the results of water-rock interaction occurred with the Mz units. The wells in this area are very productive and can sustain pumping rates of >1500 gallon-per-min for several days. The rocks in the area are reported to be highly fractured and it is likely that the wells in the area also tap groundwater from the deeper Mz rock units through the fracture-dominated permeable zones.

6.4 Geothermometric results

The quartz, chalcedony, and Na-K-Ca temperature estimates for east Idaho Falls area range from 115 to 143 °C, 86 to 117 °C, and 45 to 74 °C, respectively (Appendix D). For these water samples, RTest was applied using a mineral assemblage of clay mineral(s), calcite, chalcedony, clinoptilolite, and K-feldspar. The Mg concentrations in these waters are found to be controlled by mineral equilibria with clay minerals such as chlorite, saponite, illite, and beidellite. The RTest temperature estimates for these 6 water samples are very similar with a range from 136-143 °C (Appendix D). East Idaho Falls waters are diluted by 1.5 to 2.5 times with the dilute water. Similarly, RTest modeling of these samples indicate that these waters are subjected with high fugacity of CO₂ (6-20 bar) in the reservoir at depth. The gas rich Comore

Loma and Blackhawk samples also support the RTest results that indicate high fugacity of CO₂ in the reconstructed fluids.

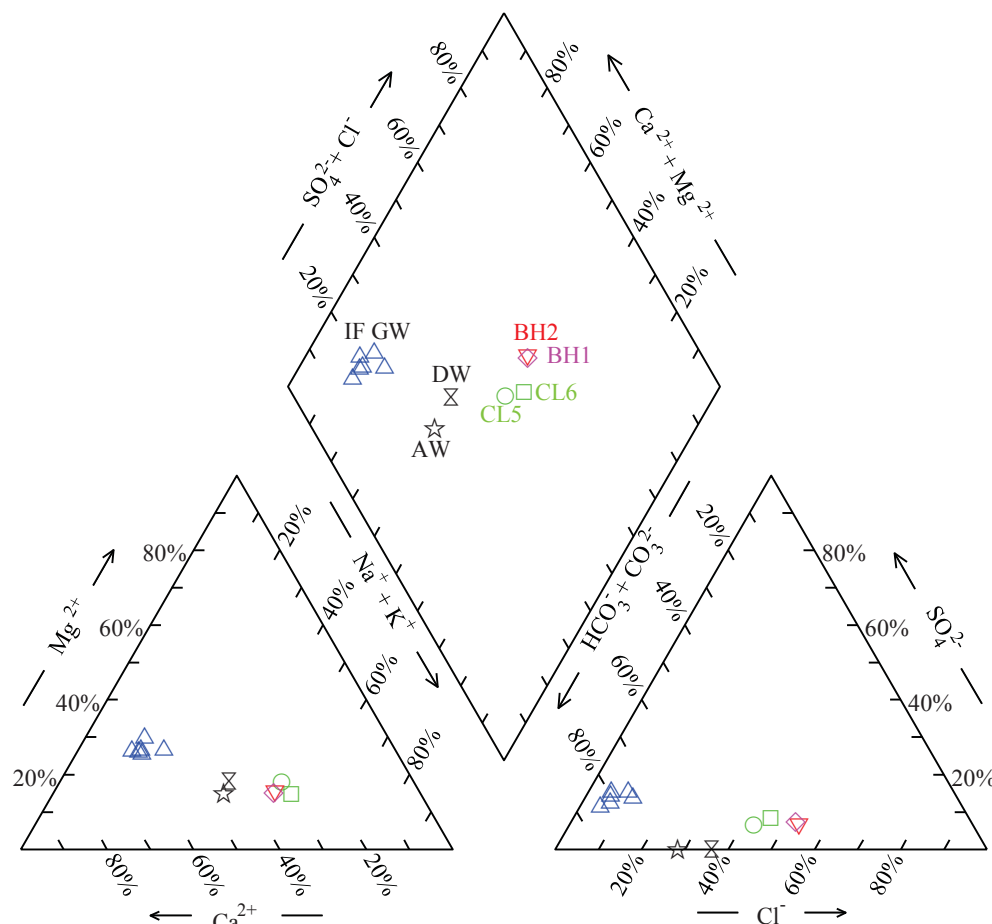


Figure E14. Chemical composition of water samples from Idaho Falls and from foothills on the east of Idaho Falls area plotted on Piper diagram. IF GW: Groundwater from Idaho Falls and Ammon; wells from foothills are - DW: Dryer well, AW: Anderson well, CL5: Comore Loma well #5, CL6: Comore Loma well #6, BH1: Blackhawk well #1, and BH2: Blackhawk well #2.

7. Butte City area

7.1 General

The Butte City geothermal area (Figure 1) is located about 16 km to the west from Idaho National Laboratory desert site along route 26 in Butte County, Idaho. This area is about 100 km west from Idaho Falls and about 5 km east from Arco. The thermal anomaly of the area was identified when a well drilled by Butte City intercepted warm water (Ross, 1970). The area has several warm wells that produce water at 23-36 °C. The two hottest wells in the area, Butte City Well and Greenhouse Well, are currently used for municipal water supply and heating greenhouses, respectively. Previously, a hot water producing well (41 °C, the Lewis Rothwell Well) from an area about 22 km west from Butte City was reported by Young and Mitchell (1973).

7.2 Geologic setting

The Butte City geothermal area lies near the ESRP margins. Surficial Quaternary alluvial deposits are mapped around Butte City, but tholeiitic Quaternary basalts are mapped to the south of this area (Kuntz et al., 1994). Therefore, it is likely that alternating sequences of Quaternary basalts and alluvial deposits constitute the near subsurface materials in the area. The thickness of basalts/sediment layers in this area may range from 200-300 m (Whitehead, 1992; Blackwell et al., 1992). Paleozoic sedimentary rocks outcrop in the Arco Hills of the Lost River Range located a few kilometers to the north from the area. The geologic contact between ESRP and Lost River Range has been interpreted by different workers as being a fault, a down warp or a shear accommodation zone (Sparlin et al., 1982; Peng and Humphreys, 1998; McQuarrie and Rodgers, 1998; Payne et al., 2013). The type of contact between these two geologic and geographic provinces could make a significant effect on the type of basement rock under the basalt/sediment sequences in the area. If the contact is a fault, a thick sequence of Tertiary rhyolites may underlie the Quaternary rocks. However, if the contact is defined by a down warp, a thin sequence of rhyolite is likely to be present sandwiched between underlying Paleozoic sedimentary rocks and overlying quaternary rocks. Regardless of the type of north-south boundary between the ESRP and Lost River Range, two N-S and SE-NE striking faults that make the Arco Peaks and Arco Hills, respectively, seem to intersect or plunged down the Butte City geothermal area. this area is located within the Arco-Big Southern Butte volcanic rift zone that is characterized by linear trends of eruptive centers, eruptive and non-eruptive fissures, monoclines, and grabens (Kuntz and Kork, 1978; Kuntz et al., 1994).

7.3 Water chemistry

Two water samples from two wells (Butte City Well and Greenhouse Well) in the area were collected and analyzed during the sampling campaign of this study. Water samples from these wells have been analyzed several times over the last several decades, and their compositions are found to be consistent over time. Besides these two wells, four other water compositions measured from warm wells (23-41 °C) in the area were also compiled from existing literature (e.g., Young and Mitchell, 1973). The concentrations of major cations and anions in these samples (Appendix B) are shown on a Piper diagram (Figure E15). Waters from this area are near-neutral (pH 6.3-8.1) Ca-(Mg)-HCO₃ type with TDS ranging from 370-720 mg/kg. Silica concentrations in the water samples from Butte City are relatively low (24-38 mg/L). Similarly, F concentrations in Butte City water samples represent typical values of basalt-interacted ESRP waters with a narrow concentration range from 0.4-0.7 mg/L. However, the Lewis Rothwell Well which is located further west from Butte City has been reported to produce water with relatively higher concentrations of SiO_{2(aq)}, F, and SO₄ possibly indicating that this water may have interacted with rhyolites (or even Paleozoic sedimentary rocks as indicated by higher SO₄ content) at greater depth (and potentially at higher temperature) and latter re-equilibrated with basalts at shallow depth.

7.4 Geothermometric results

Reservoir temperatures for the Butte City geothermal area are given in Appendix D. Quartz (no steam loss) and chalcedony (Fournier, 1977) geothermometers resulted in 70-90 °C and 38-59 °C, respectively. Similarly, Mg-corrected temperature clustered around 40 °C, and for one sample locally re-equilibrated temperature is indicated. Silica-enthalpy mixing model (no-steam loss) temperatures are 75 and 124 °C obtained with chalcedony and quartz solubility curves, respectively. The fractions of thermal water in the sampled waters as indicated by silica-enthalpy mixing models are 40% and 25%, respectively. However, RTest modeling showed good convergence with no mixing scenarios for the Butte City area samples. RTest modeling for Butte City area samples were performed using a mineral assemblage consisting of calcite, chalcedony, clinoptilolite, dolomite, phengite, and saponite. The RTest modeling resulted in temperatures around 60 °C for these samples. When compared, RTest temperature estimates are more aligned with chalcedony and Na-K-Ca temperatures, and slightly warmer than the temperatures of the water that these wells produce. Moreover, Blackwell et al. (1992) recorded a temperature of about 53 °C for the lower part of the Greenhouse well (reported as the Richardson well). Therefore, the Butte City

wells are tapping water from a reservoir that is located at a shallow depth and is equilibrated at lower temperature. Notwithstanding the cooler geothermometric temperatures from water samples from this area, Dobson et al. (2015) reported an unusually high $^3\text{He}/^4\text{He}$ ratio for one sample (Greenhouse Well) from this area, indicating that the area may have a deep magmatic heat source. The sulfate-water oxygen isotope temperatures for these two wells were similar, but somewhat higher than the RTest temperatures at 95 °C for the Greenhouse well and 92 °C for the Butte City wells (Appendix D).

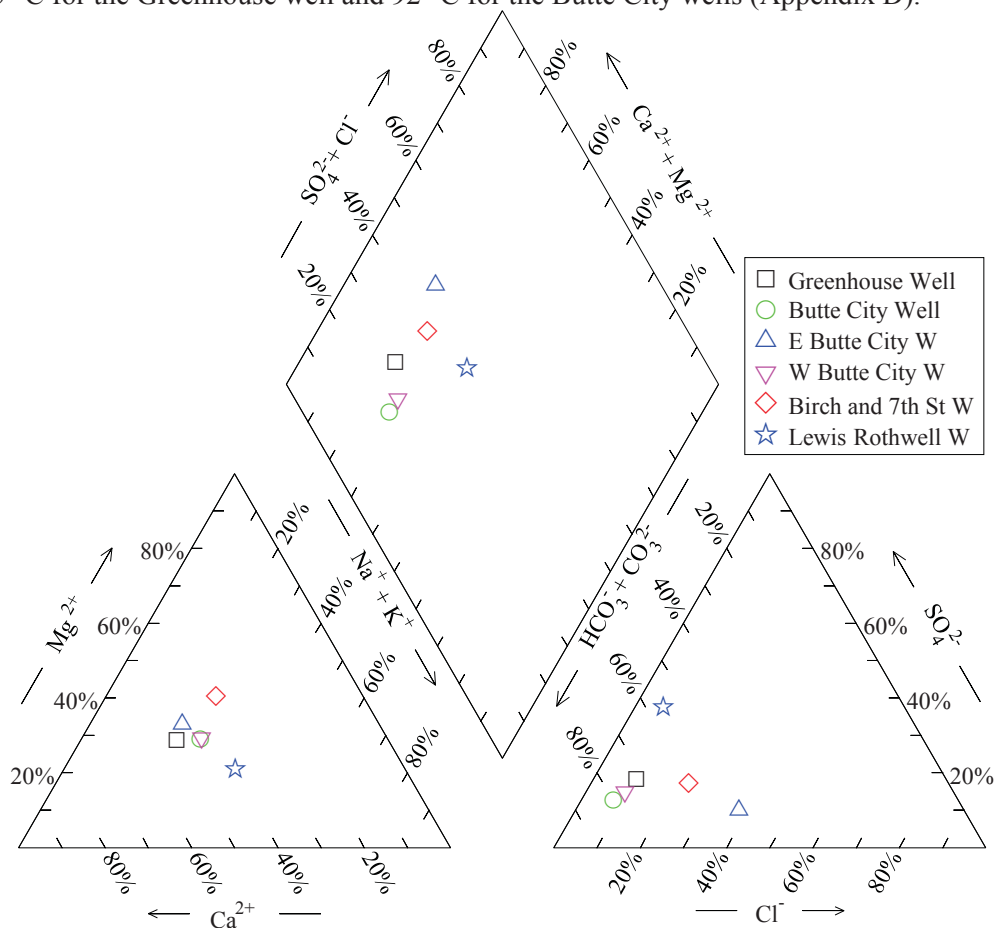


Figure E15. Piper diagram representing chemistry of water samples from Butte City area

The Lewis Rothwell Well yielded lower temperatures. Estimated reservoir temperatures for this well with chalcedony, quartz, Na-K-Ca, and RTest geothermometers are 77, 106, 49, and 80 ± 3 °C, respectively. Low estimated temperature but higher concentration of F in water indicate that the Lewis Rothwell Well may be tapping water that has interacted with rhyolites at greater depth and potential higher temperature but latter modified by interactions with basalts at lower temperature.

It is likely that the heat source for the Butte City geothermal area is a mid-crustal mafic sill complex identified with regional seismic studies (Sparlin et al., 1982; Peng and Humphreys, 1998) and petrochemical analysis of sequences of ESRP basalt (Shervais et al., 2006). Another likely possibility for the elevated temperature in the area is its hydrogeological setting. Groundwater modeling of the ESRP aquifer system indicates rather low transmissivity for this area (Whitehead, 1992). Thinner aquifers with lower transmissivity and longer residence times may help produce a local thermal anomaly.

8. Condie Hot Spring

8.1 General

The Condie Hot Spring (CHS) geothermal area (Figure 1) is located about 3.5 km northeast of Carey in Blain County, Idaho. This area sits at about 1450 m above sea level along the Route 26/93. The area is characterized by three hot springs. The main geothermal feature of the area is the CHS which issues water at 50.5 °C. Two additional spring systems in the area – Milford Sweat Hot Spring (MS) and Rush Warm Springs (RWS) – issue water at 38.1 and 29 °C, respectively. None of the hot springs in the area are currently being used for any economical or recreational activities.

8.2 Geologic setting

The CHS geothermal area is located along the north-central margin of the ESRP. A generalized geological section for the area is shown in Figure E16. To the ESRP side of the cross-section, Quaternary alluvial and flood basalt layers are present at shallow depth. However, non-ESRP area (Basin and Range type geographic province) to the north, the Tertiary Challis volcanic rocks outcrop. Underneath the both Tertiary and Quaternary rocks/sediments are the Paleozoic sedimentary units. The contact between the ESRP and Basin and Range in this area is not properly understood, and cross-section is constructed based on geologic interpretation made by McQuarrie and Rodgers (1998) that the Paleozoic rock units warp down into the ESRP rocks. Other competing views either consider fault(s) (Sparlin et al., 1982) or a shear zone (Payne et al., 2013) as the boundary that separates the ESRP from the Basin and Range in this area.

Because of the lack of well log data from the area, the thickness of the Quaternary basalts is not known. Similarly, whether any rhyolite units exist between the basalt layers and Paleozoic rocks is not known. The thickness of basalt layers (or aquifer thickness) as depicted in Figure E16 is based on the information provided by Whitehead (1992). Similarly, no rhyolite sequence is shown underneath the basalt layers because of the lack of geochemical signatures in the water compositions from the CHS area geothermal waters that would indicate the presence of felsic volcanic rock at depth. However, the lack of rhyolite signatures in thermal waters may stem from the fact that the area does have very thick basalt layers and the felsic volcanic rocks are buried at greater depth. This scenario seems equally valid if the contact between ESRP and the area to the north (Basin and Range Province) is a structural fault or caldera ring fracture(s).

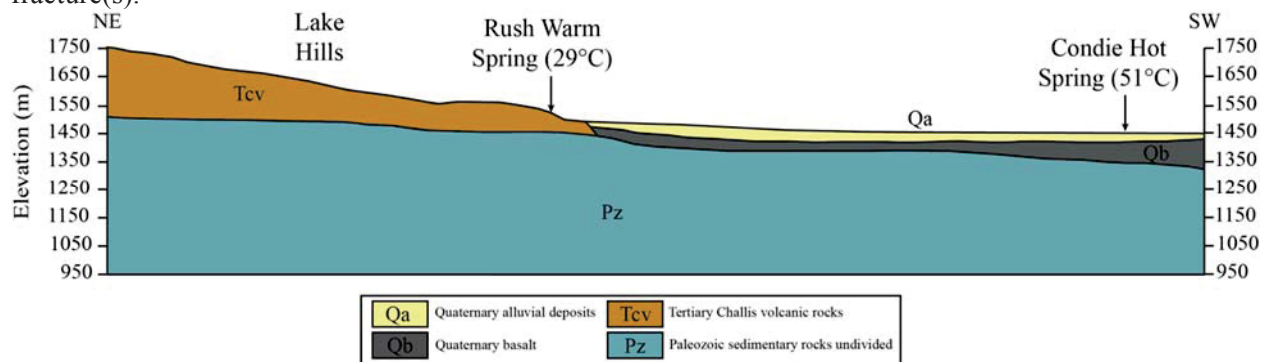


Figure E16. Geologic cross-section of the Condie Hot Spring geothermal area

The geologic map of the area shows a fault extending to the MS, however there were no mapped faults in the vicinity of CHS and RWS (Lewis et al., 2012). The Tertiary Challis volcanic rocks in the vicinity of RWS are highly jointed. The warm water that these springs issue may have been moving from depth along the joint openings or along the gravel/conglomerate layer between Paleozoic units and Challis volcanic rocks. Similarly, the CHS may have flow paths controlled by deep joints in the basalt layers or the area may have unmapped fault(s).

8.3 Water chemistry

We collected four water samples from three hot springs systems representing the CHS geothermal area (Appendix B). Field temperatures of these samples range from 23.2 °C (RWS2) to 50.5 °C (CHS). In addition to these samples with elevated temperatures, several water compositions measured from cooler (11-15 °C) wells around the area are also compiled from NWIS database. Chemical compositions of major cation and anions in these samples are depicted in Figure E17. Both warmer and cooler sampling features in this area produce near neutral (pH 6.7-7.7) Ca-HCO₃ type waters with TDS levels ranging from 300 to 500 mg/L. Since CHS geothermal area waters have relatively low F (1.5-1.8 mg/L) concentrations and are near neutral in pH, these waters might have had limited exposure to felsic volcanic rocks. However, the water isotope composition of the CHS sample ($\delta D = -150\text{‰}$, $\delta^{18}O = -18.6\text{‰}$) falls significantly to the right of the Meteoric Water Line and is consistent with high levels of high-temperature interaction with rocks. This was not the case with the MS sample ($\delta D = -141\text{‰}$, $\delta^{18}O = -18.3\text{‰}$) which lies very close to the Meteoric Water Line, suggesting they followed different pathways in the subsurface.

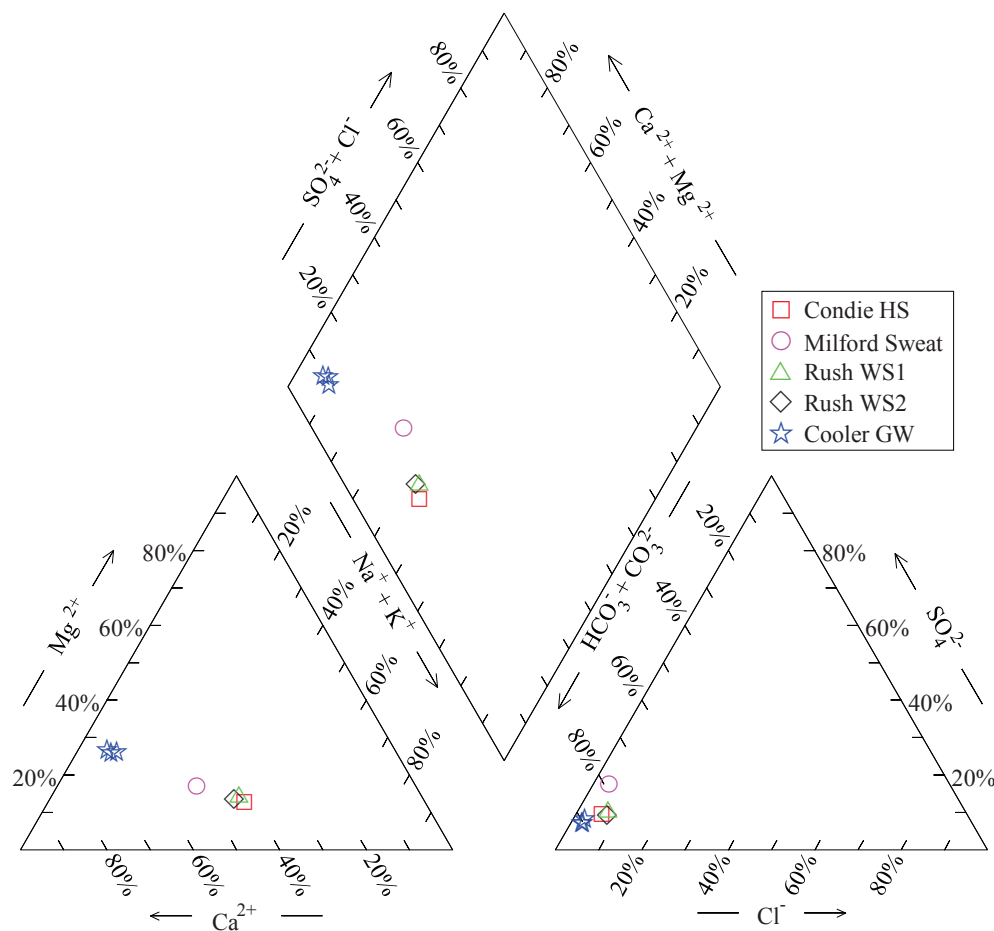


Figure E17. Piper diagram representing chemistry of water samples from Condie Hot Spring area

8.4 Geothermometric results

Reservoir temperature estimates of the CHS area are given in Appendix D. All thermal features in the area resulted in very similar temperature with traditional geothermometers. The quartz (no steam loss), chalcedony, and Na-K-Ca (Mg corrected) temperatures ranges are 71-82 °C, 40-51, and 71-83 °C, respectively. Reservoir temperature estimates with chalcedony geothermometer are similar to the hottest

feature (CHS) in the area. Silica-enthalpy (chalcedony-enthalpy) mixing model using four samples from thermal features and three additional cooler (field temperature 10-15 °C) samples from shallow wells from this area also resulted in reservoir temperature (52 °C) similar to CHS field temperature with essentially no mixing with cooler water. However, quartz-enthalpy mixing model resulted in reservoir temperature of about 100 °C with 50% dilution with cooler water.

Multicomponent geothermometric tool RTest was applied to these water samples using a mineral assemblage consisting of beidellite, calcite, clinoptilolite, chalcedony, illite, and fluorite with three optimization parameters (mass of water, fugacity of CO₂ and temperature). For the optimization of mass of thermal water, a composition of water based on a local groundwater (10.4 °C) was used during RTest modeling. The Milford Sweat hot spring resulted in the lowest (73±9 °C) and Rush Warm Spring¹ resulted in the highest (106±9 °C) reservoir temperatures for the area. The RTest results also indicate that the CHS area thermal features are issuing waters that may have diluted 50- 65% with local groundwater. Sulfate-water oxygen isotope geothermometry for the CHS and MS samples yielded temperatures of 102 and 105 °C, respectively. These temperatures are somewhat higher than the RTest temperatures.

9. Magic Hot Spring

9.1 General

The Magic Hot Spring (MHS) area (Figure 1) is located on the northern margins of the central ESRP near the Camas-Blaine county line, Idaho. It sits at 1470 m above sea level on the edge of the Magic Reservoir approximately 40 km south of Ketchum, Idaho and is located on the eastern end of the Camas Prairie. Until a 79 m deep well (Magic Reservoir Landing Well, MRLW) was drilled for direct heating purpose in 1965, the MHS was issuing 36°C water (Ross, 1970). However, with the operation of well, MHS dried out (Mitchell, 1976). At the beginning, the MRLW was producing water at 66°C, however, the water temperature subsequently increased to 74 °C by 1975 (Mitchell, 1976; Mitchell et al., 1980). The most recent (2014) temperature record for the well is 75 °C.

9.2 Geologic setting

The MHS area consists predominantly of Miocene-Quaternary silicic volcanic rocks and basalt flows. The Pliocene-Miocene Poison Creek Tuff (Tpct) is the uppermost unit in the immediate vicinity of Magic Reservoir and is underlain by the Miocene Tuff of City of Rocks (Tcort), a rhyolite tuff from the Idavada Group (Figure E18). Other rhyolites and basalt flows are abundant in the surrounding areas but are not shown in the cross-section. The Cretaceous Idaho Batholith granitic rocks (Kg) form the basement throughout the region.

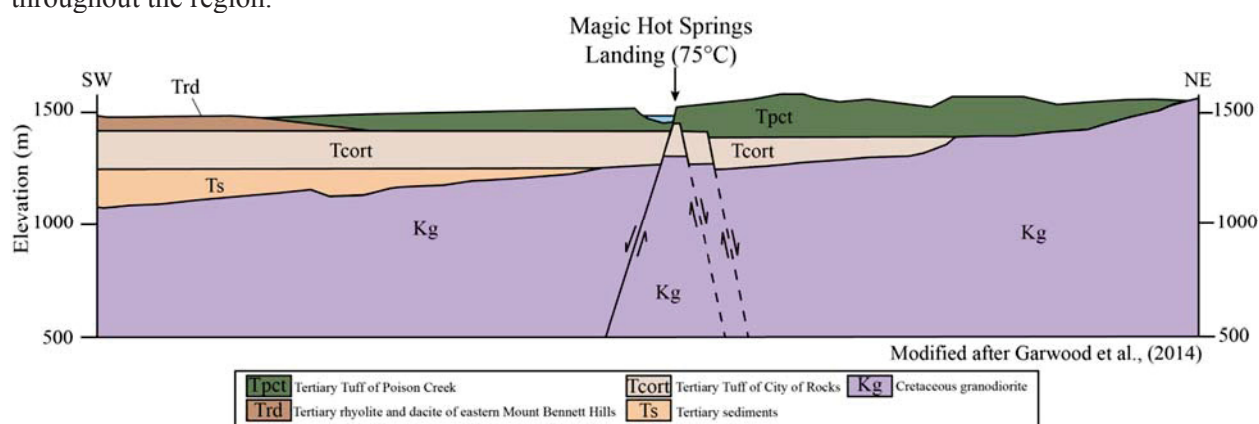


Figure E18. Geologic cross-section of the Magic Reservoir Hot Springs area

Structurally, this area is interesting because of its location at the inter-section of several regional to local geographic and geologic features including the ESRP, Camas Prairies, eastern part of Mt. Bennett Hills, and Idaho Batholith. The MHS area is in a tensional stress regime and includes many high-angle normal faults that create block-faulted configurations (Struhsacker, 1982). Mitchell (1976) recognized two curvilinear features from Landsat false color infrared satellite imagery and discusses their controlling nature in the immediate area. The Magic Reservoir Fault trends northwest and extends the length of the reservoir and into the northern Soldier Mountains. Another fault extends at a slightly less northwest trend along the Clay Bank Hills and intersects the Magic Reservoir fault near the location of the MHS landing well (Malde et al., 1963). Struhsacker et al. (1982) refer to the resulting structure as the Hot Springs Landing horst. These structures are interpreted to have occurred prior to Quaternary volcanism due to the lack of deformation in the flat lying young basalts and sediments. They may also be related to a buried caldera inferred from stratigraphic thicknesses and basalt vent locations in the surrounding regions (Leeman, 1982).

9.3 Water chemistry

Two sets of samples were collected from this well- one sample was directly collected from a shallow leak in the MHS-RLW and another sample collected from a runoff channel (Appendix B). Both of the samples show similar chemical results except for slightly higher pH and lower recorded temperature for the sample collected from runoff channel indicating a higher degree of degassing of CO₂ and cooling. The MHS-RLW produces near neutral (pH 6.79, degassed sample pH 8.61) Na-HCO₃ type water (Figure E19) with higher amount of TDS (1500 mg/L). The well water contains higher concentrations of SiO₂ (103 mg/L) and Cl (75 mg/L).

9.4 Geothermometric results

Reservoir temperatures of the MHS area are given in Appendix D. Quartz (no steam loss), chalcedony, and Mg-corrected Na-K-Ca geothermometers resulted in 139 and 142 °C, and 113 and 116 °C, and 153 and 152 °C with compositions measured in water samples from the well leak and leak runoff channel, respectively. Silica-enthalpy mixing models were applied with compositions measured in water samples from well leak and a well producing cooler groundwater. The runoff channel sample was not considered because of the apparent heat loss. The chalcedony-enthalpy mixing model resulted in 145 °C reservoir temperature with about 50% dilution. Similarly, the quartz-enthalpy mixing model resulted in 181 °C reservoir temperature with about 60% dilution.

The RTest modeling of MHS samples were performed using a local groundwater composition to optimize the mass of water along with two other optimization parameters - fugacity of CO₂ and temperature. A mineral assemblage consisting of beidellite, clinoptilolite, chalcedony, dolomite, and K-feldspar was used. The RTest results (Appendix D) indicate that the MHS geothermal area has a reservoir temperature of about 163 °C. However, the RTest temperature estimate with the runoff water composition is about 10 °C cooler than the temperature estimate with composition water directly collected from the well leak. Similar to the estimated degree of dilution derived from the chalcedony-enthalpy mixing model, the RTest modeling indicates that the MHS-RLW water is diluted by almost 50% with local groundwater.

Sulfate-water isotope temperatures for both the well and runoff samples were quite high at 237 and 233 °C, respectively. Although these temperatures are high, there are other isotope indicators that these samples underwent significant high temperature water rock interaction. The water isotope composition of the well water ($\delta D = -151\text{‰}$, $\delta^{18}O = -16.9\text{‰}$) is significantly shifted off the meteoric water line (the runoff sample was also shifted, but was also clearly evaporated during cooling). In addition, the isotopic composition of dissolved methane in the water ($\delta D = -203\text{‰}$, $\delta^{13}C = -22.0\text{‰}$) is typical of methane produced in a magmatic system, suggesting that these fluids interacted with magmatic rocks at depth.

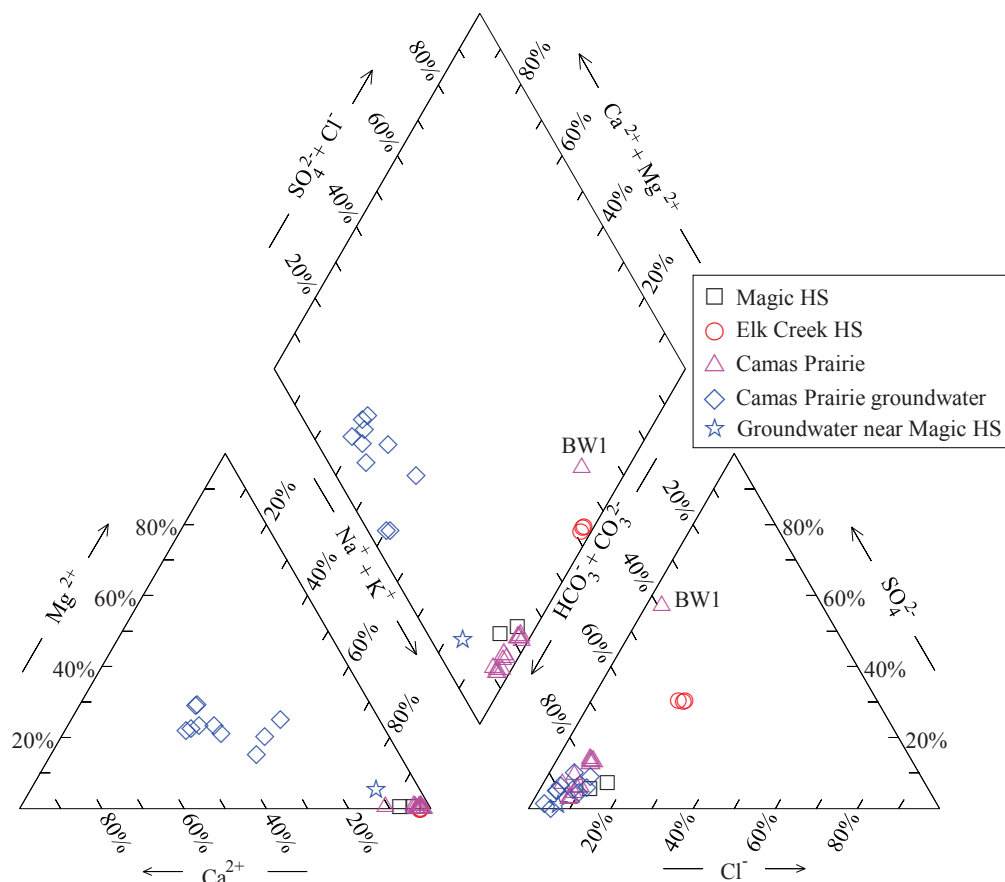


Figure E19. Piper diagram representing chemistry of water samples from Camas Prairies area. Composition of water measured from Barron Well 1 (BW1) has high SO_4 concentration compared to the concentration of SO_4 in all other Camas Prairie samples.

10. Elk Creek Hot Springs

10.1 General

The Elk Creek Hot Springs (ECHS) area (Figure 1) is located in the southern Soldier Mountains near the Elk Creek drainage in Camas County, Idaho. It sits at 1730 m above sea level approximately 15 km northeast of Fairfield, Idaho. There are a series of springs in the area that issue thermal waters from fractures in granitic rock that range in temperature from 45-55°C. Currently, the geothermal resource at this site is not utilized for any commercial activities.

10.2 Geologic setting

The ECHS area is located on the southeastern margin of the Idaho Batholith region near the eastern part of Camas Prairie. Rocks in the area include - Miocene Tuff of Cannonball Mountain Formation (Tcm) of the Idavada Group, Eocene dacite and rhyodacite of the Challis Volcanic Group (Tcvd), a diorite and gabbro unit (Tdg), and the Cretaceous Idaho Batholith granodiorite (Kg) (Garwood et al., 2014). Various Tertiary dacite and rhyolite dikes (Td) are mapped throughout the area intruding into batholith granodiorites and based on local abundance, are inferred in cross-section. Alluvial fan deposits are localized to slopes and valleys.

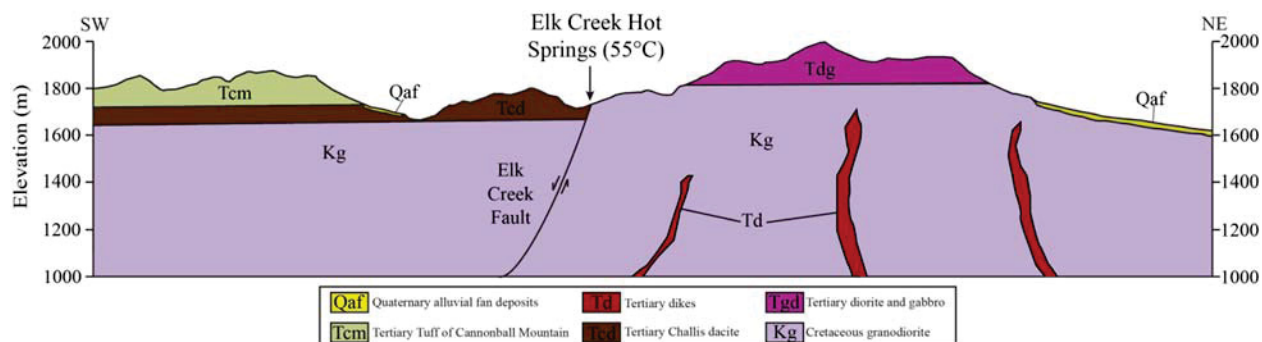


Figure E20. Geologic cross-section through the Elk Creek Hot Springs area

Many NW trending normal faults with orientations similar to Basin and Range extensional structures dominate. Locally, the SW dipping, NW trending Elk Creek Fault extends from the Camas Prairie north into the Soldier Mountains. This fault and associated breccia and gouge facilitate flow from deeply jointed and fractured granodiorite (Figure E20). Also, the presence of numerous dikes in the area represents planes of weakness within the batholith and could be analogous to geothermal flow pathways.

10.3 Water chemistry

In our sampling campaigns, we collected samples from two thermal expressions- ECHS1 and ECHS2 (Appendix B). Previously, Mitchell (1976) reported chemical compositions of three ECHS features. Over time, the compositions and field temperature of water from these hot springs remain unchanged. All ECHS expressions issue alkaline ($\text{pH} \geq 9$), Na-HCO_3 type water at 50-55 °C with TDS about 340 mg/L. Concentrations of Mg, Ca, and K are low compared to the concentration of Na (Figure E19). Concentration of F in these hot springs is very high (>15 mg/L). Generally, alkaline pH and very high F concentration are used as distinct chemical characteristics of waters that interact with Idaho batholith. The F-bearing accessory minerals in the granite/granodiorite of the Idaho batholith (Figure E20) are thought to be the source of unusually high F content in these waters (Mitchell, 1976).

10.4 Geothermometric results

When plotted on Giggenbach diagram (figure not shown), the ECHS samples appear as partially equilibrated waters that may have interacted with reservoir rocks at 120-140 °C (Figure 5). Both ECHS1 and ECHS2 samples result in very similar quartz (no steam loss) (115 °C), chalcedony (86 °C), and Na-K-Mg (99 °C) reservoir temperatures (Appendix D).

The RTest was applied to the ECHS water samples using a mineral assemblage consisting of beidellite, calcite, clinoptilolite, chalcedony, K-feldspar, and paragonite with three optimization parameters (mass of water, fugacity of CO_2 and temperature). Pure water is used during RTest modeling because the water samples from ECHS geothermal area contain very low concentrations of Ca and Mg (major cations in local ground water) indicating that pristine water is diluting the thermal waters. The RTest temperature estimates for the ECHS geothermal are about 125 °C (Appendix D) with almost 50% dilution. A sulfate-water temperature of 136°C was calculated for one the samples.

11. Camas Prairie area

11.1 General

Camas Prairie (Figure 1) is an east-west elongated (about 50 km by 15 km) intermontane valley in Camas and Elmore Counties, Idaho. Besides the Magic Hot Spring and the Elk Creek Hot Springs that are located in the eastern part of Camas Prairie, the area has several other hot springs and hot wells. The Sheep and Wolf Hot Springs (SWHS) are located in the western part of Camas Prairie, about 4 km north

from Hill City in Idaho. These two hot springs, separated by approximately 100 m, sit at 1565 m above sea level and issue hot water at about 50°C. The Wardrop Hot Springs (WHS) (60°C) located near the base of the Soldier Mountains is approximately 10 km northeast from SWHS whereas the Barron Hot Spring (BHS) (73 °C) located near the base of the Mount Bennett Hills (MBH) is approximately 12 km to the southwest from SWHS. Numerous hot wells are located in the vicinity of BHS. Currently, these resources are not used for any commercial activities.

11.2 Geologic setting

Camas Prairie is bounded by the MBH to the south and the Soldier Mountains to the north. The MBH are composed predominantly of Miocene rhyolitic ash flows and lava flows of the Idavada Volcanic Group (Tfv) that overlies Idaho Batholith granodiorite (Kg). Local basalt flows and fluvial/lacustrine sediments are also present. The Soldier Mountains are composed of mostly of Kg with minor amounts of younger intrusives. Camas Prairie is host to an unknown thickness of Quaternary alluvial, fluvial, and lacustrine sediments (Qs) with local lenses of basalt (Qb) encountered in the shallow subsurface (Figure E21).

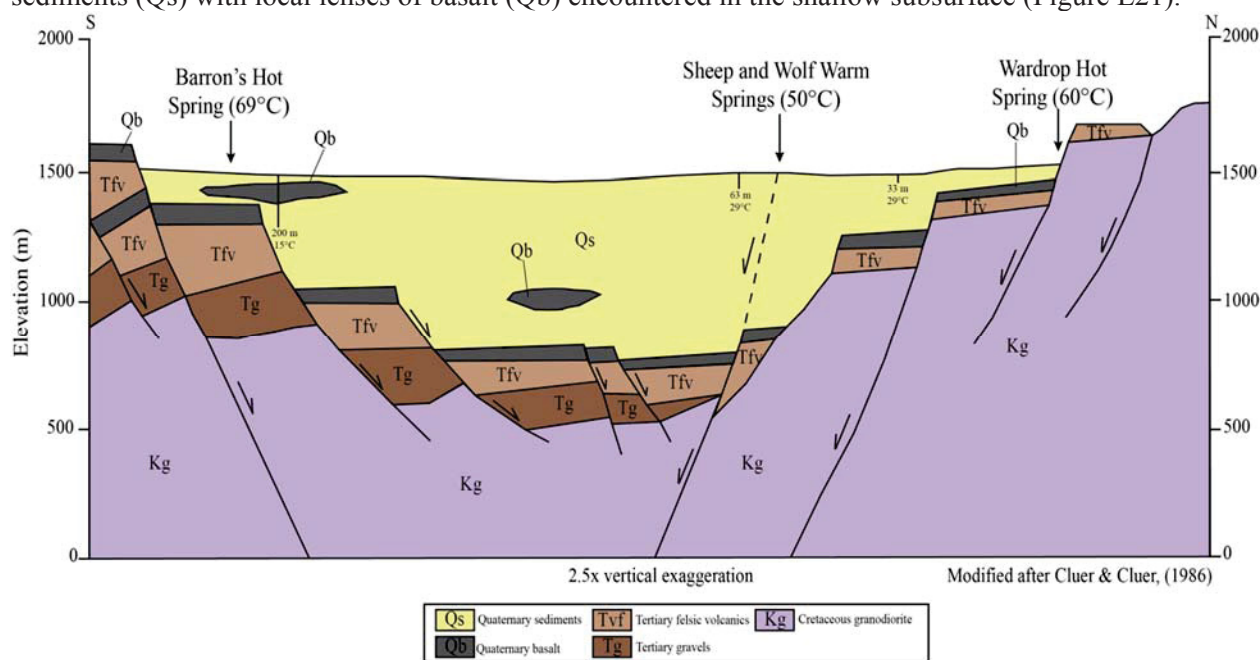


Figure E21. Schematic geologic cross-section of Camas Prairie (after Cluer and Cluer, 1986).

The Camas Prairie experienced north-south extensional tectonics during recent geologic time. Cluer and Cluer (1986) make an argument for a “Camas Prairie Rift” which they believe to have occurred between 2-5 Ma and lasted a relatively short time. The loading and down-warping of the SRP to the south created an extensional regime along the Camas Prairie region that created marginal faulting and development of rift valley separating the SRP from the Idaho Batholith region. Subsequently, basalt and sediment layers filled in the rift valley and shaped the present day Camas Prairie (Figure E21). Although the schematic diagram (Figure E21) shows almost a kilometer of valley-fill sediments at the center of Camas Prairie, preliminary results of the ongoing Snake River Play Fairway Phase II project indicate that the valley-fill sediments may be much thinner (a few hundred meters at the deepest parts). Concerted efforts combining seismic, electromagnetic, and gravity surveys could help define the structural setting of this area. In general, faults that parallel the SRP with opposite senses of displacement are present in the MBH and along the edge of the Soldier Mountains. One of these faults is inferred to be continuous but concealed through the prairie in close proximity to SWHS. The spring waters have likely migrated upward from a deeply buried fracture zone in the granodiorite along this fault. The water could also be under slight artesian pressure because most of the Camas Prairie is below the potentiometric surface (Mitchell, 1976).

11.3 Water chemistry

Besides water samples from MHS-RLW and ECHS, compositions of water measured from several thermal (26-73 °C) and groundwater (10-15.5 °C) sampling features are assembled for Camas Prairie (Appendix B). All thermal waters except Barron Well 1 (BW1) are of Na-HCO₃ type water (Figure E19). The BW1 sample is Na-SO₄ type that contains unusually high concentration (210 mg/L) of SO₄. Thermal water samples in Camas Prairie can be separated into two groups. The first group of samples is collected from the hot springs located in the northern parts of Camas Prairie. These hot springs include Wardrop, Hot Spring Ranch 1-3, Wolf, and Sheep (Figure E21). These hot springs issue waters with high pH (9.0-9.9), relatively low level of TDS (220-350 mg/L), low concentrations of both Ca and Mg, and intermediate concentration of F (1.9-3.7 mg/L). The second group of samples is collected from the hot springs and wells located in the southern parts of Camas Prairie. The notable sampling features of this group are Barron Hot Springs and wells (Figure E21). These samples are near-neutral to slightly alkaline (pH 7.4-8.5) with slightly higher level of TDS (380-640 mg/L), low concentration of Mg, and high concentration of F (7-13 mg/L).

The majority of groundwater samples in Camas Prairie are of Ca-HCO₃ type; however, Na-HCO₃ type groundwater samples are not uncommon in the area (Figure E19). In general, the Camas Prairie groundwater samples have near neutral pH (6.9-8.4), low level of TDS (125-270 mg/L), higher concentrations of Ca and Mg, and low concentrations of F (<0.8 mg/L).

11.4 Geothermometric results

All Camas Prairie thermal water samples provide similar reservoir temperatures with the same traditional geothermometers (Appendix D). The quartz, chalcedony, and Na-K-Ca geothermometers results in temperature estimates in the range of 103-128, 74-99, and 70-124 °C, respectively. Despite the similar temperature estimates with traditional geothermometers, the silica-enthalpy model was applied separately to water samples from the northern and central-southern parts of Camas Prairie. Nevertheless, both groups result in similar temperature estimates with chalcedony-enthalpy (126-133 °C) and quartz-enthalpy (162-173 °C) models.

The RTest was applied to Camas Prairie thermal water samples using a mineral assemblage consisting of calcite, clinoptilolite, chalcedony, fluorite, and K-feldspar. Analcime was added to the mineral assemblage while running RTest for northern area samples whereas beidellite was added to the mineral assemblage while running RTest for southern area samples. All RTest runs were performed with three optimization parameters (mass of water, fugacity of CO₂ and temperature) using pure water as an end member cooler water while optimizing the mass of thermal water. Unlike the traditional geothermometers and mixing models, RTest temperature estimates of Camas Prairie area samples show bimodal distribution- higher temperatures for the samples from northern parts and lower temperatures for the samples from southern parts (Appendix D). The RTest reservoir temperature estimates for hot springs in the northern part are 181-204 °C with dilution up to 75% whereas RTest reservoir temperature estimates for hot springs and wells in the southern parts are much cooler at 79-108 °C with negligible dilution. Sulfate-water oxygen isotope temperatures for a sample from Wardrop Hot Spring of the northern Camas Prairie and the Barron Well of the southeastern Camas Prairie yielded temperatures of 133 and 419°C, respectively. The Barron Well temperature exceeds the effective range of the geothermometer, but does indicate a very high temperature source for the sulfate. This is supported by the δ³⁴S of the sulfate, which at -8.3‰ was by far the lowest of any of the measured samples. This is very low value for the sulfate usually indicates that it is formed from oxidation of pyrite, suggesting it might be a reliable indicator of formation in a hydrothermal system. In addition to the high sulfate-water oxygen isotope temperature, the isotopic composition of the water is shifted off the meteoric water line indicating the possibility of high temperature water-rock interaction. The Wardrop Hot Spring temperature is lower than the RTest

temperatures, but that sample had a very low concentration of sulfate and could have been compromised (see Appendix C).

The chemical compositions of thermal waters indicate that the northern and central-southern parts of the Camas Prairie have different hydrogeological and geochemical settings at depth. In general, both surface and subsurface waters of the Camas Prairie area flow from west to east to the Big Wood River and ultimately to the Magic Reservoir (Wallace, 1972). Precipitation falling in the Soldier Mountains to the north provides the majority of recharge water to the northern Camas Prairie groundwater/geothermal systems. The thermal water that moves up along the range forming faults near/along the northern boundary of the Prairie is significantly diluted with pristine water that several south flowing creeks from the mountains bring in to the Prairie. On the other hand, the MBH to the south offers only minor recharge to the Camas Prairie. Unlike the northern part of the Prairie, the groundwater/geothermal aquifers in the southern parts the Prairie are likely to have longer residence times. Although a long residence time results in higher field temperatures (the hottest hot spring in the area is Barron Hot Spring II with a reported temperature of 73 °C, Mitchell, 1976), it also helps re-equilibrate the thermal water at lower temperature. Because of the structural and hydrogeological controls, the hot springs in the northern parts of the Prairie are issuing diluted thermal water whereas the sampling features in the southern part are issuing re-equilibrated water. The RTest results also support this argument. Despite the cooler temperature estimates for the southern part, this part of the Camas Prairie is likely to have similar geothermal resources at depth as the northern parts of the Camas Prairie. This is consistent with the high temperature calculated with from the sulfate-water oxygen isotope temperature, which would not be strongly impacted by equilibration with the rock as it moved to the surface.

12. South Mount Bennett Hills

12.1 General

Several hot springs are located along the southwestern-southern base of the MBH (Figure 1) in Elmore, Gooding, and Lincoln Counties in Idaho. Some of the known hot springs in the area are the Prince Albert (Coyote) (PAHS, 57.7 °C), Latty (LHS, 65 °C), and White Arrow (WAHS, 65 °C). Another hot spring (named Hot Spring) is located further to the west, but is reportedly dried out recently. Similarly, some hot wells [e.g., Northwest Pipeline (38 °C), Dave Archer (43 °C), Shannon (47 °C), etc.] are also reported from this area. The Bostic 1-A well (2950 m) drilled to the south from this area indicated the presence of hot rock (Arney et al., 1982). Presence of several hot springs and hot rock at depth suggests that the areas along the southern base of the MBH have great potential for geothermal resources. However, except for WAHS and LHS, none of the other resources in the area have been used for any commercial purpose. The WAHS has been used for heating greenhouses and LAHS is currently being used for space heating by local ranchers.

12.2 Geologic setting

This geothermal area extends over 70 km along the northern margins of the SRP (some parts of both WSRP and ESRP) abutting the MBH. A geologic cross-section shown in Figure E22 is constructed for the western part of the area near LHS and PAHS. Rocks underlying the LHS area mainly consist of mafic and felsic volcanic rock with thick sequences of sediments and gravels. The MBH to the north consists of predominantly of Miocene rhyolitic ash flows and lava flows of the Idavada Volcanic Group (Tir) that overlie the Idaho Batholith granodiorite (Kg). At the base of the MBH, the WSRP basalt flows are intercalated with quaternary sediments (Qs) from the Pleistocene-Pliocene Lake Idaho and the Tertiary Glenn's Ferry Formation (Tgf) sandstones and shales. At depth, an older basalt unit (Banbury basalt, Tbb) and Idavada volcanics are reported from a 2950 m deep oil and gas wildcat well (Bostic 1-A, Arney, 1984). Although, not penetrated, Kg is inferred to make up the basement underlying the WSRP.

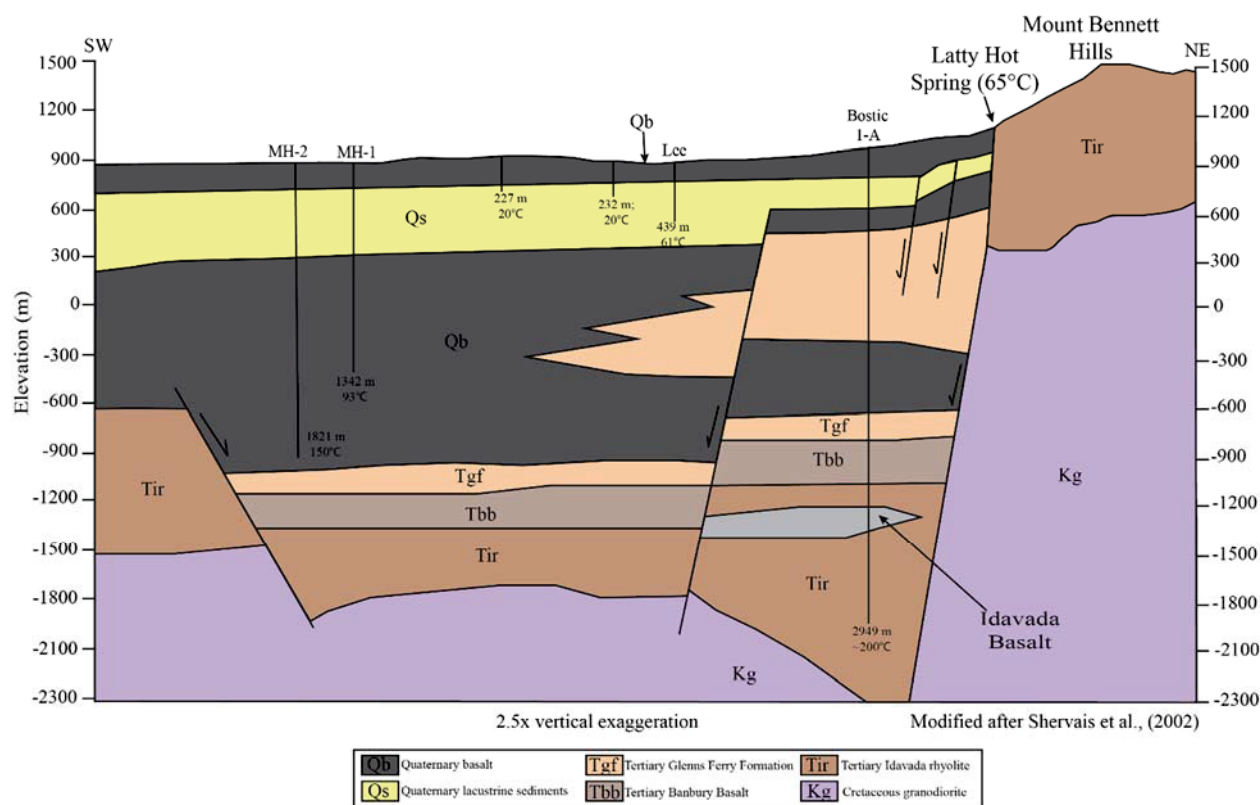


Figure E22. Geologic cross-section through the WSRP and Latty Hot Springs area along with three deep geothermal wells (MH-1, MH-2 and Bostic 1-A) (modified from Shervais et al., 2002).

Regionally, extensional tectonics dominate with many high-angle northwest trending normal faults that parallel the WSRP and dip to the southwest. These are responsible for the uplift of the MBH and have a cumulative throw along the major range-front fault of approximately 2900 m based on the presence of Idavada volcanics in the Bostic 1-A well (Arney et al., 1984). The hot springs in the area are mostly distributed along the base of the MBH whereas hot wells are distributed further south from the base of the MBH. The range-front fault(s) and associated fracture zones are most likely facilitating fluid flow from deep circulation in the batholith to the surface as hot springs. The hot water wells further south are likely tapping water that flow and is potentially re-equilibrated in the basalt and sediment layers.

12.3 Water chemistry

During our sampling campaign, we collected and analyzed three samples from the PAHS, LHS, and WAHS. Similarly, the compositions of thermal waters measured from hot wells from this area are assembled from Young and Mitchell (1973) (Appendix B). The water compositions assembled for this area given in Appendix B. Thermal waters from this area are neutral to slightly alkaline in pH (7-9.4) with TDS range 270-720 mg/L. All thermal waters are Na-HCO₃ type water with field temperature in the range of 26.5-68 °C. In general, these water samples share low concentrations of Ca, K, Mg, and Cl, and higher concentrations of Na and SiO₂(aq). However, they have variable F concentration. Specifically, the hot spring waters and a few hot well waters are low to moderately high (1-12 mg/L) in concentration of F whereas the majority of the hot wells have very high F concentrations (13-20 mg/L). The high F waters are at or near saturation with fluorite at their field temperatures.

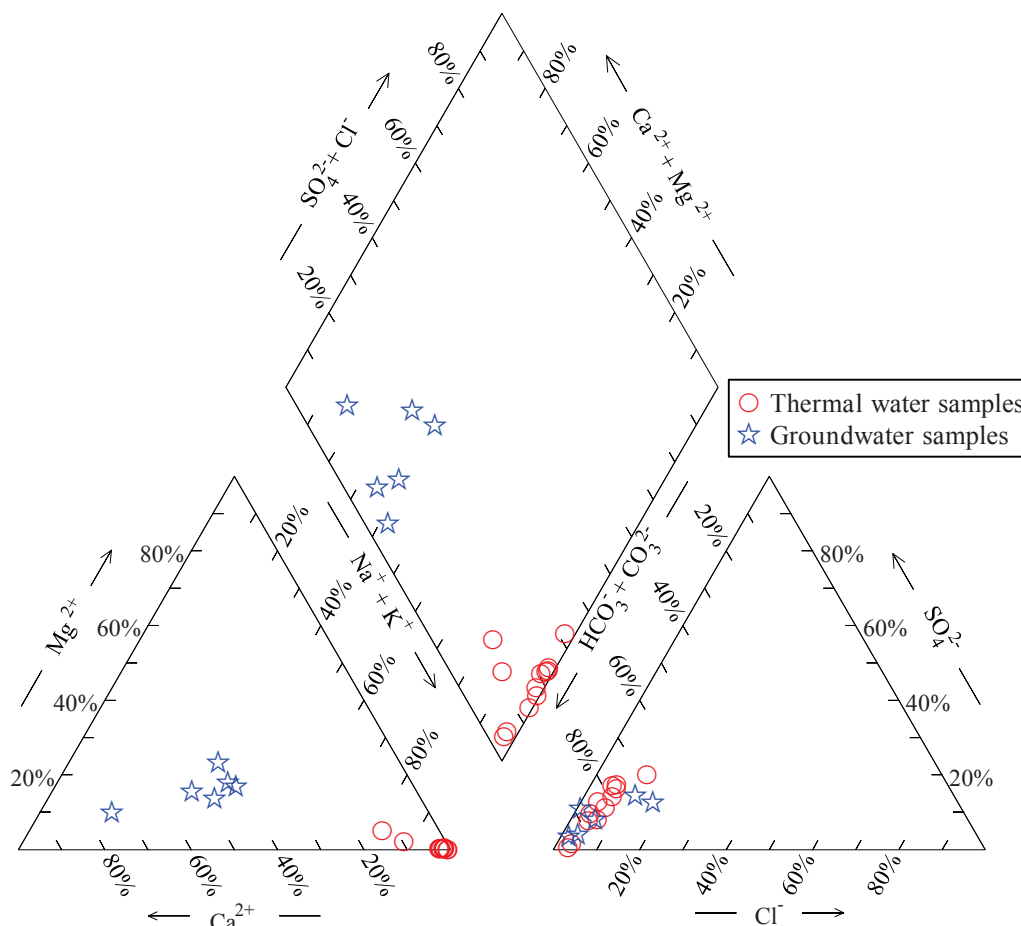


Figure E23. Piper diagram representing chemistry of water samples from Camas Prairies area.

12.4 Geothermometric results

Reservoir temperature estimates for this area calculated from several water samples are given in Appendix D. Quartz, chalcedony, and Na-K-Ca geothermometers resulted in 110-143, and 80-117, and 72-160 °C, respectively. The PAHS and LHS resulted in highest temperatures for the area with these traditional geothermometers. Silica-enthalpy mixing models with chalcedony and quartz solubility curves resulted in 150 and 182 °C temperature estimates for the area.

RTEst temperature estimates for the area are developed using two separate mineral assemblages – one for the hot spring (and Shannon Well) waters and another for hot well waters. For hot springs, a mineral assemblage consisting of calcite, chalcedony, chlorite, clinoptilolite, K-feldspar, and phengite was used, whereas for hot wells, a mineral assemblage consisting of calcite, chalcedony, clinoptilolite, K-feldspar, kaolinite, and beidellite was used. As with the traditional geothermometers, the RTEst modeling of waters from hot springs yielded higher temperatures. The three hot springs in the area, PAHS, LHS, and WAHS resulted in reservoir temperatures at 193 ± 8 , 197 ± 5 , and 177 ± 6 °C, respectively. A sulfate-water oxygen isotope temperature of 154°C was calculated for PAHS which is lower than the RTEst temperature, but still relatively high. Similarly, RTEst temperature estimate for Shannon well is 137 ± 10 °C. All the other wells resulted in lower reservoir temperatures (82-122 °C). The reservoir temperature estimates using hot spring waters are similar to the bottom hole temperature (~200 °C, Arney et al., 1984) measured in Bostic 1-A Well. It is likely that these hot springs are issuing deep thermal waters that ascent along the range forming faults. Along the flow path, these deep thermal waters get mixed with dilute water. RTEst results indicate that the hot spring waters are issuing diluted (up to 70%) thermal waters. On the other hand, the

hot wells are producing re-equilibrated or low-temperature equilibrated waters with small (<20%) or negligible dilution.

13. Glenns Ferry area

The Glenns Ferry area is located at the junction between ESRP and WSRP in southern Idaho (Figure 1). The prospect is an elongate area along the Interstate 84 from King Hill to Hammett covering Glenns Ferry town in Elmore County, Idaho. The presence of a few shallow hot wells in the area were noted in earlier previous reports. The hottest feature in the area is the Johnston well which produces water at 39 °C. Besides this feature, we sampled two additional shallow hot wells during our sampling campaign. In addition, chemical data for two additional wells were taken from previous reports (e.g., Young and Mitchell, 1973).

The shallow hot wells (32.5-39 °C) of this area are producing near-neutral to slightly alkaline (pH 7.64-9.26) Na-HCO₃ type waters. The Glenns Ferry area water samples contain very minute amounts of Mg, and consequently, these samples plot as partially equilibrated waters on Giggenbach diagram (see Figure 5 of the report). Some samples also contain a large amount of F that indicates that presence of volcanic ash/rhyolite rocks in the reservoir. One of the samples contains a large amount of NO₃, which indicates surface water contamination of well water.

Reservoir temperature estimates with traditional as well as RTest (Appendix D) geothermometric approaches indicate a moderately hot geothermal system in the area. Temperature estimates with quartz, chalcedony, and Na-K-Ca geothermometers are 80-109, 48-79, and 74-138 °C, respectively. Silica enthalpy mixing models using chalcedony and quartz solubility curves yield reservoir temperatures of about 108 and 150 °C, respectively. The RTest reservoir temperatures (67-85 °C) of the Glenns Ferry samples are within the range of temperature estimates of the traditional geothermometers. Two samples were collected for isotope analyses, but the sulfate concentrations were too low for calculating temperatures.

14. Banbury Hot Springs-Twin Falls area

The southwestern periphery of the ESRP near Twin Falls and Buhl is one of the Known Geothermal Resource Areas in southern Idaho (more detailed information can be found in Appendix J). The area is comprised of two dense clusters of geothermal surface features, Banbury Hot Springs (BHS in Figure 1) and Twin Falls (TF in Figure 1). Discharging thermal waters range in temperature from 25 °C to 70 °C. These thermal waters are being used for space heating, agriculture, and recreation.

The Tertiary rhyolitic volcanic rocks underlie the Quaternary and Tertiary basaltic units in these prospect areas. Paleozoic metasedimentary rocks are thought to underlie the entire area (Lewis and Young, 1989). The thermal aquifer system in the area is located beneath basalt units within the Idavada volcanics and is under artesian conditions with the temperatures of the waters increasing to the northwest. Thermal waters (Appendix B) are thought to originate from deep circulation paths from the Cassia Mountain recharge zone to the south through fractures in the overlying basalts of the thermal area (Street and DeTar, 1987).

Reservoir temperature estimates obtained with traditional geothermometers and RTest are given in Appendix D for both the Banbury Hot Springs and Twin Falls prospects. The highest reservoir temperatures (ca. 160 °C) for the Banbury Hot Springs prospect are obtained for Banbury Hot Spring, Miracle Hot Spring well, and Salmon Falls Hot Spring with RTest as well as other geothermometers. Sulfate-water oxygen isotope temperatures calculated for the Banbury samples range from 115 to 159 °C and are very similar to the RTest temperature. For the Twin Falls prospect, the highest reservoir temperatures (ca. 135 °C) are obtained for samples from two hot shallow wells (used for direct heating – Neely, 1996) within the premises of the College of Southern Idaho. A sulfate-water isotope temperature for one of College of Southern Idaho waters was 133 °C.

15. Cedar Hill area

A series of shallow hot wells and a hot spring (Nat-So-Pah) located on the northern to northwestern base of the Cassia Mountains from Artesian City-Rock Creek (in Cassia County) to Hollister (in Twin Falls County) are grouped in the Cedar Hill geothermal prospect (Figure 1). The Hollister area contains the Nat-So-Pah Hot Spring and a few hot (32-38 °C) shallow (65-180 m) wells. Additional shallow wells near towns of Rock Creek and Artesian City have also encountered hot water. The chemical compositions of thermal waters from this prospect were taken from previous reports/papers (e.g., Ross, 1970; Young and Mitchell, 1973; Mitchell et al. 1980).

Geologically, all sampling features from this prospect are located in areas with or without thin basaltic and rhyolite surface layers. The basement rocks for all these wells are the Paleozoic marine limestone, dolomite, siltstone, quartzite, and chert that are exposed in the Cassia Mountains. The area has several NE dipping faults. The Nat-So-Pah Hot Spring is located along a NE-SW fault east of Hollister. Furthermore, a NW-SE striking (NE dipping) fault may have intersected the NE-SW fault at this hot spring. An unnamed well located northeast of Hollister likely intersects the NW-SW fault at depth. The wells near Rock Creek and Artesian City are located at the NW terminals of NW-SE faults that are mapped in the Cassia Mountains and likely to have plunged down to the Quaternary sediments.

Compositions of all thermal waters of this prospect are given in Appendix B. In general, thermal waters of this prospect are neutral (pH 6.6-7.6) Ca-HCO₃ or Na-HCO₃ type. Specifically, the hot spring and a nearby unnamed well produce Na-HCO₃ type water. However, concentrations of silica in these two water samples are relatively low compared to other three Ca-HCO₃ type water samples.

Geothermometric results for these water samples are given in Appendix D. The reservoir temperature estimates range from 75 to 127 °C, 62 to 116 °C, 29 to 87 °C, and 50 to 73 °C with RTEst, quartz, chalcedony, and Na-K-Ca-(Mg) geothermometers, respectively. No isotope samples were taken from these thermal features.

16. Murphy Hot Spring

The Murphy Hot Spring (MHS) geothermal prospect (Figure 1) is located in southeastern part of Owyhee County along the East Fork of the Jarbidge River in southern Idaho near its border with Nevada. The small unincorporated town Murphy Hot Spring is the only nearby establishment in the area. A road (Three Creek Road) links this small town to Rogerson, Idaho and Jarbidge, Nevada. Currently, the hot spring is used as a recreational facility for local people and campers.

Geologically, the MHS area is located within the Bruneau-Jarbidge super volcanic field associated with the past (11-13 Ma) Yellowstone hotspot activities (Pierce and Morgan, 1992; Beranek et al., 2006). The hot spring sits in rhyolite lava flows and ignimbrites produced from the Bruneau-Jarbidge eruptive center. The Basin and Range type extensional post-volcanic tectonics has been active in the area creating several NW-SE trending normal faults. A N-S fault that passes through the MHS area (Rember and Bennett, 1979) may provide the subsurface plumbing for the hot spring.

For geothermometric calculations, the composition of the MHS water (Appendix B) was obtained from Young and Lewis (1982). The hot spring issues near-neutral (pH 8.5) Na-HCO₃ type water at about 55 °C. The reservoir temperature estimates with quartz, chalcedony, and Na-K-Ca geothermometers are 148, 122, and 62 °C, respectively. The RTEst results for this hot spring indicate a reservoir temperature estimates about 117 °C (Appendix D).

17. Oakley Hot Spring

The Oakley Hot Spring geothermal prospect (Figure 1) is located near town of Oakley in Cassia County, Idaho. The prospect area extends to the south from the Oakley Fan along the southern margins of the SRP

in the Goose Creek basin, a down-dropped basin surrounded by the Albion Mountains-Middle Mountains to the east and Cassia Mountains to the west.

Previously, the USGS performed reconnaissance drilling (95-197 m) and conducted a geological investigation for coal and uranium-bearing lignite beds in this area (Hilderbrand, 1983). Using previously available regional information (e.g., Mapel and Hail, 1959; Axelrod, 1964), Hildebrand (1983) suggested a general stratigraphy for the area with the Idavada Volcanics containing shale, tuff, and lacustrine sediments underlain by Tertiary rhyolite and Paleozoic meta-sediments. The geologic map of Cassia County Idaho compiled by Link (2002c) shows several intersecting normal faults in the region of these geothermal features that may have provide flow paths for the hot water to the surface (e.g., Oakley Hot Spring) and shallow wells (e.g., Richard Austin well and others).

Three thermal features (one hot spring and two wells) in this area were sampled for this study. In addition, water compositions from two additional shallow wells in the area were taken from the literature. All water compositions for the thermal features in this prospect are given in Appendix B. The hot spring and wells in this area issuing Na-HCO₃ (or Na-Cl-HCO₃) type waters with neutral to slightly alkaline pH (7.85-9.32) and temperatures ranging from 31-47 °C. Geothermometric results (Appendix D) of these water samples indicate moderately hotter reservoir temperatures. Quartz and chalcedony geothermometers indicate temperatures in the range from 77-125 ° and 45-97 °C, respectively. Mg-corrected Na-K-Ca temperatures show a much wider range of temperatures (45-155 °C). Sulfate-water oxygen isotope and RTest multicomponent geothermometers resulted in reservoir temperature estimates in the range of 92-157 °C and 77-130 °C, respectively.

18. Durfee Hot Spring

The Durfee Hot Spring (DFS) geothermal prospect is also located at Almo in Cassia County, Idaho (Figure 1). This hot spring has been in use for recreational purposes since the early 1900s. Geologically, the hot spring is located along a fault at the southeastern base of the Albion Mountains (Link, 2002c). The reservoir rock is likely to be the metamorphosed quartz monzonite rocks of the Archean basement underneath the Quaternary valley (basin) fill sediments.

During our sampling campaign, the DFS was sampled and analyzed. Similarly, the composition of water from a nearby well (Harold Ward well) was obtained from Young and Mitchell (1973). Both of these features produce near neutral (pH 7.4-8.8) Na-Cl-HCO₃ type water at 38-45 °C (Appendix B). Geothermometric reservoir temperature estimates for the hot spring are 117, 88, 80, 104, and 138 °C with quartz, chalcedony, Na-K-Ca (Mg-corrected), sulfate-water oxygen isotope, and RTest multicomponent geothermometers, respectively. The reservoir temperature estimates from the well water composition are cooler than temperature estimates for the hot spring (Appendix D).

19. Marsh Creek area

The Marsh Creek geothermal prospect is located to the east of Burley in Cassia County, Idaho (Figure 1). The area covers both sides of the northern end of the Cottrell Mountains. Two hot springs (Marsh Creek Hot Springs and Marsh Gulley Hot Springs) and some shallow hot wells Ross (1970) are located in the western part of the area. In the report, Ross (1970) refers this area as the Albion Basin (prospect). The eastern part of the area (eastern side of the Cottrell Mountains) is also characterized by the presence of several shallow wells that produce hot water.

Geologically, this area consists of three formations- Quaternary sediments, the Salt Lake Formation (ash, tuff, conglomerate, sand, clay, and marl), and Precambrian basement rocks. The Cottrell Mountains is a faults-bounded horst (Link, 2002c), and the thermal activities in the area may be related to the fluid movement along these faults.

During our sampling campaign, we collected water samples from two wells- one on each side of the Cotterel Mountains. We were not able to collect water samples from the hot springs reported to be present in this area by Ross (1970), but water chemistry data for four additional shallow hot wells were obtained from literature. All of these composition data are given in Appendix B. Thermal wells in this area produce near neutral (pH 7.6-8.3), Na-HCO₃ type water at temperatures up to 60 °C. The reservoir temperature estimates (Appendix D) with geothermometers quartz, chalcedony, and Na-K-Ca range from 96-113 °C, 66-83 °C, and 48-89 °C, respectively. Similarly, a sulfate-water oxygen isotope temperature for a sample from the Marsh Creek well was calculated to 142 °C. RTest temperature estimates range from 96 to 141 °C. It is likely that the western part of the prospect may have geothermal system with reservoir temperature as high as 140 °C.

20. Wybenga Dairy area

The Wybenga Dairy prospect is located west of Burley on the southern side of the Snake River in Cassia County, Idaho (Figure 1). We sampled the Wybenga Dairy well (34 °C) for this study. The Kimberley hotspot well (Shervais et al., 2013, 1958 m) was located about 26 km west from Wybenga Dairy area in a similar geologic setting. Shervais et al. (2013) reported that the areas around Kimberley (including Wybenga Dairy) lie on the southern margin of the Twin Falls eruptive complex. The lithologic logs recorded for the Kimberley well show pre-dominantly rhyolite lava and welded ash flow tuffs beneath the surface basalts and sediments. The temperature measurements made during drilling of this well indicate an isothermal zone with temperatures between 55-60 °C from 400 m to bottom of the well (Shervais et al., 2013). No hot springs have been reported in this area, but several hot shallow wells are present to the southwest (>13 km) of this area near the base of the Cassia Mountains (these features are included in Cedar Hill prospect).

The Wybenga Dairy well produces near neutral (pH 7.45), Ca-HCO₃ water (Appendix B). The reservoir temperature estimates with quartz, chalcedony, Na-K-Ca, and RTest geothermometers are 118, 89, 189, and 132 °C, respectively (Appendix D). An unpublished RTest temperature for a water sample from the Kimberley well was 137 °C. However, as mentioned above, the highest measured temperature in the Kimberley well was about 60 °C. Therefore, we believe it is likely that there is hotter reservoir in this part of the ESRP at > 2 km depth.

21. Indian Hot Spring

The Indian Hot Springs (IHS) area is located south of American Falls in Power County, Idaho (Figure 1). This area is reported to have two hot springs, each discharging just under 3785 L/min (Ross, 1970). Ross (1970) also mentioned the presence of additional warm shallow wells in the area. However, during our sampling campaign, we collected water sample only from the main hot spring of the area that is currently used to fill a recreational pool.

Figure E24 shows the simplified geologic cross-section of the IHS area. Quaternary basalts cover the area, but underneath the basalt lie 400-600 m of the Tertiary Starlight and Salt Lake Formations consisting of sediments and ash deposits. Paleozoic rocks underlie these rocks. Ross (1970) shows two west dipping normal faults in the area. The subsurface plumbing of the IHS system seems to be controlled by the western normal fault (Figure E24).

The IHS issues neutral (pH 7.23), Na-Cl-HCO₃ type water at 33 °C (Appendix B). Several geothermometers are used to estimate reservoir temperatures. All geothermometers but sulfate-water oxygen isotope geothermometer, which resulted in about 174 °C, yielded potential reservoir temperature <80 °C (Appendix D).

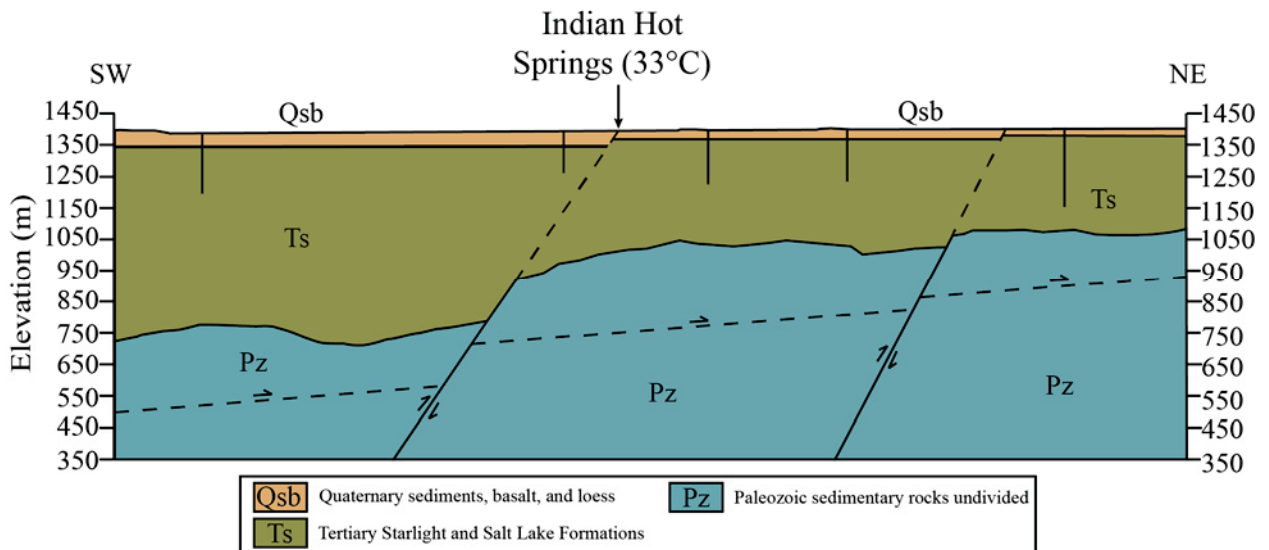


Figure E24. Generalized geologic cross-section through the Indian Hot Springs area, south of American Falls in Idaho

22. Tyhee area

This area is located near the small town of Tyhee, north of Pocatello, in Bannock County, Idaho. The prospect area (Figure 1) extends further to the north into the Fort Hall Indian Reservation along Interstate Highway 15. Earlier, Ross (1970) reported the presence of some hot shallow wells in the area, including the Fort Hall well, which produces water at 41 °C. Similarly, within the Tyhee town, two warm (21-25 °C) wells (Robert Brown well 1 and 2) are reported by Young and Mitchell (1973).

The area around Tyhee and Fort Hall is covered by young ESRP flood basalts (of unknown thickness) that are likely underlain by rhyolite and ash-tuff deposits. Geologically, the hottest well (Fort Hall thermal well) in the area is located at the northwestern base of the Pocatello Range. However, no fault is mapped between the Pocatello Range and the ESRP rocks (Bond et al., 1978; Lewis et al., 2012).

For this project, we collected samples from the hottest well in the area. Chemical data for samples from two other wells were obtained from Young and Mitchell (1973) (Appendix B). Geothermometers applied to these chemical data indicate a moderately hot (up to 93 °C) reservoir temperature for this geothermal system (Appendix D).

23. Quidop-Yandell Warm Springs

The Quidop-Yandel prospect (Figure 1) is located southeast of Blackfoot in Bingham County, Idaho. The area has several warm/hot springs with temperatures ranging from 21 to 38 °C. The Yandell Warm Spring (YWS) system has been sampled multiple times over the years. However, the thermal resource in the area has never been used.

The area is covered by thin layers of the Quaternary loess deposits (Trimble, 1982). Underlying the loess deposits are Paleozoic sedimentary rocks. An inferred fault shown in the cross-section (Figure E25) likely controls fluid movement to the YWS and other springs in the area.

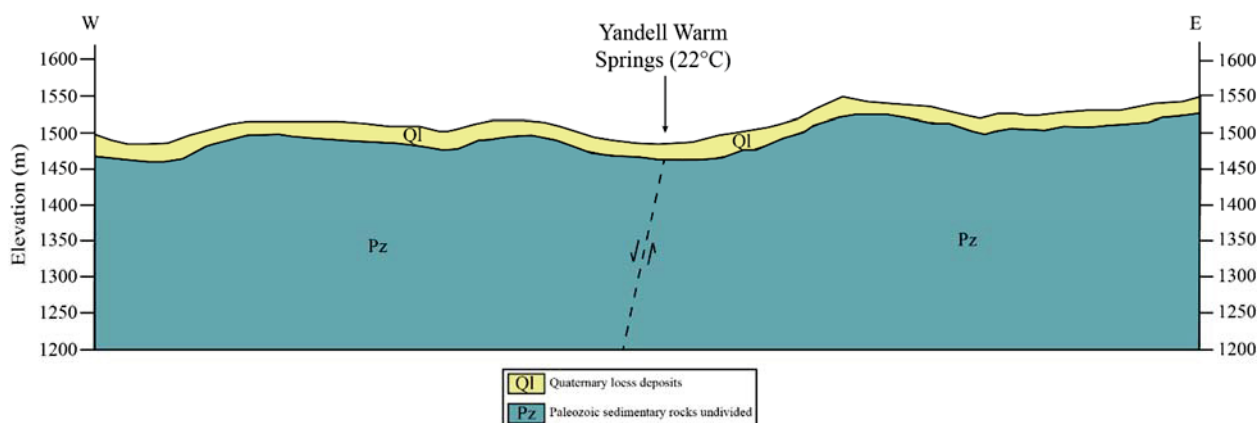


Figure E25. Generalized geologic cross-section through the Yandell Warm Spring area, southwest of Balckfoot, Idaho.

During our sampling campaign, we were able to collect samples from three thermal features (YWS and two Quidop springs) in the area. Similarly, water chemistry data for an additional feature (Alkali Flat Warm Spring) were obtained from Mitchell et al. (1980). All water compositions are given in Appendix B. The RTest multicomponent chemical geothermometric approach resulted in a moderately hot (59-90 °C) reservoir temperature for the area. Other traditional geothermometers applied to this area water samples resulted in low temperature (23-63 °C) estimates (Appendix D).

References

- Allmendinger, R.W., 1982. Sequence of late Cenozoic deformation in the Blackfoot Mountains, Southeastern Idaho. In: Bonnicksen and R.M. Breckenridge, eds., *Cenozoic Geology of Idaho*. Idaho Bureau of Mines and Geology Bulletin 26, p 505-516.
- Anders, M. H., Rodgers, D. W., Hemming, S. R., Saltzman, J., DiVenere, V. J., Hagstrum, J. T., Embree, G. F., and Walter, R. C., 2014. A fixed sublithospheric source for the late Neogene track of the Yellowstone hotspot: Implications of the Heise and Picabo volcanic fields. *Journal of Geophysical Research: Solid Earth*, 119, 2871–2906.
- Arney, B., 1982. Evidence of former higher temperatures from alteration minerals, Bostic 1-A well, Mountain Home, Idaho. *GRC Transactions*, 6, 3-6.
- Arney, B. H. and Goff, F., 1982. Evaluation of the hot-dry-rock geothermal potential of an area near Mountain Home, Idaho. LA-9365-HDR, Los Alamos National Laboratory.
- Arney, B.H., Gardner, J.N., Belluomini, S.G., 1984, Petrographic analysis and correlation of volcanic rocks in Bostic 1-A well near Mountain Home, Idaho, LA-9966-HDR, Los Alamos National Laboratory.
- Arnórsson, S., 1985. The use of mixing models and chemical geothermometers for estimating underground temperature in geothermal systems. *J. Volc. Geotherm. Res.*, 23, 299-335.
- Arnórsson, S., Gunnlaugsson, and Svavarsson, H., 1983. The chemistry of geothermal waters in Iceland. III. Chemical geothermometry in geothermal investigations. *Geochim. Cosmochim. Acta*, 47, 567-577.
- Axelrod, D. I., 1964. The Miocene Trapper Creek flora of southern Idaho. University of California, Publications in Geological Sciences, 51, 148 p.
- Beranek, L. P., Link, P. K., & Fanning, C. M., 2006. Miocene to Holocene landscape evolution of the western Snake River Plain region, Idaho: Using the SHRIMP detrital zircon provenance record to track eastward migration of the Yellowstone hotspot. *Geological Society of America Bulletin*, 118(9-10), 1027-1050.

- Blackwell, D.D., Kelley, S., and Steele, J.L., 1992. Heat flow modeling of the Snake River Plain, Idaho. US Department of Energy Report for contract DE-AC07-761DO1570, 109.
- Bond, J. G., Kauffman, J. D., Miller, D. A., and Venkatakrishnan, R., 1978. Geologic Map of Idaho: Moscow. Idaho, Idaho Bureau of Mines and Geology Map GM-1.
- Brott, C.A., Blackwell, D.D. and Mitchell, J.C., 1976. Geothermal Investigations in Idaho, Part 8, Heat Flow in the Snake River Plain Region, Idaho. Idaho Department of Water Resources, Water Information Bulletin No.30.
- Cannon, C., Wood, T., Neupane, G., McLing, T., Mattson, E., Dobson, P., and Conrad, M., 2014. Geochemistry Sampling for Traditional and Multicomponent Equilibrium Geothermometry in Southeast Idaho. *GRC Transactions* 38, 524-431.
- Christiansen, R.L., 2001. The Quaternary and Pliocene Yellowstone plateau volcanic field of Wyoming, Idaho, and Montana, United States Geological Survey Professional Paper 729-G.
- Cluer, J.K. and Cluer, B.L., 1986. The late Cenozoic Camas Prairie Rift south-central Idaho. *Contributions to Geology*, University of Wyoming, 24(1), 91-101.
- Dobson, P.F., Kennedy, B.M., Conrad, M.E., McLing, T., Mattson, E., Wood, T., Cannon, C., Spackman, R., van Soest, M., and Robertson, M., 2015. He isotopic evidence for undiscovered geothermal systems in the Snake River Plain. *Proceedings*, 40th Workshop on Geothermal Reservoir Engineering, Stanford University, Stanford, CA.
- Embree, G.F., and Hoggan R.D., 1999. Secondary deformation within the Huckleberry Ridge Tuff and subjacent Pliocene units near the Teton Dam: Road log to the regional geology of the eastern margin of the Snake River plain, Idaho. In S.S. Hughes and G.D. Thackray, eds., *Guidebook to the Geology of Eastern Idaho*, Idaho Museum of Natural History, Pocatello, Idaho, p. 181-202.
- Embree, G.F., Phillips, W.M., and Welhan, J.A., 2011. Geologic map of the Newdale quadrangle, Fremont and Madison Counties, Idaho. Idaho Geological Survey, University of Idaho, Moscow, Idaho 83844-3014.
- Faulds, J. E., Hinz, N. H., Coolbaugh, M. F., Cashman, P. H., Kratt, C., Dering, G., Edwards, J., Mayhew, B., and McLachlan, H., 2011. Assessment of favorable structural settings of geothermal systems in the Great Basin, western USA. *GRC Transactions*, 35, 777-783.
- Fournier, R. O., and Potter, R.W. II, 1982. Revised and expanded silica (quartz) geothermometer. *Geotherm. Resour. Coun. Bullet.* 11(10), 3-12.
- Fournier, R.O., 1977. Chemical geothermometers and mixing models for geothermal systems. *Geothermics* 5, 41-50.
- Fournier, R.O., 1979. A revised equation for the Na/K geothermometer. *GRC Transactions*, 3, 221-224.
- Fournier, R.O. and Truesdell, A.H., 1973. An empirical Na-K-Ca geothermometer for natural waters. *Geochim. Cosmochim. Acta* 37, 1255-1275.
- Fournier, R.O. and Potter II, R.W., 1979. Magnesium correction to the Na-K-Ca chemical geothermometer. *Geochim. Cosmochim. Acta* 43, 1543-1550.
- Garwood, D.L., Kauffman, J.D., Othberg, K.L., Lewis, R.S., 2014 Geologic map of the Fairfield 30x60 Minute Quadrangle, Idaho, Idaho Geological Survey.
- GeothermEx, Inc., 2010. Independent technical report: Resource evaluation of the Newdale geothermal prospect, Madison and Fremont Counties, Idaho, USA. Geothermix, Inc., Richmond, California, USA, 101 p.
- Giggenbach, W.F., 1988. Geothermal solute equilibria. Derivation of Na-K-Mg-Ca geoindicators. *Geochim. Cosmochim. Acta*, 52, 2749-2765.
- Hildebrand, R. T., 1983. Reconnaissance drilling during 1980 in the Goose Creek coal field, Cassia County, Idaho. US Geological Survey Open-File Report 83-477, 28 p.
- Lewis, R.E. and Young, H.W., 1989. The hydrothermal system in central Twin Falls County, Idaho: U.S. Geological Survey Water Resources Investigations Report 88-4152, 44 p.

- Lewis, R.S., Link, P.K., Stanford, L.R., and Long, S.P., 2012. Geologic map of Idaho. Idaho Geological Survey, Geologic Map 9.
- Link, P.K., 2002a. Clark County, Idaho. Digital Atlas of Idaho, Idaho State University, Geosciences Department, 3 p.
- Link, P.K., 2002b. Fremont County, Idaho. Digital Atlas of Idaho, Idaho State University, Geosciences Department, 3 p.
- Link, P.K., 2002c. Cassia County, Idaho. Digital Atlas of Idaho, Idaho State University, Geosciences Department, 3 p.
- Kellogg, K.S., Harlan, S.S., Mehnert, H.H., Snee, L.W., Pierce, K.L., Hackett, W.R., and Rodgers, D.W., 1994. Major 10.2-Ma rhyolitic volcanism in the Eastern Snake River Plain Idaho-Isotopic age and stratigraphic setting of the Arbon Valley Tuff Member of the Starlight Formation. US Geological Survey Bulletin 2091, 28 p.
- Kuntz, M. A., and Kork, J. O., 1978. Geology of the Arco-Big Southern Butte area, eastern Snake River Plain, and volcanic hazards to the radioactive waste management complex, and other waste storage and reactor facilities at the Idaho National Engineering Laboratory, Idaho (No. 78-691). US Geological Survey.
- Kuntz, M. A., Covington, H. R., and Schorr, L. J., 1992. An overview of basaltic volcanism of the eastern Snake River Plain, Idaho. *Geological Society of America Memoirs* 179, 227-268.
- Kuntz, M.A., Skipp, B.A., Lanphere, M.A., Scott, W.E., Pierce, K. L., Dalrymple, G.B., Champion, D.E., Embree, G.F., Page, W.R., Morgan, L.A., Smith, R.P., Hackett, W.R., and Rodgers, D.W., 1994. Geologic map of the Idaho National Engineering Laboratory and adjoining areas, eastern Idaho. US Geological Survey, Miscellaneous Investigations Series, Map I-2330.
- Leeman, W.P., 1982. Geology of the Magic Reservoir area, Snake River Plain, Idaho, in Bill Bonnichsen and R.M. Breckenridge, *Cenozoic Geology of Idaho*, Idaho Bureau of Mines and Geology Bulletin 26, 369-376.
- Mabey, D.R., 1978. Gravity and aeromagnetic anomalies in the Rexburg area of eastern Idaho. U.S. Geological Survey Open-File Report 78-382, 19p.
- Malde, H. E., 1991. Quaternary geology and structural history of the Snake River Plain, Idaho and Oregon. *The Geology of North America*, 2, 251-281.
- Malde, H. E., Powers, H. A., and Marshall, C. H., 1963. Reconnaissance geologic map of west-central Snake River Plain, Idaho (No. 373).
- Mansfield, G. R., 1927. Geography, geology, and mineral resources of part of southeastern Idaho, with description of Carboniferous and Triassic fossils. U.S. Geological Survey Prof. Pap., 928, 92 p.
- Mapel, W. J., and Hail, W. J., Jr., 1959. Tertiary geology of the Goose Creek district, Cassia County, Idaho, Box Elder County, Utah, and Elko County, Nevada. US Geological Survey Bulletin 1055-H, 217-254.
- Mattson, E.D., Smith, R.W., Neupane, G., Palmer, C.D., Fujita, Y., McLing, T.L., Reed, D.W., Cooper, D.C., and Thompson, V.S., 2015. Improved geothermometry through multivariate reaction-path modeling and evaluation of geomicrobiological influences on geochemical temperature indicators: final report (No. INL/EXT-14-33959). Idaho National Laboratory (INL).
- McLing, T.L., Smith, R.W., and Johnson, T.M., 2002. Chemical characteristics of thermal water beneath the eastern Snake River Plain. In: *Geology, Hydrogeology, and Environmental Remediation: Idaho National Engineering and Environmental Laboratory, Eastern Snake River Plain, Idaho*, P.K. Link and L.L. Mink, eds. *Geological Society of America Special Paper* 353, 205-211.
- McLing, T., McCurry, M., Cannon, C., Neupane, G., Wood, T., Podgorney, R., Welhan, J., Mines, G., Mattson, E., Wood, R., Plamer, C., and Smith, R., 2014. David Blackwell's Forty Years in the Idaho Desert, The Foundation for 21st Century Geothermal Research. *GRC Transactions* 38, 143-153.

- Mitchell, J.C., 1976. Geothermal investigations in Idaho Part 7: Geochemistry and geologic setting of the thermal waters of the Camas Prairie Area, Blaine and Camas Counties, Idaho, Idaho Department of Water Resources, Water Information Bulletin No. 30
- Mitchell, J.C., Johnson, L.L., and Anderson, J.E., 1980. Geothermal investigations in Idaho Part 9: Potential for direct heat application of geothermal resources, Idaho. Idaho Department of Water Resources, Water Information Bulletin No. 30.
- Morgan, L.A., and McIntosh, W.C., 2005. Timing and development of the Heise volcanic field, Snake River Plain, Idaho, western USA. *Geological Society of America Bulletin* 117, 288-306.
- Neely, K.W., 1996. Geothermal heat keeps students warm at the College of Southern Idaho. *GRC Transactions*, 20, 129-136.
- Neupane, G., Mattson, E.D., McLing, T.L., Palmer, C.D., Smith, R.W., and Wood, T.R., 2014. Deep Geothermal Reservoir Temperatures in the Eastern Snake River Plain, Idaho using Multicomponent Geothermometry. *Proceedings*, Thirty-Ninth Workshop on Geothermal Reservoir Engineering, Stanford University, Stanford, California, February 24-26, 2014.
- Neupane, G., E.D. Mattson, T.L. McLing, C.D. Palmer, R.W. Smith, T.R. Wood, and R.K. Podgorney, 2015a. Geothermal reservoir temperatures in southeastern Idaho using multicomponent geothermometry. *Proceedings*, World Geothermal Congress 2015a, Melbourne, Australia, 19-25 April 2015.
- Neupane, G., J.S. Baum, E.D. Mattson, G.L. Mines, C.D. Palmer, and R.W. Smith, 2015b. Validation of multicomponent equilibrium geothermometry at four geothermal power plants. *Proceedings*, Fortieth Workshop on Geothermal Reservoir Engineering Stanford University, Stanford, California, January 26-28, 2015.
- Neupane, G., Mattson, E.D., Mines, G.L., McLing, T.L., Dobson, P.F., Conrad, M.E., Wood, T.R., Cannon, C., Worthing, W., 2015c. Geothermometric temperature comparison of hot springs and wells in southern Idaho. *GRC Transactions* 39, 495-502.
- Occidental Geothermal, Inc., 1979. Sturm 1, Computer Processed Log. Department of Water Resources, Idaho, 18 p.
- Oriel, S.S. and Platt, L.B., 1980. Geologic map of the Preston 1 X 2 quadrangle, southeastern Idaho and western Wyoming. US Geological Survey, Miscellaneous Investigation Series, Map I-1127.
- Palmer, C.D., Ohly, S.R., Smith, R.W., Neupane, G., McLing, T., Mattson, E., 2014. Mineral Selection for Multicomponent Equilibrium Geothermometry. *GRC Transactions* 38, 453-459.
- Peng, X., and Humphreys, E.D., 1998. Crustal velocity structure across the eastern Snake River Plain and the Yellowstone swell. *Journal of Geophysical Research* 103, 7171-7186.
- Phillips, W.M., Moore, D.K., and Feeney, D.M., 2016a. Geologic map of the Poplar Quadrangle, Bonneville County, Idaho. Idaho Geological Survey.
- Phillips, W.M., Moore, D.K., Feeney, D.M., and Embree, G.F., 2016b. Geologic map of the Heise Quadrangle, Bonneville, Jefferson, and Madison Counties, Idaho. Idaho Geological Survey.
- Pierce, K. L., and Morgan, L. A., 1992. The track of the Yellowstone hot spot: Volcanism, faulting, and uplift. *Geological Society of America Memoirs* 179, 1-54.
- Piety, L.A., Sullivan, J.T., and Anders, M.H., 1992. Segmentation and paleoseismicity of the Grand Valley fault, southeastern Idaho and western Wyoming in Regional Geology of Eastern Idaho and Western Wyoming. *Geological Society of America Memoirs*, 179, 155-182.
- Prostka, H.J. and Embree, G.F., 1978. Geology and geothermal resources of the Rexburg area, eastern Idaho. U.S. Geological Survey Open-File Report 78-1009.
- Ralston, D.R., Arrigo, J.L., Baglio, J.V. Jr., Coleman, L.M., Souder, K., Mayo, A.L., 1981. Geothermal evaluation of the thrust area zone in southeastern Idaho, Idaho Water and Energy Research Institute, University of Idaho.
- Rember, W.C. and Bennett, E.H., 1979. Geologic map of the Twin Falls quadrangle, Idaho. Idaho Bureau of Mines and Geology, Geologic Map Series, Twin Falls 2 Quadrangle, scale 1:250,000, Reference ID-R274.

- Ross, S.H., 1970. Geothermal Potential of Idaho. *Geothermics*, 2, 975-1008.
- Shervais, J.W., Shroff, G., Vetter, S.K., Matthews, S., Hanan, B.B., McGee, J.J., 2002. Origin and Evolution of the Western Snake River Plain: Implications from stratigraphy, faulting, and the geochemistry of basalts near Mountain Home, Idaho, in Bill Bonnichsen, C.M., White, and Michael McCurry eds., Tectonic and magmatic evolution of the Snake River Plain Volcanic Province: Idaho Geological Survey Bulletin 30, p. 343-361.
- Shervais, J.W., Vetter, S.K., and Hanan, B.B., 2006. Layered mafic sill complex beneath the eastern Snake River Plain: Evidence from cyclic geochemical variations in basalt, *Geology*, vol. 34, no. 5, p 365-368.
- Shervais, J. W., Schmitt, D.R., Nielson, D., Evans, J.P., Christiansen, E.H., Morgan, L., Shanks, W.C.P, Blackwell, D.D., Glen, J.M., Champion, D., Potter, K.E., and Kessler, J.A., 2013. First results from HOTSPOT: The Snake River Plain scientific drilling project, Idaho, USA. *Sci. Drill.*, 15, 36–45.
- Skipp, B., 1985. Contraction and extension faults in the southern Beaverhead Mountains, Idaho and Montana. US Geological Survey, Open-File Report 85-545, 183 p.
- Souder, K.C., 1985. The hydrochemistry of thermal waters of southeastern Idaho, western Wyoming, and northeastern Utah. MS Thesis, University of Idaho, Moscow, Idaho, 139 p.
- Sparlin, M.A., Braile, L.W., and Smith, R.B., 1982. Crustal structure of the Eastern Snake River Plain determined from ray trace modeling of seismic refraction data, *Journal of Geophysical Research*, 87, 2619-2633.
- Street, L. V., & DeTar, R. E. (1987). Geothermal investigations in Idaho: Geothermal resource analysis in Twin Falls County, Idaho. Idaho Dept. of Water Resources, Twin Falls (USA); Bureau of Land Management, Boise, ID (USA), 106 p.
- Struhsacker, D.W., Jewell, P.W., Zeisloft, J., Evans, S.H., 1982. The geology and geothermal setting of the Magic Reservoir area, Blaine and Camas Counties, Idaho, in Bill Bonnichsen and R.M. Breckenridge, Cenozoic Geology of Idaho, Idaho Bureau of Mines and Geology, Bulletin 26, 377-393.
- Trimble, D.E., 1982. Geologic map of the Yandell Springs quadrangle, Bannock and Bingham Counties, Idaho. US Geological Survey, Geologic Quadrangle Map, Yandell Springs Quadrangle, Idaho GQ-1553.
- Truesdell, A.H., 1976. Summary of Section III. Geochemical techniques in exploration. Proceedings of the Second United Nations Symposium on the Development and Use of Geothermal Resources, San Francisco 1975, 1, liii – lxxix.
- Wallace, R.W., 1972. A finite-element, planar-flow model of Camas Prairie, Idaho. Doctoral dissertation, University of Idaho, Moscow, Idaho, 178 p.
- Young, H.W. and Lewis, R.E., 1982. Hydrology and geochemistry of thermal groundwater in southwestern Idaho and north-central Nevada. US Geological Survey Professional Paper 1044-J, 26 p.
- Young, H. W., and Mitchell, J. C., 1973. Geothermal investigations in Idaho. Part 1. Geochemistry and geologic setting of selected thermal waters. Idaho Dept. of Water Admin., Water Inf Bul, 30, 24 p.

Appendix F.

Neupane, G., Mattson, E.D., Mines, G.L., McLing, T.L., Dobson, P.F., Conrad, M.E., Wood, T.R., Cannon, C., Worthing, W., 2015c. Geothermometric temperature comparison of hot springs and wells in southern Idaho. GRC Transactions, 39, 495-502.

Geothermometric Temperature Comparison of Hot Springs and Wells in Southern Idaho

Ghanashyam Neupane^{1,2}, Earl D. Mattson¹, Travis L. McLing^{1,2}, Patrick F. Dobson³,
Mark E. Conrad³, Thomas R. Wood^{2,4}, Cody Cannon^{2,4}, and Wade Worthing^{2,4}

¹Idaho National Laboratory, Idaho Falls ID, USA

²Center for Advanced Energy Studies, Idaho Falls ID, USA

³Lawrence Berkeley National Laboratory, Berkeley CA, USA

⁴University of Idaho-Idaho Falls, Idaho Falls ID, USA

ghanashyam.neupane@inl.gov

Keywords

Geothermal sites, hot springs, wells, reservoir temperature, Snake River Plain, RTEst

ABSTRACT

Conventional geothermal resource prospecting often begins with geochemical analysis of geothermal fluids sampled from surface expressions (hot springs and fumaroles). Similarly, water samples from hot wells located near the surface expressions are also routinely collected and analyzed as a part of regional exploration efforts. The chemical compositions of these water samples can be used to assess the likely reservoir temperatures of the geothermal sites as well as to understand other reservoir characteristics. In this paper, we present comparative results of geothermometric reservoir temperatures based on water compositions measured from pairs of hot springs and nearby wells of 10 potential geothermal sites in southern Idaho using both traditional and multicomponent equilibrium geothermometric approaches. Our results show that the reservoir temperatures estimated using water compositions measured surface thermal features and wells produce similar results. However, for two of the 10 sites, Durfee Hot Spring and Fairchild Hot Spring, the estimated reservoir temperatures based on water compositions measured from hot springs were significantly higher than the estimated reservoir temperatures using the well water sample. In the case of the Durfee system, the well water may have chemically re-equilibrated within the aquifer resulting in a lower estimated temperature than that calculated using the hot spring. Similarly, in the case of the Fairchild system, the hot spring and well water chemistry are chemically distinct and had the greatest distance between the hot spring and well pairs of the examined geothermal sites. The difference in fluid chemistry suggests that the Fairchild Hot Spring reservoir is compartmentalized and the two expressions are issuing waters migrated from two separate portions of the reservoir. Although the majority of the hot spring/well pairs in southern Idaho provided concordant reservoir temperatures, it is imperative to consider the consistency of the water types and distance between the sources when estimating reservoir temperatures.

1. Introduction

Sampling of water from surface thermal features (hot springs, fumaroles) as well as hot shallow wells for geochemical analyses may constitute an early prospecting phase of geothermal exploration. Geochemical data of water samples collected from geothermal can provide insights into diverse reservoir characteristics such as age of water, residence time, recharge, and subsurface temperatures. Geothermometric calculations use chemical concentrations of single (e.g., silica), a limited number (e.g., Na/K, Na-K-Ca, etc.), or multiple species in water and gas samples collected from surface expressions to assess reservoir temperatures.

In many cases, geothermal resources manifest their deeper hydrothermal activities in the form of surface expressions such as hot springs and fumaroles (e.g., Roosevelt Hot Springs). However, in some cases there have been no prior natural surface expressions (i.e., hidden systems), such as in Raft River Geothermal field where shallow wells drilled for domestic/irrigation purposes produced hot water and prompted further study to evaluate the potential geothermal resource.

Therefore, it is also important to assess the water compositions of warm- or hot-water producing shallow wells to evaluate geothermal potential of an area.

The United States Geological Survey (USGS), state geological surveys and water resource departments, and research groups supported by the US Department of Energy have conducted multiple campaigns to collect and analyze water samples from numerous sources including hot springs and hot shallow wells located throughout the western US. In this paper, we report comparative geothermometric results of water samples from hot springs and nearby hot shallow wells from numerous geothermal sites located near and along the margin of the Snake River Plain (SRP) in southern Idaho (Figure 1). The main objective of this study was to evaluate whether the chemical compositions of hot water measured from hot shallow wells are also equally useful in determining reservoir temperatures as those of compositions of water measured from hot springs.

2. Water Samples

Compositions of water samples measured from paired sources which are assumed to represent individual geothermal sites in southern Idaho were assembled for this study (Table 1). Nine of the paired sources were composed of hot springs and hot shallow wells. In the case of one example (Magic Reservoir Hot Spring), both compositions represent water derived from a well with one sample directly collected from a shallow leak in the well whereas the other sample was collected from a runoff channel that has experienced cooling and degassing.

Most of the sites considered in this study represent the geothermal systems located within and along the margins of the eastern and western SRP except two sites (Battle Creek HS and Durfee HS) that are located south-southeast from the SRP in the Basin and Range Province (Figure 1).

3. Geothermometric Approaches

The underlying assumption of geothermometry is that waters collected from geothermal expressions maintain a chemical signature that reflects equilibrium with the minerals in the deeper reservoir (Fournier *et al.*, 1974). There are numerous empirical and semi-empirical traditional geothermometers (e.g., silica geothermometers (Fournier, 1977), Na-K-Ca geothermometer (Truesdell and Fournier, 1973), and so on) routinely used within the geothermal prospecting community. Although many of the traditional geothermometers are fitted relationships, there have been some geochemical postulations supporting these relationships. For example, silica geothermometers are based on the assumption of the solubility of solid-phase silica (e.g., quartz, chalcedony, etc.) controlling the aqueous concentration of silica (Fournier, 1977). Similarly, several variations of sodium-potassium geothermometers are based on water-rock interaction involving albite and potassium feldspar. The reliability, sensitivity, and responsiveness of traditional geothermometers to various composition altering processes (such as boiling, mixing, degassing, etc.) vary. For example, geothermometers based on cation concentration ratios (e.g., Na/K geothermometer) are minimally sensitive to boiling or mixing with dilute water; while geothermometers based directly on the concentration of component(s) (e.g., quartz geothermometer) are highly sensitive to these processes ((D'Amore and Arnórsson, 2000)). A drawback to many existing geothermometry approaches is that they do not adequately account for physical processes (e.g., mixing, boiling) and geochemical processes (e.g., mineral dissolution, precipitation, degassing) that may occur after the water leaves the reservoir and thereby alter its composition. If these changes are not taken into account, predictions of *in-situ* reservoir conditions (e.g., temperature, $f\text{CO}_2$) based on the chemical composition of water samples taken from shallower depths or at the surface may be erroneous, or too imprecise to be useful.

In addition, it is difficult to quantify uncertainties associated with temperatures estimated with these geothermometers. As a result, it is not uncommon to find diverse temperature estimates for the same water using multiple traditional geothermometers. Nevertheless, because these

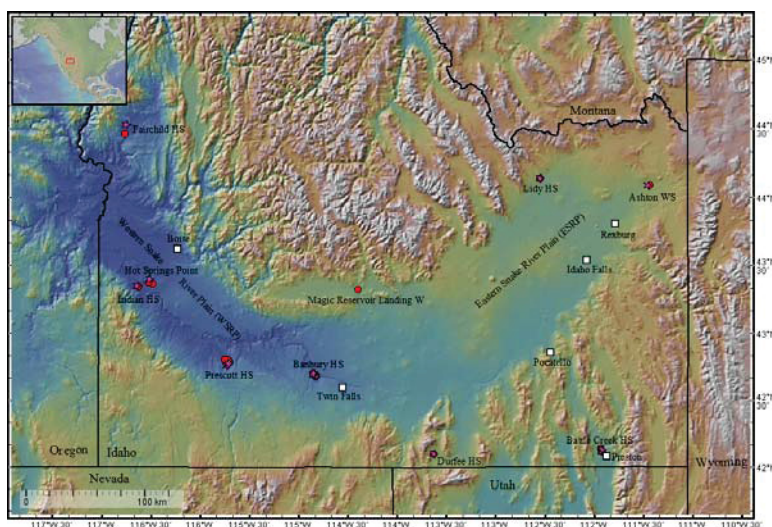


Figure 1. Shaded relief map of southern Idaho with locations of hot springs and nearby wells used in this study. Purple stars represent the hot springs whereas red circles represent the wells. The map was prepared from NASA 10-m DEM data in GeoMapApp.

Table 1. Composition of water samples (mg/L). Hot springs are italicized. Bold-faced names represent the geothermal sites.

Samples	T ¹	pH	Al ²	Na	K	Ca	Mg	B	Li	SiO ₂ (aq)	HCO ₃	SO ₄	Cl	F	Ref ³
Ashton WS⁴	41.0	7.60		36	1.6	1.1	0.10			110	92	4.7	2.9	2.2	a
Sturm W ⁵	31.4	8.73	0.005	33	0.89	3.2	0.05	0.04	0.05	63	66	5.8	3.3	2.1	b
Lidy HS1⁶	56.1	7.17	0.001	25	13	66	16	0.09	0.05	38	132	102	7.3	4.6	b
Lidy HS2	52.3	7.21	0.001	28	13	64	16	0.09	0.05	34	163	98	6.9	4.7	b
Lidy HS W	59.0	7.60		24	12	55	14	0.09	0.04	37	180	100	7.1	4.4	c
Magic Reservoir HS Landing W	75.0	6.79	0.009	311	20	22	1.4	1.2	1.2	104	703	50	74	9.9	b
Magic Reservoir HS Landing Runoff	39.1	8.61	0.007	333	21	13	1.3	1.2	1.2	109	710	53	79	11	b
Banbury HS	58.5	9.15	0.01	95	1.6	1.0	0.001	0.22	0.03	103	168	24	17	11	b
Hot Sulphur Miracle HS	57.0	9.40		130	1.5	0.9	0.1	0.34	0.04	86	59	34	34	21	d
Salmon Falls HS	70.5	9.10		140	1.1	1.2	0.1	0.44	0.06	89	70	32	50	27	c
Miracle HS W	58.4	9.53	0.02	128	1.9	0.8	0.001	0.33	0.05	100	93	34	32	22	b
Banbury HS Well	58.8	9.24	0.01	97	1.6	0.9	0.001	0.22	0.03	103	249	23	17	11	d
Near Banbury Natatorium W5	30.0	9.30		97	1.6	0.9	0.1	0.21	0.03	64	85	28	20	13	d
Near Banbury Natatorium W2	42.5	9.30		90	1.7	1.3	0.1	0.17	0.04	67	85	28	14	9	d
Near Banbury Natatorium W4	44.5	9.40		100	1.8	3.3	0.1	0.23	0.04	88	83	27	22	12	d
Near Banbury Natatorium W3	42.0	9.20		100	2.1	3.7	0.2	0.23	0.03	94	88	27	23	13	d
Near Banbury Natatorium W1	45.5	9.10		100	1.8	0.9	0.1	0.23	0.04	86	100	29	30	26	d
Banbury Natatorium W	59.0	9.30		110	1.6	1.1	0.1	0.26	0.04	88	78	30	23	15	d
Harry Huttanus W2	59.0	9.00		100	1.5	1.1	0.1	0.23	0.04	100	90	27	25	14	c
Sliger W	72.0	9.37	0.07	136	1.6	0.9	0.004	0.50	0.05	94	212	30	50	24	b
Unnamed W1 near SFHS ⁷	72.0	9.30		140	1.2	0.9	0.1	0.47	0.06	86	59	35	51	27	d
Unnamed_W_SF CREEK	62.0	9.40		150	1.4	0.7	0.1	0.49	0.05	84	56	35	48	15	d
Unnamed W2 near SFHS	71.5	9.50		140	1.5	1.5	0.1	0.51	0.06	82	56	33	51	27	d
Durfee HS	44.9	8.78	0.003	84	3.3	8.2	0.35	0.08	0.09	68	107	28	59	6.2	b
Harold Ward W	38.0	7.40		70	3.1	37	9.3			44	169	33	80	2.9	d
Battle Creek HS1	77.0	7.00		3100	660	160	16			80	699	50	5400	12	e
Battle Creek HS2	43.0	6.50		3071	535	166	15	7.3		107	697	29	5048	6.0	e
Battle Creek HS3	81.0	6.50		3053	533	162	19	7.2		109	757	37	5034	6.0	e
Battle Creek HS5	82.0	6.70		3161	552	174	19	7.6		109	696	35	5241	6.0	e
Battle Creek HS4	84.0	6.80		4184	686	215	24	10		97	610	33	6967	6.4	e
Squaw HS1	69.0	6.50		4184	708	135	23	7.3		126	816	27	6877	4.3	e
Squaw HS2	73.0	6.60		3844	533	241	26	9.7		126	866	23	6396	4.8	e
Bosen W	90.0	6.65	0.08	4523	795	207	18	5.6	6.1	95	583	49	7129	5.2	b
Squaw HS W1	82.0	7.80		4300	880	250	23			130	733	54	7700	7.0	e
Squaw HS W2	84.0	6.50		4368	782	279	24	8.1		124	791	35	7398	4.3	e
Squaw HS W3	82.0	6.90		3996	694	261	21			139	725	35	7291	4.9	e
Indian HS	71.5	9.40		80	0.8	1.3	0.1	0.11	0.06	71	56	23	9.1	16.0	d
Earl Foote W	45.0	9.20		130	1.2	1.4	0.1	0.25	0.01	61	140	45	22	12.0	d
Prescott HS	41.0	9.10		55	5.5	6.2	0.3	0.01		83	103	18	8.8	8.5	d
Prescott WS	40.0	8.50		43	6.7	13	1.8	0.11	0.01	89	126	15	8.8	4.5	d
Indian Bathtub HS	39.0	8.30		53	6.7	6.5	0.6	0.08	0.01	87	113	15	9.1	6.0	d
Owens W7	38.0	8.00		36	6.9	16	2.8	0.10	0.02	82	134	15	8.6	3.1	d
Prescott W	43.0	9.20		48	6.2	12	1.1	0.08	0.01	84	129	17	8.6	5.4	d
Rose W	44.0	8.30		53	7.2	12	1.1	0.12	0.02	100	126	17	8.7	8.2	d
HS Ranch W	43.0	8.50		54	4.6	6	0.3	0.07		82	91	18	9.0	12	d
Unnamed W NE of Bat HS	45.0	8.00		40	6.3	16	1.9	0.09	0.02	86	124	15	8.4	3.7	d
Owens W2	42.5	8.50		49	5.1	7.4	0.4	0.06	0.01	81	99	18	9.0	8.9	d
HS Point	60.0	6.90		285	56	46	40	2.9	0.99	70	949	116	48	7.0	d
Charters W	25.5	8.20		48	4.7	16	6.9			43	133	41	15	0.5	d
Melba City W	25.0	8.20		88	3.8	9.1	2.3			42	200	34	17	1.4	d
Fairchild HS	50.0	8.50		80	1.9	8.0	0.8			55	81	110	15	0.8	d
Fairchild Lumber W	26.9	8.70	0.3	80	9.1	3.5	0.2	0.18		69	187	14	3.8	0.7	d

¹Field temperature in °C; ²Potassium feldspar was used for missing Al during RTest modeling; ³Ref: Reference (a: Young and Mitchell, 1973; b: this study; c: Mitchell et al., 1980; d: Parlman and Young, 1992; e: Mitchell, 1976); ⁴WS: warm spring; ⁵W: Well; ⁶HS: hot spring; ⁷SFHS: Salmon Falls hot spring.

geothermometers are easy to use and sometimes provide good results, they are considered to be an essential part of the geothermal exploration toolkit (D'Amore and Arnórsson, 2000).

A more advanced geothermometric approach is multicomponent equilibrium geothermometry (MEG). The MEG approach of geothermometry utilizes multiple chemical constituents measured in water samples for inverse geochemical modeling considering a suite of selected minerals (selected based on some knowledge of the system) so as to provide more robust temperature estimates with quantifiable uncertainties. Geothermal temperature predictions using MEG provide ap-

parent improvement in reliability and predictability of temperature over traditional geothermometers. The basic concept of this method was developed in 1980s (e.g., Michard and Roekens, 1983; Reed and Spycher, 1984). Some previous investigators (e.g., D'Amore et al., 1987; Hull et al., 1987; Tole et al., 1993) have used this technique for predicting geothermal temperature in various geothermal sites. Other researchers have used the basic principles of this method for reconstructing the composition of geothermal fluids and formation brines (Pang and Reed, 1998; Palandri and Reed, 2001). More recent efforts by some researchers (e.g., Bethke, 2008; Spycher et al., 2011; Smith et al., 2012; Cooper et al., 2013; Neupane et al., 2013, 2014; Spycher et al., 2014; Peiffer et al., 2014; Palmer et al., 2014; Neupane et al., 2015a,b) have been focused on improving temperature predictability of the MEG.

For this study, both traditional [e.g., quartz (no steam loss) (Fournier, 1977), chalcedony (Fournier, 1977), and Na-K-Ca (Truesdell and Fournier, 1973; Fournier and Potter II, 1979)] and multicomponent (Palmer et al., 2014) geothermometric approaches were applied to the water compositions measured from paired sources (hot springs and nearby wells) to estimate reservoir temperatures. Specifically, the MEG approach implemented in Reservoir Temperature Estimator (RTEst) (Palmer et al., 2014) was used to assess the reservoir temperatures of several geothermal sites in southern Idaho. While applying RTEst to each water sample, a mineral assemblage with 5-7 representative minerals (Mg bearing minerals – clinchlore, illite, saponite, beidellite, talc; Na bearing minerals – paragonite, saponite; K-bearing minerals – K-feldspar, mordenite-K, illite; Ca bearing minerals – calcite; and chalcedony) was used for the development of each reservoir temperature estimate. For each site, the same mineral assemblage was used for all samples. For the selected compositions of southeastern Idaho thermal waters that do not have measured Al concentrations (Table 1), a value determined by assuming equilibrium with K-feldspar (Pang and Reed, 1998) was used in the geochemical modeling.

4. Results and Discussion

4.1 Southern Idaho waters

Compositions of water samples measured from hot springs and wells in southern Idaho are presented in Table 1. The pH values of the southern Idaho thermal waters range from 6.5 to 9.5. Similarly, the field temperatures of southern Idaho springs/wells range between 25 to 90 °C. The aqueous chemistry of these southeastern Idaho thermal waters show a large range in total dissolved solids (TDS) from about 100 mg/L (Sturm Well) to >14,000 mg/L (Bosen Well).

The dominant cations in the southern Idaho thermal waters are Na and Ca whereas bicarbonate is the dominant anion for most of the samples except Battle Creek group water samples where Cl is by far the dominant anion species. A limited number of other water samples (e.g., Fairchild and Indian Hot Springs) have SO₄ or F as the dominant anions.

When specifically comparing water chemistry from hot springs and nearby wells, it is not unusual to find some variations in the concentration of a particular solute in water from different sources representing the same site. For example, the pH of water from Sturm Well is more alkaline (>1 unit of pH) than water from the neighboring Ashton Warm Spring. Similarly, Ashton Warm Spring water contains significantly higher concentrations of SiO₂(aq) and HCO₃. On the other hand, waters from these two expressions have similar concentrations of Na, SO₄, Cl, and F. In some cases (e.g., Durfee Hot Spring), the concentration of Mg in well water is significantly higher than the concentration in the hot spring. At the Hot Spring Point site, the total dissolved solid (TDS) in hot spring water is several times higher than the TDS value in nearby wells. Despite these differences, our data from southern Idaho suggests that most of the water samples from hot springs and nearby well(s) representing the same site are typically the same type waters with the exception of the Fairchild site where different water types from the hot springs and a well ~7 km from the spring were found.

Due to these variations in solute concentrations in water samples collected from hot springs and nearby wells, non-ratio traditional geothermometers (e.g., silica variants, Na-K-Ca) provide diverse temperature estimates from their paired thermal expressions. Based on previous geothermometric studies of south/southeastern Idaho waters (e.g. Neupane et al., 2014; Neupane et al., 2015a), traditional geothermometers based on cation ratios (specifically, the variants of Na/K geothermometers) rarely provide acceptable reservoir temperatures in the region because of the likely violation of underlying geochemical assumptions for these geothermometers. However, it has been reported in our previous studies that MEG as implemented in RTEst consistently provides acceptable temperature estimates for numerous sites in the south/southeastern Idaho and other producing geothermal areas in the western US.

4.2 Reservoir Temperatures

4.2.1 Giggenbach Diagram

When plotted on a Giggenbach Na-K-Mg diagram (Giggenbach, 1988), water samples representing Battle Creek, Magic, Banbury, and Indian Hot Springs geothermal sites plot in the partially equilibrated zone whereas water samples from rest of the other sites lie in the immature zone (Figure 2). Water-rock interaction associated with the Battle Creek (Preston) reservoir could have occurred at a temperature range of 260-300 °C. Other partially equilibrated water samples may have

interacted with rock at about 200 °C (Magic Reservoir Hot Spring well waters) and between 80-140 °C (Banbury Hot Spring site), and at about 100 °C (Indian Hot Spring site).

The perceived lack of equilibrium (immaturity) of water samples from other sites could be related to low Na content, as suggested by Giggenbach (1988), as well as to their relatively higher Mg content. The waters containing high Mg content are deemed to be poor for some traditional solute geothermometry (this often indicates mixing with shallow, cooler fluids); although there have been some efforts made to implement an Mg correction in the estimated temperature (e.g., Fournier and Potter, 1979).

Immature waters from both springs and wells representing each site are either clustered or aligned together along an isotherm (e.g., Prescott Hot Springs system, Figure 2) with two exceptions being the Fairchild and Durfee sites. In the case of the Fairchild site, spring water appears to be relatively more immature; however, the opposite trend is found for the Durfee site. It is likely that the clustered or aligned immature samples representing the same site may have undergone similar geochemical consequences (e.g., mixing) along the flow path.

4.2.2 Temperature Estimated by Traditional Geothermometers

Temperature estimates with quartz (no steam loss; Fournier, 1977), chalcedony (Fournier, 1977), and Mg-corrected Na-K-Ca (Fournier and Truesdell, 1973; Fournier and Potter II, 1979) are presented in Table 2. In general, the two variants of silica geothermometers resulted in similar (with respect to each geothermometer and each site) reservoir temperatures with water compositions measured from springs and wells for the majority of the geothermal sites. For some sites (e.g., Ashton, Durfee, and HS Point), however, temperature estimates based on spring

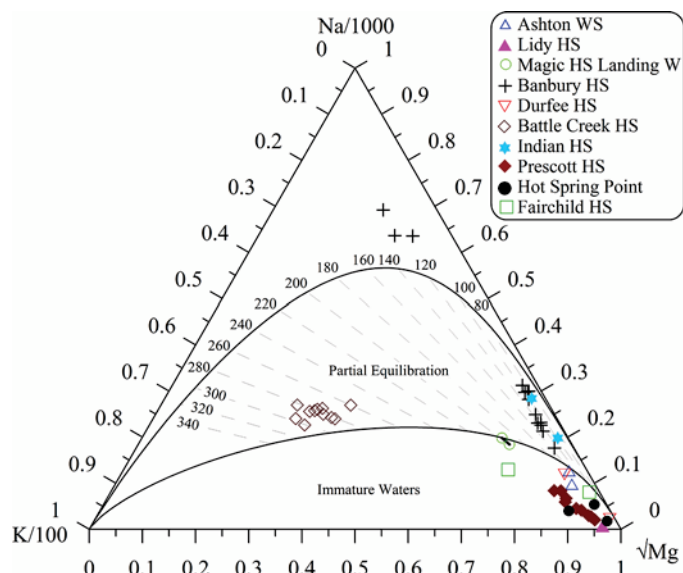


Figure 2. Water samples from south Idaho hot springs and wells plotted on a Giggenbach diagram (Giggenbach, 1988).

Table 2. Estimated reservoir temperatures obtained from compositions of water from hot springs and wells at ten geothermal sites in southern Idaho. Mean estimated temperatures are also included for geothermal sites with more than one sample from the same type of source.

Sampling sites	¹ T±σ _T	² Quartz	³ Chalcedony	⁴ Na-K-Ca
Ashton WS	147±5	143	116	130
Sturm W	152±14	113	84	109
Lidy HS1	111±6	89	58	77
Lidy HS2	105±6	85	54	71
Lidy HS W	106±5	88	57	71
Mean: Spring	108	87	56	74
Magic HS Landing Well	133±8	139	113	149
Magic HS Landing Runoff	132±4	142	116	143
Banbury HS	159±9	139	112	112
Hot Sulphur Miracle HS	150±4	129	101	103
Salmon Falls HS	148±5	131	103	92
Miracle HS W	161±3	137	110	112
Banbury HS Well	159±10	139	113	114
Near Banbury Natatorium W5	145±6	114	85	113
Near Banbury Natatorium W2	139±7	116	87	114
Near Banbury Natatorium W4	139±7	130	103	108
Near Banbury Natatorium W3	142±8	134	107	113
Near Banbury Natatorium W1	157±6	129	101	116
Banbury Natatorium W	148±6	130	103	108
Harry Huttanus W2	155±8	137	110	108
Sliger W	134±2	133	106	103
Unnamed W1 near SFHS	150±3	129	101	102
Unnamed_W_SF CREEK	152±2	128	100	115
Unnamed W2 near SFHS	135±5	126	99	98
Mean: Spring	152	133	105	102
Mean: Well	147	129	102	110
Durfee HS	138±8	117	88	131
Harold Ward W	101±6	96	66	60
Battle Creek HS1	175±6	125	97	230
Battle Creek HS2	169±5	141	115	215
Battle Creek HS3	170±5	142	116	202
Battle Creek HS5	171±4	142	116	205
Battle Creek HS4	175±5	136	109	204
Squaw HS1	179±9	151	125	204
Squaw HS2	157±6	151	125	183
Bosen Well	175±4	134	107	227
Squaw HS W1	175±5	152	127	229
Squaw HS W2	174±6	150	124	217
Squaw HS W3	171±7	156	132	216
Mean: Spring	171	141	115	206
Mean: Well	174	148	123	222
Indian HS	98±1	119	90	73
Earl Foote W	103±4	111	82	90
Prescott HS	110±4	127	99	158
Prescott WS	112±6	131	103	110
Indian Bathub HS	122±2	130	102	143
Owens W7	112±11	126	99	94
Prescott W	104±6	128	100	131
Rose W	107±3	137	110	135
HS Ranch W	105±5	126	99	151
Unnamed W NE of Bat HS	102±6	129	101	115
Owens W2	104±3	126	98	152
Mean: Spring	115	129	101	137
Mean: Well	106	129	101	130
HS Point	144±9	118	90	24
Charters W	159±7	95	64	35
Melba City W	147±14	94	63	66
Mean: Well	153	95	64	51
Fairchild HS	196±2	106	77	107
Fairchild Lumber W	144±8	117	89	179

¹RTes temperature and standard error; ²Quartz no steam loss, Fournier (1977); ³Fournier (1977); ⁴Fournier and Truesdell (1973), Mg correction applied according to Fournier and Potter II (1979).

water compositions are warmer than the temperature estimates with well water compositions (Table 2). This variation in estimated temperature is also true with Na-K-Ca geothermometer for the Ashton and Durfee sites (Table 2). On the other hand, one hot spring within the Battle Creek (Preston) site resulted in slightly lower reservoir temperature estimates compared to other hot springs or wells.

For some geothermal sites, the Na-K-Ca temperatures estimates for spring water and well water compositions are more diverse compared to the temperature estimates with silica geothermometers. For example, regardless of the source, silica geothermometer specific temperature estimates for the Prescott site are very similar. However, Na-K-Ca temperatures for this site are not similar for many samples. In general, Na-K-Ca temperatures for this system fall into two- slightly cooler temperature (94-115 °C) and warmer temperature (131-158 °C) groups. However, the cooler and warmer Na-K-Ca temperatures cannot be grouped according to the type of source since both wells and spring(s) resulted in cooler (Prescott WS, Owens W7, and Unnamed W NE of Bat HS) and warmer (all other expressions for this site) temperatures.

4.2.3 Temperature Estimated by RTest

RTest estimated reservoir temperatures are shown in Figure 3. With the exceptions of Durfee and Fairchild systems, RTest temperatures for all other sites are similar regardless of the sampling source. Several samples representing the Banbury

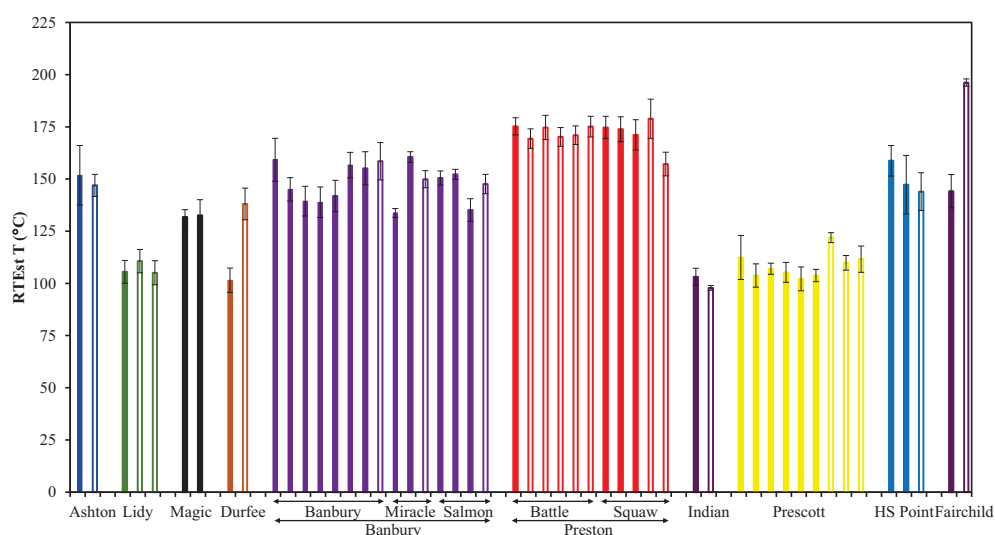


Figure 3. RTest (Palmer et al., 2014) temperature estimates for several geothermal sites in southern Idaho using composition of water samples collected from hot springs (open bars) and nearby wells (solid bars). For Magic Reservoir Hot Spring geothermal site, both temperature estimates are based on the composition of water samples derived from the same well (one from the shallow leak, and the other from surface runoff).

to 179 °C. With the exception of the relatively cooler temperature estimate from the composition of Squaw HS2, all other hot springs and wells in the area resulted in reservoir temperature estimates within a tight temperature range from 169 to 179 °C. The Prescott site, which has a large number of samples from various sources, also resulted in similar reservoir temperatures within a range of 102 to 122 °C (Figure 3). Similarly, reservoir temperature estimates obtained from spring and well water composition pairs for the Lidy, Indian, and HS Point sites are similar (Figure 6). The difference in mean reservoir temperatures estimated from water compositions of hot springs and wells for the Banbury, Battle Creek, Prescott, Lidy, and Indian sites are about 5, 3, 9, 2, 5, and 9 °C, respectively (Table 2).

Although variants of silica geothermometers and the Na-K-Ca geothermometer resulted in discordant reservoir temperature estimates for the Ashton geothermal site when using water compositions from Ashton Warm Spring and Sturm Well, RTest provided similar reservoir temperatures (Figure 3, Table 2) obtained from the compositions of water from these two sources. Since the traditional geothermometers only use a limited numbers of solute(s) present in the water for the development of reservoir temperature estimates, they tend to have limited capability to address physico-chemical processes that may have affected the composition of water along the flow path, it is likely that we can get discordant temperature estimates with water samples collected from different expressions if they have different flow paths and are subjected to different physico-chemical processes. However, MEG uses multiple components and a suite of minerals in estimating equilibrated reservoir temperatures, and RTest has the ability to reconstruct reservoir fluid as a function of fugacity of CO₂, mass of water, and temperature and uses that reconstructed fluid to estimate reservoir temperature.

An interesting example we considered in this paper is the Magic Reservoir Hot Spring site. For this site, paired water samples do not represent a spring and a well but only a single well. Water samples were directly collected from a shallow

leak in the well and from the surface runoff (outflow) of the well. Although the field temperature of the runoff water was much cooler than the temperature of well water, the chemistries of both samples are very similar (except higher pH of the runoff water because of enhanced degassing of CO₂) indicating no significant water loss due to evaporation upon cooling. The RTEst temperature estimates based on these two waters are identical with a slightly higher uncertainty value in the reservoir temperature estimated using runoff water.

As noted above, RTEst estimated reservoir temperatures obtained using the composition of paired sources of waters for two sites (Durfee and Fairchild) are different. For the Durfee site, the composition of water measured from a hot spring resulted in reservoir temperature that is 37 °C hotter than the reservoir temperature that the composition of water measured from a nearby hot shallow well produced (Table 2). At this site, the hot spring (Durfee Hot Spring) and a nearby well (Harold Ward Well) are located about 220 m apart. Both expressions issue Na-Cl-HCO₃ type water at similar temperatures (Table 1). Based on the concentrations of non-conservative components Na and SiO₂(aq) in these waters, it appears that the Harold Ward Well water may have been diluted slightly more than the Durfee Hot Spring. However, the concentration of Cl (a conservative component), which has been detected at higher concentration in well water than its concentration in spring water, does not support this hypothesis. Furthermore, these two waters have distinctively different Ca and Mg concentrations (well water having significantly higher concentration of Mg and Ca than their concentrations in spring water). Although it is inconclusive to implicate further dilution of reservoir fluid before it issues to the well, it is likely that the well produces reservoir fluid that may have re-equilibrated to lower temperature.

Similar to the Durfee site, estimated reservoir temperature for the Fairchild site obtained from the composition of hot spring water is 52 °C hotter (Table 2) than that obtained from the composition of water measured from a hot well located at a relatively large distance (over 7 km). These two sources issue different types of water, with the spring issuing Na-SO₄ type water and well issuing Na-HCO₃ type water. The diverse reservoir temperature estimates with these two water compositions may be related to that they represent different reservoir systems, as they are located fairly far apart. It is not uncommon to have compartmentalized reservoir systems with distinct chemical composition within a small area. Ayling and Moore (2013) reported such a compartmentalized reservoir system at the Raft River geothermal field in south Idaho. However, unlike the Fairchild site situation, water samples from different Raft River geothermal field wells (deep wells) with high and low TDS result in similar temperature estimates for the reservoir. Nevertheless, the results of the Durfee and Fairchild site indicate that it is important to consider (compare) the chemistry of water from different sources and the distance between these sources while using the compositions of water measured from multiple sources to evaluate the geothermal potential of a prospect.

5. Conclusions

Our geothermometric study of multiple geothermal sites in southern Idaho indicates that the water chemical compositions from hot shallow wells can be as useful in determining reservoir temperatures using multicomponent geothermometry as those from hot springs. Seven of the nine geothermal sites that had paired hot springs and nearby wells in southern Idaho calculated similar reservoir temperatures. For these sites, the largest difference in the mean estimated reservoir temperatures (calculated when more than one spring and well are present) was less than ≤9°C.

Two geothermal sites exhibited a large difference in the calculated reservoir temperature between the hot spring and the nearby well. At the Durfee and Fairchild sites, the estimated reservoir temperatures using RTEst from hot springs are higher than nearby hot shallow wells by 37 °C and 52 °C, respectively. In the case of the Durfee site, water from the well may have re-equilibrated with the minerals in the aquifer at a lower temperature along its flow path. Similarly, for the Fairchild site, the water may have re-equilibrated with different mineral assemblages along its flow path to the well, or that the hot spring and well expressions are issuing waters migrated from two separate geothermal reservoirs. The water composition of the hot spring and the well are chemically distinct types of water and may not be located close enough together (>7 km distance between them) to be considered an appropriate pair for this study.

Although the majority of southern Idaho geothermal sites have water compositions from hot springs and nearby wells that provide concordant reservoir temperatures, it is imperative to consider the water types, variations in water chemistry, and distance between the sources prior to assessing potential geothermal reservoir temperatures. These results suggest that besides the existing hot springs thermal expressions that have used to assess the potential geothermal reservoir temperatures in the past, there exist a large number of wells that can be used to develop a more complete picture of the subsurface geothermal reservoir temperature.

Acknowledgments

Funding for this research was provided by the U.S. Department of Energy, Office of Energy Efficiency & Renewable Energy, Geothermal Technologies Office.

References

- Ayling, B. and J. Moore, 2013. "Fluid geochemistry at the Raft River geothermal field, Idaho, USA: New data and hydrogeological implications." *Geothermics*, 47, 116-126.
- Bethke, C.M., 2008. "*Geochemical and Biogeochemical Reaction Modeling*." Cambridge University Press, 547 pp.
- Cooper, D.C., C.D. Palmer, R.W. Smith, and T.L. McLing, 2013. "Multicomponent equilibrium models for testing geothermometry approaches." Proceedings, 38th Workshop on Geothermal Reservoir Engineering Stanford University, Stanford, February 11-13, 2013 SGP-TR-198.
- D'Amore, F. and S. Arnórsson, 2000. "Geothermometry." In: *Isotopic and chemical techniques in geothermal exploration, development and use*, Ed. S. Arnórsson. International Atomic Energy Agency, Vienna, Australia.
- D'Amore, F., R. Fancelli, and R. Caboi, 1987. "Observations on the application of chemical geothermometers to some hydrothermal systems in Sardinia." *Geothermics*, 16, 271-282.
- Fournier, R.O., D.E. White, and A.H. Truesdell, 1974. "Geochemical indicators of subsurface temperature – I, Basic assumptions." *U.S. Geol. Survey J. Res.*, 2, 259-262.
- Fournier, R.O., 1977. "Chemical geothermometers and mixing models for geothermal systems." *Geothermics*, 5, 41-50.
- Fournier, R.O., and R.W. Potter II, 1979. "Magnesium correction to the Na-K-Ca chemical geothermometer." *Geochimica et Cosmochimica Acta*, 43, 1543-1550.
- Fournier, R.O. and A.H. Truesdell, 1973. "An empirical Na-K-Ca geothermometer for natural waters." *Geochimica et Cosmochimica Acta*, 37, 1255-1275.
- Giggenbach, W.F., 1988. "Geothermal solute equilibria. Derivation of Na-K-Mg-Ca geothermometers." *Geochimica et Cosmochimica Acta*, 52, 2749-2765.
- Hull, C.D., M.H. Reed, and K. Fisher, 1987. "Chemical geothermometry and numerical unmixing of the diluted geothermal waters of the San Bernardino Valley Region of Southern California." *GRC Transactions*, 11, 165-184.
- Michard, G. and E. Roekens, 1983. "Modelling of the chemical components of alkaline hot waters." *Geothermics*, 12, 161-169.
- Mitchell, J.C., 1976. "Geothermal Investigations in Idaho: Part 5, Geochemistry and geologic setting of the thermal waters of the northern Cache valley area, Franklin county, Idaho." Idaho Dep. Water Resources, *Water Inf. Bull.*, No. 30.
- Mitchell, J.C., L.L. Johnson, and J.E. Anderson, 1980. "Geothermal Investigations in Idaho, Part 9, Potential for direct heat application of geothermal resources." Idaho Dep. Water Resources, *Water Inf. Bull.*, No. 30.
- Neupane, G., R.W. Smith, C.D. Palmer, and T.L. McLing, 2013. "Multicomponent equilibrium geothermometry applied to the Raft River geothermal area, Idaho: preliminary results." Geological Society of America *Abstracts with Programs*, 45(7), 859.
- Neupane, G., E.D. Mattson, T.L. McLing, C.D. Palmer, R.W. Smith, and T.R. Wood, 2014. "Deep geothermal reservoir temperatures in the Eastern Snake River Plain, Idaho using multicomponent geothermometry." *Proceedings*, Thirty-Ninth Workshop on Geothermal Reservoir Engineering, Stanford University, Stanford, California, February 24-26, 2014 SGP-TR-202.
- Neupane, G., E.D. Mattson, T.L. McLing, C.D. Palmer, R.W. Smith, T.R. Wood, and R.K. Podgorney, 2015a. "Geothermal reservoir temperatures in southeastern Idaho using multicomponent geothermometry." *Proceedings*, World Geothermal Congress 2015, Melbourne, Australia, 19-25 April 2015.
- Neupane, G., J.S. Baum, E.D. Mattson, G.L. Mines, C.D. Palmer, and R.W. Smith, 2015b. "Validation of multicomponent equilibrium geothermometry at four geothermal power plants." *Proceedings*, Fortieth Workshop on Geothermal Reservoir Engineering Stanford University, Stanford, California, January 26-28, 2015.
- Palmer, C.D., S.R. Ohly, R.W. Smith, G. Neupane, T. McLing, E. Mattson, 2014. "Mineral selection for multicomponent equilibrium geothermometry." *GRC Transactions*, 38, 453-459.
- Palandri, J.L. and M.H. Reed, 2001. "Reconstruction of in situ composition of sedimentary formation waters." *Geochimica et Cosmochimica Acta*, 65, 1741-1767.
- Pang, Z.H. and M. Reed, 1998. "Theoretical chemical thermometry on geothermal waters: Problems and methods." *Geochimica et Cosmochimica Acta*, 62, 1083-1091.
- Parlman, D.J. and H.W. Young, 1992. "Compilation of selected data for thermal-water wells and springs, 1921 through 1991." US Geological Survey, Open-File Report 92-175.
- Peiffer, L., C. Wanner, N. Spycher, E. Sonnenthal, B.M. Kennedy, J. Iovenitti, 2014. "Optimized multicomponent vs. classical geothermometry: insights from modeling studies at the Dixie Valley geothermal area." *Geothermics*, 51, 154-169.
- Reed, M. and Spycher, N. (1984): Calculation of pH and mineral equilibria in hydrothermal waters with application to geothermometry and studies of boiling and dilution. *Geochimica et Cosmochimica Acta*, 48, 1479-1492.
- Smith, R.W., C.D. Palmer, and D. Cooper, 2012. "Approaches for multicomponent equilibrium geothermometry as a tool for geothermal resource exploration." AGU Fall Meeting, San Francisco, 3-7 December 2012.
- Spycher, N.F., E. Sonnenthal, and B.M. Kennedy, 2011. "Integrating multicomponent chemical geothermometry with parameter estimation computations for geothermal exploration." *GRC Transactions*, 35, 663-666.
- Spycher, N., L. Peiffer, E.L. Sonnenthal, G. Saldi, M.H. Reed, and B.M. Kennedy, 2014. "Integrated multicomponent solute geothermometry." *Geothermics*, 51, 113-123.
- Tole, M.P., H. Ármannsson, Z.H. Pang, and S. Arnórsson, 1993. "Fluid/mineral equilibrium calculations for geothermal fluids and chemical geothermometry." *Geothermics* 22, 17-37.
- Young, H.W. and J.C. Mitchell, 1973. "Geothermal investigations in Idaho. Part 1. Geochemistry and geologic setting of selected thermal waters." U.S. Geological Survey and Idaho Dept. of Water Administration.

Appendix G.

Neupane, G., Mattson, E.D., Cannon, J.C., Atkinson, T.A., McLing, T.L., Wood, T.R., Worthing, W.C., Dobson, P.F., and Conrad, M.E., 2016b. Potential hydrothermal resource areas and their reservoir temperatures in the Eastern Snake River Plain, Idaho. Proceedings, 41st Workshop on Geothermal Reservoir Engineering, Stanford University, Stanford, CA.

Potential Hydrothermal Resource Areas and Their Reservoir Temperatures in the Eastern Snake River Plain, Idaho

^{1,2}Ghanashayam Neupane*, ¹Earl D. Mattson, ^{2,3}Cody J. Cannon, ⁴Trevor A. Atkinson, ^{1,2}Travis L. McLing, ^{2,3}Thomas R. Wood, ^{2,3}Wade C. Worthing, ⁵Patrick F. Dobson, and ⁵Mark E. Conrad

¹Idaho National Laboratory, Idaho Falls, ID 83415, USA

²Center for Advanced Energy Studies, Idaho Falls, ID 83401, USA

³University of Idaho-Idaho Falls, Idaho Falls, ID 83402, USA

⁴Ormat Technologies Inc., Reno, NV 89511, USA

⁵Lawrence Berkeley National Laboratory, Berkeley, CA 94720 USA

E-mail: Ghanashayam.Neupane@inl.gov

Keywords: Eastern Snake River Plain, ESRP, RTEst, geothermal, geothermometer

ABSTRACT

The Eastern Snake River Plain (ESRP) in southern Idaho is a region of high heat flow. Sustained volcanic activities in the wake of the passage of the Yellowstone Hotspot have turned this region into an area with great potential for geothermal resources as evidenced by numerous hot springs scattered along the margins of the plain and several hot-water producing wells and hot springs within the plain. Despite these thermal expressions, it is hypothesized that the pervasive presence of an overlying groundwater aquifer in the region effectively masks thermal signatures of deep-seated geothermal resources. The dilution of deeper thermal water and re-equilibration at lower temperature are significant challenges for the evaluation of potential resource areas in the ESRP. Over the past several years, we collected approximately 100 water samples from springs/wells for chemical analysis as well as assembled existing water chemistry data from the literature. We applied several geothermometric and geochemical modeling tools to these chemical compositions of ESRP water samples. Geothermometric calculations based on principles of multicomponent equilibrium geothermometry with inverse geochemical modeling capability (e.g., Reservoir Temperature Estimator, RTEst) have been useful for evaluating reservoir temperatures, and have indicated numerous potential moderate to high temperature geothermal prospects in the ESRP. Specifically, areas around southern/southwestern side of the Mount Bennett Hills and within the Camas Prairie in the western-northwestern regions of the ESRP and its margins suggest temperatures in the range of 140-200°C. In the northeastern portions of the ESRP, Lidy Hot Springs, Ashton, Newdale, and areas east of Idaho Falls have expected reservoir temperatures ≥ 140 °C. In the southern ESRP, areas near Buhl and Twin Falls are found to have temperatures as high as 160 °C. These areas are likely to host potentially economic geothermal resources; however, further detailed study is warranted at each site to evaluate hydrothermal suitability for economic use.

1. INTRODUCTION

The eastern Snake River Plain (ESRP) in southeastern Idaho is a region of high heat flow with great potential for significant geothermal resources (Figure 1). A limited number of deep wells (such as INEL-1) and several hot springs and wells along the margin of ESRP also provide direct evidence of a high-temperature regime at depth in the area. However, most of the shallow wells within the ESRP generally have low field-measured temperature, and it is likely that the Eastern Snake River Plain Aquifer (ESRPA) is obscuring geothermal signature from depth. The ESRPA is a prolific aquifer hosted in a thick sequence of thin-layered, highly transmissive basalt flows. The aquifer rapidly transports cold water from the Yellowstone Plateau and surrounding mountain basins to springs along the Snake River Canyon west of Twin Falls, Idaho. The flush of cold water through the overlying ESRPA masks the geothermal signature of the heat existing at depth (e.g., Smith, 2004). Importantly, the geothermal gradient below the ESRP aquifer system increases rapidly (Blackwell, 1989; McLing et al., 2002; Nielson et al., 2012) providing additional evidence of the presence of a deep geothermal resource in the area.

Previously, we made an initial geothermometric assessment of the ESRP using limited water chemistry dataset (Neupane et al., 2014; Cannon et al., 2014). We followed on that work by collecting several new water samples from numerous geothermal features in the ESRP and surrounding areas. In this paper, we provide geothermometric assessment of some potential geothermal resource areas in the ESRP. Specifically, we present geothermometric temperatures of geothermal areas distributed around southern/southwestern side of the Mount Bennett Hills, Camas Prairie, Lidy Hot Springs, Ashton area, Newdale area, and areas east of Idaho Falls. Similarly, we also present geothermometric results of geothermal areas around Buhl and Twin Falls area in the southern ESRP. The reservoir temperatures of these geothermal sites were estimated with traditional (e.g., Fournier, 1977) as well as a multicomponent geothermometry tool [e.g., Reservoir Temperature Estimator (RTEst) (Palmer et al., 2014; Mattson et al., 2015)] based on the chemical composition of thermal water samples.

2. GEOLOGIC AND GEOTHERMAL SETTING OF EASTERN SNAKE RIVER PLAIN

The Snake River Plain (SRP) is a topographic depression along the Snake River (Figure 1) in southern Idaho. The SRP is divided into two parts, the western Snake River Plain (WSRP) and the ESRP. The WSRP is a basalt- and sediment-filled tectonic feature defined by

a normal fault-bounded graben whereas the ESRP is formed by crustal down-warping, faulting, and successive caldera formation that is linked to the middle Miocene to Recent volcanic activities associated with the relative movement of the Yellowstone Hot Spot (Figure 1) (Pierce and Morgan, 1992; Hughes et al., 1999; Rodgers et al., 2002). The 100 km wide ESRP extends over 600 km (Hughes et al., 1999). Four events in the late Tertiary are important for creation and shaping the ESRP (Hughes et al., 1999): (1) successive Miocene-Pliocene rhyolitic volcanic eruptive centers from southwest near the common border of Idaho, Oregon, and Nevada trending northeast to Yellowstone National Park in northwest Wyoming, (2) Miocene to Holocene crustal extension which produced the Basin and Range province, (3) Quaternary basaltic flows, and (4) Quaternary glaciation and associated eolian, fluvial, and lacustrine sedimentation and catastrophic flooding.

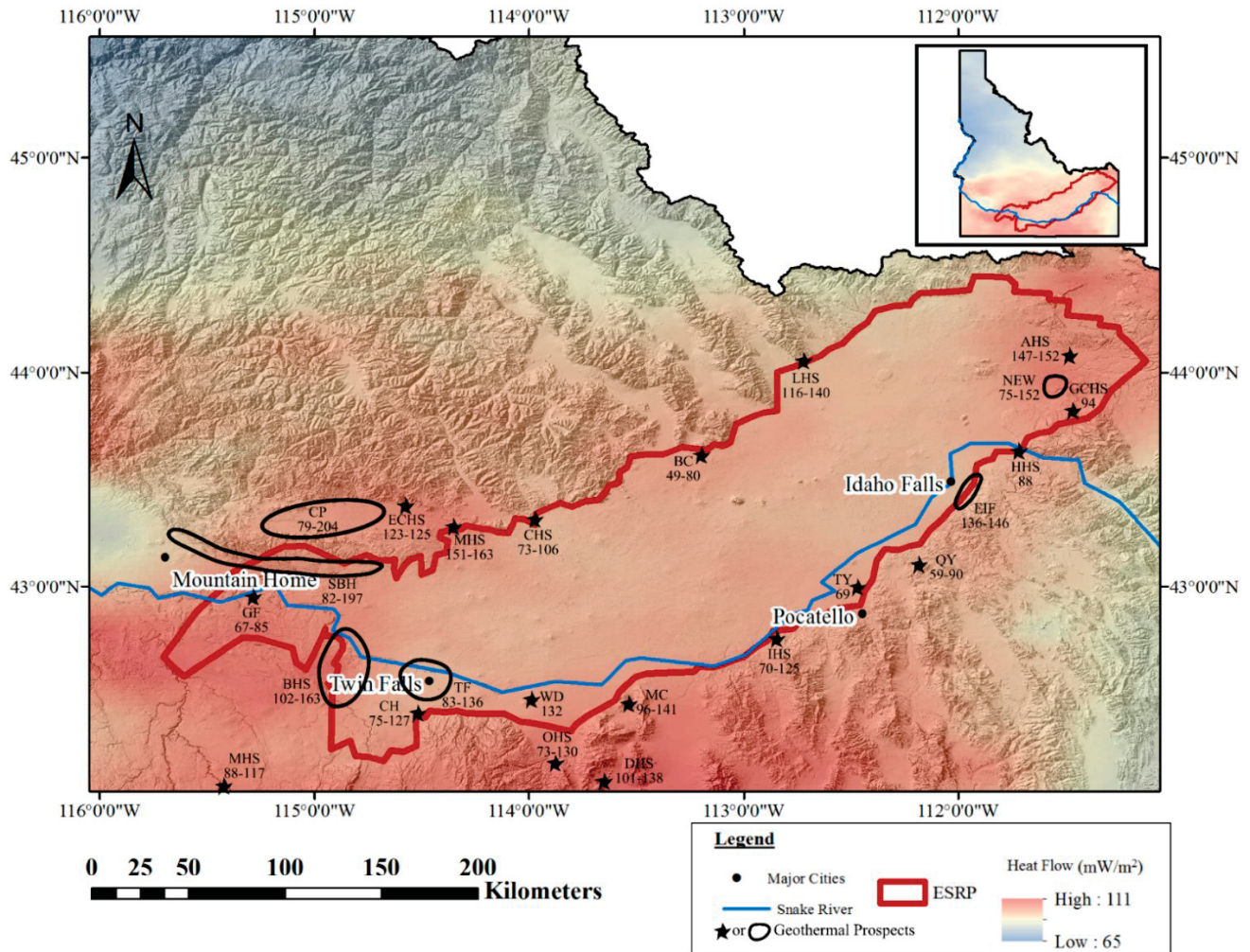


Figure 1. Map of the southern Idaho was prepared by draping heat flow map (Williams and DeAngelo, 2011) over DEM. The thick red line demarcates the margins of the ESRP from the surrounding Basin and Range province. Stars and polygons represent geothermal prospects (codenames are given in Table 1) in and around ESRP. The number or range of numbers associated with each geothermal prospect is the RTEst estimated reservoir temperature (°C).

The ESRP consists of thick volcanic ash-flow tuffs, which are overlain by >1 km of Quaternary basaltic flows (Figure 2). The felsic volcanic rocks at depth are the product of super volcanic eruptions associated with the Yellowstone Hotspot. These rocks progressively become younger to the northeast towards the Yellowstone Plateau (Pierce and Morgan, 1992; Hughes et al., 1999). The younger basalt layers are the result of several low-volume, monogenetic shield-forming eruptions of short-duration that emanated from northwest trending volcanic rifts in the wake of the Yellowstone Hot Spot (Hughes et al., 1999). The thick sequences of coalescing basalt flows with interlayered fluvial and eolian sediments in the ESRP constitute a very productive cold water aquifer system above the volcanic ash-flow tuffs (Whitehead, 1992).

Recent volcanic activity, a high heat flux [$\sim 110 \text{ mW/m}^2$ (Blackwell, 1989; Smith, 2004)], and the occurrence of numerous peripheral hot springs suggest the presence of undiscovered geothermal resources in the ESRP. As a consequence of these geologic indicators, we hypothesize that the ESRP at depth hosts a large geothermal resource with the potential for one or more viable conventional or enhanced geothermal reservoirs. In particular, we consider the lower welded rhyolite ash-flow tuff zone (Figure 2) to have exploitable heat sources that can be tapped by EGS development.

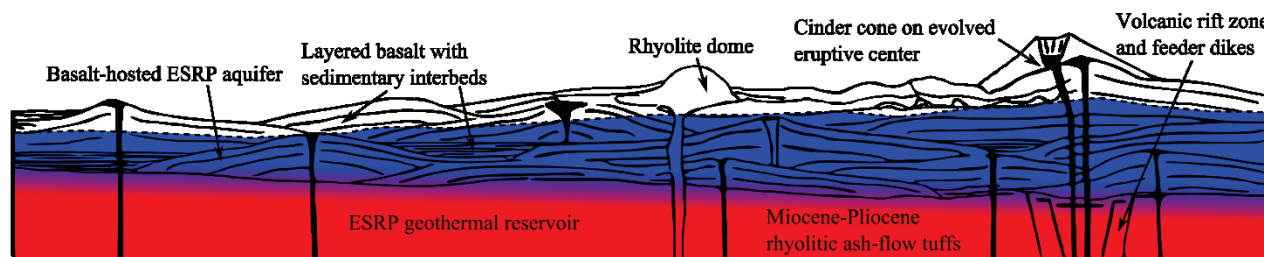


Figure 2. Schematic cross-section across the ESRP (modified from Hughes et al., 1999; Neupane et al., 2014) showing underlying rhyolitic ash-flow tuffs and overlying basalt flows with few sedimentary layers. The underlying rhyolite ash-flow tuffs are assumed to be the ESRP geothermal resource. Small amount of thermal waters are considered to be upwelling from underlying reservoir into the overlying basalt-hosted ESRP aquifer system. The presence of very productive, cold groundwater aquifer system is regarded to mask the underlying geothermal regime in the ESRP.

The ESRP system as a whole (including the deep geothermal reservoir and the overlying cold-water aquifer system) is an open and dynamic hydrogeologic system. Most water from shallow wells and springs in the ESRP are mixed waters of multiple sources, particularly a mix of meteoric water and deep-sourced reservoir water (McLing et al., 2002; Smith, 2004; Welhan, 2015). The upwelling thermal waters interact with the basalt at the base of the regionally extensive cold water aquifer (Morse and McCurry, 2002), with the altered basalt forming a permeability barrier: this helps mask the expression of the deep thermal resource (Figure 2).

3. GEOTHERMOMETRY

One of the tools used to prospect for geothermal resources is geothermometry, which uses the chemical compositions of water from springs and wells to estimate reservoir temperature. As an exploration tool, geothermometry offers a cost effective method to decrease exploration risk by evaluating a potential geothermal reservoir's temperature. To conduct geothermometry, measured chemical compositions of water from wells and springs that exhibit some level of elevated temperatures are needed. The application of geothermometry requires several assumptions. The most important assumptions are that the reservoir minerals and fluid attain a chemical equilibrium and as the water moves from the reservoir to sampled location, it retains its chemical composition (Fournier et al., 1974). The first assumption is generally valid (provided a long residence time); however, the second assumption is more likely to be violated because of composition altering processes, such as, re-equilibration at lower temperature, dilution (mixing), and loss of fluids (boiling) and volatiles (e.g., CO_2) with the decrease in pressure.

Traditional geothermometers such as silica geothermometers, Na/K geothermometer, etc., are empirical to semi-empirical approaches where a user enters the measured concentration of certain component(s) into the geothermometer equation. The reliability, sensitivity, and responsiveness of traditional geothermometers to various composition altering processes vary. For example, geothermometers based on cation concentration ratios (e.g., Na/K geothermometer) are minimally sensitive to boiling or mixing with dilute water; while geothermometers based directly on the concentration of component(s) (e.g., quartz geothermometer) are highly sensitive to these processes (D'Amore and Arnórsson, 2000). A drawback of many existing geothermometry approaches is that they do not adequately account for physical processes (e.g., mixing, boiling) and geochemical processes (e.g., mineral dissolution, precipitation, degassing) that may occur after the water leaves the reservoir and thereby alters its composition. If these changes are not taken into account, predictions of in-situ reservoir conditions (e.g., temperature, $f\text{CO}_2$) based on the chemical composition of water samples taken from shallower depths or at the surface may be erroneous, or too imprecise to be useful.

In addition, it is difficult to quantify uncertainties associated with temperatures estimated with these geothermometers. As a result, it is not uncommon to find diverse temperature estimates for the same water using multiple traditional geothermometers. Nevertheless, because these geothermometers are easy to use and sometimes provide good results, they are considered to be an essential part of the geothermal exploration toolkit (D'Amore and Arnórsson, 2000).

A more advanced geothermometric approach is multicomponent equilibrium geothermometry (MEG). The MEG approach of geothermometry utilizes multiple chemical constituents measured in water samples for inverse geochemical modeling considering a suite of selected minerals (selected based on some knowledge of the system) so as to provide more robust temperature estimates with quantifiable uncertainties. Geothermal temperature predictions using MEG provide apparent improvement in reliability and predictability of temperature over traditional geothermometers. The basic concept of this method was developed in 1980s (e.g., Michard and Roekens, 1983; Reed and Spycher, 1984). Some previous investigators (e.g., D'Amore et al., 1987; Hull et al., 1987; Tole et al., 1993) have used this technique for predicting reservoir temperatures in various geothermal sites. Other researchers have used the basic principles of this method for reconstructing the composition of geothermal fluids and formation brines (Pang and Reed, 1998; Palandri and Reed, 2001). More recent efforts by some researchers (e.g., Bethke, 2008; Spycher et al., 2011; Smith et al., 2012; Cooper et al., 2013; Neupane et al., 2013, 2014; Cannon et al., 2014; Spycher et al., 2014; Peiffer et al., 2014; Palmer et al., 2014; Neupane et al., 2015a,b,c; Mattson et al., 2015; Neupane et al., 2016a,b) have been focused on improving temperature predictability of the MEG.

For this study, both traditional [e.g., quartz (no steam loss) (Fournier, 1977), chalcedony (Fournier, 1977), and Na-K-Ca (Truesdell and Fournier, 1973; Fournier and Potter, 1979)] and RTest (Palmer et al., 2014; Mattson et al., 2015) geothermometric approaches were applied to estimate reservoir temperatures. For the silica geothermometers, pH correction on silica concentrations was not applied. While applying RTest to each water sample, a mineral assemblage consisting of 5-7 representative minerals (Mg bearing minerals – clinocllore, illite, saponite, beidellite, talc; Na bearing minerals – paragonite, saponite; K-bearing minerals – K-feldspar, clinoptilolite-

K, illite; Ca bearing minerals – calcite; fluorite, and chalcedony) was used for the development of the reservoir temperature estimate for each sample. For each site, the same mineral assemblage was used for all samples using the same thermodynamic database (e.g., LNNL database based thermo.dat database of Geochemist's Workbench). In general, the mineral assemblage is selected based on available information such as water chemistry (e.g., pH), likely reservoir rock types and temperature range, etc. For more detailed information on selection of the mineral assemblage, see Palmer et al. (2014).

4. WATER SAMPLES

4.1 New data

As a major part of this work, we initiated a sampling campaign during the spring and summer of 2014 and 2015 (Cannon et al., 2014; Dobson et al., 2015; Neupane et al., 2015c). The sampling campaign was aimed at collecting samples from thermal features that either have incomplete available data or were not sampled/analyzed previously. Our goal was to develop an extensive thermal expression chemistry data set to be used for geothermometry calculations using RTest as well as for analyzing for other trace elements, isotopes, and noble gases. Over the course of the project period, we collected and analyzed over 90 samples from thermal features in the ESRP and surrounding area. The water chemistry data will be available from the National Geothermal Data System (NGDS) web portal.

4.2 Historical data

Existing southeast Idaho water composition data have been obtained from the Idaho Department of Water Resources, literature searches from the Web of Science, and examining dissertations at the University of Idaho. Existing water composition data were evaluated for their quality (e.g., charge balance, etc.) and completeness (except Al) for MEG. Almost all of the historical data lacked measured concentration of Al, and for these samples, a value determined by assuming equilibrium with K-feldspar (Pang and Reed, 1998) was used in the geochemical modeling. In some instances, the Al values measured in new samples collected from nearby hot springs or hot wells were used.

Existing data and new chemical data were used for the estimation of reservoir temperatures with traditional geothermometers as well as with RTest. In the past, we used historical data for preliminary evaluation of geothermal resources along the margins of the ESRP (e.g., Neupane et al., 2014). Some of the geothermal features with available good quality and complete geochemical data were also sampled during our sampling campaigns, and for most of these features, the existing data were found to be similar to the new chemical data.

4.3 Hot springs and nearby hot wells

Both compositions of water samples collected from hot springs as well as shallow hot wells were used with equal importance for the temperature estimation of several geothermal prospects in ESRP. It is generally assumed that the geothermal system manifest some kind of surface signals such as hot springs or fumaroles, however, there have been some hidden or blind geothermal systems. For example, the Raft River geothermal system was identified when shallow (120-150 m deep) wells that were drilled for domestic and stock use encountered boiling water (Williams et al., 1976). Similarly, in the ESRP, the Newdale prospect (NEW in Figure 1) was first identified by the presence of numerous hot shallow wells in the area. However, how useful hot shallow waters can be for geothermometric calculations in the southern Idaho was an issue for us when we started this work. Recently, we compared the temperature estimates of hot springs and nearby wells in southern Idaho (Neupane et al., 2015c). That study indicated that the reservoir temperatures estimated using water compositions measured from surface thermal features and wells produce similar results. However, there are a few systems where the estimated reservoir temperatures based on water compositions measured from hot springs and hot wells are different. Neupane et al. (2015c) emphasized that when such differences exist, it is imperative to consider the consistency of the water types and distance between the sources when estimating reservoir temperatures. With the exception of the Durfee Hot Spring prospect [the same system was also noted by Neupane et al. (2015c) as one of two systems examined in southern Idaho that have divergent temperature estimates with hot spring and hot well compositions] (DHS in Figure 1), all other prospects with measured compositions from samples collected from hot springs and hot wells in the ESRP yielded similar results (see section 5).

4.4 Geothermal prospects

Based on the distribution of samples, 24 geothermal prospects are identified (Figures 1, 3, and Table 1). The number of samples in each prospect (Table 1) vary such that some prospects have multiple samples (e.g., Banbury Hot Springs prospect has 37 samples) from different sources where as some prospects have few number of samples (e.g., Wybenga Diary prospect has only one sample). Much more detailed descriptions of these prospects are forthcoming.

5. RESULTS

5.1 Water chemistry

Compositions of waters from hot/warm springs and wells in southeastern Idaho are presented in Figure 3. All springs/wells (with few exceptions such as Spackman well in Newdale prospect) that we sampled represent the expression of geothermal activities (field T >20 °C) in the ESRP. The highest field temperature within and along the margins of ESRP was recorded at the Magic Hot Spring Landing well (75 °C) in Magic Hot Spring prospect (MHS in Figure 1). The pH of ESRP thermal waters ranges from 6.3 to 9.6. These thermal waters show a large range in total dissolved solids (TDS) from about 106 mg/L (Sturm well in Ashton prospect, AHS in Figure 1) to more than 7,000 mg/L (Heise Hot Spring, HHS in Figure 1).

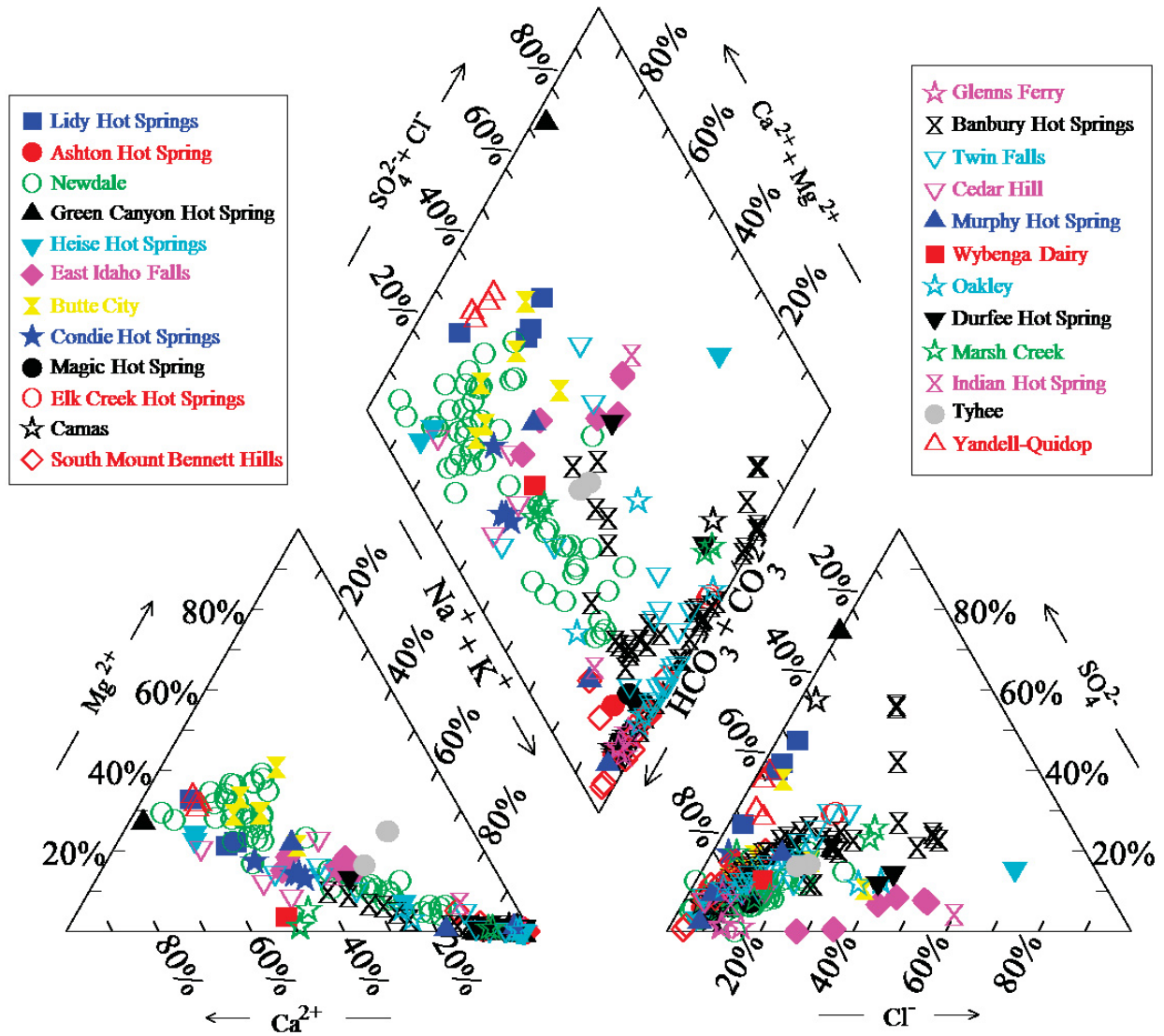


Figure 3. Chemistry of the ESRP thermal water samples shown on Piper diagram

Based on the dominant ions (Figure 3Error! Reference source not found.) in water, ESRP waters can be grouped into 10 water types. These are Ca-HCO₃, Mg-HCO₃, Ca-Mg-HCO₃, Na-HCO₃, Ca-SO₄, Na-SO₄, Na-Cl, Na-K-HCO₃, Na-K-Cl-SO₄, and Ca-Na-HCO₃ type waters. In general, ESRP waters have either Ca-Mg or Na as the dominant cations and HCO₃ as the dominant anion. The ESRP waters with dominant HCO₃ may have been the product of carbonated water-rock interaction at low to high temperatures. Specifically, Na-HCO₃ waters are considered deeper ESRP water whereas Ca-Mg-HCO₃ water are shallower ESRP water. The few water samples (e.g., Heise Hot Spring, Green Canyon Hot Spring, etc.) with Cl and/or SO₄ as dominant anions may have originated with water-rock interaction involving Paleozoic evaporite beds.

5.2 Geothermometric assessments

5.2.1 Giggenbach diagram

The sample compositions are also plotted on a Giggenbach ternary diagram (Giggenbach, 1988) to determine evidence of equilibration and/or mixing (Error! Reference source not found.) as well as to illustrate the likely water-rock interaction temperatures in the reservoirs. This plot is useful to classify waters into fully equilibrated waters, partially equilibrated, and immature waters. The diagram uses the full range of equilibrium relationships between Na, K, and Mg to determine the degree of equilibration between the water and the rock at depth. The plot suggests that the waters from several ESRP wells and springs are partially equilibrated that may have interacted with the reservoir rocks at temperatures ranging from 100 °C to 180 °C. However, majority of the ESRP waters are immature waters, as indicated by elevated Mg contents. The immature waters may indicate significant mixing with cool meteoric waters, and traditional geothermometers may not be suitable tools for temperature estimation for these waters.

5.2.2 Temperature estimates with traditional geothermometers

Traditional geothermometers were applied to measured water compositions for general assessment of the geothermal temperature at each sampling site. There have been several established empirical/semi-empirical geothermometers based on the relationship between concentrations (or concentration ratios) of chemical components with temperature. Even though majority of these geothermometers are based on empirically fitted curves, there have been some postulated geochemical basis (assumptions) supporting these relationships. For example, silica geothermometers are based on solubility of solid-phase silica (e.g., quartz, chalcedony, etc.) controlling the aqueous concentration of silica. Similarly, several variations of sodium-potassium geothermometers are based on water-rock interaction involving albite and K-feldspar. Similarly, the sensitivity and responsiveness of geothermometers to various composition-altering processes are not similar. For example, geothermometers based on cation concentration ratios are not sensitive to boiling or mixing with dilute water; however, geothermometers based directly on the concentration of component(s) show large temperature sensitivity to these processes. In practice, it is not uncommon to find diverse temperature estimates for the same water with multiple traditional geothermometers. Therefore, whenever the assumptions on which a geothermometer is based on are not satisfied, temperature estimates with it are likely to be erroneous.

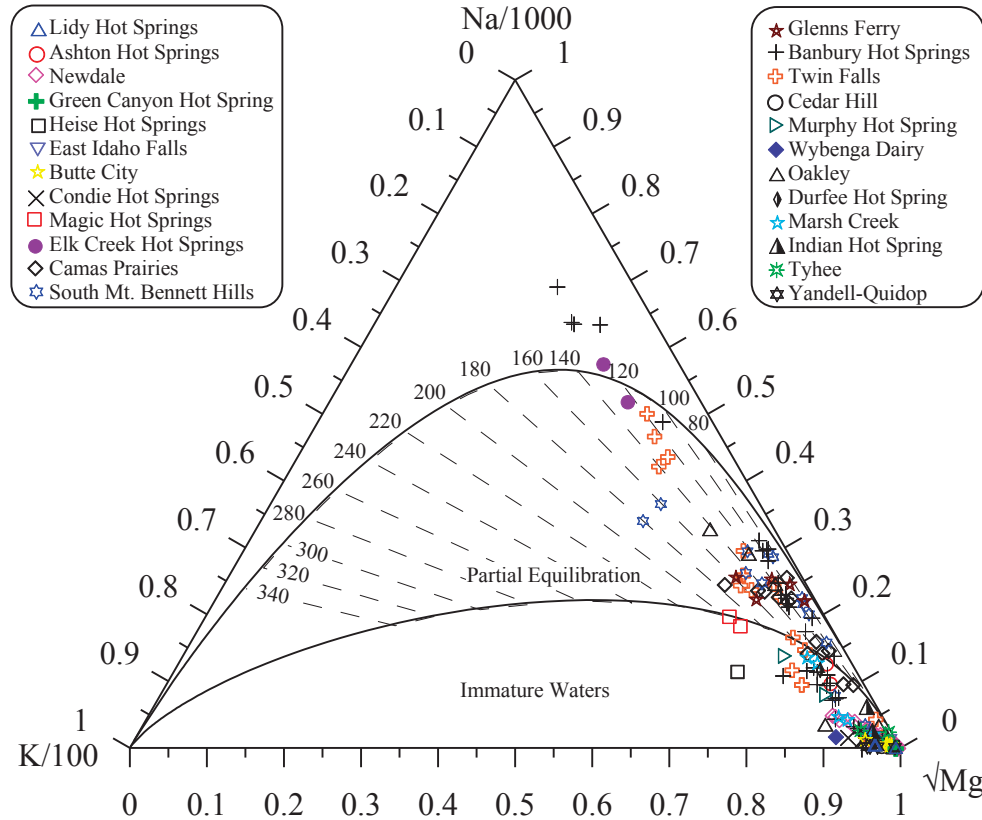


Figure 4. Giggenbach ternary diagram for the ESRP thermal water samples

For the ESRP, the traditional geothermometer-based temperatures can be difficult to use to assess the geothermal potential of prospects. For example, estimated temperature values for the Heise Hot Spring, range from 53 °C using chalcedony to 243 °C using Na/K ratios. Nevertheless, for some samples from other prospects, such as a well at the College of Southern Idaho (CSI Well2) representing the Twin Falls geothermal prospect, the range of estimated temperatures is from 85 °C to 140 °C suggesting relatively good agreement between the traditional geothermometry temperature estimates. In general, we have found that ESRP thermal estimated temperatures using the Na/K ratios are higher than estimated temperatures obtained with other geothermometers.

5.2.3 Temperature estimates with RTEst

All water samples collected during the sampling campaigns of 2014 and 2015 as well as useful water compositions assembled from literature for this study were used for the temperature estimation with RTEst. For each sample, 5-7 minerals (consisting mainly of silica-polymorphs, clays, zeolites, carbonates, sulfates, feldspars, etc.) were selected as a mineral assemblage.

An example of the RTEst results for a water sample collected from Miracle Hot Spring well located in Banbury Hot Springs prospect (BHS in Figure 1) is shown in 5a shows log Q/K_T curves of the reservoir mineral assemblage (calcite, chalcedony, beidellite, mordenite, and paragonite) used for the Miracle Hot Spring water composition. The log Q/K_T curves of these minerals intersect the log $Q/K_T = 0$ at a wide range of temperatures, making the log Q/K_T curves derived from the reported water chemistry minimally useful for estimating temperature. The range of equilibration temperature for the assemblage minerals is a reflection of physical and chemical processes that may have modified the Miracle Hot Spring water composition during its ascent to the sampling point.

To account for possible composition altering processes, RTest was used to simultaneously estimate a reservoir temperature and optimize the amount of dilute near-surface H₂O mixed with the thermal water (a physical process) and the fugacity of CO₂ change (a chemical process) that may have occurred during its ascent to the surface. Using these two additional optimization parameters, the results for the corrected fluid composition of Miracle Hot Spring are shown in Figure 5b. Compared to the log Q/KT curves calculated using the reported water compositions (Figure 5a), the optimized curves (Figure 5b) converge to log Q/KT = 0 within a narrow temperature range (i.e., 161±3 °C).

The optimized temperatures and composition parameters for the other ESRP waters were estimated using RTest in the same manner. The RTest estimated temperatures for the ESRP geothermal samples range from about 60 °C to 204 °C. The hottest reservoir temperature estimate is obtained for Wardrop Hot Spring located in north-central part of Camas Prairie (CP in Figure 1). Similarly, hot springs located on the southern side of the Mount Bennett Hills (e.g., Prince Albert Hot Spring, Latty Hot Spring) (SBH in Figure 1) also have reservoir temperature estimates as high as 200 °C.

Table 1. Estimated temperatures (°C) for several geothermal prospects in the ESRP

Prospects	Measured ^a	RTest ^b	Quartz (nsl) ^c	Chalcedony ^d	Na-K-Ca ^e	Map Code ^f
Lidy Hot Springs (4) ^g	56	116-140	57-89	25-58	44-65	LHS
Ashton Hot Spring (2)	63	147-152	113-143	84-116	109-117	AHS
Newdale (50)	87	75-152	66-134	26-112	29-111	NEW
Green Canyon Hot Spring (1)	44	94	75	44	65	GCHS
Heise Hot Spring (1)	48	88	84	53	89	HHS
East Idaho Falls (6)	28	136-146	115-143	86-117	45-74	EIF
Butte City (6)	41	49-80	70-106	38-77	37-43	BC
Condie Hot Spring (4)	51	73-106	71-82	40-51	71-83	CHS
Magic Hot Spring (2) ^h	75	151-163	139-142	113-116	143-149	MHS
Elk Creek Hot Springs (2)	56	123-125	114-115	86	107-110	ECHS
Camas Prairie (13)	73	79-204	103-128	74-100	70-124	CP
South Mount Bennett Hills (13)	68	82-197	110-143	80-117	72-160	SBH
Glenns Ferry (5)	39	67-85	80-109	48-79	74-138	GF
Banbury Hot Springs (37)	72	102-163	98-139	67-127	69-165	BHS
Twin Falls (21)	43	83-136	77-119	45-91	70-132	TF
Cedar Hill (4)	38	75-127	62-116	29-87	50-129	CH
Murphy Hot Spring (3)	55	88-117	119-148	90-122	57-144	MHS
Oakley Hot Spring (5)	47	73-130	77-125	45-97	82-155	OHS
Durfee Hot Spring (2)	45	101-138	96-117	66-88	46-131	DHS
Marsh Creek (5)	60	96-141	96-113	66-83	128-134	MC
Wybenga Dairy (1)	34	132	118	89	189	WD
Indian Hot Spring (2)	39	70-125	64-110	32-80	60-64	IHS
Tyhee (3)	41	69	63-93	31-62	52	TY
Quidop-Yandell (4)	38	59-90	55-63	23-31	43-63	QY

^aMaximum measured temperature for the prospects; ^b RTest estimated temperature range; ^cquartz (no steam loss) geothermometer temperature (Fournier, 1977); ^d chalcedony geothermometer temperature (Fournier, 1977); ^e Mg-corrected (where applicable) Na-K-Ca geothermometer temperature (Truesdell and Fournier, 1973; Fournier and Potter, 1979); ^fthese map codes are used to represent geothermal prospects in Figure 1; ^gnumber of samples representing the prospect; ^hboth samples represent the same well, one sample was collected directly from the well leak whereas other sample was collected from the runoff channel.

5.3 Geothermal prospects and their reservoir temperatures

Table 1 summarizes likely reservoir temperature range for all geothermal prospects within and along the margins of the ESRP identified in this study. The RTest estimated temperature range for each prospect is also given in Figure 1. Some of the hottest prospects in the ESRP region are Lidy Hot Springs (LHS), Magic Hot Spring (MHS), Camas Prairie (CP), south of Mount Bennett Hills (SBH), Banbury Hot Springs (BHS), east Idaho Falls (EIF), Newdale (NEW), and Ashton Hot Spring (AHS) (Figure 1). The geothermal potential of some of these prospects are also identified by the first phase of the SRP Play Fairway analysis (Shervais et al., 2015). Below we provide brief summaries for some of the promising geothermal prospects in the ESRP region.

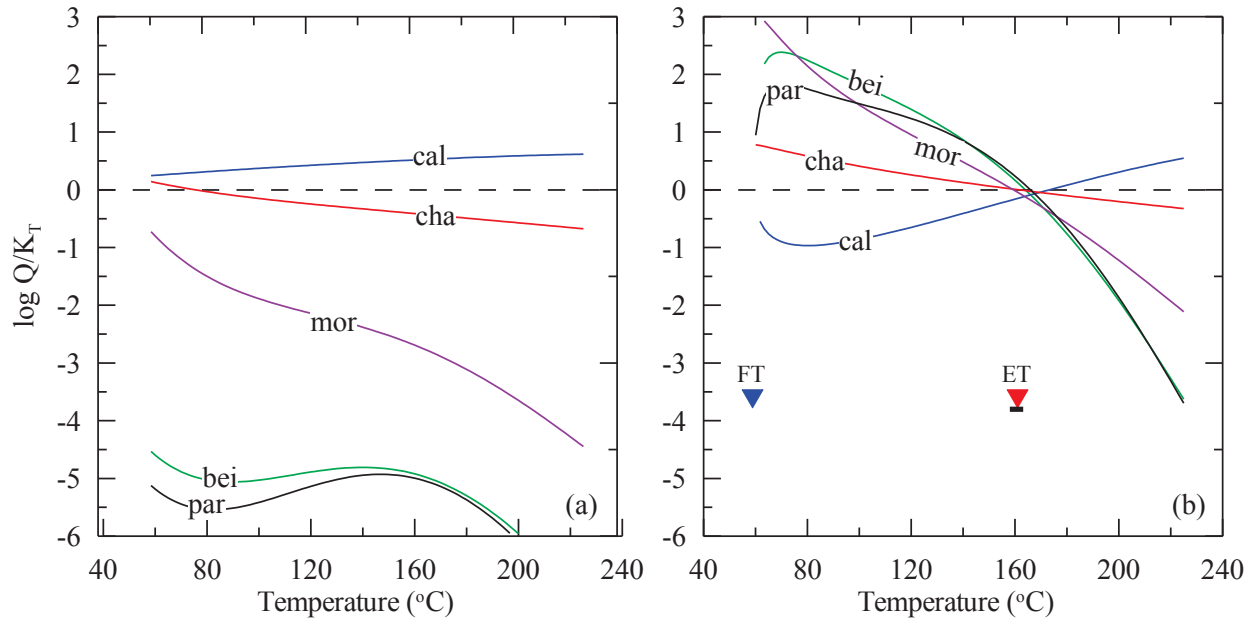


Figure 5. Graphical representation of RTest analysis of Miracle Hot Spring well located in the Banbury Hot Springs prospect (see Figure 1). a) $\log Q/K_T$ plot for assemblage minerals using observed fluid composition, b) $\log Q/K_T$ plot for assemblage minerals using RTest optimized fluid composition. In this diagram, FT is field temperature, ET is estimated temperature, and the horizontal solid bar underneath ET represents two-standard error in estimated temperature. Mineral assemblage includes: bei: beidellite-Mg, cal: calcite, cha: chalcedony, mor: mordenite-Na, and par: paragonite.

5.3.1 Lidy Hot Springs

The Lidy Hot Springs prospect (LHS in Figure 1) is located at the southeastern end of the Beaverhead Mountains in Clark County in Idaho. From the early 20th century, the area was gradually developed into a commercial recreation site that provided services such as swimming, soaking, dancing, dining, and lodging to public. However, with the transfer of ownership in the early 1960s, the site ceased to offer those recreational services, and started a travertine mining activity. Two hot springs in the area are still issuing thermal water (52-56 °C). Similarly, in the vicinity of the Lidy Hot Springs, there are other springs (e.g., Warm Spring (29 °C)) issuing warm to cooler waters.

Rocks underlying the Lidy Hot Springs area consist of young volcanics and older meta-sedimentary rocks (Link, 2002). The younger rocks (Upper Miocene and Pliocene) consist of fluvial and lacustrine deposits, felsic volcanic rocks, rhyolite flows, tuffs, ignimbrites. Thick sequences of Paleozoic sedimentary rocks (Pz) underlie the Tertiary rock types, and likely constitute the geothermal reservoir in the area.

The RTest estimated reservoir temperature for the Lidy Hot Springs prospect is about 140 °C (Table 1). RTest modeling result shows that the Lidy Hot Springs water may contain up to 60% cooler water and 40% deeper thermal water. Similarly, no-steam loss silica-enthalpy mixing model with the quartz solubility curve (Fournier, 1977; Fournier and Porter, 1982) yields a reservoir temperature of about 130°C. However, silica-enthalpy mixing model with the chalcedony solubility curve (modified from Fournier, 1977; Fournier and Porter, 1982) yields a rather cooler temperature (about 60 °C).

5.3.2 Ashton Hot Spring

The Ashton Hot Spring and associated geothermal area (AHS in Figure 1) is located at northern side of Ashton in Fremont County in Idaho. The existence of Ashton Hot Spring with a surface water temperature of 41 °C was previously reported by Mitchell et al. (1980). A 1220 m deep geothermal exploratory well (Sturm Well-1) was drilled about 2 km NE from the Ashton Hot Spring in 1979 (Occidental Geothermal Inc., 1979). Driller's records indicate a bottom-hole temperature of about 63 °C.

Geologic mapping of the area shows thin layers of Quaternary sediments covering underlying volcanic rocks (Link, 2002). Borehole records from the area reveal presence of thick sequences of flood basalts and felsic volcanics. Specifically, along the Sturm Well-1, the Quaternary sediments near surface are followed by layers of flood basalts (up to a depth of 82 m), felsic volcanics (82-808 m), and again flood basalts (808 -1220+ m) with depth (Occidental Geothermal Inc., 1979).

Quartz and chalcedony geothermometers yielded reservoir temperatures of 143 °C and 116 °C for Ashton Hot Spring and 113 °C and 84 °C for the Sturm Well, respectively. For these two sampled features, Na-K-Ca geothermometer resulted in 117 °C and 109 °C, respectively. Similarly, the RTest produced reservoir temperatures for the Sturm Well and Ashton Hot Spring are 152 ± 14 °C and 147 ± 5 °C, with nearly 70% and 35% admixing of cooler water, respectively. All of these temperatures are significantly higher than the

bottom hole temperature measured for the Sturm Well (66 °C). Given the measured temperature gradient (48 °C/km, Blackwell, 1989), such temperature conditions might be found at depths of about 3 km.

5.3.3 Newdale area

The Newdale geothermal prospect (NEW in Figure 1) in Madison and Fremont Counties in Idaho represents a blind geothermal system, as it has no hot springs. The geothermal potential of Newdale area was identified in late 1970s by several researchers (e.g., Brott et al., 1976), based on the discovery of relatively high heat flow (167 mW/m²). The area from Newdale town to NE across the Teton River has been considered as a potential area for geothermal energy (Brott et al., 1976, GeothermEx, 2010; Neupane et al., 2016b)). During 1979-1981, Union Oil of California (Unocal) drilled several geothermal test wells in the area ranging in depth from 183 m (Newdale No. 79-3) to 1204 m (Madison Geothermal No.1 near Rexburg, ID). The highest recorded temperature in the Unocal wells was 87.2 °C (Well # State 2591-07-79-1).

Surficial geologic map of this area shows presence of Quaternary sediments, Quaternary flood basalts, and Quaternary felsic volcanic rocks (Bond, 1978; Link, 2002; Embree et al., 2011). Early Pleistocene flood basalts are mapped around the town of Newdale whereas felsic volcanic rocks of similar ages (Huckleberry Ridge Tuff) are mapped NE from Newdale. In geologic cross-section, Embree et al. (2011) show Huckleberry Ridge Tuff lying underneath the Early Pleistocene basalt at Newdale. Below the Huckleberry Ridge Tuff lie the Tertiary sediments intercalated with Tertiary basalt. Subsurface lithologic records of numerous wells in the area as compiled by Idaho Geological Survey indicate the presence of thick sequences of rhyolites and tuff at greater depths.

Quartz, chalcedony, and Na-K-Ca (Mg corrected) geothermometers resulted reservoir temperatures in the range of 66-134 °C, 28-112 °C, 29-111 °C, respectively. A silica (chalcedony)-enthalpy mixing model using all Newdale area samples results in reservoir temperature of about 174 °C. Similar mixing models using quartz solubility results in even higher temperature estimates (224 °C). The RTest temperature estimates for the Newdale area samples range 75-152 °C (Table 1). The lower end RTest temperature estimates of this area are similar to the bottom hole temperatures (83-87 °C) measured at two relatively deeper (~1000 m) Unocal wells. Moreover, it is likely that the area hosts even higher temperatures at greater depths that would correspond to the higher end RTest temperatures. Assuming an 80 °C thermal gradient (as indicated by two Unocal wells), the higher end RTest temperatures would be present at about 2 km below ground surface.

5.3.4 East Idaho Falls area

The foothills (1480-1580 m above sea level) along the margins of the ESRP east of Idaho Falls (EIF in Figure 1) in Bonneville County have been known to have some wells producing warm water. The geothermal potential of the area was initially reported by Ralston et al. (1981). Specifically, they reported the existence of two wells in Rim Rock Estate that produce ≥20 °C water. Recently drilled shallow (depth up to 244 m) wells in the Comore Loma and Blackhawk communities few kilometers south from Rim Rock Estate also produce warm (21-28 °C) water.

The area lies on the edge of the SRP where pronounced volcanism has taken place throughout the past 6.5 Ma. The foothills to the east of Idaho Falls consist predominantly of tuffs, ignimbrites, and ash flows related to the Miocene-Pliocene Heise volcanic field (Morgan and McIntosh, 2005). Although all shallow wells in the area bottomed out within the volcanic rocks, the volcanic rocks in the area are thought to be about 300 m in thickness. Mesozoic sedimentary rocks that include the limestones, sandstones, siltstones, conglomerates, and evaporite beds underneath the young volcanic rocks are assumed to be the geothermal reservoir in this area.

Quartz, chalcedony, and Na-K-Ca temperature estimates for east Idaho Falls area range from 115-143 °C, 86-117 °C, and 45-74 °C, respectively. The Mg-corrected Na-K-Ca temperature estimates for these samples are lower because of the presence of high concentrations of Mg. The RTest temperature estimates of east Idaho Falls water samples are very similar with a range from 136-143 °C (Table 1).

5.3.5 Magic Hot Spring

The Magic Hot Spring prospect (MHS in Figure 1) is located on the northern margin of the ESRP in Camas and Blaine Counties in Idaho. Until a 79 m deep well (Magic Reservoir landing well) was drilled for direct use purposes in 1965, the hot spring issued 36°C water (Ross, 1970). However, with the operation of the well, the hot spring dried out (Mitchell, 1976). At the beginning, the well was producing water at 66°C, however, the water temperature subsequently increased to 74 °C by 1975 (Mitchell, 1976; Mitchell et al., 1980). The most recent (2014) temperature record for the surface discharge of the well is 75 °C.

The Magic Hot Spring area consists predominantly of Miocene-Quaternary silicic volcanic rocks and basalt flows (Struhsacker et al., 1982). The Pliocene-Miocene Poison Creek Tuff is the uppermost unit in the immediate vicinity of Magic Reservoir and is underlain by the Miocene Tuff of the Idavada Group. Other rhyolites and basalt flows are abundant in the surrounding areas but not shown in cross-section. The Cretaceous Idaho Batholith granitic rocks form the basement throughout the region.

Quartz (no steam loss), chalcedony, and Mg-corrected Na-K-Ca geothermometers resulted in 139 and 142 °C, and 113 and 116 °C, and 153 and 152 °C with compositions measured in water samples from the well leak and leak runoff channel, respectively. The chalcedony-enthalpy mixing model resulted in an estimated 145 °C reservoir temperature with about 50% dilution. Similarly, the quartz-enthalpy mixing model resulted in 181 °C reservoir temperature with about 60% dilution. The RTest results indicate that the Magic Hot Spring geothermal area has a reservoir temperature about 163 °C (Table 1).

5.3.6 Camas Prairie area

Camas Prairie (CP in Figure 1) is an east-west elongated (about 50 km by 15 km) intermontane valley in Camas and Elmore Counties in Idaho. The area has several hot springs [besides the Elk Creek Hot Springs (ECHS in Figure 1) in the northeastern part of the prairie]. The Sheep and Wolf Hot Springs are located in the western part of Camas Prairie, about 4 km north of Hill City in Idaho. These two hot springs, separated approximately 100 m from each other, issue hot water at about 50 °C. Two additional hot springs in the area are Wardrop Hot Springs (60°C), located on the northern side of prairie near the base of the Soldier Mountains, and Barron Hot Spring (73 °C), located on the southern side of the prairie near the base of the Mount Bennett Hills. The area also has several hot shallow wells, specifically scattered around the Wardrop and Barron Hot Spring areas.

Camas Prairie is bounded by the Mount Bennett Hills to the south and the Soldier Mountains to the north. The Mount Bennett Hills are composed predominantly of Miocene rhyolitic ash flows and lava flows of the Idavada Volcanic Group that overlies granodiorite of the Idaho Batholith. Local basalt flows and fluvial/lacustrine sediments are also present. The Soldier Mountains are composed mostly of granodiorite of the Idaho Batholith with minor amounts of younger intrusive rocks. Camas Prairie is host to an unknown thickness of Quaternary alluvial, fluvial, and lacustrine sediments with local lenses of basalt encountered in the shallow subsurface (Cluer and Cluer, 1986).

All Camas Prairie thermal water samples provide similar reservoir temperatures with the same traditional geothermometer. The quartz, chalcedony, and Na-K-Ca geothermometers results in temperature estimates in the range of 103-128, 74-99, and 70-124 °C, respectively. The silica-enthalpy model with chalcedony solubility and quartz solubility curves resulted in temperature estimates of about 133 °C and 173 °C, respectively.

Unlike the traditional geothermometers, RTest temperature estimates of Camas Prairie area samples show a bimodal distribution—higher temperatures for the samples from northern parts and lower temperatures for the samples from southern parts. Specifically, the hot springs from the areas along the northern part of Camas Prairie that abuts the prairie with the foothills of the Soldier Mountains (e.g., Wardrop Hot Spring, Wolf/Sheep Hot Spring) results in higher (181-204 °C) RTest reservoir temperatures. On the other hand, RTest reservoir temperature estimates for hot springs and wells (e.g., Barron Hot Spring) in the southern parts are 79-108 °C.

5.3.7 Southern side of Mount Bennett Hills

Several hot springs are located along the southern side of the Mount Bennett Hills in Elmore, Gooding, and Lincoln Counties in Idaho extending over 70 km represent this prospect (SBH in Figure 1). Some of the known hot springs in the area are the Prince Albert (Coyote) (58 °C), Latty (65 °C), and White Arrow (65 °C). The Bostic 1-A well (2950 m) drilled to the south from this area indicated the presence of hot (ca. 200 °C) rock at depths of about 3 km (Arney, 1982; Arney and Goff, 1982; Arney et al., 1984). The presence of several hot springs and hot rock at depth suggests that this part the SRP has great potential for geothermal resources.

Rocks in the area consist mainly of mafic and felsic volcanic rock with thick sequences of sediments and gravels. The Mount Bennett Hills to the north consist of predominantly of Miocene rhyolitic ash flows and lava flows of the Idavada Volcanic Group that overlies Idaho Batholith granodiorite. At the base of the Mount Bennett Hills, the basalt flows are intercalated with quaternary lacustrine sediments deposited in the Pleistocene-Pliocene Lake Idaho and the sandstones and shales of the Tertiary Glenn's Ferry Formation. At depth, an older basalt unit (Banbury basalt) and Idavada volcanics are encountered at Bostic 1-A well (Arney et al., 1984). The basement rock in the area is considered to be the Idaho Batholith granodiorite.

Reservoir temperature estimates for this area calculated with several water samples are given in Table 1. Quartz (no steam loss), chalcedony, and Na-K-Ca geothermometers resulted in 110-143, and 80-117, and 72-160 °C, respectively. The Prince Albert and Latty Hot Springs resulted in highest temperatures for the area with these traditional geothermometers. Silica-enthalpy mixing models with chalcedony and quartz solubility curves resulted in 150 and 182 °C temperature estimates for the area. As with the traditional geothermometers, the RTest modeling of waters from hot springs yielded higher temperature. The three hot springs in the area, Prince Albert, Latty, and White Arrow Hot Springs resulted in reservoir temperatures at 193±8, 197±5, and 177±6 °C, respectively. Similarly, RTest temperature estimate for a well (Shannon well) in the area is 137±10 °C. All other wells resulted in lower reservoir temperature estimates (82-122 °C). The reservoir temperature estimates using the hot spring waters are similar to the bottom hole temperature (~200 °C, Arney et al., 1984) measured in the Bostic 1-A well. It is likely that these hot springs are sourced by deep thermal waters that ascend along the range-forming faults.

5.3.8 Twin Falls area and Banbury Hot Springs

The southwestern periphery of the ESRP near Twin Falls and Buhl is one of the Known Geothermal Resource Areas in southern Idaho. The area is comprised of two dense clusters of geothermal surface manifestations, Banbury Hot Springs (BHS in Figure 1) and Twin Falls (TF in Figure 1). Discharging thermal waters range in temperature from 25 °C to 70 °C. Locally, thermal waters are being used for space heating, agriculture, and recreation.

The Twin Falls and Banbury hydrothermal areas show characteristics of both the ESRP and Basin and Range regional extension. Tertiary rhyolitic volcanic rocks underlie younger Quaternary and Tertiary basaltic units throughout the study area. Paleozoic metasedimentary rocks are thought to underlie the entire area (Lewis and Young, 1989). The thermal aquifer system in the area is located beneath basalt units within the Idavada volcanics and is under artesian conditions with temperatures of the waters increasing to the northwest. Thermal waters are thought to originate from deep circulation paths from the Cassia Mountain recharge zone to the south and through fractures in the overlying basalts of the thermal area. The waters are subsequently heated by either a regionally high

gradient (Lewis and Young, 1989) or the young basaltic sill complexes associated with ESRP volcanism (McLing et al., 2014, Dobson et al., 2015).

Reservoir temperature estimate ranges obtained with traditional geothermometers and RTest are given in Table 1 for both the Banbury Hot Springs and Twin Falls prospects. The highest reservoir temperatures (ca. 160 °C) for the Banbury Hot Springs prospect are obtained for Banbury Hot Spring, Miracle Hot Spring well, and Salmon Falls Hot Spring with RTest as well as other geothermometers. Similarly, for the Twin Falls prospect, the highest reservoir temperatures (ca. 135 °C) are obtained for samples from two hot shallow wells (used for direct heating – Neely, 1996) within the premises of the College of Southern Idaho.

6. SUMMARY

Geothermometric calculations of ESRP thermal water samples indicate numerous potential geothermal areas with elevated reservoir temperatures. Specifically, RTest results of thermal water samples from areas around the southern/southwestern side of the Mount Bennett Hills and within the Camas Prairie in the southwestern portion of the ESRP suggest temperatures of 140-200°C. In the northern portion of the ESRP, Lidy Hot Springs, Ashton, Newdale, and areas east of Idaho Falls have expected reservoir temperatures ≥ 140 °C. Resource temperatures in the southwestern ESRP, specifically, areas near Buhl and Twin Falls are estimated to as high as 160 °C. These areas are likely to host potentially economic geothermal resources; however, further detailed study is warranted for each site to evaluate their suitability for economic use.

ACKNOWLEDGMENTS

This work was supported by funding by the Assistant Secretary for Energy Efficiency and Renewable Energy, Geothermal Technologies Office of the U.S. Department of Energy under the U.S. Department of Energy Contract Nos. DE-AC07-05ID14517 with Idaho National Laboratory and DE-AC02-05CH11231 with Lawrence Berkeley National Laboratory. We thank landowners who provided access to sampling locations. We also thank Dr. Ross Spackman (Brigham Young University-Idaho) for his assistance in coordinating with landowners and filed work. Chemical analyses of the samples were conducted by Ms. Debbie Lacroix (University of Idaho) at Center for Advanced Energy Studies (CAES). We appreciate the discussion with Drs. Bill Phillips (Idaho Geological Survey), Glenn Embree (BYU-Idaho), and Dan Moore (BYU-Idaho).

REFERENCES

- Arney, B.: Evidence of former higher temperatures from alteration minerals, Bostic 1-A well, Mountain Home, Idaho. *GRC Transactions*, **6**, (1982), 3-6.
- Arney, B.H., Gardner, J.N., Belluomini, S.G.: 1984, Petrographic analysis and correlation of volcanic rocks in Bostic 1-A well near Mountain Home, Idaho. LA-9966-HDR, Los Alamos National Laboratory, (1984).
- Arney, B. H. and Goff, F.: Evaluation of the hot-dry-rock geothermal potential of an area near Mountain Home, Idaho. LA-9365-HDR, Los Alamos National Laboratory (1982).
- Bethke, C.M.: *Geochemical and Biogeochemical Reaction Modeling*. Cambridge University Press, pp. 547, (2008).
- Blackwell, D.D.: Regional implications of heat flow of the Snake River Plain, northwestern United States. *Tectonophysics*, **164**, (1989), 323-343.
- Blackwell, D., Steele, J.L., and Carter, L.S.: Heat flow patterns of the North American continent: A discussion of the DNAG geothermal map of North America. In *Neotectonics of North America*, eds. D.B. Slemmons, E. R. Engdahl, and D. D. Blackwell, Geological Society of America, DNAG, Map, 1:423437, (1991).
- Bond, J. G.: Geologic map of the state of Idaho, scale 1:500,000. Idaho Bur. of Mines and Geology, (1978).
- Brott, C.A., Blackwell, D.D., and Mitchell J.C.: Geothermal investigations in Idaho, Part 8: Heat flow study of the Snake River Plain, Idaho, Idaho Department of Water Resources. *Water Information Bulletin*, **30**, (1976), 195 pp.
- Cannon, C., Wood, T., Neupane, G., McLing, T., Mattson, E., Dobson, P., and Conrad, M.: Geochemistry sampling for traditional and multicomponent equilibrium geothermometry in southeast Idaho. *GRC Transactions*, **38**, (2014), 524-431.
- Cluer, J.K., Cluer, B.L.: The late Cenozoic Camas Prairie Rift south-central Idaho, Contributions to Geology, University of Wyoming, **24(1)**, (1986), 91-101.
- Cooper, D.C., Palmer, C.D., Smith, R.W., and McLing, T.L.: Multicomponent equilibrium models for testing geothermometry approaches. *Proceedings*, 38th Workshop on Geothermal Reservoir Engineering Stanford University, Stanford, CA (2013).
- D'Amore, F. and Arnórsson, S.: Geothermometry, in *Isotopic and Chemical Techniques in Geothermal Exploration, Development and Use* (S. Arnórsson, ed.): IAEA (Editorial), Vienna, pp. 152-199, (2000).
- D'Amore, F., Fancelli, R., and Caboi, R.: Observations on the application of chemical geothermometers to some hydrothermal systems in Sardinia. *Geothermics*, **16**, (1987), 271-282.
- Dobson, P.F., Kennedy, B.M., Conrad, M.E., McLing, T., Mattson, E., Wood, T., Cannon, C., Spackman, R., van Soest, M., and Robertson, M.: He isotopic evidence for undiscovered geothermal systems in the Snake River Plain. *Proceedings*, 40th Workshop on Geothermal Reservoir Engineering, Stanford University, Stanford, CA (2015).

- Embree, G.F., Phillips, W.M., and Welhan, J.A.: Geologic map of the Newdale quadrangle, Fremont and Madison Counties, Idaho. Idaho Geological Survey, University of Idaho, Moscow, Idaho 83844-3014, (2011).
- Fournier, R.O. and Truesdell, A.H.: An empirical Na-K-Ca geothermometer for natural waters. *Geochim. Cosmochim. Acta*, **37**, (1973), 1255-1275.
- Fournier, R.O.: Chemical geothermometers and mixing models for geothermal systems. *Geothermics*, **5**, (1977) 41-50.
- Fournier, R.O.: A revised equation for the Na/K geothermometer. *GRC Transactions*, **3**, (1979), 221-224.
- Fournier, R.O. and Potter, R.W. II: Magnesium correction to the Na-K-Ca chemical geothermometer. *Geochim. Cosmochim. Acta*, **43**, (1979), 1543-1550.
- GeothermEx, Inc.: Independent technical report: Resource evaluation of the Newdale geothermal prospect, Madison and Fremont Counties, Idaho, USA. Geothermix, Inc., Richmond, California, USA, February 10, 2010, p. 101, (2010).
- Giggenbach, W.F.: Geothermal solute equilibria. Derivation of Na-K-Mg-Ca geothermometers. *Geochim. Cosmochim. Acta*, **52**, (1988), 2749-2765.
- Hughes, S.S., Smith, R.P., Hackett, W.R., and Anderson, S. R.: Mafic volcanism and environmental geology of the eastern Snake River Plain. *Idaho Guidebook to the Geology of Eastern Idaho*. Idaho Museum of Natural History, (1999), 143-168.
- Hull, C.D., Reed, M.H., and Fisher, K.: Chemical geothermometry and numerical unmixing of the diluted geothermal waters of the San Bernardino Valley Region of Southern California. *GRC Transactions*, **11**, (1987), 165-184.
- Lewis, R.E. and Young, H.W.: The hydrothermal system in central Twin Falls County, Idaho: U.S. Geological Survey Water Resources Investigations Report 88-4152, p. 44, (1989).
- Link, P.K.: Clark County, Idaho. Digital Atlas of Idaho, Idaho State University, Geosciences Department, p. 3, (2002).
- Mattson, E.D., Smith, R.W., Neupane, G., Palmer, C.D., Fujita, Y., McLing, T.L., Reed, D.W., Cooper, D.C., and Thompson, V.S.: Improved geothermometry through multivariate reaction-path modeling and evaluation of geomicrobiological influences on geochemical temperature indicators: Final Report No. INL/EXT-14-33959, Idaho National Laboratory (INL), Idaho Falls, Idaho, (2015).
- McLing, T.L., Smith, R.W., and Johnson, T.M.: Chemical characteristics of thermal water beneath the eastern Snake River Plain. In: *Geology, Hydrogeology, and Environmental Remediation: Idaho National Engineering and Environmental Laboratory, Eastern Snake River Plain, Idaho*, P.K. Link and L.L. Mink, eds. *Geological Society of America Special Paper* **353**, (2002), 205-211.
- McLing, T., McCurry, M., Cannon, C., Neupane, G., Wood, T., Podgorney, R., Welhan, J., Mines, G., Mattson, E., Wood, R., Palmer, C. and Smith, R.: David Blackwell's Forty Years in the Idaho Desert, The Foundation for 21st Century Geothermal Research; Geothermal Resources Council Transactions, **38**, (2014), 143-153.
- Michard, G. and Roekens, E.: Modelling of the chemical components of alkaline hot waters. *Geothermics*, **12**, (1983), 161-169.
- Mitchell, J.C.: Geothermal Investigations in Idaho – Part 7: Geochemistry and geologic setting of the thermal waters of the Camas Prairie Area, Blaine and Camas Counties, Idaho. Idaho Department of Water Resources, *Water Information Bulletin* **30**, (1976).
- Mitchell, J.C., Johnson, L.L., and Anderson, J.E.: Geothermal Investigations in Idaho – Part 9: Potential for direct heat applications of geothermal resources. Idaho Department of Water Resources, *Water Information Bulletin* **30**, (1980).
- Morgan, L.A., and McIntosh, W.C.: Timing and development of the Heise volcanic field, Snake River Plain, Idaho, western USA. *Geological Society of America Bulletin*, **117**, (2005), 288-306.
- Morse, L.H. and McCurry, M.: Genesis of alteration of Quaternary basalts within a portion of the eastern Snake River Plain aquifer. *Special Papers Geological Society of America*, (2002) 213-224.
- Neely, K.W.: Geothermal heat keeps students warm at the College of Southern Idaho. *GRC Transactions*, **20**, (1996), 129-136.
- Neupane, G., Smith, R. W., Palmer, C. D., and McLing, T. L.: Multicomponent equilibrium geothermometry applied to the Raft River geothermal area, Idaho: preliminary results. In *Geological Society of America Abstracts with Programs*, **45** (7), (2013).
- Neupane, G., Mattson, E.D., McLing, T.L., Palmer, C.D., Smith, R.W., and Wood, T.R.: Deep geothermal reservoir temperatures in the Eastern Snake River Plain, Idaho using multicomponent geothermometry. *Proceedings, Thirty-Ninth Workshop on Geothermal Reservoir Engineering*, Stanford University, Stanford, California, February 24-26, 2014 SGP-TR-202, (2014).
- Neupane, G., Mattson, E.D., McLing, T.L., Palmer, C.D., Smith, R.W., Wood, T.R., and Podgorney, R.K.: Geothermal reservoir temperatures in southeastern Idaho using multicomponent geothermometry. *Proceedings, World Geothermal Congress 2015*, Melbourne, Australia, 19-25 April 2015, (2015a).
- Neupane, G., Baum, J.S., Mattson, E.D., Mines, G.L., Palmer, C.D., and Smith, R.W.: Validation of multicomponent equilibrium geothermometry at four geothermal power plants. *Proceedings, Fortieth Workshop on Geothermal Reservoir Engineering* Stanford University, Stanford, California, January 26-28, 2015, (2015b).

- Neupane, G., Mattson, E.D., Mines, G.L., McLing, T.L., Dobson, P.F., Conrad, M.E., Wood, T.R., Cannon, C., Worthing, W.: Geothermometric temperature comparison of hot springs and wells in southern Idaho. *GRC Transactions*, **39**, 495-502 (2015c).
- Neupane, G., Mattson, E.D., McLing, T.L., Palmer, C.D., Smith, R.W., Wood, T.R., and Podgorney, R.K.: Geothermometric evaluation of geothermal resources in southeastern Idaho. *Geoth. Energ. Sci*, **4**(1), (2016a), 11-22.
- Neupane, G., Mattson, E.D., Cannon, J.C., Atkinson, T.A., McLing, T.L., Wood, T.R., Worthing, W.C., and Conrad, M.E.: Mixing effects on geothermometric calculations of the Newdale Geothermal area in the Eastern Snake River Plain, Idaho. *Proceedings*, 41st Workshop on Geothermal Reservoir Engineering, Stanford University, Stanford, California, February 22-24, 2016 SGP-TR-209 (2016b).
- Nielson, D.L., Delahunty, C., and Shervais, J.W.: Geothermal systems in the Snake River Plain, Idaho, characterized by the Hotspot project. *GRC Transactions*, **36**, (2012) 727-730.
- Occidental Geothermal, Inc.: Sturm 1, Computer Processed Log. Department of Water Resources, Idaho, p. 18, (1979)
- Palandri, J.L. and Reed, M.H.: Reconstruction of in situ composition of sedimentary formation waters. *Geochim. Cosmochim. Acta*, **65**, (2001), 1741-1767.
- Palmer, C.D., Ohly, S.R., Smith, R.W., Neupane, G., McLing, T., Mattson, E.: Mineral selection for multicomponent equilibrium geothermometry. *GRC Transactions*, **38**, (2014), 453-459.
- Pang, Z.H. and Reed, M.: Theoretical chemical thermometry on geothermal waters: Problems and methods. *Geochim. Cosmochim. Acta*, **62**, (1998), 1083-1091.
- Peiffer, L., Wanner, C., Spycher, N., Sonnenthal, E., Kennedy, B.M., Iovenitti, J.: Optimized multicomponent vs. classical geothermometry: insights from modeling studies at the Dixie Valley geothermal area. *Geothermics*, **51**, (2014), 154-169.
- Pierce, K. L., and Morgan, L. A.: The track of the Yellowstone hot spot: Volcanism, faulting, and uplift. *Geological Society of America Memoirs*, **179**, (192), 1-54.
- Ralston, D.R., Arrigo, J.L., Baglio, J.V. Jr., Coleman, L.M., Souder, K., and Mayo, A.L.: Geothermal evaluation of the thrust area zone in southeastern Idaho, Idaho Water and Energy Research Institute, University of Idaho, (1981).
- Reed, M. and Spycher, N.: Calculation of pH and mineral equilibria in hydrothermal waters with application to geothermometry and studies of boiling and dilution. *Geochim. Cosmochim. Acta*, **48**, (1984), 1479-1492.
- Rodgers, D.W., Ore, H.T., Bobo, R.T., McQuarrie, N., and Zentner, N.: Extension and subsidence of the eastern Snake River Plain, Idaho. Tectonic and Magmatic Evolution of the Snake River Plain Volcanic Province. *Idaho Geological Survey Bulletin*, **30**, (2002), 121-155.
- Ross, S.H.: Geothermal potential of Idaho. *Geothermics Special Issue* **2**, (1970), 975-1008.
- Shervais, J.W., Glen, J.M., Liberty, L.M., Dobson, P., Gasperikova, E., Sonnenthal, E., Visser, C., Garg, S., Evans, J.P., Siler, D., DeAngelo, J., Athens, N., and Burns, E.: Snake River Plain play fairway analysis – Phase 1 Report. *GRC Transactions*, **39**, (2015), 761-769.
- Smith, R.P.: Geologic setting of the Snake River Plain aquifer and vadose zone. *Vadose Zone Journal*, **3**, (2004), 47-58.
- Smith, R.W., Palmer, C.D., and Cooper, D.: Approaches for multicomponent equilibrium geothermometry as a tool for geothermal resource exploration. *Abstracts*, AGU Fall Meeting, San Francisco, 3-7 December 2012, (2012).
- Spycher, N.F., Sonnenthal, E., and Kennedy, B.M.: Integrating multicomponent chemical geothermometry with parameter estimation computations for geothermal exploration. *GRC Transactions*, **35**, (2011), 663-666.
- Spycher, N., Peiffer, L., Sonnenthal, E. L., Saldi, G., Reed, M. H., and Kennedy, B. M.: Integrated multicomponent solute geothermometry. *Geothermics*, **51**, (2014), 113-123.
- Struhsacker, D.W., Jewell, P.W., Ziesloft, J., and Evans, S.H. Jr.: The geology and geothermal setting of the Magic Reservoir area, Blaine and Camas Counties, Idaho. In: Cenozoic geology of Idaho, B. Bonnicksen and R.M. Breckenridge, eds., *Idaho Bureau of Mines and Geology Bulletin* **26**, (1982), 377-393.
- Tole, M.P., Ármannsson, H., Pang, Z.H., & Arnórsson, S.: Fluid/mineral equilibrium calculations for geothermal fluids and chemical geothermometry. *Geothermics*, **22**, (1993), 17-37.
- Welhan, J.A.: Thermal and Trace-Element Anomalies in the Eastern Snake River Plain aquifer: toward a conceptual model of the EGS resource. *GRC Transactions*, **39**, (2015), 363-375.
- Whitehead, R.L.: Geohydrologic framework of the Snake River Plain regional aquifer system, Idaho and eastern Oregon. Regional aquifer system analysis-Snake River Plain, Idaho. *US Geological Survey Professional Paper* 1408-B, (1992).
- Williams, C.F., and DeAngelo, J.: Evaluation of Approaches and Associated Uncertainties in the Estimation of Temperatures in the Upper Crust of the Western United States, *GRC Transactions*, **35**, (2011), 1599-1605.

Neupane et al.

Williams, P.L., Mabey, D.R., Zohdy, A.A.R., Ackermann, H., Hoover, D.B., Pierce, K.L., and Oriel, S.S.: Geology and geophysics of the southern Raft River Valley geothermal area, Idaho, USA. *Proceedings*, Second UN Symposium on the Development and Use of Geothermal Resources, San Francisco, Lawrence Berkeley National Laboratory, (1976), 1273-1282.

Appendix H.

Neupane, G., Mattson, E.D., Cannon, J.C., Atkinson, T.A., McLing, T.L., Wood, T.R., Worthing, W.C., and Conrad, M.E., 2016b. Mixing effects on geothermometric calculations of the Newdale Geothermal area in the Eastern Snake River Plain, Idaho. Proceedings, 41st Workshop on Geothermal Reservoir Engineering, Stanford University, Stanford, CA.

Mixing Effects on Geothermometric Calculations of the Newdale Geothermal Area in the Eastern Snake River Plain, Idaho

^{1,2}Ghanashayam Neupane*, ¹Earl D. Mattson, ^{2,3}Cody J. Cannon, ⁴Trevor A. Atkinson, ^{1,2}Travis L. McLing, ^{2,3}Thomas R. Wood, ^{2,3}Wade C. Worthing, and ⁵Mark E. Conrad

¹Idaho National Laboratory, Idaho Falls, ID 83415, USA

²Center for Advanced Energy Studies, Idaho Falls, ID 83401, USA

³University of Idaho-Idaho Falls, Idaho Falls, ID 83402, USA

⁴Ormat Technologies Inc., Reno, NV 89511, USA

⁵Lawrence Berkeley National Laboratory, Berkeley, CA 94720 USA

E-mail: Ghanashayam.Neupane@inl.gov

Keywords: Eastern Snake River Plain, Newdale, RTEst, geothermal, geothermometer

ABSTRACT

The Newdale geothermal area in Madison and Fremont Counties in Idaho is a known geothermal resource area whose thermal anomaly is expressed by high thermal gradients and numerous wells producing hot water (up to 51 °C). Geologically, the Newdale geothermal area is located within the Eastern Snake River Plain (ESRP) that has a time-transgressive history of sustained volcanic activities associated with the passage of Yellowstone Hotspot from the southwestern part of Idaho to its current position underneath Yellowstone National Park in Wyoming. Locally, the Newdale geothermal area is located within an area that was subjected to several overlapping and nested caldera complexes. The Tertiary caldera forming volcanic activities and associated rocks have been buried underneath Quaternary flood basalts and felsic volcanic rocks. Two southeast dipping young faults (Teton Dam Fault and an unnamed fault) provide the structural control for this localized thermal anomaly zone. Geochemically, water samples from numerous wells in the area can be divided into two broad groups – Na-HCO₃ and Ca-(Mg)-HCO₃ type waters. Each type of water can further be subdivided into two groups depending on their degree of mixing with other water types or interaction with other rocks. For example, some bivariate plots indicate that some Ca-(Mg)-HCO₃ water samples have interacted only with basalts whereas some samples of this water type also show limited interaction with rhyolite or mixing with Na-HCO₃ type water. Traditional geothermometers [e.g., silica variants, Na-K-Ca (Mg-corrected)] indicate lower temperatures for this area; however, a traditional silica-enthalpy mixing model results in higher reservoir temperatures. We applied a new multicomponent equilibrium geothermometry tool (e.g., Reservoir Temperature Estimator, RTEst) that is based on inverse geochemical modeling which explicitly accounts for boiling, mixing, and CO₂ degassing. RTEst modeling results indicate that the well water samples are mixed with up to 75% of the near surface groundwater. Relatively, the Ca-(Mg)-HCO₃ type water samples are more diluted than the Na-HCO₃ type water samples. However, both water types result in similar reservoir temperatures, up to 150 °C. Samples in the vicinity of faults produced higher reservoir temperatures than samples away from the faults. Although both the silica-enthalpy mixing and RTEst models indicated promising geothermal reservoir temperatures, evaluation of the subsurface permeability and extent of the thermal anomaly is needed to better define the hydrothermal potential of the Newdale geothermal resource.

1. INTRODUCTION

The Newdale geothermal area in Madison and Fremont Counties in Idaho represents a blind geothermal system in the north-eastern part of Eastern Snake River Plain (ESRP) (Figure 1). The ESRP is a region of high heat flow with great potential for significant geothermal resources (Brott et al., 1976; Blackwell, 1989). In general, the ESRP consists of thick volcanic ash-flow tuffs, which are overlain by >1 km of Quaternary basaltic flows (Hughes et al., 1999; Anders et al., 2014; McLing et al., 2014). The felsic volcanic rocks at depth are the product of super volcanic eruptions associated with the Yellowstone Hotspot. These rocks progressively become younger to the northeast towards the Yellowstone Plateau (Pierce and Morgan, 1992; Hughes et al., 1999). The younger basalt layers are the result of several low-volume, fissure type or monogenetic shield-forming eruptions of short-duration that emanated from northwest trending volcanic rifts in the wake of the Yellowstone Hot Spot (Hughes et al., 1999). The thick sequences of coalescing basalt flows with interlayered fluvial and eolian sediments in the ESRP constitute a very productive aquifer system above the volcanic ash-flow tuffs (Whitehead, 1992).

The geothermal potential of Newdale area was identified in 1970s by several researchers (e.g., Brott et al., 1976), specifically, with the discovery of relatively high heat flow (167 mW/m²). Subsequent studies on geology, geophysics, and geochemistry of the area identified a zone called Newdale thermal anomaly zone (Mabey, 1978; Prostka and Embree, 1978; Mitchel et al., 1980). The area around the town of Newdale and NE across the Teton River (Figure 1) has been considered as a potential area for geothermal energy (Brott et al., 1976, GeothermEx, 2010). During 1979-1981, Union Oil of California (Unocal) drilled several geothermal test wells in the area ranging in depth from 183 m to 1025 m (Well St 08 in Figure 1). The highest recorded temperature in Unocal wells was 87.2 °C (Well St-07 in Figure 1). Currently, Standard Steam Trust LLC (SST) holds a set of leases for further exploration and development in an area of about 53.4 km² around Newdale and defines this area as ‘Newdale geothermal energy prospect’ (GeothermEx, 2010).

In this paper, we present geochemical and geothermometric assessments of the Newdale geothermal area. The geochemical evaluation of the area was conducted by employing graphical presentations of water compositions of hot shallow wells. Specifically, the ternary and bivariate plots of various aqueous species and their ratios were used to understand types of water and mixing trends in the area. Geothermometric evaluation of the area was conducted using traditional as well as multicomponent equilibrium geothermometry (MEG) tools. Specifically, the effect of mixing of cooler water in the thermal water on geothermometric results was evaluated with an MEG code, Reservoir Temperature Estimator (RTEst) (Palmer et al., 2014).

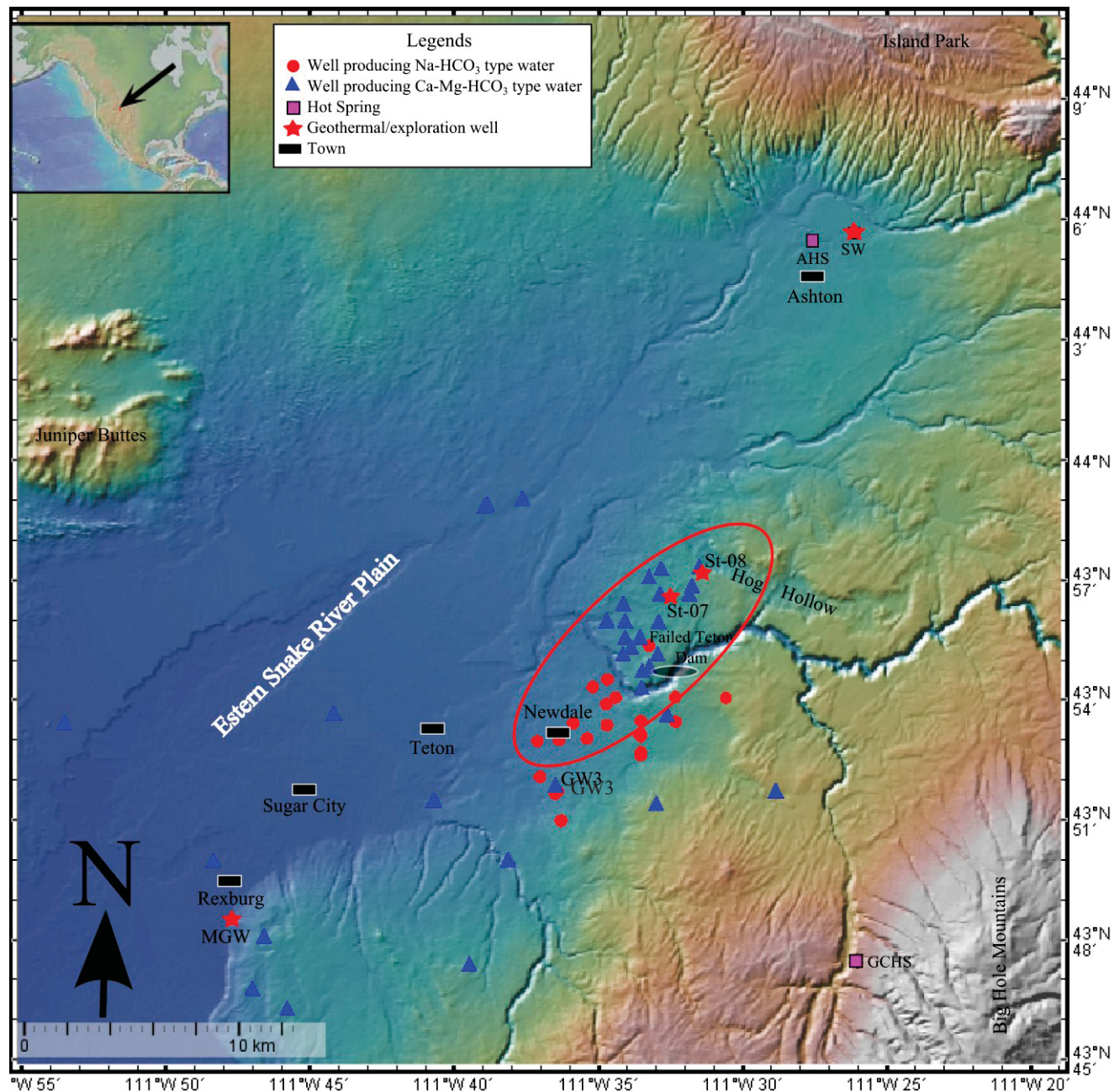


Figure 1. Location of Newdale geothermal prospect in the Eastern Snake River Plain. St-07: State 2591-07-79-1 well, St-08: State 2591-08-79-1 well, MGW: Madison Geothermal well (1204 m), SW: Sturm Well, AHS: Ashton Hot Spring, and GCHS: Green Canyon Hot Spring. GW3 is a groundwater well. Hog Hollow is a geographically depressed area in the northeastern part of prospect.

2. GEOLOGIC SETTING

Surficial geologic map of this area shows presence of Quaternary sediments, Quaternary flood basalts, and Quaternary felsic volcanic rocks (Bond, 1978; Link, 2002; Embree et al., 2011). Early Pleistocene flood basalts are mapped around the town of Newdale whereas felsic volcanic rocks of similar ages are mapped NE from Newdale. In geologic cross-section, Embree et al. (2011) show Huckleberry Ridge Tuff lying underneath the Early Pleistocene basalt at Newdale. Below the Huckleberry Ridge Tuff lie the Tertiary sediments intercalated with Tertiary basalt (Figure 2). Subsurface lithologic records of numerous wells in the area as compiled by the Idaho Geological Survey indicate the presence of thick sequences of rhyolites and tuff at greater depths.

Based on geologic, geomorphologic (Prostka and Embree, 1978) and gravity anomaly features (Mabey, 1978), a series of overlapping and intersecting calderas that developed during 4.45-6.62 Ma (Morgan and McIntosh, 2005) have been inferred as Rexburg Caldera Complex (RCC) covering a large area including Rexburg, Teton, Sugar City, and Newdale areas, and possibly even extending north to the Ashton area (Malde, 1991; Blackwell et al., 1992; Anders et al., 2014). Specifically, the Newdale geothermal area is located along the three inferred caldera margins (Prostka and Embree, 1978). Recently, Anders et al. (2014) mapped the Blacktail Creek Tuff caldera (a caldera unit of RCC) rim that passes through the Newdale geothermal area along the Teton River. It is important to note that the Teton River within the thermal anomaly area acts as a boundary for surficial rock types (Embree et al., 2011) as well as geochemical boundary for the water types (Figure 1). Specifically, the surficial rocks to the north/northeastern side of the river are felsic volcanic rocks associated with the Quaternary Huckleberry Ridge Tuff (Qyh in Figure 2) whereas surficial rocks to the southern side are Quaternary flood basalts. The geologic cross-section (Figure 2) does not show any surficial basalts because it traverses exclusively through the northern part of the prospect where the Quaternary Huckleberry Ridge Tuff and Quaternary sediments are mapped as surficial rocks (Embree et al., 2011).

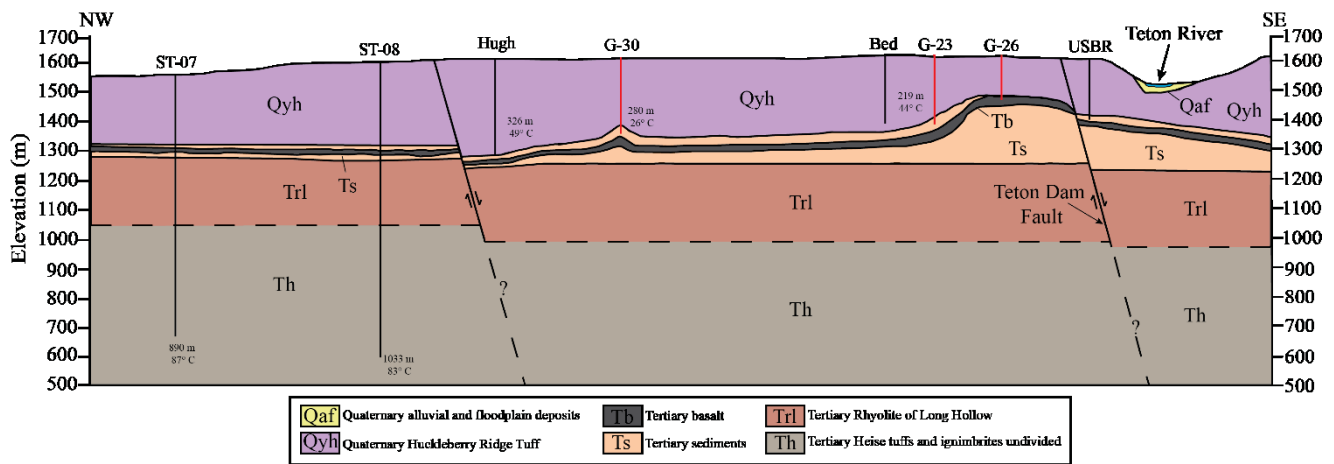


Figure 2. Geologic cross-section through Newdale geothermal area. The cross-section line passes through between two Unocal wells (St-07 and St-08 in Figure 1) and does not encounter Quaternary basalts. Stratigraphic architecture of the cross-section is constrained with available lithologic records of wells and geologic cross-section of Embree et al. (2011). The locations of two faults were adapted from geologic map (Embree et al., 2011).

It is likely that this area has highly fractured zones at depth because of the presence of intersecting caldera-ring fractures (Prostka and Embree, 1978; Anders et al., 2014). However, at present, the fractured zone has been buried underneath the thick sequences of post-RCC volcanic and sedimentary sequences. Besides the likely presence of buried caldera ring fractures at depth, two southeast dipping parallel faults are mapped in the area (Embree et al., 2011). Specifically, the Teton Dam Fault has been traced along a stretch of Teton River near the failed Teton dam (Figure 1) and extended further to NE and SW (Prostka and Embree, 1978; Embree et al., 2011). The other fault is located NW of the Teton Dam Fault. Prostka and Embree (1978) also show a NW striking and SW dipping fault (Warm Creek Fault) that extends from the Big Hole Mountains to the SE and intersects the NE terminus of the Teton Dam Fault. However, this fault has not been shown on the new geologic map prepared by Embree et al. (2011). Moreover, Embree and Hogan (1999) show a series of shallow and short faults inferred from surface lineaments that transect the Hog Hollow area (Figure 1) located in the northeastern part of the Newdale geothermal area. The significance of Teton Dam Fault and other associated faults for the Newdale geothermal system has yet to be fully evaluated. In general, these faults may act as structural control for the geothermal setting by providing upward pathways for migration of hotter fluid from depth. However, the Teton Dam Fault and the other faults in the area may have a limited role in circulating hotter fluids from depth to the surface such that these faults may have been located within the post-RCC zone without providing a continuous flow path from ring fracture zones to the surface. Moreover, the lack of surface expressions (e.g., hot springs) in the area may be related to a lack of sufficient hydraulic/convective head gradient because the water table in the area is located several tens of meters below ground surface.

3. GEOTHERMOMETRY

One of the prospecting tools for geothermal resources is geothermometry, which uses the chemical compositions of water from springs and wells to estimate reservoir temperature. As an exploration tool, geothermometry offers a cost effective method to decrease exploration risk by evaluating a potential geothermal reservoir's temperature. To conduct geothermometry, measured chemical composition of water from wells and springs that exhibit some level of elevated temperatures are needed. The application of geothermometry requires several assumptions. The most important assumptions are that the reservoir minerals and fluid attain a chemical equilibrium and as the water moves from the reservoir to sampled location, it retains its chemical compositions (Fournier et al., 1974). The first assumption is generally valid (provided a long residence time); however, the second assumption is more likely to be violated because of composition altering processes, such as, re-equilibration at lower temperature, dilution (mixing), and loss of fluids (boiling) and volatiles (e.g., CO₂) with the decrease in pressure.

Traditional geothermometers such as silica geothermometers, Na/K geothermometer, etc., are empirical to semi-empirical approaches where a user enters the measured concentrations of certain component(s) into the geothermometer equation. The reliability, sensitivity, and responsiveness of traditional geothermometers to various composition altering processes vary. For example, geothermometers based on cation concentration ratios (e.g., Na/K geothermometer) are minimally sensitive to boiling or mixing with dilute water; while geothermometers based directly on the concentration of component(s) (e.g., quartz geothermometer) are highly sensitive to these processes (D'Amore and Arnórsson, 2000). A drawback of many existing geothermometry approaches is that they do not adequately account for physical processes (e.g., mixing, boiling) and geochemical processes (e.g., mineral dissolution, precipitation, degassing) that may occur after the water leaves the reservoir and thereby alter its composition. If these changes are not taken into account, predictions of in-situ reservoir conditions (e.g., temperature, fCO₂) based on the chemical composition of water samples taken from shallower depths or at the surface may be erroneous, or too imprecise to be useful.

In addition, it is difficult to quantify uncertainties associated with temperatures estimated with these geothermometers. As a result, it is not uncommon to find diverse temperature estimates for the same water using multiple traditional geothermometers. Nevertheless, because these geothermometers are easy to use and sometimes provide good results, they are considered to be an essential part of the geothermal exploration toolkit (D'Amore and Arnórsson, 2000).

A more advanced geothermometric approach is MEG. This approach utilizes multiple chemical constituents measured in water samples for inverse geochemical modeling considering a suite of selected minerals (selected based on some knowledge of the system) so as to provide more robust temperature estimates with quantifiable uncertainties. Geothermal temperature predictions using MEG provide apparent improvement in reliability and predictability of temperature over traditional geothermometers. The basic concept of this method was developed in 1980s (e.g., Michard and Roekens, 1983; Reed and Spycher, 1984). Some previous investigators (e.g., D'Amore et al., 1987; Hull et al., 1987; Tole et al., 1993) have used this technique for predicting reservoir temperature in various geothermal sites. Other researchers have used the basic principles of this method for reconstructing the composition of geothermal fluids and formation brines (Pang and Reed, 1998; Palandri and Reed, 2001). More recent efforts by some researchers (e.g., Bethke, 2008; Spycher et al., 2011; Smith et al., 2012; Cooper et al., 2013; Neupane et al., 2013, 2014; Cannon et al., 2014; Spycher et al., 2014; Peiffer et al., 2014; Palmer et al., 2014; Neupane et al., 2015a,b,c; Mattson et al., 2015; Neupane et al., 2016a,b) have been focused on improving temperature predictability of the MEG.

For this study, both traditional [e.g., quartz (no steam loss) (Fournier, 1977), chalcedony (Fournier, 1977), and Na-K-Ca (Truesdell and Fournier, 1973; Fournier and Potter, 1979)] and RTest (Palmer et al., 2014; Mattson et al., 2015) geothermometric approaches were applied to estimate reservoir temperatures. For the silica geothermometers, pH correction on silica concentrations was not applied. While applying RTest to each water sample, a mineral assemblage consisting of 5-7 representative minerals was used for the development of reservoir temperature estimate using the LLNL based thermodynamic database (thermo.dat database of Geochemist's Workbench). In general, the mineral assemblage was selected based on available information such as water chemistry (e.g., pH), likely reservoir rock types and temperature range, etc. For more detailed information on selection of the mineral assemblage, see Palmer et al. (2014).

4. WATER SAMPLES

4.1 General

Locations of Newdale area water samples are shown in Figure 1. The water compositions used in this study represent both wells producing waters at elevated temperatures (≥ 20 °C) and cooler water (< 20 °C). The temperatures of the wells with warmer water range from 21-51 °C whereas temperatures of cooler wells range from 8.5-17.5 °C.

4.2 Water Chemistry

All Newdale area wells produce dilute (TDS ranging from 200 to 520 mg/kg with an average value of 375 ± 80 mg/kg) and near-neutral (pH ranging from 6.4 to 8.5) water. Major cations in Newdale water samples are Na, Ca, and Mg whereas major anions are HCO₃, Cl, F, and SO₄. Water samples in the area are of two types: Na-HCO₃ and Ca-(Mg)-HCO₃ (Figure 3). In the ESRP, the Na-HCO₃ and Ca-(Mg)-HCO₃ type waters are often related to deeper water that have interacted with rhyolite at relatively higher temperature and shallower ESRP groundwater that have mostly interacted with basalt at cooler temperature, respectively (Mann, 1986; McLing et al., 2002; Welhan, 2015). Recently, Cannon (2015) showed that the Ca-Mg-HCO₃ groundwater gradually changes to Na-HCO₃ type water when interacted with ESRP basalts at 70 °C for a long time. Therefore, the water types in the ESRP region are more likely to reflect the degree of thermal influence on water-rock interaction independent of rock types. The Na-HCO₃ waters have slightly higher TDS (ranging from 340 to 520 mg/kg with an average value of 440 ± 60 mg/kg) than Ca-(Mg)-HCO₃ waters (ranging from 200 to 480 mg/kg with an average value of 330 ± 60 mg/kg).

The cations ternary and the diamond plots in Figure 3 show that these two groups of water aligned along a trend from Na+K vertex to Ca-Mg baseline; however, such trend is missing in the anions ternary plot. Nevertheless, the anions ternary diagram shows a type-water independent trend that extends from the HCO_3^- vertex towards the Cl-SO_4 baseline. A similar type-water independent trend can be found on a bivariate plot constructed for HCO_3^- and Cl (Figure 4a). The trend depicted in Figure 4a reflects the intensity of water-rock interaction (regardless of the rock types) that a water sample might have experienced. In general, the higher the degree of water-rock interaction, the higher the concentrations of HCO_3^- and Cl in water. Other bivariate plots (Figure 4b through Figure 4e), however, show linear alignment of Na- HCO_3 and Ca-(Mg)- HCO_3 type water samples. Traditionally, such linear alignment of water samples on bivariate plots is considered to be the result of mixing of the two end member water compositions at different proportions. Figure 4f indicates that the both Na- HCO_3 and Ca-(Mg)- HCO_3 type waters are meteoric in origin and the variations in major ion concentrations in them is a reflection of the varying degrees of water-rock interaction involving different rock types, temperatures, and mixing with other water types.

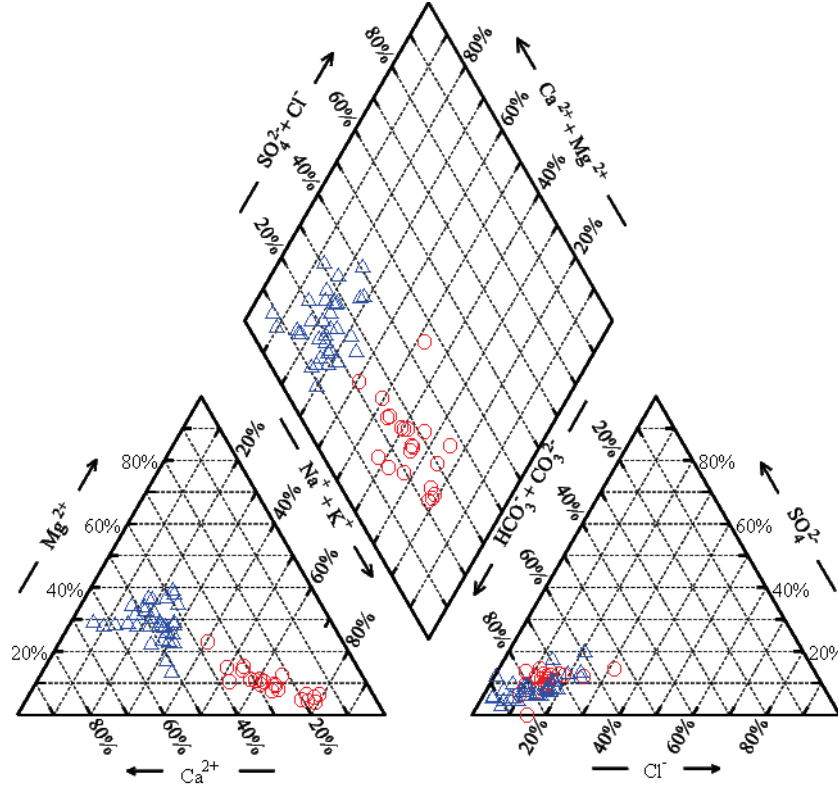


Figure 3. Piper diagram representing chemistry of water samples from Newdale geothermal area. Red circles and blue triangles represent Na- HCO_3 and Ca-(Mg)- HCO_3 type waters, respectively.

Although bivariate plots shown in Figure 4b through Figure 4f depict the apparent linear alignment of Na- HCO_3 and Ca-(Mg)- HCO_3 type waters, some additional bivariate plots with other components and ratios (Figure 5a through Figure 5f) show two distinct mixing (and/or degree of water rock interactions) trends, one for the Na- HCO_3 and other for the Ca-(Mg)- HCO_3 type waters. These diagrams indicate that for Ca-(Mg)- HCO_3 type waters, one end-member (dilute one) can be represented by a pristine water (rain/snow melt). However, the composition of other end member (towards higher TDS) is not known, but such composition for each sample can be reconstructed with RTest modeling. All intermediate waters have formed either by mixing of low and high TDS end-member waters at various proportions, or by varying degree of water-rock interaction.

Some bivariate plots (e.g., Figure 5b, d, and f) that includes Cl (concentration or as part of ratio) in their construction indicate that the cooler end member water that mixed with the Na- HCO_3 type waters is very dilute Ca-(Mg)- HCO_3 type water or pristine water. However, other bivariate plots that do not include Cl in their construction (e.g., Figure 5a, c, and e) indicate that the end member water that mixed with Na- HCO_3 type waters may have a composition similar to some intermediate Ca-(Mg)- HCO_3 type water. Since RTest does not handle complex geochemical behavior (e.g., precipitation, cation exchange, and so on), we assume that some variant of intermediate Ca-(Mg)- HCO_3 type water is the end member water that is mixed with Na- HCO_3 type waters. As with the cases of Ca-(Mg)- HCO_3 type waters, the higher TDS end member composition of Na- HCO_3 type waters are not known, and for each sample, the original thermal water is reconstructed with RTest modeling.

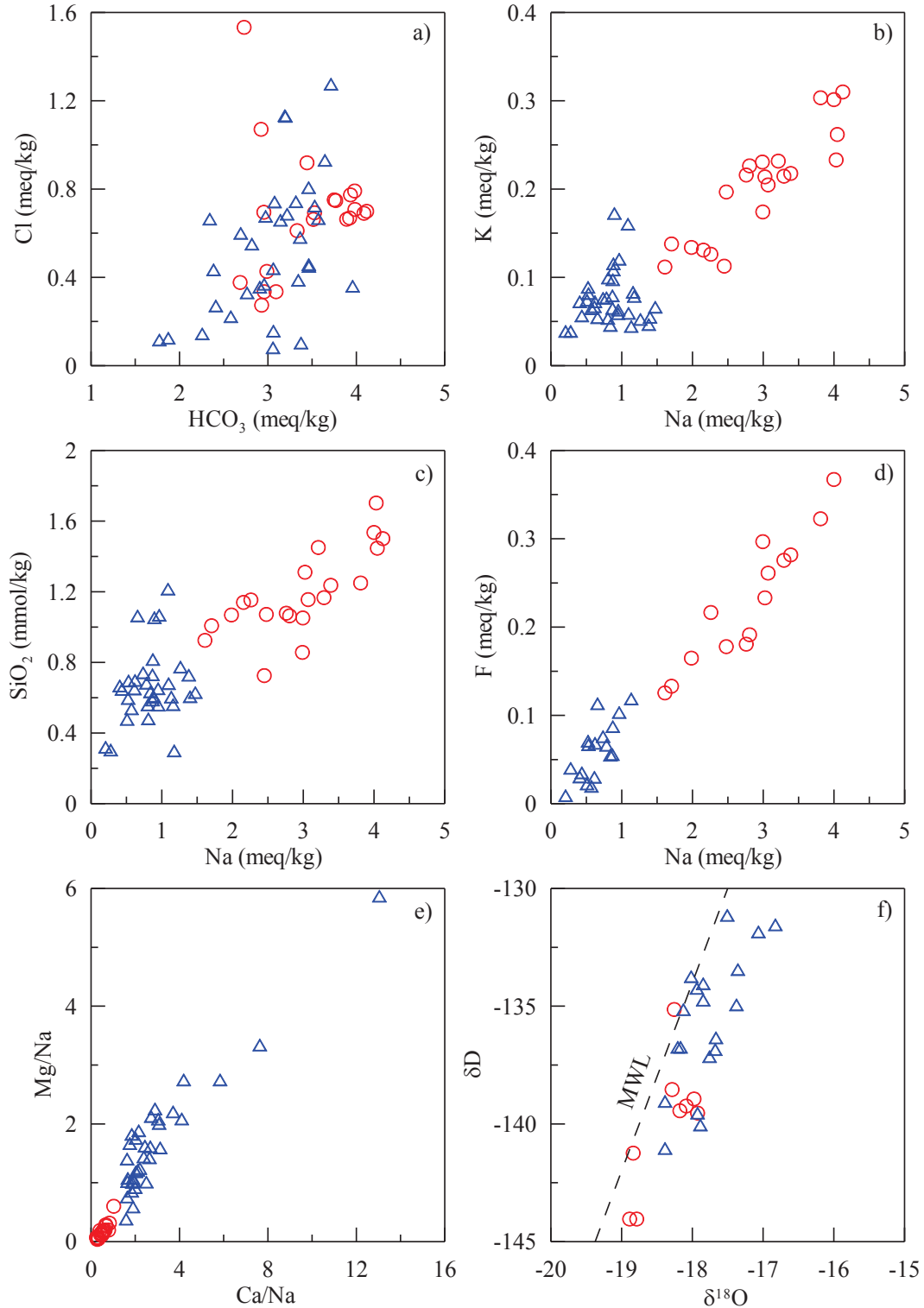


Figure 4. Bivariate diagrams constructed for some components, isotopes, and components ratios in Newdale and surrounding area water samples. Red circles and blue triangles represent Na-HCO₃ and Ca-(Mg)-HCO₃ type waters, respectively.

Bivariate plots shown on Figure 6 also supports this assumption that some intermediate Ca-(Mg)-HCO₃ type water is likely to be the end member water that is mixed with Na-HCO₃ type waters at different proportions. Figure 6a indicate that the Na-HCO₃ type water may be divided into two groups showing slightly different mixing trends. Figure 6b indicates that the Ca-(Mg)-HCO₃ waters may have two sub-groups with two mixing/water rock interaction trends. The first group of Ca-(Mg)-HCO₃ type water samples has low F, and these water samples do not show further enrichment in F with progression of water-rock interaction. On the other hand, the second

group of water samples shows a tendency of slightly increasing F with increasing concentration of Ca (and TDS as well, figure not shown); however, it may be difficult to discern whether the increasing F concentration merely reflects the fact that these waters may have had limited water-rhyolite interaction or they receive increasing amounts of Na-HCO₃ type water.

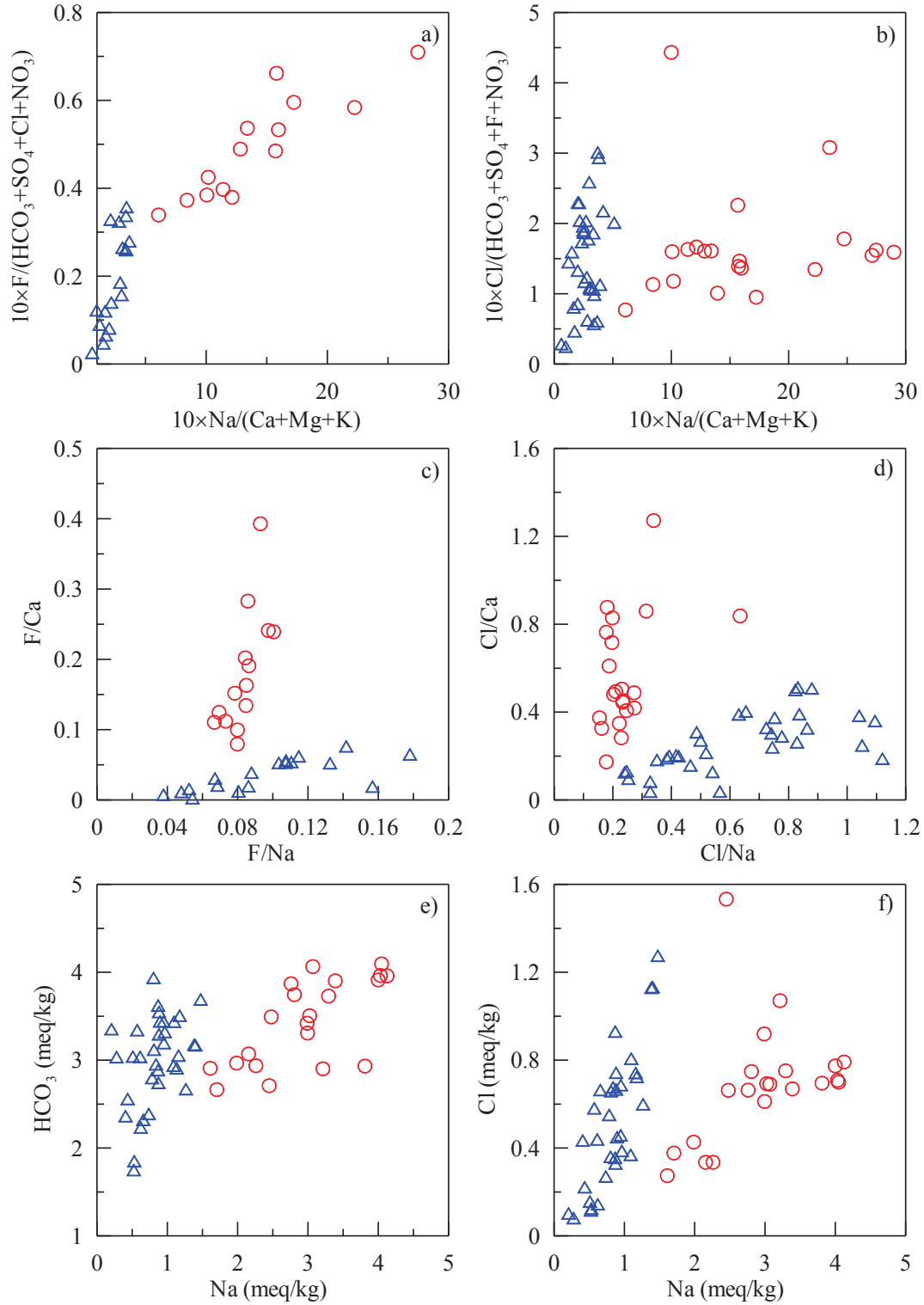


Figure 5. Bivariate diagrams constructed for some components and components ratios in Newdale and surrounding area water samples. Red circles and blue triangles represent Na-HCO₃ and Ca-(Mg)-HCO₃ type waters, respectively.

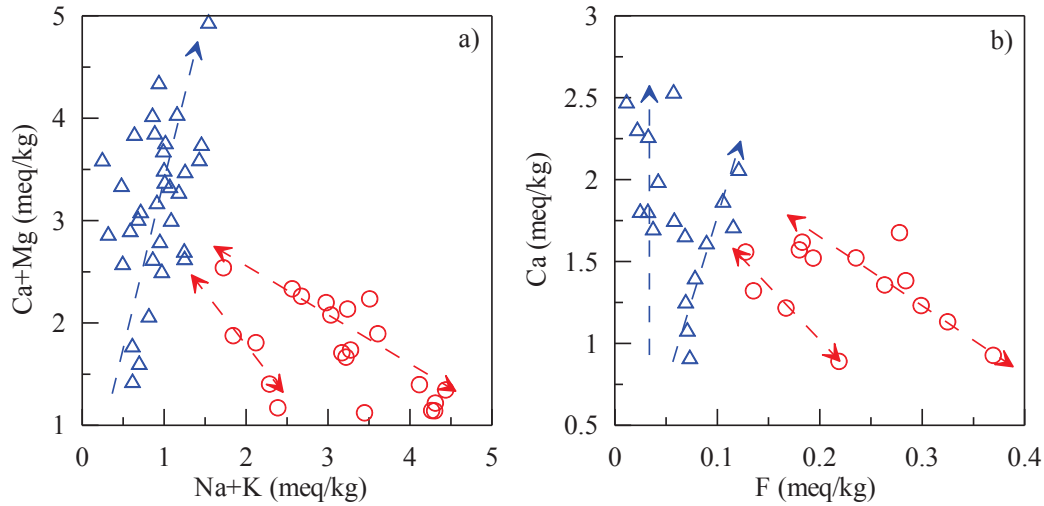


Figure 6. Bivariate diagrams constructed for some components in Newdale and surrounding area water samples. Red circles and blue triangles represent Na-HCO₃ and Ca-(Mg)-HCO₃ type waters, respectively.

Concentration of F in water samples is highly influenced by the degree of past interaction with felsic volcanic rocks. However, the majority of low F water samples are from the area north of Teton River where the subsurface lithology is dominated with felsic rocks. At first, it appears incongruent with the near surface rock types, however, the wells located north of Teton River tap water from a sediment-basalt aquifer sandwiched between pre-Huckleberry Ridge and Huckleberry Ridge felsic volcanic rocks (Figure 2). Similarly, wells distributed on the southern side of the Teton River where near surface rocks are basalts mostly tap Na-HCO₃ type water from felsic volcanic rock units underneath the basalts.

4. GEOTHERMOMETRIC CALCULATIONS

4.1.1 Traditional geothermometers

On a Giggenbach diagram, all Newdale water samples plot in immature water field (Figure 7). For this geothermal prospect, this diagram is minimally useful except indicating that these waters may be less suitable for traditional geothermometry.

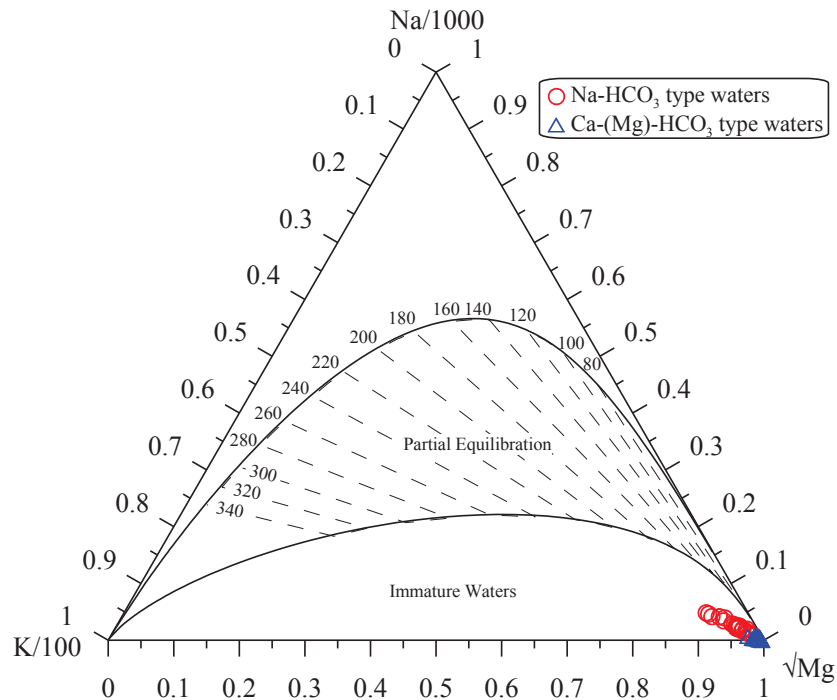


Figure 7. Newdale area water samples plotted on Giggenbach diagram.

Reservoir temperature estimates obtained with quartz, chalcedony, and Na-K-Ca (Mg-corrected) geothermometers for Ca-(Mg)-HCO₃ type waters are lower when compared to the temperature estimates obtained with the respective geothermometers for the Na-HCO₃ type waters (Table 1). The range of temperatures with quartz, chalcedony, and Na-K-Ca (Mg-corrected) geothermometers for Ca-(Mg)-HCO₃ type waters are 66-119 °C, 28-93 °C, 29-81 °C, respectively. Similarly, range of estimated temperature with these geothermometers for Na-HCO₃ type waters are 97-134 °C, 65-112 °C, and 50-111 °C, respectively. A silica (quartz)-enthalpy mixing model (Fournier, 1977; Fournier and Porter, 1982) using all samples resulted in a reservoir temperature of about 224 °C. However, the silica (chalcedony)-enthalpy mixing model resulted in reservoir temperature of about 174 °C (Figure 8).

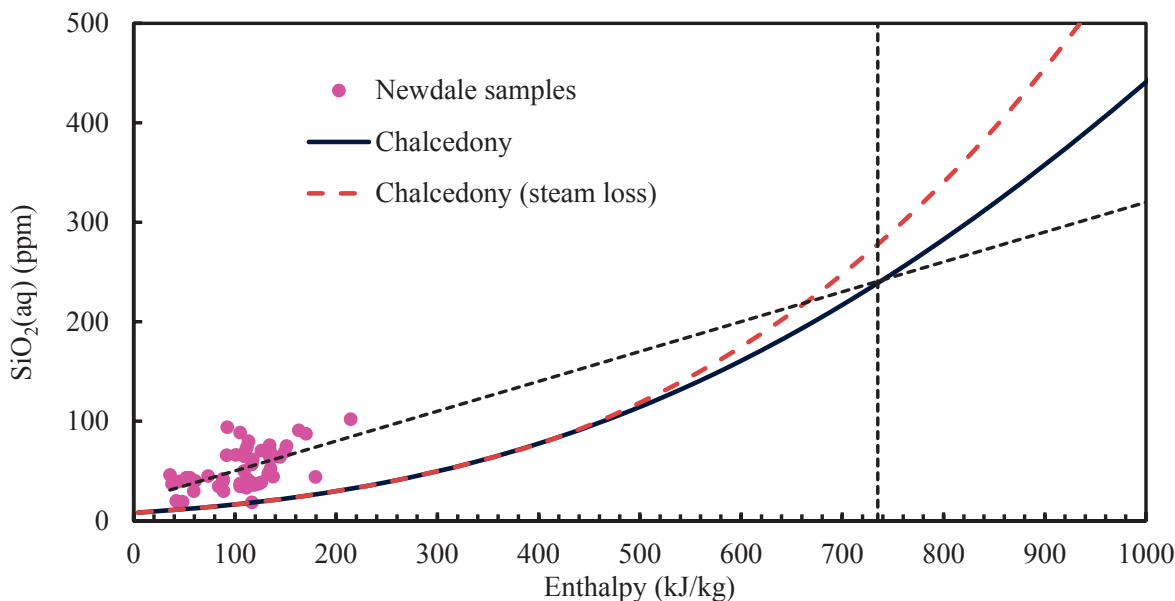


Figure 8. Silica (chalcedony)-enthalpy mixing model (modified from Fournier, 1977; Fournier and Porter, 1982) applied to all Newdale area samples.

4.2 Multicomponent geothermometry

Since Na-HCO₃ type waters show mixing trends (Figure 6) with a variant of Ca-(Mg)-HCO₃ type water; RTest modeling of these samples were performed using the option that helps reconstruct thermal fluid using mixing, fugacity of CO₂, and T as optimization parameters. The Groundwater well-3 (GW3 in Figure 1) water composition was selected to define the end member cooler water composition for RTest modeling of Na-HCO₃ type waters. The GW3 water is a Ca-(Mg)-HCO₃ type water that approximately falls along the mixing trends for both types of water on some bivariate plots (Figure 4, Figure 5a,b,e,f). During RTest modeling, some variant of this water composition is found applicable to all Na-HCO₃ type waters as well as to majority of Ca-(Mg)-HCO₃ type waters. Specifically, SiO₂(aq) concentration in GW3 water, which has unusually high concentration of 46 mg/L at 8.5 °C, was not included in the end member cooler water composition for RTest modeling. The same approach was used for most of the Ca-(Mg)-HCO₃ type waters, however, for some Ca-(Mg)-HCO₃ type waters (Remington Produce, Schwendiman, Pauline, Mark Ricks, and Laverie Ricks wells), RTest modeling was performed using pure water to account for the mixing. For these samples, use of GW3 based end member water resulted in similar estimated temperatures as with the pure water but similar or poor convergence (large standard error). As noted in the previous section, the assumption of some pristine water as end member cooler water for Ca-(Mg)-HCO₃ type waters is geochemically satisfactory to all bivariate plots (Figure 4, Figure 5, and Figure 6).

The RTest estimated temperature for all water compositions are given in Table 1. The ranges of RTest temperature estimates for Na-HCO₃ and Ca-(Mg)-HCO₃ type waters are 75-152 °C and 85-138 °C, respectively. RTest results indicate that Newdale area samples contained 10 to 75% of cooler water fractions. Relatively, Ca-(Mg)-HCO₃ type waters have greater fractions (30-75%) of cooler water than Na-HCO₃ type waters (10-50%). The relatively cooler temperatures obtained with the traditional geothermometers for the Ca-(Mg)-HCO₃ type waters may have resulted because they are more diluted with cooler waters than the Na-HCO₃ type waters.

The lower RTest temperature estimates obtained for some samples from this area are similar to the bottom hole temperatures (83-87 °C) measured at two relatively deeper (~1000 m) Unocal wells (St-07 and St-08 in Figure 1). Moreover, it is likely that the area hosts hotter zone at greater depth reaching to the higher RTest temperature estimates. Assuming an 80 °C thermal gradient (as indicated by two Unocal wells), the higher RTest temperature estimates would be available at about 2 km depth.

Table 1. Geothermometric reservoir temperatures (in °C) estimated using water compositions from several sampling features in northeastern ESRP

Wells	RTEst T $\pm\sigma^a$	Quartz (nsl) ^b	Chalcedony ^c	Na-K-Ca ^d
Newdale City W ^e	96 \pm 4	117	90	85
Wanda Woods W2	141 \pm 7	122	97	65
Walz Enterprises W	131 \pm 8	113	86	70
Wanda Woods W1	110 \pm 7	114	86	71
Wallace Little W	106 \pm 4	120	93	70
Henry Harris W	133 \pm 5	113	85	68
Donanld Trupp W	115 \pm 3	120	94	108
Wayne Larson W	122 \pm 3	130	107	111
Schwendiman W	137 \pm 4	111	83	63
Clyde W	139 \pm 5	113	86	56
Cinder Block W	119 \pm 3	117	90	79
G21	138 \pm 3	116	89	69
G23	75 \pm 6	97	65	83
G25	135 \pm 3	134	112	68
G41	138 \pm 3	127	103	79
G43	136 \pm 5	117	90	75
G44	102 \pm 4	104	74	50
G50	113 \pm 3	128	105	110
G54	118 \pm 2	126	102	80
G78	152 \pm 5	108	78	44
G80	103 \pm 2	114	86	60
<i>Remington Produce W^e</i>	<i>134\pm7</i>	<i>113</i>	<i>86</i>	<i>39</i>
<i>Dean Swindelman W</i>	<i>129\pm12</i>	<i>113</i>	<i>86</i>	<i>44</i>
<i>Pauline W</i>	<i>85\pm5</i>	<i>94</i>	<i>61</i>	<i>44</i>
<i>Mark Ricks W</i>	<i>125\pm4</i>	<i>103</i>	<i>72</i>	<i>50</i>
<i>Lavere Ricks W</i>	<i>116\pm8</i>	<i>96</i>	<i>63</i>	<i>49</i>
G22	104 \pm 10	98	66	53
G24	117 \pm 6	119	93	74
G26	118 \pm 13	91	57	49
G28	122 \pm 2	83	48	29
G30	101 \pm 10	66	28	33
G31	92 \pm 7	88	54	41
G36	110 \pm 8	94	61	31
G37	138 \pm 3	113	85	41
G38	98 \pm 3	88	54	46
G39	121 \pm 1	91	58	44
G55	104 \pm 5	100	69	81
G56	102 \pm 8	91	57	57
G64	96 \pm 4	88	54	58
G65	89 \pm 7	90	56	45
G66	102 \pm 7	91	58	49
G67	134 \pm 12	92	59	33

^aRTEst estimated temperature with associated standard error; ^b quartz (no steam loss) geothermometer temperature (Fournier, 1977); ^c chalcedony geothermometer temperature (Fournier, 1977); ^d Mg-corrected (where applicable) Na-K-Ca geothermometer temperature (Truesdell and Fournier, 1973; Fournier and Potter II, 1979); ^e wells with regular and *italicized* fonts produce Na-HCO₃ and Ca-Mg-HCO₃ type waters, respectively.

5. CONCLUSIONS

The Newdale geothermal area in Madison and Fremont Counties in Idaho is a known geothermal resource area whose thermal anomaly is expressed by high thermal gradients and numerous wells producing warm water (up to 51 °C). Geochemical evaluations of water samples from numerous wells in the area indicate that the area has two types of waters – Na-HCO₃ and Ca-(Mg)-HCO₃. These two water types are considered to be the product of water-interactions involving felsic and basic volcanic rocks and mixing with dilute and cooler groundwater. Each water type can further be subdivided into two groups depending on their degree of mixing with other water types or interaction with other rocks. For example, some bivariate plots indicate that some Ca-(Mg)-HCO₃ water samples have interacted only with basalts whereas some samples of this water type also show limited interaction with rhyolite or mixing with Na-HCO₃ type water. Traditional geothermometers [e.g., silica variants, Na-K-Ca (Mg-corrected)] indicate lower temperatures for this area; however, a traditional silica-enthalpy mixing model results in higher reservoir temperatures. Multicomponent geothermometry (e.g., RTEst) results indicate that the well water samples are mixed with up to 75% of the near surface groundwater. Relatively, Ca-(Mg)-HCO₃ type water samples are more diluted than the Na-HCO₃ type water samples. However, both water types result in similar reservoir temperatures, up to 150 °C. Geothermometric results and the available geothermal gradient data of the area indicate that the reservoir is

likely to be located at a depth of about 2 km. However, further evaluation of the subsurface permeability and extent of the thermal anomaly is needed to better define the hydrothermal potential of this geothermal resource.

ACKNOWLEDGMENTS

This work was supported by funding by the Assistant Secretary for Energy Efficiency and Renewable Energy, Geothermal Technologies Office of the U.S. Department of Energy under the U.S. Department of Energy Contract Nos. DE-AC07-05ID14517 with Idaho National Laboratory and DE-AC02-05CH11231 with Lawrence Berkeley National Laboratory. We thank landowners who provided access to sampling locations. We also thank Dr. Ross Spackman (Brigham Young University-Idaho) for his assistance in coordinating with landowners and filed work. Chemical analyses of the samples were conducted by Ms. Debbie Lacroix (University of Idaho) at Center for Advanced Energy Studies (CAES). We appreciate the discussion with Drs. Bill Phillips (Idaho Geological Survey), Glenn Embree (BYU-Idaho), and Dan Moore (BYU-Idaho).

REFERENCES

- Anders, M. H., Rodgers, D. W., Hemming, S. R., Saltzman, J., DiVenere, V. J., Hagstrum, J. T., Embree, G. F., and Walter, R. C.: A fixed sublithospheric source for the late Neogene track of the Yellowstone hotspot: Implications of the Heise and Picabo volcanic fields, *Journal of Geophysical Research: Solid Earth*, **119**, (2014), 2871–2906.
- Bethke, C.M.: *Geochemical and Biogeochemical Reaction Modeling*. Cambridge University Press, pp. 547, (2008).
- Blackwell, D.D.: Regional implications of heat flow of the Snake River Plain, northwestern United States. *Tectonophysics*, **164**, (1989), 323-343.
- Bond, J. G.: Geologic map of the state of Idaho, scale 1:500,000. Idaho Bur. of Mines and Geology, (1978).
- Brott, C.A., Blackwell, D.D., and Mitchell, J.C.: Geothermal Investigations in Idaho, Part 8, Heat Flow in the Snake River Plain Region, Idaho. *Water Information Bulletin* No.30, Idaho Department of Water Resources, (1976).
- Cannon, C., Wood, T., Neupane, G., McLing, T., Mattson, E., Dobson, P., and Conrad, M.: Geochemistry sampling for traditional and multicomponent equilibrium geothermometry in southeast Idaho. *GRC Transactions*, **38**, (2014), 524-431.
- Cooper, D.C., Palmer, C.D., Smith, R.W., and McLing, T.L.: Multicomponent equilibrium models for testing geothermometry approaches. *Proceedings*, 38th Workshop on Geothermal Reservoir Engineering Stanford University, Stanford, CA (2013).
- D'Amore, F. and Arnórsson, S.: Geothermometry. In S. Arnórsson, ed., *Isotopic and Chemical Techniques in Geothermal Exploration, Development and Use*, IAEA (Editorial), Vienna, p. 152-199, (2000).
- D'Amore, F., Fancelli, R., and Caboi, R.: Observations on the application of chemical geothermometers to some hydrothermal systems in Sardinia. *Geothermics*, **16**, (1987), 271-282.
- Embree, G.F., and Hoggan R.D.: Secondary deformation within the Huckleberry Ridge Tuff and subjacent Pliocene units near the Teton Dam: Road log to the regional geology of the eastern margin of the Snake River plain, Idaho. In S.S. Hughes and G.D. Thackray, eds., *Guidebook to the Geology of Eastern Idaho*, Idaho Museum of Natural History, Pocatello, Idaho, p. 181-202, (1999).
- Embree, G.F., Phillips, W.M., and Welhan, J.A.: Geologic map of the Newdale quadrangle, Fremont and Madison Counties, Idaho. Idaho Geological Survey, University of Idaho, Moscow, Idaho 83844-3014, (2011).
- Fournier, R.O.: Chemical geothermometers and mixing models for geothermal systems. *Geothermics*, **5**, (1977) 41-50.
- Fournier, R.O.: A revised equation for the Na/K geothermometer. *GRC Transactions*, **3**, (1979), 221-224.
- Fournier, R.O. and Truesdell, A.H.: An empirical Na-K-Ca geothermometer for natural waters. *Geochim. Cosmochim. Acta*, **37**, (1973), 1255-1275.
- Fournier, R.O. and Potter, R.W. II: Magnesium correction to the Na-K-Ca chemical geothermometer. *Geochim. Cosmochim. Acta*, **43**, (1979), 1543-1550.
- Fournier, R. O. and Potter, R.W. II: Revised and expanded silica (quartz) geothermometer. *Geotherm. Resour. Counc. Bullet.*, **11(10)**, (1982), 3-12.
- GeothermEx, Inc.: Independent technical report: Resource evaluation of the Newdale geothermal prospect, Madison and Fremont Counties, Idaho, USA. Geothermix, Inc., Richmond, California, USA, February 10, 2010, p. 101, (2010).
- Giggenbach, W.F.: Geothermal solute equilibria. Derivation of Na-K-Mg-Ca geoindicators. *Geochim. Cosmochim. Acta*, **52**, (1988), 2749-2765.
- Hughes, S.S., Smith, R.P., Hackett, W.R., and Anderson, S. R.: Mafic volcanism and environmental geology of the eastern Snake River Plain. *Idaho Guidebook to the Geology of Eastern Idaho*. Idaho Museum of Natural History, (1999), 143-168.
- Hull, C.D., Reed, M.H., and Fisher, K.: Chemical geothermometry and numerical unmixing of the diluted geothermal waters of the San Bernardino Valley Region of Southern California. *GRC Transactions*, **11**, (1987), 165-184.
- Mabey, D.R.: Gravity and aeromagnetic anomalies in the Rexburg area of eastern Idaho. *Open-File Report 78-382*, U.S. Geological Survey, (1978).

- Mann, L.J.: Hydraulic properties of rock units and chemical quality of water for INEL-1: a 10,365-foot deep test hole drilled at the Idaho National Engineering Laboratory, Idaho (No. IDO-22070). Geological Survey, Idaho Falls, ID (USA), Water Resources Div. (1986).
- Mattson, E.D., Smith, R.W., Neupane, G., Palmer, C.D., Fujita, Y., McLing, T.L., Reed, D.W., Cooper, D.C., and Thompson, V.S.: Improved geothermometry through multivariate reaction-path modeling and evaluation of geomicrobiological influences on geochemical temperature indicators: final report (No. INL/EXT-14-33959). Idaho National Laboratory (INL), (2015).
- McLing, T.L., Smith, R.W., and Johnson, T.M.: Chemical characteristics of thermal water beneath the eastern Snake River Plain. In: Geology, Hydrogeology, and Environmental Remediation: Idaho National Engineering and Environmental Laboratory, Eastern Snake River Plain, Idaho, P.K. Link and L.L. Mink, eds. *Geological Society of America Special Paper* **353**, (2002), 205-211.
- McLing, T., Mc Curry, M., Cannon, C., Neupane, G., Wood, T., Podgorney, R., Welhan, J., Mines, G., Mattson, E., Wood, R., Palmer, C. and Smith, R.: David Blackwell's Forty Years in the Idaho Desert, The Foundation for 21st Century Geothermal Research; Geothermal Resources Council Transactions, **38**, (2014), 143-153.
- Michard, G. and Roekens, E.: Modelling of the chemical components of alkaline hot waters. *Geothermics*, **12**, (1983), 161-169.
- Mitchell, J.C., Johnson, L.L, and Anderson, J.E.: Geothermal Investigations in Idaho – Part 9: Potential for direct heat applications of geothermal resources. Idaho Department of Water Resources, *Water Information Bulletin* **30**, (1980).
- Morgan, L.A. and McIntosh, W.C.: Timing and development of the Heise volcanic field, Snake River Plain, Idaho, western USA. *GSA Bulletin*, **117**, (2005), 288-306.
- Neupane, G., Smith, R. W., Palmer, C. D., and McLing, T. L.: Multicomponent equilibrium geothermometry applied to the Raft River geothermal area, Idaho: preliminary results. In *GSA Abstracts with Programs*, 45 (7), (2013) 0).
- Neupane, G., Mattson, E.D., McLing, T.L., Palmer, C.D., Smith, R.W., and Wood, T.R.: Deep geothermal reservoir temperatures in the Eastern Snake River Plain, Idaho using multicomponent geothermometry. *Proceedings*, Thirty-Ninth Workshop on Geothermal Reservoir Engineering, Stanford University, Stanford, California, February 24-26, 2014 SGP-TR-202 (2014).
- Neupane, G., Mattson, E.D., McLing, T.L., Palmer, C.D., Smith, R.W., Wood, T.R., and Podgorney, R.K.: Geothermal reservoir temperatures in southeastern Idaho using multicomponent geothermometry. *Proceedings*, World Geothermal Congress 2015, Melbourne, Australia, 19-25 April 2015 (2015a).
- Neupane, G., Baum, J.S., Mattson, E.D., Mines, G.L., Palmer, C.D., and Smith, R.W.: Validation of multicomponent equilibrium geothermometry at four geothermal power plants. *Proceedings*, Fortieth Workshop on Geothermal Reservoir Engineering Stanford University, Stanford, California, January 26-28, 2015 (2015b).
- Neupane, G., Mattson, E.D., Mines, G.L., McLing, T.L., Dobson, P.F., Conrad, M.E., Wood, T.R., Cannon, C., Worthing, W.: Geothermometric temperature comparison of hot springs and wells in southern Idaho. *GRC Transactions*, **39**, 495-502 (2015c).
- Neupane, G., Mattson, E.D., McLing, T.L., Palmer, C.D., Smith, R.W., Wood, T.R., and Podgorney, R.K.: Geothermometric evaluation of geothermal resources in southeastern Idaho. *Geoth. Energ. Sci.*, **4**(1), (2016a), 11-22.
- Neupane, G., Mattson, E.D., Cannon, J.C., Atkinson, T.A., McLing, T.L., Wood, T.R., Worthing, W.C., Dobson, P.F., and Conrad, M.E.: Potential hydrothermal resource areas and their reservoir temperatures in the Eastern Snake River Plain, Idaho. *Proceedings*, 41st Workshop on Geothermal Reservoir Engineering, Stanford University, Stanford, California, February 22-24, 2016 SGP-TR-209 (2016b).
- Palandri, J.L. and Reed, M.H. (2001). Reconstruction of in situ composition of sedimentary formation waters. *Geochim. Cosmochim. Acta*, **65**, 1741-1767.
- Palmer, C.D., Ohly, S.R., Smith, R.W., Neupane, G., McLing, T., Mattson, E.: Mineral selection for multicomponent equilibrium geothermometry. *GRC Transactions*, **38**, (2014), 453-459.
- Pang, Z.H. and Reed, M.: Theoretical chemical thermometry on geothermal waters: Problems and methods. *Geochim. Cosmochim. Acta*, **62**, (1998), 1083-1091.
- Peiffer, L., Wanner, C., Spycher, N., Sonnenthal, E., Kennedy, B.M., Iovenitti, J.: Optimized multicomponent vs. classical geothermometry: insights from modeling studies at the Dixie Valley geothermal area. *Geothermics*, **51**, (2014), 154–169.
- Pierce, K. L., and Morgan, L. A.: The track of the Yellowstone hot spot: Volcanism, faulting, and uplift. *Geological Society of America Memoirs*, **179**, (192), 1-54.
- Prostka, H.J. and Embree, G.F.: Geology and geothermal resources of the Rexburg area, eastern Idaho. *Open-File Report 78-1009*, U.S. Geological Survey, (1978).
- Reed, M. and Spycher, N.: Calculation of pH and mineral equilibria in hydrothermal waters with application to geothermometry and studies of boiling and dilution. *Geochim. Cosmochim. Acta*, **48**, (1984), 1479-1492.
- Smith, R.W., Palmer, C.D., and Cooper, D.: Approaches for multicomponent equilibrium geothermometry as a tool for geothermal resource exploration. *Abstracts*, AGU Fall Meeting, San Francisco, 3-7 December 2012.

- Spycher, N.F., Sonnenthal, E., and Kennedy, B.M.: Integrating multicomponent chemical geothermometry with parameter estimation computations for geothermal exploration. *GRC Transactions*, **35**, (2011), 663-666.
- Spycher, N., Peiffer, L., Sonnenthal, E. L., Saldi, G., Reed, M. H., and Kennedy, B. M.: Integrated multicomponent solute geothermometry. *Geothermics*, **51**, (2014), 113-123.
- Tole, M.P., Ármannsson, H., Pang, Z.H., & Arnórsson, S.: Fluid/mineral equilibrium calculations for geothermal fluids and chemical geothermometry. *Geothermics*, **22**, (1993), 17-37.
- Welhan, J.A.: Thermal and Trace-Element Anomalies in the Eastern Snake River Plain aquifer: toward a conceptual model of the EGS resource. *GRC Transactions*, **39**, (2015), 363-375.
- Whitehead, R.L.: Geohydrologic framework of the Snake River Plain regional aquifer system, Idaho and eastern Oregon. Regional aquifer system analysis-Snake River Plain, Idaho. *US Geological Survey Professional Paper 1408-B*, (1992).

Appendix I.

Conrad, M.E., Dobson, P.F., Sonnenthal, E.L., Kennedy, B.M., Cannon, C., Worthing, W., Wood, T., Neupane, G., Mattson E., and McLing, T., 2016. Application of isotopic approaches for identifying hidden geothermal systems in southern Idaho. Proceedings, 41st Workshop on Geothermal Reservoir Engineering, Stanford University, Stanford, CA.

Application of Isotopic Approaches for Identifying Hidden Geothermal Systems in Southern Idaho

Mark E. Conrad¹, Patrick F. Dobson¹, Eric L. Sonnenthal¹, B. Mack Kennedy¹, Cody Cannon², Wade Worthing², Thomas Wood², Ghanashyam Neupane³, Earl Mattson³ and Travis McLing³

¹Earth and Environmental Sciences Area, Lawrence Berkeley National Laboratory, Berkeley, CA

²University of Idaho – Idaho Falls, ID

³Idaho National Laboratory, Idaho Falls, ID

Corresponding author: msconrad@lbl.gov

Keywords: Isotopes, geothermometry, Snake River Plain, high-temperature water-rock interaction

ABSTRACT

Southern Idaho is an area of high heat flow with significant potential geothermal resources. However, shallow cold groundwater effectively masks thermal signatures of deep-seated geothermal systems in the area. In order to attempt to see through the shallow groundwater, we are applying a combination of geochemical and isotopic tools relying on dissolved gas and chemical species that have low concentrations in the dilute groundwater to prospect for high-temperature systems in the deep subsurface. For the first phase of the project, our efforts were focused in and around the eastern Snake River Plain (ESRP). We have collected and analyzed the isotopic compositions of more than 40 samples from thermal springs and wells from the region. Of potential isotope geothermometers, the sulfate-water oxygen isotope geothermometer has given the most promising results, yielding calculated temperatures similar to multi-component chemical geothermometers. Other isotopic tools that have proven useful are shifts in the isotopic compositions (δD and $\delta^{18}O$) of groundwater away from the local meteoric water line indicating high-temperature interaction with reservoir rocks or mixing with a magmatically derived fluid. In addition, the δD and $\delta^{13}C$ of dissolved methane in several of the samples indicate that the methane formed in a high temperature magmatic system. Taken together with the analyses of multi-component chemical geothermometry and a separate study of the $^3He/^4He$ from the same features, the results have identified two promising areas warranting more concentrated study in the Twin Falls area and the Camas Prairie region between the ESRP and the Idaho batholith.

1. INTRODUCTION

The western United States has been identified as an area with high potential for geothermal development (Blackwell et al., 2011) and the eastern Snake River Plain (ESRP) in southern Idaho is one of the most promising regions. The ESRP extends from the Twin Falls area in south-central Idaho northeast to the Yellowstone area (Figure 1). The geology of the ESRP consists of thick deposits of Miocene-Eocene rhyolitic tuff deposits produced from a series of volcanic centers formed by migration of the Yellowstone hotspot to its current location (Pierce and Morgan, 1992; Hughes et al., 1999). The rhyolitic rocks are overlain by Quaternary basalt flows generated from northwest trending volcanic rifts formed from extensional activity following passage of the Yellowstone hotspot (Hughes et al., 1999). The basalt flows and accompanying sedimentary interbeds can reach thicknesses of greater than 1 km. These highly permeable rocks host a major aquifer carrying run-off water from the mountainous regions surrounding the ESRP (Whitehead, 1992).

The high heat flux in the ESRP ($\sim 110 \text{ mW/m}^2$; Smith, 2004) and abundant hot springs along the margins of the plain suggest that there should be significant, exploitable geothermal reserves in the area. The deep rhyolitic rocks are the likely host rocks for the geothermal reservoir, with the high heat flow resulting from underlying young basaltic sill intrusions (e.g., Nielson and Shervais, 2014; Welhan, 2015; Shervais et al., 2015), but the high-volume, rapidly flowing shallow aquifer in the overlying basalts makes it difficult to use heat flow measurements to pinpoint areas of high potential. Most water from shallow wells and springs in the ESRP are mixed waters of multiple sources, dominated by meteoric water that may mask or significantly attenuate the thermal signal of any deep geothermal waters (McLing et al., 2002; Welhan, 2015). However, due to the dilute nature of the meteoric water, some of the chemical signatures of the high temperature systems may persist.

We are conducting this study to test the hypothesis that geochemical signatures of deep geothermal activity can be used to “see through” the shallow aquifer in the ESRP. Results of related efforts to compare the results of traditional chemical geothermometry to temperatures calculated using RTEst (Palmer et al., 2014), an advanced multi-component equilibrium geothermometer, are presented elsewhere (Neupane et al., 2016). Briefly, where traditional geothermometry does not account for physical relationships (e.g., boiling, mixing) or chemical equilibrium with complex mineral assemblages typical of real rock systems, RTEst does account for these parameters. In addition, the results of a survey of helium isotope ratios in the samples collected for this project are presented in a previous paper (Dobson et al., 2015). In this paper, the results of isotopic analyses of water (δD and $\delta^{18}O$), dissolved inorganic carbon ($\delta^{13}C$), sulfate ($\delta^{34}S$ and $\delta^{18}O$) and dissolved methane (δD and $\delta^{13}C$) are presented and discussed. The locations of samples collected for this project along with those of previous sampling efforts are plotted on Figure 1 below.

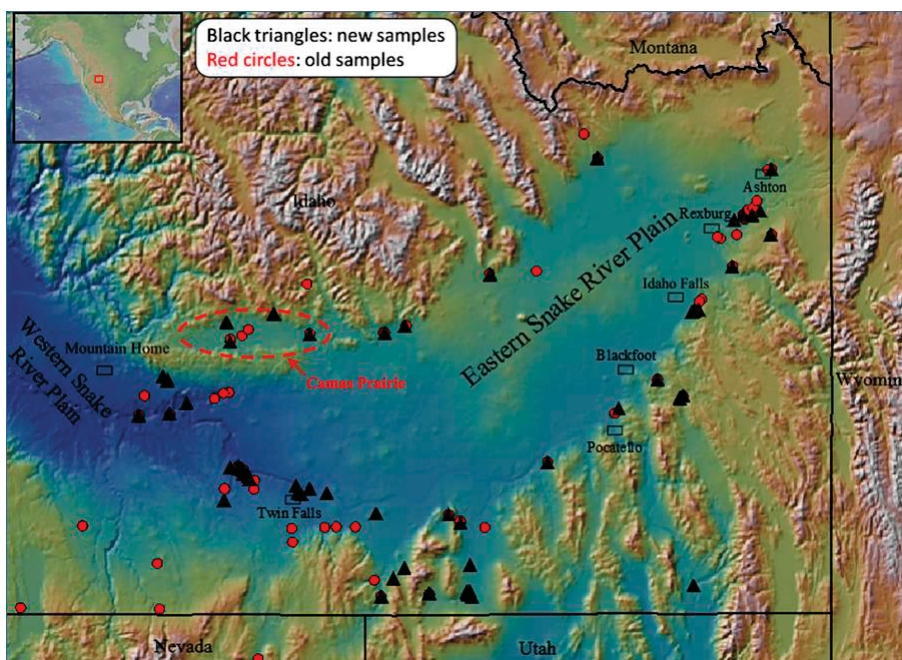


Figure 1: Map of southeastern Idaho showing the Eastern Snake River Plain and the locations of prior geothermal samples plus those collected and analyzed for this project. Note the Camas Prairie area highlighted on the map.

2. FIELD AND LABORATORY METHODS

2.1 Sampling Methods

Samples for this investigation were collected from both groundwater thermal wells and hot springs. Samples from groundwater wells were collected as near the outlet as possible following purging of at least 3 times the volume of water in the well casing. Spring samples were taken as close to the outlet as possible, determined by the hottest point within the features. At each sampling site, 3 types of samples were collected. For δD and $\delta^{18}O$ of water and $\delta^{13}C$ of total dissolved inorganic carbon (DIC), a sample of water was collected directly into a 60 ml syringe rinsed once with water from the source. The sample was then passed through a 0.2 μm filter and injected into a 40 ml amber vial filled to the top and immediately capped. The sample was then stored at 4 °C until it could be analyzed. For analyses of the $\delta^{34}S$ and $\delta^{18}O$ of dissolved sulfate, a 40 ml centrifuge tube was filled with water and HCl added to drop the pH down to ~2 to preserve the sample and drive off any dissolved inorganic carbon in the sample. For dissolved gas samples, filtered water was injected into 60 or 160 ml evacuated vials capped with thick, blue butyl rubber stoppers until the bottle was filled. The sample was stored at 4 °C until it could be analyzed.

2.2 Isotope Analyses

2.2.1 Water Isotope Measurements

The hydrogen and oxygen isotopic compositions of the water samples were analyzed separately at the Center for Stable Isotope Biogeochemistry (CSIB) at the University of California, Berkeley. δD values of water are analyzed using a hot chromium reactor unit (H/Device™) interfaced with a Thermo Delta Plus XL mass spectrometer. The $\delta^{18}O$ in water is analyzed by continuous flow using a Thermo Gas Bench II interfaced to a Thermo Delta Plus XL mass spectrometer. The precision of these analyses determined by repeated analysis of internal standards is $\pm 0.8\text{‰}$ (1 σ) for δD and $\pm 0.12\text{‰}$ (1 σ) for $\delta^{18}O$. Results are presented relative to V-SMOW.

2.2.2 Dissolved Sulfate Isotope Analyses

Following delivery of the acidified samples in the lab, ~1 ml of 1N BaCl₂ solution was added to each sample resulting in the precipitation of BaSO₄. After waiting >1 day for the precipitates to settle, the supernatant solution is decanted off and de-ionized water added to container and the sample re-suspended. The resulting sample is then centrifuged, the supernatant removed and the sample dried for >1 day. The sulfur and oxygen isotopic composition of the BaSO₄ is then analyzed. The sulfur isotope compositions of the samples were analyzed at the Center for Isotope Geochemistry (CIG) at Lawrence Berkeley National Laboratory by combustion in a Costech Elemental Analyzer with the $\delta^{34}S$ values of the resulting SO₂ analyzed on a Thermo Delta V Plus mass spectrometer. The precision of those measurements is $\pm 0.2\text{‰}$ (1 σ). The $\delta^{18}O$ values of the BaSO₄ precipitates were analyzed at CSIB using an Elementar PYRO Cube interfaced to a Thermo Delta V mass spectrometer. The precision of those measurements is $\pm 0.5\text{‰}$ (1 σ). Sulfur isotope analyses of H₂S in the samples were also attempted, but the concentrations in the samples were too low.

2.2.3 Dissolved Inorganic Carbon (DIC) Isotope Analyses

The DIC in the samples were analyzed by addition of 0.1 to 1.0 ml of sample to a He-purged vial containing 1 ml of 70% H₃PO₄. The $\delta^{13}C$ values of the resulting CO₂ were then analyzed by injection into a Micromass Trace Gas pre-concentration system interfaced to a

Micromass JA series isotope ratio mass spectrometer at CIG. The precision of those measurements is $\pm 0.3\%$ (1σ). Concentrations of DIC in the samples were also determined from these analyses by comparison with standards of known concentrations. These measurements are good to approximately $\pm 10\%$ of the measured value (1σ).

2.2.4 Dissolved Methane Isotopic Analyses

The dissolved gas samples were prepared for analysis by creating a headspace in the sample followed by addition of He gas to the headspace. For isotopic analyses, samples of the headspace gas were flushed through a sample loop on a 6-port Valco Vici valve and then injected into the column of a Thermo Trace Gas Ultra connected to the Delta V Plus mass spectrometer. For $\delta^{13}\text{C}$ analyses, the methane was separated chromatographically, and combusted to CO_2 , which was then analyzed in the mass spectrometer (1σ precision = $\pm 0.2\%$). δD analyses were done by pyrolysing the CH_4 to H_2 gas, which was then analyzed in the mass spectrometer (1σ precision = $\pm 5\%$). Concentrations of CH_4 in the headspace were calculated by comparing the total peak areas of the samples to those of known standards. Those concentrations were then converted to dissolved concentrations using Henry's law. Hydrogen isotope analyses of H_2 in the samples were also attempted, but the concentrations were too low.

3. RESULTS AND DISCUSSION

3.1 Sulfate-Water Oxygen Isotope Geothermometer

The difference between the oxygen isotopic compositions of sulfate and water can be used to calculate the temperature of formation of the sulfate (McKenzie and Truesdell, 1977; Fowler et al., 2013). There are, however, several secondary factors that can change the isotopic composition of one or the other of these two phases after the sulfate has formed. For sulfate, mixing with another source of sulfate along the pathway to the surface (e.g., gypsum/anhydrite in evaporite beds) can shift the oxygen isotopic composition of the dissolved sulfate. This can sometimes be inferred based on knowledge of the subsurface geology and/or the sulfur isotope composition of the sulfate. Sulfur in igneous/magmatic systems generally has much lower sulfur isotopic composition than sedimentary gypsum. Microbial reduction of sulfate can also shift the isotopic composition of the residual sulfate, but requires highly anaerobic conditions and will also shift the isotopic composition of the sulfur. The oxygen isotopic composition of the sulfate can also re-equilibrate with the water at lower temperatures, but this is a relatively slow process and is likely only an issue where the thermal waters have a long residence time in a shallower, cooler reservoir. For the water, the biggest issue is mixing with another source of water with a different oxygen isotope composition than the reservoir water. In the ESRP, the isotopic compositions of waters are similar between deep reservoirs and the shallow groundwater. The $\delta^{18}\text{O}$ of the water can also be shifted by boiling and/or significant water-rock interaction after formation of the sulfate, but these effects can often be seen by comparison with the hydrogen isotopic composition of the water.

For our temperature calculations, we used the revised sulfate-water oxygen isotope geothermometer formulated by Fowler et al. (2013). To test the applicability of this geothermometer, we collected and analyzed the oxygen isotopic compositions of sulfate and water in fluids injected during a fracture stimulation experiment conducted at the Newberry Volcano in the Oregon Cascades (Cladouhos et al., 2015). About 2.5 million gallons of water were injected under pressure into a subsurface zone at the site and allowed to equilibrate with the rock for 3 weeks. At that point the water was allowed to flow back out of the well and samples were collected for chemical and isotopic analyses. The calculated temperatures using the sulfate-water oxygen isotope geothermometer are plotted on Figure 2 with an average down-hole temperature calculated using GeoT, a multi-component chemical geothermometer (Spycher et al., 2014). The isotope geothermometry values are a bit lower, possibly due to background sulfate, but in general the temperatures appear to be approaching equilibrium for the final samples.

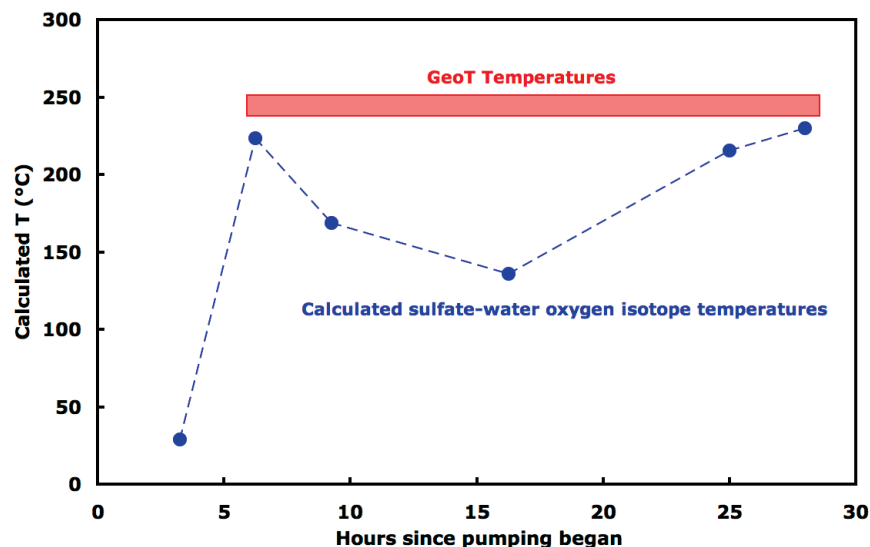


Figure 2: Temperatures calculated for flow-back samples from the Newberry Volcano EGS stimulation test.

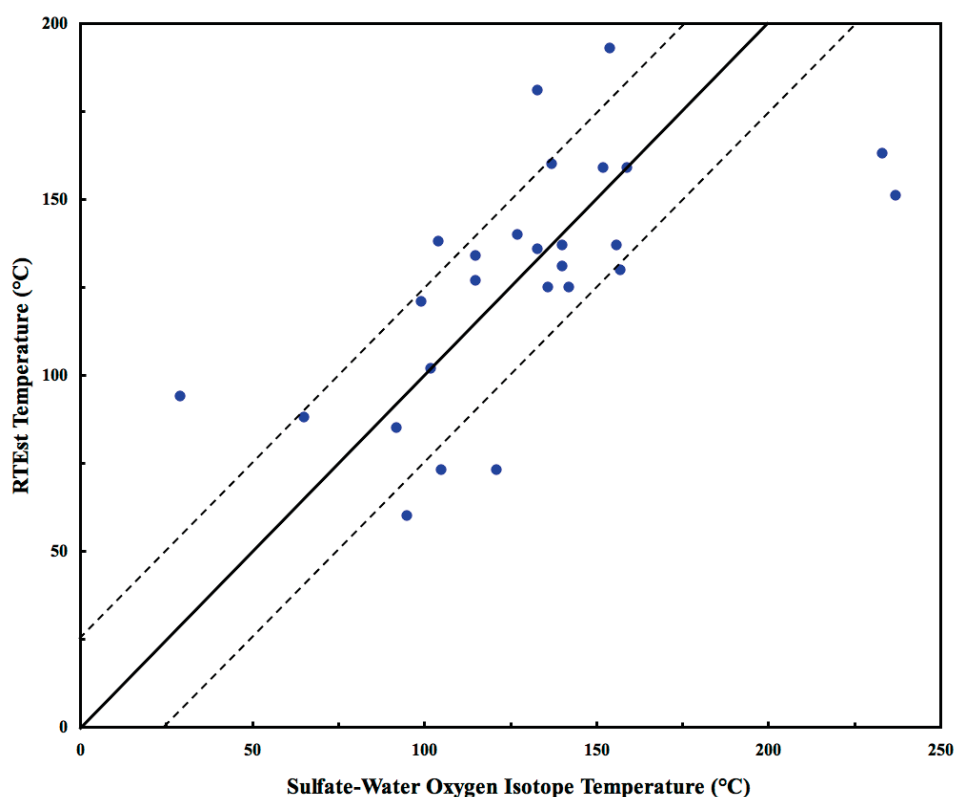


Figure 3: Comparison between temperatures calculated using the sulfate-water oxygen isotope geothermometer versus temperatures calculated using the RTest. The solid line represents a 1:1 comparison and the dashed lines indicate the range of temperatures within $\pm 25^{\circ}\text{C}$ of each other.

Temperatures calculated using the sulfate-water oxygen isotope geothermometer for samples collected for this project that contained sufficient sulfate for isotopic analyses are given in Table 1. Also included are RTest temperatures calculated for the same samples. Given all of the uncertainties associated with both techniques, there is a remarkable correlation between the two geothermometers with most being within $\pm 25^{\circ}\text{C}$ of each other (Figure 3). In some cases such as Green Canyon Hot Springs and Heise Hot Springs, the sulfate concentrations were high, likely representing interaction with sedimentary evaporite interbeds in the basalts which would result in low calculated temperatures for the sulfate-water oxygen isotope geothermometer. Otherwise, there are no clear explanations for some of the samples with much higher sulfate-water temperatures, suggesting that they might represent deep, hot geothermal systems.

Results calculated with both geothermometers indicate two areas with widespread high temperature geothermal fluids at depth. Temperatures calculated with the sulfate-water oxygen isotope geothermometer for the Twin Falls region average 137°C which is essentially identical to the average temperature calculated with RTest of 138°C . These values are higher than those reported by Mariner et al. (1997) ($90\text{--}106^{\circ}\text{C}$) for the same region using the sulfate-water oxygen isotope geothermometer. Although these temperatures are on the low side, especially for electricity generation, they come from several features spread across a large area, suggesting there may be hotspots within the region that might be suitable for power generation. The Camas Prairie is the other highly encouraging area with sulfate-water temperatures exceeding 200°C and RTest temperatures approaching that level. This area was also identified as a geothermal prospect through geothermal play fairway analysis (Shervais et al., 2015).

3.2 Water Isotopes and Water-Rock Interaction

During high-temperature water-rock interaction, the isotopic composition of the water can be shifted to the right of the meteoric water line (Taylor, 1974). The change in the isotopic composition of the water is mostly limited to the oxygen isotopic composition of the water due to the fact that most igneous/volcanic rocks contain very little hydrogen compared to water but have significant oxygen. Mixing with water derived from cooling, degassing magmas can also produce a similar effect (Giggenbach, 1992). Boiling/evaporation will also shift the residual water off the meteoric water line, but these changes will also significantly affect the hydrogen isotopic compositions of the water. It is important to note that mixing with shallower, non-thermal waters can dilute these signals.

The water isotope compositions of the samples collected for this project are plotted on Figure 4. Most of the samples plot close to the meteoric water line (precipitation in this region tends to be slightly offset to the right of the global meteoric water line), but there are several samples that have oxygen isotope composition shifted 1–3‰ to the right of the meteoric water line. Four of these samples collected from three locations are from the Camas Prairie region and are some of those with anomalously high temperatures calculated with the sulfate-water oxygen isotope geothermometer. A water sample associated with a flow zone at 1745 m depth collected from the MH-2 well (which encountered temperatures of 150°C ; Nielson and Shervais, 2014) also exhibited a similar shift in its oxygen isotope composition (Freeman, 2013).

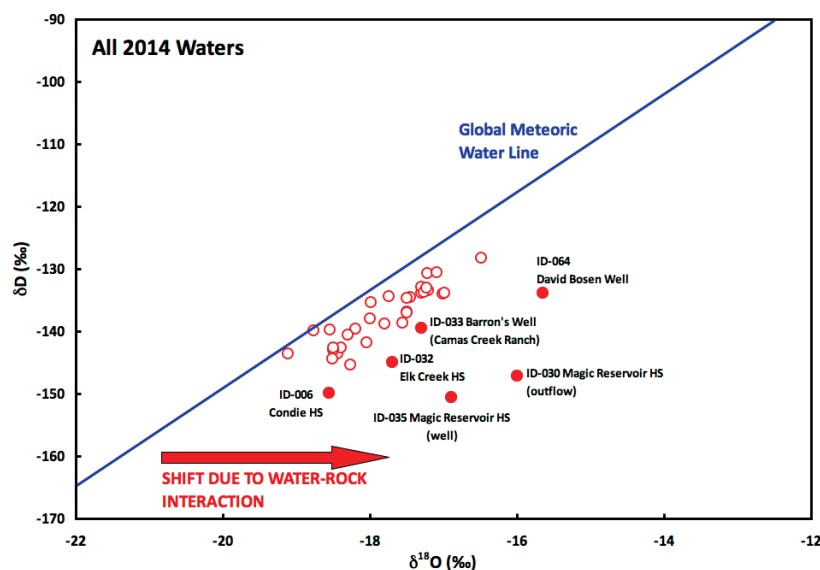


Figure 4: Hydrogen and oxygen isotopic compositions of water from ESRP samples with the global meteoric water line for comparison. Most waters fall very close to the meteoric water line, but there are several that are significantly shifted to the right of the meteoric water line, which is an indication of oxygen isotope exchange during high-temperature water-rock interaction in hydrothermal systems or mixing with magmatically-derived fluids.

3.3 Methane Isotope Signatures of High-Temperature Sources

The carbon and hydrogen isotopic compositions of CH_4 can offer clues as to the mechanism of formation and its post-formation history. Figure 5 is modified from Whiticar et al. (1986) and outlines the primary field of methane formed under thermogenic conditions in hydrocarbon reservoirs and the two primary microbial mechanisms for low-temperature methanogenesis (acetoclastic versus CO_2 reduction). Also shown on this plot is the general field of methane formed abiotically in high-temperature magmatic or hydrothermal systems outlined by Welhan et al. (1988). It is also important to note that the isotopic compositions of the methane can be significantly altered by microbial oxidation in aerobic groundwater.

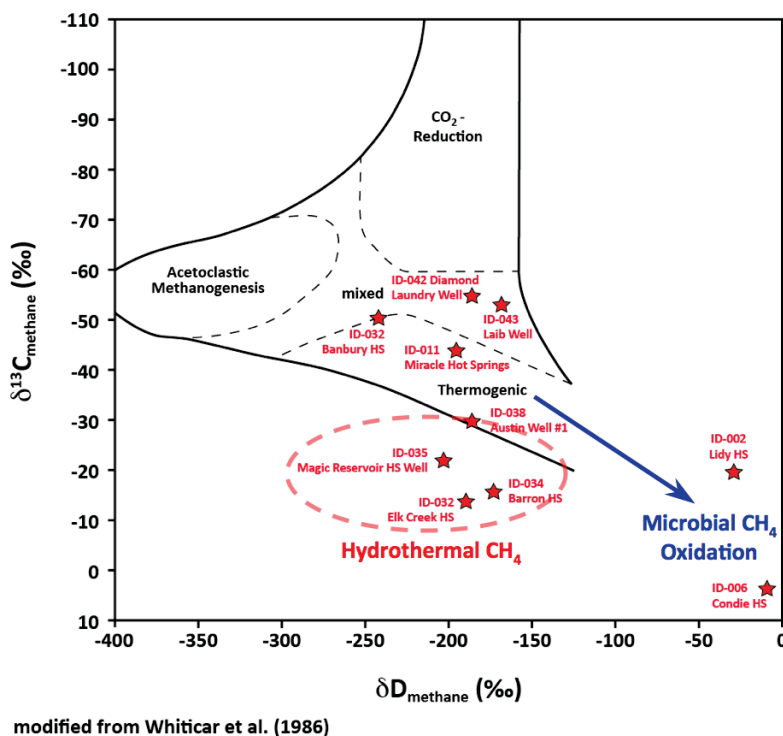


Figure 5: Carbon and hydrogen isotopic compositions of dissolved methane in samples collected from the ESRP plotted with the ranges of values expected for methane formed by different mechanisms. Most notable are the samples outlined by the red dashed line (all from the Camas Prairie) with isotopic compositions typical of methane formed in high-temperature hydrothermal systems.

The isotopic compositions of samples for which we were able to analyze both the hydrogen and carbon isotopes of CH₄ are plotted on Figure 5. Of this group, there are a couple of samples (Condie Hot Springs and Lidy Hot Springs) that have clearly undergone significant methane oxidation. This is not surprising since both sampling points were from open-air pools of water. The most interesting thing about these samples is that despite significant oxidation, there were still high enough concentrations of methane remaining for isotopic measurements. There are also a number of samples in the thermogenic/mixed origin areas of the plot. These are all from the Twin Falls area and could have been formed from thermal degradation of organic matter in the subsurface. Most interestingly, the remaining 3 samples plot in the field of high temperature hydrothermal methane. These samples are the same three from the Camas Prairie area with the water with the strongly shifted oxygen isotope composition and also have high sulfate-water oxygen isotope temperatures.

4. CONCLUSIONS

The results of study demonstrate the value of isotopic data for identifying areas with high potential for geothermal exploitation, especially when combined with other tools such as multi-component chemical geothermometers. Through this work, we have identified two very promising areas for further study.

1. Numerous intermediate temperature geothermal springs and wells characterize the Twin Falls region. These thermal features yield calculated temperatures in the range of 140±20°C across a wide area and may be indicating the existence of higher temperature hotspots in the region. In addition, helium isotope data collected from some of the same thermal springs and wells (Dobson et al., 2015) indicate the presence of mantle helium that may be related to recent basaltic intrusions that may be providing the heat driving the geothermal activity in the area.
2. Both RTEst and the sulfate-water isotope geothermometer indicate temperatures into the 200°C range at several thermal features in the Camas Prairie. Further, shifts in the isotopic compositions of the thermal waters indicating high-temperature water-rock interaction or mixing with magmatically-derived fluids may be occurring at depth and isotopic signatures of hydrothermal methane also point to significant geothermal resources in the area. Finally, several of these features also had elevated ³He/⁴He values indicating the potential presence of a mantle-derived heat source.

ACKNOWLEDGMENTS

This work was conducted with funding from the Assistant Secretary for Energy Efficiency and Renewable Energy, Geothermal Technologies Program, of the U.S. Department under the U.S. Department of Energy Contract Nos. DE-AC02-05CH11231 with Lawrence Berkeley National Laboratory and DE-AC07-05ID14517 with Idaho National Laboratory.

Table 1. Sample data

Location	CAES sample ID	Collection date	Sample Type	Latitude (N)	Longitude (W)	Elevation (m)	Feature type	T (°C)	$\delta^{18}\text{O H}_2\text{O}$	$\delta\text{D H}_2\text{O}$
Lidy Hot Springs	002	3/11/14	Water	44.1456	112.5549	1630	outflow	56	-18.2	-140
Green Canyon H.S.	004	3/11/14	Water	43.7918	111.4395	1794	outflow	44	-18.8	-140
Sturm Well	005	3/11/14	Water	44.0932	111.4351	1617	well	31	-18.6	-140
Condie H.S.	006	3/12/14	Water	43.3329	113.9173	1462	hot spring	51	-18.6	-150
Condie H.S.	006	3/12/14	Gas	43.3329	113.9173	1462	hot spring	51		
Green House Well	007	3/12/14	Water	43.6024	113.2422	1621	well	36	-18.4	-144
Eckart Office Well	008	3/13/14	Water	42.6994	114.9104	1039	well	25	-18.3	-145
Campbell Well #1	009	3/13/14	Water	42.6445	114.7830	961	well	35	-17.0	-134
Campbell Well #2	010	3/13/14	Water	42.6450	114.7870	976	well	35	-17.2	-133
Miracle H.S.	011	3/13/14	Water	42.6942	114.8567	893	well	58	-18.0	-142
Driscoll H.S.	013	3/13/14	Water	42.5436	114.9489	1044	hot spring	40	-17.0	-134
CSI campus well #2	014	3/14/14	Water	42.5830	114.4748	1119	well	38	-17.3	-134
Heise Hot Springs	001	6/9/14	Water	43.6428	-111.6877	1527	hot spring		-17.6	-139
RRG1	020	6/11/14	Water	42.1021	-113.3843	1478	Well	150	-17.3	-133
RRG2	021	6/11/14	Water	42.1104	-113.3752	1479	Well	150	-17.5	-134
RRG4	023	6/11/14	Water	42.0979	-113.3854	1479	Well	150	-17.3	-134
Indian Springs	024	6/17/14	Water	42.7259	-112.8738	1374	Thermal	33	-17.2	-131
Grush Dairy	025	6/18/14	Water	42.2367	-113.3697	1418	Well	55		
Milford Sweat H.S.	029	6/23/14	Water	43.3648	113.7888	1520	hot spring	38	-18.3	-141
Magic Reservoir H.S. Outflow	030	6/23/14	Water	43.3278	114.4003	1464	outflow	39	-16.0	-147
Elk Creek H.S.	032	6/23/14	Water	43.4232	114.6286	1733	hot spring	57	-17.7	-145
Barron well	033	6/24/14	Water	43.2924	114.9100	1549	well	38	-17.3	-140
Wardrop HS	034	6/24/14	Water	43.3829	114.9322	1580	hot spring	66	-18.4	-143
Wardrop HS	034	6/24/14	Gas	43.3829	114.9322	1580	hot spring	66		
Magic Reservoir H.S. Well	035	6/24/14	Water	43.3285	114.3997	1472	well	74	-16.9	-151
Magic Reservoir H.S. Well	035	6/24/14	Gas	43.3285	114.3997	1472	well	74		
Prince Albert H.S.	036	6/24/14	Water	43.1297	115.3384	1316	hot spring	58	-18.5	-143
Oakley Warm Spring Well	037	6/25/14	Water	42.1733	113.8616	1619	warm	47	-18.0	-138
Austin Well #1	038	6/25/14	Water	42.0853	113.9398	1469	well	46	-18.5	-143
Marsh Creek Well	039	6/25/14	Water	42.4766	113.5077	1373	well	60	-17.5	-135
Sliger's 1000 Springs Well	040	6/26/14	Water	42.7040	114.8570	892	well	72	-17.8	-139
Banbury Well	041	6/26/14	Water	42.6884	114.8268	894	well	59	-17.5	-137
Banbury H.S.	042	6/26/14	Gas	42.6884	114.8268	894	hot spring	59	-17.5	-137
Diamond Laundry	043	7/16/14	Water	42.9554	-115.3000	783	Well	35	-18.5	-144
Leo Ray Road	046	7/17/14	Water	42.6678	-114.8267	943	Well	36	-17.2	-133
Laib Well	050	7/17/14	Water	42.9463	-115.4942	762	Well	33	-16.5	-128
Durfee H.S.	061	7/24/14	Water	42.1001	-113.6335	1646	Thermal	45	-17.7	-134
Basin Cemetery	062	7/24/14	Water	42.2233	-113.7917	1595	Well	31	-17.1	-131
Wybenga Dairy	063	7/24/14	Water	42.4822	-113.9734	1323	Well	34	-18.0	-135
David Bosen Well	064	7/25/14	Water	42.1394	-111.9371	1444	Well	90	-15.7	-134

Table 1 (continued). Sample data

Location	$\delta^{34}\text{S}_{\text{SO}_4}$ (‰)	$\delta^{18}\text{O}_{\text{SO}_4}$	$\Delta^{18}\text{O}_{\text{SO}_4}$	T_{SO_4} (°C)	RT _{Est} T (°C)	DIC (mM)	$\delta^{13}\text{C}_{\text{DIC}}$ (‰)	Dissolved CH_4 (mM)	Gas CH_4 (ppm)	$\delta^{13}\text{C}_{\text{CH}_4}$ (‰)	$\delta\text{D}_{\text{CH}_4}$ (‰)
Lidy Hot Springs	3.8	-3.4	14.8	127	140	5.4	-1.5	2.6		-19.7	-29
Green Canyon H.S.	22.6	11.6	30.3	29	94	4.2	-2.8	0.4		-16.1	
Sturm Well					152	1.6	-11.6				
Condie H.S.	18.2	-0.9	17.6	102	91	9.9	-2.1	1.4		3.6	-9
Condie H.S.									1282	3.7	27
Green House Well	14.4	0.1	18.6	95	60	9.4	-3.5				
Eckart Office Well	5.5	-2.2	16.1	115	127	1.9	-3.1				
Campbell Well #1	6.2	-3.4	13.6	140	137	3.7	-7.5				
Campbell Well #2	6.3	-3.6	13.6	140	131	3.7	-7.2				
Miracle H.S.	6.6	-4.2	13.8	137	160	1.5	-4.6	2.2		-44.0	-195
Driscoll H.S.	5.7	-4.8	12.2	156	137	2.9	-11.2				
CSI campus well #2	6.6	-3.0	14.3	133	136	2.6	-7.2				
Heise Hot Springs	20.3	5.4	23.0	65	88	21.4	3.7				
RRG1	13.9	-9.0	8.3	214	162	1.2	-5.4	0.6		-49.1	
RRG2	13.2	1.5	19.0	92	148	0.7	-5.0	0.9		-55.5	
RRG4	14.6	-9.6	7.7	224	139	0.9	-2.6				
Indian Springs	5.2	-6.4	10.8	174	70	2.0	-4.4				
Grush Dairy					102	1.6	-2.2	1.6		-55.5	
Milford Sweat H.S.	15.8	-1.0	17.3	105	73	3.2	-1.6				
Magic Reservoir H.S. Outflow	21.6	-8.7	7.3	233	163						
Elk Creek H.S.	13.1	-3.7	14.0	136	125	1.4	-4.2	6.8		-13.8	-189
Barron well	-8.3	-15.9	1.4	419	79	2.1	-6.9	2.6		-48.9	
Wardrop HS	7.0	-4.2	14.2	133	181	1.0	-7.0	2.8		-12.8	
Wardrop HS									2016	-15.8	-173
Magic Reservoir H.S. Well	21.9	-9.8	7.1	237	151	13.1	-0.9				
Magic Reservoir H.S. Well									3160	-22.0	-203
Prince Albert H.S.	8.3	-6.1	12.4	154	193	0.9	-8.6	0.5		-23.7	
Oakley Warm Spring Well	13.4	-5.9	12.1	157	130						
Austin Well #1	14.8	0.4	18.9	92	85	1.5	-2.7	12.9		-29.8	-186
Marsh Creek Well	10.2	-4.1	13.4	142	125	1.7	-4.4	2.4		-31.5	
Sliger's 1000 Springs Well	11.6	-1.7	16.1	115	134	1.2	-4.2	2.2		-47.6	
Banbury Well	6.0	-5.6	11.9	159	159	1.9	-5.9	1.7		-51.3	
Banbury H.S.									2140	-50.5	-242
Diamond Laundry	4.7	-5.0	12.5	152	159					-54.9	
Leo Ray Road					70						
Laib Well		0.8	18.0	99	121					-53.1	
Durfee H.S.		-0.4	17.4	104	138						
Basin Cemetery		-1.6	15.5	121	73						
Wybenga Dairy					132						
David Bosen Well					175					-37.8	

REFERENCES

- Blackwell, D.D., M.C. Richards, Z.S. Frone, J.F. Batir, M.A. Williams, A.A. Ruzo, R.K. Dingwall (2011), SMU Geothermal Laboratory Heat Flow Map of the Conterminous United States, 2011: Available at <http://www.smu.edu/geothermal>.
- Cladouhos, T.T., Petty, S., Swyer, M.W., Uddenberg, M.E., Grasso, K., and Nordin, Y.: Results from Newberry Volcano EGS Demonstration, 2010–2014. *Geothermics* (2015), <http://dx.doi.org/10.1016/j.geothermics.2015.08.009>.
- Dobson, P.F., B.M. Kennedy, M.E. Conrad, T. McLing, E. Mattson, T. Wood, C. Cannon, R. Spackman, M. van Soest and M. Robertson (2015) He Isotopic Evidence for Undiscovered Geothermal Systems in the Snake River Plain, *Proceedings*, Fortieth Workshop on Geothermal Reservoir Engineering, Stanford University, Stanford, California, January 26-28, 2015.
- Freeman, T.G. (2013) Evaluation of the geothermal potential of the Snake River Plain, Idaho, based on three exploration holes. MS thesis, Utah State University, 90 p.
- Fowler, A.P.G., L.B. Hackett, C.W. Klein (2013) Reformulation and performance evaluation of the sulfate-water oxygen isotope geothermometer: *CRC Transactions* **37**, 393-401.
- Giggenbach, W.F. (1992) Isotopic shifts in waters from geothermal and volcanic systems along convergent plate boundaries and their origins. *Earth and Planetary Science Letters* **113**, 495-510.
- Hughes, S.S., Smith, R.P., Hackett, W.R., and Anderson, S. R.: Mafic volcanism and environmental geology of the eastern Snake River Plain. *Idaho Guidebook to the Geology of Eastern Idaho*. Idaho Museum of Natural History, (1999), 143-168.
- Mariner, R.H., Young, H.W., Bullen, T.D., and Janik, C.J.: Sulfate-water isotope geothermometry and lead isotope data for the regional geothermal system in the Twin Falls area, south-central Idaho. *Geothermal Resources Council Transactions* **21**, (1997), 197-201.
- McLing, T.L., Smith, R.W., and Johnson, T.M.: Chemical characteristics of thermal water beneath the eastern Snake River Plain. In: *Geology, Hydrogeology, and Environmental Remediation: Idaho National Engineering and Environmental Laboratory, Eastern Snake River Plain, Idaho*, P.K. Link and L.L. Mink, eds. *Geological Society of America Special Paper* **353**, (2002), 205-211.
- McKenzie, W.F., and Truesdell, A.H.: Geothermal reservoir temperatures estimated from the oxygen isotope compositions of dissolved sulfate and water from hot springs and shallow drillholes. *Geothermics* **5**, 51-61.
- Neupane, G., Mattson, E.D., Cannon, J.C., Atkinson, T.A., McLing, T.L., Wood, T.R., Dobson, P.F., and Conrad, M.E.: Potential hydrothermal resource areas and their reservoir temperatures in the Eastern Snake River Plain, Idaho. *Proceedings*, 41st Workshop on Geothermal Reservoir Engineering, Stanford University, Stanford, California, February 22-24, 2016 SGP-TR-209 (2016).
- Nielson, D.L., and Shervais, J.W. (2014) Conceptual model for Snake River Plain geothermal systems, *Proceedings*, 39th Workshop on Geothermal Reservoir Engineering, Stanford University, Stanford, CA, SGP-TR-202.
- Palmer, C.D., Ohly, S.R., Smith, R.W., Neupane, G., McLing, T., Mattson, E.: Mineral selection for multicomponent equilibrium geothermometry. *GRC Transactions*, **38**, (2014), 453-459.
- Pierce, K. L., and Morgan, L. A.: The track of the Yellowstone hot spot: Volcanism, faulting, and uplift. *Geological Society of America Memoirs*, **179**, (192), 1-54.
- Shervais, J.W., Glen, J.M., Liberty, L.M., Dobson, P., Gasperikova, E., Sonnenthal, E., Visser, C., Nielson, D., Garg, S., Evans, J.P., Siler, D., DeAngelo, J., Athens, N., and Burns, E. (2015) Snake River Plain Play Fairway Analysis – Phase I report. *Geothermal Resources Council Transactions* **39**, 761-769.
- Smith, R.P.: Geologic setting of the Snake River Plain aquifer and vadose zone. *Vadose Zone Journal*, **3**, (2004), 47-58.
- Spycher, N., Peiffer, L., Saldi, G., Sonnenthal, E., Reed, M.H., and Kennedy, B.M. (2014) Integrated multicomponent solute geothermometry. *Geothermics* **51**, 113–123.
- Taylor, H.P. (1974) Application of oxygen and hydrogen isotope studies to problems of hydrothermal alteration and ore deposition. *Econ. Geol.* **69**, 843-883.
- Welhan, J.A. (2015) Thermal and trace-element anomalies in the Eastern Snake River Plain aquifer: Towards a conceptual model of the EGS resource. *GRC Transactions* **39**, 363-376.
- Welhan, J.A., R.J. Poreda, W. Rison, H. Craig (1988) Helium isotopes in geothermal and volcanic gases of the western United States: I. Regional variability and magmatic origin: *J. Volcanology Geotherm. Res.* **34**, 185–199.
- Whitehead, R.L.: Geohydrologic framework of the Snake River Plain regional aquifer system, Idaho and eastern Oregon. Regional aquifer system analysis-Snake River Plain, Idaho. *US Geological Survey Professional Paper* **1408-B**, (1992).
- Whiticar, M.J., E. Faber and M. Schoell (1986) Biogenic methane formation in marine and fresh-water environments – CO₂ reduction versus acetate fermentation isotope evidence. *Geochim. Cosmochim. Acta* **50**, 693-709.

Appendix J.

Cannon, C.J., 2015. Evidence for mixing and re-equilibration in the Twin Falls – Banbury hydrothermal system and its effects on reservoir temperature estimation. MS Thesis, University of Idaho, 184 p.

EVIDENCE FOR MIXING AND RE-EQUILIBRATION IN THE TWIN
FALLS – BANBURY HYDROTHERMAL SYSTEM AND ITS EFFECTS ON
RESERVOIR TEMPERATURE ESTIMATION

A Thesis

Presented in Partial Fulfillment of the Requirements for the

Degree of Master of Science

with a

Major in Hydrology

in the

College of Graduate Studies

University of Idaho

by

Cody J Cannon

Major Professor: Thomas R. Wood, Ph.D.

Committee Members: Ghanashyam Neupane, Ph.D., Robert W. Smith, Ph.D.

Department Administrator: Mickey E. Gunter, Ph.D.

November 2015

AUTHORIZATION TO SUBMIT THESIS

The thesis of Cody J. Cannon, submitted for the degree of Master of Science with a major in Hydrology and titled, “EVIDENCE OF MIXING AND RE-EQUILIBRATION IN THE TWIN FALLS – BANBURY HYDROTHERMAL SYSTEM AND ITS EFFECTS ON RESERVOIR TEMPERATURE ESTIMATION,” has been reviewed in final form.

Permission, as indicated by the signatures and dates given below, is now granted to submit final copies to the College of Graduate Studies for approval.

Major Professor: _____ Date: _____
Thomas R. Wood, Ph.D.

Committee Members: _____ Date: _____
Ghanashyam Neupane, Ph.D.

_____ Date: _____
Robert W. Smith, Ph.D.

Department
Administrator: _____ Date: _____
Mickey E. Gunter, Ph.D.

ACKNOWLEDGEMENTS

I am forever grateful to all the selfless people who made this study possible.

First, I must thank my major professor Dr. Tom Wood of whom I have the utmost respect and admiration. I am immeasurably indebted to him for all of his long hours spent working with me, his invaluable advice, continuous support and reassurance, and for always having his door open to my incessant questions and worries. I have learned countless lessons from him not only pertaining to scientific research but life in general. He is highly regarded as an expert hydrogeologist throughout the region, a skilled research scientist, and by those lucky enough, a good friend. He is a great man and a consummate professional.

I recognize the unyielding support of Dr. Hari Neupane without whose broad geochemical and geothermal knowledge; none of this work would be possible. He is not only a brilliant mind, but also a very caring person who sacrificed much of his valuable time. The scientific research competence of Dr. Bob Smith has proven vitally important to this study. He has a special knack for seeing beneath the surface of problems and has given me direction when I needed it the most. I am extremely grateful for the guidance provided by Travis McLing, whose expertise as a geologist in the field and in the laboratory have been a source of inspiration for me throughout this process. Dr. Earl Mattson has been a continual source of guidance and support throughout this process and was instrumental in providing focus to an otherwise broad collection of data. I also acknowledge the support and guidance of Dr. Pat Dobson and Dr. Mark Conrad of the Lawrence Berkeley National Laboratory.

Lastly, I must send out a very special thank you to Debbie Lacroix, whose analytical chemistry expertise is responsible for the original data in this study, Dr. Ross Spackman whose study area field expertise and incredible relational skills resulted in the collection of samples in this study, and to Eric Hass of the Department of Energy's Geothermal Technologies Office for funding this project.

DEDICATION

This work is dedicated to my incredible wife, Emily Cannon, for her unconditional love, unwavering support, and steadfast belief in me even through the tough times when I don't believe in myself. She is my best friend and the best friend any man could ask for. To my parents, Ellen and Gary Cannon, for believing in me from the beginning, convincing me that nothing is impossible, and teaching me that I am never alone. To my sister, Christi Cannon, for reminding me to never take myself too seriously. Lastly and chiefly, this thesis is dedicated to Jesus Christ in whose mighty company I am blessed to be counted. For making me a new man, His constant companionship, and grace through His selfless finished work, I am and will continue to be eternally grateful.

“He is a man in a way that we have forgotten men can be; truthful, blunt, emotional, nonmanipulative, sensitive, compassionate.” – Brennan Manning

ABSTRACT

The Twin Falls - Banbury area is one of many Known Geothermal Resource Areas located along the periphery of the Eastern Snake River Plain (ESRP). The ESRP is a topographical plain, which was formed by the bimodal volcanism of successive caldera formations associated with the migration of the Yellowstone Hot Spot over the last 16 Ma. Despite temperature gradients of 45-60 °C/km (double the global average) and high heat flow values (110 mW/m²), geothermal utilization within the ESRP is largely limited to direct use with no commercial geothermal development. A gradational trend between deep rhyolite derived Na-K-HCO₃ waters of the deep system and basalt hosted Ca-Mg-HCO₃ thermal water is observed in deep exploration wells. Mixing between the fluids of the deep system and cooler overlying groundwater as well as re-equilibration of thermal fluids during ascension are considered possibilities that may explain this trend and the low geothermometry temperature estimations of the area. The Twin Falls – Banbury area was chosen as the location for an in depth investigation into the possibility of geothermal mixing and re-equilibration as an explanation for the lower than expected geothermometry.

Evidence for mixing is provided by partial equilibration conditions in most thermal samples as well as a variety of linear mixing trends between both conservative chemical species (Cl, B, δD, etc.) and more reactive species (Ca, Mg, Na, and K). The reactive species show two distinct chemical trends between the two water types that may constitute evidence for different flow paths and/or re-equilibration of thermal fluids at lower temperatures. Multicomponent equilibrium geothermometry (MEG) analysis through the inverse modeling tool RTest (Palmer, 2013) provides more reliable reservoir temperature estimates for the area through the use of likely reservoir mineral assemblages and the compensation of a mixing component. Results from MEG also support the possibility of re-equilibration. The combination of MEG, high temperature water-rock interaction experiments, and local geological and hydrological data have resulted in a revised conceptual flow model of the Twin Falls – Banbury hydrothermal system.

TABLE OF CONTENTS

Authorization to Submit.....	ii
Abstract	iii
Acknowledgements	iv
Dedication	v
Table of Contents	vi
List of Figures	viii
List of Tables.....	x
 CHAPTER 1. Introduction.....	 1
 CHAPTER 2. Literature Review.....	 8
2.1 <i>Geology</i>	8
2.2 <i>Hydrology</i>	12
2.3 <i>Geochemistry</i>	13
2.4 <i>Methods</i>	15
2.4.1 <i>Solute Chemical Geothermometry</i>	15
2.4.2 <i>Silica-Enthalpy Mixing Models</i>	17
2.4.3 <i>Multicomponent Equilibrium Geothermometry</i>	18
2.4.5 <i>High Temperature Water-Rock Interaction Experiments</i>	20
 CHAPTER 3. Geochemistry of Thermal Waters in the Twin Falls – Banbury Thermal Area	 22
3.1 <i>Sample Chemistry</i>	22
3.2 <i>Principle Component and Hierarchical Cluster Analysis</i>	28
3.3 <i>Evidence for Mixing Between Thermal Water and Groundwater</i>	33
3.4 <i>Binary Diagram Mixing Trend Analysis</i>	36
3.5 <i>Aerial and Geologic Distribution of Water Types</i>	43
 CHAPTER 4. Geothermometry Estimation of Reservoir Temperatures in the Twin Falls – Banbury Thermal Area	 48
4.1 <i>Conventional Geothermometers</i>	48
4.1.1 <i>Silica Geothermometers</i>	49
4.1.2 <i>Cation Geothermometers</i>	53
4.2 <i>Silica-Enthalpy Mixing Models for the Twin Falls – Banbury Thermal Area</i>	63
4.3 <i>MEG Analysis of the Twin Falls – Banbury Thermal Area</i>	66
4.4 <i>RTEst Results for the Twin Falls – Banbury thermal Area</i>	71
 CHAPTER 5. Conceptual Models	 77
5.1 <i>No Mixing</i>	77

5.2 Simple Mixing.....	77
5.3 Reactive Mixing.....	78
5.4 Re-equilibration	79
5.5 Hydrogeology.....	83
5.5.1 Aquifer Test Analysis	87
CHAPTER 6. Water-Rock Interaction and Mixing Experiments.....	93
6.1 Rock Samples	93
6.2 Rock Sample Preparation	94
6.3 Initial Water Sample	96
6.4 Experimental Procedure: Part 1	97
6.5 Experimental Procedure: Part 2.....	100
6.6 Results	101
6.7 Discussion	106
CHAPTER 7. Summary and Conclusions	108
References	114
Appendix A. Sample Collection Procedure	125
Appendix B. Analytical Chemistry QA/QC	136
Appendix C. Charge Balance for Ca-HCO ₃ and Na-HCO ₃ waters.....	152
Appendix D. Well Logs Utilized in Geologic Cross Sections.....	154

LIST OF FIGURES

1	ESRP Reference and Sample Map	2
2	ESRP Schematic Cross Section	3
3	Twin Falls – Banbury Area Heat Flow and Sample Map	4
4	Twin Falls – Banbury Hydrothermal Area Reference Map	9
5	General Stratigraphy for the Twin Falls – Banbury Area	11
6	Principle Component Analysis Biplot Chart	31
7	Hierarchical Cluster Analysis Dendrogram for the Twin Falls – Banbury Area	32
8	Simple Water Type Dendrogram	32
9	Piper Diagram of Na-HCO ₃ and Ca-HCO ₃ Waters in the Twin Falls – Banbury Area	34
10	Giggenbach Ternary Diagram of Na-HCO ₃ and Ca-HCO ₃ Waters	36
11	Binary plot of δD vs $\delta^{18}O$ Showing Shift from Local MWL	37
12	Conservative Component (Cl ⁻ , B, $\delta^{18}O$, and δD) Binary Diagrams	38
13	Bicarbonate Alkalinity Binary Diagrams	39
14	Simple Gradational Trend Binary Diagrams of Reactive Components	41
15	Binary Diagrams Showing Complex Relationships of Na ⁺ vs Ca ²⁺ , Mg ²⁺ , and K ⁺	42
16	Map Showing Trend from Ca-HCO ₃ to Na-HCO ₃ Waters Away from Recharge	45
17	Water Type Distribution Map of the Banbury Thermal Area Along a Normal Fault	46
18	Water Type Distribution Map of the Twin Falls Thermal Area	47
19	Silica Solubility vs Temperature	52
20	Silica-Enthalpy Mixing Model (Quartz) Applied to the Twin Falls-Banbury Area	66
21	Silica-Enthalpy Mixing Model (Chalcedony) Applied to the Twin Falls-Banbury Area	67
22	Application of RTest to Banbury Hot Springs	69
23	Reconstructed (Optimized) Ca-HCO ₃ Thermal Water Binary Diagrams	74
24	Conceptual Model for the Twin Falls – Banbury Hydrothermal Area	82
25	Map Conceptual Model Cross Sectional Line	83
26	Geologic Cross Section of the Banbury Hot Springs Cluster Area	84
27	Map of the Cross Sectional Line Through the Banbury Hot Springs Area	85
28	Geologic Cross Section of the Twin Falls Thermal Cluster Area	86
29	Map of the Cross Sectional Line Through the Twin Falls Thermal Area	87
30	Aquifer Pumping Tests for the CSI 1 and 2 Thermal Wells	89
31	Plot of Temperature vs Drawdown for the CSI 1 and 2 Thermal Wells	90
32	Cooper-Jacob Solution for the CSI 1 Pump and Recovery Tests	93
33	Experimental Rock and Water Sample Location Maps	96
34	Rock Sample Preparation for Water-Rock Interaction Experiments	97
35	Reactor Cell Configuration for Water-Rock Interaction Experiments	99
36	Diagram of Water to Rock and Thermal Water to Groundwater Experimental Ratios	102
37	Experimental Results Showing Calcium Concentrations from Initial Mixing	104
38	Experimental Results Showing Magnesium Concentrations from Initial Mixing	104

39 Experimental Results Showing Silica Concentrations from Initial Mixing.....	105
40 Experimental Results Showing Sodium Concentrations from Initial Mixing	105
A1 Images Showing Sample Collection Procedure	127
A2 YSI ® Professional Plus Calibration Procedure	135
C1 CSI Well 1 Driller’s Log	154
C2 CSI Well 2 Driller’s Log	157
C3 Banbury Hot Springs Well Driller’s Log	159
C4 Dick Kaster Well 1 Driller’s Log	160
C5 Dick Kaster Well 2 Driller’s Log	161
C6 Sam Collier Well Driller’s Log	163
C7 City of Twin Falls Well Driller’s Log	168
C8 Twin Falls High School Well Driller’s Log	169
C9 Mike Archibald Well Driller’s Log	170
C10 Canyon Springs Golf Course Well Driller’s Log	172
C11 Pristine Springs Well Driller’s Log	173

LIST OF TABLES

1	Original Chemical Concentrations for Twin Falls – Banbury Thermal Waters	25
2	Selected Historical Chemical Concentrations for Twin Falls – Banbury Thermal Waters ..	26
3	Principle Component Analysis Eigen Values of Major Cations	29
4	Pearson’s Correlation Coefficients for PCA Variables	30
5	Silica Geothermometer Temperature Estimations for Na-HCO ₃ Waters	60
6	Silica Geothermometer Temperature Estimations for Ca-HCO ₃ Waters	61
7	Cation Geothermometer Temperature Estimations for Na-HCO ₃ Waters	62
8	Cation Geothermometer Temperature Estimations for Ca-HCO ₃ Waters	63
9	Alteration Mineral Assemblages and Weighting Factors Used in RTest Modeling	71
10	RTest Temperature Estimates of Na-HCO ₃ Waters Using Pure Water and Ca-HCO ₃ Waters Using Local Groundwater	77
11	Water-Rock Interaction Experimental Matrix	101
12	Initial and Post Mixing Experimental Concentrations	103
A1	Field Parameters for Data Collected in the ESRP in 2014	129
B1	Anion QC Table	143
B2	Cation QC Table	145
B3	Trace Element QC Table	146
B4	Chemical Concentrations for ESRP 2014 Hydrothermal Samples	150
C1	Charge Balances for Na-HCO ₃ Thermal Waters	152
C2	Charge Balances for Ca-HCO ₃ Thermal Waters	153

CHAPTER 1: INTRODUCTION

The Twin Falls – Banbury hydrothermal area is one of many Known Geothermal Resource Areas (KGRA) located along the periphery of the Eastern Snake River Plain (ESRP). The ESRP is considered to be one of the most favorable areas for geothermal development within the state of Idaho (Tester et al., 2006) which the USGS estimates is home to over 4,900 MWe of undiscovered geothermal resources with a mean power production potential of 30 GWe (Williams, 2008). Regional subsurface temperature gradients of 45-60 °C/km (double the global average) have been calculated throughout the region and heat flow values of over 150 mW/m² have been projected for depths to 6 km (Brott et al., 1976; Blackwell and Richards, 2004). Despite the high observed potential, utilization of geothermal fluids has been limited to direct use applications (direct use heating, greenhouses, fisheries, etc.) for over a century with no commercial geothermal development within or along the plain proper. This is likely due to the masking of the deep geothermal signature by the Eastern Snake River Plain Aquifer (ESRPA), a prolific basalt hosted aquifer system that overlies the rhyolites, which are thought to host thermal reservoirs throughout the region.

The ESRP is a topographical lowland which was formed by the middle Miocene to recent bimodal volcanism by a succession of caldera formations associated with the migration of the North American Plate over the Yellowstone Hot Spot (Hughes et. al., 2002; Rodgers et. al., 2002; Pierce and Morgan, 2009). Caldera formation resulted in a series of younger to the east rhyolite units (Morgan et al., 1984; Leeman et al., 2008) that are overlain by extensive younger basalt flows of Tertiary to Holocene age. The basalt sequence forms the ESRPA which carries cold water from the Yellowstone Plateau down gradient to the Thousand Springs area in Twin Falls, ID. Because of the thick overlying cold water aquifer, most of the

thermal springs and wells throughout the area are observed along the margins of the ESRP. It is thought that deep thermal water is able to make its way to the surface through a variety of structurally and geologically controlled conduits.



Figure 1. Map of the ESRP showing location relative to the United States (inset) and the approximate locations of caldera centers. Red points represent thermal samples collected in the 2014.

Many compositions for thermal fluids of the ESRP have been recorded (e.g., Ross, 1971; Young and Mitchell, 1973; Ralston et. al., 1981; Lewis and Young, 1982; Wood and Low, 1988; Parlman and Young, 1992; Mariner et al., 1991, 1997; McLing et al., 2002). However, most of the previous studies do not attempt to account for mixing with a cooler groundwater component though some acknowledge it. A gradational trend between Na-K-HCO₃ type waters associated with deep rhyolites and shallower Ca-Mg-HCO₃ thermal waters

has been observed in deep wells that penetrate the upper aquifer system (McLing et al., 2002; Mann, 1986). Many have explained this trend through mixing between thermal waters and groundwater where mixed waters exhibit a composition between the two end member waters (McLing et al., 2002; Neupane et al., 2014; Cannon et al., 2014).

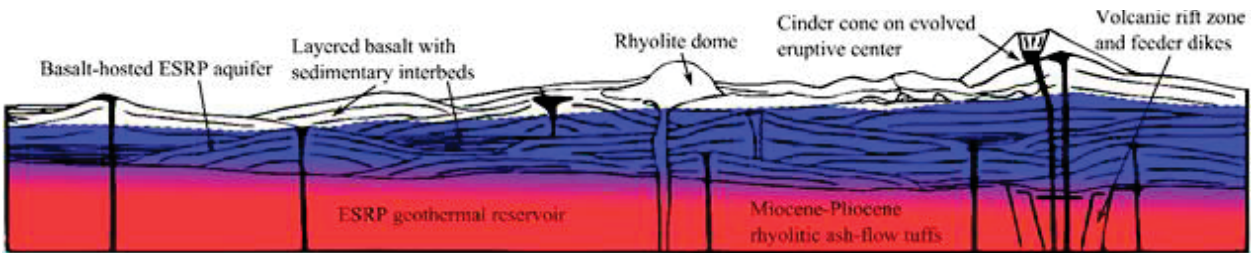


Figure 2. Schematic cross-section across the ESRP (Neupane et. al., 2014) showing underlying rhyolitic ash-flow tuffs and overlying basalt flows with few sedimentary layers. The rhyolite ash-flow tuffs underlying the basalt aquifer system are assumed to be the ESRP geothermal reservoir.

Although there are many historical thermal fluid compositions for the ESRP, many of them are incomplete in that they lack important trace elements. This study is part of a larger Department of Energy Geothermal Technologies Office funded project to provide more accurate reservoir temperature estimations throughout the ESRP by using a modern technique called multicomponent equilibrium geothermometry (MEG). MEG utilizes trace elements (particularly aluminum) to estimate temperature using the saturation states of hydrothermal alteration minerals, many of which are aluminosilicates. MEG is also capable of accounting for mixing between thermal fluids and groundwater through inverse modeling. To this end, a collaboration between the University of Idaho, the Lawrence Berkeley National Laboratory, and the Idaho National Laboratory collected samples in 2014 in order to provide more reliable temperature estimates that are corrected for the effects of mixing.

The Twin Falls – Banbury area (Figure 3) was chosen as the location for an in depth investigation into the possibility of geothermal mixing and re-equilibration as an explanation

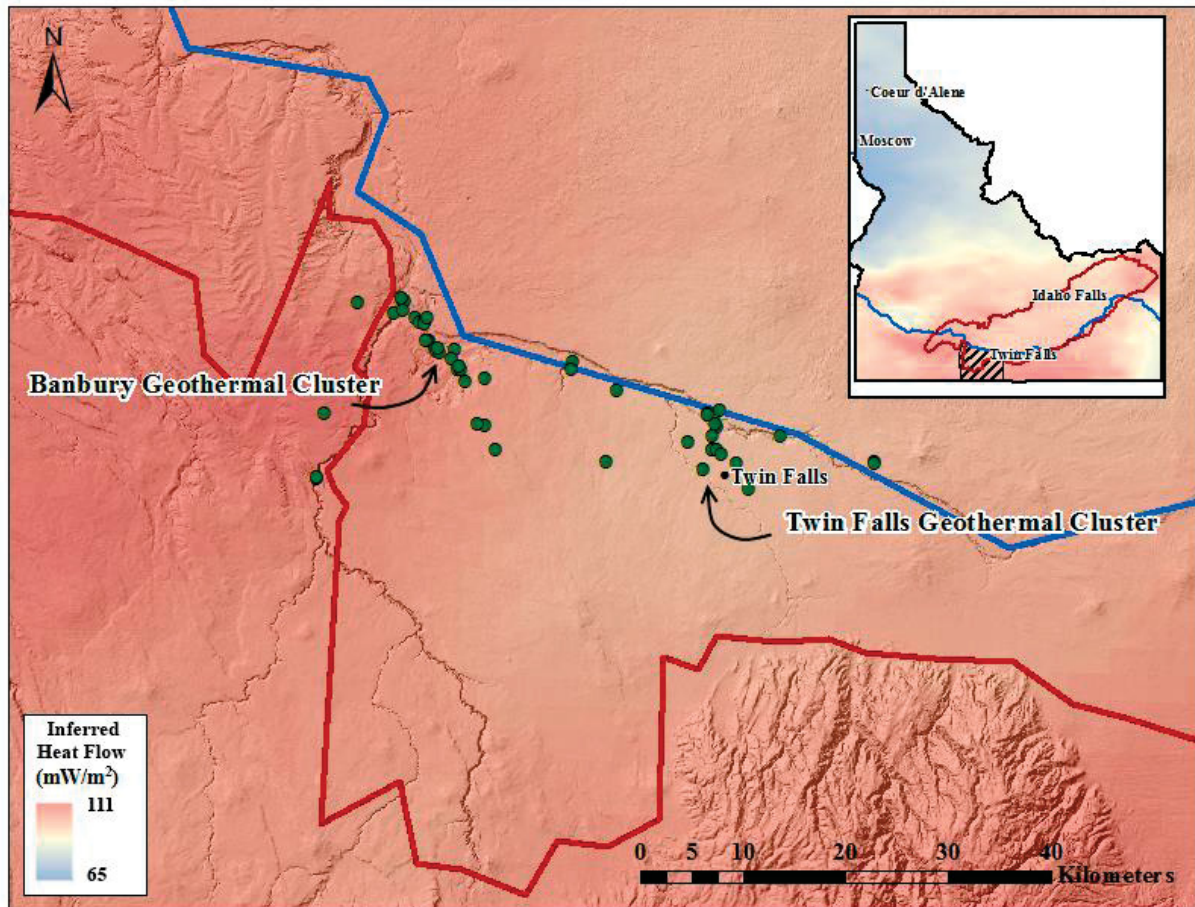


Figure 3. Study area map superimposed on the USGS heat flow map (Williams and Deangelo, 2011). Map depicts the Twin Falls – Banbury hydrothermal area relative to the ESRP margin (red line). Green points correspond to thermal waters utilized in this study.

for the lower than expected reservoir temperature estimations of the area. The area was chosen due to the high sample density obtained in the 2014 sampling campaign as well as the amount of historical data available for the area. The area is comprised of two dense clusters of geothermal surface manifestations along the trend of the Snake River near the southwestern end of the ESRP. This study attempts to combine various geochemical techniques with local hydrology and geology to provide evidence for mixing, estimate reservoir temperature while accounting for mixing, consider the possibility of re-equilibration, and refine the conceptual model for the Twin Falls – Banbury hydrothermal system. However, before investigating the

Twin falls – Banbury area in detail, it is important to identify exactly what is meant by “mixing” and the different scenarios by which mixing can occur.

Mixing Scenarios Defined

The chemical signature of geothermal water is often impacted or altered by mixing with shallower waters, thereby masking the actual reservoir temperatures calculated using geothermometry. This study examines the effects of mixing on calculated temperatures via an in-depth investigation on a relatively well known geothermal area, the Twin Falls – Banbury thermal system in south-central Idaho. Dilution corrections will be made using established mixing models and the multicomponent equilibrium geothermometry (MEG) tool RTest (Reservoir Temperature Estimator) (Palmer et al., 2013). The effect of chemical re-equilibration with rocks outside the geothermal reservoir at sub-reservoir temperatures is also considered. Mixing and re-equilibration is a practical problem facing geothermal explorationists in many areas, e.g. ESRP and similar thermal regimes. For the purposes of this work, three mixing scenarios are defined:

- 1) “simple mixing” or non-reactive mixing;
- 2) flow pathway mixing (both reactive and non-reactive)
- 3) re-equilibration.

Simple mixing involves the ascension of thermal water from depth through a conduit like a fault or fracture. The thermal water component is uninterrupted during ascension, cooling only through conduction and/or advection. Upon discharging at the surface, the thermal water is quickly mixed with surface water such as precipitation, a stream, or spring. In this case the thermal water is undiluted (no mixing prior to discharge) until it is mixed with

surface water. Most mixing models are setup to directly address this type of dilution (Fournier, 1977; Arnórsson, 1983; 1985). Solute-enthalpy mixing models developed in the 1970s and 80s can be utilized to adjust for simple mixing and refine the calculated reservoir temperatures. MEG methods including RTest can remove the influence of the cold water component based on the convergence of multiple mineral saturation indices.

The second scenario, flow path mixing, involves mixing of thermal water as it makes its way from depth to the surface. In the case of the ESRP, thermal water ascending through a fracture may be mixed with cooler groundwater as the conduit is intersected by permeable cold water zones prior to discharging at the surface or through a well. This scenario may constitute a combination of both simple and reactive mixing depending on sufficient residence times that allow for reactions to occur between the two waters and/or surrounding rock. Reactive mixing is made evident through the alteration of ratios of some chemical constituents while other more conservative species (i.e. Cl^- , B) will mix non-reactively as their ratios remain constant through dilution.

The third scenario involves the re-equilibration of thermal water or mixed thermal water with a new reservoir rock. The geochemical signature of re-equilibrated waters does not reflect the temperature of the deep thermal reservoir but only the temperature at which the waters last attained equilibrium. Because re-equilibration violates a key assumption in all geothermometry techniques (Huenges and Ledru, 2011), it has largely been ignored in geothermal investigations. Many researchers have warned about re-equilibration when discussing the applicability of their techniques (Fournier, 1977; Arnórsson, 1985; Reed and Spycher, 1984; Giggenbach, 1988; Neupane, 2015) but few have attempted to quantify or account for its effects. Unlike the previous two scenarios, re-equilibration presents a

significant problem that can't be solved by MEG nor can it be accounted for with conventional geothermometry and mixing model techniques. To better understand if re-equilibration is at play in this area, water-rock interaction and mixing experiments based on the Twin Falls – Banbury geothermal system are performed in this study.

CHAPTER 2: LITERATURE REVIEW OF THE TWIN FALLS – BANBURY HYDROTHERMAL SYSTEM

The hydrothermal system in Twin Falls, Idaho is the most utilized and perhaps the most prolific geothermal prospect throughout southern Idaho. Substantial use of the system began in the 1970s with the utilization of thermal water for fish propagation, irrigation, heating, and resorts (Street and Detar, 1987). All of these applications are still in operation today. One of the most promising areas for further development is located near Hagerman, Idaho where the Thousand Springs Resort produces 72 °C geothermal water from a 750 foot well. Electrical production and further geothermal investigations have been considered but limited due to concerns over observed declining thermal water levels although temperature declines are not evident (Fleischmann, 2006). Reservoir temperature estimations made by earlier researchers utilizing geothermometry techniques produced results that are insufficient for power production. However, preliminary results of this study show that mixing between groundwater and thermal water may have masked the true higher temperature signature of this area. The following section provides a review of the relevant literature pertaining to the Twin Falls – Banbury hydrothermal area.

2.1 Geology

Mabey (1982) stated that the Snake River Plain was one of the least understood geologic provinces in the United States. While it has been described as a graben and various rift structures, it is described by most as a regional down warping associated with the bimodal volcanism due to the successive caldera formations of the Yellowstone Hotspot beginning approximately 16 Ma (Hughes et. al., 1999; Rodgers et. al., 2002; Pierce and Morgan, 2002).

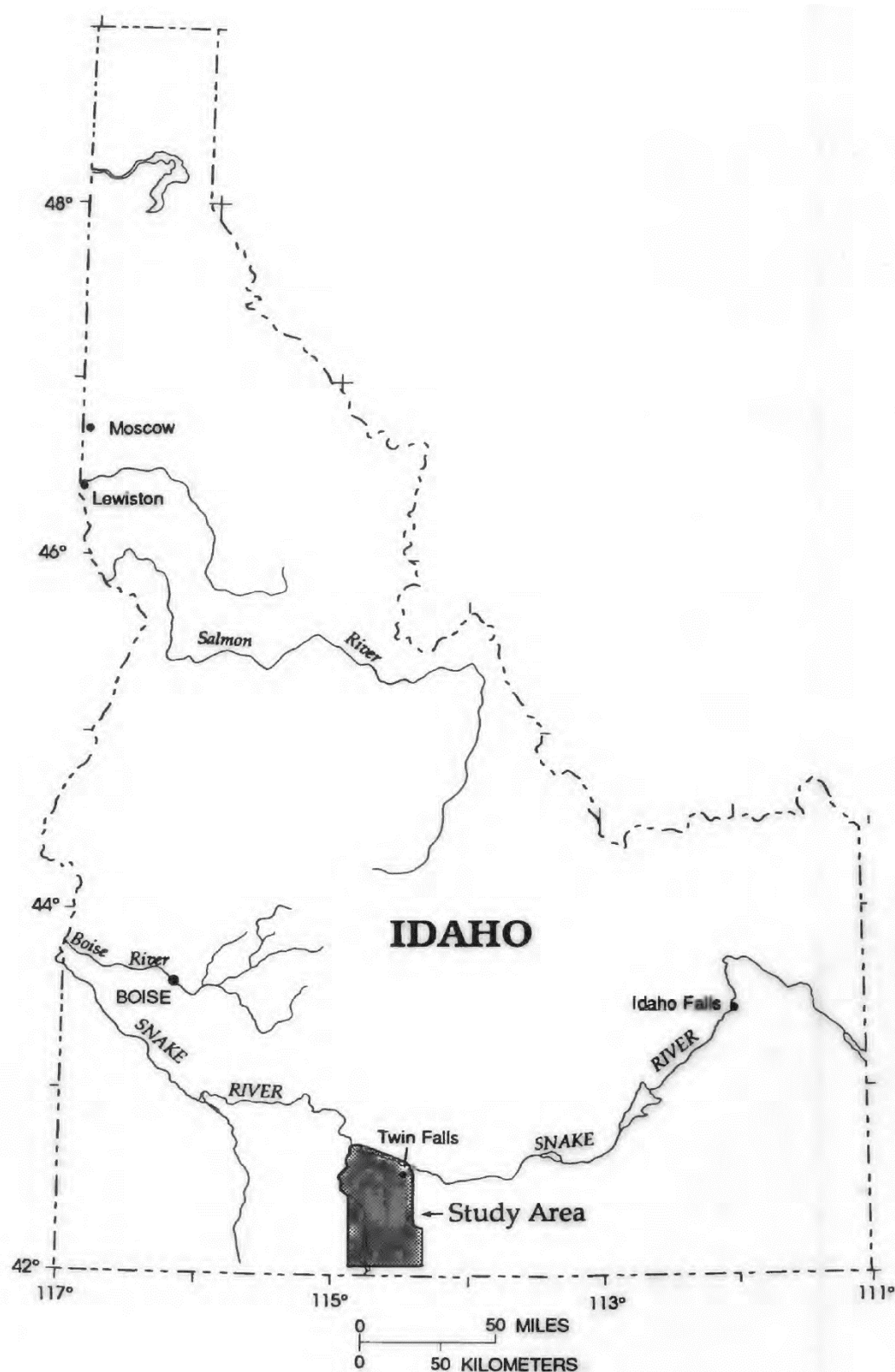


Figure 4. Map of the Twin Falls – Banbury hydrothermal study area, Lewis and Young (1982)

The Twin Falls and Banbury hydrothermal areas show characteristics of both the ESRP and basin and range regional extension. Tertiary rhyolitic volcanic rocks underlie younger quaternary and tertiary basaltic units throughout the study area. The rhyolitic units of the Idavada volcanics dip northward from the Cassia Mountains in the southern portion of the study area disappearing beneath the basaltic units of the ESRP with no clear evidence of down faulting supporting the conceptual model of ESRP regional down warping (Street and Detar, 1987). However, normal faults associated with Basin and Range extension are present in the northwestern portion of the study area. Many of these faults do not cut across basalts and are constrained to the Idavada volcanics trending north to northwest along the Salmon Falls Creek. These structures mark the beginning of the Western Snake River Plain and continue across the Bruneau Desert to the west (Kuntz, 1977).

Miocene Banbury basalts are the most predominant basalt units in the study area and may be up to 305 meters (1,000 ft.) thick (Lewis and Young, 1989). Along with overlying and interbedded Pleistocene lacustrine sediments of the Glenn's Ferry Formation (Malde and Powers, 1972), these basalts make up a locally significant shallow groundwater system. However, the most ubiquitous unit in the study area are the Tertiary volcanics of the Idavada formation which are predominantly comprised of welded rhyolitic ash flow tuff units with secondary rhyolite lava flows, andesites, and intercalated lacustrine sediments (Rember and Bennett, 1979). The Idavada volcanics are likely representative of many undifferentiated volcanic episodes from 12 to 6 Ma (Street and Detar, 1987). Electrical resistivity data shows that the Idavada volcanics are continuous over most of the area ranging in thickness from 700 to 3,000 ft. (2,000 ft average) (Lewis and Young, 1989). Lithologic logs from the recently drilled deep exploration well of Project Hotspot in nearby Kimberly, ID shows the Idavada

volcanics are at least 3,800 ft. thick and reach depths up to 6,423 ft. (Shervais et al., 2013).

General stratigraphy of the study area is depicted in Figure 5 below showing Tertiary rhyolites

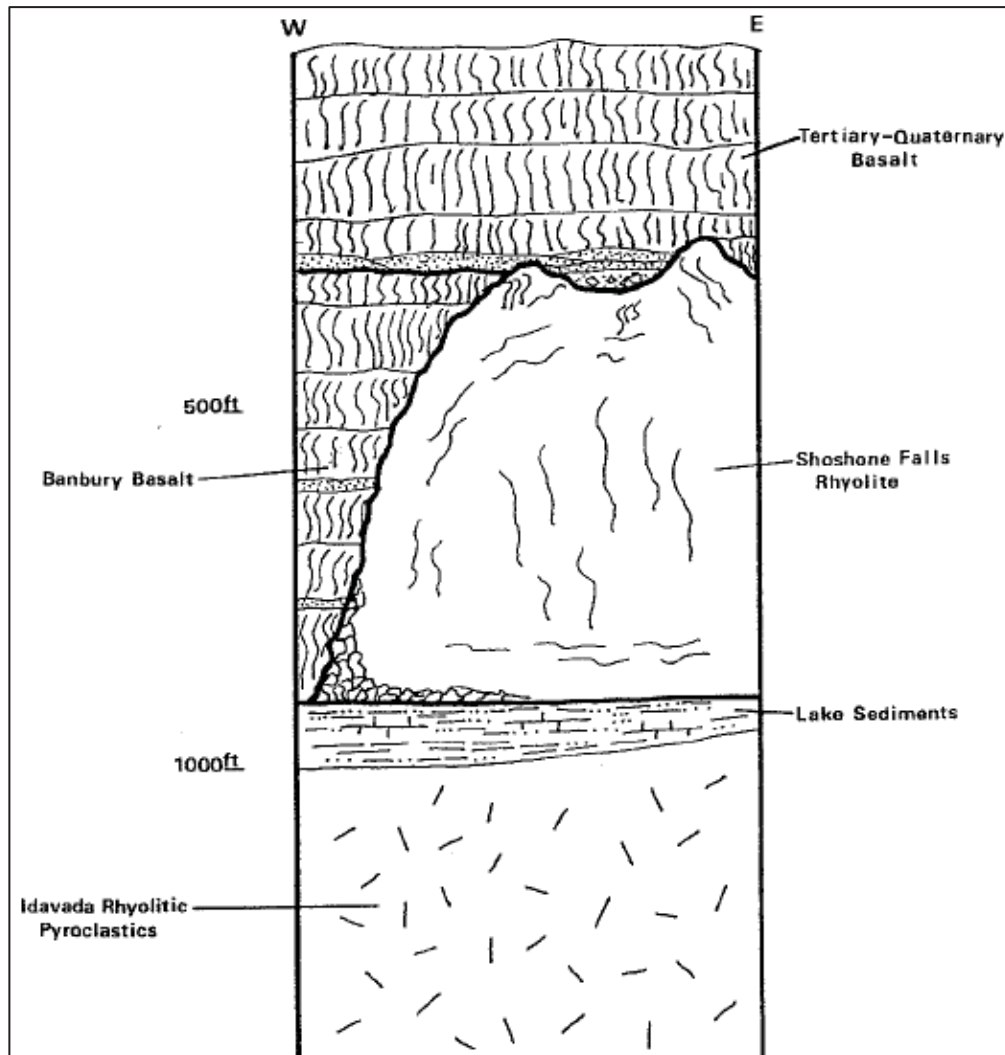


Figure 5. General stratigraphy of the Twin Falls – Banbury area (Street and DeTar, 1987).

underlying the entire study area, lacustrine sediments, Tertiary Banbury basalts, a distinct single andesitic flow layer of the Idavada called the Shoshone Falls rhyolite, and finally overlying Tertiary and Quaternary basalts.

Although none of the well logs within the study area penetrate the extent of the Idavada volcanics, Paleozoic marine sediments are thought to underlie the entire area (Lewis and Young, 1989). Pennsylvanian age carbonates outcrop just to the southeast of the town of Buhl, ID and make up the core of the Cassia Mountains near the Idaho-Nevada border to the south. The extent of the Paleozoic carbonates beneath the Idavada volcanics is unknown but over 5,000 feet of carbonates have been reported in the mountains of northern Nevada (Schroeder, 1912).

2.2 Hydrology

The Twin Falls area hydrology is separated into two separate and distinct aquifer systems. There exists a shallow, cold water aquifer system in which flow paths between areas of recharge and discharge are relatively short. This system contains aquifer sub units within Banbury Basalts and thin sedimentary interbeds. Groundwater flow direction is generally northward or northwestward (in southeastern portions of the area near the city of Twin Falls) toward the Snake River. The majority of recharge to this system comes from the south and southeast in the low hills where annual precipitation reaches 45 inches. Hydraulic heads are below land surface. The aquifer is considered to be unconfined but may be confined in some areas. Water from this shallow system is typically around 20 °C while some shallow groundwater reaches elevated temperatures due to the mixing of cooler water with thermal water (Lewis and Young, 1989).

The thermal aquifer system (20 °C to 72 °C) is located beneath basalt units within the Idavada volcanics and is under artesian conditions with temperatures of the waters increasing to the northwest. Lewis and Young (1982) produced a generalized potentiometric surface map showing an overall north and northwestern gradient in the aquifer. Permeability within the

reservoir rock itself is associated with fractures developing from tectonic movement, joints and fractures resulting from cooling during emplacement, intergranular porosity of the non-welded ash flow tuffs, and contacts between flow boundaries. Street and Detar (1987) described the results of a pumping test during the development of two deep thermal heating wells (450 and 675 meters) completed in the Idavada volcanics at the College of Southern Idaho in Twin Falls. Transmissivity ($554\text{--}923 \text{ m}^2/\text{d}$ ($44,600\text{--}74,300 \text{ gpd/ft}$)) and storativity ($5.8\text{E-}4$ to $6.2\text{E-}4$) values were measured for the Idavada rhyolites. It was concluded that no hydrologic boundaries exist between the Twin Falls and Banbury area systems.

Thermal waters are thought to originate from deep circulation paths from the Cassia Mountain recharge zone to the south and through fractures in the overlying basalts of the thermal area. The waters are subsequently heated by either a regionally high gradient (Lewis and Young, 1989) or the young basaltic sill complexes associated with ESRP volcanism (McLing et al., 2014, Dobson et al., 2015).

2.3 Geochemistry

Lewis and Young (1982) characterized the highest temperature thermal waters of this area as sodium-bicarbonate type and stated that they are slightly alkaline. In 1989, they showed that water chemistry of the thermal waters indicates mixing with a shallow cold water component through relationships of stable isotopes, chloride, and enthalpy. They highlighted a mixing trend from cooler Ca-HCO_3 to Na-HCO_3 using a Piper trilinear diagram but made no effort to address the effects of dilution on geothermometry calculations. Traditional geothermometry calculations were performed using the Na-K-Ca geothermometer and silica geothermometers (chalcedony and quartz). Mg corrections to the Na-K-Ca geothermometer were not made as the corrections were deemed insignificant for waters with around 1 ppm Mg

concentration despite a concentration of 0.2 ppm Mg being widely regarded as the boundary for correction (Fournier and Potter, 1979).

The 19 samples taken in the Lewis and Young (1982) study were near saturation with calcite thus giving skeptical temperature estimations for the Na-K-Ca geothermometer. A simple mixing analysis was done by plotting the Na-K-Ca temperature predictions versus the silica geothermometer predictions. Waters that plotted on or near the equal temperature line for these two geothermometers were considered to be representative of reservoir water (not mixed). These waters include several of the highest temperature waters including the 72 °C water of the 1000 Springs Resort. The authors drew the conclusion that 70 – 100 °C was the likely reservoir temperature from these conventional geothermometry methods. Young and Mitchell (1973) came up with a similar but slightly higher estimate of 85-135 °C.

In 1997, Mariner et al., conducted a study in Twin Falls and Jerome Counties using sulfate-water isotope geothermometry. They estimated a reservoir temperature of 90-106 °C. However, recent sulfate-water isotope geothermometry results show temperature estimates of 159 °C for this area (Conrad et al., 2015). Lead isotopic values from this study showed that thermal waters in the area have a signature reflective of Paleozoic carbonates. This suggests that despite the overprinting of a rhyolitic signature (high silica and high fluoride), thermal waters may be originating even deeper in the system within Paleozoic carbonates.

^{14}C isotopes were used to date the waters of the Twin Falls geothermal system. Age estimations for Twin Falls area thermal are around 4,000 to 10,000 years old (Mariner et al., 1991). Lewis and Young (1982) attributed low deuterium values in the waters to a historically cooler climate making the waters at least 8,000 years old and possibly up to 15,000 years old. Discharge measurements for wells in the area in early 1979 indicated a thermal water

discharge of 10,300 acre-ft annually (Lewis and Young, 1982). However, there have been significant declines to the utilization of this system for heating, low-head hydro power production, and fish propagation (Street and Detar, 1987). Fleischmann (2006) listed this area in his *Geothermal Development Needs in Idaho* stating that more exploration is warranted due to the masking of the high temperature resource by the overlying cold water system. The report states that more exploration is needed to determine the source of heat and a resource may be confirmed with deep drilling.

2.4 Methods

With advancements in geothermal science, there exists more substantial evidence for mixing in this region. Recent geothermometry studies have shown that the Twin Falls – Banbury hydrothermal system may represent a higher temperature resource than what was previously estimated (Cannon et al., 2014; Conrad et al., 2015). The following sections describe the geochemical methods utilized in this study.

2.4.1 Solute Chemical Geothermometry

Geothermal fluids have widely varied chemistries, reflecting the geologic setting and the host rock from which they emanate. Geothermometers are experimentally and empirically based equations that take advantage of specific high temperature mineral-solute reactions that are slow to equilibrate at lower temperature. These equations give geoscientists insight into the reservoir temperature achieved by the thermal water at depth prior to ascent to the surface. Several assumptions are made in order for geothermometers to be useful. The first assumption is that equilibrium between host rock and water is obtained at depth. This assumption has been proven valid through research on several commercial geothermal power plants. The second major assumption is that the thermal fluid composition is not altered by secondary

processes (boiling, mixing, reactive processes, etc.) during its ascent to the surface. This assumption is made but is often invalid and corrections need to be made to the predicted temperatures.

Utilization of geothermometers began in the late 1970s with the development of the silica geothermometers, which are perhaps the most widely used geothermometers. The quartz and amorphous silica geothermometers were first developed by Fournier (1977) and are based on the experimentally determined prograde relationship between silica concentration and increasing temperature. Different polymorphs of silica dominate at different temperatures and thus not all silica geothermometers are appropriate at all temperatures. This led to the development of the chalcedony geothermometer by Arnorsson et al. (1983). However, not all thermal fluids are hosted within silicic reservoirs leading to the development of cation geothermometers.

Cation geothermometers are based on temperature-dependent cation exchange reactions. For example, the Na-K geothermometer (Fournier, 1979; Giggenbach et al. 1988) uses the ratio of sodium to potassium based on the reaction between albite ($\text{NaAlSi}_3\text{O}_8 + \text{K}^+$) and the K-feldspar adularia ($\text{KAlSi}_3\text{O}_8 + \text{Na}^+$). The Na-K-Ca geothermometer (Fournier and Truesdell, 1973) was developed to deal with waters having high concentrations of calcium making the Na-K geothermometer unsuitable. However, high concentrations of Mg (>0.2 ppm) yield anomalously high results for the Na-K-Ca geothermometer. As a result the Mg correction for the Na-K-Ca geothermometer was developed to account for the higher Mg concentrations at temperatures less than 180°C and where Mg is present in clays and carbonates. This correction was intended for unmixed waters although high magnesium concentrations are often an indication of mixing with a cooler groundwater component. Other

cation geothermometers include the Na-Li geothermometer (Fouillac et al., 1981), which uses the ratio of sodium to lithium and is based on cation exchange reactions that take place with clays and zeolites and the K-Mg geothermometer (Giggenbach et al. 1988) which is useful when sodium and calcium have not equilibrated between fluid and rock.

2.4.2 Silica-Enthalpy Mixing Models

While the Quartz geothermometer is capable of correcting for steam loss due to boiling, none of the conventional geothermometers mentioned previously are capable of accounting for mixing. As a result, models were developed to better account for mixing. The silica-enthalpy mixing model used in this study is based on the positive relationship between silica solubility and increasing temperatures. However, in this model, respective enthalpies of sample waters calculated from field temperatures are used as plot coordinates rather than temperature because enthalpy is conserved as waters mix and boil whereas temperature is not (Fournier, 1977). This model can be applied with two separate scenarios. A trend line is drawn from the point representing the non-thermal component of the mixed water (lowest silica and enthalpy), through the mixed water from thermal springs. The intersection of this line with a silica solubility curve approximates the enthalpy of the hot-water component at reservoir conditions if there was no boiling prior to mixing. The enthalpy at the boiling temperature (100°C) which is 419 J/g is intersected with the projected trend line. From this intersection, a horizontal line is drawn to the quartz maximum steam loss line. This new enthalpy value can be used to calculate the reservoir temperature if boiling occurred prior to mixing (Fournier, 1977).

While mixing models have aided in making better predictions in areas where rapid simple mixing occurs, they are not comprehensive enough to compensate for reactive secondary

processes that may affect waters prior to or after mixing. Finally, the prediction of a reservoir temperature based solely on two or three chemical species contains more error than is desirable. Estimations that utilize an entire reservoir mineral assemblage based on likely alteration minerals within the reservoir are considered, in theory, to provide much more accurate temperature predictions.

2.4.3 Multicomponent Equilibrium Geothermometry

Reed and Spycher developed the basic concept of multicomponent equilibrium geothermometry (MEG) in 1984. The major advantage of MEG over more conventional geothermometry techniques is the use of a reservoir mineral assemblage (RMA) that represents the full suite of minerals likely to be present in a geothermal reservoir. The approach uses the calculated ion activity products (Q) of chemical species within the RMA to determine the degree of saturation ($\log Q/K_T$) where K_T is the temperature dependent mineral-water equilibrium constant. The temperature at which all minerals have near zero saturation indices is taken to be the temperature at which thermal fluid last equilibrated.

While there is an obvious advantage to utilizing an entire RMA as opposed to a few basis chemical species, MEG also allows for adjustments to be made to account for secondary alteration processes that effect calculated temperatures; including the amount of water gained (dilution/mixing) or lost (boiling) and the effects of degassing. The loss of CO_2 has been shown to affect the pH of geothermal waters and is commonly shown by the oversaturation of calcite (Palandri and Reed, 2001).

Despite the advantages of MEG over conventional geothermometry methods, there has been little application in geothermal assessment and development. Some previous investigators (e.g., D'Amore et al., 1987; Tole et al., 1993; Hull et al., 1987) have used this technique for

predicting geothermal temperature. The first two of these authors utilized a MEG technique to predict reservoir temperatures and develop conceptual models. However, both noted the difficulty that secondary processes pose to predicting an accurate equilibrium temperature. Hull et al. (1987) made an attempt to account for the dilution of thermal water by a cooler groundwater component (similar to the ESRP conceptual model). They noted that the use of a real groundwater component from a nearby source was problematic due to the production of bulk compositions with negative molalities of Mg, Al, Fe, and Ca. The use of deionized water as a mixing agent resulted in more successful temperature predictions. Hull et al. (1987) explained this phenomena by stating that either 1) the nearby cold water component is dissimilar to the actual mixing agent or 2) the mixture of thermal water and groundwater undergoes additional reactions (precipitation, exchange, etc.) and thereby re-equilibrate at a cooler temperature or within a new host rock.

More recent efforts by some researchers (e.g., Bethke, 2008; Cooper et al., 2013; Neupane et al., 2013; Spycher et al., 2014; Neupane et al., 2014) have focused on improving temperature predictability of the MEG method. The two latest tools (computer codes) are the GeoT tool developed by Spycher et al. (2014) and the Reservoir Temperature Estimator (RTEst) tool developed by Palmer (2014). RTEst is the method used in this study. RTEst couples the React module of The Geochemist's Workbench® (GWB) (Bethke and Yeakel, 2012) and the optimization program PEST (Doherty, 2013) to optimize parameters including temperature, water, and CO₂ fugacity. RTEst works to obtain an estimated reservoir temperature by repeatedly calculating mineral saturation indices while allowing temperature, solvent mass, and CO₂ fugacity to fluctuate. The ultimate goal of this inverse modeling is to minimize the objective function Φ given here by:

$$\Phi = \sum (SI_i w_i)^2 \quad \text{where } SI = (\log Q/K_T) \text{ and } w_i = \text{weighting factor for a mineral.}$$

The minimization of the objective function represents the minimization of the collective distances away from zero for all saturation indices within the RMA. In theory, the reservoir temperature is obtained when Φ is essentially zero. The weighting factor (w_i) ensures that each mineral contained in a chosen mineral assemblage is considered equally and the results are not skewed by reaction stoichiometry (Neupane et al., 2014).

2.4.4 High Temperature Water-Rock Interaction Experiments

Geothermal alteration in aqueous solutions has been extensively studied but application in geothermal reservoir characterization and development is limited. High temperature water-rock interaction experiments can provide valuable information on alteration temperature, rock composition, and especially fluid composition (Browne, 1978; Lesher et al., 1986; Reyes, 1990; Davis et al., 2003). Research into water-rock interaction at high temperatures began in the late 1950s. Khitarov (1959) investigated the interaction of high temperature waters with particular interest in granite, feldspars, and micas. Basharina (1958) successfully extracted many water-soluble constituents from an andesitic ash and in 1963, Ellis and Mahon targeted silicic volcanic rocks in particular comparing experimentally determined fluid compositions with natural ones in New Zealand.

Data from natural geothermal systems shows that local equilibria between geothermal fluids and alteration minerals controls major component concentration (except Cl^- and other mobile elements) in fluids at temperatures as low as 50 °C (Ellis, 1970; Arnórsson et al., 1983; Stefánsson and Arnórsson, 2002). Although primary rock type is important, it is

considered to have less of an effect on geothermal alteration than permeability, temperature, and fluid composition (Henley and Ellis, 1983; Rodriguez, 2001). Browne (1978) showed that Quartz, K-feldspar, albite, chlorite, Fe-epidote, calcite, illite, and pyrite were the principal alteration minerals in many rock types including rhyolites, sandstones, basalts, and andesites. However, later studies showed that significant differences occur between alteration minerals in different rock types particularly at lower temperatures ($<150^{\circ}\text{C}$) (Bethke, 1986; Reyes, 1990; Mas et al., 2006, Weisenberger and Selbekk, 2009; Rodriguez, 2011). This study utilizes the differences in alteration minerals between silicic volcanic type rocks like the Idavada volcanics and the basalts of the ESRP in which smectite clays and zeolites are dominant (Morse and McCurry, 2002; Sant, 2012).

The aforementioned geochemical techniques are utilized in this study to better understand the role of mixing and re-equilibration within the Twin Falls – Banbury hydrothermal system and the implications such secondary processes have on geothermal temperature estimation within other areas of the ESRP.

CHAPTER 3: GEOCHEMISTRY OF THE THERMAL WATERS IN THE TWIN FALLS - BANBURY GEOTHERMAL AREA

The following section details the aqueous geochemistry for the Twin Falls – Banbury hydrothermal system as it relates to the problem of mixing between the deep thermal water and shallow groundwater components of the system. Water chemistry data from previous hydrothermal studies of both the Twin Falls and Banbury Hot Springs areas are compiled and combined here with the new data obtained from the 2014 ESRP sampling campaign in order to establish sufficient sample density to:

- 1) Classify the waters based on their respective chemistries;
- 2) Observe mixing and water-rock interaction trends with both conservative and reactive chemical species through the use of binary diagrams;
- 3) Observe the areal distribution of water types and its relation to local geology and geologic structures
- 4) Apply conventional geothermometry and mixing model techniques to all of the waters; and
- 5) Delineate appropriate mixing components for use within the multicomponent equilibrium geothermometry (MEG) tool RTest.

3.1 Sample Chemistry

Sample compilation focused predominately on hydrothermal water samples within the study area but also include cooler groundwater samples from the assumed recharge zone located in the hills to south (to the east and south of the town of Robertson, ID). Interestingly, recharge area groundwater samples (4.5 – 12 °C) and cooler thermal waters within the region (< 30 °C) contain high amounts of silica (average 61 ppm) providing particularly valuable

evidence for mixing (Arnórsson, 1985) in that high silica concentrations are likely due to mixing with a thermal component. Thermal waters range in temperature from 25 °C to 70 °C. Sample selection criteria include temperature, location, and extensiveness of chemical data (possessing data from both conservative [Cl^- , F^- , Li , B , δD] and reactive [Ca^{2+} , Mg^{2+} , K^+ , Na^+ , CO_3^{3-} , SiO_2^-] species). Samples meeting the criteria were omitted only if they share the same location as a newly collected sample or lie outside of the study area. In this case is bound to the north by the Snake River which represents a groundwater boundary from the Twin Falls – Banbury area.

Chemical data for both the Banbury and Twin Falls area were compiled from four previous studies including the two isotopic studies conducted by R.H. Mariner et al. (1991 and 1997) and the USGS geothermometry studies of the Banbury (1982) and Twin Falls (1989) areas produced by R. E. Lewis and H.W. Young. These data sets are the most complete sets in terms of chemical constituents reported as compared to some of the earlier work presented in the Geothermal Investigations of Idaho series (Street and Detar, 1987; Young and Mitchell, 1974; Mitchell et al., 1980). Reported concentrations from these sources remain original and unaltered in this study with the exception of the calculation of total dissolved solids (TDS and the conversion of alkalinity listed as mg/L CaCO_3 to alkalinity as HCO_3^- from samples originating from the Geothermal Resources in the Banbury Hot Springs Area (Lewis and Young, 1982). In total, 62 samples comprise the data set including 17 new samples collected under this study. Chemical concentrations are shown in Table 2. New samples contain trace elemental analyses that are absent from previous studies. New samples were collected primarily to satisfy the need for a more extensive chemical data set (particularly Al) to more effectively utilize the MEG tool RTest. The new analyses enabled

the use of a variety of hydrothermal alteration mineral assemblages comprised of various aluminosilicates.

Information regarding the chemical analysis of new samples as well as the QA/QC reports can be found in Appendix B. Charge balance calculations show that most waters are within $\pm 15\%$ of a 1:1 charge balance and are presented in Appendix C. The waters range in TDS from as low as 62 mg/L in cold groundwater samples to 565 mg/L in thermal water samples. Waters from these samples seem to comprise two distinct groups based on differences in several constituents. One group of waters, which comprises a mix of all of the cold water samples and several thermal waters exhibit much higher calcium and magnesium concentrations and tend to have lower TDS concentrations than the other group.

Groundwaters in the area and throughout the ESRP are considered Ca-Mg-HCO₃ in type and contain similarly high magnesium concentrations. This is to be expected as magnesium is largely absent in geothermal waters. Because of increased water-rock interaction at higher temperatures, magnesium is taken up by magnesium bearing clay minerals (Ellis, 1971; Fournier and Potter, 1979; Giggenbach, 1988). The second group of waters exhibits higher sodium, silica, chloride, and TDS concentrations. This is to be expected with ESRP geothermal waters due to the prograde relationship between temperature and solubility (chloride/silica) and the increase in cation-exchange reaction within deep rhyolites (sodium) (Fournier, 1977, Arnórsson, 1985; McLing et al., 2002). These differences and others are taken into account in the classification of the waters. Thermal waters were categorized in order to investigate the effects of secondary processes on thermal waters that may be shown in chemical trends between water types. Rather than arbitrarily separate the water types (i.e. graphically), multivariate cluster analysis was performed on selected chemical data.

Table 1. Chemical concentrations of hydrothermal water samples from the Twin Falls – Banbury area taken in 2014 for this study. All concentrations are given in units of mg/L. HCO₃ and CO₃ values are alkalinity measurements given in mg/L.

Site	Lat	Long	TEMP	pH	Ca	Mg	Na	K	Li	Cl	F	SO4	B	SiO2
8	42.69940	-114.91040	24.7	9.47	5.74	0.74	112.83	4.16	0.009	46.460	12.155	90.872	0.1897	52.04
9	42.64497	-114.78706	34.5	7.98	23.47	3.00	57.54	7.69	0.057	23.094	2.213	40.459	0.1074	71.89
10	42.64432	-114.78294	34.4	7.96	26.66	3.47	55.93	8.04	0.056	20.031	2.455	31.777	0.1057	69.37
11	42.69457	-114.85592	58.4	9.53	0.84	0.00	128.20	1.87	0.046	31.692	22.368	33.720	0.3320	99.53
12	42.54479	-114.94855	37.5	8.59	11.23	0.36	149.41	1.38	0.188	53.312	2.415	188.043	0.1167	45.54
13	42.54348	-114.94897	36.2	8.65	11.14	0.79	146.61	1.92	0.190	53.588	2.445	186.647	0.1135	48.37
14	42.58318	-114.47496	38.1	8.79	4.54	0.19	94.90	3.27	0.011	26.445	9.636	46.811	0.1501	64.23
40	42.70399	-114.85699	72.0	9.37	0.94	0.00	136.44	1.59	0.054	50.446	24.222	30.057	0.4988	93.53
42	42.68841	-114.82680	58.5	9.15	1.04	0.00	94.90	1.60	0.034	16.759	11.357	23.543	0.2190	102.85
45	42.66851	-114.82436	35.0	8.69	5.95	0.19	61.69	3.41	0.060	13.972	3.423	31.303	0.1290	54.05
46	42.66778	-114.82673	35.5	8.41	7.62	0.45	56.44	4.10	0.060	11.689	3.435	24.773	0.1318	54.47
48	42.70501	-114.85701	31.8	9.55	1.93	0.01	121.63	1.62	0.043	51.925	24.128	33.132	0.5790	83.31
51	42.58050	-114.47089	37.7	8.81	3.99	0.22	86.28	2.99	0.021	25.815	8.609	45.376	0.1851	60.92
52	42.59755	-114.40018	43.0	9.16	1.22	0.01	118.11	2.19	0.027	21.127	15.821	36.321	0.2846	69.27
53	42.61390	-114.48799	43.0	9.18	1.30	0.01	109.33	2.12	0.014	26.716	16.473	30.771	0.3172	71.55
54	42.57256	-114.45175	31.0	7.77	39.91	8.98	55.41	4.92	0.031	37.515	2.353	76.026	0.1073	59.11
55	42.57750	-114.28870	37.0	9.05	1.50	0.02	126.50	3.10	0.070	34.418	23.373	37.391	0.4955	66.02
Site	HCO3	dD	dl8O	TDS	CO3	Be	Al	As	Rb	Sr	Ba	Br	NO3	
8	80.52	-145	-18.3	396.5	-	<LOD	0.00703	0.04621	0.00423	0.02194	0.0012	0.796	1.211	
9	143.96	-134	-17.0	251.6	-	<LOD	0.0001	0.00769	0.0188	0.15614	0.00356	0.374	5.372	
10	126.88	-133	-17.2	292.5	-	<LOD	0.00019	0.00678	0.01918	0.17674	0.00187	0.351	4.746	
11	92.72	-142	-18.0	422.5	-	<LOD	0.02234	0.06626	0.00617	0.00117	<LOD	ND	ND	
12	95.16	-	-	559	-	<LOD	0.00492	0.02335	0.00494	0.06262	0.00636	0.818	1.435	
13	97.6	-134	-17.0	565.5	-	<LOD	0.01628	0.02386	0.00737	0.0652	0.01489	2.975	ND	
14	127	-134	-17.3	331.5	-	<LOD	0.00136	0.01742	0.00788	0.01879	0.0005	<LOD	4.893	
40	212	-139	-17.8	494	-	0.0001	0.0744	0.0611	0.0084	0.0013	0.0004	ND	ND	
42	168	-137	-17.5	331.5	-	<LOD	0.0146	0.0420	0.0067	0.0012	0.0004	ND	ND	
45	140	-	-	227.5	-	0.0001	0.0023	0.0248	0.0085	0.0098	0.0009	0.037	ND	
46	139	-	-	221.7	-	<LOD	0.0107	0.0176	0.0104	0.0176	0.0016	0.011	0.025	
48	232	-	-	429	-	<LOD	0.0108	0.0604	0.0024	0.0074	0.0015	0.031	ND	
51	153.72	-	-	312	-	0.0001	0.0028	0.0172	0.0072	0.0168	0.0006	ND	3.501	
52	187.88	-	-	396.5	-	0.0003	0.0053	0.0143	0.0071	0.0024	0.0007	ND	36.824	
53	153.72	-	-	377	-	<LOD	0.0042	0.0292	0.0045	0.0038	0.0002	ND	1.087	
54	161.04	-	-	390	-	0.0001	0.0020	0.0060	0.0115	0.1854	0.0161	ND	6.737	
55	246.44	-	-	422.5	-	<LOD	0.0236	0.1410	0.0086	0.0039	0.0019	ND	0.100	

Table 2. Selected chemical concentrations of hydrothermal water samples from previous studies. All concentrations are given in units of mg/L. Decimal degree coordinates (WGS84) are approximated from original township and range values. Bold values correspond to TDS values generated by summing major cation and anion concentrations. Site names correspond to a particular study: LY82/89 = Lewis and Young, 1982; 89 and M91 = Mariner et al., 1991.

Site	Lat	Long	TEMP	pH	Ca	Mg	Na	K	Li	Cl	F	SO4	B	SiO2	Alkalinity as HCO3	δD	$\delta^{18}O$	TDS
M91-7	42.603164	-114.477722	39	9.3	1.6	0.06	96	2.8	0	15	11	20	-	67	145	-	-	331
M91-8	42.569362	-114.606826	27	8.6	5.1	0.17	61	4.3	0	11	3.6	16	-	77	134	-	-	253
M91-11	42.583616	-114.481118	30.5	8.6	8.6	0.4	74	6.3	0	21	11	26	-	55	121	-	-	267
M91-12	42.549979	-114.436857	30.5	7.8	37	6.8	31	4.9	0.03	31	1	51	-	50	100	-	-	266
M91-13	42.589664	-114.509924	41.5	9	1.7	0.08	130	2.5	0	36	26	28	-	60	195	-	-	408
M91-14	42.578624	-114.287802	42	9.2	1.5	0.01	120	1.9	0	17	14	32	-	66	207	-	-	-
LY89-1	42.66191	-114.812514	33	8.4	11	0.5	61	3.9	0.06	11	3.6	24	0.11	53	150	-132	-16.9	246
LY89-2	42.661228	-114.791887	37	8.1	13	1.2	58	4.1	0.06	12	3.6	25	0.09	60	140	-132	-17.2	246
LY89-3	42.654022	-114.795266	28.5	8	16	2.3	55	5.8	0.06	13	2.5	27	0.09	64	150	-	-	259
LY89-4	42.636971	-114.754192	26	8.3	7.4	0.2	62	5.6	0.08	9.9	4.8	21	0.014	82	140	-	-	262
LY89-5	42.646829	-114.785566	32.5	7.8	18	2.2	54	6	0.06	13	2.5	27	0.09	71	150	-131	-17.1	268
LY89-6	42.63448	-114.778469	25	8.1	17	1.1	53	7.5	0.05	14	2.4	22	0.02	87	160	-	-	283
LY89-7	42.597701	-114.760739	29	7.9	36	5.4	61	10	0.07	31	1.9	61	0.12	66	170	-130	-16.8	356
LY89-8	42.654938	-114.650688	44	9	1.5	0.1	96	1.5	0.03	14	16	24	0.2	75	78	-134	-17.2	304
LY89-9	42.648856	-114.652208	23	9.1	8.9	2.4	73	1.9	0.02	20	11	28	0.3	52	95	-	-	263
LY89-10	42.596158	-114.751276	31	8	39	5.6	65	11	0.07	38	1.7	75	0.1	72	160	-	-	388
LY89-11	42.631739	-114.597327	30.5	9	2	0.05	82	2.9	0.021	11	12	20	0.11	67	110	-131	-16.9	272
LY89-12	42.617975	-114.473657	27	9	1.9	0.1	110	3.5	0.02	10	22	18	0.33	82	140	-137	-17.7	341
LY89-13	42.615389	-114.488068	42	8.8	2.5	0.1	110	1.9	0.004	16	16	15	0.22	74	140	-135	-16.9	326
LY89-14	42.594962	-114.481012	39.5	9	1.9	0.1	99	1.9	0.006	15	14	25	0.16	66	110	-132	-17	301
LY89-15	42.605808	-114.478121	39	9.3	1.6	0.06	96	2.8	0	15	11	20	0.11	67	120	-138	-17	299
LY89-17	42.575903	-114.738609	25	8	35	4.5	63	12	0.07	35	1.6	69	0.08	71	160	-129	-16.4	371
LY89-18	42.566417	-114.490768	31.5	8	20	3.9	37	7	0.03	11	3.7	17	0.08	59	130	-127	-16.7	223
LY89-22	42.583859	-114.480819	30.5	9	8.6	0.4	74	6.3	0	21	11	26	0.1	55	110	-132	-17.1	262
LY89-29	42.395919	-114.691588	18.5	7.8	23	8.4	13	2.9	0.006	9	0.2	11	0.02	48	120	-123	-15.4	175
LY89-30	42.345552	-114.509176	37	8	31	13	43	11	0.05	6.3	1.9	21	0.12	19	270	-133	-17	279
LY89-32	42.27131	-114.359743	9	6.7	5.4	1.3	6	5	0.004	1.6	0.2	2	0.02	56	34	-127	-16.4	95
LY89-33	42.222385	-114.785594	12	7	7.2	1.2	5.9	2.6	0.004	3.1	0.2	5	0.02	35	30	-126	-17.1	76

Site	Lat	Long	TEMP	pH	Ca	Mg	Na	K	Li	Cl	F	SO4	B	SiO2	Alkalinity as HCO3	δD	$\delta^{18}O$	TDS
LY89-34	42.20179	-114.664984	32	7.8	21	2	18	6.9	0.034	6.8	0.7	10	0.05	58	120	-130	-16.9	200
LY89-35	42.201144	-114.697878	26	7.5	22	2.6	19	5.8	0	6.4	6	12	0.01	60	110	-131	-16.7	183
LY89-36	42.158264	-114.66585	32	7.6	18	2.3	18	4.7	0.02	6.5	0.8	8.8	0.02	65	100	-132	-16.8	174
LY89-37	42.200441	-114.586984	7.5	7.6	34	5.4	19	3.6	0.004	16	0.3	17	0.06	52	120	-120	-14.6	208
LY89-38	42.213508	-114.306916	4.5	6	2.6	0.7	3.4	2.6	0.004	1.3	0.1	3.4	0.005	38	20	-123	-16.2	62
LY82-3	42.701575	-114.856527	62	9.4	0.7	0.1	150	1.4	0.05	48	15	35	0.49	84	168	-	-	503
LY82-4	42.701842	-114.854331	71.5	9.5	1.5	0.1	140	1.5	0.06	51	27	33	0.51	82	168	-	-	505
LY82-5	42.691328	-114.866789	57	9.4	0.9	0.1	130	1.5	0.04	34	21	34	0.34	86	177	-	-	485
LY82-6	42.6881	-114.84012	45.5	9.1	0.9	0.1	100	1.8	0.04	30	26	29	0.23	86	163	-	-	438
LY82-7	42.683574	-114.834978	42.5	9.3	1.3	0.1	90	1.7	0.04	14	9.4	28	0.17	67	148	-	-	359
LY82-11	42.684873	-114.829093	44.5	9.4	3.3	0.1	100	1.8	0.04	22	12	27	0.23	88	160	-	-	414
LY82-12	42.68251	-114.82902	30	9.3	0.9	0.1	97	1.6	0.03	20	13	28	0.21	64	154	-	-	379
LY82-13	42.599928	-114.943824	42	9.2	26	3.9	35	7.9	0.05	16	1.8	35	0.06	86	120	-	-	331
LY82-15	42.669042	-114.8236	34	8.7	5.4	0.2	66	2.9	0.05	13	3.7	30	0.12	56	124	-	-	302
LY82-18	42.661493	-114.814894	32	8.4	8	0.2	62	2.8	0.05	11	3.1	26	0.11	53	144	-	-	310
LY82-19	42.660011	-114.81414	31.5	8.6	7.5	0.3	63	2.8	0.05	11	3.2	26	0.12	51	134	-	-	299
LY82-20	42.658855	-114.810791	32.5	8.3	10	0.5	62	3.5	0.05	11	2.9	25	0.11	51	150	-	-	316

3.2 Principle Component and Hierarchical Cluster Analysis

With each sample being characterized by several chemical and physical variables, the aqueous geochemistry study of the area becomes a multivariate problem. The multivariate statistical method chosen for this study is hierarchical cluster analysis (HCA). This method was chosen as an unbiased means to separate waters into discrete groupings based on concentrations of several chemical components as opposed to the more graphical means provided by Piper diagram analysis. HCA is a widely utilized data classification practice in Earth sciences (Davis, 1986) and has begun to be utilized more extensively in groundwater geochemical studies in recent years (Meng and Maynard, 2001; Cloutier et al., 2008; Kanade and Gaikwad, 2011). HCA produces a hierarchy of clusters, ranging from small clusters of very similar items to larger clusters of increasingly dissimilar items without assuming any underlying trend in the data as opposed to several partitioning methods which assume a specific number of clusters outright. The measure of similarity in this instance of HCA is provided by the Euclidean distance, given by the Pythagorean Theorem. Sample groups are joined with a linkage rule until all of the observations are sorted into different clusters. The linkage method utilized in this study is Ward's methods which uses an analysis of variance approach to establish the distance between clusters. Many studies have found that the use of the Euclidean distance and Ward's method produce the most distinctive groupings within which samples are more or less homogeneous (Adar et al., 1992; Guler et al., 2002; and Zumlot et al., 2012).

It is usually suggested that prior to HCA, some sort data reduction be done in order to both gain insight into the correlation of variables and source of major variance, and ultimately to simplify the data into a more meaningful and manageable set. Principle component analysis

(PCA) is utilized for data reduction in this study. The premise of PCA is that every sample can be represented as a single point in a K-dimensional space (depending the number of variables being analyzed). All points within the data set can essentially be approximated by a single plane (whose axes are principle components and Eigen vectors) space by a least squares regression. The result is a few orthogonal components (Eigenvalue > 1) that explain the majority of the variance within the data set (Meng and Maynard, 2001).

PCA produces factor or component scores which are essentially coordinates corresponding to individual data points within each principle component. These scores can then be utilized in HCA as opposed to clustering based on the raw values for all variables. Like the Piper diagram analysis, major cations and anions were chosen in this study as the variables for PCA. Other constituents such as SiO_4^{2-} and F^- did not account for much of the variance within the data and were omitted. Both PCA and HCA ordinarily require a normal distribution of all variables included or a transformation is suggested. Key components (K^+ and Na^+) are normally distributed within this data set while other components contain a slight right skew. A log transformation was performed prior to PCA and HCA but resulted in erroneous partitioning of water samples incongruent with Piper diagram classification. For this reason, the data presented here are not transformed. The Eigenvalues for the principle components produced are shown below in Table 3. The principle components used are highlighted in bold.

Table 3. Principle components and corresponding % variance

	F1	F2	F3	F4	F5	F6	F7
Eigenvalue	3.096	2.088	1.068	0.373	0.210	0.111	0.054
Variability (%)	44.225	29.828	15.258	5.330	3.007	1.584	0.768
Cumulative %	44.225	74.052	89.311	94.641	97.648	99.232	100.0

Pearson's correlation coefficients are shown below in Table 4. Na^+ and Cl^- , K^+ and Ca^{2+} , Mg^+ and K^+ , and SO_4^{2-} and Cl^- are all significantly and positively correlated as is the case in a majority of groundwater studies. In contrast, K^+ and Cl^- are shown to be very weakly correlated in this study where they are commonly correlated in many groundwater studies (Rani and Babu, 2008; Muthulakshmi et al., 2013). However, the groundwater samples in this study tend to have higher potassium concentrations and do not follow the $\text{Na}^+ > \text{Ca}^{2+} > \text{Mg}^+ > \text{K}^+$ trend exhibited in other studies. This source of potassium is significant in mixing trends and will be discussed further in section 3.5. Additionally, it is worth noting that bicarbonate alkalinity does not seem to be correlated strongly with any other chemical component and may not be useful in further evaluation of mixing trends. Figure 6 (below) is a biplot of the first two principle components representing about 74% of the variance within the data set. Negative and positive correlations can be seen here. It is important to note that SO_4^{2-} and HCO_3^- lie close to the principle component (F2) axis meaning they are not responsible for much of the variance within the dataset.

Table 4. Pearson's (n) correlation table of PCA variables (chemical components)

Variables	Ca	Mg	Na	K	Cl	SO4	HCO3
Ca	1	0.855	-0.568	0.784	-0.021	0.184	0.012
Mg		1	-0.507	0.631	-0.073	0.059	0.135
Na			1	-0.518	0.715	0.436	0.421
K				1	-0.160	0.007	0.100
Cl					1	0.684	0.323
SO4						1	-0.019
HCO3							1

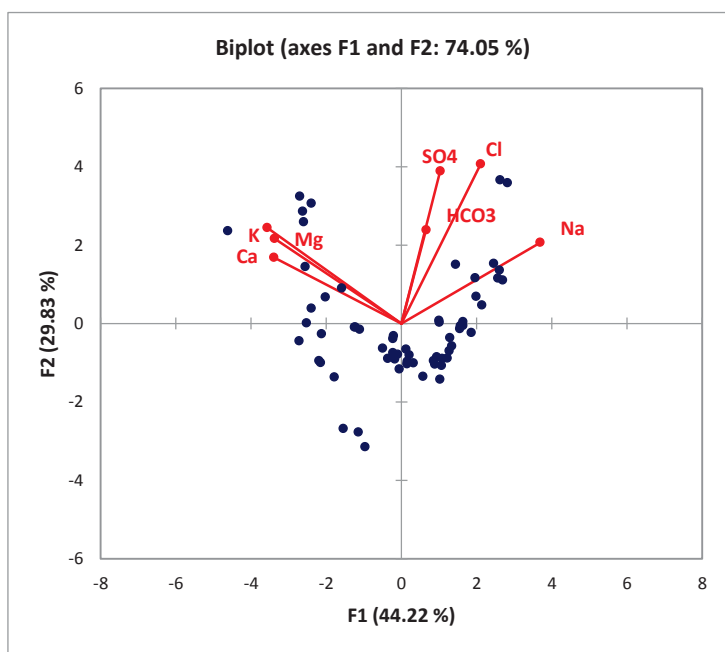


Figure 6. Biplot of principle components 1 and 2 with variables (red lines) and samples (blue dots)

HCA was run using the XLSTAT ® add-in for Microsoft ® Excel. HCA was run using both principle component scores and raw chemical data. The PCA proved valuable in producing only three water types as opposed to the six produced without data reduction. The dendrograms in Figures 7 and 8 represent the final cluster output. Water types are listed in Tables 5-8 with the corresponding author initials and dates preceding the sample numbers. Two of the waters classified as type 3 waters (CC-12 and CC-13) are believed to have been influenced by local irrigation water (evident by much higher sulfate and chloride values than surrounding areas). For this reason, they have been grouped into type 2 waters for mixing trend applications. The waters fall into two main end members:

- 1) Na-HCO₃ (Type 1) waters characterized by high temperatures, high Na⁺ concentrations, and low Ca²⁺ and Mg⁺ concentrations.
- 2) Ca-HCO₃ (Type 2) waters characterized by lower temperatures, low Na⁺ concentrations, and high Ca²⁺ and Mg⁺ concentrations.

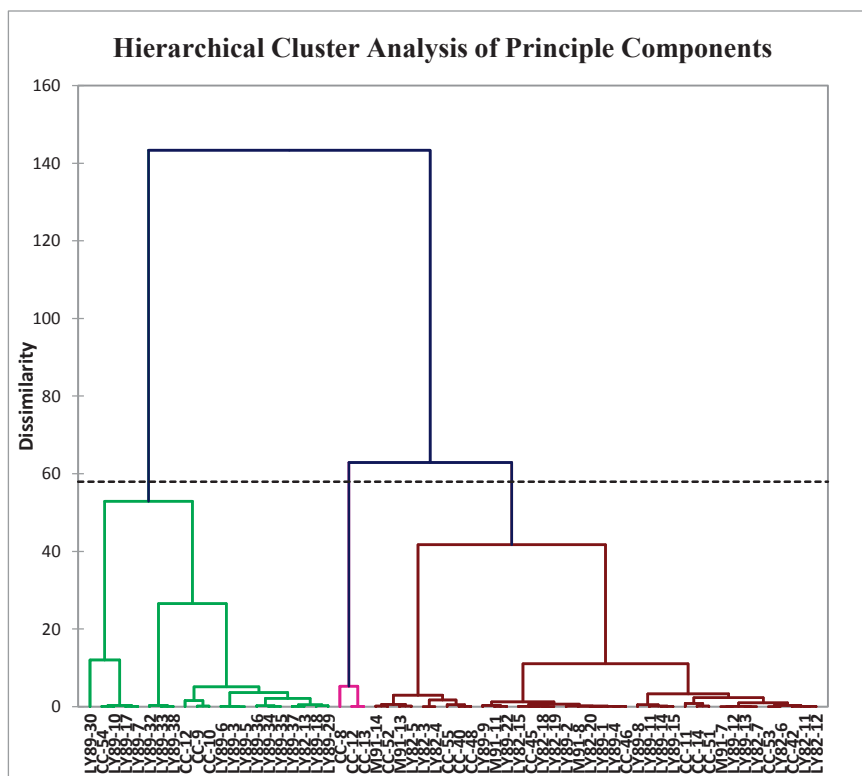


Figure 7. Dendrogram showing clusters of samples provided by HCA on principle components.

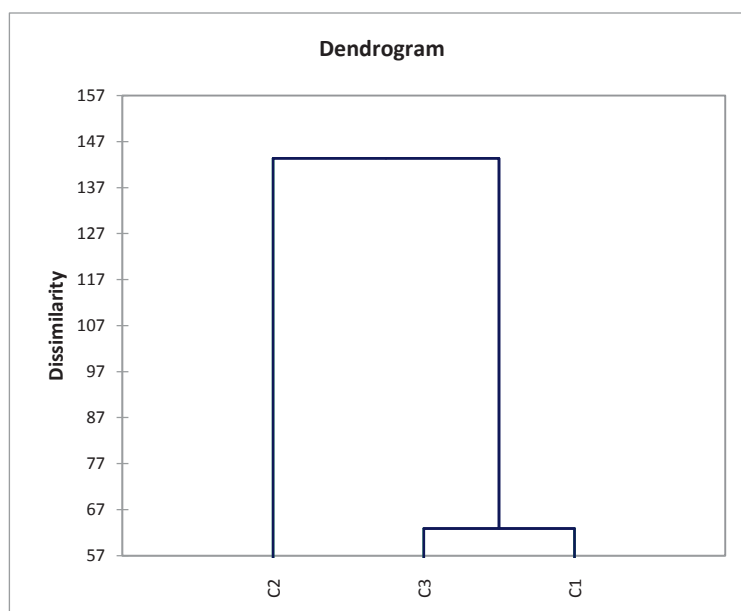


Figure 8. Simple dendrogram showing the resultant 3 water types.

3.3 Evidence for Mixing Between Thermal Water and Groundwater

After the completion of water classification by cluster analysis, the samples were plotted on a Piper diagram (Piper, 1944) to gain a visual representation of sample distribution. The Piper diagram is perhaps the most common method used in classifying waters (Fetter, 2001) due to it being an easy to comprehend graphical representation based on concentrations of all major anions (SO_4^{2-} , Cl^- , and $\text{CO}_3^{2-} + \text{HCO}_3^-$) and major cations (Ca^{2+} , Mg^{2+} , and $\text{Na}^+ + \text{K}^+$). Two separate trilinear diagrams are used to plot the relative percentages of cations and anions. These two separate points are then projected onto the Piper diagram diamond using a matrix transformation to form a single point, which can then be used to classify a water.

Earlier hydrothermal studies in regions of the ESRP have noted the characteristic trend between the two aforementioned end member waters (Mann, 1986; Wood and Lowe, 1988, Mariner et al., 1991; McLing et al., 2002). Na- HCO_3 type waters are generally associated with deeper groundwater sources with increased ion-exchange reactions replacing calcium with sodium during hydrothermal alteration of feldspars as a result of longer residence times and higher temperatures (White, 1967; Edmunds and Shand, 2009). Giggenbach (1991) described the formation of Ca-Na- HCO_3 and Ca- HCO_3 type thermal waters as a result of mixing with a ground water component like the Ca-Mg- HCO_3 waters that dominate the upper aquifer system of the ESRP (McLing et al., 2002; Wood and Lowe, 1988). Deep wells (> 1km) that penetrate the upper basalt hosted portion of the aquifer, e.g. the INEL-1 and Project Hotspot: Kimberly and Kimama wells (Shervais et al., 2013), reveal the pure Na- HCO_3 thermal end member. Mann (1986) described the change in composition from deep rhyolite hosted Na- HCO_3 water to mixed Ca-Na- HCO_3 basalt hosted water in the INEL-1. McLing et al. (2002) showed perhaps the best visual representation of this trend with a Piper diagram consisting of thermal

waters throughout the ESRP. Lewis and Young (1989) also observed this trend in the Twin Falls area. However, due to sporadic and regional sample population and small sample density, these studies lacked a significant number of mixed intermediate Ca-Na-HCO₃ type samples to fully support this mixing hypothesis (Figure 9).

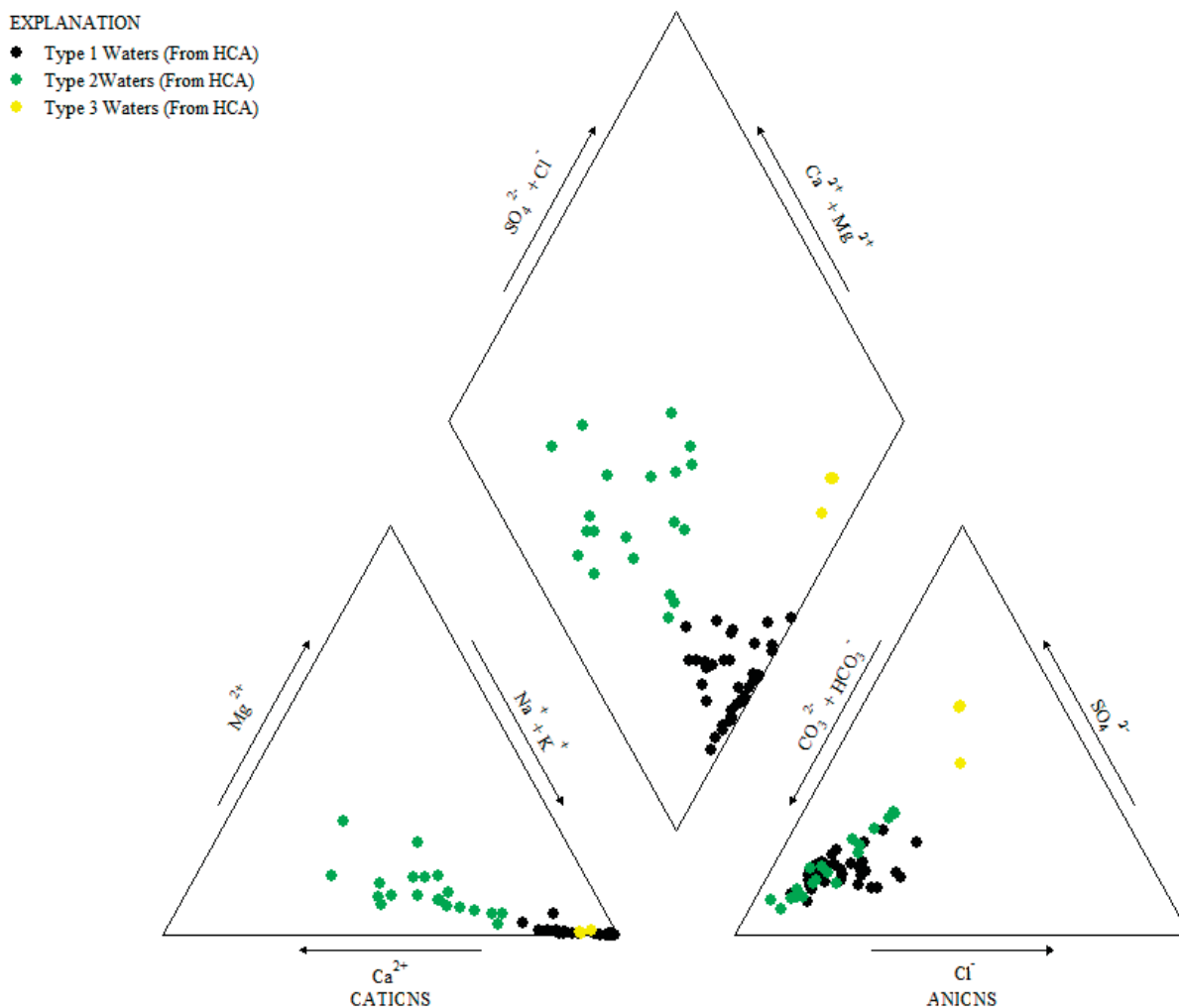


Figure 9. Piper trilinear diagram showing the relationship between Na-HCO₃ thermal waters (black) and Ca-HCO₃ thermal waters (green). Yellow samples appear to have been altered by nearby irrigation.

Piper diagram analysis for the 62 water samples utilized in this study gives a strong visual representation of the trend between water types. Figure 9 shows the distribution between Type 1 (Na-HCO₃) waters in the upper left corner of the diagram and Type 2 (Ca-

HCO₃) type waters in the lower right corner. A significant trend and overlap can be seen between water types. In particular, the trend observed in the cation portion of the diagram demonstrates the gradual exchange between Na⁺ and Ca²⁺. It is important to note that anion concentrations (Cl, HCO₃⁻, and SO₄²⁻) seem to be independent of water type and the degree of mixing.

Sample compositions are also plotted on a Giggenbach ternary diagram (Figure 10) to determine evidence of equilibration and/or mixing. The Giggenbach ternary diagram (1988) was developed as a means to classify waters into fully equilibrated (mature) waters, partially equilibrated, and immature waters (dissolution of rock without equilibration). The latter two categories show evidence of mixing with cool meteoric waters. The diagram uses the full range of equilibrium relationships between the Na, K, and Mg alteration minerals expected to form after recrystallization to determine the degree of equilibration between the water and the rock of thermal influence at depth. Few previous geothermal investigations in south central Idaho and the ESRP made use of the Giggenbach diagram as evidence for mixing. No previous studies in the Twin Falls – Banbury thermal area have utilized this diagram.

In Figure 10 below, most samples plot in the partially equilibrated and immature portions of the diagram with only a few plotting near or within the mature portion. The majority of Ca-HCO₃ type waters are grouped in the far right corner of the diagram reflecting the influence of high magnesium concentrations presumably from mixing with groundwater. Both the Piper and Giggenbach diagram sample distributions provide particularly valuable evidence for mixing in this area.

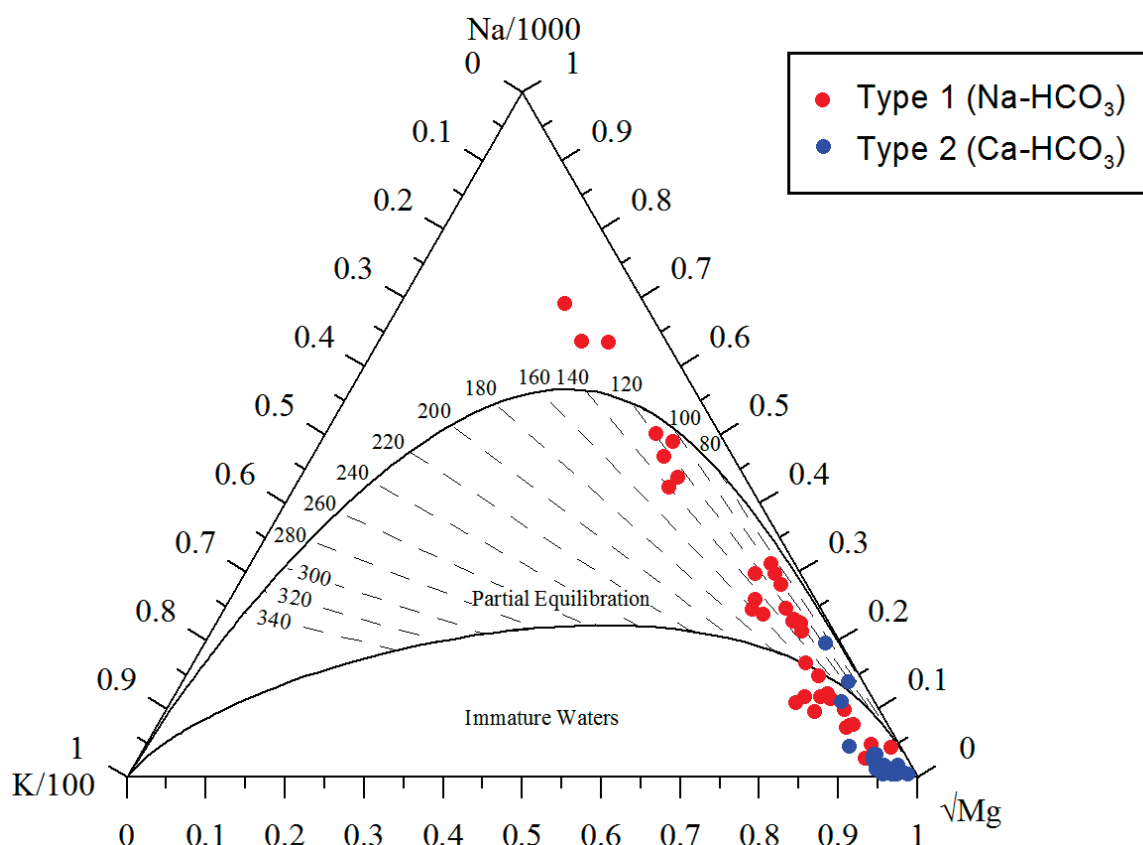


Figure 10. Giggenbach ternary diagram showing the distribution of the two water types with respect to degree of equilibration. Blue points represent Ca-HCO_3 thermal waters and red points represent Na-HCO_3 waters.

3.4 Binary Diagram Mixing Trend Analysis

Binary diagrams consisting of conservative species that are not be incorporated into geothermal minerals have been utilized in mixing evaluations for many years (Fournier, 1979; Arnórsson, 1985; Huenges and Ledru, 2011). The evaluation of linear relationships between components including Cl^- , B, F^- and δD provide particularly good evidence for mixing as the ratio between conservative elements will remain fixed as concentrations are simply lowered through dilution. This study utilizes mixing relationships between conservative components (non-reactive mixing) and also those between reactive components in order to obtain a more complete picture of the overall controls on mixing. Preliminary results show that the MEG

tool RTest does not result in satisfactory convergence of mineral saturation index lines when a local groundwater sample is mixed with Na-HCO₃ thermal waters. While Na-HCO₃ thermal waters show evidence for mixing, they may not mix directly with groundwater. Instead, an “intermediate” composition between the two thermal waters may be the mixing component. Additionally, secondary reactive processes may alter thermal waters after mixing resulting in re-equilibration. Binary diagram trends between the two water types may reveal controls on mixing in greater detail and may determine an intermediate end member composition for use in MEG reservoir temperature predictions.

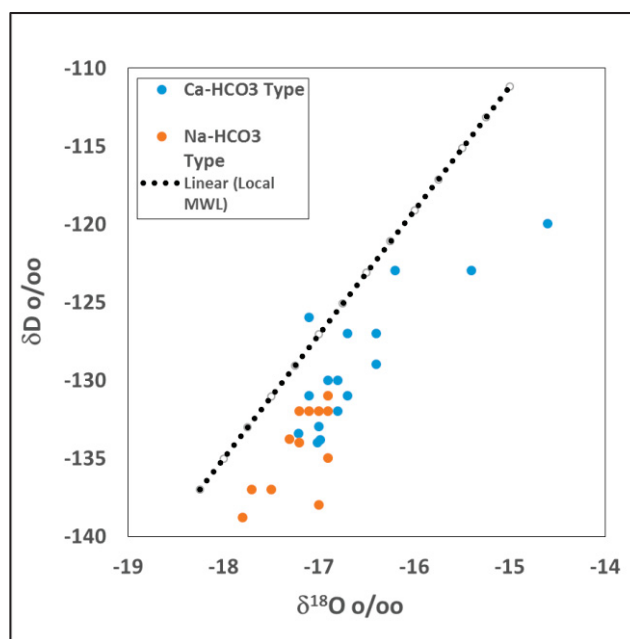


Figure 11. Plot of δD vs $\delta^{18}O$ showing the shift of sample waters from the local meteoric water line.

Thermal water samples with available deuterium and oxygen-18 isotope data are plotted in Figure 11 above. Samples display a significant right shift from the local meteoric water line (USGS, 2004). The isotopic shift in ^{18}O is typical of geothermal waters and is most likely a result of increased water-rock interaction at depth resulting in oxygen enrichment (Taylor, 1974; Clark, 2015). Deuterium shifts, on the other hand, are likely not explained by any hydrothermal process as it is conserved through these processes. A likely explanation is

that recharge occurred during an older and colder time (Pleistocene) in which precipitation concentrations were isotopically lighter with respect to deuterium. This explanation is consistent with carbon-14 age data of waters in the area provided by Mariner et al. (1991). Another possible explanation for shifts in δD concentration is the enrichment of deuterium through isotopic fractionation due to boiling (Bottinga, 1968; Taylor, 1974; Truesdell, et al.; 1978). The possibility of boiling is discussed further in chapter 4.2. The relationship between these two isotopes shows a gradational trend with waters becoming more depleted with

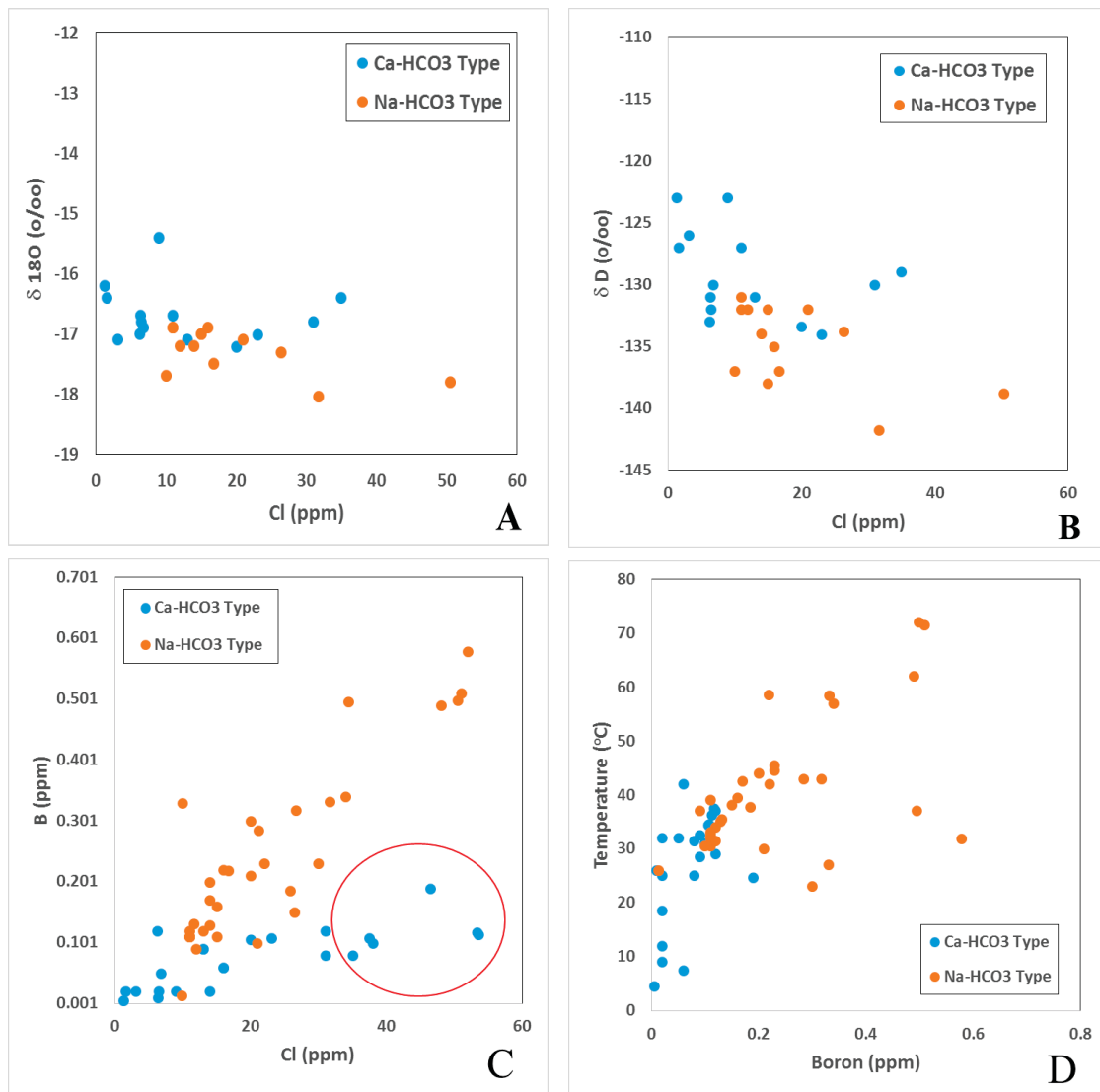


Figure 12. Plots of conservative components (Cl, B, $\delta^{18}O$, and δD).

respect to oxygen-18 in the deeper Na-HCO₃ type waters.

Gradational trends between conservative constituents such as boron and chloride are thought to constitute some of the best evidence for mixing (Huenges and Ledru, 2011). Boron and chloride concentrations are much higher in geothermal waters than in cold waters as can be seen by the linear relationship between boron and surface water temperature in the Figure 12D. The ratio of chloride to boron will not be affected by mixing, as these constituents are not considered to be incorporated into geothermal minerals. The concentrations will simply decrease with dilution from mixing between thermal and cold waters will result in a steady decline as seen in Figure 12C with a B/Cl⁻ slope of about 0.1/10 with the exception of a few circled values from the Lewis and Young (1982) study. The intersection of the Cl⁻/B trend is expected to meet the chloride axis in the range of 10 ppm (chloride precipitation and cold water range) with a 0 ppm boron concentration (Arnórsson, 1985). Linear relationships between these two components and $\delta^{18}\text{O}$ and $\delta^2\text{H}$ also constitute sufficient evidence for mixing (Huenges and Ledru, 2011).

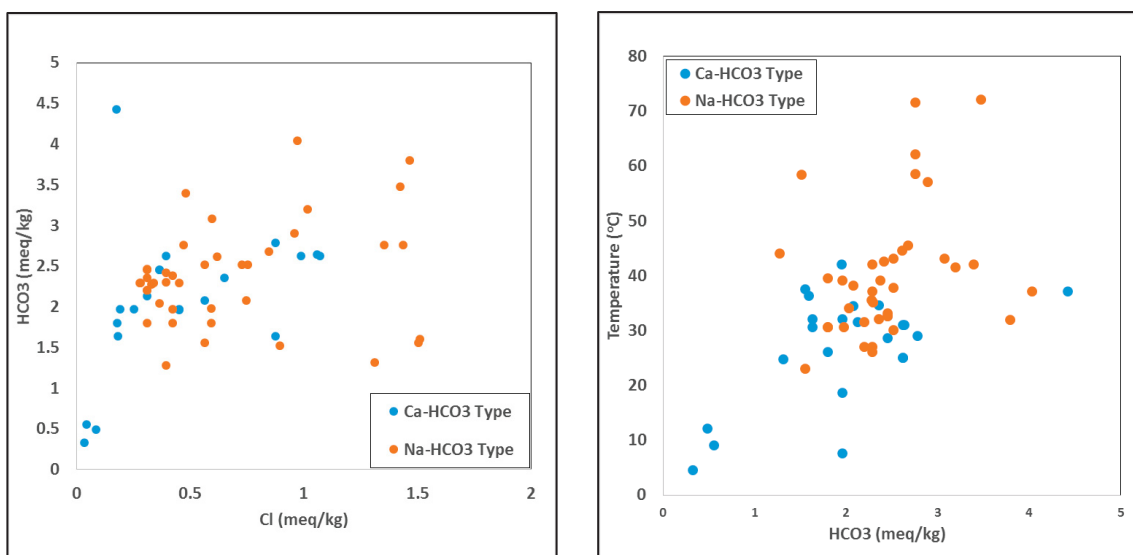
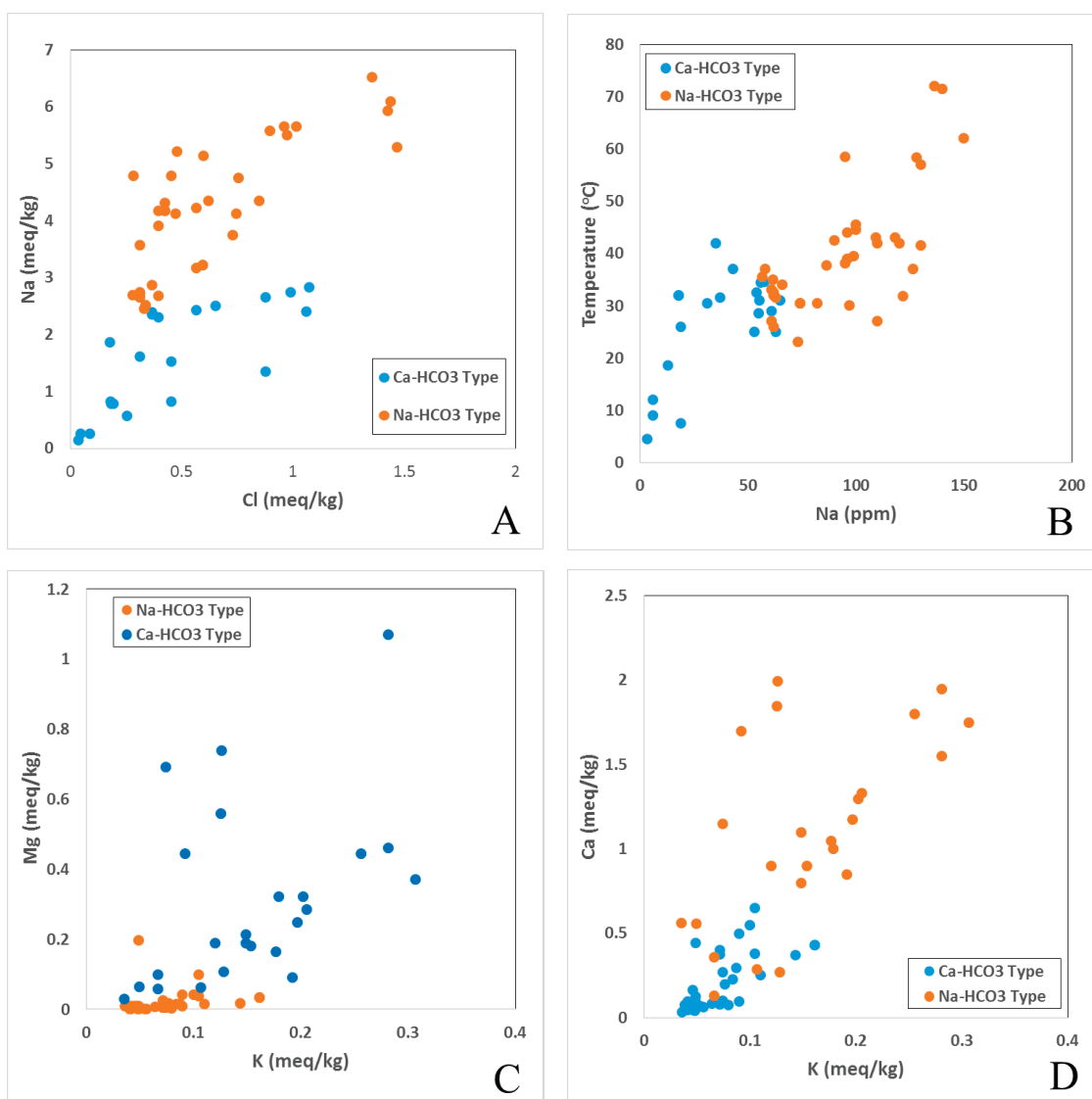


Figure 13. Plot showing the lack of relationship between HCO₃⁻ and Cl⁻ and Temperature.

It is important to note that some chemical components cannot be used in distinguishing between the two waters and that no mixing trend may manifest itself. This is the case with carbonate alkalinity of this system, seen in Figure 13 above. There does not appear to be any discernible relationship between bicarbonate concentrations and temperature or chloride. This observation signifies that bicarbonate concentration acts



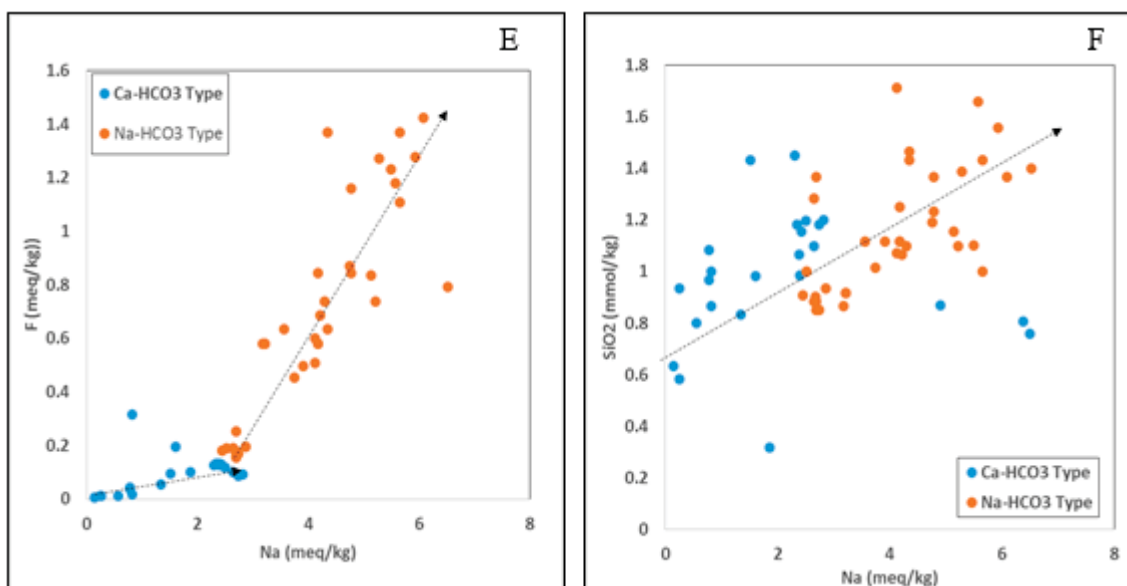


Figure 14. Binary plots between several reactive components showing simple mixing relationships.

independently of the mixing process. For this reason, either a local groundwater bicarbonate concentration or an average bicarbonate concentration should be utilized in RTest modeling.

When examining relationships between major cations and anions for the thermal water samples, some distinct linear relationships become evident. The Na^+/Cl^- relationship as well as the Na^+ vs temperature relationship observed in Figures 14A and B shows the distinct transition between the sodium rich thermal end member to cooler more dilute waters. The Na^+/Cl^- trend passes through the origin signifying that little to no sodium and chloride need to be utilized in the dilution portion of MEG modeling. Figures 14 C and D show the positive relationship between both Mg^{2+} and K^+ and Ca^{2+} and K^+ . Na-HCO₃ thermal waters are depleted with respect to Mg^+ and K^+ compared with the Ca-HCO₃ type waters. The Na-HCO₃ type waters begin with virtually no magnesium and grade into higher concentrations perhaps with increasing dilution. The same trend is seen between Ca^{2+} and K^+ where Na-HCO₃ type waters begin with little to no calcium and grade into more calcium rich waters. An important

observation gained here is that if an “intermediate” reactive mixing component is to be used in RTest modeling, it will require the addition of potassium.

Fluoride concentrations in the thermal water samples yield two separate trends. The Ca-HCO₃ type waters contain little to no amount of fluoride while the Na-HCO₃ type shows a steep trend in fluoride concentrations. Elevated fluoride concentrations are common throughout the ESRP and are often attributed to increased reaction with rhyolites (Mitchell et al., 1980). The sharp separation in fluoride trends between the two waters could signify that the Ca-HCO₃ type waters are mixed with a small amount of thermal water or have had little water-rock interaction with rhyolites. There is also a positive relationship between SiO₂⁻ and Na⁺ as shown in Figure 14 F showing increased silica concentration towards Na-HCO₃ thermal end member waters. Unlike many other solute trends, which begin at near zero concentrations, SiO₂⁻ begins at around 40 ppm corresponding to high SiO₂⁻ concentrations in the groundwater of the study area compared to most of the ESRPA (Lewis and Young, 1989).

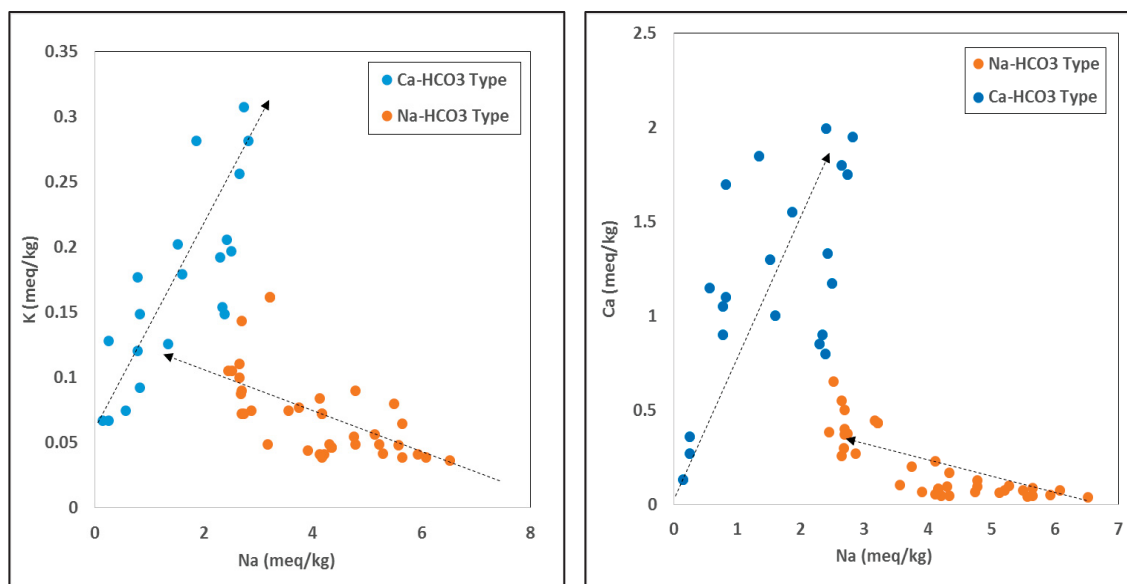


Figure 15. Binary plots showing the complex relationship between Na⁺ and K⁺ and Na⁺ and Ca²⁺

While the previously discussed relationships have been relatively simple, the relationships between K^+ , Ca^{2+} , and Mg^{2+} vs Na^+ are more complex. In both these trends (shown in Figure 15 above) there is a sharp near-vertical boundary that separates the trends of the two water types. Possible explanations for the sharp increase in Ca^{2+} and K^+ exhibited by the $Ca-HCO_3$ type waters include:

- 1) A significant source of Ca^{2+} , K^+ , and Mg^{2+} within the basalts and sediments of the Banbury formation that overly the rhyolites of the Idavada volcanics (source of $Na-HCO_3$ waters).
- 2) Re-equilibration via an exchange reaction resulting in an increase in Na^+ and K^+ and a decrease in Ca^{2+} and Mg^{2+} concentrations resulting in the formation of $Ca-HCO_3$ thermal waters.
- 3) Two separate and distinct flow paths (different temperatures and host rocks) resulting in the two thermal water types.

The use of binary diagrams presented in this section provides support for mixing between thermal water and groundwater as well as provides information about the concentrations of constituents to be used in the mixing portion of inverse MEG modeling. Mixing and/or re-equilibration mechanisms will be explored further in Chapters 4-6.

3.5 Areal and Geologic Distribution of Water Types

Water samples were plotted by type (according to HCA) on digital orthoimagery (USDA, 2011) and geologic maps (Gillerman et al., 2005; Othberg et al., 2005). The spatial distribution shown below in Figure 16 shows the progression from $Ca-HCO_3$ type waters from the Cassia Mountain recharge zone to $Na-HCO_3$ type waters towards the boundary of the Snake River. Figure 16 shows the direction of groundwater movement from a potentiometric

surface created using water level data from the USGS National Water Information System. Figures 17 and 18 show detailed views of the Banbury and Twin Falls area clusters. All of the thermal samples within the Banbury cluster fall along a major normal fault, which parallels the path of the Snake River. This distribution shows the gradation from Ca-HCO_3^- type waters to more thermal Na-HCO_3^- type waters northward along the fault away from the recharge zone. A likely scenario for this observed gradation is the ascension of thermal waters through the normal fault and the increase in the amount of mixing southward of the fault. The Twin Falls cluster shows the same gradation away from the area of recharge towards the Snake River. Shervais et al. (2013) suggest that the thermal system in the Twin Falls area is controlled by a caldera margin. The geology and hydrology of these two areas will be discussed further in Chapter 5.

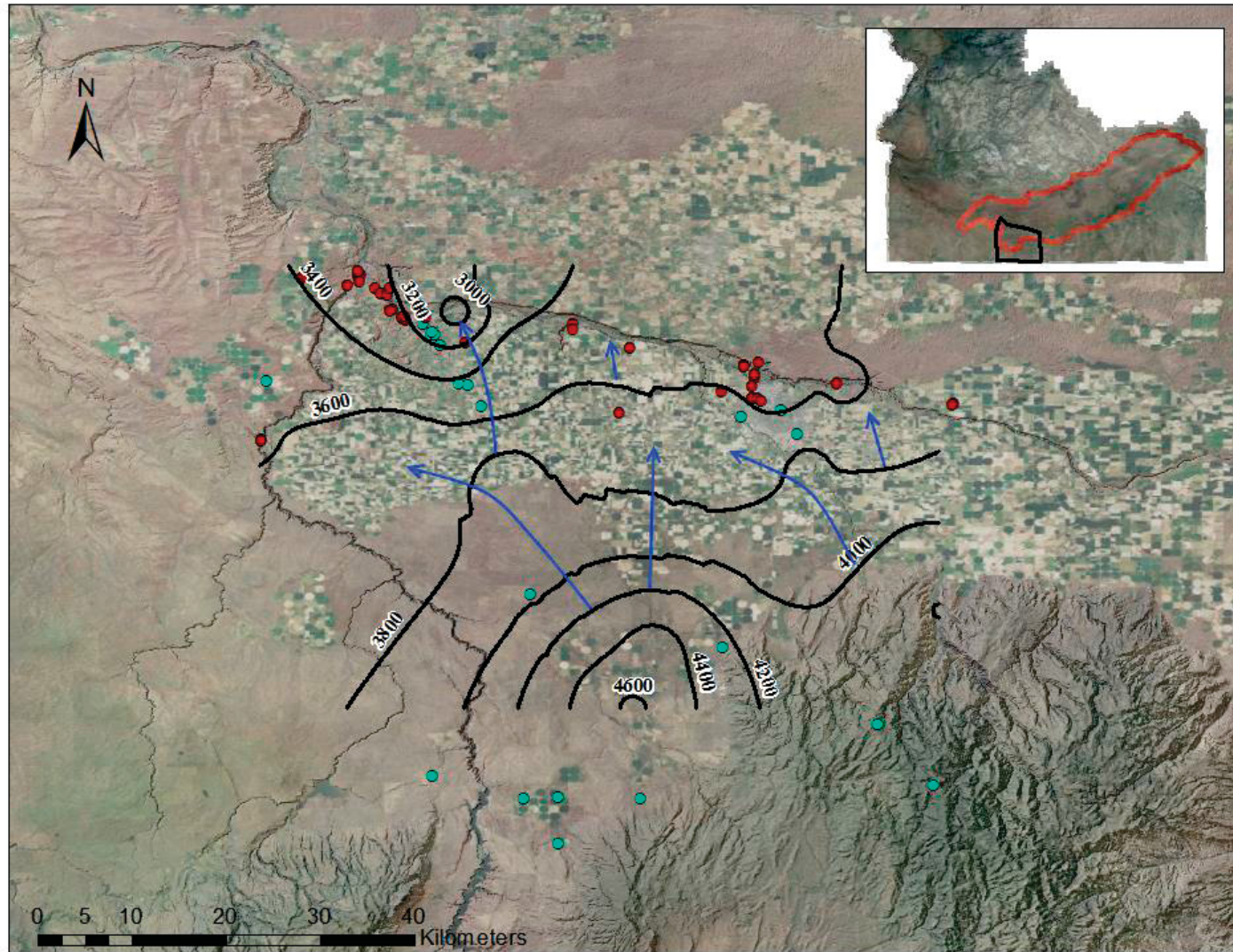


Figure 16. Map of water samples showing the gradation from Ca-HCO_3^- type (blue) waters to Na-HCO_3^- type waters (red) away from the recharge zone. Groundwater flow lines (blue) produced from inverse distance weighting of water level data from the USGS National Water Information System.

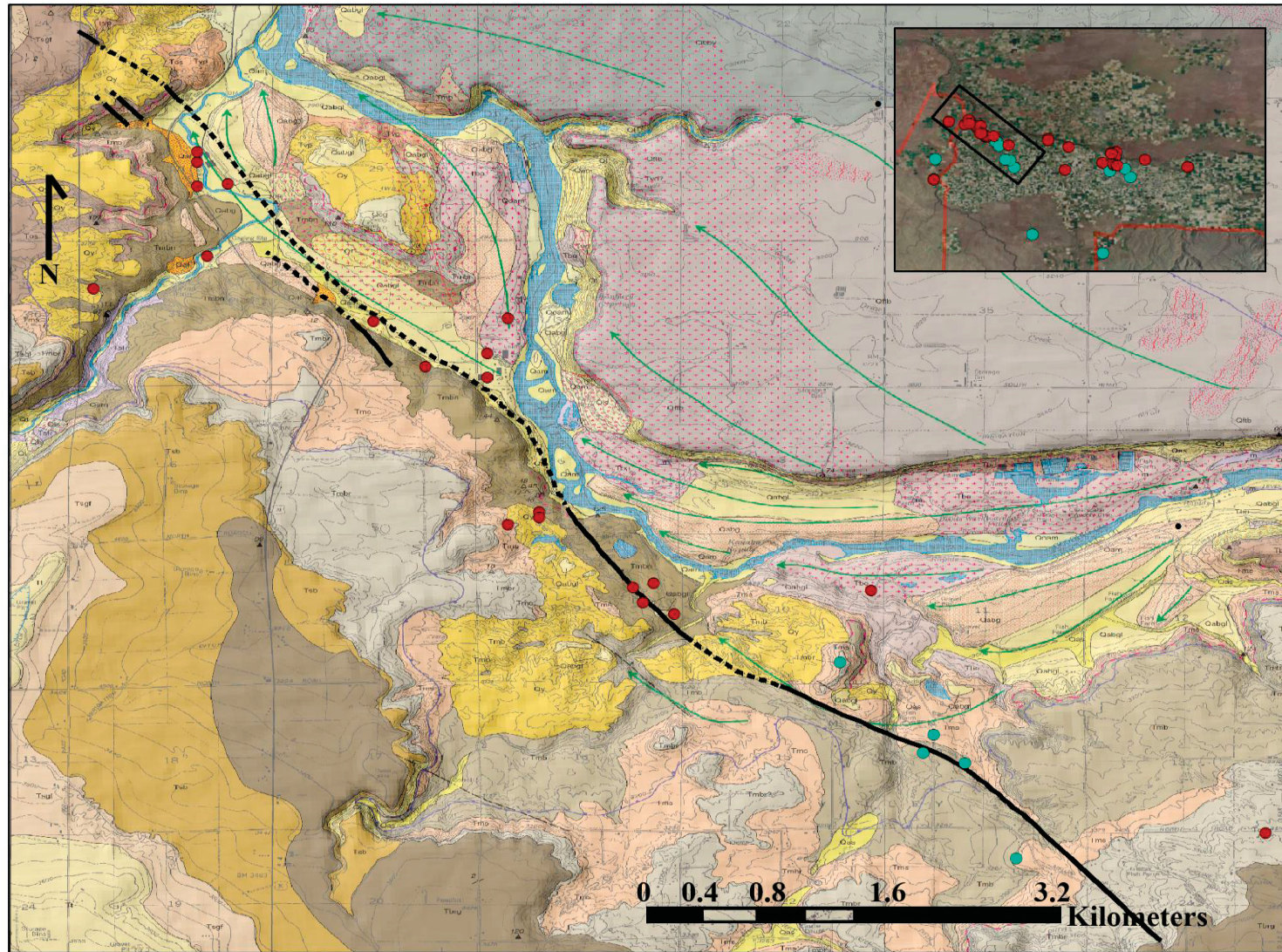


Figure 17. Banbury thermal area geologic map showing distribution of Ca-HCO_3 (blue) and Na-HCO_3 (red) waters along a normal fault. Geologic map (Gillerman et al., 2005) shows transition from Tertiary basalt flows south of the river to Quaternary basalt flows to the north. Green lines represent flood lines of the Bonneville Flood (c.15 ka). Red stipple areas correspond to dune trends.

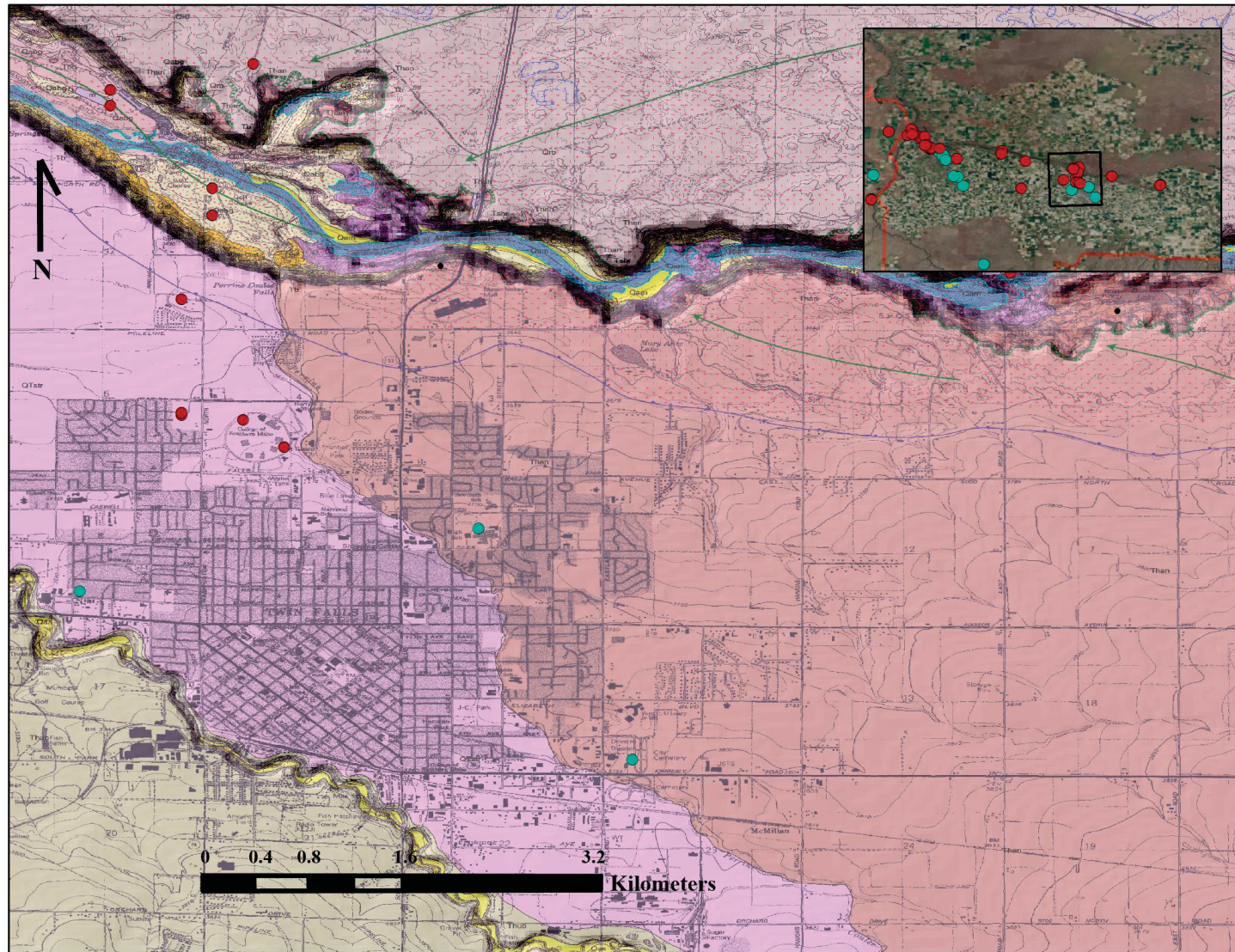


Figure 18. Twin Falls thermal area showing distribution of Ca-HCO_3^- (blue) and Na-HCO_3^- (red) waters. Geologic map (Othberg et al., 2005) shows the contacts between different Quaternary basalt flows south of the river and the outcropping of Idavada Volcanics (Shoshone Falls Rhyolite) near the river (dark purple).

CHAPTER 4: GEOTHERMOMETRY ESTIMATION OF RESERVOIR TEMPERATURES IN THE TWIN FALLS – BANBURY THERMAL AREA

The following section details the various approaches to calculate reservoir temperatures using geothermometry techniques as well as account for the effects of the mixing described in the previous section. Conventional along with recently developed techniques are utilized in order to show differences in temperature estimation and also to account for both simple and reactive mixing. While chemical and isotope geothermometry have been applied to the Twin Falls – Banbury area, mixing models and multicomponent equilibrium geothermometry techniques have not been applied prior to this study.

4.1 Conventional Geothermometry

Conventional geothermometers (as referred to in this study) are empirically or experimentally determined equations that are often utilized in geothermal exploration to predict deep reservoir temperatures from surface expressions or water wells. They are based on the relationship between fluid constituents (solutes, gases, and isotopes of elements) and fluid temperature. Most are based on temperature dependent chemical equilibrium reactions involving an assemblage of hydrothermally altered minerals. Various solute geothermometers have been continuously developed and improved upon since the 1960s. Of the many chemical and isotope geothermometers developed, the most prevalent cation geothermometers and silica geothermometers will be discussed and utilized in this study. It is important to note that all of the geothermometers discussed in this section make several key assumptions as outlined by Fournier et al. (1974):

- 1) Dissolved “indicator” constituent concentrations are fixed by temperature-dependent reactions between water and rock.
- 2) An adequate supply of all reactants is available.
- 3) Equilibrium with respect to indicator constituents in the reservoir is attained.
- 4) No re-equilibration occurs after the water leaves the reservoir
- 5) There is no mixing of different waters during ascension.

The assumption of equilibrium has been generally accepted as valid in the geothermal community through the study of well discharges among several geothermal fields. However, the assumption that no secondary processes have altered the fluid during its ascent from reservoir to the surface is rarely a reality. Fluids may cool adiabatically (boil) during ascent or mix with more dilute waters resulting in oversaturation and undersaturation of certain geothermal indicator constituents respectively. While some conventional geothermometers have attempted to account for the effects of boiling, none of the conventional geothermometers presented herein have accounted for dilution. For these reasons, it is important to keep the limitations and suitability of a particular geothermometer to a rock/fluid type in mind when utilizing for temperature estimation.

Silica Geothermometers

Silica geothermometers were first proposed by Fournier and Rowe (1966). They are based on the prograde relationship between silica solubility and rising fluid temperature. They are widely used in almost all geochemical investigations of geothermal systems around the world (Verma, 2000). Silica geothermometers have been developed for a variety of silica

mineral species but they are based on the basic reaction producing dissolved silica in the form H_4SiO_4 from various silica minerals:



Dissolved silica concentrations in most natural waters are not influenced by “common ion effects” or the formation of complex ions like other geothermal indicators (Fournier, 1977). Additionally, the assumption of adequate reactant supply is generally valid for dissolved silica. In the case of the Twin Falls – Banbury thermal area, thermal waters are hosted within rhyolites of the Idavada volcanics making the silica geothermometers the most appropriate of the conventional geothermometers for temperature estimation.

Quartz solubility seems to control the dissolved silica content of most geothermal systems $> 180^\circ\text{C}$. Quartz geothermometers are suggested for use in the temperature range of $120\text{--}330^\circ\text{C}$ if certain conditions are met: equilibrium with quartz, pore-fluid pressure fixed by vapor pressure of pure water, no mixing, no conductive cooling or adiabatic cooling (Fournier and Rowe, 1966). The quartz geothermometer was later modified to account for oversaturation produced by steam loss (Fournier, 1973). Two geothermometers were produced, one based on silica concentration with maximum steam loss at 100°C and one with no steam loss at all. However, the most widely used quartz geothermometer was developed by Fournier and Potter (1982). All are shown below where concentrations of silica (SiO_2 and S) are in units of mg/kg.

Quartz - Maximum Steam Loss (Fournier, 1977)

$$t = \frac{1522}{5.75 - \log(\text{SiO}_2)} - 273.15$$

Quartz - No Steam Loss (Fournier, 1977)

$$t = \frac{1309}{5.19 - \log(\text{SiO}_2)} - 273.15$$

Quartz Geothermometer (Fournier and Potter, 1982)

$$t = -42.198 + 2.883 \times 10^{-1} S - 3.668 \times 10^{-4} S^2 + 3.1665 \times 10^{-7} S^3 + 70.34 \log S$$

Another widely utilized silica geothermometer is the chalcedony geothermometer.

Chalcedony is widely regarded to be applicable for lower temperatures. However, Fournier (1991) pointed out the ambiguity between Quartz and Chalcedony as quartz controls solubility below 180 °C at some locations and chalcedony at others. Residence time, fluid temperature, rock type and fluid type all effect the controlling phase. Chalcedony, which is comprised largely of very fine quartz and mogonite crystals, probably all changes to quartz with time which makes the age of a thermal fluid of particular importance (Gíslason et al., 1997).

Chalcedony – Maximum Steam Loss (Arnórsson et al., 1983)

$$t = \frac{1264}{5.31 - \log(\text{SiO}_2)} - 273.15$$

Chalcedony – No Steam Loss (Arnórsson et al., 1983)

$$t = \frac{1112}{4.91 - \log(\text{SiO}_2)} - 273.15$$

A less commonly applied silica geothermometer is the amorphous silica geothermometer (Fournier, 1977). Due to the much higher solubility of amorphous silica compared to other silica polymorphs (Figure 19 below), the amorphous silica geothermometer yields very low temperature estimates for waters if amorphous silica is not the dominant species.

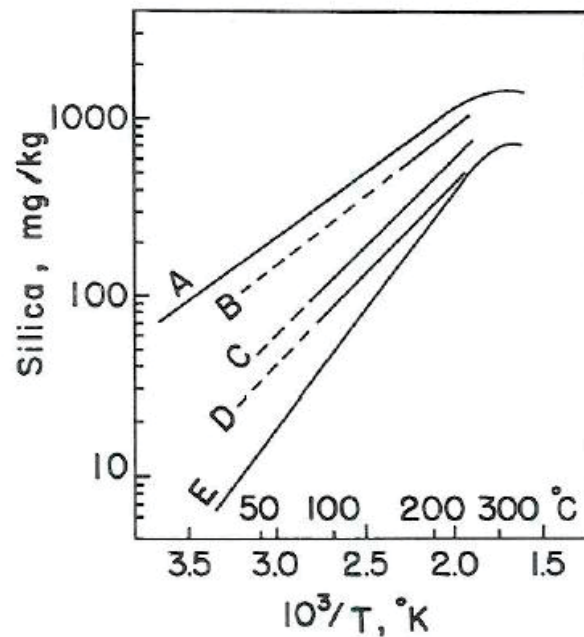


Figure 19. Solubility of silica polymorphs vs. temperature: A = Amorphous silica, B = Opal – CT, C = α -cristobalite, D = chalcedony, and E = quartz (Fournier, 1977).

Amorphous Silica (Fournier, 1977)

$$t = \frac{731}{4.52 - \log(\text{SiO}_2)} - 273.15$$

Unfortunately, there is a wide dispersion in temperature predictions amongst silica geothermometers even when applying one geothermometer to all the wells in a geothermal

field (Verma, 2000). This is primarily due to secondary alteration effects: steam loss, mixing, and re-equilibration (Truesdell and Fournier, 1977).

The silica geothermometers applied to the two water types of the Twin Falls – Banbury thermal area give varied results with the chalcedony temperature estimates being consistently less than the quartz estimates. This is to be expected and the amorphous silica estimates yielding unrealistically low (below surface temperature and negative values). Overall, The Ca-HCO₃ type waters yield lower temperature estimates than the Na-HCO₃ type waters due to the higher silica concentrations of the Na-HCO₃ type waters. Quartz temperature estimates for the Na-HCO₃ type waters averaged 117 °C with a 36 °C range between all measurements while the Ca-HCO₃ type waters yielded a 108 °C average with a much higher range of 68 °C due to the larger range of SiO₂ concentrations. Chalcedony temperature estimates yield an average of 91 °C with a 39 °C range for the Na-HCO₃ type waters while the Ca-HCO₃ type waters averaged 80 °C with a range of 73 °C. There appears to be no significant correlation between silica-based predicted temperatures and field temperatures with many cooler water samples yielding higher estimates than some hotter samples.

Cation Geothermometers

The other often utilized type of chemical geothermometers are called cation geothermometers. These geothermometers are based on empirical and experimental cation exchange reactions with temperature-dependent equilibrium constants. A widely used cation geothermometer is the Na/K geothermometer (Fournier, 1979; Giggenbach 1988; Truesdell, 1976; Arnórsson et al., 1983) based on the exchange of Na⁺ and K⁺ between two coexisting

alkali feldspars like the exchange between albite and various K-feldspars shown in the equation below.



The reaction results in a decreasing Na/K ratio with increasing fluid temperature. While ratios may be still affected by secondary processes they are considered less likely to be affected by dilution and steam loss. The Na/K geothermometer is suitable for temperatures between 100 °C and 350 °C as it is slower to re-equilibrate than the quartz geothermometers. However, the Na/K geothermometer is not useful in acidic waters which would not be in equilibrium with feldspars. More importantly for this study, the Na/K geothermometer is not useful in waters with high calcium concentrations like many of the mixed thermal waters found in and around the ESRP.

Na/K (Truesdell, 1976)

$$t = \frac{856}{\log\left(\frac{Na}{K}\right) + 0.857} - 273.15$$

Na/K (Fournier, 1979)

$$t = \frac{1217}{\log\left(\frac{Na}{K}\right) + 1.483} - 273.15$$

Na/K (Arnórsson, 1983)

$$t = \frac{933}{\log\left(\frac{Na}{K}\right) + 0.993} - 273.15$$

To account for the effects of increased calcium concentrations, Fournier and Truesdell (1973) suggested the use of a Na-K-Ca geothermometer. While the amount of total Ca in most hydrothermal systems is controlled by the solubility of calcium-bearing carbonates (usually calcite), calcium also enters into various silicate reactions and in turn is in competition with sodium and potassium. Because natural waters are generally comprised of much more sodium than potassium and aqueous potassium tends to change so as to satisfy an equilibrium expression with a given Na/Ca ratio; a change in aqueous potassium in response to an increase in calcium will be far more evident in calculations involving the Na/K ratio. If waters pick up additional calcium as they migrate upward, the temperature estimates made using the Na/K geothermometer will be too low. Waters already containing increased concentrations in calcium ($\sqrt{M_{Ca}/M_{Na}} > 1$) capable of depositing calcium carbonate upon descent will result in temperature estimations that are too high. For this reason, the reaction configurations involving only Ca^{2+} , Na^+ , K^+ were transposed into a generalized form:

$\text{Log } K_e = \log (Na/K) + \beta \log (\sqrt{Ca} / Na)$, where β depends upon the stoichiometry of the reaction.

Based on the distribution of natural thermal waters, Fournier and Truesdell (1973) originated a geothermometer equation which could be used to calculate temperatures based upon the relationship between Ca^{2+} , Na^+ , and K^+ . The equation works for two possible β values: $\beta = 1/3$ for waters equilibrating above 100 °C and $\beta = 4/3$ for waters equilibrating

under 100 °C. The user of the geothermometer must calculate $\log (\sqrt{Ca} / Na) + 2.06$. If the value is positive, the user applies $\beta = 4/3$ and if negative $\beta = 1/3$. The equation utilizes the assumptions of: 1) excess silica is present (generally valid) and 2) aluminum is conserved in solid phases (not true but so little aqueous aluminum is usually present that it can be neglected).

$$t = \frac{1647}{\log \frac{Na}{K} + \beta \log \frac{\sqrt{Ca}}{Na} + 2.24} - 273.15$$

Mg correction for the Na-K-Ca geothermometer

Because most geothermal fluids > 180 °C contain < 0.2 mg/kg magnesium, a correction is necessary for those fluids which contain higher amounts of magnesium (Fournier and Potter, 1979). The temperature dependence of magnesium is largely controlled by formation of chlorite in thermal waters and also biotite and actinolite at very high temperature. In cooler thermal systems, magnesium may be incorporated into clays and carbonates. The correction was devised empirically to account for waters that have high magnesium concentrations because they are saline or because the reservoir temperature is below 180 °C. It was not intended to deal with waters that have been subjected to mixing and have high magnesium concentrations because of cold groundwater influence. In general, the presence of high magnesium gives anomalously high temperature results when using the Na-K-Ca geothermometer. However, the use of a magnesium correction on a mixed thermal water will result in an underestimation of true reservoir temperature. The correction is applied as such:

- 1) If the temperature estimate from the Na-K-Ca geothermometer is < 70 °C, do not apply.

- 2) Calculate correction factor R using equivalent units:
- 3) Do not apply the correction if $R > 50$ and assume the water is from cool equilibrium conditions with temperatures close to measured surface temperature regardless of geothermometry.
- 4) If the Na-K-Ca estimated temperature is $> 70^\circ\text{C}$ and $R < 50$, apply the correction equation (Fournier and Potter, 1979) to obtain Δt .
- 5) Subtract Δt from the Na-K-Ca estimated temperature.

$$R = \frac{Mg}{Mg+Ca+K}(100)$$

$$\Delta t_{mg} = 10.66 - 4.7415(R) + 325.867 \log(R) - \frac{1.0321 \times 10^5 (\log R)^2}{T} - \frac{1.96683 \times 10^7 (\log R)^2}{T^2} + \frac{1.6053 \times 10^7 (\log R)^3}{T^2}$$

K-Mg Geothermometer

The K-Mg geothermometer (Giggenbach et al., 1988) was developed for application to systems where sodium and calcium are not in equilibrium between the thermal fluid and rock. Unfortunately, the K-Mg system is distinct from other geothermal indicators in that fluid-rock equilibrium is often attained at lower temperatures. Due to this fast re-equilibration, results from the K-Mg geothermometer are often underestimations particularly in mixed waters with elevated magnesium concentrations.

$$t = \frac{4410}{14.0 + \log(K^2/Mg)} - 273.15$$

Na-Li Geothermometer

The Na-Li geothermometer (Fouillac et al., 1981) is based on the decrease in the Na/Li ratio with increasing fluid temperature. Lithium is regarded as one of the more conservative elements in hydrothermal systems and is slow to re-equilibrate during ascent. The controlling equilibria of this geothermometer are based on cation exchange reactions between clays and zeolites. Two geothermometers were created: one to be applied for low to moderately saline waters (<11000 mg/kg Cl⁻) and the other for marine waters. All of the waters in this study fall in the first category with the applicable geothermometer listed below.

$$t = \frac{1195}{0.130 + \log(mNa/mLi)} - 273.15$$

When applied to the water samples collected in this study, the cation geothermometers give highly varied results for the exact same well/spring. The Na/K geothermometers tend to yield very high results for Ca-HCO₃ waters likely because of high calcium concentrations. In contrast, Na-HCO₃ waters with lower calcium concentrations likely picking up additional calcium during ascent to the surface yield much lower Na/K temperature predictions some of which are below measured field temperatures. Because of the presence of calcium and the lack of magnesium in the Na-HCO₃ waters, the Na-K-Ca geothermometer is likely to yield more realistic results for these thermal features. Temperature estimates for Na-HCO₃ waters using this technique range from 98 °C to 166 °C with an average of 126 °C. In contrast, the abundance of magnesium in the Ca-HCO₃ waters yields much higher temperature predictions ranging from 82 °C to 258 °C.

The high magnesium concentrations of the Ca-HCO₃ waters also makes the Mg-correction for the Na-K-Ca geothermometer inapplicable likely resulting in overcorrections yielding lower than actual temperature estimates according to its originators (Fournier and Potter, 1979). The Na-Li geothermometer results are highly variable while the K-Mg geothermometer yields temperature estimates that are unrealistic (below surface temperatures or negative values). All of the temperature estimates produced by conventional geothermometry are listed below in Tables 5-8. The large disparity in temperature estimates produced by these techniques highlights the shortcomings of estimators based on few chemical species under very precise conditions that may not be present in the thermal reservoir of this study area. The results from conventional geothermometry methods support further evaluation using both models to account for mixing and multicomponent equilibrium geothermometry methods that utilize reservoir specific alteration minerals to provide more realistic temperature estimates.

Table 5. Silica geothermometer temperature estimates for the Na-HCO₃ type waters of the Twin Falls – Banbury hydrothermal system. All estimates are given in degrees Celsius.

Na-HCO ₃ Type Waters	Qtz (No Steam Loss)	Qtz (Steam Loss)	Amorphous Silica	Chalcedony	Quartz	Chalcedony (Steam Loss)	Chalcedony (No Steam Loss)
	Fournier (1977)				Fournier and Potter (1982)	Amorsson et al. (1983)	Amorsson et al. (1983)
CC-11	137	132	17	110	137	108	109
CC-14	114	113	-4	85	114	88	85
CC-51	111	111	-6	82	112	85	83
CC-52	118	116	0	89	118	91	89
CC-53	119	118	1	91	120	93	91
CC-55	115	114	-2	86	116	89	87
CC-40	133	130	14	106	134	105	105
CC-42	139	134	18	112	139	110	111
CC-45	105	106	-11	76	106	80	77
CC-46	106	106	-11	76	106	81	77
CC-48	127	124	8	100	127	100	99
LY82-3	128	125	8	100	128	100	99
LY82-4	126	124	7	99	127	99	98
LY82-5	129	126	10	101	129	101	101
LY82-6	129	126	10	101	129	101	101
LY82-7	116	115	-2	87	116	90	87
LY82-11	130	127	11	103	130	102	102
LY82-12	114	113	-4	85	114	88	85
LY82-15	107	107	-9	78	108	82	79
LY82-18	105	105	-12	75	105	79	76
LY82-19	103	103	-13	73	103	78	74
LY82-20	103	103	-13	73	103	78	74
LY89-1	105	105	-12	75	105	79	76
LY89-2	111	110	-7	81	111	85	82
LY89-4	126	124	7	99	127	99	98
LY89-8	122	120	3	93	122	95	93
LY89-9	104	104	-12	74	104	79	75
LY89-11	116	115	-2	87	116	90	87
LY89-12	126	124	7	99	127	99	98
LY89-13	121	119	3	93	121	94	93
LY89-14	115	114	-2	86	115	89	87
LY89-15	116	115	-2	87	116	90	87
LY89-22	106	106	-10	77	107	81	78
M91-7	116	115	-2	87	116	90	87
M91-8	123	121	4	95	123	96	95
M91-11	106	106	-10	77	107	81	78
M91-13	111	110	-7	81	111	85	82
M91-14	115	114	-2	86	115	89	87

Table 6. Silica geothermometer temperature estimates for the Ca-HCO₃ type waters of the Twin Falls – Banbury hydrothermal system. All estimates are given in degrees Celsius.

Ca-HCO ₃ Type Waters	Qtz (No Steam Loss)	Qtz (Steam Loss)	Amorphous Silica	Chalcedony	Quartz	Chalcedony (Steam Loss)	Chalcedony (No Steam Loss)
	Fournier (1977)				Fournier and Potter (1982)	Arnorsson et al. (1983)	Arnorsson et al. (1983)
CC-8	104	104	-12	74	104	79	75
CC-9	120	118	1	91	120	93	91
CC-10	118	116	0	89	118	91	89
CC-12	98	99	-18	67	98	73	69
CC-13	100	101	-15	70	101	75	72
CC-54	110	109	-7	80	110	84	81
LY82-13	129	126	10	101	129	101	101
LY89-3	114	113	-4	85	114	88	85
LY89-5	119	117	1	90	119	92	90
LY89-6	130	126	10	102	130	102	101
LY89-7	115	114	-2	86	115	89	87
LY89-10	120	118	1	91	120	93	91
LY89-17	119	117	1	90	119	92	90
LY89-18	110	109	-7	80	110	84	81
LY89-29	100	101	-16	70	100	75	71
LY89-30	62	67	-48	29	62	40	33
LY89-32	107	107	-9	78	108	82	79
LY89-33	86	89	-28	55	86	62	57
LY89-34	109	109	-8	79	109	83	80
LY89-35	111	110	-7	81	111	85	82
LY89-36	114	113	-3	86	115	88	86
LY89-37	104	104	-12	74	104	79	75
LY89-38	89	92	-25	59	90	66	61
M91-12	102	103	-14	72	102	77	73

Table 7. Cation geothermometer temperature estimates for the Na-HCO₃ type waters of the Twin Falls – Banbury hydrothermal system. All estimates are given in degrees Celsius.

Na-HCO ₃ Type Waters	Na-K				Na-K-Ca	Na-K-Ca (Mg Corrected)	Na-Li	K-Mg
	Truesdell (1976)	Fournier (1979)	Giggenbach (1988)	Arnorsson (1983)	Fournier and Truesdell (1973)	Fournier and Potter (1979)	Fouilliac et al. (1988)	Giggenbach et al. (1988)
CC-11	45	93	114	57	112	112	119	-19
CC-14	96	140	160	107	132	132	63	7
CC-51	96	140	160	107	131	131	99	9
CC-52	58	105	126	69	118	118	95	-7
CC-53	60	108	128	72	118	118	69	-6
CC-55	74	120	141	85	129	129	144	-9
CC-40	34	83	104	46	103	103	124	-11
CC-42	52	101	121	64	112	112	119	-17
CC-45	132	171	189	141	144	144	184	6
CC-46	156	191	208	164	154	140	190	10
CC-48	40	89	110	52	102	102	118	-3
LY82-3	23	73	95	35	98	98	114	15
LY82-4	30	79	101	42	98	98	128	14
LY82-5	33	83	104	45	103	103	110	14
LY82-6	56	104	125	68	116	116	124	11
LY82-7	59	106	127	70	114	114	131	12
LY82-11	56	104	125	68	108	108	124	11
LY82-12	51	100	120	63	113	113	110	13
LY82-15	113	155	174	124	136	136	165	9
LY82-18	116	157	176	126	133	133	169	10
LY82-19	114	156	175	125	133	133	168	13
LY82-20	133	172	190	143	141	136	169	13
LY89-1	144	181	199	153	146	140	184	12
LY89-2	153	189	206	162	149	118	188	18
LY89-4	177	208	224	185	166	165	205	-1
LY89-8	48	97	118	60	107	107	111	14
LY89-9	77	124	144	89	112	61	104	38
LY89-11	98	142	161	109	136	136	100	-1
LY89-12	90	135	155	101	136	136	84	1
LY89-13	54	102	123	65	109	109	22	10
LY89-14	59	107	128	71	114	114	39	10
LY89-15	85	130	150	96	132	132	-	0
LY89-22	171	204	220	179	165	154	-	3
M91-7	85	130	150	96	132	132	-	0
M91-8	153	189	206	162	157	156	-	2
M91-11	171	204	220	179	165	154	-	3
M91-13	60	107	128	71	118	118	-	4
M91-14	49	97	118	61	110	110	-	-7

Table 8. Cation geothermometer temperature estimates for the Ca-HCO₃ type waters of the Twin Falls – Banbury hydrothermal system. All estimates are given in degrees Celsius.

Ca-HCO ₃ Type Waters	Na-K				Na-K-Ca	Na-K-Ca (Mg Corrected)	Na-Li	K-Mg
	Truesdell (1976)	Fournier (1979)	Giggenbach (1988)	Arnórsson (1983)	Fournier and Truesdell (1973)	Fournier and Potter (1979)	Fouilliac et al. (1988)	Giggenbach et al. (1988)
CC-8	101	144	163	111	135	107	50	14
CC-9	221	243	257	227	175	107	184	15
CC-10	231	250	263	235	177	106	186	16
CC-12	23	73	94	35	82	82	203	26
CC-13	39	88	110	51	94	94	206	27
CC-54	175	207	223	183	150	65	144	32
LY82-13	296	298	307	296	194	102	214	17
LY89-3	194	222	237	200	165	99	192	18
LY89-5	199	226	241	206	167	108	193	17
LY89-6	229	249	262	233	180	148	181	8
LY89-7	248	263	275	251	183	98	196	16
LY89-10	252	267	278	256	186	102	191	14
LY89-17	270	279	290	271	193	113	193	11
LY89-18	269	279	289	271	188	84	170	19
LY89-29	294	297	306	294	176	39	133	42
LY89-30	318	313	320	315	204	40	197	21
LY89-32	641	506	487	597	258	106	156	15
LY89-33	433	389	387	419	211	101	157	26
LY89-34	399	368	368	389	215	140	239	14
LY89-35	351	336	340	345	201	119	-	19
LY89-36	321	316	323	319	193	111	193	21
LY89-37	269	279	289	271	171	87	91	34
LY89-38	606	488	472	568	247	95	198	21
M91-12	243	260	272	247	169	78	183	30

4.2 Silica-Enthalpy Mixing Models for the Twin Falls – Banbury Thermal Area

The evidence for mixing provided by the use of binary diagram trends and Giggenbach diagram analysis (partial equilibration) suggests that conventional geothermometry techniques cannot be taken at face value. Adjustments for dilution should be made to enable more accurate temperature prediction. Several models have been developed to deal with simple mixing (non-reactive dilution) including the silica-enthalpy model (Fournier and Truesdell, 1974) and the silica-carbonate mixing model (Arnórsson, 1985). The silica-enthalpy diagram was chosen for use in this study due to the abundance of silica within the reservoir rocks satisfying the second geothermometry assumption discussed previously. The silica-carbonate model was excluded due to the variability in carbonate measurements from

field titrations and the effects of CO₂ degassing on carbonate concentrations. The silica-enthalpy mixing model is based on the positive relationship between silica solubility and increasing temperature. To apply the model, temperatures for both the cold water and thermal components must be known. However, in this model, respective enthalpies of sample waters calculated from field temperatures are used as plot coordinates rather than temperature because enthalpy is conserved as waters mix and boil whereas temperature is not (e.g., Fournier and Truesdell, 1974).

The model yields two temperature estimates representing one situation in which waters are subjected to boiling prior to mixing and one where no boiling occurs. Enthalpy vs quartz solubility curves are used corresponding to the two separate scenarios. A straight line is drawn from the point representing the non-thermal component of the mixed water (lowest silica and enthalpy), through the mixed water thermal samples. The intersection of this line with the quartz solubility curve gives the enthalpy of the hot-water component at reservoir conditions if there was no boiling prior to mixing. The enthalpy at the boiling temperature (100°C) which is 419 J/g is intersected with the projected trend line. From this intersection, a horizontal line is drawn to the quartz maximum steam loss line. This new enthalpy value can be used to calculate the reservoir temperature if boiling occurred prior to mixing (Fournier, 1977).

In order to better constrain the temperature estimates from the mixing models, evidence for and against the possibility of boiling must be considered. As mentioned previously, shifts in δD concentrations may be explained by boiling. Truesdell et al. (1978) demonstrated the enrichment of deuterium from fractionation due to boiling in both a single-stage and continuous steam loss scenario. They observed increases of 1.44 times and 9.1% for

chloride and δD concentrations respectively for single-stage steam loss and 1.41 times 3.1% for continuous steam loss for some of the thermal waters in Yellowstone National Park. These calculations were made utilizing a known recharge water deuterium concentration and assuming all heat loss was due to boiling from 360 °C parent water to the 93 °C boiling point.

Because local area groundwater deuterium concentrations differ from thermal water concentrations and thermal waters are likely much older (Pleistocene), a local Pleistocene deuterium concentration would be needed for such calculations. However, given a likely reservoir temperature of about 160 °C (Conrad et al., 2015) and a local boiling point of about 95 °C, one can approximate how much boiling may occur in the system. Assuming that all of the heat loss in the system is due to steam loss (not likely due to evidence for groundwater mixing), we can estimate a percentage of water lost to boiling. The total enthalpy lost due to vaporization from 160 °C to 95 °C is about 277 kJ/kg and the latent heat of enthalpy for water is about 2257 kJ/kg (Marsh, 1987). Relating heat loss and latent heat of vaporization to evaporative mass, a maximum of about 12 % of thermal water per kg could potentially be lost to boiling. Due to low chloride concentrations of thermal waters in the study area and lack of recharge deuterium values, effects from this small proportion of boiling are not likely to be evident in water chemistry. Additionally, the lack of fumaroles, sinter deposits, and supersaturation of silica suggest that influence of boiling is of minimal importance to this area.

The model developed by Fournier and Truesdell (1974) used only quartz as the controlling dissolved silica component. This approach has been modified in this study to include a chalcedony-enthalpy mixing model in addition to the quartz-enthalpy model in order to account for the possibility of chalcedony controlling silica solubility. The results are

presented below in Figures 20-21. Because there is little evidence supporting a maximum boiling scenario in the study area, temperature estimates from these models are likely constrained to the lower (no steam loss) estimates. The estimated reservoir temperatures from the quartz-enthalpy diagram are about 143 °C (no steam loss) to 175 °C (max steam loss). The fraction of thermal water incorporated into mixing for the no steam loss scenario is about 39%. The chalcedony-enthalpy model yields a lower temperature range of 120 °C (no steam loss) to 142 °C (max steam loss). The fraction of thermal water incorporated into mixing for the no steam loss scenario is about 49%. While the temperature estimates of the mixing models may be more realistic than those of conventional geothermometers, the mixing models applied in this section account only for simple non-reactive mixing and are based on only one dissolved indicator constituent.

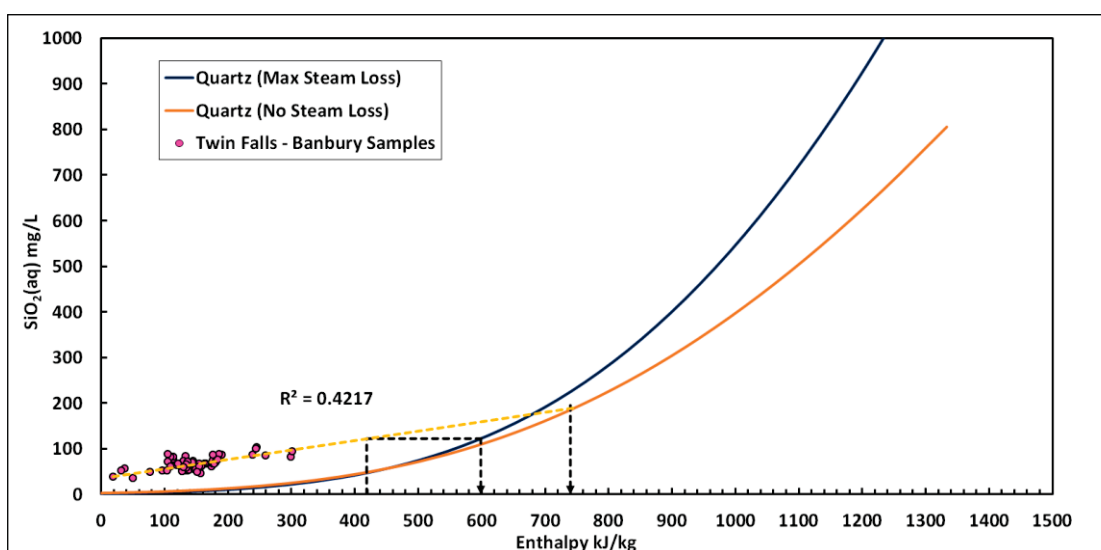


Figure 20. Silica-enthalpy model (quartz) applied to the thermal waters of the Twin Falls – Banbury system. The trend line (yellow) passes through both end member waters and is projected to the no steam loss line (orange). The intersection of the trend line with the boiling point (419 kJ/kg) is projected to the max steam loss line (blue). Temperature estimations are obtained from the resulting two enthalpy values.

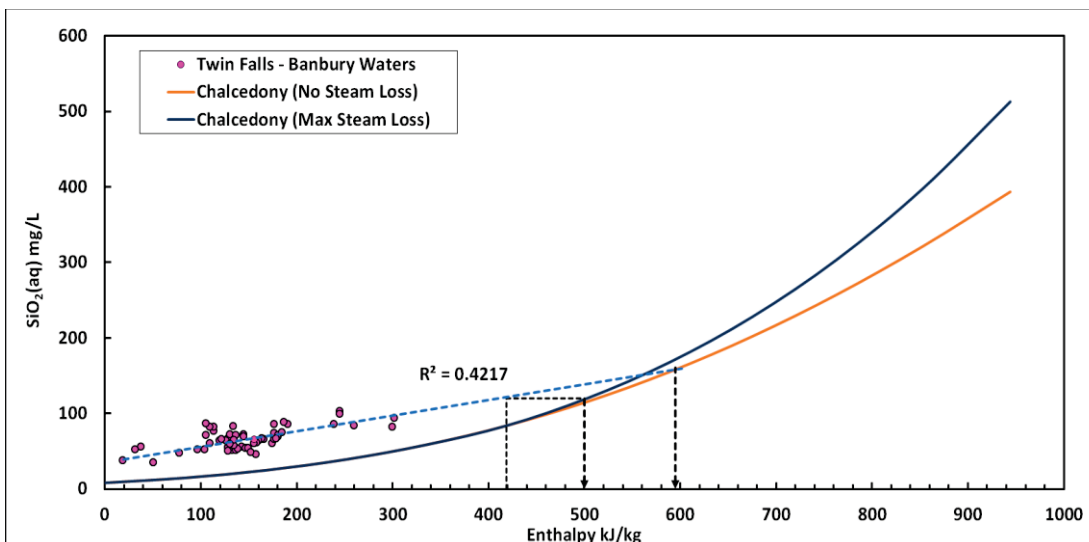


Figure 21. Silica-enthalpy model (chalcedony) applied to the thermal waters of the Twin Falls – Banbury system. The trend line (yellow) passes through both end member waters and is projected to the no steam loss line (orange). The intersection of the trend line with the boiling point (419 kJ/kg) is projected to the max steam loss line (blue). Temperature estimations are obtained from the resulting two enthalpy values.

4.3 MEG Analysis of the Twin Falls – Banbury Area

Recent developments in multicomponent equilibrium geothermometry (MEG) have led to appreciable improvement in the reliability and accuracy of reservoir temperature estimations compared with conventional geothermometry (Spycher et al., 2011; Smith et al., 2012; Neupane et al., 2013, 2014; Palmer et al., 2014; Cannon et al., 2014; Neupane et al., 2015). The concept behind MEG originated in the 1980s (Michard and Roekens, 1983; Reed and Spycher, 1984) and is based on the estimation of reservoir temperature through saturation indices of several minerals likely to be in equilibrium with the thermal water. The use of an entire chemical suite rather than a couple of basis species has an obvious advantage over conventional techniques. While MEG is still affected by the same secondary processes that violate the assumptions of geothermometry (boiling, dilution, etc.), new techniques allow for the correction of these processes if they can be identified. RTest (Reservoir Temperature

Estimator) is one such tool that can accomplish these corrections by reconstructing the last equilibrated composition of a given thermal fluid (Palmer et al., 2014; Neupane et al., 2015). Validation of the RTest tool was demonstrated by Neupane et al. (2015) through the successful matching of estimated reservoir temperatures and actual bottom-hole temperatures of five geothermal power plants.

RTest uses a likely reservoir mineral assemblage (RMA) in the prediction of the thermal fluid temperature within the reservoir. The reservoir temperature is taken to be the one in which all of the mineral saturation indices are in equilibrium shown by having a summed $\log(Q_i/K_{i,T})$ of zero where Q_i and $K_{i,T}$ are the ion activity product and temperature dependent equilibrium constant for the i^{th} mineral respectively. RTest accomplishes temperature estimation by utilizing the React module of The Geochemist's Workbench® (Bethke and Yeakel, 2012) in order to model equilibrium conditions among minerals, aqueous species, and gaseous phases with respect to geochemical reactions. RTest couples the React module with the model-independent optimization software PEST (Doherty, 2013) to optimize parameters including CO_2 fugacity, amount of water gained or lost, and temperature. These parameters correspond to secondary alteration processes that affect fluid composition. Through the use of these parameters alone, RTest is capable of compensating for the effects of boiling and simple (non-reactive mixing). However, if a cooler water end member composition is known, RTest can “extract” this end member through inverse modeling thereby accounting for reactive mixing.

The equilibrium reservoir temperature is calculated through the minimization of the objective function, Φ . The objective function is essentially a weighted sum of squares of the saturation indices of the chosen RMA where RTest acts to minimize the collective distances

away from zeros for all saturation indices. The objective function is given by the following equation:

$$\Phi = \sum (SI_i w_i)^2$$

where SI_i is the saturation index for the i^{th} mineral and w_i is the weighting factor. The weighting factor w_i is based on the number of thermodynamic components within each mineral to ensure that each mineral contributing to equilibrium with the thermal fluid is considered equally and not skewed by reaction stoichiometry (Neupane et al., 2015).

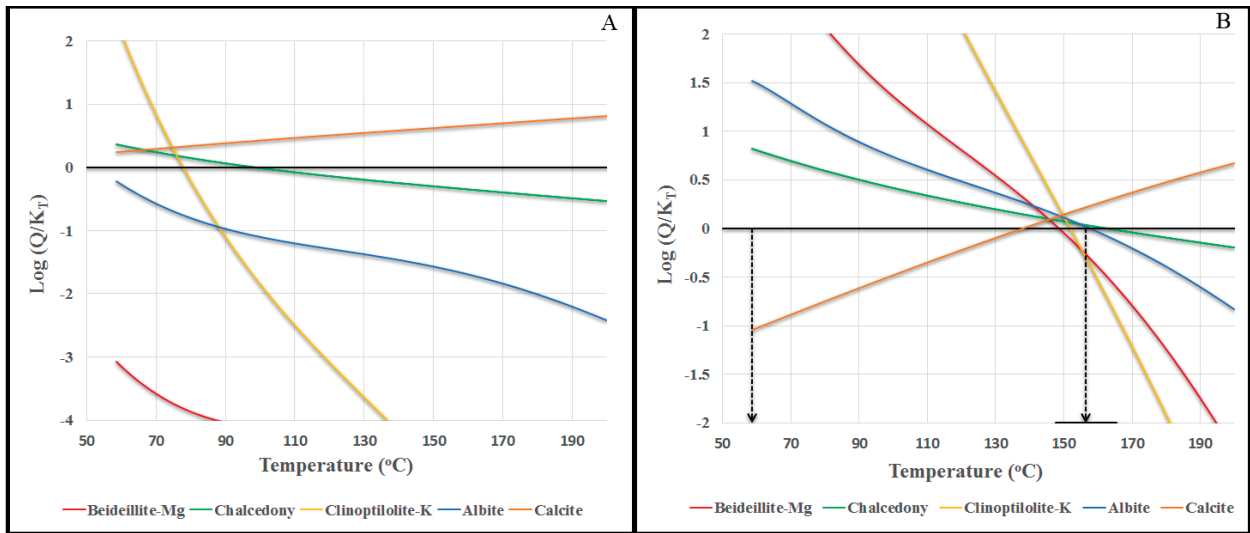


Figure 22. Temperature estimation for Banbury Hot Springs showing the $\log Q/K_T$ curves for minerals (Calcite, Chalcedony, Beidellite – Mg, Clinoptilolite-K, and Albite) calculated using original water chemistry. A) Without optimization of H_2O mass and CO_2 fugacity B) Optimized $\log Q/K_T$ curves showing field temperature (58.4°C), estimated temperature (158 °C), and error bar (black bar on x-axis).

The reservoir mineral assemblages used here are based on alteration mineral assemblages present in hydrothermally altered basalts and rhyolites. Early work has shown that rock type has less of an effect on geothermal alteration compared with temperature, fluid composition, and permeability (Browne, 1978; Henley and Ellis, 1983). Browne (1978)

demonstrated that basalts, rhyolites, andesites, and sandstones were all dominated by an alteration mineral assemblage including illite, calcite, pyrite, epidote, k-feldspar, albite, and quartz in the temperature range of 250 – 285 °C. However, there are important differences between basalt and rhyolitic alteration mineral assemblages particularly at lower (<200 °C) temperatures. At lower temperatures, secondary mineralization within geothermally altered basalts and rhyolites typically includes phyllosilicates, zeolites, oxides, hydroxides, and carbonates (Neuhoff et al., 1999; Weisenberger and Selbekk, 2009; Rodriguez, 2011). As temperatures increase, zones of mixed illite-smectite clays begin to dominate at 200-250 °C, chlorite-epidote at 250-300 °C, and epidote-actinolite at >300 °C. At temperatures < 200 °C kaolinite and smectite clays predominate with other minerals including zeolites, quartz and chalcedony, K-feldspar, calcite, and chlorite (Lonker et al., 1993; Larsson et al., 2002).

The main differences in geothermal alteration between basalts and the more silicic rhyolites and andesites are observed in clay mineralogy. Clays formed from the alteration of rhyolites and andesites are more Na⁺ and K⁺ rich compared to those formed in basalts. These clays are typically mixed illite-smectite clays as well as montmorillonites. In addition to being enriched with respect to Na⁺ and K⁺, alteration clay and zeolites in rhyolites and andesites tend to be more deficient in magnesium due to the low magnesium concentrations within these rock types (Bethke, 1986; Reyes, 1990; Mas et al., 2006).

The alteration minerals particular to this study area were based largely on the work of Sant (2012) who analyzed the alteration minerals within basalt core samples from the Kimberly well of the Project Hotspot (Shervais et al., 2013). This well lies just to the east of the study area in Burley, ID and penetrates the basalts of the upper aquifer system. Of particular importance are the smectite clays observed in core samples from 1042 meters to

1829 meters (3126 – 5487 ft.). Morse and McCurry (2002) also analyzed basalt core samples from the deep aquifer penetrating INEL-1 well located to the northeast of the study area on the Idaho National Laboratory. Both of these studies have attributed the boundary between the upper and lower aquifer systems to the development of these smectite clays. RTest provides a means of selecting minerals based on five rock types (Tholeitic, Calc-alkaline, Silicic, Siliciclastic, and Carbonates), 3 temperature ranges (low, 50-100 °C; moderate 150 to 300 °C; and high, >300 °C), and two water types (neutral and acidic) based on a review of 48 different geothermal systems (Palmer et al., 2014). Minerals used in this study along with their corresponding weighting factors are listed below in Table 9.

Table 9. Alteration minerals used in RTest inverse modeling with corresponding weighting factors (W_i)

Mineral	W_i
Calcite	1/2
Chalcedony	1
Beidellite Mg	1/6.65
Kaolinite	1/4
Clinoptilolite-Ca	1/13
Clinoptilolite-K	1/14
Saponite-Na	1/7.33
Saponite-K	1/7.165
Illite	1/6.65
Heulandite	1/7
Fluorite	1/3
Talc	1/7
Muscovite	1/7
Paragonite	1/7

4.4 RTest Results for the Twin Falls – Banbury Thermal Area

The following reservoir temperature estimates were made utilizing the MEG tool RTest in order to both better predict temperatures as compared with more conventional techniques and also test the rationale behind the three mixing scenarios presented in Chapter 1 (Simple Mixing, Flow-Pathway Mixing, and Mixing with Re-equilibration). The inverse modeling performed using RTest is capable of accounting for both simple mixing and reactive mixing through the removal of a mixing component. Pure water, local groundwater (recharge area), and an idealized intermediate water (based on binary diagram trends) were used in this study as mixing components.

No Mixing

Despite evidence for mixing, the possibility of no mixing was considered in the MEG approach. Allowing only temperature and CO₂ fugacity to fluctuate as optimization parameters, adequate convergence of saturation indices was not obtained for either Ca-HCO₃ or Na-HCO₃ type thermal waters using likely alteration mineral assemblages found in basalts and rhyolites. Results were slightly better for Ca-HCO₃ type waters but far from meaningful with objective function (Φ) values greater than or equal to 0.1.

Simple Mixing

The possibility of simple mixing between groundwater and thermal waters was considered in RTest modeling through the use of a 6 °C recharge area groundwater sample (Sample LY89-38) as the mixing component between the Ca-HCO₃ and Na-HCO₃ type thermal waters. Mixing between groundwater and the Na-HCO₃ type thermal waters is not supported through the use of RTest as all attempts of modeling this scenario resulted in a lack

of saturation index convergence for all likely mineral assemblages. However, mixing between groundwater and Ca-HCO₃ type thermal waters is supported through the use of RTest .

Objective function values (Φ) of less than 1×10^{-6} are obtained for some waters. These values are better than all previous studies utilizing RTest in MEG analyses including those which successfully validated actual bottom-hole temperatures of geothermal power plants (Cannon et al., 2014; Neupane et al., 2014; 2015). Simple mixing is also supported through the use of pure water as the mixing component in mixing with Na-HCO₃ type thermal waters.

Flow Pathway Reactive Mixing

Flow Pathway or reactive mixing was investigated using an “intermediate” composition water created from the binary diagram analysis in Chapter 3. Na-HCO₃ type thermal waters were mixed with water that contained amounts of K⁺, Ca²⁺, and Mg²⁺ taken from the intersection of the two trends presented in Figure 15. Na-HCO₃ type thermal waters were modelled with waters containing between 0.12-0.15 meq/kg K⁺, 0.5-0.7 meq/kg Ca²⁺, and 0.15-0.2 meq/kg Mg²⁺. This type of mixing was not supported in the attempts to mix thermal water with this “intermediate” composition as adequate conversion was not attained and temperatures at or near surface temperatures were predicted with standard deviations of temperatures reaching over +/- 150 °C. Additionally, mixing between Ca-HCO₃ and Na-HCO₃ type thermal waters is not supported through the use of RTest.

Re-equilibration

The possibility of re-equilibration may be gleaned from the RTest results. The reconstructed equilibrium water compositions produced by RTest modeling of the Ca-HCO₃ type thermal waters may be significant in that if the Ca-HCO₃ type thermal waters were the

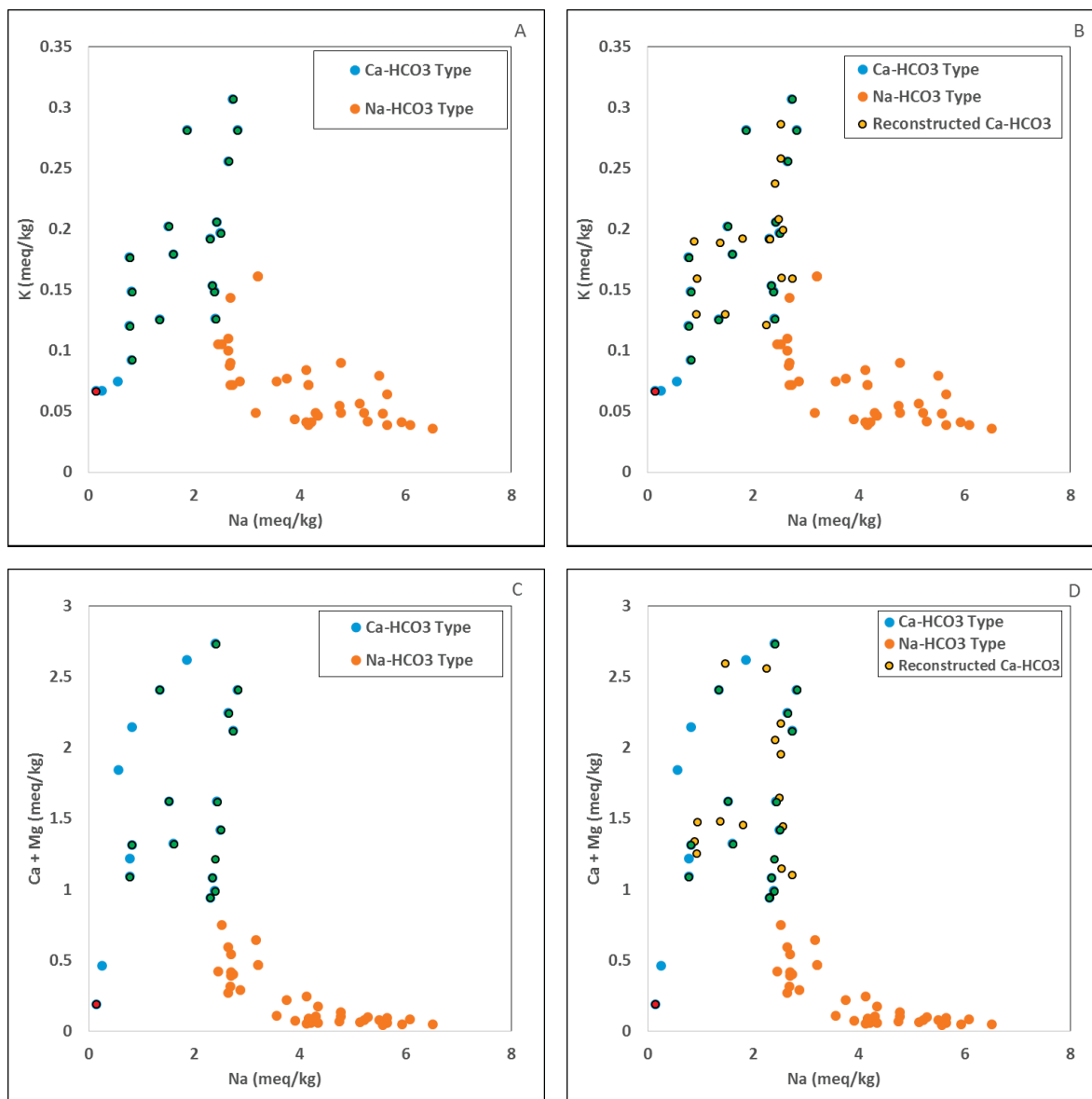


Figure 23. Initial (green) vs MEG reconstructed (yellow) compositions of Ca-HCO₃ thermal waters. A and B show the relationship between Na⁺ vs K⁺ while C and D show Ca²⁺ and Mg²⁺ vs Na⁺.

result of simple mixing between groundwater and deep Na-HCO₃ type waters, the reconstructed (optimized) waters would be similar in composition to the Na-HCO₃ type waters and follow the general trends displayed in Figure 15. However, reconstructed water compositions do not resemble Na-HCO₃ waters suggesting that re-equilibration from the Na-HCO₃ waters to the Ca-HCO₃ is a possibility. The initial and reconstructed water compositions of the Ca-HCO₃ type waters are plotted with respect to K⁺, Ca²⁺, Mg²⁺, and Na⁺ concentrations in Figure 23.

The pure water mixing with Na-HCO₃ type thermal waters mentioned previously also opens up the possibility of re-equilibration in this system. In order for pure water to mix with the deep Na-HCO₃ type thermal waters of the system, a mechanism by which recharge area groundwater transitions into pure or very dilute water prior to mixing may be needed. A reaction in which Ca²⁺ and Mg²⁺ concentrations are diminished while Na⁺ concentrations are increased would explain this phenomenon. Cation exchange reactions between alteration clays and zeolites or a precipitation reaction in which cation concentrations are diminished due to falling out of solution may be the driving forces behind this mechanism. Cation exchange reactions are more likely than reactions involving precipitation as precipitation reactions would likely result in a similar decrease of anion concentrations as both cations and anions would drop out of solution together due to the ionic bond formed during precipitation. A series of re-equilibration zones may explain the gradational change in composition from Na-HCO₃ to more Ca-rich thermal waters. This re-equilibration mechanism is supported by the apparent relationship between:

1) Mg-rich smectite clays (Beidellite-Mg) used in the Ca-HCO₃ RMA and the Na-rich smectite clays (Saponite-Na) used in the Na-HCO₃ RMA. The high cation exchange capacity of smectite clays supports these findings (Carroll, 1954; Robin et al., 2015).

2) Clinoptilolite-Ca (zeolite) used in Ca-HCO₃ RMA and Clinoptilolite-K used in the Na-HCO₃ RMA. Cation exchange between these two Clinoptilolite end members is explained by Pabalan and Bertetti (2001).

RTEst modeling of Na-HCO₃ type thermal waters mixing with pure water yields temperature estimates ranging from 108 °C to 160 °C. These results are in agreement with sulfate-water isotope geothermometry estimates of 150 °C for Banbury Hot Springs (Conrad et al., 2015). Modeling of Ca-HCO₃ type thermal waters mixing with local groundwater yields temperature estimates ranging from 84 °C to 104 °C. These results may either constitute evidence for two distinct flow paths and equilibration temperatures resulting in the two water types or relationship between the two waters defined by a re-equilibration. Possible conceptual models resulting from geothermometry results will be discussed in detail in Chapter 5. Below are the RTEst temperature estimations and mineral assemblages for both Ca-HCO₃ and Na-HCO₃ type thermal waters.

Table 10. RTest temperature estimates (a), mass of thermal water component per 1 kg solution used in mixing (c), log of CO₂ fugacity, RTest objective function (Φ), selected RMAs, and (b) associated standard deviations of each measurement.

Na-HCO ₃ Type Water RTest Results - Pure Water Mixing						
Site ID	Name	$T^a \pm \sigma^b$	$M^c \text{ H}_2\text{O} \pm \sigma^b$	$\log f_{\text{CO}_2} \pm \sigma^b$	Φ	RMA
CC-11	Miracle Hot Springs	160 ± 2.5	0.49 ± 0.01	-0.56 ± 0.058	$1.23\text{E-}4$	Beidellite-Mg, Calcite, Chalcedony, Clinoptilolite-K, Paragonite
CC-14	CSI Well 2	136 ± 11	0.43 ± 0.06	-0.23 ± 0.029	$2.05\text{E-}3$	Saponite-K, Calcite, Chalcedony, Clinoptilolite-Ca,
CC-40	1000 Springs (Sliger's Well)	134 ± 2.1	0.34 ± 0.005	-0.1 ± 0.051	$2.93\text{E-}4$	Calcite, Chalcedony, Illite, Paragonite, Heulandite, Fluorite
CC-42	Banbury Hot Springs	158 ± 9	0.49 ± 0.04	-0.26 ± 0.21	$2.25\text{E-}3$	Beidellite-Mg, Calcite, Chalcedony, Clinoptilolite-K, Albite
CC-45	Leo Ray Hill	121 ± 6	0.46 ± 0.02	-0.4 ± 0.14	$2.34\text{E-}3$	Saponite-Na, Calcite, Chalcedony, Clinoptilolite-K, Paragonite
CC-46	Leo Ray Road	120 ± 1	0.48 ± 0.045	-0.31 ± 0.02	$5.15\text{E-}5$	Saponite-Na, Calcite, Chalcedony, Clinoptilolite-K, Paragonite
CC-48	Hensley Well	134 ± 17	0.52 ± 0.09	-0.36 ± 0.47	$8.28\text{E-}3$	Beidellite-Mg, Calcite, Chalcedony, Clinoptilolite-K, Paragonite
CC-51	CSI Well 1	134 ± 11	0.42 ± 0.06	-0.14 ± 0.3	$2.28\text{E-}3$	Calcite, Chalcedony, Clinoptilolite-Ca, Saponite-K
CC-52	Larry Anderson Well	108 ± 3	0.73 ± 0.09	-1.5 ± 0.09	$5.75\text{E-}4$	Saponite-Na, Calcite, Chalcedony, Fluorite, Talc
CC-53	Pristine Springs	130 ± 10	0.54 ± 0.08	-0.92 ± 0.3	$2.18\text{E-}3$	Saponite-Na, Calcite, Chalcedony, Fluorite, Talc
CC-55	Anderson Campground Well	123 ± 3	0.56 ± 0.01	-0.77 ± 0.07	$7.43\text{E-}4$	Beidellite-Mg, Calcite, Chalcedony, Clinoptilolite-K, Paragonite

Ca-HCO ₃ Type Water RTest Results - Groundwater Mixing					
Site ID	$T^a \pm \sigma^b$	$M^c \text{ H}_2\text{O} \pm \sigma^b$	$\log f_{\text{CO}_2} \pm \sigma^b$	Φ	RMA
CC-9 (Campbell Well 1)	95 ± 0.46	0.97 ± 0.005	-1.17 ± 0.01	$1.95\text{E-}05$	Beidellite-Mg, Calcite, Chalcedony, Kaolinite, Clinoptilolite-Ca
CC-10 (Campbell Well 2)	93 ± 0.27	0.97 ± 0.003	-1.25 ± 0.007	$6.48\text{E-}06$	Beidellite-Mg, Calcite, Chalcedony, Kaolinite, Clinoptilolite-Ca
CC-54 (Twin Falls High School)	80 ± 2.3	1.0 ± 0.01	-1.32 ± 0.06	$4.11\text{E-}04$	Beidellite-Mg, Calcite, Chalcedony, Muscovite, Clinoptilolite-Ca
LY82-13	98 ± 0.91	1.0 ± 0.04	-1.06 ± 0.02	$7.35\text{E-}05$	Beidellite-Mg, Calcite, Chalcedony, Kaolinite, Clinoptilolite-Ca
LY89-3	94 ± 0.58	0.86 ± 0.006	-1.16 ± 0.01	$2.95\text{E-}05$	Beidellite-Mg, Calcite, Chalcedony, Kaolinite, Clinoptilolite-Ca
LY89-5	97 ± 0.59	0.91 ± 0.009	-1.13 ± 0.02	$3.06\text{E-}05$	Beidellite-Mg, Calcite, Chalcedony, Kaolinite, Clinoptilolite-Ca
LY89-6	104 ± 1.1	0.98 ± 0.012	-1.04 ± 0.03	$9.67\text{E-}05$	Beidellite-Mg, Calcite, Chalcedony, Kaolinite, Clinoptilolite-Ca
LY89-7	84 ± 2.1	1.0 ± 0.02	-1.23 ± 0.04	$4.08\text{E-}04$	Beidellite-Mg, Calcite, Chalcedony, Kaolinite, Clinoptilolite-Ca
LY89-10	88 ± 1.5	1.0 ± 0.008	-1.21 ± 0.02	$2.01\text{E-}04$	Beidellite-Mg, Calcite, Chalcedony, Kaolinite, Clinoptilolite-Ca
LY89-17	88 ± 1.3	1.0 ± 0.008	-1.20 ± 0.02	$1.72\text{E-}04$	Beidellite-Mg, Calcite, Chalcedony, Kaolinite, Clinoptilolite-Ca
LY89-18	89 ± 0.61	0.88 ± 0.002	-1.29 ± 0.003	$3.44\text{E-}05$	Beidellite-Mg, Calcite, Chalcedony, Kaolinite, Clinoptilolite-Ca
LY89-34	89 ± 0.69	0.88 ± 0.011	-1.33 ± 0.02	$4.66\text{E-}05$	Beidellite-Mg, Calcite, Chalcedony, Kaolinite, Clinoptilolite-Ca
LY89-35	91 ± 0.31	0.86 ± 0.0006	-1.37 ± 0.001	$9.36\text{E-}06$	Beidellite-Mg, Calcite, Chalcedony, Kaolinite, Clinoptilolite-Ca
LY89-36	98 ± 1.60	0.84 ± 0.018	-1.33 ± 0.03	$2.34\text{E-}04$	Beidellite-Mg, Calcite, Chalcedony, Kaolinite, Clinoptilolite-Ca
M91-12	80 ± 1.23	0.91 ± 0.02	-1.54 ± 0.04	$1.35\text{E-}04$	Beidellite-Mg, Calcite, Chalcedony, Kaolinite, Clinoptilolite-Ca

CHAPTER 5: CONCEPTUAL MODELS FOR THE TWIN FALLS – BANBURY HYDROTHERMAL SYSTEM

The following section details the competing possible conceptual models for the Twin Falls-Banbury hydrothermal system and provides evidence for the dismissal of all but one. Four conceptual models based on the previously defined mixing scenarios are presented herein. Results from chemical analyses, mixing analyses, reservoir temperature predictions, and regional geology are utilized to support or dismiss these models.

5.1 No Mixing Conceptual Model

Mixing between local groundwater and thermal waters is supported by the partial equilibration and immature classifications of thermal waters made by the Giggenbach ternary diagram, the linear relationships between conservative species chloride and boron, and the linear relationship between ^{18}O and Deuterium. Mixing has been attributed as a possible explanation for the masking of geothermal signatures throughout the ESRP (McLing et al., 2002; Neupane et al., 2014; Dobson et al., 2015). However, the possibility that no mixing occurs in this system is considered unlikely due to inadequate (high) Φ value for both Ca-HCO_3 and Na-HCO_3 thermal waters using only temperature and CO_2 fugacity as optimization parameters.

5.2 Simple Mixing Conceptual Model

The idea of simple mixing is supported by gradational trends exhibited by some chemical constituents (Cl/B , $^{18}\text{O/D}$, $^{18}\text{O/Cl}$, Na/Cl , Na/SiO_2 , etc.) and is accounted for by silica-enthalpy mixing diagrams in Chapter 4. RTest modeling of mixing between recharge area groundwater and Ca-HCO_3 type thermal water supports simple mixing between these

two components (Table 10). However, trends exhibited in the relationships between Na^+ , K^+ , Ca^{2+} , and Mg^{2+} among Na-HCO_3 and Ca-HCO_3 thermal waters suggest that either some reaction has taken place in addition to mixing or that the two water types are representative of two distinct flow paths. Simple mixing between local groundwater and Na-HCO_3 type thermal waters is not supported by MEG modeling through RTest while the use of pure water as the mixing component is supported. Simple mixing with pure water may be explained by dilution through precipitation as thermal water is rapidly mixed at the surface as is the case in conventional mixing models (Fournier, 1977; Arnorsson, 1985). While this concept may hold up for thermal springs, it does not provide a mechanism by which pure water is mixed with Na-HCO_3 thermal waters in deep wells.

5.3 Reactive Mixing

In order for pure water or dilute Na-HCO_3 water (as discussed in Chapter 4) to mix with thermal Na-HCO_3 type waters of the deep system, there must either be 1) a flow pathway by which pure water from precipitation infiltrates directly into the deep system and mixes with thermal water or 2) a mechanism by which Ca-Mg-HCO_3 type groundwater gradationally transitions into dilute Na-HCO_3 water during infiltration. For these reasons, a conceptual model with and without re-equilibration are investigated. Recharge area groundwater is thought to pick up its enriched Ca^+ and Mg^{2+} signature from the Paleozoic (Pennsylvanian and Permian) marine sediments that are exposed at the surface in the mountainous recharge area to the southeast of Buhl, ID (Lewis and Young, 1989; Mariner et al., 1997). While all non-thermal groundwater samples in between the recharge area and both the Twin Falls and Banbury hydrothermal areas are Ca-HCO_3 in type, the regional geology supports the possibility of a flow path for precipitation directly into the Idavada volcanics which are also

exposed in the hills to the south of the study area. The depth and extent of the Paleozoic carbonates is largely unknown although over 1,524 meters (5,000 ft.) sections of carbonate sediments are reported in the mountains of northern Nevada (Schroeder, 1912). Additionally, lead isotope data from thermal waters in the study area provide a carbonate signature providing evidence that carbonates persist beneath the Idavada volcanics throughout the study area (Mariner et al., 1997)

While the possibility exists for a rhyolite exclusive flow pathway, the likelihood of pure water remaining dilute from the surface to depths up to 3 km (Lewis and Young, 1989) is not favorable. Data from many natural geothermal systems shows that local equilibria between fluid and host rock is attained at temperatures as low as 50 °C (Arnórsson et al., 1983; Stefánsson and Arnórsson, 2002). Pure water from precipitation would likely obtain a similar signature to that of the deep Na-HCO₃ thermal waters having flowed through rhyolites to extensive depths. Without the possibility of re-equilibration at a lower temperature, it would follow that an increase in the fraction of thermal water component in MEG analysis would result in higher temperature estimations. This is not found to be the case as can be seen in the RTest results presented in Chapter 4, Table 10. For instance, Miracle Hot Springs has a predicted reservoir temperature of 160 °C with an optimized thermal water component of 0.49 whereas the Larry Anderson Well has an optimized thermal composition comprised of 73% thermal water at 130 °C.

5.4 Re-equilibration

The gradational transition between Na-HCO₃ type thermal waters of the deep system to more Ca-HCO₃ type thermal waters nearer to the surface is found throughout the ESRP (Mann, 1986; McLing et al., 2002;). A re-equilibration mechanism may explain this

relationship. As shown in the Figure 24 below, a mechanism by which Ca^{2+} and Mg^{2+} are diminished with increasing temperature and depth while Na^+ concentrations rise explains the rationale behind pure water or dilute Na-HCO_3 water mixing. Conversely, the reduction of Na^+ and rise of Ca^{2+} and Mg^{2+} during ascension may explain the transition between deep Na-HCO_3 thermal waters to more Ca-HCO_3 type thermal waters through re-equilibration. This mechanism is supported by the apparent exchange between Ca^{2+} and K^+ rich zeolites and Na^+ and Mg^{2+} rich smectite clays. For the reasons mentioned in this chapter, a conceptual model including re-equilibration is the most likely. However, the possibility of two flow paths and equilibration temperatures resulting in the two observed thermal water types cannot be ruled out.

Figure 24 shows a cross sectional view of regional geology from the recharge area in the Cassia Mountains to Banbury Hot Springs. Suggested possible flow pathways, water types, and a re-equilibration mechanism are also represented and explained through the 4 stages listed below. This cross section was created from available well log data and local geologic maps (Gillerman et al., 2005; Othberg et al. 2005). Figure 25 shows the location of the cross section line in map view.

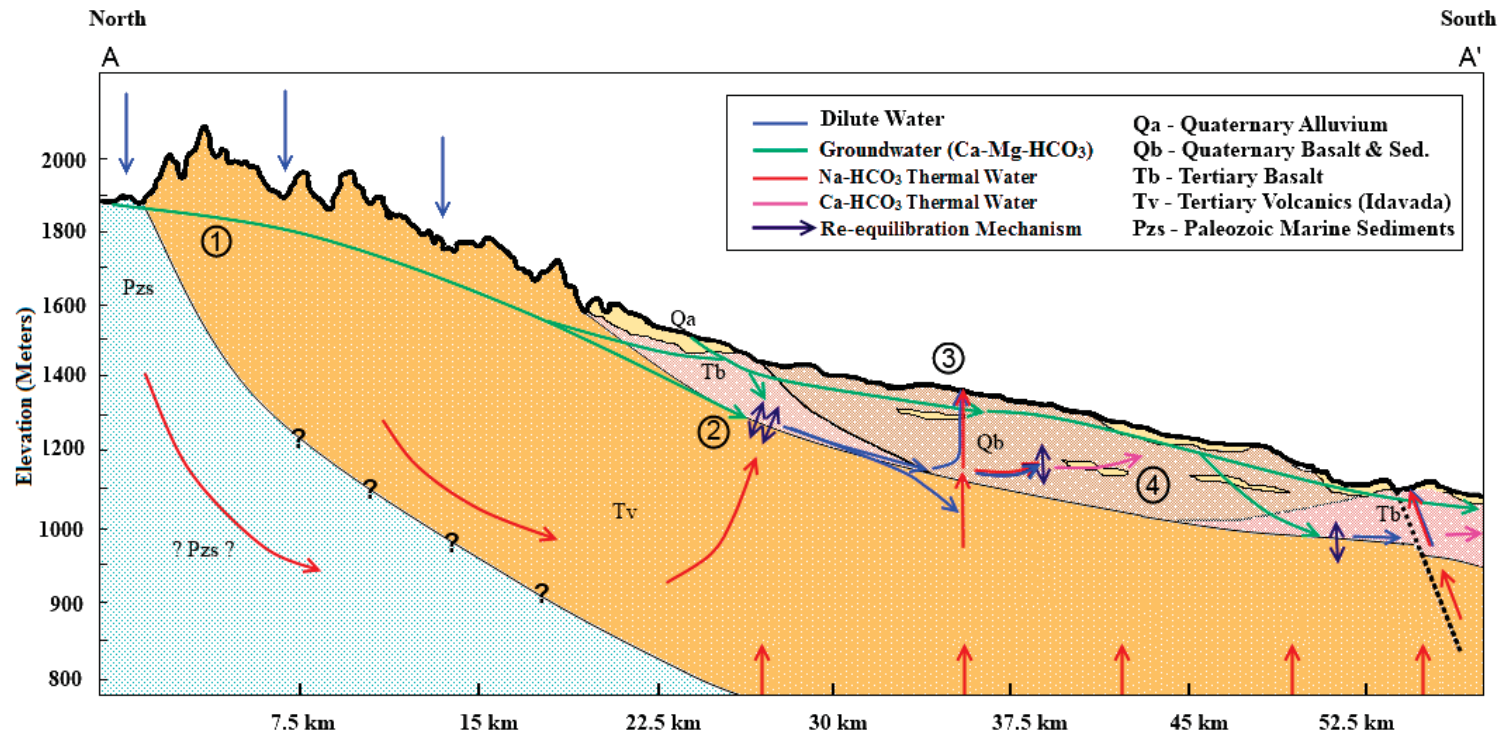


Figure 24. Conceptual model for the Twin Falls – Banbury thermal area showing possible flow pathways, water types, regional geology, and possible re-equilibration mechanism.

- 1) Precipitation infiltrates into the subsurface likely picking up Ca-Mg-HCO₃ signature from Paleozoic carbonates.
- 2) The mixing of Ca-Mg-HCO₃ groundwater with Na-HCO₃ thermal water at intermediate temperature and depth. Re-equilibration (purple arrows) results in the loss of Ca²⁺ and Mg²⁺ and the gaining of Na⁺ resulting in dilute Na-HCO₃ water.
- 3) Na-HCO₃ thermal water mixes with dilute water during ascension resulting in the manifestation of mixed Na-HCO₃ thermal water at the surface.
- 4) An alternate flow path through basalt results in the re-equilibration of Na-HCO₃ thermal water into Ca-HCO₃ thermal water.

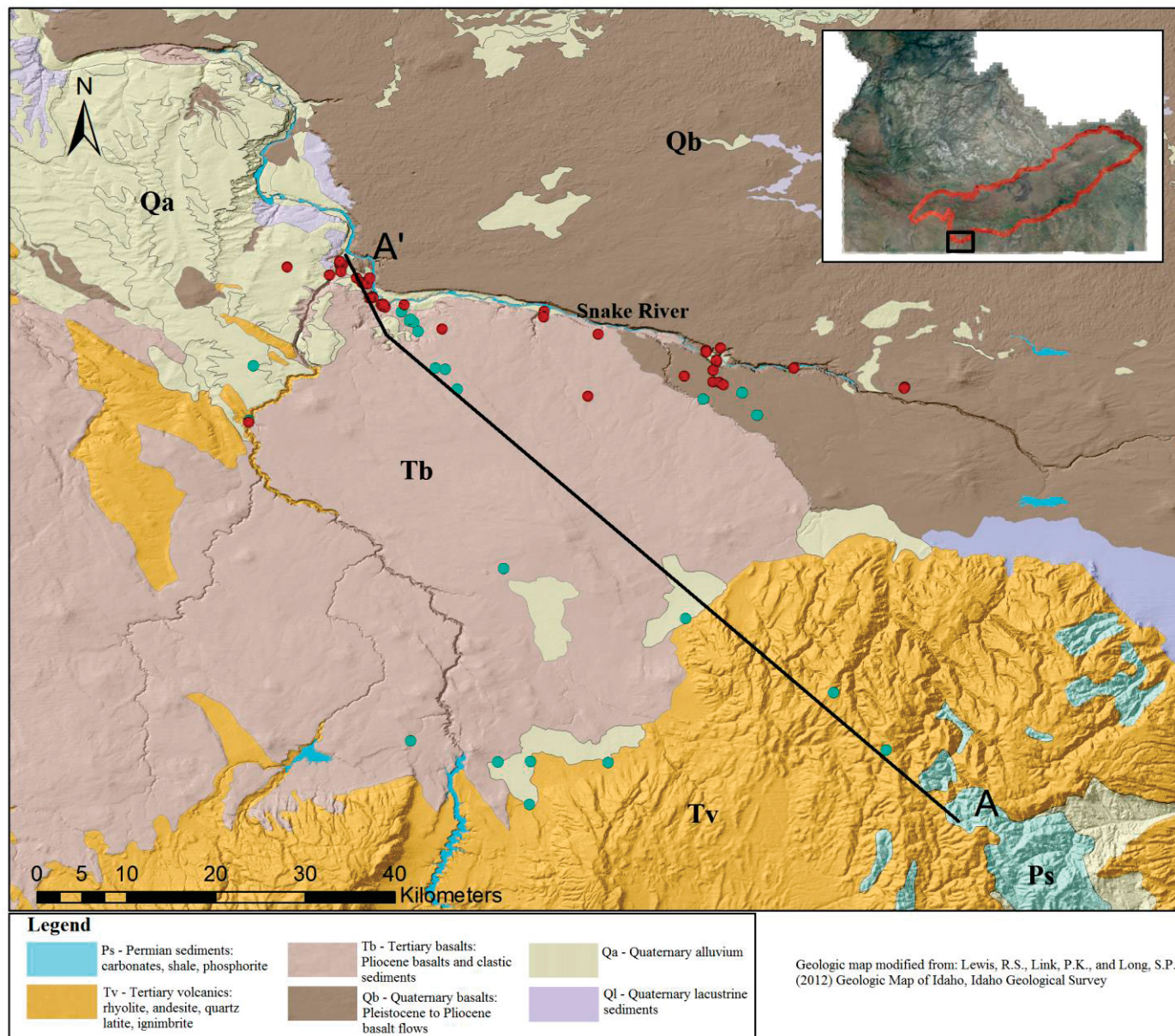


Figure 25. Cross sectional line of Figure 24 with geologic units and water type distribution (Red: Na-HCO_3 , Blue: Ca-HCO_3)

5.5 Hydrogeology

Thermal water in the Banbury hydrothermal area seems to be structurally controlled with the majority of thermal surface manifestations located along a single northwest trending normal fault associated with Basin and Range extension (Street and DeTar, 1987; Lewis and Young, 1989). According to the Idaho Geological Survey, most of the normal faults within the study area are contained within the units of the Idavada volcanics and do not offset the overlying younger basalts (Othberg et al., 2012). The normal fault near the cluster of Na-HCO₃ thermal waters near Banbury Hot Springs appears to be one of the exceptions. Offset to both overlying Quaternary and Tertiary basalts (Banbury basalt) is shown in a nearly 2 km

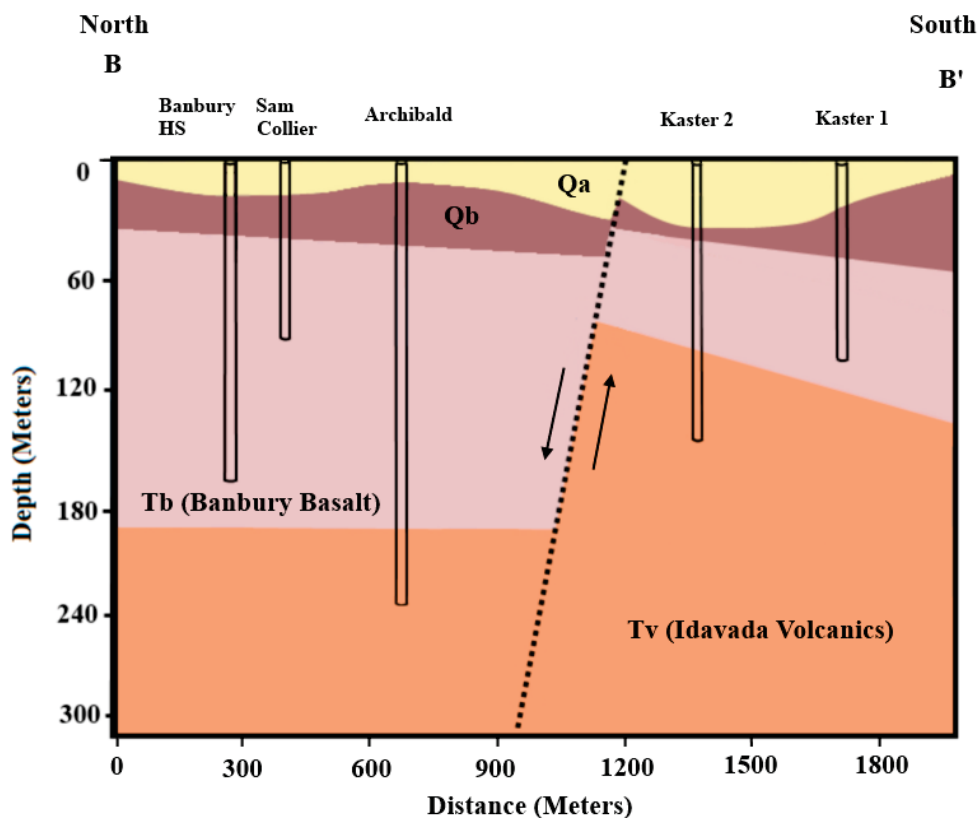


Figure 26. Geologic cross section through the Banbury Hot Springs area.

long cross section which cuts across the fault in this area. As discussed in Chapter 3, Ca-HCO_3 type thermal waters are more prevalent southward towards the area of recharge and within wells completed within basalts. A possible explanation for the spatial distribution of the two thermal waters is that the Ca-HCO_3 type thermal waters are found in areas where faults are constrained within Idavada volcanic units thus allowing for increased residence times and re-equilibration into Ca-HCO_3 type waters within basalt as shown in Figure 24. Logs of wells used in cross section construction are available in Appendix D.

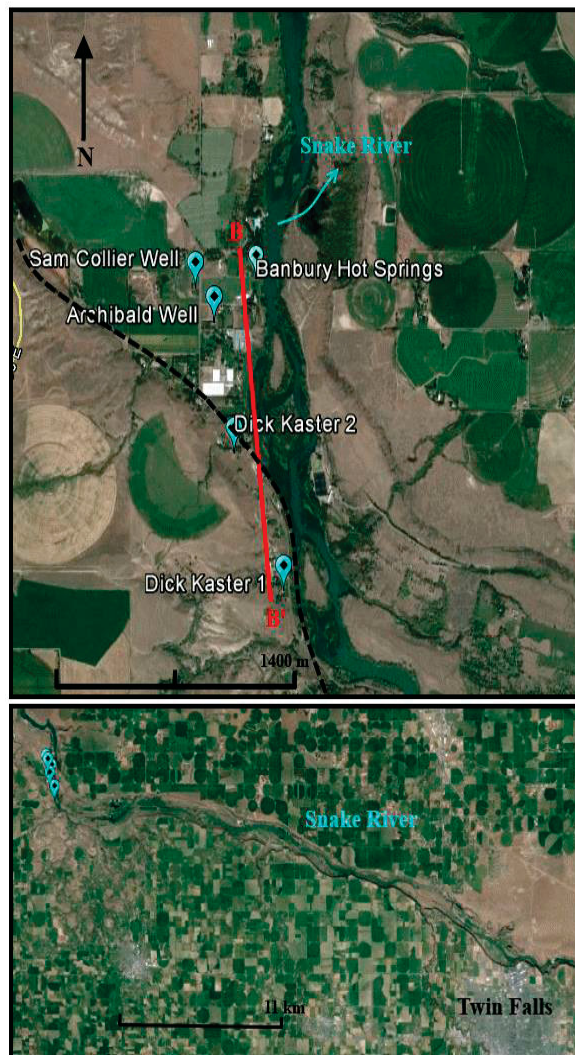


Figure 27. (Top) Map of the cross section line through the Banbury area. (Bottom) Reference map.

A similar transition from Ca-HCO_3 thermal waters to Na-HCO_3 thermal waters away from the zone of recharge is observed in the cluster of thermal expressions near the city of Twin Falls, ID. However, there is no evidence for a fault-controlled system like the one observed in the Banbury area. Figure 28 depicts the local geology of the area in cross section view with no apparent offset. Shervais et al. (2013) suggests that upflow zones in this area may be controlled by permeability associated with a buried caldera margin. The concentration of hotter Na-HCO_3 type waters near the Snake River where units of Idavada volcanics are exposed shows that thermal water occurrence may be controlled by thinning basalt units. Aside from the lack of faulting in the Twin Falls area, the other major difference in geology from the Banbury area are the presence of the Shoshone Falls Rhyolite (andesite unit of the Idavada volcanics) and a significant layer of lacustrine sediments above the rhyolites of the

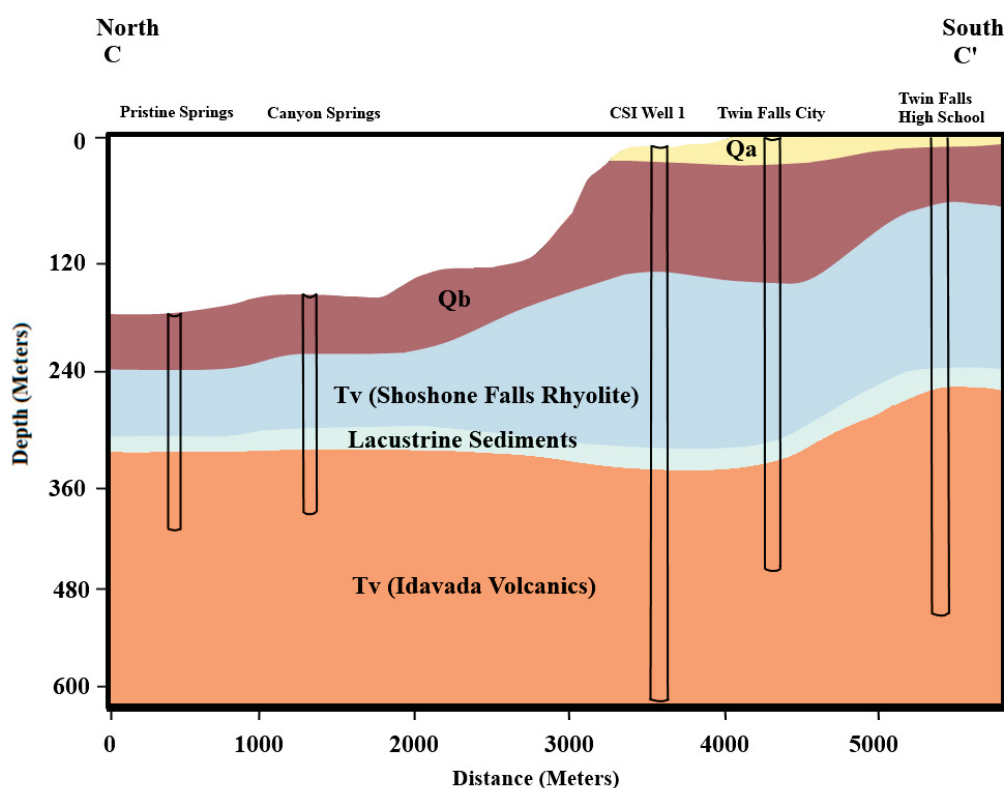


Figure 28. Geologic cross section through the Twin Falls thermal area.

Idavada volcanics. The lacustrine sedimentary layer comprised of oolitic siltstone and claystone (Street and DeTar, 1987) may serve as the confining layer for the artesian thermal aquifer in this area.

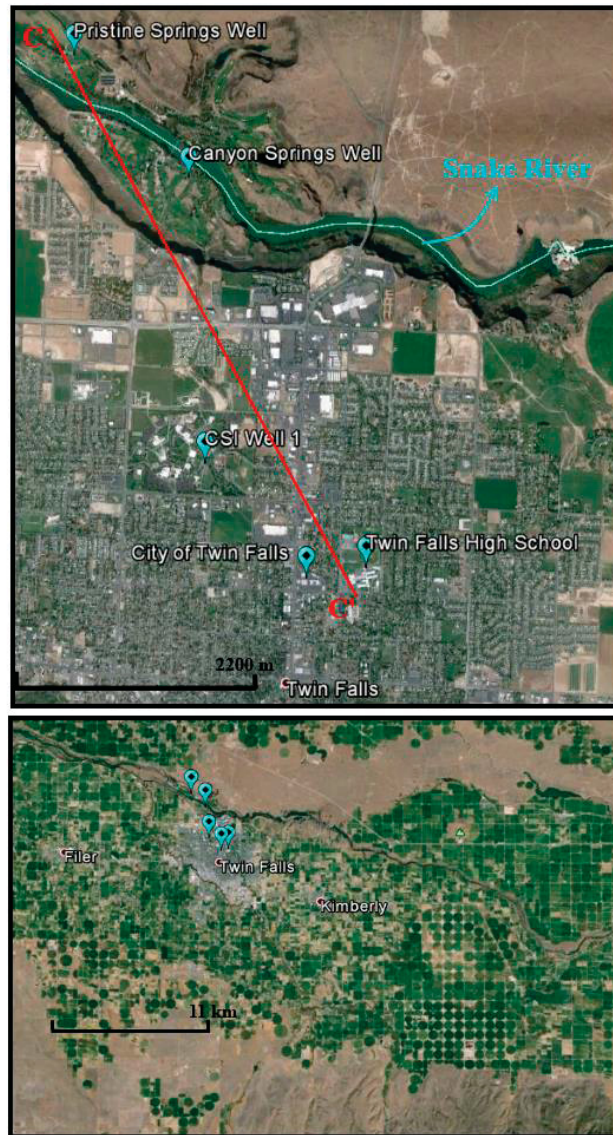


Figure 29. (Top) Map of the cross section line through the Twin Falls area. (Bottom) Reference map.

Aquifer Test and Analysis

As discussed previously, flow pathways and residence times may be very important in allowing for re-equilibration from Na-HCO₃ type waters into more Ca-rich thermal waters. Declines in hydraulic head in the Twin Falls – Banbury area have been observed for over thirty years (Lewis and Young, 1982; 1989; Street and DeTar, 1987) due to increased utilization of the resource with several areas showing hydraulic heads below land surface. Monitoring of thermal wells in the study area revealed that the Twin Falls and Banbury hydrothermal areas are interconnected with development and increased utilization in one area resulting in declines in the other. Flow throughout the aquifer is thought to be controlled primarily by fractures resulting from tectonic movement, cooling joints, porosity of non-welded ash flow tuff units, and contacts between successive flows (Street and DeTar, 1987).

Aquifer parameters of the rhyolites of the Idavada volcanics were estimated first in 1982 through a pumping test of two of the deeper wells in the area (CSI 1 and 2) performed by CH2M Hill. CSI 1 and 2 (2200 and 1480 ft. deep) are geothermal wells used for space-heating located on the campus of the College of Southern Idaho and were sampled for chemical analysis (CC-51 and CC-14) as part of this study in 2014. While water temperatures seem to have remained constant (37 °C) since drilling was completed in 1979, a significant decline in hydraulic head has been observed. Street and DeTar (1987) reported hydraulic head values around 14 meters above land surface. Both of these wells are no longer flowing artesian with water levels of about 1.2 meters below land surface at present day. Due to the observed decline in water levels and the erroneous listing of CSI 1 at 1191 ft. deep (cased portion of the well) in the initial pump test report, a new pump test was conducted for both

CSI wells from 9/1/15 – 9/5/15 in an effort to establish a vertical gradient and thermal water travel times..

A 24-hr drawdown test and a 24-hr recovery test were performed for both wells. Pumping of CSI 2 began at 10:00 AM on 9/1/15 and continued until 10:00 AM on 9/2/15 after which it was allowed to recover for a full 24 hours. CSI 1 was pumped immediately after the recovery test of CSI 2 beginning around 10:00 AM on 9/3/15 continuing until around 10:00 AM on 9/4/15. Recovery of CSI 1 was also monitored and ended on 10:00 AM on 9/5/15. Solinst ® Levelogger ® (Model 3001) pressure transducers were installed in both wells and hung at approximately 50 ft. beneath land surface from ports on the well heads. A Solinst ® Barologger ® barometric pressure transducer was kept securely at the same location as CSI 1. All transducers were set to obtain measurements every minute. Both wells were pumped at a rate of 300 gpm although data from the pressure transducers show the pumping

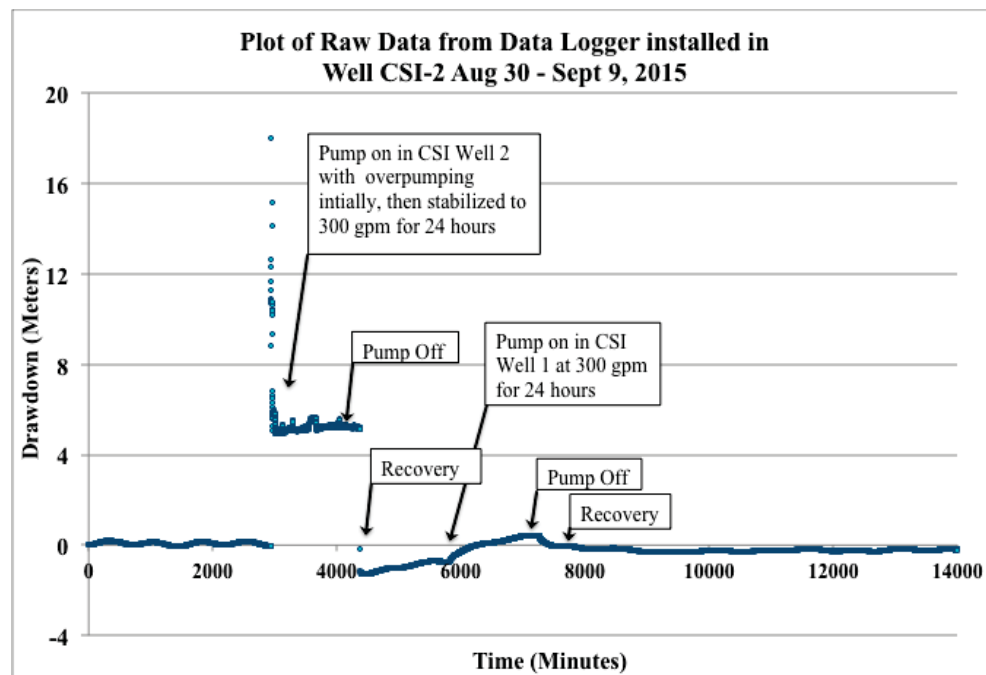


Figure 30. Plot of uncorrected drawdown from CSI Well 2 vs time since transducer installation.

rate may have taken about an hour to stabilize after initial over pumping (Figure 30).

Due to difficulty in retrieving the pressure transducer from CSI 1, only data from CSI 2 as the pumped well and observation well is available. Figure 30 shows the pressure readings (meters of water) from CSI 2 during the entirety of both pumping and recovery tests. A cyclic antecedent trend is observed prior to the start of pumping showing a sinusoidal fluctuation of about 0.1 meters every 600 minutes. This is probably caused by a pump cycling on and off somewhere within the aquifer. At the start of the test, it can be seen that 18 meters of over pumping occurred due to the pump rate exceeding the target rate of 300 gpm until flow was regulated. Drawdown was about 5 meters during the steady pumping rate of 300 gpm. When the pump was shut off at 1440 minutes, it can be seen that the water level over recovered by 1.2 meters as noted by the double headed arrow to the left in Figure 31. Also recorded in Figure 31 is the temperature (red line) during pumping which rose nearly 15 °C. There are at least two plausible explanations for the over recovery observed during the tests: 1) electronic

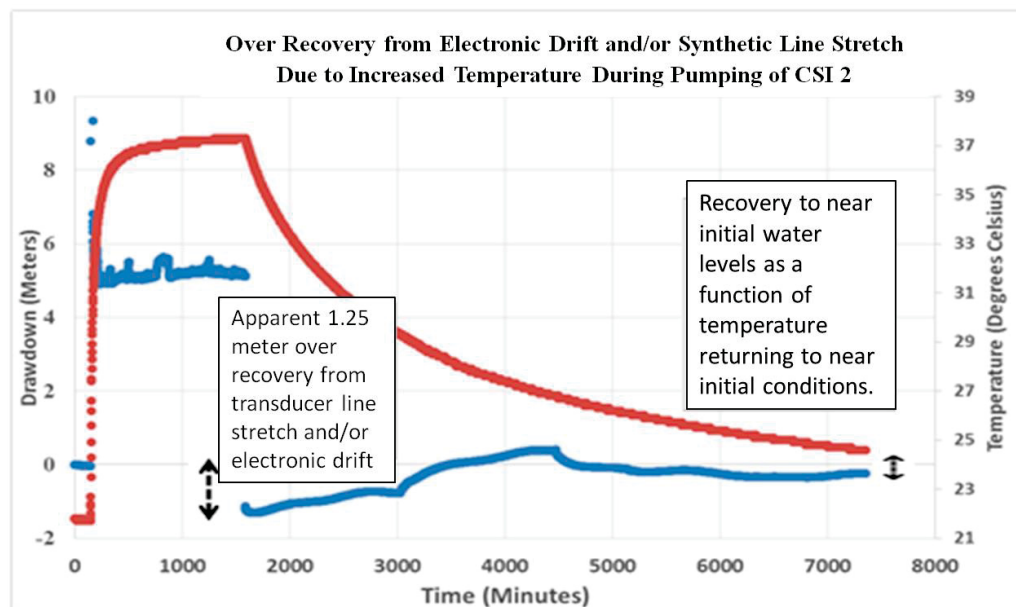


Figure 31. Plot of CSI Well 2 temperature (red) vs drawdown (blue) highlighting possibilities of electronic drift or stretch in synthetic line resulting in the observed overpumping.

instrument drift corresponding to heating; and 2) stretch in the graduated synthetic line used to hang the transducer. As temperatures approach initial values near the end of the CSI 1 pumping test, transducer water level measurements near background levels prior to pumping.

Over pumping in the early time data and the observed over recovery in the CSI 2 pumping tests deemed the data set from CSI 2 pumping as unusable. However, time-drawdown pairs were generated for both the pumping and recovery tests for this well when CSI 1 was being pumped. Aquifer parameters were estimated using the hydrologic type curve matching software AQTESOLV®. From previous hydrologic research in the area (Street and DeTar, 1987; Lewis and Young, 1989) and the local artesian conditions, analysis was focused on confined and leaky-confined aquifer solutions. Based on cross section analysis (Figure 28) and CSI well logs (Appendix D), the lacustrine sediment layer consisting of oolitic siltstone and sandstone (Street and Detar, 1987) may serve as the confining unit for this system. The best match of the data to type curves was achieved using the Cooper-Jacob (1946) straight-line method. This method is a variation of the classic Theis (1935) well function that relates the transmissivity (T), storativity, (S), radial distance of drawdown (r), and pumping time (t) to the pumping rate (Q) in an infinite series shown below:

$$W(u) = (-.5772 - \ln u + u - \frac{u^2}{2 \times 2!} + \frac{u^3}{3 \times 3!} \dots)$$

where W(u) is the well function and (u) is given by:

$$u = \frac{r^2 S}{4 T t}$$

The final relationship between drawdown and aquifer parameters is given by:

$$dd = \frac{Q}{4\pi T} W(u)$$

Cooper and Jacob (1946) approximated the relationship between drawdown and $\log(t)$ as a straight-line relationship by making the recognition that the second-order and higher terms in the infinite series become negligible with small (u) values given by long pumping times (t) or short radial distances (r). Solutions to the pumping and recovery test for the CSI 1 wells are shown below in Figure 32. Calculated transmissivity values of 930 m²/d (75,000 gpd/ft) are within the same order of magnitude and in close agreement with the values reported by Street and Detar (1987) of 554-923 m²/d (44,600 – 74,300 gpd/ft). Based on the well logs of CSI 1 and 2, thermal water appears to come from a fracture zone at approximately 350 – 370 meters (1150 – 1215 ft) below land surface. Because both wells are open across the entire water bearing zone, calculation of a vertical gradient is not possible. Available data are insufficient to define the anisotropy of the Idavada volcanics. Thus, the data set precludes making a reasonable estimate of vertical travel times. Because of the strong artesian conditions of the deep thermal aquifer, the vertical gradient is known to be upward. However, without additional well data and depth discrete pumping tests, it is not possible to accurately quantify the vertical flow rate. Future work including detailed flow path analysis within the Idavada volcanics and the investigation into possible thermal flow paths between rhyolites and basalts is highly recommended.

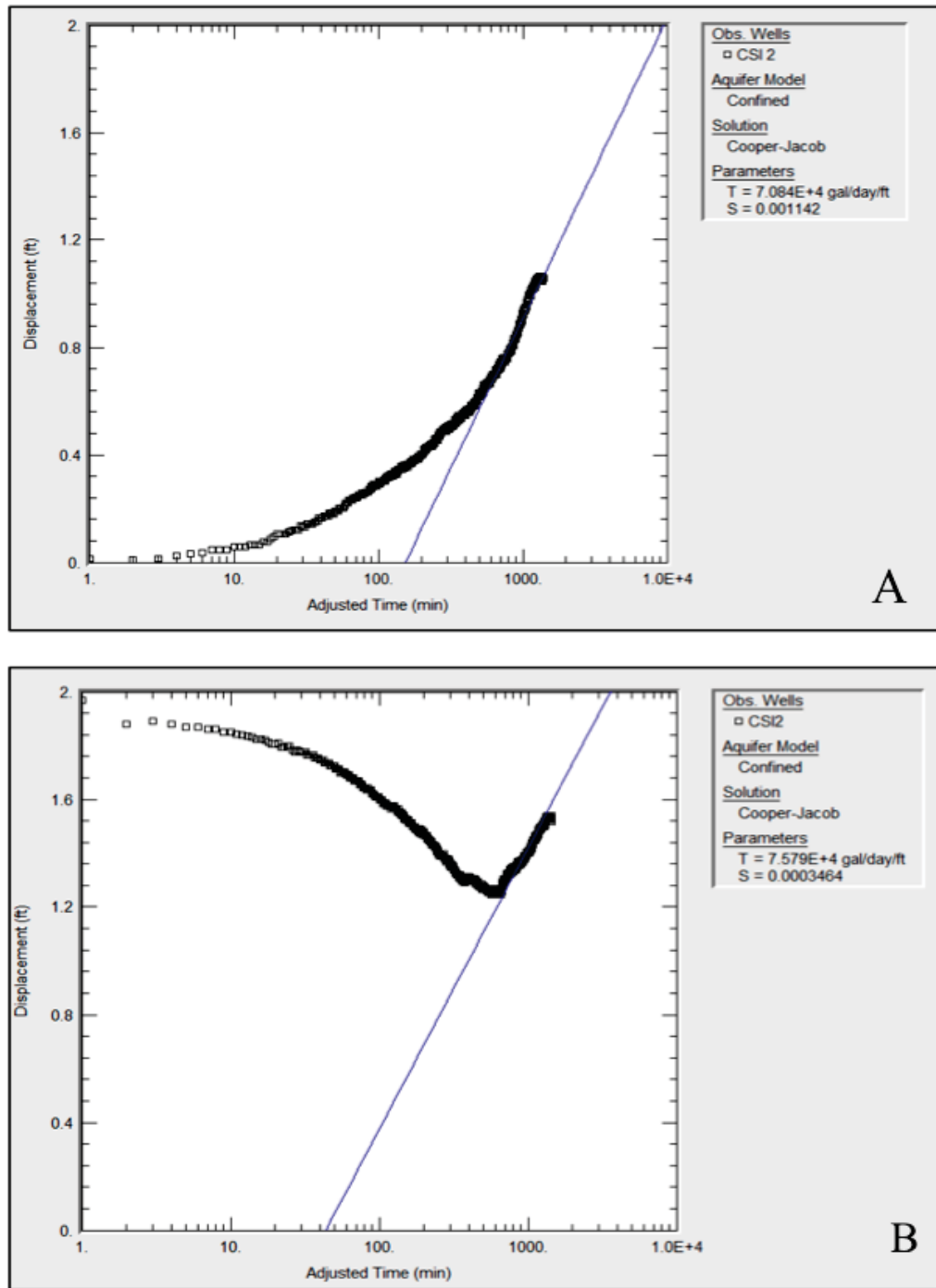


Figure 32. Cooper Jacob straight-line solution applied to barometric pressure corrected pumping (A) and recovery (B) limbs of the CSI Well 1 aquifer test.

CHAPTER 6: WATER-ROCK INTERACTION AND MIXING

EXPERIMENTS

The concept of re-equilibration in the Twin Falls – Banbury hydrothermal system may explain the modeling results of pure water mixing with Na-HCO₃ type thermal waters and the apparent gradational transition between deep Na-HCO₃ waters and shallower Ca-HCO₃ thermal waters (Figure 24). Bench scale water-rock interaction and mixing experiments were constructed in order to test the validity of the potential re-equilibration mechanism which results in the exchange of Ca and Mg with Na. This exchange results in the downward transition from local groundwater to very dilute water after mixing with Na-HCO₃ thermal waters and the re-equilibration of Na-HCO₃ thermal waters into Ca-HCO₃ thermal waters after mixing during ascension.

Experiments were modelled after the study area with an initial thermal water coming into equilibrium within the Idavada volcanics at 150 °C (Banbury Hot Springs temperature estimate) and subsequently being mixed with a local groundwater sample within the basalts of the ESRP and maintained at an intermediate temperature (70 °C). Thermal water was produced within closed system stainless steel reactor cells maintained at 150 °C and saturation vapor pressure. This water was then mixed with local groundwater in three different proportions comprised of 60%, 40%, and 20% thermal water. Chemical concentrations of mixed water samples over time are used to better understand the implications of flow pathway mixing and re-equilibration.

6.1 Rock Samples

Rock sample for the initial water-rock interaction were collected from the Shoshone Falls Rhyolite within the Idavada volcanics. Because core samples in sufficient quantity were

possible to obtain, samples were obtained from an outcropping unit of Idavada volcanics near the city of Twin Falls, ID. Street and Detar (1987) gave a sample location (42.598158°, -114.463464°) and detailed description of an easily accessed portion of the Shoshone Falls Rhyolite within the Snake River Canyon. Despite the apparent misnomer, this rock is actually thought to constitute a single andesitic flow unit within the Idavada volcanics. The sample location can be seen in Figure 33A below. Basalt rock samples for the second portion of the experiment were collected from an outcrop within the ESRP at the Pleistocene Hell's Half Acre basalt flow (Figure 33C). Samples were collected here and used as a proxy for Twin Falls area basalts due to difficulty in gaining access to basaltic outcrops on private property.

6.2 Rock Sample Preparation

In order to increase reaction rates through increased particle surface area (Savage et al., 1992; Neupane et al., 2013), blocky samples from outcrops were reduced to a finer grain size prior to heating and interaction with sample water. Rock samples were first cut using a rock saw into manageable sized pieces prior to being crushed into approximately 5 cm diameter pieces using a ball peen hammer (Figure 34). Samples were then reduced to finer grain sizes using a Braun ® Chipmunk rock crusher. The pulverized samples were then sieved (dry) and wet sieved (Figure 34) through brass (ASTM Sieve # 60– 120) sieves to separate out 0.25 – 0.125 mm particle sizes. Grain sizes in this range have been utilized for past water-rock interaction experiments to increase reaction rates (Savage et al. 1992, Rodriguez, 2011; Neupane et al., 2013). Samples were then decanted using deionized water to remove any suspended fine-grained particles and organic material. Samples were then allowed to dry for 48 hours prior to obtaining dry mass values by scale.

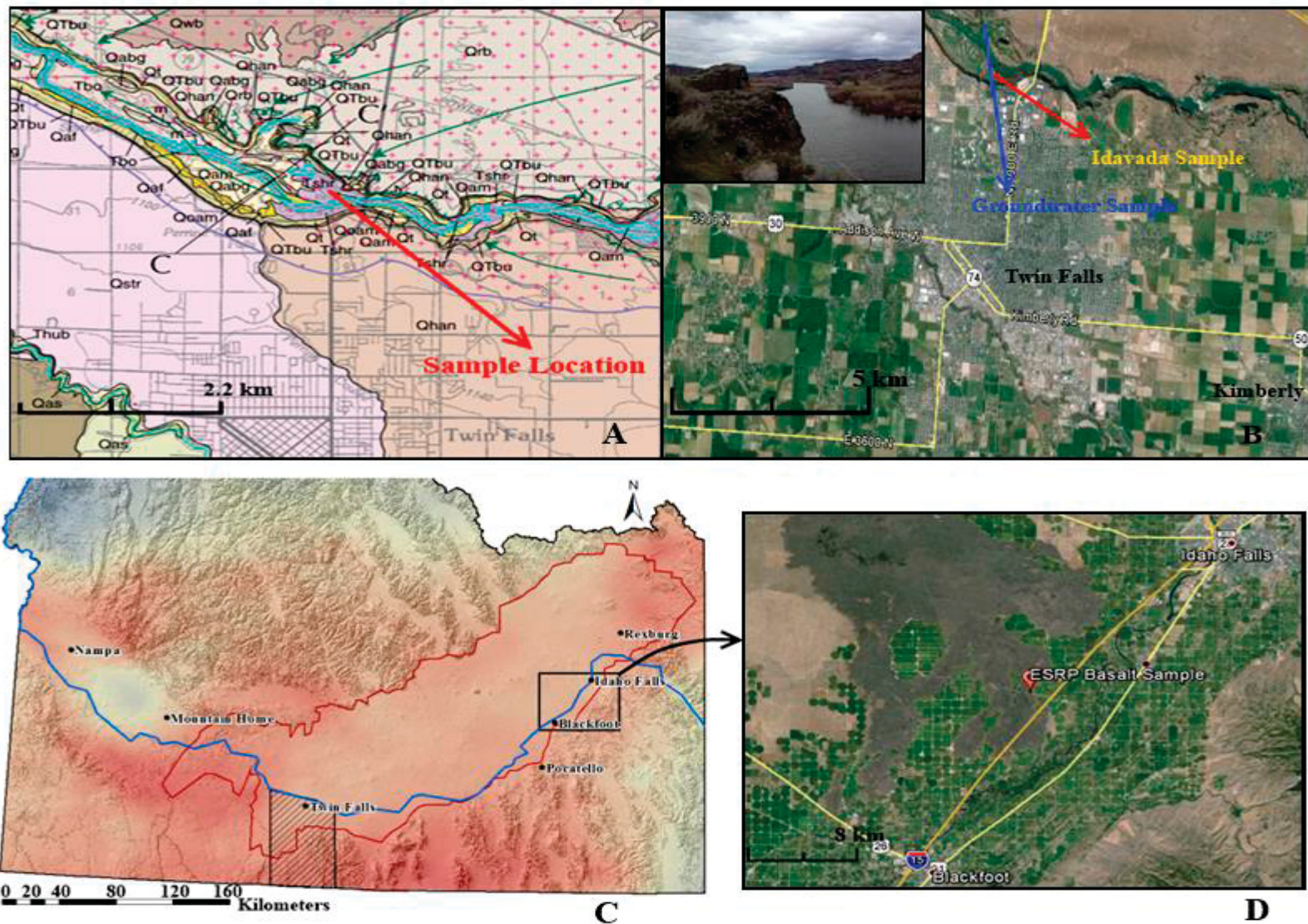


Figure 33. A) Idavada volcanics sampling location on a geologic map showing unit outcrop (dark pink). B) Idavada and groundwater sample locations map view. Inset – View of Idavada volcanics outcrop C) Reference map showing Hell's Half Acre location compared to study area. D) ESRP basalt sample location map view.

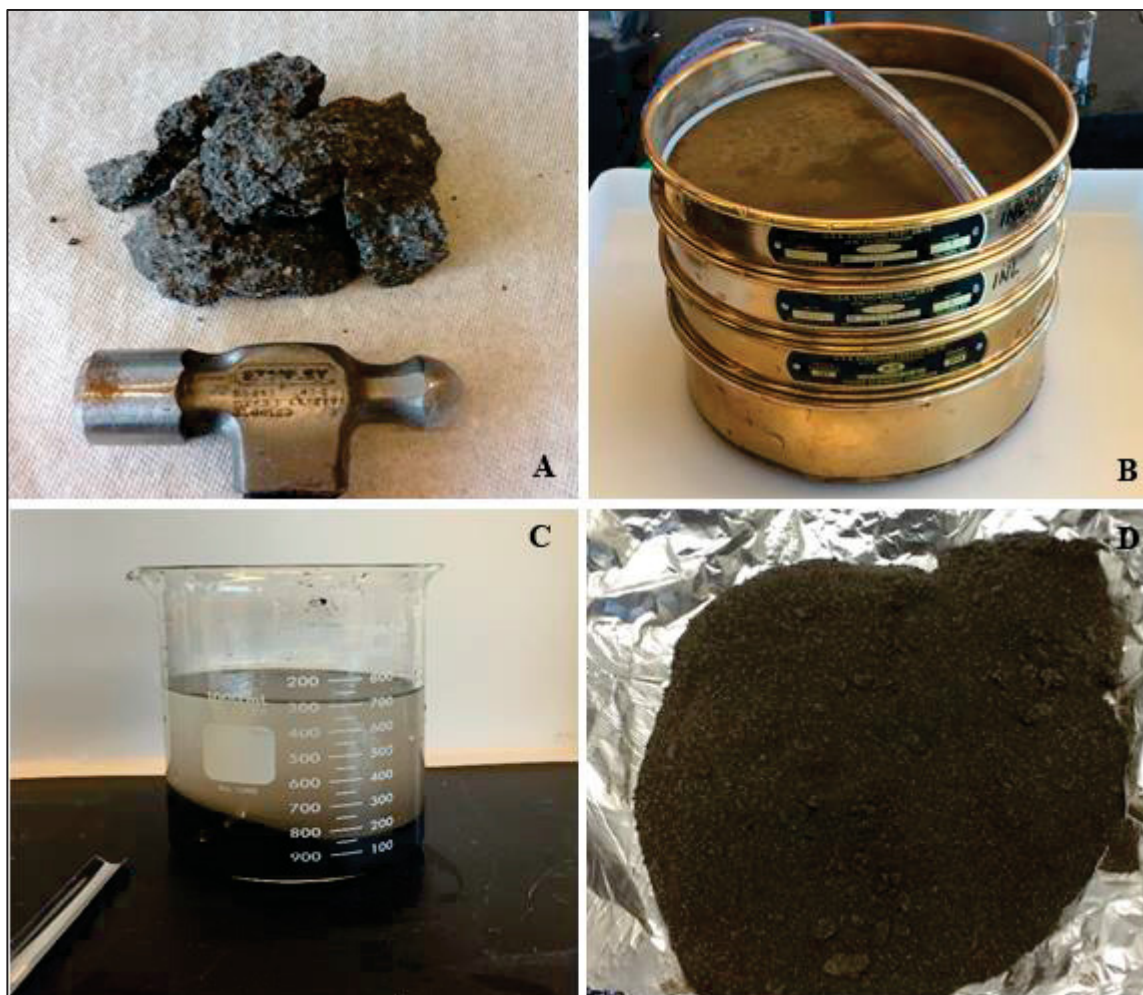


Figure 34. A) Idavada volcanics sample preparation prior to crushing. B) Wet sieving setup with deionized water line. C) Decanting process of rock sample after wet sieving. D) Final dry Idavada sample.

6.3 Initial Water Sample

A local groundwater sample was collected in order to use as both the source water for the formation of the Na-HCO_3 thermal water and as the mixing component in the second phase of the experiment. Samples were collected from a city water supply well (Blue Lakes Well) in coordination with the Twin Falls Department of Water Resources office. Sample location can be seen in Figure 33B. Samples were collected for major cation, major anion, and trace element analysis in the same manner as other geothermal samples throughout this study

(Appendix A). Five additional 1 liter non-acidified samples were collected for use in both portions of the experiment. Initial water chemistry is presented in Table 12 and is comparable to cooler groundwater samples from earlier studies of the area (Chapter 3, Table 2).

6.4 Experimental Procedure: Part I

The thermal water component for the mixing experiment was created using two stainless steel 1.0 L (Type 316) reaction vessels (Model 4523 Parr® Instrument) in which temperature, pressure, and stirring within the reactors were controlled independently. Maximum operating pressures and temperatures of these reactors are rated at 1900 psig (131 bars) and 350 °C, respectively (Parr Instruments Company, 2011). These reaction vessels are constructed so that fluids can be sampled at operating pressure and temperature without disassembling the reactor or affecting experimental conditions. Reactor vessels were cleaned thoroughly through sanding, acid washing with a 5% HNO₃ solution, rinsing with Milli-Q Nanopure water, and finally heating at 150 °C while partially filled with Milli-Q Nanopure water for 24 hours. Additionally, reactor vessels were pressurized with ultra-pure N₂ gas and left for 24 hours in order to monitor any pressure leaks due to faulty connections and/or gaskets.

After assuring the reactor vessels were clean and there were no apparent pressure leaks or temperature losses in the test runs, samples were added to two clean and empty reactor vessels (4/8/2015). 60 grams of Idavada volcanics samples were added to each vessel with 600 mL of groundwater sample in accordance with Parr® instrument fill volume limitations. Reactors were then gradually heated to 150 °C and a stirring frequency of 200 rpm for 30 seconds every hour was established in order for the fluid-rock mixture to remain well mixed. Temperature and pressure were monitored remotely to assure there were no deviations from

the set temperature and saturation vapor pressure at 150 °C (~4.76 bars). Reactors ran for a total of 101 days with sampling taking place at 82 days (6/28/15) and 101 days (7/17/15). Based on previous silicic water-rock interaction experiments where equilibrium conditions were observed in as few as 1-32 days (Rodriguez, 2011; Neupane et al., 2013) and personal communication with Dr. Hari Neupane, 101 days was deemed a sufficient time frame to

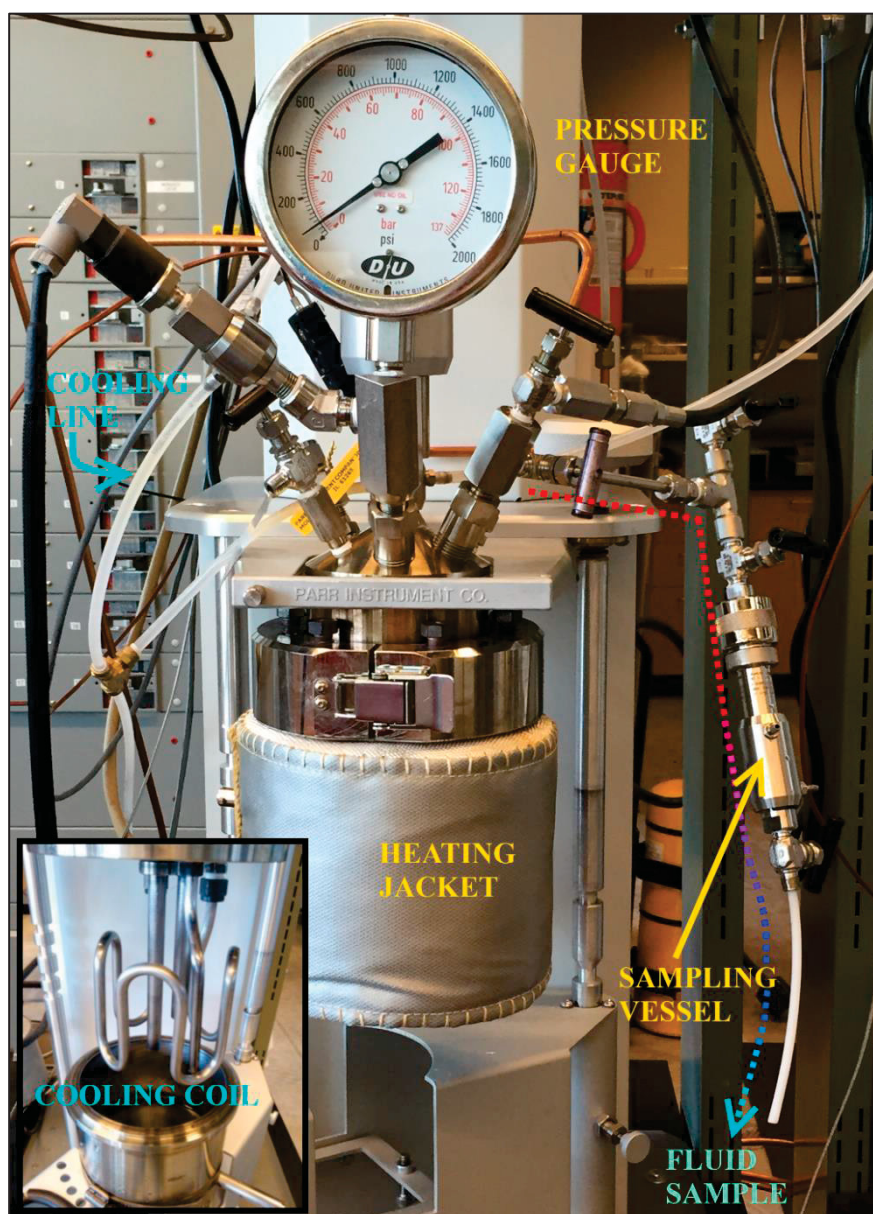


Figure 35. Water-rock interaction experiments conducted at 150 °C using bench top Parr 1 L reactor vessels. Inset – a reactor vessel and its cooling coil.

obtain equilibrium at 150 °C. Equilibrium conditions are also supported by reaction path modeling using The Geochemist's Workbench (Bethke and Yeakel, 2013) where calculated near zero saturation index values are observed for chalcedony, calcite, and fluorite. The absence of apparent equilibrium conditions with the clays and zeolites mentioned previously in Chapters 3 and 4 may be explained by the use of the andesitic Shoshone Falls Rhyolite sample as opposed to the more abundant rhyolites within the Idavada volcanics. Additionally, the remarkably high silica concentrations observed in initial water samples may suggest that volcanic silicic glass is controlling silica equilibrium. Future work examining secondary alteration mineralization within experimental rock samples along with experimental runs with varied rock types would aid in reducing uncertainties regarding equilibrium.

Prior to sample collection, a small 5-10 mL volume was extracted in order to purge the sampling vessel of "dead sample" stuck from the previous sample collection. Three samples of approximately 5-8 mL were taken for cation, anion, and trace elemental analyses in pre-washed 25 mL HDPE bottles. All samples were filtered through a 0.45 μm filter. Cation and trace metal samples were preserved through acidification to a $\text{pH} < 2$ with concentrated optima grade HNO_3 . An additional 3-4 mL sample was taken to obtain a pH measurement immediately after sampling. Major anions were analyzed with ion chromatography (Dionex ICS-2100), major cations were analyzed with Inductively Coupled Plasma-Optical Emission Spectroscopy (ICP-OES iCAP 6500), and trace elements were analyzed with Inductively Coupled Plasma-Mass Spectroscopy (ICP-MS Agilent 7500ce). Water chemistry results for the initial thermal component are shown in Table 12.

6.5 Experimental Procedure: Part 2

Prior to mixing thermal waters from Reactors #5 and #6 with groundwater and new host rock samples, the cleaning and leak test procedure described above was repeated for four new reactor vessels (#s 1,3,4, and 8). The water rock ratio of 600 mL water to 60 g of rock sample was maintained throughout the mixing portion of the experiment. Reactors #5 and #6 were brought down to 70°C individually and transferred rapidly (5 min) into new reactors with cold groundwater where the mixture was heated to 70 °C, maintained at saturation vapor pressure, and stirred for 30 seconds at 200 rpm every hour. Thermal to mixed water ratios of 60%, 40%, and 20% thermal water were utilized for reactor #s 4, 3, and 1 respectively. Reactor #8 was established as the experimental control in which no ESRP basalt rock sample was added. Water to rock and thermal water to groundwater ratios are presented in Table 11.

Table 11. Water-rock Interaction Experimental Matrix

Initial Experimental Waters						
Reactor	T (°C)	P_{H_2O} (bars)	Idavada Sample Mass (g)	Solution Volume (mL)	Duration (days)	
# 5	150	4.76	60	600	101	
# 6	150	4.76	60	600	101	
Mixed Experimental Waters						
Reactor	T (°C)	P_{H_2O} (bars)	Basalt Sample Mass (g)	Thermal Solution Volume (mL)	Groundwater Solution Volume (mL)	Duration (days)
# 1	70	0.31	60	120	480	4
# 3	70	0.31	60	240	360	40
# 4	70	0.31	60	360	240	40
# 8	70	0.31	0	240	360	40

Because reactor #s 3 and 8 contained thermal water derived from reactor #5, the thermal water to groundwater ratio of 40 % thermal water to 60% groundwater was utilized in control reactor # 8 to match the ratio of reactor # 3. 60 g of ESRP basalt sample was added to

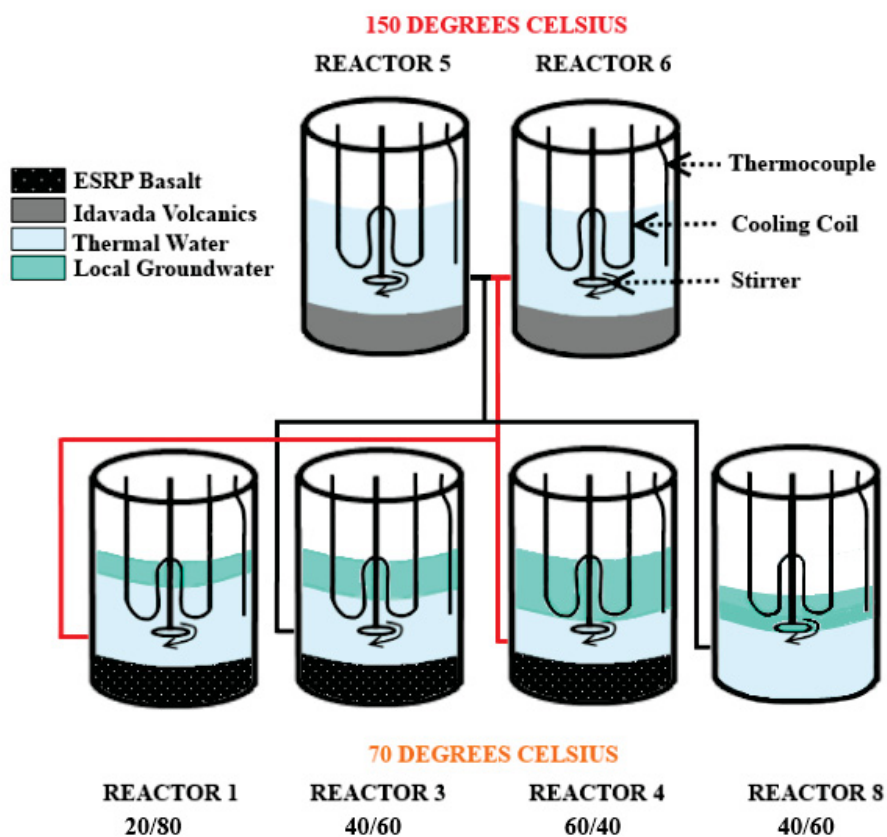


Figure 36. Experimental diagram showing the transfer of thermal water to mixed water reactors. Water to groundwater ratios are shown for Reactors # 1, 3, 4, and 8.

each reactor vessel. All reactors were sampled at 4 hr, 8 hr, 24 hr, 48 hr, 96 hr, 10 days, 20 days, 30 days, and 40 days with the exception of reactor # 1 which ran dry after the 96 hr sample most likely due to the development of a pressure leak. Samples were taken for major cations, anions, and trace metals and analyzed in the same manner as the first portion of the experiment. The water chemistry results for all reactors are presented in Table 12 below.

6.6 Results

Experimental results with respect to solution concentration over time are shown in Table 12 for all analyzed chemical constituents. Results are presented graphically for select chemical constituents of interest in Figures 37-40.

Table 12. Chemical analysis results from initial and mixed experimental waters.

Initial Experimental Waters													
Sample	pH	Temp °C	F mg/L	Cl mg/L	SO4 mg/L	NO3 mg/L	Ca mg/L	Mg mg/L	Na mg/L	K mg/L	SiO2 mg/L	Al mg/L	B mg/L
Groundwater Sample	7.47	15.9	0.5	46.2	59.3	9.36	57.2	19.78	35.4	6.45	41.6	1.00E-04	-
CC-150-5 (6-28-15)	6.85	150	2.61	42.5	57.4	7.30	12.3	0.11	42.5	21.4	242	0.41	-
CC-150-6 (6-28-15)	6.91	150	3.42	49.3	61.8	9.26	2.65	0.21	69.1	38.6	270	1.79	-
CC-150-5 (7-17-15)	6.88	150	3.02	46.77	63.87	8.23	16.5	0.10	47.9	23.5	255	0.60	0.107
CC-150-6 (7-17-15)	6.96	150	3.55	47.48	58.71	8.95	<10	0.10	70.4	35.9	235	1.98	0.107
Mixed Experimental Waters													
Sample	pH	Temp °C	F mg/L	Cl mg/L	SO4 mg/L	NO3 mg/L	Ca mg/L	Mg mg/L	Na mg/L	K mg/L	SiO2 mg/L	Al mg/L	B ug/L
CC-1-20/80-7-17-15 (4 Hr)	7.59	70	2.32	50.0	71.4	22.5	23.6	5.66	61.5	23.3	127	1.045	0.114
CC-1-20/80-7-17-15 (8 Hr)	7.96	70	2.08	48.9	70.4	9.12	22.4	5.31	66.7	24.0	109	0.119	0.136
CC-1-20/80-7-18-15 (24 Hr)	7.62	70	1.84	50.0	86.2	9.25	18.9	4.25	79.5	24.4	77.7	0.161	0.166
CC-1-20/80-7-19-15 (48 Hr)	7.35	70	1.29	49.7	107	8.99	13.9	2.82	91.7	23.8	60.5	0.221	0.162
CC-1-20/80-7-21-15 (96 Hr)	7.72	70	0.544	48.6	168	8.58	<1	1.21	138	23.6	27.9	0.476	0.150
CC-3-40/60-7-17-15 (4 Hr)	7.94	70	1.63	48.1	63.2	9.17	34.5	9.59	54.9	21.1	127	0.351	0.117
CC-3-40/60-7-17-15 (8Hr)	7.91	70	1.64	48.5	63.9	9.24	38.3	10.85	51.6	18.3	110	0.184	0.100
CC-3-40/60-7-18-15 (24 Hr)	7.75	70	1.58	47.9	66.1	9.12	37.2	10.32	51.8	17.8	103	0.074	0.119
CC-3-40/60-7-19-15(48 Hr)	7.28	70	1.53	48.5	70.1	9.26	39.6	10.41	55.6	18.4	109	0.072	0.104
CC-3-40/60-7-21-15 (96 Hr)	7.35	70	1.30	48.3	77.4	9.15	34.9	10.29	60.3	18.6	101	0.101	0.114
CC-3-40/60-7-28-15 (10Day)	7.1	70	1.01	48.7	90.0	9.10	29.7	10.26	70.6	19.1	94.1	0.130	0.122
CC-3-40/60-8-5-15 (20 Days)	6.86	70	0.851	48.2	98.8	9.09	27.2	9.91	75.6	19.2	90.3	0.110	0.122
CC-3-40/60-8-16-15 (30 Day)	6.98	70	0.771	48.3	104	8.91	25.8	9.23	83.0	18.7	91.2	0.130	0.111
CC-3-40/60-8-29-15 (40 Day)	7.15	70	0.65	47.95	107.18	8.98	21.1	8.58	87.4	18.9	78.7	0.117	0.126
CC-4-60/40-7-17-15 (4 Hr)	7.92	70	1.48	51.0	69.4	9.22	42.1	10.74	47.7	14.6	130	0.078	0.156
CC-4-60/40-7-17-15 (8 Hr)	7.82	70	1.49	50.8	70.2	9.18	40.6	10.37	46.5	14.3	119	0.050	0.157
CC-4-60/40-7-18-15 (24 Hr)	7.75	70	1.41	50.7	73.0	9.11	41.3	10.05	49.8	15.1	114	0.050	0.155
CC-4-60/40-7-19-15(48 Hr)	7.45	70	1.28	52.0	80.0	9.10	38.2	9.32	53.6	15.2	112	0.059	0.144
CC-4-60/40-7-21-15 (96 Hr)	7.36	70	0.939	51.9	91.7	9.06	31.0	8.54	60.6	15.2	93.6	0.092	0.342
CC-4-60/40-7-28-15 (10 day)	7.21	70	<0.5	50.6	122	9.05	25.6	7.56	72.0	15.7	74.9	0.067	0.175
CC-4-60/40-8-5-15 (20 Day)	7.01	70	<0.5	49.1	125	8.59	21.3	5.86	83.7	15.6	61.2	0.105	0.256
CC-4-60/40-8-16-15 (30 Day)	7.06	70	<0.5	47.6	127	8.33	14.6	3.80	96.6	16.2	47.3	0.192	0.162
CC-4-60/40-8-29-15 (40 Day)	7.21	70	<0.5	46.37	139.66	8.01	10.7	3.00	105	16.1	50.8	0.198	0.183
CC-8-NoRock-7-17-15- (4 Hr)	8.18	70	1.57	47.7	63.0	8.97	39.2	9.77	41.9	15.4	145	0.155	0.119
CC-8-NoRock-7-17-15 (8 Hr)	8.14	70	1.57	47.7	63.5	8.93	41.0	10.72	43.6	16.0	146	0.097	0.086
CC-8-NoRock-7-18-15 (24 Hr)	8.04	70	1.52	47.7	62.1	8.92	39.6	10.41	42.6	15.2	139	0.091	0.208
CC-8-NoRock-7-19-15 (48 Hr)	7.86	70	1.48	47.4	61.3	8.77	37.2	10.17	42.6	15.0	134	0.075	0.102
CC-8-NoRock-7-21-15 (96 Hr)	7.84	70	1.45	47.6	61.2	8.76	33.9	9.47	41.8	14.6	126	0.051	0.110
CC-8-NoRock-7-28-15 (10 Day)	7.44	70	0.872	46.8	54.9	8.64	19.2	5.68	36.1	12.6	69.9	0.050	0.144
CC-8-NoRock-8-5-15 (20 Day)	7.48	70	<0.5	44.1	45.5	8.09	<10	2.49	30.6	10.1	15.9	0.050	0.100
CC-8-NoRock-8-16-15 (30 Day)	7.5	70	<0.5	40.5	37.7	7.31	<10	1.12	26.2	8.5	<10	0.081	0.100
CC-8-NoRock-8-29-15 (40 Day)	7.4	70	<0.5	31.41	28.18	5.61	<10	1.07	35.4	11.8	<10	0.076	0.100

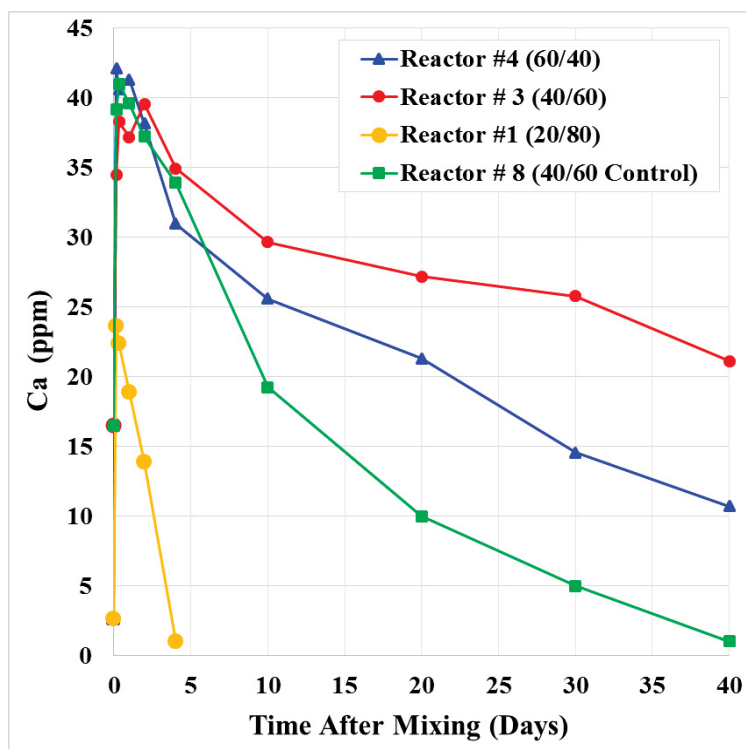


Figure 37. Calcium concentrations of experimental mixed thermal water samples over time. Ratios of thermal to groundwater are given in parentheses.

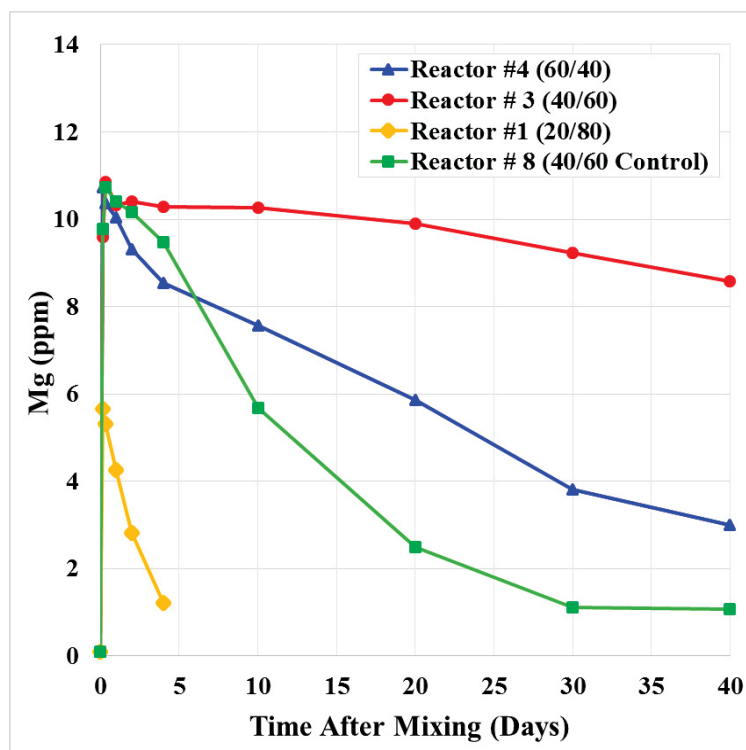


Figure 38. Magnesium concentrations of experimental mixed thermal water samples over time. Ratios of thermal to groundwater are given in parentheses.

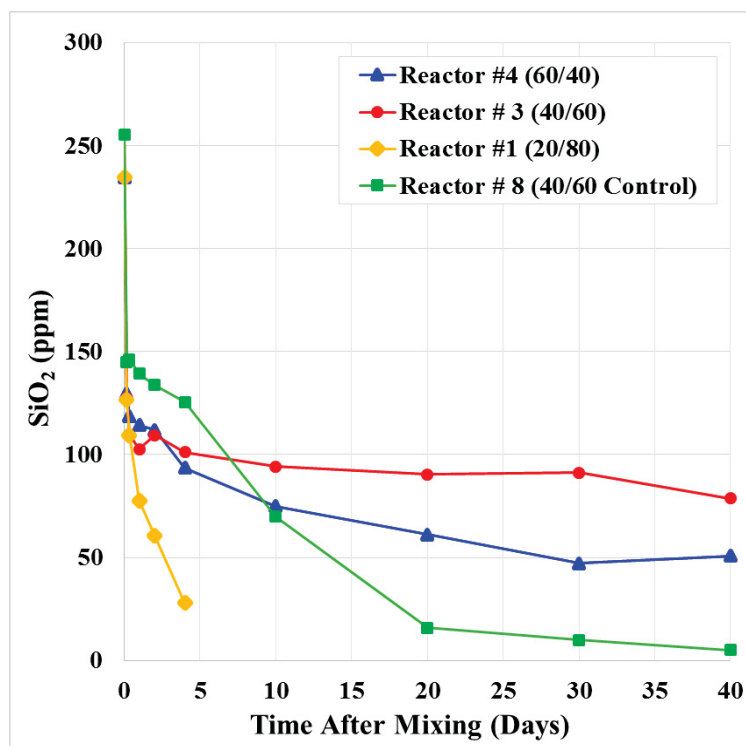


Figure 39. Silica concentrations of experimental mixed thermal water samples over time. Ratios of thermal to groundwater are given in parentheses.

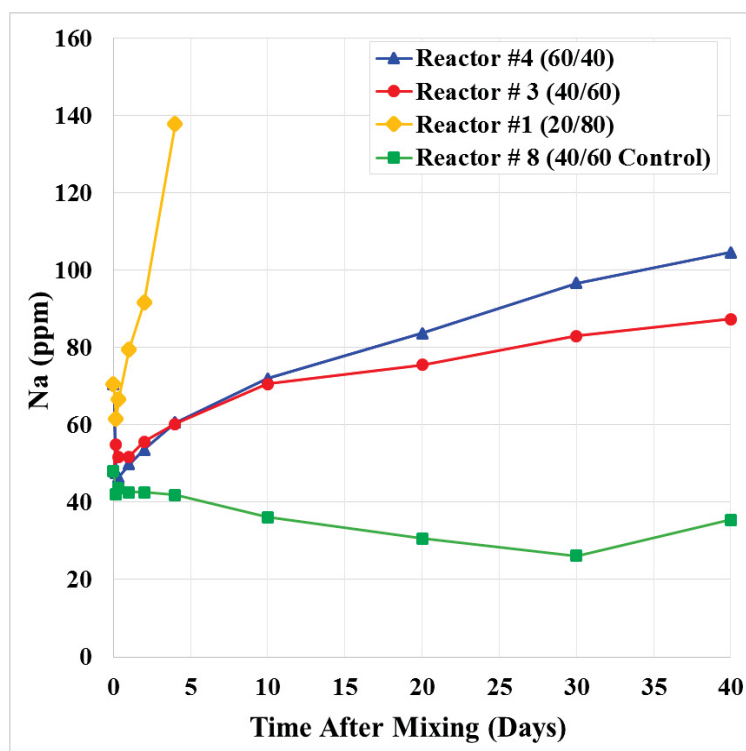


Figure 40. Sodium concentrations of experimental mixed thermal water samples over time. Ratios of thermal to groundwater are given in parentheses.

Ca and Mg concentrations show an immediate increase after initial mixing with groundwater progressing from initial concentrations ($< 10 - 16.5$ ppm Ca and 0.1 ppm Mg) to values around $35-40$ ppm Ca and $9.5 - 10.5$ ppm Mg (Reactors # 3,4, and 8). Reactor # 1, containing 20 % thermal water, exhibits a less prominent initial increase in Ca and Mg concentrations rising to only about 23.6 ppm Ca and 5.66 ppm Mg. After fluctuating about the initial point of increase, all reactors show significant declines in Ca and Mg concentration after the 4 day mark. The rate of decline of Ca and Mg seems to be effected by the ratio of initial thermal water to groundwater as a sharper decline for both constituents is exhibited in Reactor # 4 containing the highest ratio (60% thermal water) compared to Reactor # 3 (40 % thermal water). Reactor # 8 (control) shows a steeper decline than the previous two reactors for both Ca and Mg. Due to sample loss from a likely vessel leak, Reactor # 1 only has available data for 4 days. A very steep decline in both Ca and Mg is observed in Reactor # 1 but the rate of decline may be influenced by the open system created by the apparent leak.

SiO₂ concentrations show a dramatic decline after the initial mixing of thermal water and groundwater samples dropping from between $235-255$ ppm SiO₂ to between about $130-145$ ppm at the 4 hour mark in all reactors. However, unlike Ca and Mg concentration trends which show no sign of leveling off, SiO₂ seem to level off in Reactors # 3 and 4 at around the 20 day mark. Again, Reactor # 3 (60 % thermal water) with a greater percentage of thermal water component results in lower concentrations compared with Reactor # 4 (40% thermal water). Reactor # 8 (control) does not appear to be leveling off given its sharp decline.

In contrast to the previously discussed trends, Na concentrations increase in Reactor #s 1, 3, and 4 after initial mixing. Reactor # 4 (60 % thermal water) exhibits a steeper rate of increase over time than Reactor # 3 (40% thermal water). Reactor # 8 (control) is the only

reactor which exhibits a fairly constant decline in Na concentrations over time. The steepest rate of increase of sodium concentrations is observed in Reactor # 1. However, this trend may or may not be significant due to the aforementioned equipment malfunctions manifesting around the 4 day mark.

6.7 Discussion

The experiments conducted in this chapter replicated the mixing of a felsic volcanic derived thermal water (150 °C) with a more dilute Ca-Mg-HCO₃ type groundwater at an intermediate temperature (70 °C) and the subsequent composition altering processes of the mixed water. These experiments show that the rates of change for select cations (Ca, Mg, and Na) and SiO₂ within mixed thermal waters may be dependent on the ratio of thermal water to groundwater within solution. A greater percentage of thermal water is correlated to a steeper rate of decline in Ca, Mg, and SiO₂ concentrations and a steeper rate of increase in Na concentrations. An increase number of experiments with varying thermal water to groundwater ratios may show whether this correlation is significant or not. Significant differences in concentrations between thermal water, groundwater, and mixed water are observed almost immediately.

After the 4 day mark, waters begin showing significant decreasing trends with respect to Ca, Mg, and SiO₂ concentrations and a significant rising trend with respect to Na concentrations. Reactor #8, which contained no basalt rock samples, is the only experiment to not show an increasing Na trend after mixing which may suggest that the transition into a more mafic rock type is necessary for the observed trends. With the exception of SiO₂, these trends do not show signs of levelling off. This observation is congruent with a mechanism for re-equilibration by a precipitation or cation exchange reaction explaining the apparent mixing

between pure or dilute Na-HCO_3 water with thermal Na-HCO_3 type waters of the Twin Falls – Banbury hydrothermal system. The inverse of the trends displayed above may explain the possible re-equilibration of rising Na-HCO_3 type water into more Ca-HCO_3 type thermal waters at cooler temperatures.

CHAPTER 7: SUMMARY AND CONCLUSIONS

The Eastern Snake River Plain, formed by successive caldera formation associated with the migration of the Yellowstone hotspot, is considered to have some of the highest geothermal potential within the state of Idaho and the entire country (Tester et al., 2006). Geothermal potential is made evident through the many hydrothermal expressions (springs and wells) that line the periphery of the plain, anomalously high geothermal gradients (Brott et al., 1976) and heat flow values (Blackwell and Richards, 2004), and high mantle signature $^3\text{He}/^4\text{He}$ ratios (Dobson et al., 2015). Despite all of the potential within the region, geothermal development has been limited to low temperature resources and attempts at reservoir temperature estimation have resulted in lower than expected estimates. Many believe that this is due to the masking of the deep geothermal signature by the prolific overlying groundwater aquifer of the ESRPA (McLing et al., 2002; Neupane et al., 2014; Cannon et al., 2014; Dobson et al., 2015). While previous studies have acknowledged the possibility of mixing between ascending thermal waters and groundwater, few have attempted to compensate for its effects on reservoir temperature estimation through geothermometry. Because of sample density and preliminary temperature estimation results, the Twin Falls – Banbury hydrothermal system was chosen as the location for an in depth investigation into the possibility of mixing and re-equilibration in thermal waters of the ESRP.

Through principle component and hierarchical cluster analyses, two distinct thermal water types (Na-HCO_3 and Ca-HCO_3) were identified in the Twin Falls – Banbury area. Na-HCO_3 waters are separated by from Ca-HCO_3 waters by higher temperatures, higher TDS, and higher Na^+ concentrations. Ca-HCO_3 waters are characterized by high Ca^{2+} and Mg^{2+} concentrations and cooler temperatures. Na-HCO_3 waters emanate exclusively from thermal

springs and a select few wells that are completed within the rhyolites of the Idavada volcanics whereas the Ca-HCO_3 thermal waters are found in wells completed within the overlying basalts. This is consistent with the trend from Na-K-HCO_3 thermal waters and Ca-Na-HCO_3 thermal waters with decreasing temperature and depth observed in the deep INEL-1 well that penetrates the basalt units of the ESRPA (Mann, 1986; McLing et al., 2002).

Evidence for mixing in the study area is provided by a linear trend between these two water types on a Piper diagram (Piper, 1944), partial equilibration and immature classification of most thermal water samples on the Giggenbach ternary diagram (Giggenbach, 1988), and linear trends between several conservative chemical constituents (Cl, B, δD , etc.). In addition to the evidence for simple mixing between the two water types, relationships between some reactive chemical constituents (Na, K, Mg, and Ca) display two separate and distinct trends for the two water types which suggests either:

- 1) The waters may be the result of two separate and unrelated flow pathways, host rocks, and/or equilibration temperatures.

Or

- 2) The waters have undergone some form of reactive mixing and/or re-equilibration resulting in the transition from Na-HCO_3 thermal waters to Ca-HCO_3 thermal waters and vice versa depending on the reservoir temperature, rock types, and thermal water to groundwater ratio.

Reservoir temperature estimations were made utilizing conventional geothermometry techniques, silica-enthalpy mixing models, and multicomponent equilibrium geothermometry. Silica and cation conventional geothermometers yield highly varied results and many of them are limited in their application due to high calcium and magnesium concentrations of many

thermal water samples. Silica-enthalpy mixing models are capable for accounting for dilution effects from simple mixing and are considered to yield more reliable temperature estimations. However, these models yield a wide range of possible reservoir temperatures and are incapable of accounting for the apparent reactive mixing and/or re-equilibration. In contrast, MEG through the use of the inverse modeling tool RTest, is capable of accounting for a mixing component while utilizing an entire assemblage of likely reservoir alteration minerals to obtain a reservoir temperature. RTest was utilized for both Ca-HCO₃ and Na-HCO₃ thermal waters. Simple mixing between groundwater and thermal water is not supported for Na-HCO₃ thermal waters yet is supported for Ca-HCO₃ thermal waters yielding temperature estimates between around 90 – 100 °C. The reconstructed compositions for Ca-HCO₃ waters produced by inverse modeling do not resemble the compositions of the Na-HCO₃ waters signifying that the Ca-HCO₃ thermal waters may be the result of re-equilibration if there exists a relationship between the two thermal water types.

An “intermediate” composition obtained from the intersection of the reactive constituent trends was utilized as the mixing component in RTest modeling of Na-HCO₃ waters. This type of mixing is not supported through the use of RTest as adequate saturation index convergence of likely reservoir minerals is not obtained. However, the use of pure water as the mixing component in RTest modeling of Na-HCO₃ results in adequate saturation index convergence and reservoir temperatures as high as 160 °C. The same results are achieved when dilute Na-HCO₃ water is used as the mixing component for Na-HCO₃ RTest modeling. In order to explain this phenomenon, a mechanism for re-equilibration was proposed in which groundwater (Ca-Mg-HCO₃ type) loses Ca²⁺ and Mg²⁺ and gains Na⁺ upon mixing with a Na-HCO₃ thermal water with increasing temperature and depth resulting in

dilute water that further mixes with Na-HCO₃ thermal waters. Conversely, this re-equilibration mechanism explains the transition from Na-HCO₃ thermal waters into more Ca-HCO₃ thermal waters by the increase of Ca²⁺ and Mg²⁺ and decrease of Na⁺ from mixing during ascension through a series of equilibration zones. The RMAs utilized in MEG inverse modeling show that Ca-HCO₃ waters in equilibrium with Ca²⁺ and Mg²⁺ rich smectite clays and zeolites gradually shift to Na-HCO₃ waters in equilibrium with Na⁺ and K⁺ rich smectite clays and zeolites through several zones of re-equilibration resulting in thermal water types in between the two end members.

A possible re-equilibration mechanism was tested using high temperature water-rock interaction experiments. In the experiments, a 150 °C thermal water derived from equilibration with Idavada volcanics was mixed with a local groundwater at an intermediate 70 °C within the basalts of the ESRP. Samples taken over 40 days reveal that Ca²⁺, Mg²⁺, and SiO₂ concentrations decrease significantly at about 4 days after initial mixing. Na⁺ concentrations increase dramatically within the same observation time thus providing support for the possibility of re-equilibration of thermal waters within the Twin Falls – Banbury hydrothermal area.

A detailed look into local geology and hydrology reveals that the thermal system is likely recharged from the Cassia Mountains to the south of the study area. Groundwater likely picks up its Ca-Mg-HCO₃ signature from the Paleozoic carbonates exposed in the area before travelling northwesterly towards the Twin Falls and Banbury thermal clusters. The Banbury hydrothermal system appears to be controlled by a single northwest trending normal fault with Ca-HCO₃ thermal waters grading into Na-HCO₃ thermal waters away from the recharge zone. A similar distribution of thermal waters is observed in the Twin Falls thermal area without the

presence of a major fault. Na-HCO₃ thermal waters are located near the Snake River where overlying Quaternary and Tertiary basalt units thin allowing for Tertiary Idavada volcanics to be exposed at the surface. A pumping test was performed on two deep rhyolite-penetrating wells on the campus of the College of Southern Idaho. Estimates of aquifer transmissivity from pump/recovery test analysis agree with a previous area study (Street and DeTar, 1987) at values of 930 m²/d (7.5×10^4 gpd/ft). While there appears to be no decline in temperature of the Twin Falls area resource in the last 30 years, a significant decline in hydraulic head of about 15 meters (50 ft.) is observed with head values dropping from about 14 meters (45 ft.) above land surface to about 1.2 meters (4 ft.) below land surface at present day.

In its entirety, this work has resulted in the redefining of the conceptual model for the Twin Falls – Banbury thermal system. Advanced geothermometry techniques have been utilized to provide evidence for a high temperature (150+ °C) resource in the Twin – Falls Banbury area, historic and newly collected geochemical data have been used to provide evidence for both mixing and re-equilibration of thermal waters, and the possibility of a re-equilibration mechanism has been tested through a series of high temperature water-rock interaction and mixing experiments. The RTest temperature estimates made for Na-HCO₃ waters are consistent with an estimate of 150 °C for Banbury Hot Springs made using sulfate-water isotope geothermometry earlier this year (Conrad et al., 2015).

In addition to providing new insights into reservoir temperature and mixing relationships, this study has raised questions that may be answered by future work. Although the possibility of the two thermal water types being unrelated and the product of two separate flow paths is considered unlikely, it cannot be ruled out from the work presented here. Additionally, the results of the mixing portion of the water-rock interaction experiments lead

to the assumption that the transition from silicic volcanics to basalt is necessary for re-equilibration to take place. Further work regarding possible flow paths between the Idavada volcanics and overlying basalts is warranted to answer both of these questions. An expansion of the experiment to include the possibility of re-equilibration without mixing, rhyolite exclusive mixing, and temperature decreases in rhyolites and basalts without mixing may also aid in the understanding of the system. Lastly, x-ray powder diffraction (XRD) and scanning electron microscopy (SEM) analysis of post experimental rock samples would aid in both the understanding of alteration mineral assemblages and the exchange or precipitation reactions responsible for re-equilibration.

REFERENCES

- Adar, E.M., E. Rosenthal, A.S. Issar, and Batelaan, O. (1992). Quantitative assessment of the flow pattern in the Southern Arava Valley (Israel) by environmental tracers and a mixing cell model. *J. Hydrol.*, 136, p. 333-352.
- Arnórsson, S., Gunnlaugsson, E., and Svavarsson, H. (1983). The chemistry of geothermal waters in Iceland. II. Mineral equilibria and independent variables controlling water compositions. *Geochim. Cosmochim. Acta*, 47, p. 547-566.
- Arnórsson, S. (1985). The use of mixing models and chemical geothermometers for estimating underground temperature in geothermal systems. *J. Volc. Geotherm. Res.*, 23, p. 299-335.
- Basharina, L.A. (1958). Water extracts of the ashes and the ash-cloud gases of the Bezymyannyi volcano: Akad. Nauk SSSR, Lab. Vulkanol., Vulkanol. Stantsii Biull, v. 27, p. 38-42.
- Bethke, C.M. (2008). *Geochemical and Biogeochemical Reaction Modeling*. Cambridge University Press, p 547.
- Bethke, C.M. and Yeakel, S. (2012). The Geochemist's Workbench ® Release 9.0. Reaction Modeling Guide. *Aqueous Solutions, LLC*, Champaign, Illinois.
- Blackwell, D.D., and M.C. Richards. (2004). "Geothermal Map of North America." American Association of Petroleum Geologists, 1 sheet, scale 1:6,500,000.
- Bottinga, Y. (1968). Hydrogen isotope equilibria in the system hydrogen-water. *Journal of Physical Chemistry*, v. 72, p. 4338-4340.
- Brott, C.A., D.D. Blackwell, and J.C. Mitchell. (1976). Geothermal Investigations in Idaho Part 8: Heat Flow in the Snake River Plain Region, Southern Idaho. *Water Information Bulletin* 30, Idaho Department of Water Resources.
- Browne, P.R.L. (1978). Hydrothermal Alteration in Active Geothermal Fields. *Annual Review of Earth and Planetary Sciences*, 6: p. 229-250.
- Cannon, C., Wood, T., Neupane, G., McLing, T., Mattons, E., Dobson, P., and Conrad, M. (2014). Geochemical Sampling for Traditional and Multicomponent Equilibrium Geothermometry in Southeast Idaho. *Geothermal Resources Council Transactions*, Vol. 38, p. 425.

- Carroll, D. (1959). Ion exchange in clays and other minerals. Geological Society of America, v. 70, p. 749-779.
- Clark, I.D. (2015). *Groundwater Geochemistry and Isotopes*. "Tracing the Water Cycle. Taylor and Francis Group, LLC, p. 127-129.
- Cloutier, V., Lefebvre, R., Therrien, R., and Savard, M.M. (2008). Multivariate statistical analysis of geochemical data as indicative of the hydrogeochemical evolution of ground water in a sedimentary rock aquifer system. *J. Hydrol.*, 353, p. 294-313.
- Cooper, H.H. and Jacob, C.E. (1946). A generalized graphical method for evaluating formation constants and summarizing well field history, *Am. Geophys. Union Trans.*, vol. 27, p. 526-534.
- Cooper, D.C., Palmer, C.D., Smith, R.W., & McLing, T.L. (2013). Multicomponent equilibrium models for testing geothermometry approaches. *Proceedings*. 38th Workshop on Geothermal Reservoir Engineering Stanford University, Stanford, CA.
- Conrad, M.E., Dobson, P.F., Sonnenthal, E.L., Cannon, C., Wood, T., McLing, T., Neupane, G., and Mattson, E. (2015) Isotopic Insights into Deep Geothermal Systems in the Snake River Plain in Southeastern Idaho. *25th Goldschmidt Conference, Prague, Czech Republic*.
- D'Amore, F., Fancelli, R., and Caboi, R. (1987). Observations on the application of chemical geothermometers to some hydrothermal systems in Sardinia. *Geothermics*, 16, p. 271-282.
- Davis, J. (1986). *Statistics and Data Analysis in Geology*. 2nd Edn. Wiley, New York, p. 646
- Davis, A.C., Bickle, M.J. and Teagle, D.A.H. (2003). Imbalance in the oceanic strontium budget. *Earth and Planetary Science Letters*, 211(1-2) p. 173-187.
- Dobson, P.F., Kennedy, M.B., Conrad, M.E., McLing, T., Mattson, E., Wood, T., Cannon, C., Spackman, R., van Soest, M., and Robertson, M. (2015). The Isotopic Evidence for Undiscovered Geothermal Systems in the Snake River Plain. *Proceedings*, 40th Workshop on Geothermal Reservoir Engineering, Stanford University, Stanford, CA, p. 2-4
- Doherty J.: PEST, Model-Independent Parameter Estimation User Manual, 5th Edition. Watermark Numerical Computing, www.pesthomp.org, (2005)

- Edmunds, M.W., and Shand, P. (2009). *Natural Groundwater Quality*, “Geochemical Modeling of Processes Controlling Baseline Compositions. John Wiley & Sons, p. 85-89.
- Ellis, A.J. (1970). Quantitative interpretation of chemical characteristics of hydrothermal systems. *Geothermics*, 2(Part 1),p. 516-528.
- Ellis, A. J. (1971). Magnesium ion concentrations in the presence of magnesium chlorite, calcite, carbon dioxide, quartz. *Amer. J. Sci.* 271, p. 481-489.
- Ellis A. J. and Mahon W. A. J. (1967) Natural hydrothermal systems and experimental hot water-rock interactions (Part II). *Geochim. Cosmochim. Acta* 31, p. 519–538.
- Fetter, C.W., 2001. *Applied Hydrogeology (4th ed.)*, Prentice-Hall, Upper Saddle River, New Jersey, p. 374.
- Fleischmann, D.J. (2006). Geothermal development needs in Idaho. Geothermal Energy Association report for the U.S. Department of Energy, p. 51
- Fouilliac, C., and Michard, G. (1981). Sodium/lithium ratio in water applied to geothermometry of geothermal reservoirs, *Geothermics*, 10, p. 55-70.
- Fournier, R.O. (1977). Chemical geothermometers and mixing model for geothermal systems. *Geothermics*, 5, 41-50.
- Fournier, R.O., and A.H. Truesdell. (1973). “An empirical Na-K-Ca geothermometer for natural waters.” *Geochim. Cosmochim. Acta*, v. 37 p. 1255-1275.
- Fournier, R.O., and R.W. Potter. (1979). “Magnesium correction to the Na-K-Ca chemical geothermometer.” *Geochim. Cosmochim. Acta* v. 43, p. 1543-1550
- Fournier R.O., and R.W. Potter II. (1982). “A revised and expanded silica (quartz) geothermometer.” *Geotherm. Resourc. Counc. Bull.*, v. 11, p.3-12
- Fournier, R. O. and Rowe, J.J. (1966). Estimation of underground temperatures from the silica content of water from hot springs and wet steam wells. *Am. J. Sci.*, 264, p. 685-691.
- Fournier, R.O., and Truesdell, A.H., (1973): An empirical Na-K-Ca geothermometer for natural waters. *Geochim. Cosmochim. Acta*, 37, 1255-1275.
- Fournier, R.O., and Truesdell, A.H. (1974). Geochemical indicators of subsurface temperature Part 2, Estimation of temperature and fraction of hot water mixed with cold water: U.S. GeoLSurvey Jour. Research, v.2, no.3, p. 263 270

- Giggenbach, W.F. (1988). Geothennal solute equilibria. Deviation of Na-K-Mg-Ca geoindicators. *Geochim. Cosmochim. Acta*, 52, p. 2749-2765
- Giggenbach, W.F. (1991). Chemical techniques in geothermal exploration; Application of Geochemistry in Geothermal Reservoir Development (D'Amore F., Ed.), UNITAR/UNDP Center on Small Energy Resources, Rome, p. 119-144.
- Gillerman, V.S., Kauffman, J.D., and Othberg, K.L. (2005) Geologic Map of the Thousand Springs Quadrangle, Gooding and Twin Falls Counties, Idaho. Idaho Geological Survey
- Gíslason, S.R., Heaney, P.J., Oelkers, E.H., Schott, J. (1997). Kinetic and thermodynamic properties of moganite, a novel silica polymorph. *Geochimica et Cosmochimica Acta*, (6), p.1193-1204.
- Guler, C., Thyne, G., McCray, J. and Turner, K. (2002). Evaluation of graphical and multivariate statistical methods for classification of water chemistry data. *Hydrogeol. J.*, 10, p. 455-474.
- Henley, R.W. and Ellis, A.J. (1983). Geothermal Systems Ancient and Modern – a Geochemical Review. *Earth-Science Reviews*, 19(1): 1-50.
- Huenges, E., and Ledru, P. (2011). *Geothermal Energy Systems: Exploration, Development, and Utilization*. Wiley Publishing, pp. 97-100
- Hughes, S.S., R.P. Smith, W.R. Hackett, and S. R. Anderson. (1999). “Mafic volcanism and environmental geology of the eastern Snake River Plain.” *Idaho Guidebook to the Geology of Eastern Idaho*. Idaho Museum of Natural History, p. 143-168
- Hughes, S.S., Wetmore, P.H. and Casper, J.L. (2002). Evolution of Quaternary Tholeiitic Basalt Eruptive Centers on the Eastern Snake River Plain, Idaho. In B. Bonnichsen, C.M. White, and M. McCurry, eds., *Tectonic and Magmatic Evolution of the Snake River Plain Volcanic Province*, Idaho Geological Survey Bulletin **30**, p. 23.
- Hull, C.D., Reed, M.H., and Fisher, K. (1987). Chemical geothermometry and numerical unmixing of the diluted geothermal waters of the San Bernardino Valley Region of Southern California. *GRC Transactions*, 11, p. 165-184.
- Kanade, S. and Gaikwad V.B. (2011). A multivariate statistical analysis of bore well chemistry data-Nashik and Niphad Taluka of Maharashtra, India. *Univer. J. Env. Res. Technol.*, 1, 193-202.

- Khitarov, N.I., Lebedev, E.B., Rengarten, E.B., and Arsena, R.V. (1959). The solubility of water in basaltic and granitic melts. *Geochemistry*, 5, p. 479-492.
- Kuntz, M.A, Covington, H.R., and Schorr, L.J. (1992) Chapter 12 – An Overview of Basaltic Volcanism of the Eastern Snake River Plain, Idaho. In Link, P.K., Kuntz, M.A., and Platt, L.B., eds., *Regional Geology of Eastern Idaho and Western Wyoming*, *Geological Society of America Memoir* 179, p. 227–267.
- Larsson, D., Grönvold, K., Oskarsson, N. and Gunnlaugsson, E. (2002). Hydrothermal alteration of plagioclase and growth of secondary feldspar in the Hengill Volcanic Centre, SW Iceland. *Journal of Volcanology and Geothermal Research*, 114, p. 275-290.
- Leeman, W.P., Annen, C. and Dufek, J. (2008). Snake River Plain – Yellowstone Silicic Volcanism: Implications for Magma Genesis and Magma Fluxes. In Annen, C. and Zellmer, G. F. (eds) *Dynamics of Crustal Magma Transfer, Storage and Differentiation*. Geological Society, London, Special Publications, **304**, p. 235–259.
- Lewis, R.E., and H.W. Young (1982). “Geothermal resources in the Banbury Hot Springs Area, Twin Falls County, Idaho.” U.S. Geological Survey Water-Supply Paper 2186, p. 27.
- Lewis, R.E. and H.W. Young. (1989). The hydrothermal system in central Twin Falls County, Idaho: U.S. Geological Survey Water Resources Investigations Report 88-4152, p. 44
- Leshner, C.M., Gibson, H.L. and Campbell, I.H. (1986). Composition-volume changes during hydrothermal alteration of andesite at Buttercup-Hill, Noranda-District, Quebec. *Geochimica Et Cosmochimica Acta*, 50(12), p. 2693-2705.
- Lonker, S.W., Franzson, H. and Kristmannsdottir, H., 1993. Mineral-Fluid Interactions in the Reykjanes and Svartsengi Geothermal Systems, Iceland. *American Journal of Science*, 293(7): 605-670.
- Mabey, D.R. (1982) Geophysics and tectonics of the Snake River Plain, Idaho, in Bonnicksen, B., and Breckenridge, R.M., eds., *Cenozoic Geology of Idaho: Idaho Bureau of Mines and Geology Bulletin* 26, p. 139
- Malde, H. E., and Powers, H. A. (1972). Geologic map of the Glens Ferry-Hagerman area, west-central Snake River Plain, Idaho: U.S. Geol. Survey Misc. Geol. Inv. Map 1-696

- Mann, L.J. (1986). Hydraulic properties of rock units and chemical quality of water for INEL-1: A 10,365-foot-deep test hole drilled at the Idaho National Engineering Laboratory, Idaho: U.S. Geological Survey Water Resources Investigations Report 86-4020, p. 23.
- Marsh, K.N. (1987) Recommended Reference Materials for the Realization of Physiochemical Properties. Blackwell, Oxford.
- Mas, A., Guisseau, D., Patrier Mas, P., Beaufort, D., Genter, A., Sanjuan, B. and Girard, J.P. (2006). Clay minerals related to the hydrothermal activity of the Bouillante geothermal field (Guadeloupe). *Journal of Volcanology and Geothermal Research*, 158(3-4) p. 380
- Mariner, R.H., H.W. Young, W.C. Evans, and D.J. Parlman. (1991). "Chemical, isotopic, and dissolved gas compositions of the hydrothermal system in Twin Falls and Jerome Counties, Idaho. *Geothermal Resources Council Transactions*, v. 15, p. 257-263.
- Mariner, R.H., H.W. Young, T.D. Bullen, and C.J. Janik. (1997). Sulfate-water isotope geothermometry and lead isotope data for regional geothermal system in the Twin Falls area, south-central Idaho. *Geothermal Resources Council Transactions*, v. 21, p. 197-201.
- McLing, T.L., R.W. Smith, and T.M. Johnson. (2002). "Chemical Characteristics of Thermal Water Beneath the Eastern Snake River Plain Aquifer." GSA Special Paper 353, p.13.
- McLing, T., McCurry, M., Cannon, C., Neupane, G., Wood, T., Podgorney, R., Welhan, J., Mines, G., Mattson, E., Wood, R., Palmer, C. and Smith, R. (2014) David Blackwell's Forty Years in the Idaho Desert, The Foundation for 21st Century Geothermal Research. *Geothermal Resources Council Transactions*, 38, p. 143–153.
- Meng, S.X., and Maynard, J.B. (2001). Use of statistical analysis to formulate conceptual models of geochemical behavior: Water chemical data from the Botucatu aquifer in Sao Paulo state. Brazil. *J. Hydrol.*, 250, p. 78-97.
- Mitchell, J.C., Johnson, L.L., and Anderson, J.E. (1980). Geothermal Investigations in Idaho Part 9: Potential for Direct Heat Application of Geothermal Resources. *Idaho Department of Water Resources Water Information Bulletin No. 30*
- Morgan, L.A., Doherty, D.J., and Leeman, W.P. (1984). Ignimbrites of the eastern Snake River Plain, Idaho: Evidence for major caldera-forming eruptions: *Journal of Geophysical Research*, v. 89, p. 8665–8678.

- Morse, L.H. and McCurry, M. (2002). Genesis of alteration of Quaternary basalts within a portion of the eastern Snake River Plain aquifer. *Special Papers Geological Society of America*, p. 213-224.
- Muthulakshmi, L., Ramu, A., Kannan, N., and Murugan, A. (2013). Application of Correlation and Regression Analysis in Assessing Ground Water Quality. *International Journal of ChemTech Research Vol. 5*, p. 355-356.
- Neuhoff, P.S., Fridriksson, T., Arnorsson, S. and Bird, D.K. (1999). Porosity evolution and mineral paragenesis during low-grade metamorphism of basaltic lavas at Teigarhorn, eastern Iceland. *American Journal of Science*, 299(6): 467-501.
- Neupane, G., Smith, R.W., McLing, T.L., Palmer, C.D., and Smith, W.W. (2013). Constraining Multicomponent Equilibrium Geothermometer Temperature Using Laboratory Experiments: Preliminary Results. *Geological Society of America*, v. 45, p.774.
- Neupane, G., Smith, R. W., Palmer, C. D., and McLing, T. L (2013). Multicomponent equilibrium geothermometry applied to the Raft River geothermal area, Idaho: preliminary results. In *Geological Society of America Abstracts with Programs*, 45.
- Neupane, G., E.D. Mattson, T.L. McLing, C.D. Palmer, R.W. Smith, and T.R. Wood. (2014). Deep geothermal reservoir temperatures in the Eastern Snake River Plain, Idaho using multicomponent geothermometry. *Proceedings, 39th Workshop on Geothermal Reservoir Engineering*, Stanford University, Stanford, California, February 24-26, 2014 SGP-TR-202, p.12.
- Neupane, G., Baum, J.S., Mattson, E.D., Mines, G.L., Palmer, C.D., and Smith, R.W., (2015). Validation of Multicomponent Equilibrium Geothermometry at Four Geothermal Power Plants. *Fortieth Workshop on Geothermal Reservoir Engineering* Stanford University, Stanford, California, January 26-28, SGP-TR-204, p. 1-9.
- Othberg, K.L., Kauffman, J.D., and Gillerman, V.S. (2005) *Geologic Map of the Twin Falls Quadrangle, Jerome, and Twin Falls Counties, Idaho*. Idaho Geological Survey.
- Othberg, K.L., Kauffman, J.D., and Gillerman, V.S. and Garwood, D.L. (2012) *Geologic Map of the Twin Falls 30 x 60 Minute Quadrangle, Idaho*. Idaho Geological Survey.
- Geologic Map 49

- Pabalan, R.T., and Bertetti, P.F. (2001). *Cation-Exchange Properties of Natural Zeolites*. Mineralogical Society of America, v. 45, p. 453-518.
- Palmer, C.D. 2013. Installation manual for Reservoir Temperature Estimator (RTEst), Idaho National Laboratory, Idaho Falls, ID.
- Parlman, D.J. and Young H.W. (1992). Compilation of Selected Data for Thermal-Water Wells and Springs in Idaho, 1921 through 1991. *U.S. Geological Survey Open-File Report 92-175*, p. 201.
- Pierce, K.L. and Morgan, L.A. (2009). Is the Track of the Yellowstone hotspot Driven by a Deep Mantle Plume? – Review of Volcanism, Faulting, and Uplift in Light of New Data, *Journal of Volcanology and Geothermal Research*, 188, p. 1–25.
- Piper, A. M. (1944). A graphic procedure in the geochemical interpretation of water analyses. *Transactions. American Geophysical Union* 25, p. 914.
- Ralston, D.R., J.L. Arrigo, J.V. Baglio Jr., L.M. Coleman, K. Souder, and A.L. Mayo. (1981). “Geothermal evaluation of the thrust area zone in southeastern Idaho.” Idaho Water and Energy Research Institute, University of Idaho, p. 110.
- Rani, A.L. and Babu S. (2008). A statistical evaluation of ground water chemistry from the west coast of Tamil Nadu, India. *Indian Journal of Marine Sciences* vol 37. p. 189-192.
- Reed, M. and Spycher, N. (1984). Calculation of pH and mineral equilibria in hydrothermal waters with application to geothermometry and studies of boiling and dilution. *Geochimica et Cosmochimica Acta*, 48, p. 1479-1492.
- Rember, W.C., and Bennett, E.H. (1979) Geologic map of the Twin Falls quadrangle, Idaho: Moscow, Idaho, Idaho Bureau of Mines and Geology, Geologic Map Series, Twin Falls Quadrangle, scale 1:250,000.
- Reyes, A.G. (1990). Petrology of Philippine geothermal systems and the application of alteration mineralogy to their assessment. *Journal of Volcanology and Geothermal Research*, 43 p. 279-309.
- Robin, V., Tertre, E., Beaufort, D., Regnault, O., Sardini, P., and Descostes, M. (2015). Ion exchange reactions of major cations (H^+ , Na^+ , Ca^{2+} , Mg^{2+} , and K^+) on beidellite: Experimental results and new thermodynamic database. Toward a better prediction of contaminant mobility in natural environments. *Applied Geochemistry* v. 59, p. 74-84.

- Rodgers, D.W., H.T. Ore, R.T. Bobo, N. McQuarrie, and N. Zentner. (2002). "Extension and subsidence of the eastern Snake River Plain, Idaho." In: C.M. White and M. McCurry, eds., *Tectonic and Magmatic Evolution of the Snake River Plain Province: Idaho Geologic Survey Bulletin 30*, p. 121-155.
- Rodriguez, A. (2011). *Water-Rock Interaction of Silicic Rocks: An Experimental and Geochemical Modeling Study. United Nations University Training Programme* Reykjavik, Iceland. P. 2-21.
- Ross, S.H. (1971). "Geothermal potential of Idaho." Idaho Bureau of Mines and Geology, Pamphlet 150, p. 72.
- Rounds, S.A., and Wilde, F.D. (2001). U.S. Geological Survey TWRI Book 9. Chapter 6.6: Alkalinity and Acid Neutralizing Capacity.
- Sant, C.J. (2012). *Geothermal Alteration of Basaltic Core from the Snake River Plain, Idaho.* Utah State University. All Graduate Theses and Dissertations Paper 1451.
- Savage, D., Bateman, K., and Richards, H.G. (1992). Granite-water interactions in a flow-through experimental system with applications to the Hot Dry Rock geothermal system at Rosemanowes, Cornwall, U.K. *Applied Geochemistry*, v. 7 p. 226
- Schroeder, F.C. (1912) *A reconnaissance of the Jarbidge, Contact, and Elk Mountain mining districts, Elko County, Nevada: U.S. Geological Survey Bulletin 497*, p. 36
- Shervais, J.W., Schmidt, D.R., Nielson, D., Evans, J.P., Christiansen, E.H., Morgan, L., Shanks, W.C.P., Prokopenko, A.A., Lachmar, T., Liberty, L.M., Blackwell, D.D., Glen, J.M., Champion, D., Potter, K.E. and Kessler, J.A. (2013). First Results from HOTSPOT: The Snake River Plain Scientific Drilling Project, Idaho, U.S.A., *Scientific Drilling*, 15, p. 36–45.
- Smith, R.W., Palmer, C.D., and Cooper, D.: Approaches for multicomponent equilibrium geothermometry as a tool for geothermal resource exploration. AGU Fall Meeting, San Francisco, 3-7 December 2012.
- Spycher, N.F., Peiffer, L., Sonnenthal, E.L., Saldi, G., Reed, M.H., Kennedy, B.M. (2014) Integrated multicomponent solute geothermometry), *Geothermics*, 51, p. 113–123

- Street, L.V., and DeTar, R.E. (1987). Geothermal Resource Analysis in Twin Falls County, Idaho: Idaho Department of Water Resources: Water Information Bulletin No. 30, Part 15, p. 46
- Stefánsson, A. and Arnórsson, S. (2002). Gas pressures and redox reactions in geothermal fluids in Iceland. *Chemical Geology*, 190(1-4), p. 251-27
- Taylor, H. P., Jr. (1974). The Application of Oxygen and Hydrogen Isotope Studies to Problems of Hydrothermal Alteration and Ore Deposition: *Economic Geology*, vol. 69, p. 843-883.
- Tester, J.W., Anderson, B.J., Batchelor, A.S., Blackwell, D.D., DiPippo, R., Drake, E.M., Garnish, J., Livesay, B., Moore, M.C., Nichols, K., Petty, S., Toksöz, M.N., and Veatch, R. W. (2006). The future of geothermal energy - impact of enhanced geothermal systems (EGS) on the United States in the 21st century. Massachusetts Institute of Technology, p. 372.
- Theis, C.V. (1935). The relation between the lowering of the piezometric surface and the rate and duration of discharge of a well using groundwater storage, Am. Geophys. Union Trans., vol. 16, p. 519-524.
- Tole, M.P., Ármannsson, H., Pang, Z.H., and Arnórsson, S. (1993). Fluid mineral equilibrium calculations for geothermal fluids and chemical geothermometry. *Geothermics* 22, p. 17-37.
- Truesdell, A.H., 1976. "Summary of section III - geochemical techniques in exploration." Proceedings of the 2nd U.N. Symposium on the Development and Use of Geothermal Resources, San Francisco, v. 1, p. 31.
- Truesdell, A.H., and Fournier, R.O., 1977: Procedure for estimating the temperature of a hot water component in a mixed water using a plot of dissolved silica vs. enthalpy. U.S. Geol. Survey J. Res., 5, p. 49- 52.
- Truesdell, A.H., M. Nathenson, and R.O. Rye. 1977. The effects of subsurface boiling and dilution on the isotopic compositions of Yellowstone thermal waters. *Journal of Geophysical Research* 82, p. 3694–3704.
- USDA (2011). Digital Orthoimagery Series of Idaho (2011, 1-meter, Natural and False Color) USDA-FSA-APFO Aerial Photography Field Office. Salt Lake City, Utah.

- USGS (2004) Development of a local meteoric water line for southeastern Idaho, western Wyoming, and southcentral Montana. Scientific Investigations Report 2004-5126
- Verma, M.P. (2000). Limitations in applying silica geothermometers for geothermal reservoir estimation. 25th Workshop on Geothermal Reservoir Engineering. Stanford University, Stanford, California, January 24-26, 2000. SGP-TR-165
- Weisenberger, T. and Selbekk, R.S., 2009. Multi-stage zeolite facies mineralization in the Hvalfjordur area, Iceland. *International Journal of Earth Sciences*, 98(5) p. 985-999.
- White, D.E. (1968). Thermal Waters of Volcanic Origin. *Bulletin of the Geological Society of America* vol. 58, p. 1649-1650.
- Williams, C.F., and DeAngelo, J. (2011). Evaluation of Approaches and Associated Uncertainties in the Estimation of Temperatures in the Upper Crust of the Western United States, *Geothermal Resources Council Transactions*, 35, p. 1599–1605.
- Williams, C.F., Reed, M.J., Mariner, R.H., DeAngelo, J. and Galanis, S.P., Jr. (2008). Assessment of Moderate- and High-Temperature Geothermal Resources of the United States, *U.S. Geological Survey Fact Sheet* 2008-3082, p. 4.
- Wood, W.W., and W.H. Low. (1988). “Solute chemistry of the Snake River Plain Regional Aquifer System, Idaho and Eastern Oregon.” U.S. Geological Survey Professional Paper 1408-D, p. 79.
- Young, H.W., and J.C. Mitchell (1973). “Geothermal Investigations in Idaho Part 1: Geochemistry and Geologic Setting of Selected Thermal Waters.” USGS, *IDWR Water Information Bulletin* No. 30, p. 23-28.
- Zumlot, T., Batayneh, A., Nazal, Y., Ghrefat, H., Mogren, S., Zaman, H., Elawadi, E., and Laboun A. (2012). Using multivariate statistical analyses to evaluate groundwater contamination in the northwestern part of Saudi Arabia. *Environ Earth Sci.* DOI 10.1007/s12665-013-2392-1

APPENDIX A: SAMPLE COLLECTION

Sampling Phase 1: Field Parameters, Filtration, and Collection

A mobile field sampling trailer was constructed to protect equipment and staff from harsh environmental conditions often present in southern Idaho. Sampling took place in a two phase fashion. Phase one includes the measurement of field parameters, rinsing of bottles with sample water, and bottling of samples. If sampling from a thermal spring, a piece of 0.25-inch stainless steel pipe attached to MasterFlex ® peristaltic tubing (both prewashed in 10% trace grade HNO₃) was used as an inlet. The stainless steel tubing often includes a non-reactive Nalgene ® bottle cap acting as a stabilizer to keep the inlet above sediment or algal mats and may be extended to the center of the spring using an extendable swimming pool cleaning rod. The spring water is then pumped from the source using a Geotech ® Geopump Peristaltic Pump (Series II). If measuring from a thermal well, a variety of prewashed spigot fittings and couples can be used to connect to the well head outlet. Thermal water is pumped from the source into a flow through cell (YSI® 6850) where the YSI Professional Plus Multi-parameter Meter is used to record the field parameters. The YSI multimeter is calibrated daily prior to sampling. The calibration procedure and checklist can be found on page 131. If warranted, the sample water may be cooled to < 60 °C (YSI sensor limitation) using a coiled stainless steel rod submerged in ice water within a 5-gallon cooler as shown in the picture below. Relevant field parameters include pH, oxidation-reduction potential, dissolved oxygen, temperature, conductivity, and total dissolved solids. Once field parameters are stabilized and logged, sample water travels through an EMD Millipore ® 0.45 µm Groundwater Capsule filter prior to bottling in order to rid the sample of various suspended particles.

Three separate water samples are taken from each source in order to analyze for major cations (Ca, K, Mg, Na, and SiO₂ (aq)), major anions (F, Cl, SO₄, and NO₃), and various trace elements (Al, B, Li, Br, Sr, Se, Rb, Ba, and Bi). Bottles are prepared prior any sampling campaign. Cation and anion samples are collected in 250 mL HDPE bottles whereas trace element samples are collected in 1 L HDPE bottles. All bottles are filled with nanopure (18.2 MΩ) deionized water and left to sit for 24 hours. They are subsequently rinsed with this same solution before preparation. Major cation and trace element bottles are partially filled with a 10% trace grade HNO₃ solution and agitated to clean the entirety of the bottle. Anion sample bottles are simply filled with nanopure deionized water once more due to the impending analyses of NO₃ and NO₂. Prior to being filled with sample water in the field, all bottles are emptied of their cleaning solutions (neutralized in waste container with baking soda to a pH of >6). Once emptied bottles are rinsed 3 times with sample water before being capped and preserved.



Figure A1. (A) Sample team comprised of U of I graduate student Cody Cannon (mid left), INL scientist Travis McLing (mid right), Dr. Mark Conrad (foreground) of the LBNL, and Dr. Pat Dobson (background) of the LBNL. (B) Sample equipment set up showing the peristaltic pump and tubing, 0.45µm filter, YSI ® Professional Plus Multimeter and Flow-Through Cell, and three sample bottles. (C) Sampling of Driscoll Spring near Twin Falls, ID. (D) Utilization of a coiled cooling system prior to sampling collection at Worswick Hot Springs, ID.

Sampling Phase 2: Preservation and Titration

A separate 50 mL filtered sample will be collected in an acid-washed graduated cylinder to be used in titration in order to determine the amount of dissolved carbonate (as CO_3 and HCO_3).

A Hach ® Digital Titrator (Model 1690001) equipped with either 1.6N or 0.16N sulfuric acid

is used to titrate the sample. A pH meter is rinsed with sample water and then used to monitor the samples pH as the acid is applied. The number of titrations it takes for the sample water to be lowered to a pH of 4.5 is recorded from the titrator and subsequently used to calculate the amount of carbonate in the sample. The total alkalinity calculation procedure for a digital titrator can be found in the USGS field manual chapter 6.6 (Rounds and Wilde, 2001).

Simultaneously or soon after titration is complete, the major cation and trace element bottles are preserved with 70% optima grade nitric acid until a pH of ≤ 2 is reached. Preservation is done to prevent precipitation of constituents or adsorption onto the bottle walls. Anion samples are not preserved and should be analyzed within approximately 28 days of sample collection as per EPA method 300.1. Cation and trace element samples have a shelf life of 6 months as per EPA Methods SW-846 and 200.8 respectively. After preservation and capping, water samples are sealed with strips of ParaFilm® and refrigerated at 4 °C until chemical analysis. Upon completion of sampling, all used tubing is cleaned by pumping 10% trace grade nitric acid from one carboy into a baking soda laden waste carboy.

All field parameters for samples utilized in this study are listed below.

Table A1. Field parameters for select ESRP thermal samples collected in 2014.

Timestamp	Date In Lab	Lat	Long	Site	Unit ID	Temperature (C)	pH	Conductivity (uS/cm)	Dissolved Oxygen (mg/L)	ORP (mV)	TDS (g/L)	Alkalinity (mg/L as HCO ₃)
3/10/2014 13:30	3/14/2014	43.64283	-111.68768	001	Heise Hot Springs	48.2	6.3	14789	0.43	-269.2	7.0005	986
3/11/2014 8:13	3/14/2014	44.14558	-112.55494	002	Lidy Hot Springs 1	56.1	7.2	836	0.34	-177.5	0.364	132
3/11/2014 9:13	3/14/2014	44.14166	-112.55240	003	Lidy Hot Springs 2	52.3	7.2	815	0.87	-140.9	0.3835	163
3/11/2014 13:12	3/14/2014	43.79211	-111.44009	004	Green Canyon Hot Springs	44	7.2	1152	2.84	96.9	0.585	137
3/11/2014 16:40	3/14/2014	44.09325	-111.43534	005	Sturm Well	31.4	8.7	183	4.5	44.5	0.106	66
3/12/2014 12:15	3/14/2014	43.33278	-113.91790	006	Condie Hot Springs	50.5	7	1075	0.6	-71.8	0.481	315
3/12/2014 15:09	3/14/2014	43.60234	-113.24214	007	Greenhouse Well	36.3	7.1	882	2.89	101.5	0.481	285
3/13/2014 8:53	3/14/2014	42.69940	-114.91040	008	Eckart Office Well	24.7	9.5	610	4.71	39.7	0.3965	81
3/13/2014 10:30	3/14/2014	42.64497	-114.78706	009	Campbell 1	34.5	8	457.7	4.06	64.2	0.2516	144
3/13/2014 11:13	3/14/2014	42.64432	-114.78294	010	Campbell 2	34.4	8	527	4.57	64.6	0.2925	127
3/13/2014 14:34	3/14/2014	42.69457	-114.85592	011	Miracle Hot Springs	58.4	9.5	1002	0.29	-162.1	0.4225	93
3/13/2014 16:19	3/14/2014	42.54479	-114.94855	012	Driscoll Well	37.5	8.6	1070	5.36	-13.8	0.559	95
3/13/2014 16:52	3/14/2014	42.54348	-114.94897	013	Driscoll Spring	36.2	8.7	1027	4.62	27.8	0.5655	98
3/14/2014 8:13	3/14/2014	42.58318	-114.47496	014	CSI Well 2	38.1	8.8	631	3.97	75.5	0.3315	127
6/6/2014 9:14	6/6/2014	43.44244	-111.90484	015	Comore Loma #6	20.9	6.7	828	6.82	176.6	0.585	222
6/6/2014 10:56	6/6/2014	43.43774	-111.93018	016	Comore Loma #5	27.7	6.9	943	6.28	121.5	0.585	251
6/6/2014 12:56	6/6/2014	43.43142	-111.94501	017	Blackhawk #2	26.8	6.6	1249	6.55	114.2	0.83683	271
6/6/2014 12:56	6/6/2014	43.43121	-11.94469	018	Blackhawk #1	25.1	6.8	1176	7.14	109.7	0.7605	268
6/11/2014 11:01	6/11/2014	42.10207	-113.38434	020	Raft River Geothermal # 1	150	7.1	5972	0.06	-217.8	2.3335	34
6/11/2014 11:52	6/11/2014	42.11042	-113.37519	021	Raft River Geothermal # 2	150	6.9	4079	0.07	-218.8	1.846	38
6/11/2014 12:44	6/11/2014	42.08359	-113.35865	022	Raft River Geothermal # 7	150	6.3	11474	0.08	-218.8	5.1805	33
6/11/2014 13:39	6/11/2014	42.09787	-113.38541	023	Raft River Geothermal # 4	150	7.1	4846	0.09	-219.3	2.1775	44
6/17/2014 13:33	6/17/2014	42.72589	-112.87381	024	Indian Hot Springs	32.7	7.2	1452	2.38	-61.2	0.8255	223
6/18/2014 9:57	6/18/2014	42.23667	-113.36971	025	Grush Dairy	54.7	9.2	1196	0.04	-146.5	0.494	283
6/18/2014 11:31	6/18/2014	42.107989	-113.39206	026	Raft River USGS Well	79.6	8.1	5463	1.5	-179.8	2.5805	95
6/18/2014 12:07	6/18/2014	42.10776	-113.39186	027	Raft River Frasier Well	78.6	7.7	4900	0.2	-175.2	2.444	60
6/18/2014 13:18	6/18/2014	42.09656	-113.37800	028	Raft River Crook Well	81	8.3	7297	0.46	-85.5	4.6475	35
6/23/2014 10:18	6/26/2014	43.36414	-113.78943	029	Milford Sweat	38.1	7.3	792	-	69.3	0.416	251
6/23/2014 12:48	6/26/2014	43.32777	-114.39941	030	Magic Hot Springs Landing Runoff	39.1	8.6	2227	-	-24.6	1.1375	710
6/23/2014 15:46	6/26/2014	43.42341	-114.62857	031	Elk Creek 1	50.0	9.1	758	-	-126	0.338	93
6/23/2014 16:15	6/26/2014	43.42322	-114.62865	032	Elk Creek 2	55.5	9.1	812	-	-82.6	0.3445	90
6/24/2014 9:13	6/26/2014	43.29241	-114.91002	033	Barron Well	38.0	8	1195	-	-104.8	0.624	181
6/24/2014 10:24	6/26/2014	43.38290	-114.93224	034	Wardrop Hot Springs (Gonzales' House)	67.5	9	553	-	-130.8	0.2145	193
6/24/2014 13:10	6/26/2014	43.32777	-114.39941	035	Magic Hot Springs Landing Well	75.0	6.8	2951	-	-84	1.183	703

Timestamp	Date In Lab	Lat	Long	Site	Unit ID	Temperature (C)	pH	Conductivity (uS/cm)	Dissolved Oxygen (mg/L)	ORP (mV)	TDS (g/L)	Alkalinity (mg/L as HCO3)
6/24/2014 16:48	6/26/2014	43.12966	-115.33841	036	Prince Albert Hot Springs	57.7	9.1	472.9	-	-134.6	0.1963	105
6/25/2014 10:44	6/26/2014	42.17334	-113.86163	037	Oakley Warm Spring	46.9	9.3	667	-	-172.7	0.3185	107
6/25/2014 13:30	6/26/2014	42.08533	-113.93984	038	Richard Austin Well 1	45.7	9	733	-	-107.6	0.351	205
6/25/2014 16:28	6/26/2014	42.47663	-113.50770	039	Marsh Creek Well	59.6	8.2	1055	-	-147.7	0.429	124
6/26/2014 10:14	6/26/2014	42.70399	-114.85699	040	1000 Springs (Sliger's Well)	72.0	9.5	1266	-	-127.2	0.494	212
6/26/2014 11:55	6/26/2014	42.68841	-114.82680	041	Banbury Hot Springs Well	58.8	9	798	-	-112.8	0.3315	249
6/26/2014 12:16	6/26/2014	42.68841	-114.82680	042	Banbury Hot Springs	58.5	9	820	-	-115	0.3315	168
7/15/2014 15:01	7/17/2014	42.95543	-115.29997	043	Diamond Laundry	35.0	8.9	829	0.1	-290.2	0.442	315
7/15/2014 18:48	7/17/2014	43.00294	-115.19222	044	Johnston Well	39.0	9.3	499.4	0.2	-212.1	0.2626	117
7/16/2014 12:02	7/17/2014	42.66851	-114.82436	045	Leo Ray Hill	35.0	8.7	414.9	0.1	-24.1	0.2275	140
7/16/2014 12:34	7/17/2014	42.66778	-114.82673	046	Leo Ray Road	35.5	8.4	409.7	0.3	-89.4	0.2217	139
7/16/2014 13:32	7/17/2014	42.65772	-114.79054	047	Kanaka Rapids (Zigler's House)	30.1	8	427.3	3.8	69.3	0.2529	120
7/16/2014 14:29	7/17/2014	42.70501	-114.85701	048	Hensley Well	31.8	9.6	741	0.6	-263.5	0.429	232
7/16/2014 17:38	7/17/2014	43.11025	-115.31258	049	Latty Hot Prings	65.0	9.3	323.1	1.7	-96.2	0.1735	107
7/16/2014 19:50	7/17/2014	42.94632	-115.49423	050	Laib Well	32.5	7.6	1621	0.1	-203.7	0.923	886
7/17/2014 10:03	7/17/2014	42.58050	-114.47089	051	CSI Well 1	37.7	8.8	586	3.3	38.7	0.312	154
7/17/2014 11:25	7/17/2014	42.59755	-114.40018	052	Larry Anderson Well	43.0	9.2	816	0	-205.1	0.3965	188
7/17/2014 12:42	7/17/2014	42.61390	-114.48799	053	Pristine Springs	43.0	9.2	769	0.3	-107.2	0.377	154
7/17/2014 15:16	7/17/2014	42.57256	-114.45175	054	Twin Falls High School	31.0	7.8	660	5.6	-13.7	0.39	161
7/17/2014 16:49	7/17/2014	42.57750	-114.28870	055	Anderson Campground Well	37.0	9.1	786	1.2	-191.1	0.4225	246
7/22/2014 14:00	7/22/2014	43.60827	-113.24432	056	Butte City Well	32.5	7.4	720	4.2	611.2	0.432	386
7/23/2014 14:45	7/23/2014	43.02583	-112.02551	057	Quidop Springs 1	21.0	6.7	1288	2.3	324.4	0.9165	617
7/23/2014 15:49	7/23/2014	43.03717	-112.00427	058	Quidop Springs 2	38.1	6.6	2112	0.5	-139.1	1.0985	710
7/23/2014 18:03	7/23/2014	43.11448	-112.16660	059	YaNDell Warm Springs	22.2	7.3	635	3.2	-22.2	0.4355	266
7/24/2014 12:07	7/24/2014	42.43758	-113.43432	060	Skaggs Ranch	33.3	7.7	396.6	0.4	-28.8	0.2223	181
7/24/2014 14:02	7/24/2014	42.10008	-113.63354	061	Durfee Hot Springs	44.9	8.8	690	4.1	119.3	0.325	107
7/24/2014 18:01	7/24/2014	42.22333	-113.79167	062	Basin Cemetery	30.7	7.9	482	3.3	-15.8	0.2827	122
7/24/2014 19:17	7/24/2014	42.48216	-113.97341	063	Wybenga Dairy	33.9	7.5	331.3	3.7	22	0.1839	115
7/29/2014 12:00	7/29/2014	42.13944	-111.93709	064	David Bosen Well	90.0	6.7	22609	2.56	147	14.5	583
7/30/2014 12:00	7/30/2014	43.87717	-111.55890	065	SchweNDiman Well	28.0	7.6	363	5.9	156	0.3	165
7/30/2014 12:00	7/30/2014	43.88566	-111.55949	066	Clyde Well	32.7	7.5	398	4.11	147	0.3	183
7/30/2014 12:00	7/30/2014	43.90127	-111.50967	067	Cinder Block Well	26.3	7.4	360	3.66	146	0.3	182
7/30/2014 12:00	7/30/2014	43.88308	-111.6186	068	Newdale City Well	30.0	7.3	575	4.45	575	0.3	251
7/30/2014 12:00	7/30/2014	43.85840	-111.67870	069	Spackman Well	14.1	7.2	336	7.15	145	0.2	190
8/15/2014 12:00	8/15/2014	42.97813	-112.41654	070	Fort Hall Thermal Well	21.1	7.9	557	6.6	160.1	0.39	223
6/17/2015 14:10	6/19/2015	43.33723	-115.04430	077	Wolf H.S.	50	9.5	400.5	2.9	-27.3	0.1898	107

YSI® Professional Plus Calibration Procedure

The following contains the order and manner in which the YSI Professional Plus instrument should be calibrated. Tips and troubleshooting not covered in this guide can be found in the YSI Professional Plus Manual and Dissolved Oxygen Handbook.

Temperature:

The YSI temperature sensor does not need to be calibrated as it is accurate to ± 0.15 °C and does not drift. However, you should verify that the temperature sensor is reading accurately by comparing it to a traceable thermometer before calibrating any of the other sensors.

Conductivity:

The conductivity calibration should be verified every day the instrument is used. However, the conductivity sensor is very stable and may hold its calibration for several weeks. Whether calibrating in the lab or in the field, you should use a conductivity standard and ensure that you calibrate conductivity and not specific conductance as you will most likely not be in exactly 25.0 °C water. Never use a calibration fluid that is more than a month old after opening. Rinse the cal cup and all sensors with DI water and then rinse with conductivity calibration solution. Fill the cal cup to where the top vent holes of the conductivity sensor are fully submerged. Input the standard value into the YSI calibration menu. Allow enough time for the temperature and conductivity values to stabilize and accept the calibration. Record the calibration values on the calibration sheet.

pH:

The pH calibration should be verified every day the instrument is used. However, a new pH sensor may be capable of holding its calibration for several days. If you're absolutely certain that the waters being sampled will all be over or below pH 7, then a 2 point calibration is all that is necessary. Otherwise, it is best to use a 3 point calibration. Rinse the cal cup and all sensors with DI water. Proceed to rinse the cal cup and sensors with a small amount of pH 7 buffer solution. Next, fill the cal cup with enough pH 7 buffer so that the pH sensor tip and temperature sensor are submerged. Input the buffer standard into the pH calibration menu in the YSI. Allow enough time for pH values and temperature values to stabilize. Accept the calibration value. Repeat this process for pH 4 and 10 buffers to complete the calibration. Record the stabilized pH values as well as the pH values in mV. Ensure the mV values fall within the accepted range listed on the calibration sheet.

ORP:

The ORP calibration should be verified every day the instrument is used. However, a new ORP sensor may be capable of holding its calibration for several days. Rinse the cal cup and all sensors with DI water. Proceed to rinse the cal cup and sensors with a small amount of ORP Zobell calibration solution. Fill the cal cup with enough ORP calibration solution so that the ORP sensor is fully submerged. Input the standard value into the YSI handheld. Allow enough time for the temperature and ORP values to stabilize and accept the calibration. Record the pre-calibrated stabilized ORP value and ensure the post-calibrated value matches the standard.

DO:

The dissolved oxygen sensor should be calibrated every day the instrument is used. It is not necessary to calibrate in both % and mg/L or ppm. Calibrating in % will simultaneously calibrate mg/L and ppm and vice versa. Before calibrating the DO sensor note the age of the DO membrane from previous calibrations. If it has not been changed within 8 weeks, change it. If any silver chloride has built up on the silver anode, try to simply mechanically clean it with the YSI cleaning brush. If the buildup is too heavy, use wet 400-grit sandpaper to clear away any build up. If you require chemical cleaning, soak the silver anode in a 3% (household ammonium cleaner) for 8-12 hours. Following the soak, rinse thoroughly with DI water and wipe the residue with a paper towel ensuring that no build up is trapped under the membrane. For correct sensor operation, the gold cathode must be textured properly. Use wet 400-grit sandpaper to remove build up and lightly scratch the cathode to allow more surface area for the electrolyte solution under the membrane (2-3 twists of sandpaper is usually sufficient). If any cleaning is required, make sure to record this information in the notes section of the calibration sheet.

The best way to calibrate the DO sensor is by using water saturated air. Fill the cal cup with about 1/8 inches of DI water. Ensure that the DO sensor and temperature sensor are not submerged. Engage 1 or 2 threads to allow for venting into the cal cup. Wait about 10 minutes for the calibration chamber to become completely saturated. While waiting, determine the calibration % value by dividing the true barometric pressure by 760 (cal. value will only be 100% at sea level or 760 mmHg) and multiplying by 100. Allow time for readings to stabilize around calibration value and accept calibration. Record values on calibration sheet.

Note: Chemical cleaning should be performed as infrequently as possible (1 or 2 times per year depending on use).

Post Calibration Values:

After completing calibration record the following values from the .glp file for the day's calibration to ensure the calibration was successful: Conductivity Cal Cell Constant (Range 5.0 +/- 1.0 acceptable), DO Sensor Value (yellow membrane: 4.31 μ A - 8.00 μ A), pH Slope (\approx 55 to 60 mV/pH, 59 ideal).

YSI Professional Plus Calibration						
Date of Calibration:				Technician:		
Temperature:						
		Reading:		Accurate:	Y	N
Conductivity:						
		Standard (µS/cm):		Pre Cal:		Post Cal:
pH:						
		pH 7	Pre Cal:		pH mV:	
		pH 4	Pre Cal:		pH mV:	
		pH 10	Pre Cal:		pH mV:	
		pH 7	Range: 0 mV ± 50 mV			
		pH 4	Range: +165 to +180 from 7 buffer mV value			
		pH 10	Range: -165 to -180 from 7 buffer mV value			
ORP:						
		Standard (mV):		Pre Cal:		Post Cal:
DO:						
		DO Membrane Age:		Changed:	Y	N
		Sensor Anode Cleaned:	Y N	*Chemically:	Y	N
		Sensor Cathode Cleaned:	Y N	*Chemically:	Y	N
		Barometric Pressure:		Standard %		
		Calibrated %				
Post Calibration Values						
Conductivity Cell Constant: Range: 5.0 +/- 1.0			Y	N	Value:	
DO Current Value (µA): (4.31µA - 8.00µA)			Y	N	Value:	
pH Slope: (≈ 55 to 60 mV/pH, 59 ideal)			Y	N	Value:	
Notes:						

Figure A2. YSI® Professional Plus Calibration Form

APPENDIX B: CHEMICAL ANALYSIS AND QUALITY CONTROL

Chemical analysis was performed by Cody Cannon under the supervision of analytical chemist Debbie Lacroix and the analytical chemistry laboratory lead Joanna Taylor at the Center for Advanced Energy Studies, Idaho Falls, Idaho. Samples were analyzed in accordance with their respective holding times (preserved and non-preserved) and appropriate dilutions were made to each sample when necessary. Calibration standards for each analytical instrument were prepared from various batch solutions provided by Inorganic Ventures TM in order to obtain valid concentrations in the desired range based upon previous geothermal research (0.1 to 500+ ppm for major cations and anions) and trace elemental needs for multicomponent equilibrium geothermometry calculations (1 ppb to 1ppm) for constituents including aluminum, magnesium, boron, etc. Analyses were conducted using the Dionex TM ICS-2100 Ion Chromatograph (IC) for major anions, the Thermo iCAP TM 6500 Inductively-Coupled Plasma Optical Emission Spectrometer (ICP-OES) for major cations, and the Agilent TM 7500ce Inductively-Coupled Plasma Mass Spectrometer (ICP-MS) for trace elements. The following sections detail the analysis and processing of samples 001-070.

Ion Chromatography for Major Anions

Samples are injected into a stream of eluent, passed through a series of ion exchange columns, and into a conductivity detector. The first column, a guard column, protects the analytical column by removing particulate and organic matter. The analytical column separates anions or cations by their relative affinities for column resins. The suppressor (between the analytical column and the conductivity detector) provides continuous suppression of background conductivity of the eluent and enhances response of the target analytes. The separated anions

or cations are measured by conductivity. The compounds are identified based on retention times and quantified by conductivity or absorbance. Control of the instrument is provided by PC-based Chromeleon software

Ion-exchange chromatography is a means of retaining target analytes by separating out the target anions from cations in a separator column. Once separated in the column, the Dionex™ ICS-2100 IC detects the concentrations of chosen anions by means of measuring conductivity. Calibration standards 1-7 were prepared from an Inorganic Ventures™ stock solution IC-FAS-1A containing the solutes: F^- , Cl^- , NO_2^- , NO_3^- , Br^- , SO_4^{2-} , and PO_4^{3-} . Solutions were prepared by means of dilutions by weight, resulting in seven standards ranging in concentrations from 0 ppm Cl^- (nanopure water) to 100 ppm Cl^- . Standard concentrations are listed below in Table 1. Analysis was carried out using a modified form of the EPA 300.1 Method (Hautman and Munch, 1997). Each run began with the analysis of 3 blank samples (nanopure water) followed by the seven standards in order to establish background levels and a calibration curve. A calibration curve coefficient of determination value of $R^2 = 0.995$ was used for all analyses in accordance with EPA 300.1. A laboratory control standard (LCS) was analyzed following the calibration standards to verify the validity of the calibration curve, followed by a nanopure dilution blank. The dilution blank was analyzed to ensure there was no analyte contamination in the water use to dilute the samples. Every ten samples, a blank sample was analyzed followed by all seven standards analyzed as samples. The blank analysis was used to verify there was no carryover during the run and the reanalysis of standards as samples was used to determine instrument drift and to aid in the LOD calculation for each analyte in the analytical run. Samples were diluted prior to analysis based on any previous water chemistry for specific samples or surrounding areas (diluted for >100 ppm Cl^- and

SO₄²⁻). Samples were diluted and re-run after initial analysis if necessary so that the concentrations would fall within the calibration range. Duplicate samples were run at a frequency of one sample per run, modified from the 10% recommended by EPA 300.1. Adherence to the recommended 90-110% recovery and 10% difference values for spikes and duplicates respectively was obtained for adequate quality control. Conductivity peak analysis was performed for each sample to ensure no interference or deviation in baseline provided by the calibration curve influenced sample concentration readings. Quality control information for standard solutions and LOD values for anions are provided in Table 1.

ICP-OES analysis for Major Cations

Samples are pumped through a nebulizer to produce a fine spray. The large droplets are removed by a spray chamber and the small droplets then pass through to the plasma. The plasma is formed by an intense magnetic field produced by radio frequency (RF) passing through a copper coil. The plasma generates photons of light by the excitation of atoms and ions. The emission of light which occurs as discrete lines, are separated according to their wavelength by diffractive optics using an Echelle optical design. The analytical signals are measured using a Charge Injection Device (CID) as the detector. The samples can be analyzed using either the radial or axial plasma views depending on the sensitivity needed. Various interferences must be considered and addressed appropriately. Control of the spectrometer is provided by PC-based iTEVA software.

Inductively-Coupled Plasma Optical Emission Spectrometry is performed by ionizing argon gas in an intense electro-magnetic field and “igniting” the plasma. Water samples are then transported via a peristaltic pump into the analytical nebulizer where the sample is made into an aerosol and forced to collide directly with the plasma flame. The sample is thereby broken

down into charged ions after collision with electrons and charged ions of the plasma. The continuous breaking up of molecules into their respective atoms emits signature wavelengths of light that can be read and quantified by the spectrometer (Huang and Hieftje, 1989). In a similar manner to the IC analysis, standards were prepared from an Inorganic Ventures™ stock solution: QCP-CICV-1 containing the cations Ca^{2+} , K^+ , Mg^+ , Na^+ , Ba^{2+} , Al^{3+} , and Fe^{3+} . However, concentrations of aluminum and magnesium proved to be too low in many samples to obtain a reading above the LOD. For this reason, these elements were analyzed separately using the ICP-MS. Standards were prepared in the ranges of 1-25 ppm Ca^{2+} , K^+ , Mg^+ , Na^+ and 1-20 ppm SiO_2^- . Additional standards were added to account for geothermal waters with high (100+ ppm) SiO_2^- and waters with higher TDS with elevated Na^+ (up to 1500 ppm) concentrations. A calibration curve was established with a 99.5% confidence, $R^2 = 0.995$ in accordance with EPA Method 200.7 (Martin et al., 1994). Analysis began with the running of blanks followed by all calibration standards in order to establish background levels and a calibration curve. Blanks and standards were analyzed again after every 10 samples to determine carryover, instrument drift and LODs. Duplicate and spiked samples were added randomly and run at a frequency of one sample per run, modified from the 10% recommended by EPA 200.7. Adherence to the recommended 70-130% recovery and 10% difference values for spikes and duplicates respectively was obtained for adequate quality control.

Multiple wavelengths of every constituent are read by the ICP-OES for each run as some wavelengths have more interferences than others. In order to pick the appropriate wavelength for each constituent, percent difference deviations from true values were calculated for each standard and the wavelength with the least percent difference ($< 10\%$ difference) were chosen

and concentrations were reported from each respective wavelength. Quality control information for standard solutions and LOD values for major cations are provided in Table 2.

ICP-MS analysis for Trace Elements

The sample is pumped with a peristaltic pump into a nebulizer where it is converted into a fine aerosol. The fine droplets are separated from the larger droplets by means of a spray chamber. From there, it is transported into the plasma torch. The plasma is formed by an intense magnetic field produced by radio frequency passing through a copper coil. The plasma generates positively charged ions. The ions are directed through the interface region, kept at a vacuum that consists of two metallic cones (sampler and skimmer) that allow the ions to pass through to the electrostatic lenses called the ion optics. These optics stop photons, particulates, and neutral species from reaching the detector. The ions travel through the octapole in the reaction cell which minimizes polyatomic spectral interferences. The ions reach the quadrupole where they are separated according to their mass-to-charge ratio (m/z) by electrostatically steering the ions of a selected mass down the middle of the rods to the detector while ejecting the other unstable ions (Greenfield, 1994). The ions are converted into an electronic signal with a detector called an electron multiplier. Control of the spectrometer is provided by PC-based MassHunter® software.

Standards were prepared from Inorganic Ventures™ stock solutions: CCS-4 (alkali, alkaline, non-transition elements) and CCS-5 (fluoride soluble elements). CCS-4 was utilized for the constituents: Li, Be, Al, Mg, Se, As, Rb, Sr, Ba, and Bi. CCS-5 was utilized solely for boron. Boron is often regarded as an important conservative tracer in geothermal fluids. Standards utilizing CCS-4 solution were prepared for the range of 1-500 ppb of all elements. CCS-5 standards were prepared for the range 1 ppb to 1 ppm boron based on previous ESRP

geothermal studies which included boron. Magnesium and aluminum were analyzed separately for all samples in order to fill in data gaps where concentrations fell below the LOD with the ICP-OES. Magnesium and aluminum standards were prepared in the range of 1 ppb to 1 ppm for both elements.

Analysis was accomplished using a modified form of EPA method 200.8 (Creed et al., 1994). Collision cell technology was utilized to eliminate interference from polyatomic ions due to the high TDS nature of geothermal waters. A calibration curve was established with a 99.5% confidence, $R^2 = 0.995$ in accordance with EPA method 200.8. Analysis began with the running of blanks followed by all calibration standards in order to establish background levels and a calibration curve. Blanks and standards were run again after every 10 samples to verify lack any contamination, to determine drift and establish the LOD for the run an internal standard of rhodium (Rh) was analyzed with the samples to correct for any matrix interferences. Duplicate and spiked samples were added randomly and run at a frequency of one sample per run, modified from the 10% recommended by EPA 200.8. Adherence to the recommended 70-130% recovery and 10% difference values for spikes and duplicates respectively was obtained for adequate quality control. Unless a deviation greater than 10% occurred for a particular QC standard, concentration values for samples were reported from raw data. Quality control information for standard solutions and ILOD values for trace elements are provided in Table 3.

Limit of Detection, Precision and Accuracy

The Limit of detection is the lowest concentration of a given analyte that is likely to be consistently distinguished from analysis (Needleman et al., 1990). Ordinarily, it is calculated from background analyte levels provided by blank samples. In this study, ILOD was

calculated using a "limit of blank" approximation where a Gaussian distribution of blank concentrations is assumed. An approximation assuming infinite degrees of freedom would use the student's t distribution value of 1.645 for a 95% confidence interval where $LOD = \text{Average}_{\text{blank}} + (1.645 \times \text{Standard Deviation}_{\text{blank}})$. However, in an effort to produce a more conservative approximation due to sample sizes of blanks varying from 4-5 blanks to 20, the standard deviation of blank was multiplied by 3 instead. ILOD values for all chemical constituents in 5% HNO_3 can be seen with the blank values in Tables B1-3.

Tables B1-3 also provides information on average instrument precision and accuracy.

Accuracy refers to the closeness of a measured value to a standard or known value. Accuracy can be seen in the % Recovery column in Tables 1-3. Sample data was considered valid if the % recoveries were $\pm 10\%$ of the known value. Therefore, data not within the 10% acceptable window was not considered valid and the data was not used. Precision refers to the closeness of two or more measurements to each other. Precision was determined by calculating the standard deviation(s) of the standards. The standard deviation provides an indication of the range of variation in the measurements. The relative standard deviation (RSD), expresses the standard deviation as a percentage, with the smaller the relative standard deviation (or standard deviation), the more precise the measurements. The average precision for this sample set can be seen in the %RSD column in tables 1-3 below.

Table B1. Anion QC Table

Fluoride							
True Concentration (mg/L)	# of points	Average Concentration (mg/L)	% Recovery	RSD (%)	Standard Deviation (mg/L)	3 Times Standard Deviation (mg/L) (ILOD)	10 Times Standard Deviation (mg/L) (ILOQ)
Blank	25	0.027	NA	133%	0.036	0.108	0.361
0.05	5	0.052	104%	13%	0.007	0.020	0.066
0.2	5	0.199	100%	7%	0.014	0.043	0.143
0.5	19	0.565	113%	19%	0.105	0.316	1.053
1.0	17	1.10	110%	21%	0.236	0.708	2.359
2.0	5	2.07	104%	2%	0.050	0.151	0.502
3.0	12	3.19	106%	7%	0.238	0.713	2.378
5.0	12	5.45	109%	15%	0.796	2.388	7.961
7.0	12	7.23	103%	3%	0.229	0.688	2.293
10	12	9.94	99%	2%	0.219	0.657	2.189
Chloride							
Blank	25	0.060	NA	112%	0.067	0.200	0.666
2.5	5	2.53	101%	10%	0.253	0.759	2.53
5.0	14	5.22	104%	4%	0.191	0.573	1.91
10	17	10.1	101%	4%	0.390	1.17	3.90
25	17	25.1	100%	4%	1.03	3.08	10.3
50	17	51.7	103%	3%	1.40	4.20	14.0
75	12	75.9	101%	2%	1.14	3.42	11.4
101	16	102	101%	3%	3.04	9.12	30.4
Nitrite							
Blank	16	0.088	NA	130%	0.114	0.343	1.14
0.2	5	0.203	102%	7%	0.015	0.046	0.154
1.0	17	0.850	85%	9%	0.080	0.241	0.802
2.0	5	2.18	109%	1%	0.032	0.096	0.321
5.0	15	5.12	102%	11%	0.586	1.76	5.86
10	15	10.2	102%	11%	1.14	3.43	11.4
20	10	20.5	103%	1%	0.271	0.712	2.71
35	10	36.0	103%	1%	0.461	1.38	4.61
50	9	49.5	99%	1%	0.326	0.979	3.26
Sulfate							
Blank	16	0.045	NA	171%	0.077	0.232	0.772
0.4	5	0.400	100%	8%	0.031	0.094	0.314
1.0	9	1.07	107%	15%	0.161	0.483	1.61
1.5	5	1.55	103%	5%	0.084	0.252	0.839
4.0	5	3.85	96%	2%	0.068	0.205	0.684

8.0	5	7.83	98%	1%	0.092	0.276	0.919
10	11	10.0	100%	4%	0.352	1.06	3.52
16	5	15.6	98%	1%	0.144	0.432	1.44
25	12	25.5	102%	1%	0.308	0.925	3.09
50	12	49.8	100%	1%	0.648	1.95	6.49
75	12	75.1	100%	1%	0.995	2.99	9.96
100	11	99.1	99%	1%	1.25	3.75	12.5
Bromide							
True Concentration (mg/L)	# of points	Average Concentration (mg/L)	% Recovery	RSD	Standard Deviation (mg/L)	3 Times Standard Deviation (mg/L) (ILOD)	10 Times Standard Deviation (mg/L) (ILOQ)
Blank	16	0.040	NA	393%	0.157	0.472	1.58
0.25	5	0.236	94%	2%	0.004	0.011	0.035
1.0	17	1.04	104%	10%	0.104	0.313	1.04
2.5	5	2.47	99%	2%	0.060	0.180	0.601
5.0	15	4.78	96%	7%	0.355	1.07	3.55
10	15	9.74	97%	5%	0.472	1.42	4.72
20	10	20.1	101%	2%	0.354	1.06	3.54
35	10	35.7	102%	2%	0.714	2.14	7.14
50	9	50.8	102%	2%	1.09	3.27	10.9
Nitrate							
Blank	16	0.024	NA	175%	0.042	0.126	0.421
0.25	5	0.261	104%	2%	0.005	0.016	0.053
1.0	17	1.16	116%	4%	.0510	1.53	5.10
2.5	5	2.76	110%	5%	0.142	0.427	1.42
5.0	15	5.02	100%	13%	0.661	1.98	6.61
10	19	10.1	101%	9%	0.871	2.61	8.71
20	10	20.0	100%	3%	0.520	1.56	5.20
35	10	35.7	102%	2%	0.804	2.41	8.04
50	9	50.8	102%	1%	0.655	1.97	6.56

Table B2. Cation QC Table

Calcium							
True Concentration (mg/L)	# of points	Average Concentration (mg/L)	% Recovery	RSD	Standard Deviation (mg/L)	3 Times Standard Deviation (mg/L) (ILOD)	10 Times Standard Deviation (mg/L) (ILOQ)
Blank	16	-0.052	NA	-79%	0.041	0.124	0.413
1.0	7	0.994	99%	8%	0.083	0.248	0.825
2.5	2	2.86	114%	5%	0.154	0.462	1.54
5.0	6	5.13	103%	6%	0.319	0.957	3.19
10	6	10.7	107%	19%	2.02	6.06	20.2
25	3	26.0	104%	11%	2.95	8.85	29.5
50	4	48.5	97%	1%	0.650	1.95	6.50
Potassium							
Blank	16	0.278	NA	72%	0.200	0.599	2.00
1.0	7	1.28	128%	20%	0.258	0.773	2.58
2.5	2	2.74	110%	13%	0.368	1.10	3.68
5.0	6	5.22	104%	5%	0.237	0.710	2.37
10	7	10.3	103%	4%	0.442	1.33	4.42
25	3	24.3	97%	5%	1.13	3.40	11.3
50	4	48.4	97%	2%	0.951	2.85	9.51
Magnesium							
Blank	16	-0.071	NA	-96%	0.068	0.204	0.680
1.0	7	0.980	98%	19%	0.182	0.546	1.82
2.5	2	2.91	116%	11%	0.319	0.958	3.19
5	6	5.28	106%	8%	0.438	1.31	4.38
10	7	10.5	105%	12%	1.22	3.65	12.2
25	3	26.3	105%	16%	4.12	12.4	41.2
50	4	49.0	98%	1%	0.582	1.75	5.81
Sodium							
Blank	16	0.711	NA	74%	0.529	1.59	5.30
1.0	7	1.76	176%	23%	0.404	1.21	4.04
2.5	2	3.22	129%	4%	0.127	0.380	1.27
5	6	5.22	104%	6%	0.311	0.934	3.11

10	7	10.5	105%	4%	0.432	1.30	4.32
25	3	24.7	99%	3%	0.713	2.14	7013
50	4	47.5	95%	2%	0.803	2.41	8.03
Silica							
Blank	16	-0.029	NA	-186%	0.054	0.161	0.536
1.0	6	1.08	108%	11%	0.119	0.358	1.20
5.0	7	5.24	105%	6%	0.317	0.951	3.17
10	7	10.4	104%	5%	0.494	1.48	4.94
20	7	20.9	105%	4%	0.846	2.54	8.47

Table B3. Trace Element QC Table

Boron							
True Concentration (ug/L)	# of points	Average Concentration (ug/L)	% Recovery	RSD %	Standard Deviation (ug/L)	3 Times Standard Deviation (ug/L) (ILOD)	10 Times Standard Deviation (ug/L) (ILOQ)
Blank	19	3.98	NA	40%	1.58	4.7	16
1.0	13	3.03	303%	76%	2.29	6.9	23
5.0	13	5.95	119%	26%	1.56	4.7	16
10	13	11.1	111%	13%	1.43	4.3	14
20	13	24.8	124%	7%	1.85	5.6	19
50	13	49.0	98%	7%	3.35	10	33
100	13	108	108%	8%	8.86	27	89
500	13	541	108%	9%	46.9	141	469
1000	13	1022	102%	8%	84.7	254	847
Lithium							
Blank	18	0.392	NA	145%	0.57	1.71	5.70
1.0	7	1.35	135%	97%	1.31	3.93	13.1
5.0	5	5.67	113%	5%	0.257	0.770	2.57
25	5	26.8	107%	4%	1.08	3.25	10.8
50	13	48.1	96%	11%	5.47	16.4	54.7
100	5	105	105%	4%	3.89	11.7	38.9
150	7	144	96%	11%	15.2	45.6	152
200	5	197	99%	3%	4.99	15.0	49.9
250	8	238	95%	9%	21.3	64.0	213
300	7	293	98%	10%	29.2	87.5	292
350	7	338	97%	9%	30.5	91.4	305
400	7	398	100%	7%	26.1	78.4	261
500	12	495	99%	5%	22.7	68.0	227
Beryllium							
Blank	18	0.214	NA	114%	0.244	0.732	2.44

1.0	7	1.33	133%	52%	0.694	2.08	6.94
5.0	5	5.38	108%	4%	0.195	0.584	1.95
25	5	25.9	104%	3%	0.892	2.68	8.92
50	13	49.3	99%	10%	4.98	14.9	49.8
100	5	99.9	100%	2%	2.31	6.92	23.1
150	7	151	101%	2%	3.13	9.39	31.3
200	5	196	98%	2%	3.25	9.74	32.5
250	8	248	99%	4%	9.26	27.8	92.6
300	7	308	103%	4%	11.5	34.4	115
350	7	353	101%	3%	10.2	30.5	102
400	7	410	103%	3%	10.5	31.4	105
500	12	505	101%	3%	15.7	47.0	157
Magnesium							
Blank	17	0.120	NA	233%	0.28	0.839	2.80
1.0	8	5.00	500%	74%	3.72	11.2	37.2
5.0	13	4.53	91%	44%	2.00	6.00	20.0
25	5	27.0	108%	4%	1.01	3.04	10.1
50	13	54.1	108%	14%	7.78	23.3	77.8
100	5	103	103%	3%	2.62	7.85	26.2
150	7	165	110%	3%	4.67	14.0	46.7
200	5	194	97%	2%	3.92	11.8	39.2
250	7	272	109%	1%	4.06	12.2	40.6
350	7	329	94%	2%	5.92	17.7	59.2
400	7	384	96%	1%	3.21	9.64	32.1
450	6	440	98%	1%	4.93	14.8	49.3
500	5	482	96%	2%	10.6	31.7	106
Aluminum							
Blank	25	0.76	NA	NA	0.861	2.58	8.61
1.0	15	2.26	226%	113%	1.23	3.70	12.3
5.0	13	3.53	71%	54%	2.32	6.97	23.2
25	5	27.3	109%	66%	1.20	3.61	12.0
50	20	55.2	110%	4%	5.37	16.1	53.7
100	5	104	104%	10%	3.37	10.1	33.7
150	14	159	106%	3%	6.13	18.4	61.3
200	5	195	98%	4%	5.16	15.5	51.6
250	15	260	104%	3%	12.1	36.2	121
300	7	311	104%	5%	7.11	21.3	71.1
350	21	356	102%	2%	22.5	67.6	225
400	7	417	104%	6%	8.56	25.7	85.6
450	6	440	98%	2%	4.35	13.0	43.5
500	12	504	101%	1%	17.2	51.7	172
Arsenic							
Blank	18	0.35	NA	125%	0.437	1.31	4.37
1.0	7	1.57	157%	40%	0.623	1.87	6.23

5.0	5	5.16	103%	6%	0.311	0.93	3.11
25	5	25.8	103%	2%	0.580	1.74	5.80
50	13	48.6	97%	8%	3.84	11.5	38.4
100	5	99.1	99%	2%	1.53	4.60	15.3
150	7	145	97%	3%	3.84	11.5	38.4
200	5	191	96%	2%	3.67	11.0	36.7
250	7	239	96%	2%	5.75	17.2	57.5
300	7	295	98%	3%	8.27	24.8	82.7
350	7	340	NA	2%	6.99	21.0	69.9
400	7	402	157%	3%	13.4	40.2	134
500	12	496	103%	2%	11.1	33.3	111
Selenium							
Blank	18	0.55	NA	119%	0.654	1.96	6.54
1.0	7	1.93	193%	33%	0.638	1.91	6.38
5.0	5	5.35	107%	9%	0.507	1.52	5.07
25	5	25.7	103%	2%	0.441	1.32	4.41
50	13	49.5	99%	8%	4.06	12.2	40.6
100	5	102	102%	2%	1.76	5.29	17.6
150	7	147	98%	3%	3.77	11.3	37.7
200	5	197	99%	1%	2.85	8.55	28.5
250	8	240	96%	4%	8.42	25.3	84.2
300	7	296	99%	3%	7.53	22.6	75.3
350	7	339	97%	1%	4.35	13.1	43.5
400	7	403	101%	3%	10.8	32.3	108
500	12	494	99%	2%	9.50	28.5	95.0
Rubidium							
Blank	18	0.35	NA	106%	0.371	1.11	3.71
1.0	7	1.40	140%	48%	0.668	2.00	6.68
5.0	5	5.61	112%	2%	0.120	0.36	1.20
25	5	26.9	108%	1%	0.274	0.82	2.74
50	12	50.1	100%	6%	3.21	9.63	32.1
100	5	105	105%	1%	1.03	3.10	10.3
150	7	151	101%	2%	2.54	7.62	25.4
200	5	199	100%	1%	1.86	5.57	18.6
250	8	245	98%	3%	7.16	21.5	71.6
300	7	303	101%	1%	4.20	12.6	42.0
350	7	345	99%	1%	3.90	11.7	39.0
400	7	403	101%	2%	6.09	18.3	60.9
500	12	499	100%	2%	8.90	26.7	89.0
Strontium							
Blank	18	0.22	NA	110%	0.243	0.728	2.43
1.0	7	1.38	138%	46%	0.630	1.89	6.30
5	5	5.62	112%	2%	0.121	0.362	1.21
25	5	26.8	107%	1%	0.267	0.801	2.67

50	13	50.1	100%	6%	3.18	9.53	31.8
100	5	105	105%	1%	0.989	2.97	9.89
150	7	151	101%	2%	2.60	7.80	26.0
200	5	197	99%	1%	1.63	4.90	16.3
250	8	243	97%	3%	6.95	20.9	69.5
300	7	300	100%	1%	3.70	11.1	37.0
350	7	344	98%	1%	4.02	12.1	40.2
400	7	402	101%	1%	4.96	14.9	49.6
500	12	499	100%	2%	7.97	23.9	79.7
Barium							
Blank	18	0.25	NA	105%	0.263	0.788	2.63
1.0	7	1.32	132%	52%	0.691	2.07	6.91
5.0	5	5.40	108%	3%	0.138	0.414	1.38
25	5	25.9	104%	1%	0.372	1.12	3.72
50	13	48.7	97%	8%	4.03	12.1	40.3
100	5	101	101%	2%	1.94	5.83	19.4

Table B4. Chemical concentrations for geothermal samples collected throughout the ESRP in 2014.

Site	Lat	Long	Unit ID	Alkalinity as HCO3	ICP-OES					ICP-MS								IC				
					Ca	Mg	Na	K	SiO2(aq)	Li	Be	Al	As	Rb				Sr	Ba	B	F	Cl
001	43.64283	-111.68768	Heise Hot Springs	985.76	487.66	93.79	1539.72	206.21	33.63	2.48	1.17E-03	0.131	0.032	0.652	5.466	0.057	4.550	4.00	2267.48	712.26	ND	
002	44.14558	-112.55494	Lidy Hot Springs 1	131.76	66.24	15.58	25.43	13.22	37.76	0.05	<LOD	0.001	0.014	0.019	0.597	0.086	0.093	4.60	7.29	101.91	ND	
003	44.14166	-112.55240	Lidy Hot Springs 2	163.48	64.16	16.34	27.65	13.47	34.21	0.05	<LOD	0.001	0.014	0.019	0.611	0.078	0.092	4.68	6.94	98.28	ND	
004	43.79211	-111.44009	Green Canyon Hot Springs	136.64	144.20	33.75	4.99	4.46	27.01	0.01	<LOD	<LOD	0.003	0.007	1.172	0.034	0.020	1.46	0.94	314.24	2.12	
005	44.09325	-111.43534	Sturm Well	66.12	3.18	0.05	33.25	0.89	63.14	0.05	<LOD	0.005	0.012	0.004	0.005	0.001	0.039	2.09	3.28	5.77	0.63	
006	43.33278	-113.91790	Condie Hot Springs	314.76	61.09	11.47	62.40	22.49	29.51	0.09	<LOD	0.003	0.005	0.047	0.932	0.284	0.258	1.58	13.97	33.47	2.69	
007	43.60234	-113.24214	Greenhouse Well	285.48	77.81	27.75	33.83	9.36	31.58	0.04	<LOD	<LOD	0.010	0.021	0.723	0.096	0.151	0.74	22.24	57.52	6.59	
008	42.69940	-114.91040	Eckart Office Well	80.52	5.74	0.74	112.83	4.16	52.04	0.01	<LOD	0.007	0.046	0.004	0.022	0.001	0.190	12.16	46.46	90.87	1.21	
009	42.64497	-114.78706	Campbell 1	143.96	23.47	3.00	57.54	7.69	71.89	0.06	<LOD	0.000	0.008	0.019	0.156	0.004	0.107	2.21	23.09	40.46	5.37	
010	42.64432	-114.78294	Campbell 2	126.88	26.66	3.47	55.93	8.04	69.37	0.06	<LOD	0.000	0.007	0.019	0.177	0.002	0.106	2.46	20.03	31.78	4.75	
011	42.69457	-114.85592	Miracle Hot Springs	92.72	0.84	0.00	128.20	1.87	99.53	0.05	<LOD	0.022	0.066	0.006	0.001	<LOD	0.332	22.37	31.69	33.72	ND	
012	42.54479	-114.94855	Driscoll Well	95.16	11.23	0.36	149.41	1.38	45.54	0.19	<LOD	0.005	0.023	0.005	0.063	0.006	0.117	2.42	53.31	188.04	1.44	
013	42.54348	-114.94897	Driscoll Spring	97.60	11.14	0.79	146.61	1.92	48.37	0.19	<LOD	0.016	0.024	0.007	0.065	0.015	0.113	2.45	53.59	186.65	ND	
014	42.58318	-114.47496	CSI Well 2	126.88	4.54	0.19	94.90	3.27	64.23	0.01	<LOD	0.001	0.017	0.008	0.019	0.001	0.150	9.64	26.44	46.81	4.89	
015	43.44244	-111.90484	Comore Loma #6	222.04	50.80	15.25	96.66	15.97	65.34	0.12	<LOD	0.002	0.003	0.042	0.311	0.163	0.216	0.38	126.11	32.19	5.90	
016	43.43774	-111.93018	Comore Loma #5	251.32	51.96	18.54	89.75	15.77	85.12	0.09	<LOD	0.002	0.004	0.042	0.243	0.225	0.215	0.27	120.31	25.60	2.76	
017	43.43142	-111.94501	Blackhawk #2	270.84	77.43	22.10	124.43	17.29	83.67	0.13	<LOD	0.002	0.004	0.045	0.405	0.247	0.341	0.23	204.93	36.98	2.84	
018	43.43142	-11.94469	Blackhawk #1	268.40	75.34	21.04	122.23	16.74	81.99	0.13	<LOD	0.002	0.004	0.044	0.430	0.229	0.335	0.26	196.52	39.07	3.48	
020	42.10207	-113.38434	Raft River Geothermal # 1	34.16	59.89	0.16	567.72	39.89	132.81	1.57	1.31E-03	0.085	0.010	0.420	1.527	0.028	0.269	9.08	956.09	58.43	1.40	
021	42.11042	-113.37519	Raft River Geothermal # 2	38.06	52.49	0.10	418.22	37.89	157.34	1.05	5.92E-04	0.086	0.005	0.388	1.224	0.015	0.193	9.49	979.92	63.69	6.30	
022	42.08359	-113.35865	Raft River Geothermal # 7	32.94	199.21	0.10	1258.19	150.28	226.84	2.57	9.33E-04	0.069	0.018	1.306	4.931	0.080	0.488	6.05	2197.12	59.30	1.33	
023	42.09787	-113.38541	Raft River Geothermal # 4	44.41	59.79	0.14	542.55	38.82	133.60	1.57	6.62E-04	0.066	0.007	0.396	1.413	0.023	0.249	7.15	790.36	59.32	0.06	
024	42.72589	-112.87381	Indian Hot Springs	222.53	80.84	19.52	126.03	11.48	20.37	0.08	<LOD	0.002	0.025	0.028	2.115	0.288	0.104	0.50	216.27	19.81	0.36	
025	42.23667	-113.36971	Grush Dairy	283.04	0.90	0.09	164.01	2.49	72.97	0.15	<LOD	0.112	0.003	0.011	0.016	0.006	0.093	6.70	68.97	24.02	ND	
026	42.108	-113.39206	Raft River USGS Well	95.16	70.72	0.14	621.47	24.85	84.27	1.50	6.77E-04	0.040	0.006	0.287	1.612	0.017	0.274	7.04	976.46	56.47	0.05	
027	42.10776	-113.39186	Raft River Frasier Well	59.78	67.22	0.21	598.27	22.61	77.42	1.45	1.08E-03	0.033	0.007	0.280	1.543	0.017	0.264	5.82	857.85	54.42	0.06	
028	42.09656	-113.37800	Raft River Crook Well	35.38	157.70	0.31	1186.92	35.88	95.91	2.57	1.45E-03	0.059	0.015	0.430	3.117	0.118	0.480	6.07	1679.69	56.51	0.18	
029	43.36414	-113.78943	Milford Sweat	251.32	66.49	13.68	42.95	8.45	24.58	0.04	5.82E-05	0.003	0.073	0.021	0.449	0.092	0.172	1.85	6.61	49.92	0.01	
030	43.3278	-114.39941	Magic Hot Springs Runoff	709.59	13.17	1.29	333.02	20.93	109.44	1.17	1.39E-03	0.007	0.006	0.123	0.646	0.147	1.237	10.57	79.07	52.95	ND	
031	43.42341	-114.62857	Elk Creek 1	92.72	2.33	0.00	90.18	1.66	65.02	0.21	<LOD	0.022	0.005	0.008	0.109	0.001	0.254	15.13	23.17	42.57	ND	
032	43.42322	-114.62865	Elk Creek 2	90.28	2.27	0.00	91.23	1.57	65.30	0.21	<LOD	0.026	0.005	0.008	0.112	0.001	0.252	15.17	23.14	42.60	ND	
033	43.29241	-114.91002	Barron Well	180.56	16.90	0.62	156.25	2.97	51.70	0.36	1.83E-04	0.010	0.001	0.020	0.356	0.009	0.173	7.08	9.48	210.93	ND	
034	43.38290	-114.93224	Wardrop Hot Springs	192.76	1.18	0.27	56.01	0.88	76.82	0.05	<LOD	0.086	0.003	0.005	0.045	0.000	0.047	3.35	5.06	11.49	0.00	
035	43.3278	-114.39941	Magic Hot Springs Well	702.72	22.34	1.39	310.54	19.79	103.74	1.18	2.37E-03	0.009	0.004	0.126	0.931	0.223	1.200	9.95	74.11	50.34	ND	

Site	Lat	Long	Unit ID	Alkalinity as HCO3	ICP-OES					ICP-MS								IC			
					Ca	Mg	Na	K	SiO2(aq)	Li	Be	Al	As	Rb				Sr	Ba	B	F
036	43.12966	-115.33841	Prince Albert Hot Springs	104.92	0.26	0.01	55.28	2.67	110.10	0.01	1.24E-04	0.017	0.009	0.007	0.001	0.001	0.037	6.95	2.55	8.42	ND
037	42.17334	-113.86163	Oakley Warm Spring	107.36	2.23	0.02	85.72	2.18	79.21	0.03	1.26E-04	0.015	0.001	0.015	0.053	0.001	0.052	7.61	52.57	21.40	ND
038	42.08533	-113.93984	Richard Austin Well 1	204.96	2.14	0.06	105.97	1.89	29.71	0.07	1.01E-04	0.025	0.007	0.006	0.038	0.014	0.071	2.42	16.17	22.80	ND
039	42.47663	-113.50770	Marsh Creek Well	124.44	9.08	0.41	107.78	4.28	62.55	0.07	1.69E-04	0.007	0.001	0.029	0.094	0.012	0.063	13.18	51.77	50.26	ND
040	42.70399	-114.85699	1000 Springs (Sliger's Well)	212.28	0.94	0.00	136.44	1.59	93.53	0.05	5.54E-05	0.074	0.061	0.008	0.001	0.000	0.499	24.22	50.45	30.06	ND
041	42.68841	-114.82680	Banbury Hot Springs Well	248.88	0.88	0.00	96.77	1.65	103.40	0.03	8.87E-05	0.014	0.042	0.007	0.001	0.000	0.216	11.39	16.86	23.50	ND
042	42.68841	-114.82680	Banbury Hot Springs	168.36	1.04	0.00	94.90	1.60	102.85	0.03	<LOD	0.015	0.042	0.007	0.001	0.000	0.219	11.36	16.76	23.54	ND
043	42.95543	-115.29997	Diamond Laundry	314.76	1.66	0.18	142.30	1.29	30.13	0.02	<LOD	0.013	0.000	0.002	0.007	0.001	0.890	13.07	23.26	4.30	304.06
044	43.00294	-115.19222	Johnston Well	117.12	2.42	0.05	77.41	1.27	40.93	0.02	<LOD	0.009	0.002	0.002	0.002	0.000	0.329	16.96	5.95	10.29	0.44
045	42.66851	-114.82436	Leo Ray Hill	140.30	5.95	0.19	61.69	3.41	54.05	0.06	5.11E-05	0.002	0.025	0.008	0.010	0.001	0.129	3.42	13.97	31.30	ND
046	42.66778	-114.82673	Leo Ray Road	139.08	7.62	0.45	56.44	4.10	54.47	0.06	<LOD	0.011	0.018	0.010	0.018	0.002	0.132	3.44	11.69	24.77	0.02
048	42.70501	-114.85701	Hensley Well	231.80	1.93	0.01	121.63	1.62	83.31	0.04	<LOD	0.011	0.060	0.002	0.007	0.001	0.579	24.13	51.93	33.13	ND
049	43.11025	-115.31258	Latty Hot Prings	107.36	0.20	0.01	53.91	1.90	103.21	0.02	5.64E-05	0.020	0.009	0.006	0.001	0.000	0.043	6.85	2.73	11.45	0.09
050	42.94632	-115.49423	Laib Well	885.72	9.43	0.55	291.73	9.84	57.73	0.34	4.50E-04	0.176	0.002	0.018	0.093	0.094	2.167	1.74	66.20	10.37	164.00
051	42.58050	-114.47089	CSI Well 1	153.72	3.99	0.22	86.28	2.99	60.92	0.02	8.49E-05	0.003	0.017	0.007	0.017	0.001	0.185	8.61	25.81	45.38	3.50
052	42.59755	-114.40018	Larry Anderson Well	187.88	1.22	0.01	118.11	2.19	69.27	0.03	3.12E-04	0.005	0.014	0.007	0.002	0.001	0.285	15.82	21.13	36.32	36.82
053	42.61390	-114.48799	Pristine Springs	153.72	1.30	0.01	109.33	2.12	71.55	0.01	<LOD	0.004	0.029	0.005	0.004	0.000	0.317	16.47	26.72	30.77	1.09
054	42.5726	-114.4518	Twin Falls High School	161.04	39.91	8.98	55.41	4.92	59.11	0.03	1.04E-04	0.002	0.006	0.012	0.185	0.016	0.107	2.35	37.51	76.03	6.74
055	42.57750	-114.28870	Anderson Campground Well	246.44	1.50	0.02	126.50	3.10	66.02	0.07	<LOD	0.024	0.141	0.009	0.004	0.002	0.495	23.37	34.42	37.39	0.10
056	43.6083	-113.24432	Butte City Well	385.52	51.55	20.88	32.45	7.53	33.17	0.03	<LOD	0.002	0.006	0.016	0.558	0.118	0.164	0.62	19.81	49.43	3.78
057	43.02583	-112.02551	Quidop Springs 1	617.32	165.42	55.84	28.40	22.96	16.05	0.13	2.45E-04	0.005	0.009	0.034	1.824	0.026	0.094	0.81	23.30	223.91	1.97
058	43.0372	-112.0043	Quidop Springs 2	710.04	199.48	68.95	33.80	34.11	19.61	0.21	1.15E-02	0.416	0.027	0.050	2.598	0.125	0.129	0.81	15.16	344.95	8.84
059	43.11448	-112.16660	Yandell Warm Springs	265.96	72.47	26.33	13.55	3.95	16.57	0.02	<LOD	0.000	0.003	0.004	0.489	0.045	0.036	0.60	16.29	90.37	1.97
060	42.4376	-113.4343	Skaggs Ranch	180.56	27.73	1.99	32.62	3.86	44.06	0.02	<LOD	0.000	0.001	0.007	0.134	0.075	0.031	1.52	20.37	14.52	ND
061	42.1001	-113.63354	Durfee Hot Springs	107.36	8.21	0.35	84.27	3.30	67.87	0.09	5.88E-05	0.003	0.002	0.025	0.124	0.012	0.075	6.19	59.19	28.16	0.34
062	42.2233	-113.7917	Basin Cemetery	122.00	18.33	2.42	57.98	1.98	40.20	0.01	1.81E-04	0.001	0.002	0.003	0.168	0.013	0.064	3.58	47.41	21.01	1.40
063	42.4822	-113.97341	Wybenga Dairy	114.68	25.03	1.07	20.90	8.71	69.43	0.01	8.25E-05	0.002	0.002	0.016	0.212	0.129	0.052	0.70	13.13	15.74	0.83
064	42.1394	-111.9371	David Bosen Well	583.16	206.92	18.48	4523.31	794.93	95.12	6.07	6.75E-03	0.078	0.076	4.972	20.351	3.235	5.555	5.21	7128.94	49.19	ND
065	43.8772	-111.55890	Schwendiman Well	164.70	26.86	6.87	39.27	5.49	61.53	0.05	<LOD	0.002	0.007	0.017	0.080	0.022	0.087	2.57	13.67	25.25	4.50
066	43.8857	-111.5595	Clyde Well	183.00	24.67	7.29	45.65	5.32	65.03	0.06	6.09E-05	0.002	0.010	0.018	0.078	0.027	0.119	3.17	15.41	22.97	5.62
067	43.9013	-111.50967	Cinder Block Well	181.78	18.17	3.50	52.25	5.04	70.48	0.07	8.85E-05	0.002	0.013	0.018	0.050	0.021	0.151	4.18	12.18	17.19	1.08
068	43.8831	-111.6186	Newdale City Well	251.32	27.56	4.70	70.89	8.12	70.41	0.12	5.39E-05	0.002	0.012	0.031	0.086	0.052	0.215	5.03	24.86	29.74	7.18
069	43.85840	-111.67870	Spackman Well	190.32	37.16	13.68	11.64	3.00	29.60	<LOD	<LOD	0.001	0.002	0.004	0.108	0.033	0.065	0.46	5.82	12.91	7.71
070	42.9781	-112.4165	Fort Hall Thermal Well	223.26	55.35	21.27	29.30	7.14	49.98	0.03	< 0.0001	< 0.01	0.005	0.311	0.311	0.065	0.054	ND	ND	ND	ND

APPENDIX C: WATER TYPES AND CHARGE BALANCE

Table C1. Major cations and anions for Na-HCO₃ type thermal waters utilized in this study. Charge balances listed are given as the ratio of cations to anions calculated from meq/L units. Values with more than a 20% difference from a 1:1 balance are highlighted in red.

Site	Lat	Long	T (°C)	pH	Ca	Mg	Na	K	Cl	F	SO4	Alkalinity as HCO ₃	TDS	Charge Balance
M91-7	42.60316	-114.477722	39	9.3	1.6	0.06	96	2.8	15	11	20	145	331	1.14
M91-8	42.56936	-114.606826	27	8.6	5.1	0.17	61	4.3	11	4	16	134	253	1.00
M91-11	42.58362	-114.48118	30.5	8.6	8.6	0.4	74	6.3	21	11	26	121	267	1.04
M91-13	42.58966	-114.509924	41.5	9	1.7	0.08	130	2.5	36	26	28	195	408	0.94
M91-14	42.57862	-114.287802	42	9.2	1.5	0.01	120	1.9	17	14	32	207	272	1.01
LY89-11	42.63174	-114.597327	30.5	9	2	0.05	82	2.9	11	12	20	110	272	1.18
LY89-12	42.61798	-114.473657	27	9	1.9	0.1	110	3.5	10	22	18	140	341	1.21
LY89-13	42.61539	-114.488068	42	8.8	2.5	0.1	110	1.9	16	16	15	140	326	1.27
LY89-14	42.59496	-114.481012	39.5	9	1.9	0.1	99	1.9	15	14	25	110	301	1.28
LY89-15	42.60581	-114.478121	39	9.3	1.6	0.06	96	2.8	15	11	20	120	299	1.28
LY89-22	42.58386	-114.480819	30.5	9	8.6	0.4	74	6.3	21	11	26	110	262	1.09
CC-14	42.58318	-114.47496	38.1	8.79	4.54	0.19	95	3.3	26	10	47	127	332	1.03
CC-51	42.58050	-114.47089	37.7	8.81	3.99	0.22	86	3.0	26	9	45	154	312	0.87
CC-52	42.59755	-114.40018	43.0	9.16	1.22	0.01	118	2.2	21	16	36	188	397	1.00
CC-53	42.61390	-114.48799	43.0	9.18	1.30	0.01	109	2.1	27	16	31	154	377	1.02
CC-55	42.57750	-114.28870	37.0	9.05	1.50	0.02	126	3.1	34	23	37	246	423	0.81
LY82-3	42.70158	-114.856527	62	9.4	0.7	0.1	150	1.4	48	15	35	168	503	1.17
LY82-4	42.70184	-114.854331	71.5	9.5	1.5	0.1	140	1.5	51	27	33	168	505	0.98
LY82-5	42.69133	-114.866789	57	9.4	0.9	0.1	130	1.5	34	21	34	177	485	1.01
LY82-6	42.6881	-114.84012	45.5	9.1	0.9	0.1	100	1.8	30	26	29	163	438	0.81
LY82-7	42.68357	-114.834978	42.5	9.3	1.3	0.1	90	1.7	14	9	28	148	359	1.04
LY82-11	42.68487	-114.829093	44.5	9.4	3.3	0.1	100	1.8	22	12	27	160	414	1.03
LY82-12	42.68251	-114.82902	30	9.3	0.9	0.1	97	1.6	20	13	28	154	379	0.99
LY82-15	42.66904	-114.8236	34	8.7	5.4	0.2	66	2.9	13	4	30	124	302	1.00
LY82-18	42.66149	-114.814894	32	8.4	8	0.2	62	2.8	11	3	26	144	310	0.94
LY82-19	42.66001	-114.81414	31.5	8.6	7.5	0.3	63	2.8	11	3	26	134	299	1.00
LY82-20	42.65886	-114.810791	32.5	8.3	10	0.5	62	3.5	11	3	25	150	316	0.97
LY89-1	42.66191	-114.812514	33	8.4	11	0.5	61	3.9	11	4	24	150	246	0.97
LY89-4	42.63697	-114.754192	26	8.3	7.4	0.2	62	5.6	10	5	21	140	262	0.99
LY89-8	42.65494	-114.650688	44	9	1.5	0.1	96	1.5	14	16	24	78	304	1.43
CC-40	42.70399	-114.85699	72.0	9.5	0.94	0.00	136	1.59	50	24	30	212	494	0.89
CC-42	42.68841	-114.82680	58.5	9	1.04	0.00	95	1.60	17	11	24	168	332	0.98
CC-45	42.66851	-114.82436	35.0	8.69	5.95	0.19	62	3.41	14	3	31	140	228	0.87
CC-46	42.66778	-114.82673	35.5	8.41	7.62	0.45	56	4.10	12	3	25	139	222	0.90
CC-48	42.70501	-114.85701	31.8	9.55	1.93	0.01	122	1.62	52	24	33	232	429	0.75
LY89-2	42.66123	-114.791887	37	8.1	13	1.2	58	4.1	12	4	25	140	246	1.01
CC-11	42.69457	-114.85592	58.4	9.53	0.84	0.00	128	1.87	32	22	34	93	423	1.32
LY89-9	42.64886	-114.652208	23	9.1	8.9	2.4	73	1.9	20	11	28	95	263	1.18

Table C2: Major cations and anions for Ca-HCO₃ type thermal waters utilized in this study. Charge balances listed are given as the ratio of cations to anions calculated from meq/L units.

Site	Lat	Long	T (°C)	pH	Ca	Mg	Na	K	Cl	F	SO ₄	Alkalinity as HCO ₃	TDS	Charge Balance
LY89-17	42.5759	-114.738609	25	8	35	4.5	63	12	35	2	69	160	371	1.01
LY82-13	42.59993	-114.943824	42	9.2	26	3.9	35	7.9	16	2	35	120	331	1.03
LY89-3	42.65402	-114.795266	28.5	8	16	2.3	55	5.8	13	3	27	150	259	1.00
CC-9	42.64497	-114.78706	34.5	7.98	23.47	3.00	58	7.69	23	2	40	144	252	1.04
CC-10	42.64432	-114.78294	34.4	7.96	26.66	3.47	56	8.04	20	2	32	127	293	1.24
CC-12	42.54479	-114.94855	37.5	8.59	11.23	0.36	149	1.38	53	2	188	95	559	1.00
LY89-10	42.59616	-114.751276	31	8	39	5.6	65	11	38	2	75	160	388	1.03
LY89-5	42.64683	-114.785566	32.5	7.8	18	2.2	54	6	13	3	27	150	268	1.02
LY89-6	42.63448	-114.778469	25	8.1	17	1.1	53	7.5	14	2	22	160	283	0.95
LY89-7	42.5977	-114.760739	29	7.9	36	5.4	61	10	31	2	61	170	356	1.02
M91-12	42.54998	-114.436857	30.5	7.8	37	6.8	31	4.9	31	1	51	100	266	1.07
LY89-18	42.56642	-114.490768	31.5	8	20	3.9	37	7	11	4	17	130	223	1.04
LY89-29	42.39592	-114.691588	18.5	7.8	23	8.4	13	2.9	9	0	11	120	175	1.01
LY89-30	42.34555	-114.509176	37	8	31	13	43	11	6	2	21	270	279	0.93
LY89-32	42.27131	-114.359743	9	6.7	5.4	1.3	6	5	2	0	2	34	95	1.17
LY89-33	42.22239	-114.785594	12	7	7.2	1.2	6	2.6	3	0	5	30	76	1.13
LY89-34	42.20179	-114.664984	32	7.8	21	2	18	6.9	7	1	10	120	200	0.90
LY89-35	42.20114	-114.697878	26	7.5	22	2.6	19	5.8	6	6	12	110	183	0.90
LY89-36	42.15826	-114.66585	32	7.6	18	2.3	18	4.7	7	1	9	100	174	0.97
LY89-37	42.20044	-114.586984	7.5	7.6	34	5.4	19	3.6	16	0	17	120	208	1.10
LY89-38	42.21351	-114.306916	4.5	6	2.6	0.7	3	2.6	1	0	3	20	62	0.91
CC-54	42.57256	-114.45175	31.0	7.77	39.91	8.98	55	4.92	38	2	76	161	390	0.97
CC-8	42.69940	-114.91040	24.7	9.47	5.74	0.74	113	4.16	46	12	91	81	397	1.04
CC-13	42.54348	-114.94897	36.2	8.65	11.14	0.79	147	1.92	54	2	187	98	566	0.99

APPENDIX D: SELECT WELL DRILLER'S LOGS

Form 238-7
1/78

RECEIVED

STATE OF IDAHO
DEPARTMENT OF WATER RESOURCES

WELL DRILLER'S REPORT

State law requires that this report be filed with the Director, Department of Water Resources, within 30 days after the completion or abandonment of the well.

USE TYPEWRITER OR
BALLPOINT PEN

RECEIVED

Department of Water Resources
Southern District Office

FEB 27 1980

FEB 1 1980

1. WELL OWNER

Name College Southern Idaho

Address Twin Falls, Idaho

Owner's Permit No. _____

2. NATURE OF WORK

☒ New well ☐ Deepened ☐ Replacement
☐ Abandoned (describe method of abandoning) _____

3. PROPOSED USE

☐ Domestic ☐ Irrigation ☐ Test ☐ Municipal
☐ Industrial ☐ Stock ☐ Waste Disposal or Injection
☒ Other heating part / Campus Geothermal (specify type)

4. METHOD DRILLED

☐ Rotary ☐ Air ☐ Hydraulic ☐ Reverse rotary
☒ Cable ☐ Dug ☐ Other _____

5. WELL CONSTRUCTION

Casing schedule: ☒ Steel ☐ Concrete ☐ Other _____

Thickness	Diameter	From	To
250 inches	16 inches	1	367 feet
250 inches	12 inches	2	1191 feet
_____ inches	_____ inches	_____	_____ feet
_____ inches	_____ inches	_____	_____ feet

Was casing drive shoe used? ☒ Yes ☐ No

Was a packer or seal used? ☐ Yes ☒ No

Perforated? ☐ Yes ☒ No

How perforated? ☐ Factory ☐ Knife ☐ Torch

Size of perforation _____ inches by _____ inches

Number	From	To
_____ perforations	_____ feet	_____ feet
_____ perforations	_____ feet	_____ feet
_____ perforations	_____ feet	_____ feet

Well screen installed? ☐ Yes ☒ No

Manufacturer's name _____

Type _____ Model No. _____

Diameter _____ Slot size _____ Set from _____ feet to _____ feet

Diameter _____ Slot size _____ Set from _____ feet to _____ feet

Gravel packed? ☐ Yes ☒ No ☐ Size of gravel _____

Placed from _____ feet to _____ feet

Surface seal depth 120 Material used in seal: ☒ Cement grout ☐ Puddling clay ☐ Well cuttings

Sealing procedure used: ☐ Slurry pit ☐ Temp. surface casing ☒ Overbore to seal depth

Method of joining casing: ☐ Threaded ☒ Welded ☐ Solvent Weld

Describe access port flow line well

6. LOCATION OF WELL

Sketch map location must agree with written location.

N

W E

S

Subdivision Name _____

Lot No. _____ Block No. _____

County Twin Falls

SE 1/4 Sec. 4 T. 10 N. R. 17 E. 1/2

7. WATER LEVEL

Static water level flow line feet below land surface.

Flowing? ☒ Yes ☐ No G.P.M. flow 800

Artesian closed-in pressure _____ p.s.i.

Controlled by: ☒ Valve ☐ Cap ☐ Plug

Temperature 102 OF. Quality good

8. WELL TEST DATA

☐ Pump ☐ Bailor ☐ Air ☐ Other _____

Discharge G.P.M.	Pumping Level	Hours Pumped
_____	_____	_____
_____	_____	_____
_____	_____	_____

9. LITHOLOGIC LOG

Hole Diam.	Depth From	Depth To	Material	Water Yes No
12	0	9	Brown clay	X
	9	20	Black basalt	X
	20	24	Brown silt	X
	24	35	Black basalt	X
	35	43	Brown silt	X
	43	47	Broken basalt	X
	47	49	Black basalt	X
	49	82	Brown clay	X
	82	103	Black basalt	X
	103	120	Grey basalt	X
	120	153	Brown basalt	X
	153	162	Grey basalt	X
	162	187	Brown basalt	X
	187	227	Grey basalt (205-227 very hard)	X
	227	232	Brown clay	X
	232	235	Grey basalt	X
	235	244	Brown clay	X
	244	283	Gravel + b/c clay	X
	283	305	Grey clay	X
	305	335	Brown clay w/ some gravel	X
	335	338	Grey basalt	X
	338	343	Grey clay	X
	343	377	Grey basalt	X
	377	417	Grey basalt (cracked)	X
	417	425	Grey clay	X
	425	433	Grey basalt (cracked hard)	X
	433	445	Grey basalt (hard)	X
	445	495	Grey basalt w/ clay layers	X
	495	563	Grey basalt (very hard)	X
	563	570	Grey basalt w/ clay seams	X
	570	583	Grey basalt (hard)	X
	583	585	Grey clay	X
	585	610	Grey basalt	X
	610	625	Grey basalt (hard)	X
	625	633	Brown clay	X
	633	660	Grey basalt (very hard)	X

10. Work started 7/25/78 finished 11/21/79

11. DRILLERS CERTIFICATION

I/We certify that all minimum well construction standards were complied with at the time the rig was removed.

Firm Name Bolox Henry Firm No. 86

Address Murtavich, Idaho Date 1 Dec 1979

Signed by (Firm Official) Blaine Bolox

and
(Operator) Michael H. H.

USE ADDITIONAL SHEETS IF NECESSARY — FORWARD THE WHITE COPY TO THE DEPARTMENT


Form 238-7
1978

STATE OF IDAHO
DEPARTMENT OF WATER RESOURCES
WELL DRILLER'S REPORT

State law requires that this report be filed with the Director, Department of Water Resources within 30 days after the completion or abandonment of the well.

USE TYPEWRITER OR
BALLPOINT PEN

FEB 2 1980

1. WELL OWNER Name <u>College of Southern Idaho</u> Address <u>Twin Falls, Idaho</u> Owner's Permit No. _____	7. WATER LEVEL (Page 2) Static water level _____ feet below land surface Flowing? <input checked="" type="checkbox"/> Yes <input type="checkbox"/> No G.P.M. flow <u>800</u> Artesian closed-in pressure <u>21</u> p.s.i. Controlled by: <input checked="" type="checkbox"/> Valve <input type="checkbox"/> Cap <input type="checkbox"/> Plug Temperature <u>62</u> °F. Quality <u>good</u>																																																																																																																																																																																																																												
2. NATURE OF WORK <input type="checkbox"/> New well <input type="checkbox"/> Deepened <input type="checkbox"/> Replacement <input type="checkbox"/> Abandoned (describe method of abandoning) _____	8. WELL TEST DATA <input type="checkbox"/> Pump <input type="checkbox"/> Bailer <input type="checkbox"/> Air <input type="checkbox"/> Other _____ <table border="1"> <thead> <tr> <th>Discharge G.P.M.</th> <th>Pumping Level</th> <th>Hours Pumped</th> </tr> </thead> <tbody> <tr><td> </td><td> </td><td> </td></tr> <tr><td> </td><td> </td><td> </td></tr> <tr><td> </td><td> </td><td> </td></tr> </tbody> </table>	Discharge G.P.M.	Pumping Level	Hours Pumped																																																																																																																																																																																																																									
Discharge G.P.M.	Pumping Level	Hours Pumped																																																																																																																																																																																																																											
3. PROPOSED USE <input type="checkbox"/> Domestic <input type="checkbox"/> Irrigation <input type="checkbox"/> Test <input type="checkbox"/> Municipal <input type="checkbox"/> Industrial <input type="checkbox"/> Stock <input type="checkbox"/> Waste Disposal or Injection <input type="checkbox"/> Other <u>Geothermal</u> (specify type) _____	9. LITHOLOGIC LOG <table border="1"> <thead> <tr> <th rowspan="2">Hole Diam.</th> <th colspan="2">Depth</th> <th rowspan="2">Material</th> <th colspan="2">Water</th> </tr> <tr> <th>From</th> <th>To</th> <th>Yes</th> <th>No</th> </tr> </thead> <tbody> <tr><td>12</td><td>660</td><td>678</td><td>Grey Andesite (very hard)</td><td>X</td><td> </td></tr> <tr><td>8</td><td>678</td><td>687</td><td>Brown clay</td><td> </td><td> </td></tr> <tr><td>6</td><td>687</td><td>698</td><td>Grey basalt & old layers</td><td> </td><td> </td></tr> <tr><td>4</td><td>698</td><td>705</td><td>Grey clay</td><td> </td><td> </td></tr> <tr><td>2</td><td>705</td><td>733</td><td>Brown clay & rocks</td><td> </td><td> </td></tr> <tr><td>2</td><td>733</td><td>750</td><td>Grey basalt</td><td> </td><td> </td></tr> <tr><td>2</td><td>750</td><td>785</td><td>Grey clay</td><td> </td><td> </td></tr> <tr><td>2</td><td>785</td><td>860</td><td>Grey Andesite (very hard)</td><td> </td><td> </td></tr> <tr><td>2</td><td>860</td><td>870</td><td>Grey clay</td><td> </td><td> </td></tr> <tr><td>2</td><td>870</td><td>901</td><td>Grey rock</td><td> </td><td> </td></tr> <tr><td>2</td><td>901</td><td>903</td><td>Grey clay</td><td> </td><td> </td></tr> <tr><td>2</td><td>903</td><td>907</td><td>Grey rock</td><td> </td><td> </td></tr> <tr><td>2</td><td>907</td><td>952</td><td>Clay & rock in thin layers</td><td> </td><td> </td></tr> <tr><td>2</td><td>952</td><td>963</td><td>Grey clay</td><td> </td><td> </td></tr> <tr><td>2</td><td>963</td><td>978</td><td>Hard grey clay</td><td> </td><td> </td></tr> <tr><td>2</td><td>978</td><td>981</td><td>Grey rock</td><td> </td><td> </td></tr> <tr><td>2</td><td>981</td><td>992</td><td>Hard grey clay</td><td> </td><td> </td></tr> <tr><td>2</td><td>992</td><td>1011</td><td>Grey Andesite (very hard)</td><td> </td><td> </td></tr> <tr><td>2</td><td>1011</td><td>1012</td><td>Sticky clay</td><td> </td><td> </td></tr> <tr><td>2</td><td>1012</td><td>1020</td><td>Grey Andesite (very hard)</td><td> </td><td> </td></tr> <tr><td>2</td><td>1020</td><td>1030</td><td>Brown clay</td><td> </td><td> </td></tr> <tr><td>2</td><td>1030</td><td>1050</td><td>Tan clay</td><td> </td><td> </td></tr> <tr><td>2</td><td>1050</td><td>1055</td><td>Brown sand</td><td> </td><td> </td></tr> <tr><td>2</td><td>1055</td><td>1070</td><td>Grey brown sand</td><td> </td><td> </td></tr> <tr><td>2</td><td>1070</td><td>1085</td><td>Dark grey sand & some clay sand</td><td>X</td><td> </td></tr> <tr><td>2</td><td>1085</td><td>1105</td><td>Dark grey sand & some sticky shale</td><td>X</td><td> </td></tr> <tr><td>2</td><td>1105</td><td>1107</td><td>Grey rock</td><td> </td><td> </td></tr> <tr><td>2</td><td>1107</td><td>1110</td><td>Grey shale</td><td> </td><td> </td></tr> <tr><td>2</td><td>1110</td><td>1123</td><td>Grey rock</td><td> </td><td> </td></tr> <tr><td>2</td><td>1123</td><td>1125</td><td>Clay & sand (first flow)</td><td>X</td><td> </td></tr> <tr><td>2</td><td>1125</td><td>1155</td><td>Brown rhyolite</td><td>X</td><td> </td></tr> <tr><td>2</td><td>1155</td><td>1170</td><td>Broken brown rhyolite & sand</td><td>X</td><td> </td></tr> <tr><td>2</td><td>1170</td><td>1215</td><td>Brown rhyolite</td><td>X</td><td> </td></tr> <tr><td>2</td><td>1215</td><td> </td><td>Reduced hole from 16" to 12" at 1190</td><td> </td><td> </td></tr> <tr><td>2</td><td> </td><td> </td><td>(1215 was end of Major flow)</td><td> </td><td> </td></tr> </tbody> </table>	Hole Diam.	Depth		Material	Water		From	To	Yes	No	12	660	678	Grey Andesite (very hard)	X		8	678	687	Brown clay			6	687	698	Grey basalt & old layers			4	698	705	Grey clay			2	705	733	Brown clay & rocks			2	733	750	Grey basalt			2	750	785	Grey clay			2	785	860	Grey Andesite (very hard)			2	860	870	Grey clay			2	870	901	Grey rock			2	901	903	Grey clay			2	903	907	Grey rock			2	907	952	Clay & rock in thin layers			2	952	963	Grey clay			2	963	978	Hard grey clay			2	978	981	Grey rock			2	981	992	Hard grey clay			2	992	1011	Grey Andesite (very hard)			2	1011	1012	Sticky clay			2	1012	1020	Grey Andesite (very hard)			2	1020	1030	Brown clay			2	1030	1050	Tan clay			2	1050	1055	Brown sand			2	1055	1070	Grey brown sand			2	1070	1085	Dark grey sand & some clay sand	X		2	1085	1105	Dark grey sand & some sticky shale	X		2	1105	1107	Grey rock			2	1107	1110	Grey shale			2	1110	1123	Grey rock			2	1123	1125	Clay & sand (first flow)	X		2	1125	1155	Brown rhyolite	X		2	1155	1170	Broken brown rhyolite & sand	X		2	1170	1215	Brown rhyolite	X		2	1215		Reduced hole from 16" to 12" at 1190			2			(1215 was end of Major flow)		
Hole Diam.	Depth		Material	Water																																																																																																																																																																																																																									
	From	To		Yes	No																																																																																																																																																																																																																								
12	660	678	Grey Andesite (very hard)	X																																																																																																																																																																																																																									
8	678	687	Brown clay																																																																																																																																																																																																																										
6	687	698	Grey basalt & old layers																																																																																																																																																																																																																										
4	698	705	Grey clay																																																																																																																																																																																																																										
2	705	733	Brown clay & rocks																																																																																																																																																																																																																										
2	733	750	Grey basalt																																																																																																																																																																																																																										
2	750	785	Grey clay																																																																																																																																																																																																																										
2	785	860	Grey Andesite (very hard)																																																																																																																																																																																																																										
2	860	870	Grey clay																																																																																																																																																																																																																										
2	870	901	Grey rock																																																																																																																																																																																																																										
2	901	903	Grey clay																																																																																																																																																																																																																										
2	903	907	Grey rock																																																																																																																																																																																																																										
2	907	952	Clay & rock in thin layers																																																																																																																																																																																																																										
2	952	963	Grey clay																																																																																																																																																																																																																										
2	963	978	Hard grey clay																																																																																																																																																																																																																										
2	978	981	Grey rock																																																																																																																																																																																																																										
2	981	992	Hard grey clay																																																																																																																																																																																																																										
2	992	1011	Grey Andesite (very hard)																																																																																																																																																																																																																										
2	1011	1012	Sticky clay																																																																																																																																																																																																																										
2	1012	1020	Grey Andesite (very hard)																																																																																																																																																																																																																										
2	1020	1030	Brown clay																																																																																																																																																																																																																										
2	1030	1050	Tan clay																																																																																																																																																																																																																										
2	1050	1055	Brown sand																																																																																																																																																																																																																										
2	1055	1070	Grey brown sand																																																																																																																																																																																																																										
2	1070	1085	Dark grey sand & some clay sand	X																																																																																																																																																																																																																									
2	1085	1105	Dark grey sand & some sticky shale	X																																																																																																																																																																																																																									
2	1105	1107	Grey rock																																																																																																																																																																																																																										
2	1107	1110	Grey shale																																																																																																																																																																																																																										
2	1110	1123	Grey rock																																																																																																																																																																																																																										
2	1123	1125	Clay & sand (first flow)	X																																																																																																																																																																																																																									
2	1125	1155	Brown rhyolite	X																																																																																																																																																																																																																									
2	1155	1170	Broken brown rhyolite & sand	X																																																																																																																																																																																																																									
2	1170	1215	Brown rhyolite	X																																																																																																																																																																																																																									
2	1215		Reduced hole from 16" to 12" at 1190																																																																																																																																																																																																																										
2			(1215 was end of Major flow)																																																																																																																																																																																																																										
4. METHOD DRILLED <input type="checkbox"/> Rotary <input type="checkbox"/> Air <input type="checkbox"/> Hydraulic <input type="checkbox"/> Reverse rotary <input type="checkbox"/> Cable <input type="checkbox"/> Dug <input type="checkbox"/> Other _____ 5. WELL CONSTRUCTION Casing schedule: <input type="checkbox"/> Steel <input type="checkbox"/> Concrete <input type="checkbox"/> Other _____ <table border="1"> <thead> <tr> <th>Thickness</th> <th>Diameter</th> <th>From</th> <th>To</th> </tr> </thead> <tbody> <tr><td> </td><td> </td><td> </td><td> </td></tr> <tr><td> </td><td> </td><td> </td><td> </td></tr> <tr><td> </td><td> </td><td> </td><td> </td></tr> <tr><td> </td><td> </td><td> </td><td> </td></tr> </tbody> </table> Was casing drive shoe used? <input type="checkbox"/> Yes <input type="checkbox"/> No Was a packer or seal used? <input type="checkbox"/> Yes <input type="checkbox"/> No Perforated? <input type="checkbox"/> Yes <input type="checkbox"/> No How perforated? <input type="checkbox"/> Factory <input type="checkbox"/> Knife <input type="checkbox"/> Torch Size of perforation _____ inches by _____ inches <table border="1"> <thead> <tr> <th>Number</th> <th>From</th> <th>To</th> </tr> </thead> <tbody> <tr><td> </td><td> </td><td> </td></tr> <tr><td> </td><td> </td><td> </td></tr> <tr><td> </td><td> </td><td> </td></tr> </tbody> </table> Well screen installed? <input type="checkbox"/> Yes <input type="checkbox"/> No Manufacturer's name _____ Type _____ Model No. _____ Diameter _____ Slot size _____ Set from _____ feet to _____ feet Diameter _____ Slot size _____ Set from _____ feet to _____ feet Gravel packed? <input type="checkbox"/> Yes <input type="checkbox"/> No <input type="checkbox"/> Size of gravel _____ Placed from _____ feet to _____ feet Surface seal depth _____ Material used in seal: <input type="checkbox"/> Cement grout <input type="checkbox"/> Puddling clay <input type="checkbox"/> Well cuttings Sealing procedure used: <input type="checkbox"/> Slurry pit <input type="checkbox"/> Temp. surface casing <input type="checkbox"/> Overbore to seal depth Method of joining casing: <input type="checkbox"/> Threaded <input type="checkbox"/> Welded <input type="checkbox"/> Solvent Weld <input type="checkbox"/> Cemented between strata Describe access port _____	Thickness	Diameter	From	To																	Number	From	To										10. Work started <u>7/25/78</u> finished <u>11/21/79</u>																																																																																																																																																																																												
Thickness	Diameter	From	To																																																																																																																																																																																																																										
Number	From	To																																																																																																																																																																																																																											
6. LOCATION OF WELL Sketch map location must agree with written location.  Subdivision Name _____ Lot No. _____ Block No. _____ County <u>Twin Falls</u> <u>SE 1/4 Sec. 4, T. 10 N, R. 17 E</u>	11. DRILLERS CERTIFICATION I/We certify that all minimum well construction standards were complied with at the time the rig was removed. Firm Name <u>Boley-Henry</u> Firm No. <u>86</u> Address <u>McTavish, Ida</u> Date <u>1 Dec 1979</u> Signed by (Firm Official) <u>Blaine Boley Jr</u> and <u>Fred Thompson</u> (Operator)																																																																																																																																																																																																																												

USE ADDITIONAL SHEETS IF NECESSARY — FORWARD THE WHITE COPY TO THE DEPARTMENT

Form 238-7
1978STATE OF IDAHO
DEPARTMENT OF WATER RESOURCESUSE TYPEWRITER OR
BALLPOINT PEN

WELL DRILLER'S REPORT

State law requires that this report be filed with the Director, Department of Water Resources
within 30 days after the completion or abandonment of the well.

1. WELL OWNER
Name College of Southern Idaho
Address Twin Falls, Idaho
Owner's Permit No. _____

2. NATURE OF WORK
☒ New well ☐ Deepened ☐ Replacement
☐ Abandoned (describe method of abandoning) _____

3. PROPOSED USE
☐ Domestic ☐ Irrigation ☐ Test ☐ Municipal
☐ Industrial ☐ Stock ☐ Waste Disposal or Injection
☐ Other Geothermal (specify type) _____

4. METHOD DRILLED
☐ Rotary ☐ Air ☐ Hydraulic ☐ Reverse rotary
☐ Cable ☐ Dug ☐ Other _____

5. WELL CONSTRUCTION
Casing schedule: ☐ Steel ☐ Concrete ☐ Other _____
Thickness _____ inches Diameter _____ inches + _____ feet To _____ feet
_____ inches _____ inches _____ feet _____ feet
_____ inches _____ inches _____ feet _____ feet
Was casing drive shoe used? ☐ Yes ☐ No
Was a packer or seal used? ☐ Yes ☐ No
Perforated? ☐ Yes ☐ No
How perforated? ☐ Factory ☐ Knife ☐ Torch
Size of perforation _____ inches by _____ inches
Number _____ From _____ To _____
_____ perforations _____ feet _____ feet
_____ perforations _____ feet _____ feet
_____ perforations _____ feet _____ feet
Well screen installed? ☐ Yes ☐ No
Manufacturer's name _____
Type _____ Model No. _____
Diameter _____ Slot size _____ Set from _____ feet to _____ feet
Diameter _____ Slot size _____ Set from _____ feet to _____ feet
Gravel packed? ☐ Yes ☐ No ☐ Size of gravel _____
Placed from _____ feet to _____ feet
Surface seal depth _____ Material used in seal: ☐ Cement grout ☐ Well cuttings
☐ Puddling clay ☐ Slurry pit ☐ Temp. surface casing
Sealing procedure used: ☐ Slurry pit ☐ Temp. surface casing
☐ Overbore to seal depth ☐ Solvent ☐ Weld
Method of joining casing: ☐ Threaded ☐ Welded ☐ Cemented between strata
Describe access port _____

6. LOCATION OF WELL
Sketch map location must agree with written location.
N
W E
S
County Twin Falls
SE 1/4 Sec. 4, T. 10 N, R. 17 E

7. WATER LEVEL
Static water level _____ feet below _____ surface
Flowing? ☒ Yes ☐ No G.P.M. flow 300
Artesian closed-in pressure 89 p.s.i.
Controlled by: ☒ Valve ☐ Cap ☐ Plug
Temperature 102 °F. Quality _____

8. WELL TEST DATA
☐ Pump ☐ Bailor ☐ Air ☐ Other _____
Discharge G.P.M. _____ Pumping Level _____ Hours Pumped _____

9. LITHOLOGIC LOG

Hole Diam.	Depth From	To	Material	Water Yes No
12"	1215	1550	Reddish brown rhyolite	X
12"	1550	1655	Grey brown rhyolite	X
12"	1655	1720	Grey rhyolite	X
12"	1720	1800	Grey rhyolite	X
8"	1800	1820	Reduced hole at 1760	
	1820	1837	Grey rhyolite	
	1837	1852	Brown rhyolite	
	1852	1867	Grey rhyolite	
	1867	1907	Grey-brown rhyolite	
	1907	1928	Brown rhyolite	
	1928	1962	Grey rhyolite	
	1962	2003	Brown rhyolite (1950-60)	X
	2003	2080	Grey Andesite	X
	2080	2105	Olivine	X
	2105	2121	Grey Andesite	X
	2121	2187	Light brown rhyolite	X
	2187	2220	Light brown rhyolite covered	X

10. Work started 7/25/78 finished 11/21/78

11. DRILLERS CERTIFICATION
I/We certify that all minimum well construction standards were complied with at the time the rig was removed.
Firm Name Boley & Henry Firm No. 86
Address Murtzuch Idaho Date 1 Dec 1978
Signed by (Firm Official) Blaine Boley
and MICROFILMED
(Operator)

USE ADDITIONAL SHEETS IF NECESSARY - FORWARD THE WHITE COPY TO THE DEPARTMENT

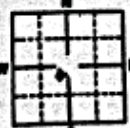
Figure C1. CSI Well 1 Driller's Log

Form 257
1/78

 STATE OF IDAHO
DEPARTMENT OF WATER RESOURCES
WELL DRILLER'S REPORT

 State law requires that this report be filed with the Director, Department of Water Resources
within 30 days after the completion or abandonment of the well.

 USE TYPEWRITER OR
BALLPOINT PEN
RECEIVED
JUN 9 1978

1. WELL OWNER Name <u>CSI # 2</u> <u>College of Southern Idaho</u> Address <u>Twain Falls, Idaho</u> Owner's Permit No. _____	7. WATER LEVEL Static water level _____ feet below land surface Flowing? <input checked="" type="checkbox"/> Yes <input type="checkbox"/> No G.P.M. flow <u>1100</u> Artesian closed-in pressure <u>30</u> p.s.i. Controlled by: <input checked="" type="checkbox"/> Valve <input type="checkbox"/> Cap <input type="checkbox"/> Plug Temperature <u>10.1</u> °F. Quality <u>good</u>																																																																																																															
2. NATURE OF WORK <input checked="" type="checkbox"/> New well <input type="checkbox"/> Deepened <input type="checkbox"/> Replacement <input type="checkbox"/> Abandoned (describe method of abandoning) _____	8. WELL TEST DATA <input type="checkbox"/> Pump <input type="checkbox"/> Sailer <input type="checkbox"/> Air <input type="checkbox"/> Other _____ <table border="1"> <thead> <tr> <th>Discharge G.P.M.</th> <th>Pumping Level</th> <th>Hours Pumped</th> </tr> </thead> <tbody> <tr> <td><u>1100</u></td> <td><u>flow</u></td> <td></td> </tr> </tbody> </table>	Discharge G.P.M.	Pumping Level	Hours Pumped	<u>1100</u>	<u>flow</u>																																																																																																										
Discharge G.P.M.	Pumping Level	Hours Pumped																																																																																																														
<u>1100</u>	<u>flow</u>																																																																																																															
3. PROPOSED USE <input type="checkbox"/> Domestic <input type="checkbox"/> Irrigation <input type="checkbox"/> Test <input type="checkbox"/> Municipal <input type="checkbox"/> Industrial <input type="checkbox"/> Stock <input type="checkbox"/> Waste Disposal or Injection <input type="checkbox"/> Other <u>geothermal</u> (specify type) _____	9. LITHOLOGIC LOG <table border="1"> <thead> <tr> <th>Depth</th> <th>Material</th> <th>Water</th> </tr> </thead> <tbody> <tr><td>0-15</td><td>Brown clay</td><td>Y</td></tr> <tr><td>15-22</td><td>Clayey brown rock</td><td>Y</td></tr> <tr><td>22-25</td><td>Grey basalt</td><td>Y</td></tr> <tr><td>25-49</td><td>Brown clay</td><td>X</td></tr> <tr><td>49-63</td><td>Grey basalt</td><td>Y</td></tr> <tr><td>63-76</td><td>Clay</td><td>X</td></tr> <tr><td>76-85</td><td>Grey basalt</td><td>X</td></tr> <tr><td>85-98</td><td>Clay</td><td>Y</td></tr> <tr><td>98-130</td><td>Grey-brown basalt</td><td>X</td></tr> <tr><td>130-164</td><td>Grey basalt</td><td>X</td></tr> <tr><td>164-181</td><td>Brown basalt</td><td>X</td></tr> <tr><td>181-218</td><td>Grey basalt</td><td>X</td></tr> <tr><td>218-220</td><td>Talc</td><td>Y</td></tr> <tr><td>220-241</td><td>Grey basalt</td><td>X</td></tr> <tr><td>241-278</td><td>Brown sandy clay, good</td><td>X</td></tr> <tr><td>278-386</td><td>Soft brown conglomerate</td><td>X</td></tr> <tr><td>386-406</td><td>Grey basalt</td><td>Y</td></tr> <tr><td>406-428</td><td>Brown clay</td><td>X</td></tr> <tr><td>428-468</td><td>Grey clay</td><td>Y</td></tr> <tr><td>468-499</td><td>Brown clay</td><td>X</td></tr> <tr><td>499-528</td><td>Grey clay</td><td>Y</td></tr> <tr><td>528-543</td><td>Grey basalt (hard)</td><td>X</td></tr> <tr><td>543-549</td><td>Brown clay</td><td>X</td></tr> <tr><td>549-640</td><td>Brown sandy clay</td><td>X</td></tr> <tr><td>640-668</td><td>Grey sandy clay</td><td>Y</td></tr> <tr><td>668-714</td><td>Grey sandy clay</td><td>X</td></tr> <tr><td>714-722</td><td>Grey sandy clay</td><td>X</td></tr> <tr><td>722-728</td><td>Grey basalt</td><td>X</td></tr> <tr><td>728-758</td><td>Reddish brown clay</td><td>Y</td></tr> <tr><td>758-778</td><td>Grey basalt</td><td>Y</td></tr> <tr><td>778-783</td><td>Brown basalt/grayish clay</td><td>Y</td></tr> <tr><td>783-788</td><td>Tan clay</td><td>X</td></tr> <tr><td>788-853</td><td>Grey basalt (hard)</td><td>X</td></tr> <tr><td>853-858</td><td>Brown basalt</td><td>X</td></tr> <tr><td>858-864</td><td>Grey basalt</td><td>X</td></tr> <tr><td>864-873</td><td>Grey clay (sticky)</td><td>Y</td></tr> </tbody> </table>	Depth	Material	Water	0-15	Brown clay	Y	15-22	Clayey brown rock	Y	22-25	Grey basalt	Y	25-49	Brown clay	X	49-63	Grey basalt	Y	63-76	Clay	X	76-85	Grey basalt	X	85-98	Clay	Y	98-130	Grey-brown basalt	X	130-164	Grey basalt	X	164-181	Brown basalt	X	181-218	Grey basalt	X	218-220	Talc	Y	220-241	Grey basalt	X	241-278	Brown sandy clay, good	X	278-386	Soft brown conglomerate	X	386-406	Grey basalt	Y	406-428	Brown clay	X	428-468	Grey clay	Y	468-499	Brown clay	X	499-528	Grey clay	Y	528-543	Grey basalt (hard)	X	543-549	Brown clay	X	549-640	Brown sandy clay	X	640-668	Grey sandy clay	Y	668-714	Grey sandy clay	X	714-722	Grey sandy clay	X	722-728	Grey basalt	X	728-758	Reddish brown clay	Y	758-778	Grey basalt	Y	778-783	Brown basalt/grayish clay	Y	783-788	Tan clay	X	788-853	Grey basalt (hard)	X	853-858	Brown basalt	X	858-864	Grey basalt	X	864-873	Grey clay (sticky)	Y
Depth	Material	Water																																																																																																														
0-15	Brown clay	Y																																																																																																														
15-22	Clayey brown rock	Y																																																																																																														
22-25	Grey basalt	Y																																																																																																														
25-49	Brown clay	X																																																																																																														
49-63	Grey basalt	Y																																																																																																														
63-76	Clay	X																																																																																																														
76-85	Grey basalt	X																																																																																																														
85-98	Clay	Y																																																																																																														
98-130	Grey-brown basalt	X																																																																																																														
130-164	Grey basalt	X																																																																																																														
164-181	Brown basalt	X																																																																																																														
181-218	Grey basalt	X																																																																																																														
218-220	Talc	Y																																																																																																														
220-241	Grey basalt	X																																																																																																														
241-278	Brown sandy clay, good	X																																																																																																														
278-386	Soft brown conglomerate	X																																																																																																														
386-406	Grey basalt	Y																																																																																																														
406-428	Brown clay	X																																																																																																														
428-468	Grey clay	Y																																																																																																														
468-499	Brown clay	X																																																																																																														
499-528	Grey clay	Y																																																																																																														
528-543	Grey basalt (hard)	X																																																																																																														
543-549	Brown clay	X																																																																																																														
549-640	Brown sandy clay	X																																																																																																														
640-668	Grey sandy clay	Y																																																																																																														
668-714	Grey sandy clay	X																																																																																																														
714-722	Grey sandy clay	X																																																																																																														
722-728	Grey basalt	X																																																																																																														
728-758	Reddish brown clay	Y																																																																																																														
758-778	Grey basalt	Y																																																																																																														
778-783	Brown basalt/grayish clay	Y																																																																																																														
783-788	Tan clay	X																																																																																																														
788-853	Grey basalt (hard)	X																																																																																																														
853-858	Brown basalt	X																																																																																																														
858-864	Grey basalt	X																																																																																																														
864-873	Grey clay (sticky)	Y																																																																																																														
4. METHOD DRILLED <input type="checkbox"/> Rotary <input type="checkbox"/> Air <input type="checkbox"/> Hydraulic <input type="checkbox"/> Reverse rotary <input checked="" type="checkbox"/> Cable <input type="checkbox"/> Dug <input type="checkbox"/> Other _____ 5. WELL CONSTRUCTION Casing schedule: <input checked="" type="checkbox"/> Steel <input type="checkbox"/> Concrete <input type="checkbox"/> Other _____ <table border="1"> <thead> <tr> <th>Thickness</th> <th>Diameter</th> <th>From</th> <th>To</th> </tr> </thead> <tbody> <tr><td>2.50 inches</td><td>16 inches</td><td>1 foot</td><td>512 feet</td></tr> <tr><td>2.50 inches</td><td>10 inches</td><td>1 foot</td><td>1348 feet</td></tr> <tr><td>2.50 inches</td><td>10 inches</td><td>1184 feet</td><td>1325 feet</td></tr> <tr><td>2.50 inches</td><td>8 inches</td><td>1223 feet</td><td>1353 feet</td></tr> </tbody> </table> Was casing drive shoe used? <input checked="" type="checkbox"/> Yes <input type="checkbox"/> No 16" solid shoe Was a packer or seal used? <input type="checkbox"/> Yes <input checked="" type="checkbox"/> No 12" Cast Steel Perforated? <input checked="" type="checkbox"/> Yes <input type="checkbox"/> No 10" " " How perforated? <input checked="" type="checkbox"/> Factory <input type="checkbox"/> Knife <input type="checkbox"/> Torch Size of perforation <u>3/8</u> inches by <u>3</u> inches 8" near bottom 16" near bottom 12" near bottom 8" near bottom 100' perforations 8" near bottom Well screen installed? <input type="checkbox"/> Yes <input checked="" type="checkbox"/> No Manufacturer's name _____ Type _____ Model No. _____ Diameter _____ Slot size _____ Set from _____ feet to _____ feet Diameter _____ Slot size _____ Set from _____ feet to _____ feet Gravel packed? <input type="checkbox"/> Yes <input checked="" type="checkbox"/> No <input type="checkbox"/> Size of gravel _____ Packed from _____ feet to _____ feet Surface seal depth <u>200</u> Material used in seal: <input type="checkbox"/> Cement grout <input type="checkbox"/> Puddling clay <input type="checkbox"/> Well cuttings Sealing procedure used: <input type="checkbox"/> Shurry pit <input type="checkbox"/> Temp. surface casing <input checked="" type="checkbox"/> Overbore to seal depth Method of joining casing: <input type="checkbox"/> Threaded <input checked="" type="checkbox"/> Welded <input type="checkbox"/> Solvent Weld <input type="checkbox"/> Cemented between strings Describe access port <u>flow line well</u>	Thickness	Diameter	From	To	2.50 inches	16 inches	1 foot	512 feet	2.50 inches	10 inches	1 foot	1348 feet	2.50 inches	10 inches	1184 feet	1325 feet	2.50 inches	8 inches	1223 feet	1353 feet	10. WORK PERIOD Work started <u>22 Apr 1978</u> Finished <u>22 Apr 1978</u> 11. DRILLER CERTIFICATION <u>cb dl</u> I/We certify that all minimum well construction standards were complied with at the time the rig was removed. Firm Name <u>Boley & Henry</u> Firm No. <u>86</u> Address <u>Murtawell, Idaho</u> Signed by (Firm Official) <u>Blaine Boley</u> and <u>Blaine Boley</u> (Operator)																																																																																											
Thickness	Diameter	From	To																																																																																																													
2.50 inches	16 inches	1 foot	512 feet																																																																																																													
2.50 inches	10 inches	1 foot	1348 feet																																																																																																													
2.50 inches	10 inches	1184 feet	1325 feet																																																																																																													
2.50 inches	8 inches	1223 feet	1353 feet																																																																																																													
6. LOCATION OF WELL Sketch map location must agree with written location.  Subdivision Name _____ Lot No. _____ Block No. _____ County <u>Twain Falls</u> <u>NE 1/4 Sec 4, T. 10 N. R. 17 W.</u>																																																																																																																

USE ADDITIONAL SHEETS IF NECESSARY - FORWARD THE WHITE COPY TO THE DEPARTMENT

STATE OF IDAHO
DEPARTMENT OF WATER RESOURCES
WELL DRILLER'S REPORT

State law requires that this report be filed with the Director, Department of Water Resources
within 30 days after the completion or abandonment of the well.

USE TYPEWRITER OR
BALLPOINT PEN
RECEIVED
JUN 10 1961

1. WELL OWNER *Page #2*
Name College of Southern Idaho
Address Twin Falls, Idaho
Owner's Permit No. _____

2. NATURE OF WORK
☐ New well ☐ Deepened ☐ Replacement
☐ Abandoned (describe method of abandoning) _____

3. PROPOSED USE
☐ Domestic ☐ Irrigation ☐ Test ☐ Municipal
☐ Industrial ☐ Stock ☐ Waste Disposal or Injection
☐ Other _____ (specify type)

4. METHOD DRILLED
☐ Rotary ☐ Air ☐ Hydraulic ☐ Reverse rotary
☐ Cable ☐ Dug ☐ Other _____

5. WELL CONSTRUCTION
Casing schedule: ☐ Steel ☐ Concrete ☐ Other _____
Thickness _____ Diameter _____ From _____ To _____
Inches _____ inches _____ feet _____ feet
Inches _____ inches _____ feet _____ feet
Inches _____ inches _____ feet _____ feet
Was casing drive shoe used? ☐ Yes ☐ No
Was a packer or seal used? ☐ Yes ☐ No
Perforated? ☐ Yes ☐ No
How perforated? ☐ Factory ☐ Knife ☐ Torch
Size of perforation _____ inches by _____ inches
Number _____ From _____ To _____
perforations _____ feet _____ feet
perforations _____ feet _____ feet
perforations _____ feet _____ feet
Well screen installed? ☐ Yes ☐ No
Manufacturer's name _____
Type _____ Model No. _____
Diameter _____ Slot size _____ Set from _____ feet to _____ feet
Diameter _____ Slot size _____ Set from _____ feet to _____ feet
Gravel packed? ☐ Yes ☐ No ☐ Size of gravel _____
Paved from _____ feet to _____ feet
Surface seal depth _____ Material used in seal: ☐ Cement grout
☐ Pudding clay ☐ Well cuttings
Sealing procedure used: ☐ Shury pit ☐ Temp. surface casing
☐ Overbars to seal depth
Method of joining casing: ☐ Threaded ☐ Welded ☐ Solvent
Weld _____
Describe screen part _____

6. LOCATION OF WELL
Sketch map location must agree with written location.
Subdivision Name _____
Lot No. _____ Block No. _____
County Twin Falls
NE 1/4 Sec 4, T. 10 N. R. 17 W.

7. WATER LEVEL
Static water level _____ feet below land surface
Flowing? ☐ Yes ☐ No G.P.M. flow _____
Artesian closed-in pressure ☐ Yes ☐ No
Controlled by: ☐ Valve ☐ Dip ☐ Plug
Temperature _____ of. Quality _____
JUL 10 1961

8. WELL TEST DATA
☐ Pump ☐ Sailer ☐ Alluvial ☐ Other Resources
Discharge G.P.M. _____ Pumping Level _____ Hours Pumped _____

9. LITHOLOGIC LOG

Well Elev.	Depth From	To	Material	Water Yes No
16	913	988	Grey basalt (very hard)	
	988	990	Grey clay	
	990	995	Grey basalt	
	995	1028	Grey clay (sticky)	
	1028	1028	Grey basalt	
	1028	1062	Clay shale of fine gravel	
	1062	1070	Black basalt	
	1070	1080	Grey brown clay (sticky)	
	1080	1090	Grey clay of shale (sticky)	
	1090	1111	Grey brown shale	
	1111	1115	Grey basalt	
	1115	1119	Grey clay	
	1119	1122	Grey basalt	
	1122	1144	Grey clay with layers	
	1144	1157	Black basalt	
	1157	1176	Grey clay shale	
	1176	1181	Grey basalt	
	1181	1186	Grey shale	
	1186	1198	Grey basalt with layers	
	1198	1202	Grey basalt	
	1202	1207	Grey basalt with layers	
	1207	1215	Grey basalt	
	1215	1230	Grey brown basalt	
	1230	1233	Grey basalt (hard)	
	1233	1248	Grey-brown basalt	
	1248	1267	Grey sandstone (very hard)	
	1267	1275	Brown shale (crustal)	
	1275	1321	Thick shale	
	1321	1325	Light brown clay	
	1325	1327	Dark brown clay	
	1327	1357	Dark brown shale	
	1357	1360	Dark brown shale	
	1360	1367	Dark brown shale	
	1367	1370	Dark brown shale	
	1370	1375	Dark brown shale	
	1375	1380	Dark brown shale	
	1380	1385	Dark brown shale	
	1385	1390	Dark brown shale	
	1390	1395	Dark brown shale	
	1395	1400	Dark brown shale	
	1400	1405	Dark brown shale	
	1405	1410	Dark brown shale	
	1410	1415	Dark brown shale	
	1415	1420	Dark brown shale	
	1420	1425	Dark brown shale	
	1425	1430	Dark brown shale	
	1430	1435	Dark brown shale	
	1435	1440	Dark brown shale	
	1440	1445	Dark brown shale	
	1445	1450	Dark brown shale	
	1450	1455	Dark brown shale	
	1455	1460	Dark brown shale	
	1460	1465	Dark brown shale	
	1465	1470	Dark brown shale	
	1470	1475	Dark brown shale	
	1475	1480	Dark brown shale	
	1480	1485	Dark brown shale	
	1485	1490	Dark brown shale	
	1490	1495	Dark brown shale	
	1495	1500	Dark brown shale	
	1500	1505	Dark brown shale	
	1505	1510	Dark brown shale	
	1510	1515	Dark brown shale	
	1515	1520	Dark brown shale	
	1520	1525	Dark brown shale	
	1525	1530	Dark brown shale	
	1530	1535	Dark brown shale	
	1535	1540	Dark brown shale	
	1540	1545	Dark brown shale	
	1545	1550	Dark brown shale	
	1550	1555	Dark brown shale	
	1555	1560	Dark brown shale	
	1560	1565	Dark brown shale	
	1565	1570	Dark brown shale	
	1570	1575	Dark brown shale	
	1575	1580	Dark brown shale	
	1580	1585	Dark brown shale	
	1585	1590	Dark brown shale	
	1590	1595	Dark brown shale	
	1595	1600	Dark brown shale	
	1600	1605	Dark brown shale	
	1605	1610	Dark brown shale	
	1610	1615	Dark brown shale	
	1615	1620	Dark brown shale	
	1620	1625	Dark brown shale	
	1625	1630	Dark brown shale	
	1630	1635	Dark brown shale	
	1635	1640	Dark brown shale	
	1640	1645	Dark brown shale	
	1645	1650	Dark brown shale	
	1650	1655	Dark brown shale	
	1655	1660	Dark brown shale	
	1660	1665	Dark brown shale	
	1665	1670	Dark brown shale	
	1670	1675	Dark brown shale	
	1675	1680	Dark brown shale	
	1680	1685	Dark brown shale	
	1685	1690	Dark brown shale	
	1690	1695	Dark brown shale	
	1695	1700	Dark brown shale	
	1700	1705	Dark brown shale	
	1705	1710	Dark brown shale	
	1710	1715	Dark brown shale	
	1715	1720	Dark brown shale	
	1720	1725	Dark brown shale	
	1725	1730	Dark brown shale	
	1730	1735	Dark brown shale	
	1735	1740	Dark brown shale	
	1740	1745	Dark brown shale	
	1745	1750	Dark brown shale	
	1750	1755	Dark brown shale	
	1755	1760	Dark brown shale	
	1760	1765	Dark brown shale	
	1765	1770	Dark brown shale	
	1770	1775	Dark brown shale	
	1775	1780	Dark brown shale	
	1780	1785	Dark brown shale	
	1785	1790	Dark brown shale	
	1790	1795	Dark brown shale	
	1795	1800	Dark brown shale	
	1800	1805	Dark brown shale	
	1805	1810	Dark brown shale	
	1810	1815	Dark brown shale	
	1815	1820	Dark brown shale	
	1820	1825	Dark brown shale	
	1825	1830	Dark brown shale	
	1830	1835	Dark brown shale	
	1835	1840	Dark brown shale	
	1840	1845	Dark brown shale	
	1845	1850	Dark brown shale	
	1850	1855	Dark brown shale	
	1855	1860	Dark brown shale	
	1860	1865	Dark brown shale	
	1865	1870	Dark brown shale	
	1870	1875	Dark brown shale	
	1875	1880	Dark brown shale	
	1880	1885	Dark brown shale	
	1885	1890	Dark brown shale	
	1890	1895	Dark brown shale	
	1895	1900	Dark brown shale	
	1900	1905	Dark brown shale	
	1905	1910	Dark brown shale	
	1910	1915	Dark brown shale	
	1915	1920	Dark brown shale	
	1920	1925	Dark brown shale	
	1925	1930	Dark brown shale	
	1930	1935	Dark brown shale	
	1935	1940	Dark brown shale	
	1940	1945	Dark brown shale	
	1945	1950	Dark brown shale	
	1950	1955	Dark brown shale	
	1955	1960	Dark brown shale	
	1960	1965	Dark brown shale	
	1965	1970	Dark brown shale	
	1970	1975	Dark brown shale	
	1975	1980	Dark brown shale	
	1980	1985	Dark brown shale	
	1985	1990	Dark brown shale	
	1990	1995	Dark brown shale	
	1995	2000	Dark brown shale	

10. MIN. FLOW 1443-1455
Work started _____ Subbed _____

11. DRILLING CERTIFICATION *CB*
I/We certify that all minimum well construction standards were
complied with at the time the rig was removed.
Pilot Name Baley-Henry Firm No. 61
Address Mullanbach, Idaho Date 24 May 1961
Signed by Pilot Official Blaine Baley
and Blaine Baley
Inspector Blaine Baley

USE ADDITIONAL SHEETS IF NECESSARY - FORWARD THE WHITE COPY TO THE DEPARTMENT

Figure C2. CSI Well 2 Driller's Log

Form 9/82
RECEIVED

STATE OF IDAHO
 DEPARTMENT OF WATER RESOURCES
WELL DRILLER'S REPORT

USE TYPEWRITER OR
 BALLPOINT PEN

JAN 12 1987
 State law requires that this report be filed with the Director, Department of Water Resources within 30 days after the completion or abandonment of the well.

Department of Water Resources

Salt Lake Region Office

1. WELL OWNER

Name Banbury Hot Springs
 Address Rt 3 Tuhl, Id.
 Owner's Permit No. _____

7. WATER LEVEL

Static water level _____ feet below land surface.
 Flowing? ☒ Yes ☐ No G.P.M. flow _____
 Artesian closed-in pressure 55 p.s.i.
 Controlled by: ☒ Valve ☐ Cap ☐ Plug
 Temperature 130 °F. Quality good
 Describe artesian or temperature zones below.

2. NATURE OF WORK

☐ New well ☒ Deepened ☐ Replacement
☐ Abandoned (describe abandonment procedures such as materials, plug depths, etc. in lithologic log)

8. WELL TEST DATA

☐ Pump ☐ Baller ☐ Air ☐ Other _____

Discharge G.P.M.	Pumping Level	Hours Pumped
<u>250 (Estimate)</u>		

3. PROPOSED USE

☐ Domestic ☐ Irrigation ☐ Test ☐ Municipal
☐ Industrial ☐ Stock ☐ Waste Disposal or Injection
☐ Other geothermal (specify type)

9. LITHOLOGIC LOG

86778

Bore Diam.	Depth		Material	Water Yes No
	From	To		
8"	273	276	Black basalt	
	276	279	Black sand	
8"	279	282	Black basalt	
8"	282	314	Red-brown clay (sticky)	
8"	314	324	Black basalt	
8"	324	333	Red clay	
8"	333	341	Brown clay	
6"	341	363	Black basalt	
6"	363	408	Black basalt, shale & clay in layers	
6"	408	416	Black Basalt	
6"	416	453	Alternating layers of shale & clay (small flow)	X
4"	453	520	Grey basalt Rhyolite	X
4"	520	535	Layers of green shale	
4"	535	543	clay & rhyolite	X
4"	543	550	Green rhyolite	X
4"	550	550	Brown rhyolite (Main flow)	X

RECEIVED
 JAN 16 1987

Department of Water Resources

4. METHOD DRILLED

☐ Rotary ☐ Air ☐ Hydraulic ☐ Reverse rotary
☒ Cable ☐ Dug ☐ Other _____

5. WELL CONSTRUCTION

Casing schedule: ☒ Steel ☐ Concrete ☐ Other _____

Thickness	Diameter	From	To
<u>250</u> inches	<u>6</u> inches	<u>1</u> feet	<u>343</u> feet
<u>250</u> inches	<u>5</u> inches	<u>253</u> feet	<u>453</u> feet
_____ inches	_____ inches	_____ feet	_____ feet

Was casing drive shoe used? ☒ Yes ☐ No
 Was a packer or seal used? ☐ Yes ☒ No
 Perforated? ☐ Yes ☒ No
 How perforated? ☐ Factory ☐ Knife ☐ Torch
 Size of perforation _____ inches by _____ inches
 Number _____ From _____ To _____
 _____ perforations _____ feet _____ feet
 _____ perforations _____ feet _____ feet
 _____ perforations _____ feet _____ feet

Well screen installed? ☐ Yes ☒ No

Manufacturer's name _____

Type _____ Model No. _____

Diameter _____ Slot size _____ Set from _____ feet to _____ feet

Diameter _____ Slot size _____ Set from _____ feet to _____ feet

Gravel packed? ☐ Yes ☒ No ☐ Size of gravel _____

Placed from _____ feet to _____ feet

Surface seal depth _____ Material used in seal: ☒ Cement grout

☐ Bentonite ☐ Pudding clay ☐ _____

Sealing procedure used: ☐ Slurry pit ☐ Temp. surface casing

☒ Overbore to seal depth

Method of joining casing: ☐ Threaded ☒ Welded ☐ Solvent

☐ Cemented between strata

Describe access port flowing well

6. LOCATION OF WELL

Sketch map location must agree with written location.

Subdivision **MICROFILMED**
 Lot No. _____ Block No. _____

County Twin Falls 33
SW 1/4 NW 1/4 Sec 29 T. 8 S. R. 14 E. NE

10.

Work started 15 Aug finished 15 Oct 1986

11. DRILLERS CERTIFICATION

I/We certify that all minimum well construction standards were complied with at the time the rig was removed.

Firm Name Boley & Henry Firm No. 86

Address Muntz Park, Id Date 8 Jan 1987

Signed by (Firm Official) Blaine Boley

and
 (Operator) Blaine Boley

USE ADDITIONAL SHEETS IF NECESSARY — FORWARD THE WHITE COPY TO THE DEPARTMENT

Figure C3. Banbury Hot Springs Well Driller's Log

USE TYPEWRITER OR
BALL POINT PEN

State of Idaho
Department of Water Resources

WELL DRILLER'S REPORT

State law requires that this report be filed with the Director, Department of Water Resources, within 30 days after the completion or abandonment of the well.

Location Corrected by IDWR To:

T09S R14E Sec. 4 SENW

By: segbert 2010-10-15

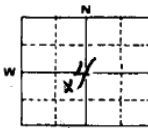
1. WELL OWNER Name: <u>DICK KASTER</u> Address: <u>HAGERMAN, IDAHO</u> Owner's Permit No. _____		7. WATER LEVEL Static water level _____ feet below land surface Flowing? <input checked="" type="checkbox"/> Yes <input type="checkbox"/> No G.P.M. flow <u>300</u> Temperature <u>104</u> ° F. Quality _____ Artesian closed-in pressure <u>58</u> p.s.i. Controlled by <input checked="" type="checkbox"/> Valve <input type="checkbox"/> Cap <input type="checkbox"/> Plug																																																																																													
2. NATURE OF WORK <input checked="" type="checkbox"/> New well <input type="checkbox"/> Deepened <input type="checkbox"/> Replacement <input type="checkbox"/> Abandoned (describe method of abandoning) _____		8. WELL TEST DATA <input type="checkbox"/> Pump <input type="checkbox"/> Bailer <input type="checkbox"/> Other <table border="1"> <thead> <tr> <th>Discharge G.P.M.</th> <th>Draw Down</th> <th>Hours Pumped</th> </tr> </thead> <tbody> <tr><td> </td><td> </td><td> </td></tr> <tr><td> </td><td> </td><td> </td></tr> <tr><td> </td><td> </td><td> </td></tr> </tbody> </table>		Discharge G.P.M.	Draw Down	Hours Pumped																																																																																									
Discharge G.P.M.	Draw Down	Hours Pumped																																																																																													
3. PROPOSED USE <input checked="" type="checkbox"/> Domestic <input type="checkbox"/> Irrigation <input type="checkbox"/> Test <input type="checkbox"/> Other (specify type) _____ <input type="checkbox"/> Municipal <input type="checkbox"/> Industrial <input type="checkbox"/> Stock <input type="checkbox"/> Waste Disposal or Injection		9. LITHOLOGIC LOG 045806 <table border="1"> <thead> <tr> <th rowspan="2">Hole Diam.</th> <th colspan="2">Depth</th> <th rowspan="2">Material</th> <th rowspan="2">Water Yes/No</th> </tr> <tr> <th>From</th> <th>To</th> </tr> </thead> <tbody> <tr><td>5"</td><td>0</td><td>10</td><td>BOULDERS</td><td>X</td></tr> <tr><td> </td><td>10</td><td>19</td><td>GREY LAVA</td><td> </td></tr> <tr><td> </td><td>19</td><td>24</td><td>CLAY</td><td> </td></tr> <tr><td> </td><td>24</td><td>26</td><td>ROCK</td><td> </td></tr> <tr><td> </td><td>26</td><td>30</td><td>CLAY</td><td> </td></tr> <tr><td> </td><td>30</td><td>32</td><td>ROCK</td><td> </td></tr> <tr><td> </td><td>32</td><td>34</td><td>CLAY</td><td> </td></tr> <tr><td> </td><td>34</td><td>38</td><td>ROCK</td><td> </td></tr> <tr><td> </td><td>38</td><td>40</td><td>CLAY</td><td> </td></tr> <tr><td> </td><td>40</td><td>60</td><td>ROCK</td><td> </td></tr> <tr><td> </td><td>60</td><td>77</td><td>WATER TALL + LAVA</td><td>X</td></tr> <tr><td> </td><td>77</td><td>81</td><td>HARD SHALE</td><td> </td></tr> <tr><td> </td><td>81</td><td>101</td><td>GREY LAVA</td><td> </td></tr> <tr><td> </td><td>101</td><td>160</td><td>SANDY + ROCK</td><td> </td></tr> <tr><td> </td><td>160</td><td>200</td><td>CLAY + HARD SHALE</td><td> </td></tr> <tr><td> </td><td>200</td><td>250</td><td>BLUE CLAY</td><td>X</td></tr> <tr><td> </td><td>250</td><td>375</td><td>BLACK LAVA + LITTLE WATER IN SPOTS</td><td>X</td></tr> </tbody> </table>		Hole Diam.	Depth		Material	Water Yes/No	From	To	5"	0	10	BOULDERS	X		10	19	GREY LAVA			19	24	CLAY			24	26	ROCK			26	30	CLAY			30	32	ROCK			32	34	CLAY			34	38	ROCK			38	40	CLAY			40	60	ROCK			60	77	WATER TALL + LAVA	X		77	81	HARD SHALE			81	101	GREY LAVA			101	160	SANDY + ROCK			160	200	CLAY + HARD SHALE			200	250	BLUE CLAY	X		250	375	BLACK LAVA + LITTLE WATER IN SPOTS	X
Hole Diam.	Depth		Material		Water Yes/No																																																																																										
	From	To																																																																																													
5"	0	10	BOULDERS	X																																																																																											
	10	19	GREY LAVA																																																																																												
	19	24	CLAY																																																																																												
	24	26	ROCK																																																																																												
	26	30	CLAY																																																																																												
	30	32	ROCK																																																																																												
	32	34	CLAY																																																																																												
	34	38	ROCK																																																																																												
	38	40	CLAY																																																																																												
	40	60	ROCK																																																																																												
	60	77	WATER TALL + LAVA	X																																																																																											
	77	81	HARD SHALE																																																																																												
	81	101	GREY LAVA																																																																																												
	101	160	SANDY + ROCK																																																																																												
	160	200	CLAY + HARD SHALE																																																																																												
	200	250	BLUE CLAY	X																																																																																											
	250	375	BLACK LAVA + LITTLE WATER IN SPOTS	X																																																																																											
4. METHOD DRILLED <input type="checkbox"/> Cable <input checked="" type="checkbox"/> Rotary <input type="checkbox"/> Dug <input type="checkbox"/> Other		10. Work started <u>10-3-75</u> finished <u>10-9-75</u>																																																																																													
5. WELL CONSTRUCTION Diameter of hole <u>8</u> inches Total depth <u>375</u> feet Casing schedule: <input checked="" type="checkbox"/> Steel <input type="checkbox"/> Concrete <table border="1"> <thead> <tr> <th>Thickness</th> <th>Diameter</th> <th>From</th> <th>To</th> </tr> </thead> <tbody> <tr> <td><u>250</u> inches</td> <td><u>8</u> inches</td> <td><u>1</u> feet</td> <td><u>28</u> feet</td> </tr> <tr><td> </td><td> </td><td> </td><td> </td></tr> <tr><td> </td><td> </td><td> </td><td> </td></tr> <tr><td> </td><td> </td><td> </td><td> </td></tr> <tr><td> </td><td> </td><td> </td><td> </td></tr> </tbody> </table> Was casing drive shoe used? <input type="checkbox"/> Yes <input type="checkbox"/> No Was a packer or seal used? <input type="checkbox"/> Yes <input type="checkbox"/> No Perforated? <input type="checkbox"/> Yes <input type="checkbox"/> No How perforated? <input type="checkbox"/> Factory <input type="checkbox"/> Knife <input type="checkbox"/> Torch Size of perforation _____ inches by _____ inches <table border="1"> <thead> <tr> <th>Number</th> <th>From</th> <th>To</th> </tr> </thead> <tbody> <tr><td> </td><td> </td><td> </td></tr> <tr><td> </td><td> </td><td> </td></tr> <tr><td> </td><td> </td><td> </td></tr> </tbody> </table> Well screen installed? <input type="checkbox"/> Yes <input type="checkbox"/> No Manufacturer's name _____ Model No. _____ Slot size _____ Set from _____ feet to _____ feet Diameter _____ Slot size _____ Set from _____ feet to _____ feet Gravel packed? <input type="checkbox"/> Yes <input type="checkbox"/> No Size of gravel _____ Placed from _____ feet to _____ feet Surface seal depth <u>28'</u> Material used in seal <input checked="" type="checkbox"/> Cement grout <input type="checkbox"/> Pudding clay <input type="checkbox"/> Well cuttings Sealing procedure used <input type="checkbox"/> Shury pit <input type="checkbox"/> Temporary surface casing <input type="checkbox"/> Overbore to seal depth		Thickness	Diameter	From	To	<u>250</u> inches	<u>8</u> inches	<u>1</u> feet	<u>28</u> feet																	Number	From	To										11. DRILLERS CERTIFICATION Firm Name <u>EISENHART DRILLING</u> Firm No. <u>31</u> Address <u>P.O. BOX 919 Tolo</u> Date <u>2/16/76</u> Signed by (Firm Official) <u>Arnold Elbing</u> and <u>Pat Gillispie</u> (Operator)																																																									
Thickness	Diameter	From	To																																																																																												
<u>250</u> inches	<u>8</u> inches	<u>1</u> feet	<u>28</u> feet																																																																																												
Number	From	To																																																																																													
6. LOCATION OF WELL Sketch map location must agree with written location. <u>47</u>  Subdivision Name _____ Lot No. <u>2000</u> Block No. _____ County <u>Twin Falls</u> NE 1/4 SW 1/4 Sec. <u>4</u> T. <u>9</u> N/S. R. <u>14</u> E/W		USE ADDITIONAL SHEETS IF NECESSARY FORWARD THE WHITE COPY TO THE DEPARTMENT																																																																																													

Figure C4. Dick Kaster Well 1 Driller's Log

IDAHO DEPARTMENT OF WATER RESOURCES WELL DRILLER'S REPORT

Use Typewriter or Ballpoint Pen


Office Use Only
Inspected by _____
Twp _____ Rge _____ Sec _____
UTATION 1/4 _____ 1/4 _____ 1/4
Lat: : : Long: : :

1. DRILLING PERMIT NO. _____
Other IDWR No. 000002000

2. OWNER:
Name _____
Address _____
City _____ State _____ Zip _____

3. LOCATION OF WELL by legal description:

Sketch map location must agree with written location.



Twp. _____ North ☐ or South ☐
 Rge. _____ East ☐ or West ☐
 Sec. _____ $\frac{1}{4}$ $\frac{1}{4}$ $\frac{1}{4}$ $\frac{1}{4}$
 Gov't Lot _____ County _____
 Lat. : : : Long. : : :
 Address of Well Site _____

City _____
(Give at least name of road + Distance to Road or Landmark)

Lt. _____ Blk. _____ Sub. Name _____

4. USE:

☐ Domestic ☐ Municipal ☐ Monitor ☐ Irrigation
☐ Thermal ☐ Injection ☐ Other _____

5. TYPE OF WORK check all that apply (Replacement etc.)

☐ New Well ☐ Modify ☐ Abandonment ☐ Other _____

6. DRILL METHOD

☐ Air Rotary ☐ Cable ☐ Mud Rotary ☐ Other _____

7. SEALING PROCEDURES

SEAL/FILTER PACK			AMOUNT	METHOD
Material	From	To	Sacks or Pounds	

Was drive shoe used? ☐ Y ☐ N Shoe Depth(s) _____
Was drive shoe seal tested? ☐ Y ☐ N How? _____

8. CASING/LINER:

Diameter	From	To	Gauge	Material	Casing	Liner	Welded	Threaded
					<input type="checkbox"/>	<input type="checkbox"/>	<input type="checkbox"/>	<input type="checkbox"/>
					<input type="checkbox"/>	<input type="checkbox"/>	<input type="checkbox"/>	<input type="checkbox"/>
					<input type="checkbox"/>	<input type="checkbox"/>	<input type="checkbox"/>	<input type="checkbox"/>

Length of Headpipe _____ Length of Tailpipe _____

9. PERFORATIONS/SCREENS

☐ Perforations Method _____

☐ Screens Screen Type _____

From	To	Slot Size	Number	Diameter	Material	Casing	Liner
						<input type="checkbox"/>	<input type="checkbox"/>
						<input type="checkbox"/>	<input type="checkbox"/>
						<input type="checkbox"/>	<input type="checkbox"/>

10. STATIC WATER LEVEL OR ARTESIAN PRESSURE:

_____ ft. below ground Artesian pressure _____ lb.
Depth flow encountered _____ ft. Describe access port or
control devices: _____

11. WELL TESTS:

☐ Pump ☐ Bailer ☐ Air ☐ Flowing Artesian

Yield gal./min.	Drawdown	Pumping Level	Time

Water Temp. _____ Bottom hole temp. _____

Water Quality test or comments: _____

Depth first Water Encountered _____

12. LITHOLOGIC LOG: (Describe repairs or abandonment)

[illegible]

13. DRILLER'S CERTIFICATION

I/We certify that all minimum well construction standards were complied with at the time the rig was removed.

Firm Name _____ Firm No. _____

Firm Official [Signature] Date _____

Supervisor or Operator _____ Date _____

(Sign once if Firm Official & Operator)

Figure C5. Dick Kaster Well 2 Driller's Log

CORRECTION
State of Idaho
Department of Water Administration

WELL DRILLER'S REPORT

State law requires that this report be filed with the Director, Department of Water Administration, within 30 days after the completion or abandonment of the well.

NOV 20 1974

RECEIVED

USE TYPEWRITER
BALL POINT PEN

1. WELL OWNER
Name SAM COLLIER
Address HAGERMAN, IDAHO
Owner's Permit No. 793028 WR 47-7279

2. NATURE OF WORK
☒ New well ☐ Deepened ☐ Replacement
☐ Abandoned (describe method of abandoning)

3. PROPOSED USE
HEAT OF HOME
☐ Domestic ☐ Irrigation ☐ Test ☒ Other (specify type)
☐ Municipal ☐ Industrial ☐ Stock ☐ Waste Disposal or Injection

4. METHOD DRILLED
☐ Cable ☒ Rotary ☐ Dug ☐ Other

5. WELL CONSTRUCTION
Diameter of hole 6 inches Total depth 300 feet
Casing schedule: ☒ Steel ☐ Concrete
Thickness 2.50 inches Diameter 6 inches From 1 feet To 52 feet
Inches inches feet feet
Inches inches feet feet
Inches inches feet feet
Inches inches feet feet
Was a packer or seal used? ☐ Yes ☐ No
Perforated? ☐ Yes ☐ No
How perforated? ☐ Factory ☐ Knife ☐ Torch
Size of perforation _____ inches by _____ inches
Number _____ From _____ To _____
_____ perforations _____ feet _____ feet
_____ perforations _____ feet _____ feet
_____ perforations _____ feet _____ feet
Well screen installed? ☐ Yes ☐ No
Manufacturer's name _____
Type _____ Model No. _____
Diameter _____ Slot size _____ Set from _____ feet to _____ feet
Diameter _____ Slot size _____ Set from _____ feet to _____ feet
Gravel packed? ☐ Yes ☐ No Size of gravel _____
Placed from _____ feet to _____ feet
Surface seal depth 51' Material used in seal ☒ Cement grout
☐ Pudding clay ☒ Well cuttings
Sealing procedure used ☐ Sherry pit ☐ Temporary surface casing
☐ Overbore to seal depth

6. LOCATION OF WELL
Sketch map location must agree with written location.
Subdivision Name _____
Lot No. _____ Block No. _____
County Twin Falls
33 Sec. 8 T. 14 N. 14 E. 36
NW SW GOVT LOT 6 ISSARY

7. WATER LEVEL
Department of Water Resources
Southern District Office
Static water level _____ feet below land surface
Flowing? ☒ Yes ☐ No G.P.M. flow 40 gpm
Temperature 86° F. Quality _____
Artesian closed-in pressure _____ p.s.i.
Controlled by ☒ Valve ☐ Cap ☐ Plug

8. WELL TEST DATA
☐ Pump ☐ Bailor ☐ Other
Discharge G.P.M. _____ Draw Down _____ Hours Pumped _____

9. LITHOLOGIC LOG
40246
Hole Diam. _____ Depth _____ Material _____ Water _____
From _____ To _____ Yes No
6 0 1 TOP SOIL X
1 16 BOULDERS
16 18 SANDSTONE
18 30 BOULDERS
30 39 GREY CLAY
39 70 RED LAVA
70 98 BLACK DIOLITE + TALC X
98 102 BROWN CLAY + BROKEN BROWN DIOLITE X
102 110 BLACK DIOLITE + WATER TALC X
110 118 GREY CLAY + BLACK DIOLITE X
118 138 GREY CLAY X
138 190 BLACK DIOLITE X
190 245 GREY CLAY X
245 255 BROKEN ROCK + RIVER SAND X
255 300 SHALE X

10. Work started 9-19-74 finished 9-24-74

11. DRILLERS CERTIFICATION
Firm Name EISINGER WELL DRILLING Firm No. 31
Address P.O. BOX 919 TWIN FALLS Date Oct 28 1974
Signed by (Firm Official) Arnold Eisinger
and Pat Gillispie
(Operator)

FORWARD THE WHITE COPY TO THE DEPARTMENT

Figure C6. Sam Collier Well Driller's Log

Well Log Form 1
7/59 - 1-64

069569

WELL LOG AND REPORT OF THE STATE RECLAMATION ENGINEER OF IDAHO

RECEIVED
AUG 23 1960

Department of Reclamation

Permit No. _____ Well No. _____ County Twin FallsOwner City of Twin FallsAddress Twin Falls, IdahoDriller Boley, Henry, Weech & Mack GrayAddress Murtaugh & Kimberly, IdahoSW SW NW 10 10S17E 18S 17E
Well location Lynwood Addition, City of Twin Falls E/WSize of drilled hole 20" to 12"

Locate well in section

NW¼	NE¼
SW¼	SE¼

Total depth of well 1530 ft.Give depth to standing water from the ground flowing water temp. 87 °Fahr.On "Pumping Test" delivery was 1000 g.p.m. or 2 c.f.s. Drawdown was 450 feet.Size of pump and motor used to make test 10" pump, 300 H.P. Diesel, 500 ft. setting.Length of time of test 15 hours _____ minutes.If flowing well, give flow _____ c.f.s. or 120 g.p.m. and of shut off pressure noIf flowing well, described control works none (TYPE AND SIZE OF VALVE, ETC.)Water will be used for Municipal Weight of casing per lineal foot _____Thickness of casing 1/2" Casing material steel (STEEL, CONCRETE, WOOD, ETC.)Diameter, length and location of casing 47 ft of 22" OD & 514 ft of 16" OD. Cemented in
at bottom. (CASING 12" IN DIAMETER OR LESS, GIVE INSIDE DIAMETER;
CASING OVER 12" IN DIAMETER, GIVE OUTSIDE DIAMETER)

CASING RECORD

Diam. Casing	From Feet	To Feet	Length	Remarks—seals, grouting, etc.
22"	0	47'	47'	Cemented
16"	0	514'	514'	12' of cement grout around the bottom.

Number and size of perforations none located _____ feet to _____ feet from groundDate of commencement of well 5/4/1959 Date of completion of well 8/1/1960

10S17E 10 SW SW NW

well

4-16-70

WELL LOG

[illegible]

WELL DRILLER'S STATEMENT

This well was drilled under my supervision and the above information is true and correct to the best of my knowledge and belief.

Signed

By _____

Dated 8/14/60, 1960.

License No. 150

Well Log Form 1
4/89 1 M

069570

SHEET NO. 2

Well Owner _____

Well Driller _____

Well Location _____

WELL LOG

From Feet	To Feet	Type of Material	Water-bearing Formation Ans. Yes or No	Casing Perforated Ans. Yes or No
0	9	Dirt and rock		
9	22	Gray lava		
22	31	Black lava		
31	56	Gray lava		
56	73	Brown clay & rocks		
73	86	Black lava		
86	93	Gray lava		
93	102	Brown clay		
102	113	Gray lava broken		
113	118	Clay		
118	140	Gray lava		
140	153	Brown lava		
153	174	Gray lava		
174	218	Brown lava		
218	258	Gray lava		
258	300	Clay & fine gravel		
300	375	Brown clay		
375	418	Gray clay		
418	458	Tan clay		
458	483	Gray clay & gravel		
483	487	Clay & rhyolite		
487	503	Brown clay		
503	579	Black rhyolite		
579	730	Gray rhyolite		
730	746	Black rhyolite		
746	758	Black rhyolite & clay		
758	775	Gray rhyolite (very hard)		

10517E



SHEET NO. 2

Well Owner

Well Driller

Well Location

WELL LOG

From Foot	To Foot	Type of Material	Water-bearing Formation Ans. Yes or No	Casing Perforated Ans. Yes or No
775	858	Brown clay & rocks		
858	876	Grey rhyolite		
876	895	Grey rhyolite (very hard)		
		The above drilled by Boley, Henry & Weech, Murtaugh, Idaho.		
		May 4, 1959 to August 4, 1959.		
		The following drilled by Mack Gray, Kimberly, Idaho.		
		April 4, 1960 to August 1, 1960.		
895	950	Hard grey basalt		
950	970	Blue shale		
970	1050	Black basalt		
1050	1120	Blue shale sticky		
1120	1140	Grey sandstone		
1140	1250	Grey shale sticky		
1250	1275	Grey basalt (very hard)		
1275	1290	Brown shale sticky		
1290	1310	White soft shale		
1310	1370	Decomposed limestone		
1370	1375	Grey sand		
1375	1400	Red rhyolite. Well started to flow at 1390'. Temp. 64°.		
1400	1510	Red rhyolite solid. Flowing 54 g.p.m. Temp. 85°.		
1510	1530	Broken loose rhyolite caving.		
		Well flowing 100 g.p.m. Water Temp. 87°.		
		Water temp. taken at bottom of well with recording thermometer gave a		
		reading of 102°. Flow increased 20 g.p.m. after testing.		

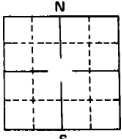
Figure C7. City of Twin Falls Well Driller's Log

Form 238-7
9/82STATE OF IDAHO
DEPARTMENT OF WATER RESOURCES
WELL DRILLER'S REPORTUSE TYPEWRITER OR
BALLPOINT PENState law requires that this report be filed with the Director, Department of Water Resources
within 30 days after the completion or abandonment of the well.

1. WELL OWNER Name <u>Twin Falls School District No. 411</u> <u>201 Main Avenue West</u> Address <u>Twin Falls, Idaho 83301</u> Owner's Permit No. <u>47-7964</u>	7. WATER LEVEL Static water level <u>0</u> feet below land surface. Flowing? <input checked="" type="checkbox"/> Yes <input type="checkbox"/> No G.P.M. flow <u>15 gpm</u> Artesian closed-in pressure <u>0</u> p.s.i. Controlled by: <input checked="" type="checkbox"/> Valve <input checked="" type="checkbox"/> Cap <input type="checkbox"/> Plug Temperature <u>96°F</u> Quality _____ <small>Describe artesian or temperature zones below</small>																																																																																																																																																																																						
2. NATURE OF WORK <input checked="" type="checkbox"/> New well <input type="checkbox"/> Deepened <input type="checkbox"/> Replacement <input type="checkbox"/> Abandoned (describe abandonment procedures such as materials, plug depths, etc. in lithologic log)	8. WELL TEST DATA <input checked="" type="checkbox"/> Pump <input type="checkbox"/> Bailer <input type="checkbox"/> Air <input type="checkbox"/> Other _____ <table border="1" style="width: 100%; border-collapse: collapse;"> <thead> <tr> <th>Discharge G.P.M.</th> <th>Pumping Level</th> <th>Hours Pumped</th> </tr> </thead> <tbody> <tr><td> </td><td> </td><td> </td></tr> <tr><td> </td><td> </td><td> </td></tr> <tr><td> </td><td> </td><td> </td></tr> </tbody> </table>	Discharge G.P.M.	Pumping Level	Hours Pumped																																																																																																																																																																																			
Discharge G.P.M.	Pumping Level	Hours Pumped																																																																																																																																																																																					
3. PROPOSED USE <input type="checkbox"/> Domestic <input type="checkbox"/> Irrigation <input type="checkbox"/> Test <input type="checkbox"/> Municipal <input type="checkbox"/> Industrial <input type="checkbox"/> Stock <input type="checkbox"/> Waste Disposal or Injection <input type="checkbox"/> Other <u>Heating</u> (specify type)	9. LITHOLOGIC LOG <u>Pg 1 of 2</u> <u>052988</u> <table border="1" style="width: 100%; border-collapse: collapse;"> <thead> <tr> <th rowspan="2">Bore Diam.</th> <th colspan="2">Depth</th> <th rowspan="2">Material</th> <th rowspan="2">Water Yes No</th> </tr> <tr> <th>From</th> <th>To</th> </tr> </thead> <tbody> <tr><td> </td><td>0</td><td>12</td><td>Top Soil</td><td> </td></tr> <tr><td> </td><td>12</td><td>48</td><td>Gray Lava</td><td> </td></tr> <tr><td> </td><td>48</td><td>53</td><td>Lava Ash</td><td> </td></tr> <tr><td> </td><td>53</td><td>130</td><td>Gray Lava</td><td> </td></tr> <tr><td> </td><td>130</td><td>137</td><td>Red Lava</td><td> </td></tr> <tr><td> </td><td>137</td><td>165</td><td>Brown Lava</td><td> </td></tr> <tr><td> </td><td>165</td><td>170</td><td>Red Lava</td><td> </td></tr> <tr><td> </td><td>170</td><td>238</td><td>Gray Lava</td><td> </td></tr> <tr><td> </td><td>238</td><td>258</td><td>Brown Lava</td><td> </td></tr> <tr><td> </td><td>258</td><td>263</td><td>Brown Lava</td><td> </td></tr> <tr><td> </td><td>263</td><td>274</td><td>Brown Rhyolite</td><td> </td></tr> <tr><td> </td><td>274</td><td>315</td><td>Gray Rhyolite</td><td> </td></tr> <tr><td> </td><td>315</td><td>438</td><td>Gray Rhyolite</td><td> </td></tr> <tr><td> </td><td>438</td><td>458</td><td>Softer Gr. Rhyolite More Water</td><td> </td></tr> <tr><td> </td><td>458</td><td>471</td><td>Red & Gray Broken Rhy.-Water</td><td> </td></tr> <tr><td> </td><td>471</td><td>518</td><td>" " " Lots of water</td><td> </td></tr> <tr><td> </td><td>518</td><td>528</td><td>Brown Rhyolite</td><td> </td></tr> <tr><td> </td><td>528</td><td>531</td><td>Broken Gray Rhy. Water</td><td> </td></tr> <tr><td> </td><td>531</td><td>557</td><td>Hard Gray Rhyolite</td><td> </td></tr> <tr><td> </td><td>557</td><td>583</td><td>Broken Softer Red Rhyolite</td><td> </td></tr> <tr><td> </td><td>583</td><td>587</td><td>Solid Gray Rhyolite</td><td> </td></tr> <tr><td> </td><td>587</td><td>606</td><td>Very Hard Gray Rhyolite</td><td> </td></tr> <tr><td> </td><td>606</td><td>612</td><td>Brown Broken Rhy. - water</td><td> </td></tr> <tr><td> </td><td>612</td><td>625</td><td>Solid Gray Rhyolite</td><td> </td></tr> <tr><td> </td><td>625</td><td>638</td><td>Broken Gray Rhy. More Water</td><td> </td></tr> <tr><td> </td><td>638</td><td>698</td><td>Hard Gray Rhyolite</td><td> </td></tr> <tr><td> </td><td>698</td><td>714</td><td>Gray Shale Some Black Rock More Water</td><td> </td></tr> <tr><td> </td><td>714</td><td>797</td><td>Black Rhy. Broken - Water</td><td> </td></tr> <tr><td> </td><td>797</td><td>803</td><td>Broken Brown Rock</td><td> </td></tr> <tr><td> </td><td>803</td><td>809</td><td>Brown Clay</td><td> </td></tr> <tr><td> </td><td>809</td><td>842</td><td>Green Clay & Shale</td><td> </td></tr> <tr><td> </td><td>842</td><td>870</td><td>Broken Black Rock</td><td> </td></tr> <tr><td> </td><td>870</td><td>879</td><td>Soft Red Rhyolite</td><td> </td></tr> <tr><td> </td><td>879</td><td>910</td><td>Medium Black Rock</td><td> </td></tr> <tr><td> </td><td>910</td><td>926</td><td>Hard Black Rock</td><td> </td></tr> </tbody> </table>	Bore Diam.	Depth		Material	Water Yes No	From	To		0	12	Top Soil			12	48	Gray Lava			48	53	Lava Ash			53	130	Gray Lava			130	137	Red Lava			137	165	Brown Lava			165	170	Red Lava			170	238	Gray Lava			238	258	Brown Lava			258	263	Brown Lava			263	274	Brown Rhyolite			274	315	Gray Rhyolite			315	438	Gray Rhyolite			438	458	Softer Gr. Rhyolite More Water			458	471	Red & Gray Broken Rhy.-Water			471	518	" " " Lots of water			518	528	Brown Rhyolite			528	531	Broken Gray Rhy. Water			531	557	Hard Gray Rhyolite			557	583	Broken Softer Red Rhyolite			583	587	Solid Gray Rhyolite			587	606	Very Hard Gray Rhyolite			606	612	Brown Broken Rhy. - water			612	625	Solid Gray Rhyolite			625	638	Broken Gray Rhy. More Water			638	698	Hard Gray Rhyolite			698	714	Gray Shale Some Black Rock More Water			714	797	Black Rhy. Broken - Water			797	803	Broken Brown Rock			803	809	Brown Clay			809	842	Green Clay & Shale			842	870	Broken Black Rock			870	879	Soft Red Rhyolite			879	910	Medium Black Rock			910	926	Hard Black Rock	
Bore Diam.	Depth		Material	Water Yes No																																																																																																																																																																																			
	From	To																																																																																																																																																																																					
	0	12	Top Soil																																																																																																																																																																																				
	12	48	Gray Lava																																																																																																																																																																																				
	48	53	Lava Ash																																																																																																																																																																																				
	53	130	Gray Lava																																																																																																																																																																																				
	130	137	Red Lava																																																																																																																																																																																				
	137	165	Brown Lava																																																																																																																																																																																				
	165	170	Red Lava																																																																																																																																																																																				
	170	238	Gray Lava																																																																																																																																																																																				
	238	258	Brown Lava																																																																																																																																																																																				
	258	263	Brown Lava																																																																																																																																																																																				
	263	274	Brown Rhyolite																																																																																																																																																																																				
	274	315	Gray Rhyolite																																																																																																																																																																																				
	315	438	Gray Rhyolite																																																																																																																																																																																				
	438	458	Softer Gr. Rhyolite More Water																																																																																																																																																																																				
	458	471	Red & Gray Broken Rhy.-Water																																																																																																																																																																																				
	471	518	" " " Lots of water																																																																																																																																																																																				
	518	528	Brown Rhyolite																																																																																																																																																																																				
	528	531	Broken Gray Rhy. Water																																																																																																																																																																																				
	531	557	Hard Gray Rhyolite																																																																																																																																																																																				
	557	583	Broken Softer Red Rhyolite																																																																																																																																																																																				
	583	587	Solid Gray Rhyolite																																																																																																																																																																																				
	587	606	Very Hard Gray Rhyolite																																																																																																																																																																																				
	606	612	Brown Broken Rhy. - water																																																																																																																																																																																				
	612	625	Solid Gray Rhyolite																																																																																																																																																																																				
	625	638	Broken Gray Rhy. More Water																																																																																																																																																																																				
	638	698	Hard Gray Rhyolite																																																																																																																																																																																				
	698	714	Gray Shale Some Black Rock More Water																																																																																																																																																																																				
	714	797	Black Rhy. Broken - Water																																																																																																																																																																																				
	797	803	Broken Brown Rock																																																																																																																																																																																				
	803	809	Brown Clay																																																																																																																																																																																				
	809	842	Green Clay & Shale																																																																																																																																																																																				
	842	870	Broken Black Rock																																																																																																																																																																																				
	870	879	Soft Red Rhyolite																																																																																																																																																																																				
	879	910	Medium Black Rock																																																																																																																																																																																				
	910	926	Hard Black Rock																																																																																																																																																																																				
4. METHOD DRILLED <input checked="" type="checkbox"/> Rotary <input checked="" type="checkbox"/> Air <input type="checkbox"/> Hydraulic <input type="checkbox"/> Reverse rotary <input type="checkbox"/> Cable <input type="checkbox"/> Dug <input type="checkbox"/> Other _____	10. (See Page 2) Work started <u>Aug. 15, 1984</u> finished <u>Sept. 1984</u>																																																																																																																																																																																						
5. WELL CONSTRUCTION Casing schedule: <input checked="" type="checkbox"/> Steel <input type="checkbox"/> Concrete <input type="checkbox"/> Other _____ <table border="1" style="width: 100%; border-collapse: collapse;"> <thead> <tr> <th>Thickness</th> <th>Diameter</th> <th>From</th> <th>To</th> </tr> </thead> <tbody> <tr> <td>16 inches</td> <td>.250 inches</td> <td>1 feet</td> <td>23 feet</td> </tr> <tr> <td>.250 inches</td> <td>12 inches</td> <td>2 feet</td> <td>900 feet</td> </tr> <tr> <td> </td><td> </td><td> </td><td> </td></tr> <tr> <td> </td><td> </td><td> </td><td> </td></tr> <tr> <td> </td><td> </td><td> </td><td> </td></tr> </tbody> </table> Was casing drive shoe used? <input checked="" type="checkbox"/> Yes <input type="checkbox"/> No Was a packer or seal used? <input type="checkbox"/> Yes <input type="checkbox"/> No Perforated? <input type="checkbox"/> Yes <input type="checkbox"/> No How perforated? <input type="checkbox"/> Factory <input type="checkbox"/> Knife <input type="checkbox"/> Torch Size of perforation _____ inches by _____ inches <table border="1" style="width: 100%; border-collapse: collapse;"> <thead> <tr> <th>Number</th> <th>From</th> <th>To</th> </tr> </thead> <tbody> <tr> <td> </td><td> </td><td> </td></tr> <tr> <td> </td><td> </td><td> </td></tr> <tr> <td> </td><td> </td><td> </td></tr> </tbody> </table> Well screen installed? <input type="checkbox"/> Yes <input checked="" type="checkbox"/> No Manufacturer's name _____ Type _____ Model No. _____ Diameter _____ Slot size _____ Set from _____ feet to _____ feet Diameter _____ Slot size _____ Set from _____ feet to _____ feet Gravel packed? <input type="checkbox"/> Yes <input type="checkbox"/> No <input type="checkbox"/> Size of gravel _____ Placed from _____ feet to _____ feet Surface seal depth <u>900</u> Material used in seal: <input checked="" type="checkbox"/> Cement grout <input type="checkbox"/> Bentonite <input type="checkbox"/> Puddling clay <input type="checkbox"/> _____ Sealing procedure used: <input type="checkbox"/> Slurry pit <input type="checkbox"/> Temp. surface casing <input checked="" type="checkbox"/> Overbore to seal depth Method of joining casing: <input type="checkbox"/> Threaded <input checked="" type="checkbox"/> Welded <input type="checkbox"/> Solvent Weld Describe access port <input checked="" type="checkbox"/> Cemented between strata <input type="checkbox"/> Valve	Thickness	Diameter	From	To	16 inches	.250 inches	1 feet	23 feet	.250 inches	12 inches	2 feet	900 feet													Number	From	To										11. DRILLERS CERTIFICATION <u>22</u> I/We certify that all minimum well construction standards were complied with at the time the rig was removed. Firm Name <u>Elsing Drilling</u> Firm No. <u>31</u> <u>Box 919</u> Address <u>Twin Falls, ID</u> Date <u>Nov. 6, 1984</u> Signed by (Firm Official) <u>Arnold Elsing</u> and _____ (Operator) <u>Lloyd Elsing</u>																																																																																																																																																		
Thickness	Diameter	From	To																																																																																																																																																																																				
16 inches	.250 inches	1 feet	23 feet																																																																																																																																																																																				
.250 inches	12 inches	2 feet	900 feet																																																																																																																																																																																				
Number	From	To																																																																																																																																																																																					
6. LOCATION OF WELL Sketch map location must agree with written location. <table border="1" style="width: 100%; border-collapse: collapse;"> <tr> <td style="text-align: center;">N</td> <td colspan="2" style="text-align: center;">Subdivision Name _____</td> </tr> <tr> <td style="text-align: center;">W</td> <td style="text-align: center;"> </td> <td style="text-align: center;">E</td> </tr> <tr> <td style="text-align: center;">S</td> <td colspan="2" style="text-align: center;">Lot No. _____ Block No. _____</td> </tr> </table> County <u>Twin Falls</u> <u>SE</u> 1/4 <u>NW</u> 1/4 Sec. <u>10</u> , T. <u>10</u> N. R. <u>17</u> E. W.	N	Subdivision Name _____		W		E	S	Lot No. _____ Block No. _____		10. (See Page 2) Work started <u>Aug. 15, 1984</u> finished <u>Sept. 1984</u>																																																																																																																																																																													
N	Subdivision Name _____																																																																																																																																																																																						
W		E																																																																																																																																																																																					
S	Lot No. _____ Block No. _____																																																																																																																																																																																						

USE ADDITIONAL SHEETS IF NECESSARY - FORWARD THE WHITE COPY TO THE DEPARTMENT

Form 238-7
9/82STATE OF IDAHO
DEPARTMENT OF WATER RESOURCESUSE TYPEWRITER OR
BALLPOINT PEN**WELL DRILLER'S REPORT**State law requires that this report be filed with the Director, Department of Water Resources
within 30 days after the completion or abandonment of the well.

1. WELL OWNER Name <u>Twin Falls School District No. 411</u> Address <u>201 Main Ave. West</u> <u>Twin Falls, Idaho 83301</u> Owner's Permit No. _____	7. WATER LEVEL Static water level _____ feet below land surface. Flowing? <input type="checkbox"/> Yes <input type="checkbox"/> No G.P.M. flow _____ Artesian closed-in pressure _____ p.s.i. Controlled by: <input type="checkbox"/> Valve <input type="checkbox"/> Cap <input type="checkbox"/> Plug Temperature _____ °F. Quality _____ <i>Describe artesian or temperature zones below.</i>																																																																											
2. NATURE OF WORK <input type="checkbox"/> New well <input type="checkbox"/> Deepened <input type="checkbox"/> Replacement <input type="checkbox"/> Abandoned (describe abandonment procedures such as materials, plug depths, etc. in lithologic log)	8. WELL TEST DATA <input type="checkbox"/> Pump <input type="checkbox"/> Bailer <input type="checkbox"/> Air <input type="checkbox"/> Other _____ <table border="1" style="width: 100%; border-collapse: collapse;"> <tr> <th>Discharge G.P.M.</th> <th>Pumping Level</th> <th>Hours Pumped</th> </tr> <tr><td> </td><td> </td><td> </td></tr> <tr><td> </td><td> </td><td> </td></tr> <tr><td> </td><td> </td><td> </td></tr> </table>	Discharge G.P.M.	Pumping Level	Hours Pumped																																																																								
Discharge G.P.M.	Pumping Level	Hours Pumped																																																																										
3. PROPOSED USE <input type="checkbox"/> Domestic <input type="checkbox"/> Irrigation <input type="checkbox"/> Test <input type="checkbox"/> Municipal <input type="checkbox"/> Industrial <input type="checkbox"/> Stock <input type="checkbox"/> Waste Disposal or Injection <input type="checkbox"/> Other _____ (specify type)	9. LITHOLOGIC LOG Page 2 of 2 <table border="1" style="width: 100%; border-collapse: collapse;"> <thead> <tr> <th>Bore Diam.</th> <th>Depth From</th> <th>Depth To</th> <th>Material</th> <th>Water Yes No</th> </tr> </thead> <tbody> <tr><td> </td><td>926</td><td>932</td><td>Soft Brown Rock</td><td> </td></tr> <tr><td> </td><td>932</td><td>991</td><td>Hard Black Rock</td><td> </td></tr> <tr><td> </td><td>991</td><td>1055</td><td>Soft Brown Sandstone</td><td> </td></tr> <tr><td> </td><td>1055</td><td>1085</td><td>Gray Decomposed Rhyolite</td><td> </td></tr> <tr><td> </td><td> </td><td> </td><td>Hit 81° F Water</td><td> </td></tr> <tr><td> </td><td>1085</td><td>1121</td><td>Gray Decomposed Rhyolite</td><td> </td></tr> <tr><td> </td><td>1121</td><td>1246</td><td>Red Rhyolite</td><td> </td></tr> <tr><td> </td><td>1246</td><td>1284</td><td>Broken Red Rhyolite 89° F</td><td> </td></tr> <tr><td> </td><td>1284</td><td>1408</td><td>Solid Brown Rhyolite</td><td> </td></tr> <tr><td> </td><td>1408</td><td>1416</td><td>Red Rhyolite</td><td> </td></tr> <tr><td> </td><td>1416</td><td>1420</td><td>Broken Green & Pink Rhyolite</td><td> </td></tr> <tr><td> </td><td> </td><td> </td><td>Some Water</td><td> </td></tr> <tr><td> </td><td>1420</td><td>1505</td><td>Solid Brown Rhyolite</td><td> </td></tr> <tr><td> </td><td>1505</td><td>1700</td><td>Gray Rhyolite</td><td> </td></tr> </tbody> </table>	Bore Diam.	Depth From	Depth To	Material	Water Yes No		926	932	Soft Brown Rock			932	991	Hard Black Rock			991	1055	Soft Brown Sandstone			1055	1085	Gray Decomposed Rhyolite					Hit 81° F Water			1085	1121	Gray Decomposed Rhyolite			1121	1246	Red Rhyolite			1246	1284	Broken Red Rhyolite 89° F			1284	1408	Solid Brown Rhyolite			1408	1416	Red Rhyolite			1416	1420	Broken Green & Pink Rhyolite					Some Water			1420	1505	Solid Brown Rhyolite			1505	1700	Gray Rhyolite	
Bore Diam.	Depth From	Depth To	Material	Water Yes No																																																																								
	926	932	Soft Brown Rock																																																																									
	932	991	Hard Black Rock																																																																									
	991	1055	Soft Brown Sandstone																																																																									
	1055	1085	Gray Decomposed Rhyolite																																																																									
			Hit 81° F Water																																																																									
	1085	1121	Gray Decomposed Rhyolite																																																																									
	1121	1246	Red Rhyolite																																																																									
	1246	1284	Broken Red Rhyolite 89° F																																																																									
	1284	1408	Solid Brown Rhyolite																																																																									
	1408	1416	Red Rhyolite																																																																									
	1416	1420	Broken Green & Pink Rhyolite																																																																									
			Some Water																																																																									
	1420	1505	Solid Brown Rhyolite																																																																									
	1505	1700	Gray Rhyolite																																																																									
4. METHOD DRILLED <input type="checkbox"/> Rotary <input type="checkbox"/> Air <input type="checkbox"/> Hydraulic <input type="checkbox"/> Reverse rotary <input type="checkbox"/> Cable <input type="checkbox"/> Dug <input type="checkbox"/> Other _____	<div style="text-align: center; font-size: 1.5em; font-weight: bold;">RECEIVED</div> <div style="text-align: center;">JAN 8 1985</div> <div style="text-align: center; font-size: 1.5em; font-weight: bold;">RECEIVED</div> <div style="text-align: center;">JAN 21 1985</div> <div style="text-align: center; font-size: 1.5em; font-weight: bold;">MICROFILMED</div> <div style="text-align: center; font-size: 0.8em;">Department of Water Resources Twin Falls District Office</div>																																																																											
5. WELL CONSTRUCTION Casing schedule: <input type="checkbox"/> Steel <input type="checkbox"/> Concrete <input type="checkbox"/> Other _____ <table border="1" style="width: 100%; border-collapse: collapse;"> <thead> <tr> <th>Thickness</th> <th>Diameter</th> <th>From</th> <th>To</th> </tr> </thead> <tbody> <tr><td>_____ inches</td><td>_____ inches</td><td>_____ feet</td><td>_____ feet</td></tr> <tr><td>_____ inches</td><td>_____ inches</td><td>_____ feet</td><td>_____ feet</td></tr> <tr><td>_____ inches</td><td>_____ inches</td><td>_____ feet</td><td>_____ feet</td></tr> <tr><td>_____ inches</td><td>_____ inches</td><td>_____ feet</td><td>_____ feet</td></tr> </tbody> </table> Was casing drive shoe used? <input type="checkbox"/> Yes <input type="checkbox"/> No Was a packer or seal used? <input type="checkbox"/> Yes <input type="checkbox"/> No Perforated? <input type="checkbox"/> Yes <input type="checkbox"/> No How perforated? <input type="checkbox"/> Factory <input type="checkbox"/> Knife <input type="checkbox"/> Torch Size of perforation _____ inches by _____ inches <table border="1" style="width: 100%; border-collapse: collapse;"> <thead> <tr> <th>Number</th> <th>From</th> <th>To</th> </tr> </thead> <tbody> <tr><td>_____ perforations</td><td>_____ feet</td><td>_____ feet</td></tr> <tr><td>_____ perforations</td><td>_____ feet</td><td>_____ feet</td></tr> <tr><td>_____ perforations</td><td>_____ feet</td><td>_____ feet</td></tr> </tbody> </table> Well screen installed? <input type="checkbox"/> Yes <input type="checkbox"/> No Manufacturer's name _____ Type _____ Model No. _____ Diameter _____ Slot size _____ Set from _____ feet to _____ feet Diameter _____ Slot size _____ Set from _____ feet to _____ feet Gravel packed? <input type="checkbox"/> Yes <input type="checkbox"/> No <input type="checkbox"/> Size of gravel _____ Placed from _____ feet to _____ feet Surface seal depth _____ Material used in seal: <input type="checkbox"/> Cement grout <input type="checkbox"/> Bentonite <input type="checkbox"/> Pudding clay <input type="checkbox"/> _____ Sealing procedure used: <input type="checkbox"/> Slurry pit <input type="checkbox"/> Temp. surface casing <input type="checkbox"/> Overbore to seal depth Method of joining casing: <input type="checkbox"/> Threaded <input type="checkbox"/> Welded <input type="checkbox"/> Solvent Weld <input type="checkbox"/> Cemented between strata Describe access port _____	Thickness	Diameter	From	To	_____ inches	_____ inches	_____ feet	_____ feet	_____ inches	_____ inches	_____ feet	_____ feet	_____ inches	_____ inches	_____ feet	_____ feet	_____ inches	_____ inches	_____ feet	_____ feet	Number	From	To	_____ perforations	_____ feet	_____ feet	_____ perforations	_____ feet	_____ feet	_____ perforations	_____ feet	_____ feet	10. Work started _____ finished <u>9/26/84</u>																																											
Thickness	Diameter	From	To																																																																									
_____ inches	_____ inches	_____ feet	_____ feet																																																																									
_____ inches	_____ inches	_____ feet	_____ feet																																																																									
_____ inches	_____ inches	_____ feet	_____ feet																																																																									
_____ inches	_____ inches	_____ feet	_____ feet																																																																									
Number	From	To																																																																										
_____ perforations	_____ feet	_____ feet																																																																										
_____ perforations	_____ feet	_____ feet																																																																										
_____ perforations	_____ feet	_____ feet																																																																										
6. LOCATION OF WELL Sketch map location must agree with written location. <div style="text-align: center;">  </div> Subdivision Name _____ Lot No. _____ Block No. _____ County <u>SE 1/4 NW 1/4 Sec. 10, T. 10 N. R. 17 E.</u>	11. DRILLERS CERTIFICATION I/We certify that all minimum well construction standards were complied with at the time the rig was removed. Firm Name <u>Eising Dr.</u> Firm No. <u>31</u> Address _____ Date _____ Signed by (Firm Official) _____ and (Operator) <u>L.</u>																																																																											

USE ADDITIONAL SHEETS IF NECESSARY — FORWARD THE WHITE COPY TO THE DEPARTMENT

Figure C8. Twin Falls High School Well Driller's Log

Form 238-7
1/78

RECEIVED

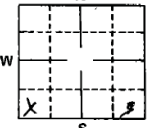
STATE OF IDAHO
DEPARTMENT OF WATER RESOURCESUSE TYPEWRITER OR
BALLPOINT PEN

WELL DRILLER'S REPORT

JUL 25 1983

State law requires that this report be filed with the Director, Department of Water Resources
Department of Water Resources 30 days after the completion or abandonment of the well.

RECEIVED

1. WELL OWNER Name <u>Mike Archibald</u> Address <u>Rt. 3 Buhl, Idaho</u> Owner's Permit No. <u>47-7577</u>	7. WATER LEVEL Static water level _____ feet below ground surface Flowing? <input checked="" type="checkbox"/> Yes <input type="checkbox"/> No G.P.M. flow _____ Artesian closed-in pressure <u>55</u> p.s.i. Controlled by: <input checked="" type="checkbox"/> Valve <input type="checkbox"/> Cap <input type="checkbox"/> Plug Temperature <u>113</u> °F. Quality <u>very good</u>																																																																																																																																																																																																												
2. NATURE OF WORK <input checked="" type="checkbox"/> New well <input type="checkbox"/> Deepened <input type="checkbox"/> Replacement <input type="checkbox"/> Abandoned (describe method of abandoning) _____	8. WELL TEST DATA <input type="checkbox"/> Pump <input type="checkbox"/> Bailor <input type="checkbox"/> Air <input type="checkbox"/> Other _____ <table border="1"> <thead> <tr> <th>Discharge G.P.M.</th> <th>Pumping Level</th> <th>Hours Pumped</th> </tr> </thead> <tbody> <tr> <td><u>27</u></td> <td><u>12</u></td> <td></td> </tr> </tbody> </table>	Discharge G.P.M.	Pumping Level	Hours Pumped	<u>27</u>	<u>12</u>																																																																																																																																																																																																							
Discharge G.P.M.	Pumping Level	Hours Pumped																																																																																																																																																																																																											
<u>27</u>	<u>12</u>																																																																																																																																																																																																												
3. PROPOSED USE <input type="checkbox"/> Domestic <input type="checkbox"/> Irrigation <input type="checkbox"/> Test <input type="checkbox"/> Municipal <input type="checkbox"/> Industrial <input type="checkbox"/> Stock <input type="checkbox"/> Waste Disposal or Injection <input checked="" type="checkbox"/> Other <u>Geothermal</u> (specify type) _____	9. LITHOLOGIC LOG <u>88526</u>																																																																																																																																																																																																												
4. METHOD DRILLED <input type="checkbox"/> Rotary <input type="checkbox"/> Air <input type="checkbox"/> Hydraulic <input type="checkbox"/> Reverse rotary <input checked="" type="checkbox"/> Cable <input type="checkbox"/> Dug <input type="checkbox"/> Other _____	<table border="1"> <thead> <tr> <th>Hole Diam.</th> <th>Depth From</th> <th>To</th> <th>Material</th> <th>Water Yes</th> <th>No</th> </tr> </thead> <tbody> <tr><td>12</td><td>0</td><td>8</td><td>Brown clay</td><td></td><td>X</td></tr> <tr><td></td><td>8</td><td>35</td><td>Brown sand</td><td>X</td><td></td></tr> <tr><td></td><td>35</td><td>48</td><td>Grey basalt</td><td></td><td>X</td></tr> <tr><td></td><td>48</td><td>67</td><td>Grey-brown clay</td><td></td><td></td></tr> <tr><td></td><td>67</td><td>72</td><td>Grey basalt</td><td></td><td></td></tr> <tr><td></td><td>72</td><td>92</td><td>Brown clay</td><td></td><td></td></tr> <tr><td>8</td><td>92</td><td>137</td><td>Grey basalt</td><td></td><td></td></tr> <tr><td>"</td><td>137</td><td>142</td><td>Brown basalt</td><td></td><td></td></tr> <tr><td>"</td><td>142</td><td>168</td><td>Grey basalt</td><td></td><td></td></tr> <tr><td>"</td><td>168</td><td>175</td><td>Dark xxx brown clay</td><td></td><td></td></tr> <tr><td></td><td>175</td><td>209</td><td>Grey basalt</td><td></td><td></td></tr> <tr><td></td><td>209</td><td>213</td><td>Brown clay & brn basalt</td><td></td><td></td></tr> <tr><td></td><td>213</td><td>219</td><td>Brown basalt</td><td></td><td></td></tr> <tr><td></td><td>219</td><td>253</td><td>Brown basalt</td><td></td><td></td></tr> <tr><td></td><td>253</td><td>257</td><td>Green clay</td><td></td><td></td></tr> <tr><td></td><td>257</td><td>270</td><td>Tan clay w/thin layers of basalt</td><td></td><td></td></tr> <tr><td>6</td><td>270</td><td>306</td><td>Tan clay w/shale layers</td><td></td><td></td></tr> <tr><td></td><td>306</td><td>327</td><td>Hard grey shale</td><td>X</td><td></td></tr> <tr><td></td><td>327</td><td>352</td><td>Grey-brn clay w/shale in layers</td><td>X</td><td></td></tr> <tr><td></td><td>352</td><td>378</td><td>Grey-brown shale w/clay in 1-2' layers</td><td></td><td>X</td></tr> <tr><td></td><td>378</td><td>409</td><td>Grey clay</td><td></td><td></td></tr> <tr><td></td><td>409</td><td>416</td><td>Light tan clay</td><td></td><td></td></tr> <tr><td></td><td>416</td><td>420</td><td>Dark green shale</td><td></td><td></td></tr> <tr><td></td><td>420</td><td>441</td><td>Light green clay</td><td></td><td></td></tr> <tr><td></td><td>441</td><td>450</td><td>Grey-brn shale</td><td></td><td></td></tr> <tr><td></td><td>450</td><td>470</td><td>Grey shale</td><td></td><td></td></tr> <tr><td></td><td>470</td><td>487</td><td>Dark grey shale</td><td></td><td></td></tr> <tr><td></td><td>487</td><td>507</td><td>Light grey shale</td><td></td><td></td></tr> <tr><td></td><td>507</td><td>510</td><td>Black rhyolite</td><td>X</td><td></td></tr> <tr><td></td><td>510</td><td>556</td><td>Brown rhyolite</td><td></td><td></td></tr> <tr><td></td><td>556</td><td>578</td><td>Black rhyolite</td><td></td><td></td></tr> <tr><td></td><td>578</td><td>584</td><td>Grey shale</td><td></td><td></td></tr> <tr><td></td><td>584</td><td>632</td><td>Black rhyolite</td><td></td><td></td></tr> </tbody> </table>	Hole Diam.	Depth From	To	Material	Water Yes	No	12	0	8	Brown clay		X		8	35	Brown sand	X			35	48	Grey basalt		X		48	67	Grey-brown clay				67	72	Grey basalt				72	92	Brown clay			8	92	137	Grey basalt			"	137	142	Brown basalt			"	142	168	Grey basalt			"	168	175	Dark xxx brown clay				175	209	Grey basalt				209	213	Brown clay & brn basalt				213	219	Brown basalt				219	253	Brown basalt				253	257	Green clay				257	270	Tan clay w/thin layers of basalt			6	270	306	Tan clay w/shale layers				306	327	Hard grey shale	X			327	352	Grey-brn clay w/shale in layers	X			352	378	Grey-brown shale w/clay in 1-2' layers		X		378	409	Grey clay				409	416	Light tan clay				416	420	Dark green shale				420	441	Light green clay				441	450	Grey-brn shale				450	470	Grey shale				470	487	Dark grey shale				487	507	Light grey shale				507	510	Black rhyolite	X			510	556	Brown rhyolite				556	578	Black rhyolite				578	584	Grey shale				584	632	Black rhyolite		
Hole Diam.	Depth From	To	Material	Water Yes	No																																																																																																																																																																																																								
12	0	8	Brown clay		X																																																																																																																																																																																																								
	8	35	Brown sand	X																																																																																																																																																																																																									
	35	48	Grey basalt		X																																																																																																																																																																																																								
	48	67	Grey-brown clay																																																																																																																																																																																																										
	67	72	Grey basalt																																																																																																																																																																																																										
	72	92	Brown clay																																																																																																																																																																																																										
8	92	137	Grey basalt																																																																																																																																																																																																										
"	137	142	Brown basalt																																																																																																																																																																																																										
"	142	168	Grey basalt																																																																																																																																																																																																										
"	168	175	Dark xxx brown clay																																																																																																																																																																																																										
	175	209	Grey basalt																																																																																																																																																																																																										
	209	213	Brown clay & brn basalt																																																																																																																																																																																																										
	213	219	Brown basalt																																																																																																																																																																																																										
	219	253	Brown basalt																																																																																																																																																																																																										
	253	257	Green clay																																																																																																																																																																																																										
	257	270	Tan clay w/thin layers of basalt																																																																																																																																																																																																										
6	270	306	Tan clay w/shale layers																																																																																																																																																																																																										
	306	327	Hard grey shale	X																																																																																																																																																																																																									
	327	352	Grey-brn clay w/shale in layers	X																																																																																																																																																																																																									
	352	378	Grey-brown shale w/clay in 1-2' layers		X																																																																																																																																																																																																								
	378	409	Grey clay																																																																																																																																																																																																										
	409	416	Light tan clay																																																																																																																																																																																																										
	416	420	Dark green shale																																																																																																																																																																																																										
	420	441	Light green clay																																																																																																																																																																																																										
	441	450	Grey-brn shale																																																																																																																																																																																																										
	450	470	Grey shale																																																																																																																																																																																																										
	470	487	Dark grey shale																																																																																																																																																																																																										
	487	507	Light grey shale																																																																																																																																																																																																										
	507	510	Black rhyolite	X																																																																																																																																																																																																									
	510	556	Brown rhyolite																																																																																																																																																																																																										
	556	578	Black rhyolite																																																																																																																																																																																																										
	578	584	Grey shale																																																																																																																																																																																																										
	584	632	Black rhyolite																																																																																																																																																																																																										
5. WELL CONSTRUCTION Casing schedule: <input checked="" type="checkbox"/> Steel <input type="checkbox"/> Concrete <input type="checkbox"/> Other _____ <table border="1"> <thead> <tr> <th>Thickness</th> <th>Diameter</th> <th>From</th> <th>To</th> <th>feet</th> </tr> </thead> <tbody> <tr><td><u>.250</u> inches</td><td><u>12</u> inches</td><td><u>1</u> feet</td><td><u>119</u> feet</td><td></td></tr> <tr><td><u>.250</u> inches</td><td><u>8</u> inches</td><td><u>12</u> feet</td><td><u>278</u> feet</td><td></td></tr> <tr><td><u>.188</u> inches</td><td><u>6</u> inches</td><td><u>185</u> feet</td><td><u>470</u> feet</td><td></td></tr> </tbody> </table> Was casing drive shoe used? <input checked="" type="checkbox"/> Yes <input type="checkbox"/> No Was a packer or seal used? <input type="checkbox"/> Yes <input checked="" type="checkbox"/> No Perforated? <input type="checkbox"/> Yes <input checked="" type="checkbox"/> No How perforated? <input type="checkbox"/> Factory <input type="checkbox"/> Knife <input type="checkbox"/> Torch Size of perforation _____ inches by _____ inches Number _____ perforations _____ feet _____ feet _____ perforations _____ feet _____ feet _____ perforations _____ feet _____ feet Well screen installed? <input type="checkbox"/> Yes <input checked="" type="checkbox"/> No Manufacturer's name _____ Type _____ Model No. _____ Diameter _____ Slot size _____ Set from _____ feet to _____ feet Diameter _____ Slot size _____ Set from _____ feet to _____ feet Gravel packed? <input type="checkbox"/> Yes <input checked="" type="checkbox"/> No <input type="checkbox"/> Size of gravel _____ Placed from _____ feet to _____ feet Surface seal depth <u>35'</u> Material used in seal: <input type="checkbox"/> Cement grout <input checked="" type="checkbox"/> Puddling clay <input type="checkbox"/> Well cuttings Sealing procedure used: <input type="checkbox"/> Slurry pit <input checked="" type="checkbox"/> Temp. surface casing <input checked="" type="checkbox"/> Overbore to seal depth Method of joining casing: <input type="checkbox"/> Threaded <input checked="" type="checkbox"/> Welded <input type="checkbox"/> Solvent Weld <input type="checkbox"/> Cemented between strata Describe access port <u>flowing well</u>	Thickness	Diameter	From	To	feet	<u>.250</u> inches	<u>12</u> inches	<u>1</u> feet	<u>119</u> feet		<u>.250</u> inches	<u>8</u> inches	<u>12</u> feet	<u>278</u> feet		<u>.188</u> inches	<u>6</u> inches	<u>185</u> feet	<u>470</u> feet		10. Work started <u>1 May 1983</u> finished <u>1 July 1983</u>																																																																																																																																																																																								
Thickness	Diameter	From	To	feet																																																																																																																																																																																																									
<u>.250</u> inches	<u>12</u> inches	<u>1</u> feet	<u>119</u> feet																																																																																																																																																																																																										
<u>.250</u> inches	<u>8</u> inches	<u>12</u> feet	<u>278</u> feet																																																																																																																																																																																																										
<u>.188</u> inches	<u>6</u> inches	<u>185</u> feet	<u>470</u> feet																																																																																																																																																																																																										
6. LOCATION OF WELL Sketch map location must agree with written location.  Subdivision Name _____ Lot No. <u>7</u> Block No. _____ County <u>Twin Falls</u> <u>SW</u> 1/4 <u>SW</u> 1/4 Sec. <u>33</u> , T. <u>8</u> N., R. <u>14</u> E.	11. DRILLERS CERTIFICATION I/We certify that all minimum well construction standards were complied with at the time the rig was removed. Firm Name <u>Boley & Henry</u> Firm No. <u>86</u> Address <u>Murtaugh, Idaho</u> Date <u>5 July, 1983</u> Signed by (Firm Official) <u>B. Boley</u> and (Operator) <u>Russ Boley</u>																																																																																																																																																																																																												

USE ADDITIONAL SHEETS IF NECESSARY - FORWARD THE WHITE COPY TO THE DEPARTMENT

[illegible]

Figure C9. Mike Archibald Well Driller's Log

Form 238-2
1/78

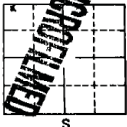
RECEIVED

STATE OF IDAHO
DEPARTMENT OF WATER RESOURCES
WELL DRILLER'S REPORTRECEIVED
USE TYPEWRITER OR
BALLPOINT PEN

JUN 7 1982

State law requires that this report be filed with the Director, Department of Water Resources, within 30 days after the completion or abandonment of the well.

JUN 10 1982

1. WELL OWNER Department of Water Resources Southern District Office Name <u>Canyon Springs Golf Course</u> <u>P. O. Box 112 % J. D. McCollum</u> Address <u>Twin Falls, ID 83301</u> Owner's Permit No. <u>47-7758</u>		7. WATER LEVEL Static water level <u>0</u> feet below land surface. Flowing? <input checked="" type="checkbox"/> Yes <input type="checkbox"/> No G.P.M. flow <u>6300</u> Artesian closed-in pressure <u>240</u> p.s.i. Controlled by: <input checked="" type="checkbox"/> Valve <input type="checkbox"/> Cap <input type="checkbox"/> Plug Temperature <u>102</u> °F. Quality <u>Good</u> <u>103</u> °F																																																																																																																				
2. NATURE OF WORK <input type="checkbox"/> New well <input checked="" type="checkbox"/> Deepened <input type="checkbox"/> Replacement <input type="checkbox"/> Abandoned (describe method of abandoning) _____		8. WELL TEST DATA <input type="checkbox"/> Pump <input type="checkbox"/> Bailor <input type="checkbox"/> Air <input checked="" type="checkbox"/> Other <u>flow</u> <table border="1"> <tr> <th>Discharge G.P.M.</th> <th>Pumping Level</th> <th>Hours Pumped</th> </tr> <tr> <td>6300</td> <td>0</td> <td></td> </tr> </table>		Discharge G.P.M.	Pumping Level	Hours Pumped	6300	0																																																																																																														
Discharge G.P.M.	Pumping Level	Hours Pumped																																																																																																																				
6300	0																																																																																																																					
3. PROPOSED USE <input type="checkbox"/> Domestic <input type="checkbox"/> Irrigation <input type="checkbox"/> Test <input type="checkbox"/> Municipal <input type="checkbox"/> Industrial <input type="checkbox"/> Stock <input type="checkbox"/> Waste Disposal or Injection <input checked="" type="checkbox"/> Other <u>Heating clubhouse</u> (specify type)		9. LITHOLOGIC LOG <u>73889</u> <table border="1"> <thead> <tr> <th>Hole Diam.</th> <th>Depth From</th> <th>To</th> <th>Material</th> <th>Water Yes No</th> </tr> </thead> <tbody> <tr><td>8</td><td>260</td><td>274</td><td>Grey basalt-very hard</td><td></td></tr> <tr><td></td><td>274</td><td>280</td><td>Brown basalt-hard</td><td></td></tr> <tr><td></td><td>280</td><td>312</td><td>Black basalt-hard</td><td></td></tr> <tr><td></td><td>312</td><td>314</td><td>Broken basalt-crevice</td><td></td></tr> <tr><td></td><td>314</td><td>315</td><td>Black basalt-some brown</td><td></td></tr> <tr><td></td><td>315</td><td>329</td><td>Black basalt-big or broken boulders</td><td></td></tr> <tr><td></td><td>329</td><td>377</td><td>Grey basalt-very hard Andesite ?</td><td></td></tr> <tr><td></td><td>377</td><td>389</td><td>Broken black basalt ? Andesite ?</td><td></td></tr> <tr><td></td><td>389</td><td>394</td><td>Black basalt ? Andesite ?</td><td></td></tr> <tr><td></td><td>394</td><td>413</td><td>Broken black basalt</td><td></td></tr> <tr><td></td><td>413</td><td>438</td><td>Grey basalt-very hard</td><td></td></tr> <tr><td></td><td>438</td><td>452</td><td>Softer broken basalt</td><td></td></tr> <tr><td></td><td></td><td></td><td>Trace of cold flowing water</td><td>T</td></tr> <tr><td></td><td>452</td><td>460</td><td>Solid basalt</td><td></td></tr> <tr><td></td><td>460</td><td>552</td><td>Layers of sandstone & clays-some warmer water</td><td>X</td></tr> <tr><td></td><td>552</td><td>592</td><td>Layers of clay & rock</td><td></td></tr> <tr><td></td><td></td><td></td><td>Water increasing-about 150 GPM temp. increase from 80° to 92°F</td><td></td></tr> <tr><td></td><td>592</td><td>670</td><td>Broken rhyolite with shale layers</td><td></td></tr> <tr><td></td><td></td><td></td><td>Water increased about 600 GPM temp 99°</td><td></td></tr> <tr><td></td><td>670</td><td>750</td><td>Broken rhyolite with shale layers</td><td></td></tr> <tr><td></td><td></td><td></td><td>Big increases in water Temp increased 102-103°</td><td></td></tr> <tr><td></td><td></td><td></td><td>See report filed by Denton Drilling 12/27/81</td><td></td></tr> </tbody> </table>		Hole Diam.	Depth From	To	Material	Water Yes No	8	260	274	Grey basalt-very hard			274	280	Brown basalt-hard			280	312	Black basalt-hard			312	314	Broken basalt-crevice			314	315	Black basalt-some brown			315	329	Black basalt-big or broken boulders			329	377	Grey basalt-very hard Andesite ?			377	389	Broken black basalt ? Andesite ?			389	394	Black basalt ? Andesite ?			394	413	Broken black basalt			413	438	Grey basalt-very hard			438	452	Softer broken basalt					Trace of cold flowing water	T		452	460	Solid basalt			460	552	Layers of sandstone & clays-some warmer water	X		552	592	Layers of clay & rock					Water increasing-about 150 GPM temp. increase from 80° to 92°F			592	670	Broken rhyolite with shale layers					Water increased about 600 GPM temp 99°			670	750	Broken rhyolite with shale layers					Big increases in water Temp increased 102-103°					See report filed by Denton Drilling 12/27/81	
Hole Diam.	Depth From	To	Material	Water Yes No																																																																																																																		
8	260	274	Grey basalt-very hard																																																																																																																			
	274	280	Brown basalt-hard																																																																																																																			
	280	312	Black basalt-hard																																																																																																																			
	312	314	Broken basalt-crevice																																																																																																																			
	314	315	Black basalt-some brown																																																																																																																			
	315	329	Black basalt-big or broken boulders																																																																																																																			
	329	377	Grey basalt-very hard Andesite ?																																																																																																																			
	377	389	Broken black basalt ? Andesite ?																																																																																																																			
	389	394	Black basalt ? Andesite ?																																																																																																																			
	394	413	Broken black basalt																																																																																																																			
	413	438	Grey basalt-very hard																																																																																																																			
	438	452	Softer broken basalt																																																																																																																			
			Trace of cold flowing water	T																																																																																																																		
	452	460	Solid basalt																																																																																																																			
	460	552	Layers of sandstone & clays-some warmer water	X																																																																																																																		
	552	592	Layers of clay & rock																																																																																																																			
			Water increasing-about 150 GPM temp. increase from 80° to 92°F																																																																																																																			
	592	670	Broken rhyolite with shale layers																																																																																																																			
			Water increased about 600 GPM temp 99°																																																																																																																			
	670	750	Broken rhyolite with shale layers																																																																																																																			
			Big increases in water Temp increased 102-103°																																																																																																																			
			See report filed by Denton Drilling 12/27/81																																																																																																																			
4. METHOD DRILLED <input checked="" type="checkbox"/> Rotary <input checked="" type="checkbox"/> Air <input checked="" type="checkbox"/> Hydraulic <input type="checkbox"/> Reverse rotary <input checked="" type="checkbox"/> Cable <input type="checkbox"/> Dug <input type="checkbox"/> Other																																																																																																																						
5. WELL CONSTRUCTION Casing schedule: <input checked="" type="checkbox"/> Steel <input type="checkbox"/> Concrete <input type="checkbox"/> Other <table border="1"> <thead> <tr> <th>Thickness</th> <th>Diameter</th> <th>From</th> <th>To</th> </tr> </thead> <tbody> <tr><td>.250 inches</td><td>24 inches</td><td>1 feet</td><td>26 feet</td></tr> <tr><td>.322 inches</td><td>16 inches</td><td>1 feet</td><td>128 feet</td></tr> <tr><td>.375 inches</td><td>12 inches</td><td>1 feet</td><td>261 feet</td></tr> <tr><td>.250 inches</td><td>8 inches</td><td>1 feet</td><td>592 feet</td></tr> </tbody> </table> Was casing drive shoe used? <input type="checkbox"/> Yes <input checked="" type="checkbox"/> No Was a packer or seal used? <input type="checkbox"/> Yes <input checked="" type="checkbox"/> No Perforated? <input type="checkbox"/> Yes <input checked="" type="checkbox"/> No How perforated? <input type="checkbox"/> Factory <input type="checkbox"/> Knife <input type="checkbox"/> Torch Size of perforation _____ inches by _____ inches <table border="1"> <thead> <tr> <th>Number</th> <th>From</th> <th>To</th> </tr> </thead> <tbody> <tr><td>_____ perforations</td><td>_____ feet</td><td>_____ feet</td></tr> <tr><td>_____ perforations</td><td>_____ feet</td><td>_____ feet</td></tr> <tr><td>_____ perforations</td><td>_____ feet</td><td>_____ feet</td></tr> </tbody> </table> Well screen installed? <input type="checkbox"/> Yes <input checked="" type="checkbox"/> No Manufacturer's name _____ Type _____ Model No. _____ Diameter _____ Slot size _____ Set from _____ feet to _____ feet Diameter _____ Slot size _____ Set from _____ feet to _____ feet Gravel packed? <input type="checkbox"/> Yes <input checked="" type="checkbox"/> No <input type="checkbox"/> Size of gravel _____ Placed from _____ feet to _____ feet Surface seal depth <u>261</u> Material used in seal: <input checked="" type="checkbox"/> Cement grout <input type="checkbox"/> Puddling clay <input type="checkbox"/> Well cuttings Sealing procedure used: <input type="checkbox"/> Slurry pit <input type="checkbox"/> Temp. surface casing <input checked="" type="checkbox"/> Overbore to seal depth <input type="checkbox"/> Solvent Weld Method of joining casing: <input type="checkbox"/> Threaded <input checked="" type="checkbox"/> Welded <input type="checkbox"/> Solvent Weld <input type="checkbox"/> Cemented between strata Describe access port _____		Thickness	Diameter	From	To	.250 inches	24 inches	1 feet	26 feet	.322 inches	16 inches	1 feet	128 feet	.375 inches	12 inches	1 feet	261 feet	.250 inches	8 inches	1 feet	592 feet	Number	From	To	_____ perforations	_____ feet	_____ feet	_____ perforations	_____ feet	_____ feet	_____ perforations	_____ feet	_____ feet																																																																																					
Thickness	Diameter	From	To																																																																																																																			
.250 inches	24 inches	1 feet	26 feet																																																																																																																			
.322 inches	16 inches	1 feet	128 feet																																																																																																																			
.375 inches	12 inches	1 feet	261 feet																																																																																																																			
.250 inches	8 inches	1 feet	592 feet																																																																																																																			
Number	From	To																																																																																																																				
_____ perforations	_____ feet	_____ feet																																																																																																																				
_____ perforations	_____ feet	_____ feet																																																																																																																				
_____ perforations	_____ feet	_____ feet																																																																																																																				
6. LOCATION OF WELL Sketch map location must agree with written location.  Subdivision Name _____ Lot No. _____ Block No. _____ County <u>TWIN FALLS</u> <u>TX</u> <u>Twin Falls</u> <u>NW</u> <u>1/4</u> <u>NW</u> <u>1/4</u> Sec. <u>33</u> , T. <u>9</u> S. R. <u>17</u> E.		10. Rotary drilling starting date Work started <u>1-26-82</u> finished <u>3-11-82</u>																																																																																																																				
		11. DRILLERS CERTIFICATION I/We certify that all minimum well construction standards were complied with at the time the rig was removed. Firm Name <u>Walker Water Systems, Inc.</u> Firm No. <u>15</u> <u>624 Pierce Street</u> Address <u>Twin Falls, Idaho 83301</u> Date <u>3/30/82</u> Signed by (Firm Official) <u>Fredrick B. Walker</u> and <u>Fredrick B. Walker</u> (Operator)																																																																																																																				

USE ADDITIONAL SHEETS IF NECESSARY - FORWARD THE WHITE COPY TO THE DEPARTMENT

Figure C10. Canyon Springs Golf Course Well Driller's Log

Form 238-7
8/90

STATE OF IDAHO
DEPARTMENT OF WATER RESOURCES
WELL DRILLER'S REPORT

State law requires that this report be filed with the Director, Department of Water Resources, within 30 days after the completion or abandonment of the well.

Location Corrected by IDWR To:

T09S R17E Sec. 29 NWNWSE

By: mciscell 2012-12-14

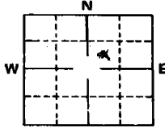
1. WELL OWNER Name <u>Pristine Springs, Inc.</u> Address <u>4074 N 2000 E Filer, ID 83328</u> Drilling Permit No. <u>36-91-Z-003</u> Water Right Permit No. <u>36-7130</u>		7. WATER LEVEL Flowing _____ Static water level _____ feet below land surface. Flowing? <input checked="" type="checkbox"/> Yes <input type="checkbox"/> No G.P.M. flow _____ Artesian closed-in pressure _____ p.s.i. Controlled by: <input type="checkbox"/> Valve <input type="checkbox"/> Cap <input type="checkbox"/> Plug Temperature _____ of Quality _____ Describe artesian or temperature zones below.																																																																																																																																					
2. NATURE OF WORK <input checked="" type="checkbox"/> New well <input type="checkbox"/> Deepened <input type="checkbox"/> Replacement <input type="checkbox"/> Well diameter increase <input type="checkbox"/> Abandoned (describe abandonment procedures such as materials, plug depths, etc. in lithologic log)		8. WELL TEST DATA <input type="checkbox"/> Pump <input type="checkbox"/> Bailer <input type="checkbox"/> Air <input type="checkbox"/> Other _____																																																																																																																																					
3. PROPOSED USE <input type="checkbox"/> Domestic <input type="checkbox"/> Irrigation <input type="checkbox"/> Test <input type="checkbox"/> Municipal <input type="checkbox"/> Industrial <input type="checkbox"/> Stock <input type="checkbox"/> Waste Disposal or Injection <input checked="" type="checkbox"/> Other <u>Fish Propagation & Power Generation</u> (specify type)		9. LITHOLOGIC LOG 83922 <table border="1"> <thead> <tr> <th>Bore Diam.</th> <th>Depth From</th> <th>To</th> <th>Material</th> <th>Water Yes</th> <th>No</th> </tr> </thead> <tbody> <tr><td>12</td><td>270</td><td>302</td><td>Very hard Andesite</td><td></td><td></td></tr> <tr><td></td><td>302</td><td>311</td><td>Slightly softer, trace brown andesite</td><td></td><td></td></tr> <tr><td></td><td>311</td><td>359</td><td>Very hard black andesite</td><td></td><td></td></tr> <tr><td></td><td>359</td><td>366</td><td>Softer black andesite</td><td></td><td></td></tr> <tr><td></td><td>366</td><td>406</td><td>Very hard</td><td></td><td></td></tr> <tr><td></td><td>406</td><td>424</td><td>Softer with little white/tan clay</td><td></td><td></td></tr> <tr><td></td><td>424</td><td>440</td><td>Greenish clay with black</td><td></td><td></td></tr> <tr><td></td><td>440</td><td>457</td><td>Grey basalt</td><td></td><td></td></tr> <tr><td></td><td>457</td><td>465</td><td>Tannish clay & grey basalt</td><td>T</td><td>80°</td></tr> <tr><td></td><td>465</td><td>480</td><td>Greenish grey sandstone with sand & some clay</td><td></td><td>88°</td></tr> <tr><td></td><td>480</td><td>484</td><td>Sand, flowing 60 gpm</td><td></td><td>92°</td></tr> <tr><td></td><td>484</td><td>490</td><td>Overnight drops to 20 gpm</td><td></td><td></td></tr> <tr><td></td><td>490</td><td>502</td><td>Whitish tan clay or shale</td><td></td><td></td></tr> <tr><td></td><td>502</td><td>530</td><td>Greenish grey sand & sandstone</td><td></td><td></td></tr> <tr><td></td><td>530</td><td>551</td><td>Soft black rhyolite</td><td></td><td></td></tr> <tr><td></td><td>551</td><td>574</td><td>Grey & greenish shale or clay</td><td>X</td><td>98°</td></tr> <tr><td></td><td>574</td><td>590</td><td>Soft grey shale with layers of sand</td><td></td><td></td></tr> <tr><td>8</td><td>590</td><td>605</td><td>Brown rhyolite</td><td></td><td></td></tr> <tr><td></td><td>605</td><td>624</td><td>Brown rhyolite</td><td>X</td><td></td></tr> <tr><td></td><td>624</td><td>630</td><td>Brown rhyolite</td><td>X</td><td>100°</td></tr> <tr><td></td><td>630</td><td>770</td><td>Brown rhyolite</td><td>X</td><td></td></tr> </tbody> </table>		Bore Diam.	Depth From	To	Material	Water Yes	No	12	270	302	Very hard Andesite				302	311	Slightly softer, trace brown andesite				311	359	Very hard black andesite				359	366	Softer black andesite				366	406	Very hard				406	424	Softer with little white/tan clay				424	440	Greenish clay with black				440	457	Grey basalt				457	465	Tannish clay & grey basalt	T	80°		465	480	Greenish grey sandstone with sand & some clay		88°		480	484	Sand, flowing 60 gpm		92°		484	490	Overnight drops to 20 gpm				490	502	Whitish tan clay or shale				502	530	Greenish grey sand & sandstone				530	551	Soft black rhyolite				551	574	Grey & greenish shale or clay	X	98°		574	590	Soft grey shale with layers of sand			8	590	605	Brown rhyolite				605	624	Brown rhyolite	X			624	630	Brown rhyolite	X	100°		630	770	Brown rhyolite	X	
Bore Diam.	Depth From	To	Material	Water Yes	No																																																																																																																																		
12	270	302	Very hard Andesite																																																																																																																																				
	302	311	Slightly softer, trace brown andesite																																																																																																																																				
	311	359	Very hard black andesite																																																																																																																																				
	359	366	Softer black andesite																																																																																																																																				
	366	406	Very hard																																																																																																																																				
	406	424	Softer with little white/tan clay																																																																																																																																				
	424	440	Greenish clay with black																																																																																																																																				
	440	457	Grey basalt																																																																																																																																				
	457	465	Tannish clay & grey basalt	T	80°																																																																																																																																		
	465	480	Greenish grey sandstone with sand & some clay		88°																																																																																																																																		
	480	484	Sand, flowing 60 gpm		92°																																																																																																																																		
	484	490	Overnight drops to 20 gpm																																																																																																																																				
	490	502	Whitish tan clay or shale																																																																																																																																				
	502	530	Greenish grey sand & sandstone																																																																																																																																				
	530	551	Soft black rhyolite																																																																																																																																				
	551	574	Grey & greenish shale or clay	X	98°																																																																																																																																		
	574	590	Soft grey shale with layers of sand																																																																																																																																				
8	590	605	Brown rhyolite																																																																																																																																				
	605	624	Brown rhyolite	X																																																																																																																																			
	624	630	Brown rhyolite	X	100°																																																																																																																																		
	630	770	Brown rhyolite	X																																																																																																																																			
4. METHOD DRILLED <input checked="" type="checkbox"/> Rotary <input type="checkbox"/> Air <input type="checkbox"/> Hydraulic <input type="checkbox"/> Reverse rotary <input type="checkbox"/> Cable <input type="checkbox"/> Dug <input type="checkbox"/> Other _____		10. WORK SCHEDULE Work started <u>3/23/92</u> finished <u>4/24/92</u>																																																																																																																																					
5. WELL CONSTRUCTION Casing schedule: <input checked="" type="checkbox"/> Steel <input type="checkbox"/> Concrete <input type="checkbox"/> Other _____ <table border="1"> <thead> <tr> <th>Thickness</th> <th>Diameter</th> <th>From</th> <th>To</th> </tr> </thead> <tbody> <tr> <td>250 inches</td> <td>8 5/8 inches</td> <td>1 feet</td> <td>582 feet</td> </tr> <tr><td> </td><td> </td><td> </td><td> </td></tr> <tr><td> </td><td> </td><td> </td><td> </td></tr> <tr><td> </td><td> </td><td> </td><td> </td></tr> <tr><td> </td><td> </td><td> </td><td> </td></tr> </tbody> </table> Was casing drive shoe used? <input type="checkbox"/> Yes <input checked="" type="checkbox"/> No Was a packer or seal used? <input type="checkbox"/> Yes <input checked="" type="checkbox"/> No Perforated? <input type="checkbox"/> Yes <input checked="" type="checkbox"/> No How perforated? <input type="checkbox"/> Factory <input type="checkbox"/> Knife <input type="checkbox"/> Torch <input type="checkbox"/> Gun Size of perforation _____ inches by _____ inches <table border="1"> <thead> <tr> <th>Number</th> <th>From</th> <th>To</th> </tr> </thead> <tbody> <tr><td> </td><td> </td><td> </td></tr> <tr><td> </td><td> </td><td> </td></tr> <tr><td> </td><td> </td><td> </td></tr> <tr><td> </td><td> </td><td> </td></tr> </tbody> </table> Well screen installed? <input type="checkbox"/> Yes <input checked="" type="checkbox"/> No Manufacturer's name _____ Type _____ Model No. _____ Diameter _____ Slot size _____ Set from _____ feet to _____ feet Diameter _____ Slot size _____ Set from _____ feet to _____ feet Gravel packed? <input type="checkbox"/> Yes <input checked="" type="checkbox"/> No <input type="checkbox"/> Size of gravel _____ Placed from _____ feet to _____ feet Surface seal depth _____ Material used in seal: <input type="checkbox"/> Cement grout <input type="checkbox"/> Bentonite <input type="checkbox"/> Puddling clay <input type="checkbox"/> _____ Sealing procedure used: <input type="checkbox"/> Slurry pit <input type="checkbox"/> Temp. surface casing <input type="checkbox"/> Overbore to seal depth <input type="checkbox"/> Solvent Method of joining casing: <input type="checkbox"/> Threaded <input type="checkbox"/> Welded <input type="checkbox"/> Solvent <input type="checkbox"/> Cemented between joints Describe access port _____		Thickness	Diameter	From	To	250 inches	8 5/8 inches	1 feet	582 feet																	Number	From	To													11. DRILLERS CERTIFICATION I/We certify that all minimum well construction standards were complied with at the time the rig was removed. Walker Water Systems, Inc. Firm Name <u>624 Pierce Street</u> Firm No. <u>15</u> Address <u>Twin Falls, Idaho 83301</u> Date _____ Signed by (Firm Official) <u>Paul Walker</u> and (Operator) _____																																																																																														
Thickness	Diameter	From	To																																																																																																																																				
250 inches	8 5/8 inches	1 feet	582 feet																																																																																																																																				
Number	From	To																																																																																																																																					
6. LOCATION OF WELL Sketch map location must agree with written location.  Subdivision Name _____ Bottom of Blue Lakes _____ Grade _____ Lot No. _____ Block No. _____ County <u>Jerome</u>		12. ADDITIONAL INFORMATION USE ADDITIONAL SHEETS IF NECESSARY - FORWARD THE WHITE COPY TO THE DEPARTMENT																																																																																																																																					

Figure C11. Pristine Springs Well Driller's Log

Appendix K.

Dobson, P.F., Kennedy, B.M., Conrad, M.E., McLing, T., Mattson, E., Wood, T., Cannon, C., Spackman, R., van Soest, M., and Robertson, M., 2015. He isotopic evidence for undiscovered geothermal systems in the Snake River Plain. Proceedings, 40th Workshop on Geothermal Reservoir Engineering, Stanford University, Stanford, CA.

He Isotopic Evidence for Undiscovered Geothermal Systems in the Snake River Plain

Patrick F. Dobson¹, B. Mack Kennedy¹, Mark E. Conrad¹, Travis McLing², Earl Mattson², Thomas Wood³, Cody Cannon³,
Ross Spackman⁴, Matthijs van Soest⁵, and Michelle Robertson¹

¹Earth Sciences Division, Lawrence Berkeley National Laboratory, Berkeley, CA

²Idaho National Laboratory, Idaho Falls, ID

³University of Idaho-Idaho Falls, Idaho Falls, ID

⁴Brigham Young University-Idaho, Rexburg, ID

⁵Arizona State University, Tempe, AZ

Corresponding author: pfdobson@lbl.gov

Keywords: He isotopes, Snake River Plain, geochemistry

ABSTRACT

The Snake River Plain is an area characterized by high heat flow and abundant Quaternary volcanism. While USGS assessments indicate that significant undiscovered geothermal resources are likely to be present in this region, no commercial geothermal development in this region has occurred. Elevated $^3\text{He}/^4\text{He}$ values reflect crustal input of mantle volatiles and may serve as a geochemical indicator of hidden geothermal systems that are masked by the presence of shallow cold water aquifers.

This study is part of an integrated geochemical investigation of thermal features in the central and eastern Snake River Plain region. Our project started by compiling existing He isotope data, regional heat flow data, and the locations of thermal wells and springs to develop compositional trends and identify new sampling opportunities where data gaps exist. Our initial field work has resulted in the highest $^3\text{He}/^4\text{He}$ measurements ever reported for the Snake River Plain, with three locations having Rc/Ra values greater than 2.0, suggesting that we can see through the effects of shallow cold water aquifers to indicate the presence of mantle-derived fluid and heat input into the shallow crust. Our new He isotopic results and previously reported data for the Snake River Plain range from 0.05 to 2.36 Rc/Ra. These results will be evaluated in conjunction with the results of conventional, isotopic, and multicomponent geothermometry studies.

1. INTRODUCTION

One of the key R&D challenges for the DOE Geothermal Technologies Office Hydrothermal program is to develop techniques that can be used to identify undiscovered geothermal resources in the US, which the USGS has estimated as having a mean power production potential of 30 GWe (Williams et al., 2008). One of the main areas with elevated heat flow in the US, the Snake River Plain (Figure 1), has no geothermal systems that have been commercially developed for energy generation. This area is characterized by abundant Quaternary volcanism associated with the migration of the Yellowstone hotspot, but in a large portion of this region there are shallow cold water aquifers that mask the presence of higher temperatures at depth.

Much of the volcanism in the Snake River Plain is associated with the migration of the Yellowstone hotspot (Pierce and Morgan, 2009), and consists of bimodal basalts and rhyolites that have been erupted over the past 17 Ma. The rhyolites were derived from a sequence of progressively younger to the east silicic volcanic centers (Morgan et al., 1984; Leeman et al., 2008). Voluminous basalt flows range in age from Tertiary to Holocene, and are found throughout both the Eastern and Western Snake River Plain. A small subset of these basalts are late Quaternary to Holocene in age, and form 8 distinct eruptive centers (Kuntz et al., 1992; Hughes et al., 2002), including the Craters of the Moon. A number of Quaternary rhyolitic domes and cryptodomes are located in the Eastern Snake River Plain – these are thought to have evolved from differentiation of basalt (McCurry et al., 2008).

While low enthalpy geothermal fluids have been harnessed for direct use in Idaho for more than a century, geothermal exploration activity in the Snake River Plain for high-enthalpy systems has been carried out sporadically over the past 50 years (Ross, 1970; Young and Mitchell, 1973; Parlman and Young, 1992), and has not yet resulted in the discovery and development of a commercial geothermal system in the area. One recent research study, Project Hotspot, drilled three deep (~2 km) wells in three different regions of the Snake River Plain (Nielson et al., 2012; Shervais et al., 2013). One of these wells (Kimama) intersected a thick (>900 m) cold water aquifer before encountering an elevated thermal gradient, while a second well (Kimberley) encountered a thick (~1500m) reservoir of 55-60°C water in rhyolitic lavas and tuffs. The third well (Mountain Home) discovered a high temperature (~150°C) geothermal system with artesian flow. None of these locations had any surface thermal features that could be used to predict the varying thermal conditions that were encountered.

With the exception of active rift zones (such as Iceland) and hot spots (Hawaii), basaltic dominated volcanic provinces are often neglected as possible hosts for productive geothermal systems (Nielson et al., 2015). This is in part due to the lack of shallow, long-

lived magma chambers that would provide a sustained source of heat to the shallow crust. However, as evidenced by the elevated heat flow, volcanic activity in the Snake River Plain region appears to be associated with magmatic intrusions in the crust that do provide a viable source of heat based on crustal models (Peng and Humphreys, 1998; DeNosaquo et al., 2009). McCurry and Welhan (2012), Nielson and Shervais (2014), and McLing et al. (2014) all postulate that basaltic sill complexes associated with these volcanic features could serve as the heat source for geothermal systems in the Snake River Plain region. However, such subsurface features are difficult to detect using standard exploration techniques. One possible way to detect such features is to use a tracer that would be present in geothermal fluids that would identify the presence of a magmatic component. Helium isotopes may serve as such a tracer for geothermal fluids in the Snake River Plain region.

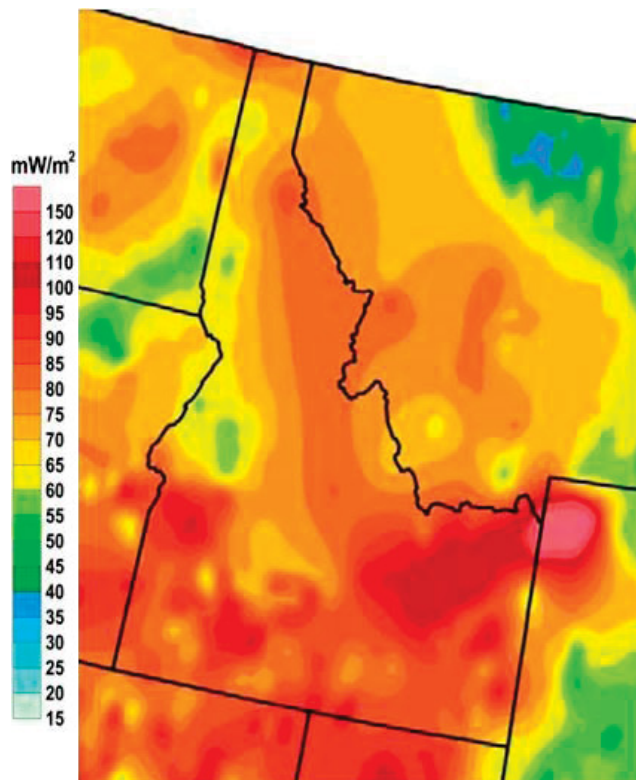


Figure 1: Heat flow map of Idaho and the surrounding region, showing elevated values in the Snake River Plain (Blackwell et al., 2011).

2. FIELD AND LABORATORY METHODS

Helium samples were collected during three field campaigns: September 2003, March 2014, and June 2014. Samples collected in 2014 were obtained from thermal springs and wells as part of a coordinated geochemical study of these features for multicomponent and isotopic geothermometry (McLing et al., 2014; Cannon et al., 2014). A type-K thermocouple was used to measure the temperature of the thermal features. Gas samples for noble gas analyses were collected from bubbling hot springs using an inverted plastic funnel that was connected with Tygon tubing to a copper tube. Gas was bubbled through the system to purge any atmospheric contamination, and the gas samples were then trapped in the copper tube using cold seal weld clamps, resulting in a gas sample volume of $\sim 9.8 \text{ cm}^3$. For water samples without a gas phase, water was collected in copper tubes to trap dissolved gases for analysis. The samples were then analyzed with a noble gas mass spectrometer at the Center for Isotope Geochemistry at LBNL using the methods described in Kennedy and van Soest (2006). Helium isotopic compositions have been corrected for air contamination (R_c) using the He/Ar and Ne/Ar ratios by assuming all of the Ne and Ar were derived from air or air saturated water.

3. RESULTS

There are very few published He isotope values for thermal waters in the Snake River Plain region. Welhan et al. (1988) reported He isotope values ranging from 0.14 to 0.51 R/R_a for four thermal springs in the Snake River Plain region. A more comprehensive unpublished study of He isotopic variations for 19 thermal springs and wells in southern Idaho was conducted by Jenkins (1979); he reported R/R_a values ranging from 0.1 to 1.56, with all but two samples having values less than 1.

The initial results of this study provide He isotope data from a wide range of thermal springs and wells in the Snake River Plain and neighboring areas. A total of 11 He samples were collected during the 2003 field season, and an additional 21 He samples were

collected in 2014. Three of the areas that were sampled in 2003 were resampled in 2014 as a check on the reproducibility of the analyses. In all cases, the Rc/Ra values for the resampled features are within 0.2 Rc/Ra of each other.

He isotope values for the features sampled thus far in this study range from a low of 0.05 Rc/Ra (for Lidy Hot Springs) up to a high value of 2.36 for the Barron's (Camas Creek Ranch) well (Figures 2 & 3). A total of eight features had Rc/Ra values greater than 1.5, with three of these having values greater than 2. The elevated (Rc/Ra > 1.5) values cluster in three distinct regions: one near Craters of the Moon (Green House well), a second in the Twin Falls area (Miracle HS, Banbury HS and well, and Sligers well), and a third located on the northern margin of the Snake River Plain north of Twin Falls (White Arrow HS, Magic Reservoir HS well, and Barron's well).

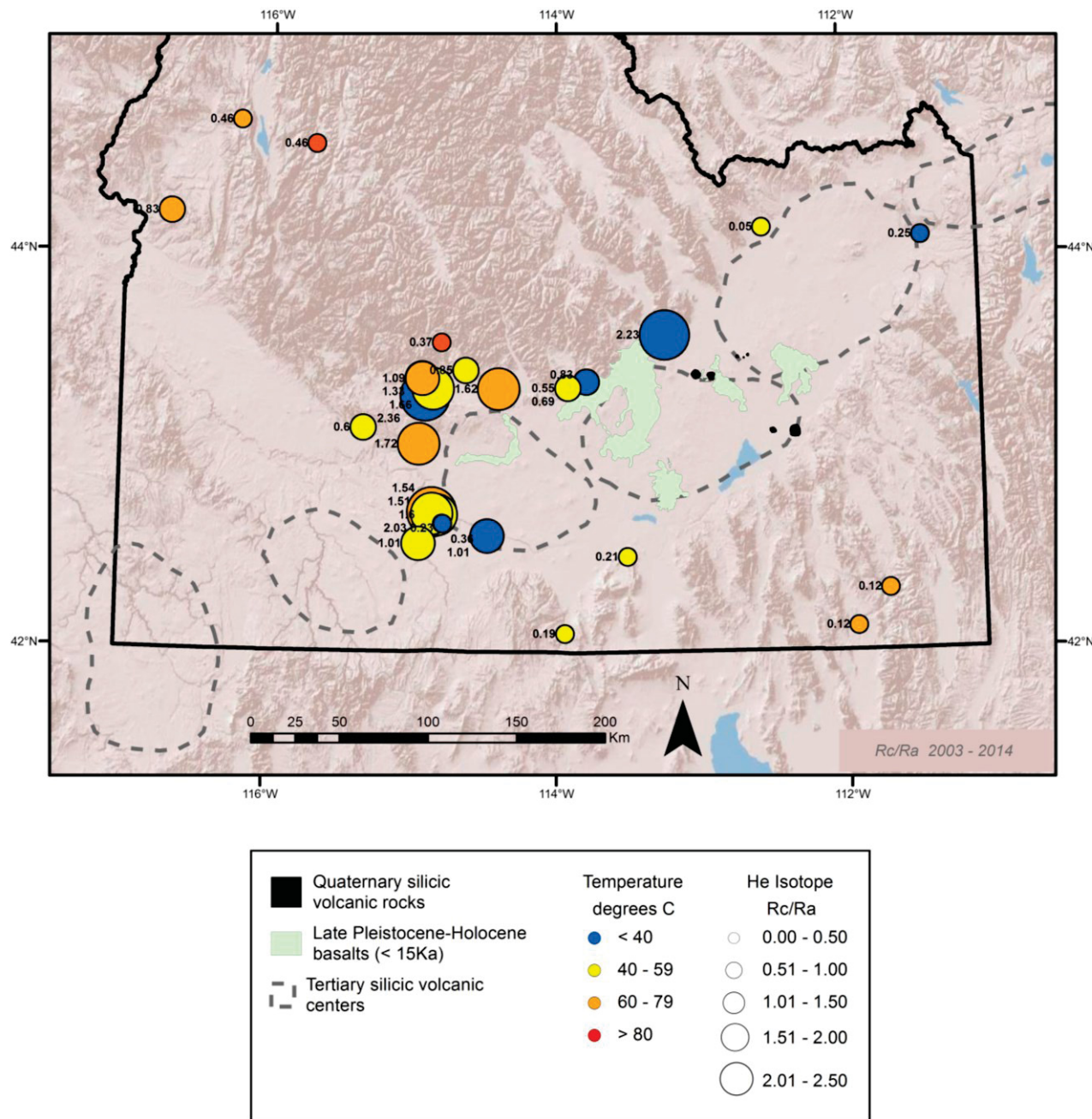


Figure 2: He isotopic values for the Snake River Plain superimposed on a digital elevation map with locations of latest Pleistocene-Holocene basalts (Kuntz et al., 1992; Hughes et al., 2002), Quaternary rhyolites (McCurry et al., 2008), and the outlines of major Tertiary silicic volcanic centers (Leeman et al., 2008). Symbol size and number indicates Rc/Ra He value, and symbol color indicates the measured surface temperature of spring or well.

4. DISCUSSION

Helium isotopes can be used to identify the source of the helium (Ballentine et al., 2002; Graham, 2002), thus facilitating its use as a tracer for the origin of geothermal fluids. There are three major reservoirs of helium: the mantle, the crust, and the atmosphere. The $^3\text{He}/^4\text{He}$ of air is 1.4×10^{-6} , and is defined as Ra. Mantle (magmatic) He values are typically enriched in ^3He , with $^3\text{He}/^4\text{He}$ ratios 7 to 9 times that of atmosphere (7-9 R/Ra). Because ^4He is produced by radiogenic decay of Th and U, crustal He ratios are typically ~ 0.02 R/Ra.

Kennedy and van Soest (2007) conducted a detailed study of He isotopic compositions of thermal features across the Basin and Range. They observed that fluids from geothermal systems located on the western margin of the Great Basin that were associated with a volcanic heat source had elevated $^3\text{He}/^4\text{He}$ values ($\text{Rc}/\text{Ra} > 3$). In contrast, amagmatic geothermal systems in the Basin and Range Province had significantly lower values (Rc/Ra from ~ 0.2 to 2); however, these values are considerably above crustal values (~ 0.02). They interpreted the slightly elevated values for the nonvolcanic systems to reflect amagmatic flow of mantle fluids through the ductile lower crust. The values increased systematically from east to west, correlating with an east-west increase in crustal strain rate suggesting a concurrent east-west increase in deep crustal permeability, enhancing fluid flow to the surface. Several regions were found to have anomalously high R/Ra values with respect to the general trend. Siler et al. (2014) looked to correlate the occurrence of major structural features in these regions to see if they might serve as localized zones of higher permeability that would further facilitate deep crustal circulation of fluids and heat.

While the Snake River Plain has a clear association with young volcanism (Figure 2), the thermal effects of this magmatic activity in the shallow crust are often masked by a thick cold water aquifer that overlies much of the Eastern Snake River Plain region (McLing et al., 2014). This cold water aquifer has a thickness reaching up to more than 900 m in places (Nielson et al., 2012; Shervais et al., 2013). Another challenge is that most of the thermal features encountered in the Snake River Plain are located along its margins. Fluids sampled from these features may have undergone cooling and mixing, thus making interpretation of fluid geothermometry challenging. Multicomponent geothermometry has been employed to better constrain the source temperatures of these complex fluids (Neupane et al., 2014; Cannon et al., 2014).

During the preliminary phase of this project, we examined the three regions with elevated He isotopic ratios to see if they coincide with areas that have evidence of young volcanism (Figure 2) or high heat flow (Figure 3). Only one of the areas (Green House well – $\text{Rc}/\text{Ra} = 2.23$, by Arco) is near young (< 15 Ka) volcanic rocks (Craters of the Moon). This well is quite unremarkable in terms of its flowing temperature (36.3°C), and multicomponent geothermometry yields a source temperature estimate of only $67 \pm 15^\circ\text{C}$ (Cannon et al., 2014). The other two high He isotope clusters (the Twin Falls area and the area near Magic Reservoir HS) are in areas with Miocene rhyolites and Plio-Pleistocene basalts (Leeman et al., 1982; Whitehead, 1992; Ellis et al., 2010) but are generally associated with higher temperature thermal features and/or wells. These clusters are located in areas with high heat flow (Figure 3).

One area that warrants future study is the region around Mountain Home, where drilling has revealed the existence of a hidden 150°C geothermal reservoir (Shervais et al., 2013). Unfortunately this well was plugged and abandoned before it could be sampled for He isotopes, but other wells in the region might contain geochemical signatures related to this system. While this area does not have Holocene volcanism, it does host Quaternary basalts (Shervais et al., 2002) and may be underlain by younger basaltic sills (Nielson and Shervais, 2014).

4. CONCLUSIONS

New helium isotope data for thermal waters in the Snake River Plain has revealed a number of elevated ($\text{Rc}/\text{Ra} > 1.5$) He isotope values that are higher than previously reported data for this region. These values suggest a significant mantle helium component. These elevated values have been observed thus far in three different areas within the Snake River Plain. There is not a clear correlation between these elevated $^3\text{He}/^4\text{He}$ values and young (< 15 Ka) volcanic features. However, this He signature may be related to basaltic intrusions that are thought to sustain the high heat flow in this region. Future work will include integration of the He data with isotope and multicomponent geothermometry and collection of additional samples in areas such as Mountain Home, where a hidden geothermal system has been discovered. Such sampling will help test whether He isotopes can help identify systems that have no surface manifestations in the Snake River Plain region.

ACKNOWLEDGMENTS

This work was conducted with funding by the Assistant Secretary for Energy Efficiency and Renewable Energy, Geothermal Technologies Program, of the U.S. Department under the U.S. Department of Energy Contract No. DE-AC02-05CH11231 with Lawrence Berkeley National Laboratory. We thank Will Smith, Hari Neupane, Wade Worthing, and Steven Levesque for their assistance in the field, and to the many property owners in Idaho who graciously allowed us access to the springs and wells on their land. We also thank Colin Williams (USGS) for sharing his heat flow maps with our team.

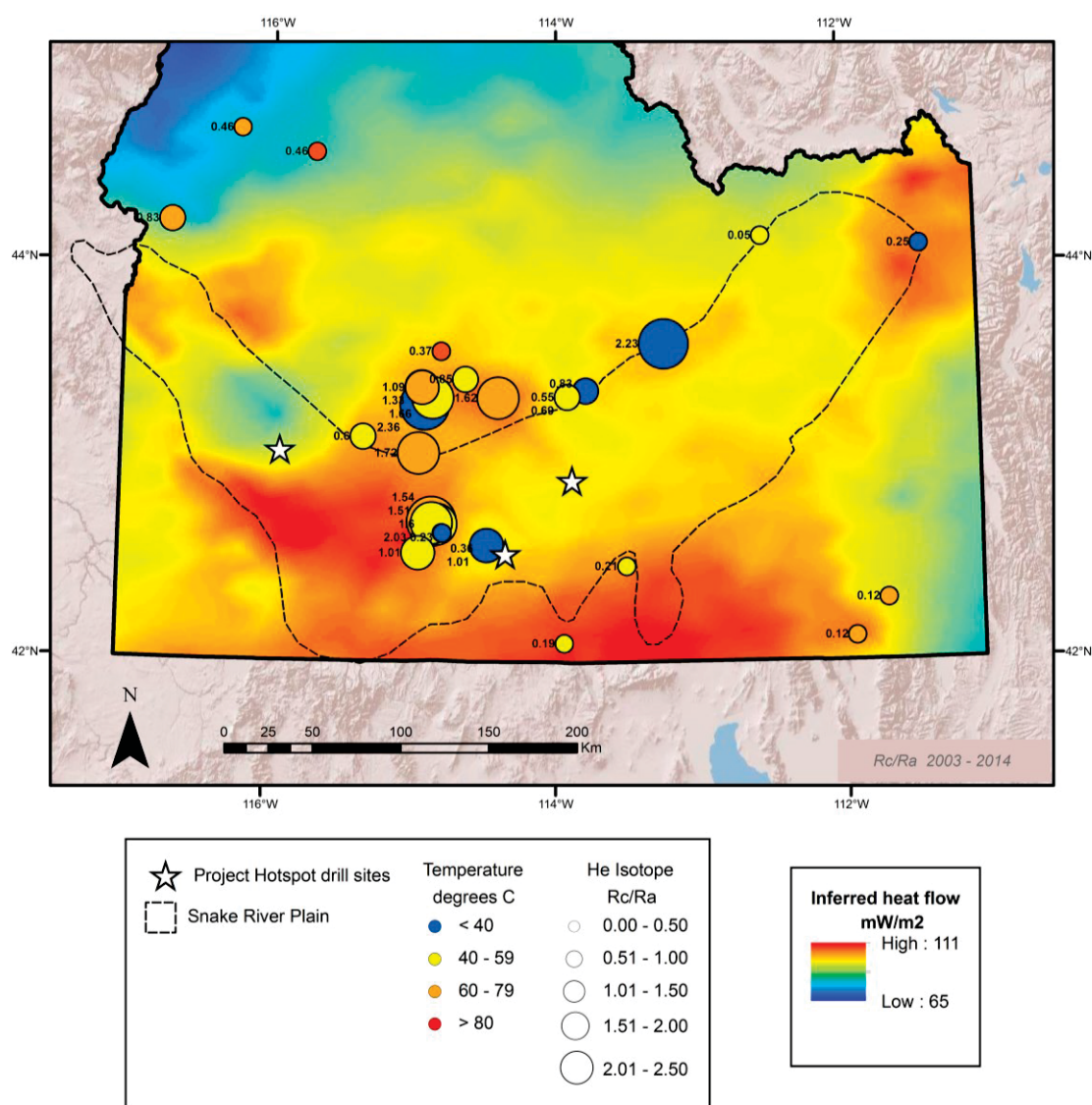


Figure 3: He isotopic values for the Snake River Plain superimposed on USGS heat flow map of the Snake River Plain (Williams and DeAngelo, 2011). Map depicts inferred heat flow below the groundwater flow system. Map was generated to identify regional-scale variations, so high heat flow in geothermal regions was capped at 120 mW/m². Outline of the Snake River Plain province from Payne et al. (2012). Symbol size and number indicates Rc/Ra He value, and symbol color indicates measured surface temperature of spring or well. The three Project Hotspot wells, depicted as stars, are (from west to east) Mountain Home, Kimberly, and Kimama (Shervais et al., 2013).

REFERENCES

- Ballentine, C.J., Burgess, R., and Marty, B.: Tracing Fluid Origin, Transport and Interaction in the Crust, in Porcelli, D., Ballentine, C.J., and Wieler, R., eds., *Reviews in Mineralogy & Geochemistry—Noble Gases in Geochemistry and Cosmochemistry*: Washington, D.C., Mineralogical Society of America, v. 47, (2002), 539–614.
- Blackwell, D.D., Richards, M.C., Frone, Z.S., Batir, J.F., Williams, M.A., Ruzo, A.A., and Dingwall, R.K.: SMU Geothermal Laboratory Heat Flow Map of the Conterminous United States, 2011, (2011), Available at <http://www.smu.edu/geothermal>
- Cannon, C., Wood, T., Neupane, G., McLing, T., Mattson, E., Dobson, P., and Conrad, M.: Geochemistry Sampling for Traditional and Multicomponent Equilibrium Geothermometry in Southeast Idaho, *Geothermal Resources Council Transactions*, **38**, (2014), 425–431.
- DeNosaquo, K.R., Smith, R.B. and Lowry, A.R.: Density and Lithospheric Strength Models of the Yellowstone-Snake River Plain Volcanic System from Gravity and Heat Flow Data. *Journal of Volcanology and Geothermal Research*, **188**, (2009), 108–127.

- Ellis, B.S., Barry, T., Branney, M.J., Wolff, J.A., Bindeman, I., Wilson, R. and Bonnicksen, B.: Petrologic constraints on the development of a large-volume, high temperature, silicic magma system: The Twin Falls eruptive centre, central Snake River Plain, *Lithos*, **120**, (2010), 475–489.
- Graham, D.W.: Noble Gas Isotope Geochemistry of Mid-Ocean Ridge and Ocean Island Basalts: Characterization of Mantle Source Reservoirs, in Porcelli, D., Ballentine, C.J., and Wieler, R., eds., *Reviews in Mineralogy & Geochemistry— Noble Gases in Geochemistry and Cosmochemistry*: Washington, D.C., Mineralogical Society of America, v. 47, (2002), 481–538.
- Hughes, S.S., Wetmore, P.H. and Casper, J.L.: Evolution of Quaternary Tholeiitic Basalt Eruptive Centers on the Eastern Snake River Plain, Idaho. In B. Bonnicksen, C.M. White, and M. McCurry, eds., *Tectonic and Magmatic Evolution of the Snake River Plain Volcanic Province*, Idaho Geological Survey Bulletin **30**, (2002), 23 p.
- Jenkins, W.J.: Mapping of Volcanic and Conducted Heat Flow Sources for Thermal Springs in the Western United States Using Helium Isotopes and other Rare Gases. U.S. Geological Survey unpublished report, (1979). Data reported in Kennedy and van Soest (2007) supplemental materials (www.sciencemag.org/cgi/content/full/318/5855/1433/DC1)
- Kennedy, B.M., and van Soest, M.C.: Flow of Mantle Fluids through the Ductile Lower Crust: Helium Isotope Trends, *Science*, **318**, (2007), 1433–1436.
- Kuntz, M.A., Covington, H.R., and Schorr, L.J.: Chapter 12 – An Overview of Basaltic Volcanism of the Eastern Snake River Plain, Idaho. In Link, P.K., Kuntz, M.A., and Platt, L.B., eds., *Regional Geology of Eastern Idaho and Western Wyoming*, *Geological Society of America Memoir* 179, (1992), 227–267.
- Leeman, W.P.: Geology of the Magic Reservoir Area, Snake River Plain, Idaho. In B. Bonnicksen and R.M. Breckenridge, eds., *Cenozoic Geology of Idaho*, Idaho Bureau of Mines and Geology Bulletin **26**, (1982), 369–376.
- Leeman, W.P., Annen, C. and Dufek, J.: Snake River Plain – Yellowstone Silicic Volcanism: Implications for Magma Genesis and Magma Fluxes. In Annen, C. and Zellmer, G. F. (eds) *Dynamics of Crustal Magma Transfer, Storage and Differentiation*. Geological Society, London, Special Publications, **304**, (2008), 235–259.
- McCurry, M., Hayden, K.P., Morse, L.H. and Mertzman, S.: Genesis of Post-Hotspot, A-Type Rhyolite of the Eastern Snake River Plain Volcanic Field by Extreme Fractional Crystallization of Olivine Tholeiite. *Bulletin of Volcanology* **70**, (2008), 361–383.
- McCurry, M. and Welhan, J.: Do Magmatic-Related Geothermal Energy Resources Exist in Southeast Idaho? *Geothermal Resources Council Transactions*, **36**, (2012), 699–707.
- McLing, T., McCurry, M., Cannon, C., Neupane, G., Wood, T., Podgorney, R., Welhan, J., Mines, G., Mattson, E., Wood, R., Palmer, C. and Smith, R.: David Blackwell’s Forty Years in the Idaho Desert, The Foundation for 21st Century Geothermal Research. *Geothermal Resources Council Transactions*, **38**, (2014), 143–153.
- Neupane, G., Mattson, E.D., McLing, T.L., Palmer, C.D., Smith, R.W. and Wood, T.R.: Deep Geothermal Reservoir Temperatures in the Eastern Snake River Plain, Idaho using Multicomponent Geothermometry, *Proceedings*, 39th Workshop on Geothermal Reservoir Engineering, Stanford University, Stanford, CA, (2014), 12 p.
- Nielson, D.L., Delahunty, C. and Shervais, J.W.: Geothermal systems in the Snake River Plain, Idaho, Characterized by the Hotspot Project, *Geothermal Resources Council Transactions*, **36**, (2012), 727–730.
- Nielson, D.L., and Shervais, J.W.: Conceptual Model for Snake River Plain Geothermal Systems, *Proceedings*, 39th Workshop on Geothermal Reservoir Engineering, Stanford University, Stanford, CA, (2014), 7 p.
- Nielson, D.L., Shervais, J., Evans, J., Liberty, L., Garg, S.K., Glen, J. Visser, C., Dobson, P., Gasperikova, E., and Sonnenthal, E.: Geothermal Play Fairway Analysis of the Snake River Plain, Idaho, *Proceedings*, 40th Workshop on Geothermal Reservoir Engineering, Stanford University, Stanford, CA, (2015), 9 p.
- Parlman, D.J. and Young H.W.: Compilation of Selected Data for Thermal-Water Wells and Springs in Idaho, 1921 through 1991. *U.S. Geological Survey Open-File Report* **92-175**, (1992), 201 p.
- Payne, S.J., McCaffrey, R., King R.W. and Kattenhorn, S.A.: A New Interpretation of Deformation Rates in the Snake River Plain and Adjacent Basin and Range Regions Based on GPS Measurements. *Geophysical Journal International*, **189**, (2012), 101–122.
- Peng, X. and Humphreys, E.D.: Crustal Velocity Structure across the Eastern Snake River Plain and the Yellowstone Swell. *Journal of Geophysical Research, B, Solid Earth and Planets*, **103(4)**, (1998), 7171–7186.
- Pierce, K.L. and Morgan, L.A.: Is the Track of the Yellowstone hotspot Driven by a Deep Mantle Plume? – Review of Volcanism, Faulting, and Uplift in Light of New Data, *Journal of Volcanology and Geothermal Research*, **188**, (2009), 1–25.
- Ross, S.H.: Geothermal Potential of Idaho. *Geothermics*, Special Issue **2**, v. 2, part 2, (1970), 975–1008.
- Shervais, J.W., Schmidt, D.R., Nielson, D., Evans, J.P., Christiansen, E.H., Morgan, L., Shanks, W.C.P., Prokopenko, A.A., Lachmar, T., Liberty, L.M., Blackwell, D.D., Glen, J.M., Champion, D., Potter, K.E. and Kessler, J.A.: First Results from HOTSPOT: The Snake River Plain Scientific Drilling Project, Idaho, U.S.A., *Scientific Drilling*, **15**, (2013), 36–45.
- Shervais, J.W., Shroff, G., Vetter, S.K., Matthews, S., Hanan B.B., and McGee, J.J.: Origin and Evolution of the Western Snake River Plain: Implications from Stratigraphy, Faulting, and the Geochemistry of Basalts near Mountain Home, Idaho. In B. Bonnicksen,

- C.M. White, and M. McCurry, eds., Tectonic and Magmatic Evolution of the Snake River Plain Volcanic Province: Idaho Geological Survey Bulletin **30**, (2002), 343–361.
- Siler, D.L., Kennedy, B.M. and Wannamaker, P.E.: Regional Crustal Discontinuities as Guides for Geothermal Exploration, *Geothermal Resources Council Transactions*, **38**, (2014), 39–47.
- Welhan, J.A., Poreda, R.J., Rison, W., and Craig, H.: Helium Isotopes in Geothermal and Volcanic Gases of the Western United States, I. Regional Variability and Magmatic Origin, *Journal of Volcanology and Geothermal Research*, **34**, (1988), 185–199.
- Whitehead, R.L.: Geohydrologic Framework of the Snake River Plain Regional Aquifer System, Idaho and Eastern Oregon, *U.S. Geological Survey Professional Paper* **1408-B**, (1992), 32 p.
- Williams, C.F., and DeAngelo, J.: Evaluation of Approaches and Associated Uncertainties in the Estimation of Temperatures in the Upper Crust of the Western United States, *Geothermal Resources Council Transactions*, **35**, (2011), 1599–1605.
- Williams, C.F., Reed, M.J., Mariner, R.H., DeAngelo, J. and Galanis, S.P., Jr.: Assessment of Moderate- and High-Temperature Geothermal Resources of the United States, *U.S. Geological Survey Fact Sheet* **2008-3082**, (2008), 4 p.
- Young, H.W. and Mitchell, J.C.: Geothermal Investigations in Idaho Part 1: Geochemistry and Geologic Setting of Selected Thermal Waters. Idaho Department of Water Administration, Water Information Bulletin **30**, (1973), 43 p.